昭和33年12月25日　昭和36年11月8日　印刷［毎月1回
第3種郵便物認可　昭和36年11月15日　発行　15日発行］

OHIO STATE UNIVERSITY
FEB 21 1962
LIBRARY

BULLETIN OF THE CHEMICAL SOCIETY OF JAPAN

Vol. 34 No. 11 November 1961

CHEMISTRY HALL LIBRARY

CONTENTS

General and Physical

Stress Relaxation of Gels of Polyvinyl Alcohol-Glycerin-Water System . . . . . K. Arakawa 1549
The Infrared Absorption Spectrum of 1,2,4,5-Tetrachlorobenzene in Vapor State . . . S. Saëki 1552
π Electronic Structure of Cinnamaldehyde . . . . . K. Inuzuka 1557
The Diamagnetic Susceptibility of Benzoate, Salicylate, Propionate, Butyrate and Succinate Ions . . . . . S. Sriraman and S. Thiruvengadathan 1560
Semiconductivity and Absorption Spectrum of Perylene Single Crystal . . . . . M. Sano and H. Akamatu 1569
Thermodynamical Studies on Binary Systems Consisting of Polar and Non-polar Liquids. IV. Estimation of the Electrostatic Part of the Excess Enthalpy from the Observed Values and Comparison with the Calculated Values . . . . . K. Amaya 1584
Thermodynamical Studies on Binary Systems Consisting of Polar and Non-polar Liquids. V. The Anomalies in the Binary Systems of Polar Liquid with Aromatic Non-polar Liquid. . . . . K. Amaya 1592
Mass-spectrometric Study on Ionization and Dissociation of Diethyl Ether by Electron Impact . . . . . I. Kanomata 1596
Proton Magnetic Resonance Spectra of *p*-Cresol . . . . . I. Yamaguchi 1602
Nuclear Magnetic Resonance in Amino-group of Aniline Derivatives . . . . . I. Yamaguchi 1606
Infrared and Raman Spectra of Dialkoxy Methanes in Various Phases and the Assignment of Spectra of Methoxy Ethoxy Methane. . . . . K. Nukada 1615
Infrared and Raman Spectra of Diethoxy Methane and Diethoxy Methane-d_2 . . . K. Nukada 1624
Oxidation of Ferrous Ions in Aqueous Solutions by Cobalt-60 Gamma Rays. II. Effect of Anions at High Dose . . . . . H. Hotta and S. Ohno 1640
Synthesis of Several Tertiary Alcohols from Propanol-2 and Ethylene by Gamma-ray Irradiation . . . . . K. Hirota and M. Hatada 1644
Photoreduction of Methylene Blue by the Visible Light in the Aqueous Solution Containing Certain Kinds of Inorganic Salts. III. Kinetic Treatment of the Reaction . . . . . Y. Usui and M. Koizumi 1651
Raman Spectra of *p*-Dichlorobenzene and *p*-Dichlorobenzene-d_4 . . . . . S. Saëki 1658
Decomposition of Mono- and Diethanolamine Carbamate in Glycerol Solution . . M. Matsuda 1665
Photoconductivity of Polycyclic Aromatic Compounds . . . . . M. Sano 1668
Studies on Phenolic Resins. IV. Physical and Chemical Properties of Coating Films of Japanese Lac (*Urushi*) (Rigidity Modulus-Temperature Relations Measured by Tortional Pendulum Method) . . . . . T. Kuwata, J. Kumanotani and S. Kazama 1978
Non-Emprirical Calculation of the π-Electronic Structure of Cyclobutadiene Molecule by Valence Bond Method . . . . . S. Takekiyo 1686
Statistical Thermodynamics of Solutions of Optically Active Substances. I. Excess Free Energy of Binary Solution of *d*- and *l*-Isomers. . . . . K. Amaya 1689
Spectroscopic Studies on Molecular Configurations of Some Aliphatic Dinitriles. I. Infrared Spectra of Succinonitrile and Bis(succinonitrilo)copper(I) Nitrate. . . . . I. Matsubara 1710
Spectroscopic Studies on Molecular Configurations of Some Aliphatic Dinitriles. II. Infrared Spectra of Glutaronitrile and Bis(glutaronitrilo)copper(I) Nitrate. . . . . I. Matsubara 1719

(Continued on inside cover)

Published by the Chemical Society of Japan

THE CHEMICAL SOCIETY OF JAPAN
(NIPPON KAGAKUKAI)

Founded in 1948

Successor to the former Chemical Society of Japan founded in 1878 and to the Society of Chemical Industry, Japan founded in 1898.

BULLETIN OF THE CHEMICAL SOCIETY OF JAPAN

Editor: Tadao SHIBA, Tokyo Institute of Technology, Tokyo
Assistant Editor: Tadashi SUEHIRO, Gakushuin University, Tokyo
Editorial Board:

Yoshié BANSHO	Hidehiro GOTÔ	Keniti HIGASI
Yoshimasa HIRATA	Hiroo INOKUCHI	Tatsujiro ISHIMORI
Tadashi KAMIKUBO	Michio KOBAYASHI	Ichiro MIYAGAWA
Masazumi NAKAGAWA	Shigeru OAE	Shigeru OHASHI
Kazuo SATAKE	Syûzô SEKI	Osamu SIMAMURA
Yoshitada TOMODA	Iwao YASUMORI	Koshiro YOSHIOKA

(Continued from outside cover)

Synthesis and Physical Properties of Normal Higher Primary Alcohols. IV. Thermal and X-Ray Studies on the Polymorphism of the Alcohols of Even Carbon Numbers from Dodecanol to Tetratriacontanol . . . . . A. WATANABE 1728

Analytical and Inorganic

Refractometric Study of Some Cyano and Oxalato Complex Anions . . . . . Y. MATSUNAGA 1563
Hot-atom Chemistry of Hexamminechromium(III) Nitrate in the Solid State . . . . . N. IKEDA, K. YOSHIHARA, H. EBIHARA and K. SUZUKI 1705

Organic and Biological

The Preparation of *cis*- and *trant*-4-*tret*-Butylcyclohexyl-1-carbinols . . . . . N. MORI 1567
Syntheses of γ-Ionone Analogues. I–II . . . . . A. ARAI and I. ICHIKIZAKI 1571
Proton Magnetic Resonance Spectra of Methylthiophenesulfonylchlorides . . . . . K. TAKAHASHI, Y. MATSUKI, Y. MIYAKE and G. HAZATO 1599
Synthesis and Reactions of Cyano- and Carboxytropones . . . . . K. KIKUCHI 1610
Structure of Enteromycin. III. Structure of Demethoxyenteromycin. . . . . K. MIZUNO 1631
Structure of Enteromycin. IV. . . . . K. MIZUNO 1633
Syntheses and Ultraviolet Spectra of Aromatic Azo Compounds. I. Bromo-methylazobenzenes . . . . . Y. NOMURA 1648
Stereoregular Polymers. IX. Polymerization of Optically Active α-Olefins . . . . . S. NOZAKURA, S. TAKEUCHI, H. YUKI and S. MURAHASHI 1673
Forschung über die katalytische Entwässerung des Isoamylalkohols. III. Prüfung über die Bestandteile der durch Zinksulfat-Katalysator-Entwässerung entstehenden Produkten . . . . . A. MITSUTOMI 1693
Forschung über die katalytische Entwässerung des Isoamylalkohols. IV. Quantitative Untersuchung der durch unterm Einsatz des Zinksulfat-Katalysators erfolgende Dehydratisierung gebildeten Produkte auf ihre Bestandteile . . . . . A. MITSUTOMI und E. FUNAKUBO 1698

Short Communications

A New Rapid Method of Determining Molecular Weight of Water Soluble Linear Polymers by the Measurement of Rate of Settling of Clay Suspensions . . . . . Y. TOYOSHIMA 1734
Cation-exchange Properties of Phosphoantimonic(V) Acid . . . . . T. ITO and M. ABE 1736
Chemical Constitution of Enmein a Bitter Principle from Isodon trichocarpus Kudo . . . . . T. KUBOTA, T. MATSUURA, T. TSUTSUI and K. NAYA 1737
Tritium and Carbon-14 in the Tree Rings. . . . . K. KIGOSHI and Y. TOMIKURA 1738
Variation of the Atmospheric Carbon-14 in Recent Years at Tokyo . K. KIGOSHI and K. ENDO 1739
Dipole Moment and Infrared Spectrum of 2, 3, 5, 6-Tetraisopropylnitrobenzene . . . . . R. NAKASHIMA, S. WATARAI and T. KINUGASA 1740
On the pH Dependence of Transport Behavior of Weak Acids and Weak Bases across Ion-exchange Membranes . . . . . M. SENŌ and T. YAMABE 1741

Stress Relaxation of Gels of Polyvinyl Alcohol-Glycerin-Water System

By Kiyoshi ARAKAWA

(Received March 2, 1961)

In the previous paper[1] the results of the stress relaxation study on the gels of the polyvinyl alcohol-glycerin-water system were reported. This was taken as an example of non-electrolytic thermo-reversible gel systems of polymeric nature, and some discussions were held concerning the concentration dependence of relaxation spectrum.

The average molecular weight of the sample of polyvinyl alcohol used in the previous study was 1.1×10^4, which was comparatively low as a polymer. Another study on the mechanical behavior of polyvinyl alcohol-glycerin-water gels has been attempted for a polyvinyl alcohol sample of higher molecular weight in order to investigate the effect of the molecular weight difference on its mechanical behavior and to obtain further knowledge concerning the concentration dependence of relaxation spectrum.

Experimental

Sample. — A commercial sample of polyvinyl alcohol was used. The amount of residual acetyl group of this powder sample was 1.0% by mole, which was determined by the titration method. The intrinsic viscosity $[\eta]_{25}$ obtained by means of a capillary viscometer of Ostwald type was 1.27 (100 cc./g.), and the viscosity average molecular weight which was calculated from the value of viscosity by Diew's formula[2] was 8.5×10^4.

The preparation of specimen gels was made according to the same procedure as that described in the previous paper[1] and also the mixing ratio of glycerin and water was made to be precisely the same as before. Gels of three different concentrations of polyvinyl alcohol were prepared, namely: 6.05, 7.95 and 9.07% by weight.

Apparatus and Procedure for Measurements. — The same relaxometer as has been used in the preceding studies[3] on the rheological properties of thermo-reversible gels was used in this experiment. The measurement of relaxation Young's modulus under a given constant strain was carried out for two hours after sudden imposition of the strain. The imposed strain was 5% for 7.95% and 9.07% gels, and 20% for 6.05% gels, respectively. The temperature was varied with about 10°C interval.

1) K. Arakawa, This Bulletin, **31**, 842 (1958).
2) H. Diew, *J. Polymer Sci.*, **12**, 147 (1954).
3) K. Arakawa, This Bulletin, **32**, 1248 (1959); ibid., **33**, 1568 (1960); K. Arakawa and K. Atsumi, *J. Chem. Soc. Japan, Pure Chem. Sec.* (*Nippon Kagaku Zasshi*) **80**, 133 (1959).

Results and Discussion

Relaxation Data. — The relaxation Young's modulus under constant compressional strain at various temperatures is plotted in the form of $(298/T)E_r$ versus log t, where $(298/T)$ is a reduction factor to 25°C concerning rubber-like elasticity. The results are shown in Figs. 1(a), 1(b), and 1(c) for each concentration.

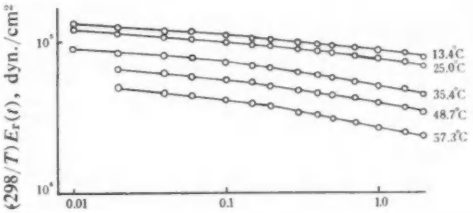

Fig. 1 (a). Reduced relaxation Young's modulus $(298/T)E_r(t)$ of 6.05% gel.

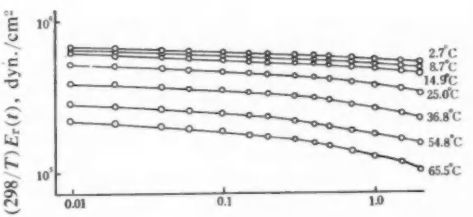

Fig. 1 (b). Reduced relaxation Young's modulus $(298/T)E_r(t)$ of 7.95% gel.

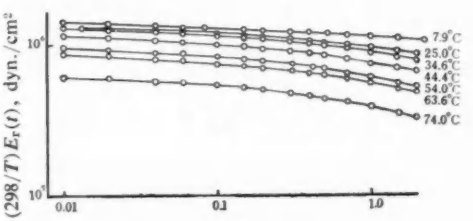

Fig. 1 (c). Reduced relaxation Young's modulus of 9.07% gel.

According to the time-temperature superposition principle[4], a master relaxation curve at 25°C for each concentration is obtained by shifting the relaxation curves at different temperatures horizontally along the $\log t$ axis. The master relaxation curves, thus obtained, are shown in Fig. 2. The coincidence of each relaxation curve by superposition is good as seen in Fig. 2.

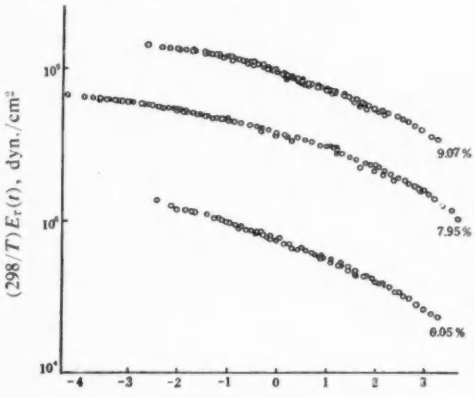

Fig. 2. Master relaxation curves at 25°C.

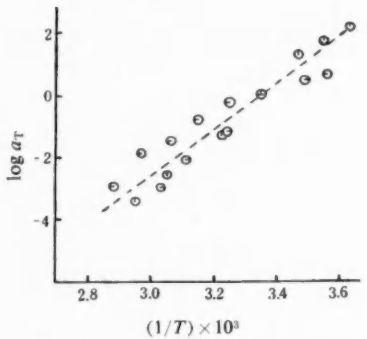

Fig. 3. $\log a_T$ versus $1/T$ relation.
⊖ 6.05%, ⊙ 7.95%, ⊖ 9.07%

The shift factors $\log a_T$ are plotted against $1/T$ in Fig. 3. This plotting shows a nearly linear relation, as in the case of the previous study[1], where the molecular weight of the polyvinyl alcohol was 1.1×10^4. Thus, the apparent activation energy H_a calculated from the gradient of the $\log a_T$ versus $1/T$ curve is kept constant within the temperature and concentration ranges in the present study. When the apparent activation energy is constant, shift factors a_T are expressed as follows,

$$a_T = A\exp(H_a/RT) \quad (1)$$

The values of $\log A$ and H_a are given in Table I, together with those of molecular weight 1.1×10^4 in the previous paper[1].

TABLE I. VALUES OF $\log A$ AND H_a

Mol. wt. of polyvinyl alcohol	8.5×10^4	1.1×10^4
$\log A$	−25.7	−43.8
H_a (kcal./mol.)	35	60

The constancy of H_a as well as the good coincidence of each relaxation curve by superposition is said to support the adequacy of the application of the superposition method, which exhibits the equality of the temperature dependence of all relaxation mechanisms within these ranges of temperature and concentration[5].

In order to compare the temperature dependence of shift factors in this case with the equation of the WLF form[6], the values of $\log a_T$ referred to T_S are plotted against $T-T_S$ in Fig. 4, where T_S is a reference temperature. The values of $\log a_T$ agree with the curve of

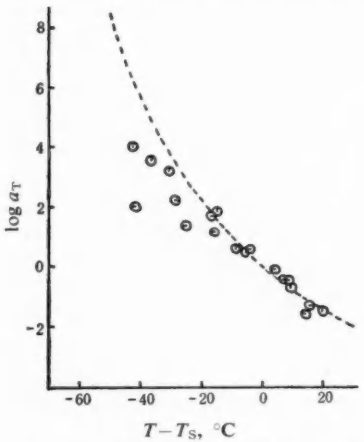

Fig. 4. $\log a_T$ versus $T-T_S$ relation.
⊖ 6.05%, ⊙ 7.95%, ⊖ 9.07%
---- Equation of WLF form, C_1: 8.86, C_2: 101.6
Values of T_S 315°K for 6.05%
319°K for 7.95%
323°K for 9.07%

WLF equation within the range of $(T-T_S)=-20\sim20$°C, but outside of this range they deviate from the curve.

Concentration Dependence of Distribution Functions of Relaxation Times.—From the

4) A. V. Tobolsky, "Properties and Structure of Polymers", John Wiley and Sons, Inc., Publishers, New York (1960), Chapter 4, Sec. 2 and 3.

5) C. A. Dahlquist and M. R. Hatfield, *J. Colloid Sci.*, **7**, 253 (1952).

6) M. L. Williams, R. F. Landel and J. D. Ferry, *J. Am. Chem. Soc.*, **77**, 3701 (1955).

master curves shown in Fig. 2 distribution functions of relaxation times, $H(\log\tau)$, which are defined by Eq. 2 are obtained by Alfrey's first order approximation, Eq. 3.

$$E_r(t)=\int_0^\infty H(\log\tau)e^{-(t/\tau)}\mathrm{d}\log\tau \qquad (2)$$

$$H(\log\tau)=-2.303\left[E_r\frac{\mathrm{d}\log E_r}{\mathrm{d}\log t}\right]_{t=\tau} \qquad (3)$$

The distribution functions, thus obtained, are shown in Fig. 5. As is seen clearly, they are of typical box type character. When seen in details, there appears a fairly broad flat region in the curve for the gel of 7.95% and a peak in the curve for the gel of 9.07%. The curve for the gel of 6.05% is regarded as the one in the rubbery flow region which follows after the flat region. The distribution functions of the gels described in the previous paper[1] are shown together for comparison by dotted lines.

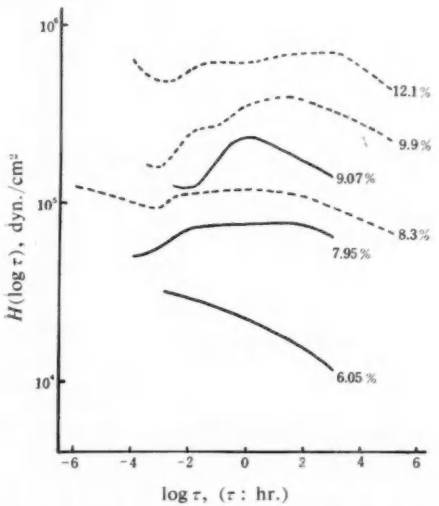

Fig. 5. Distribution functions of relaxation times.
—— Molecular weight, 8.5×10^4
---- Molecular weight, 1.1×10^4

When we see in detail the change in the shape of the curves with increase of concentration, it may certainly be said that the simple reduction rule concerning concentration which was proposed by Ferry et al.[7] and also the modified reduction rule by DeWitt et al.[8] on polymer solutions do not hold in this case, and that the circumstances are more complicated. However, when we seen all curves including dotted lines, it is found that the curves change their shapes continuously with the increase of concentration and that there is no marked difference among them in the tendency of the change in shape in spite of the fairly great difference in molecular weight.

The curve for the gel of 6.05% decreases monotonously. This corresponds to the rubbery flow region, and there appears a broad flat region in the curve of the gel of 7.95%, and the broad flat region is levelled up for the gel of 8.3%. Then there appears a peak in the flat region for the gel of 9.9%, and the peak shifts with the increase of concentration, accompanying the ascent of the curve.

Then it may be said that the difference in molecular weight has no marked effect on the distribution functions of relaxation times and that there are two or more mechanisms which behave differently with the increase of concentration.

In order to investigate the concentration dependence of distribution functions, the average values of $H(\log\tau)$ in the whole box type region, $\bar{H}$, which is regarded as the height of the idealized box type spectrum, are calculated and plotted in the form of $\log\bar{H}$ versus $\log C$, where C is concentration in weight %, in Fig. 6, including those for the case of molecular weight 1.1×10^4. Then we see in Fig. 6 that a linear relation holds between $\log\bar{H}$ and $\log C$ as follows,

$$\log\bar{H}=\alpha+\beta\log C \qquad \alpha=0.45,\ \beta=5 \qquad (4)$$

As is shown in the equation above described, the value of $\bar{H}$ is proportional to the fifth

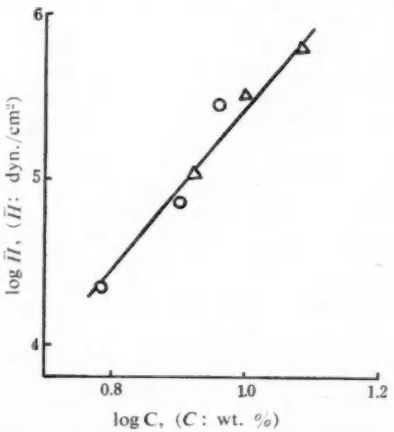

Fig. 6. Concentration dependence of average value of distribution functions of relaxation times in box type region.
○ Molecular weight, 8.5×10^4
△ Molecular weight, 1.1×10^4

7) J. D. Ferry, ibid., **72**, 3746 (1950).
8) T. W. DeWitt, H. Markovitz, F. J. Padden and L. J. Zapas, *J. Colloid Sci.*, **10**, 174 (1955).

power of concentration. Then it is said that in the case of thermo-reversible gels there exists much more sensitive dependence of distribution functions on concentration, compared with the case of concentrated polymer solutions[7,8].

Summary and Conclusion

A stress relaxation study was made for the gels of the polyvinyl alcohol-glycerin-water system using a chainomatic balance relaxometer, where the molecular weight of polyvinyl alcohol was 8.5×10^4. Relaxation Young's moduli under constant strain were measured up to two hours after sudden imposition of the strain for the gels of three different concentrations of polyvinyl alcohol: 6.05, 7.95 and 9.07% by weight. The relaxation curves at various temperatures were successfully superposed to a master relaxation curve for each concentration, and relaxation spectra were obtained from the master curves by Alfrey's approximation. The main results obtained are as follows.

1) The relaxation spectrum of the gel of the polyvinyl alcohol-glycerin-water system has a typical box type character.

2) The difference in molecular weight of polyvinyl alcohol has no marked effect on the relaxation spectrum of the gel.

3) The concentration dependence of the relaxation spectrum are fairly complicated in its details.

4) The average value of the distribution function of relaxation times in the box type region is proportional to the fifth power of concentration, rather than to the first or the second power.

Department of Chemical Industry
Faculty of Engineering
Shizuoka University
Oiwake, Hamamatsu

The Infrared Absorption Spectrum of 1, 2, 4, 5-Tetrachlorobenzene in Vapor State

By Shinnosuke SAËKI*

(Received March 4, 1961)

The molecular spectra of 1, 2, 4, 5-tetrachlorobenzene have been studied by some investigators[1]. All of these studies were, however, mainly concerned with a number of benzene derivatives to find the relation between the position of substituents in the benzene ring and C–H out-of-plane characteristic frequencies. Also 1, 2, 4, 5-tetrachlorobenzene was treated only as a member of the substituted benzenes. The assignment of the observed bands of this substance has been little discussed with the exception of its out-of-plane C–H vibration. Besides, all the spectra were taken in solid or liquid state or in solution, and the spectra taken in these states are not suitable to be used for the assignment of the bands. We measured the spectra of ordinary and deuterated 1, 2, 4, 5-tetrachlorobenzene in vapor state with the aid of a high temperature cell to make some tentative assignments of the observed infrared absorption bands.

Experimental and Results

The measurements were carried out on ordinary and deuterated 1, 2, 4, 5-tetrachlorobenzenes, from 5000 to 2000 cm^{-1} with a lithium fluoride prism, from 2000 to 700 cm^{-1} with a sodium chloride prism and from 700 to 400 cm^{-1} with potassium bromide prism using the Perkin-Elmer 112 infrared spectrometers. As the boiling points of these substances are considerably high, in order to observe the spectra in vapor state we used the high temperature cell which was described in a previous paper[2]. The partial pressure of each substance was not measured. The substance was simply put in the cell which has been previously heated but not evacuated, and regulated the quantity of the substance in the cell so that it might give a good spectrum.

The ordinary 1, 2, 4, 5-tetrachlorobenzene used in this experiments was extra pure grade on the market, and the deuterated one was kindly provided by Dr. Leitch in Canada.

* Present address: Government Chemical Industrial Research Institute, Shibuya-ku, Tokyo.

1) For example, E. K. Plyler, H. C. Allen, Jr. and E. D. Tidwell, *J. Research Nat. Bur. Standards*, **58**, 255 (1957).

2) S. Saëki, This Bulletin, 33, 1021 (1960).

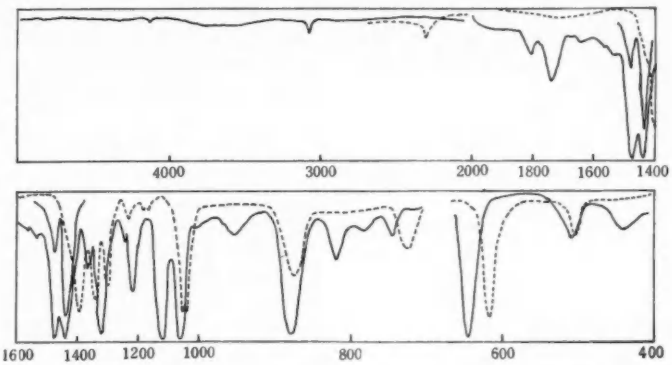

Fig. 1. Infrared absorption spectra of ordinary and deuterated 1,2,4,5-tetrachlorobenzenes.
$C_6H_2Cl_4$ —— $C_6D_2Cl_4$ ----

Table I. Infrared absorption bands of 1,2,4,5-tetrachlorobenzenes

$C_6H_2Cl_4$	$C_6D_2Cl_4$	$C_6H_2Cl_4$	$C_6D_2Cl_4$
3094 m	2300 m		1175 w
2775 w		1116 s	1054 s, 1047 s
2680 w		1060 s	
2630 w		947 w	
1802 w		880 s	874 s
1740 w		820 m	725 m
1474 m	1425 w	782 w	
1436 s	1392 s	745 w	
1367 m	1345 s	645 s	617 s
1319 s	1297 s	509 m	504 m
1241 w	1235 m	440 w	
1218 m	1187 w		

The observed spectra of each substance are shown in Fig. 1, and the observed frequencies are shown in Table I.

Assignment

The symmetry of this substance belongs to the point group V_h as *p*-dichlorobenzene does. So it has thirteen infrared active normal vibrations of which five belong to the species B_{1u} (in-plane), five to the species B_{2u} (in-plane) and three to the species B_{3u} (out-of-plane)*. These expected vibrational modes are listed in Table II.

Among these vibrations, the C–Cl bending vibration of each species is expected to be unobservable under the experimental conditions because of its low frequency, and some of the ring deformation frequencies might also exist beyond the experimental region. Therefore we should expect to observe from seven to ten fundamental frequencies under the experimental conditions. In the spectra nine or ten strong bands were observed for $C_6H_2Cl_4$ and eight strong bands for $C_6D_2Cl_4$. In addition to these strong bands a medium or weak band in shorter wavelength region was observed; that is, a band at 3094 cm^{-1} of $C_6H_2Cl_4$ and at 2300 cm^{-1} of $C_6D_2Cl_4$ which are evidently the fundamental bands of C–H and C–D stretching vibrations respectively.

Between 1500 and 1200 cm^{-1} three fundamental bands, might be expected that is, the ring stretching vibrations of the species B_{1u} and B_{2u} and the ring in-plane deformation vibration of the species B_{2u}. It should be mentioned here that the third vibration, which is called a ring deformation vibration, might probably have a considerably high frequency, because the mode of this ring deformation is necessarily accompanied by a ring stretching mode. Taking into account the relative intensities of these bands and the product rule, we consider that the

Table II. Infrared active normal vibrations of 1,2,4,5-tetrachlorobenzenes

Species	Mode
B_{1u} (in-plane)	C–H or C–D stretching
	Ring stretching
	Ring deformation
	C–Cl stretching
	C–Cl bending
B_{2u} (in-plane)	C–H or C–D bending
	Ring stretching
	Ring deformation
	C–Cl stretching
	C–Cl bending
B_{3u} (out-of-plane)	C–H or C–D bending
	Ring deformation
	C–Cl bending

* In this case, x axis was taken along the symmetry axis perpendicular to the molecular plane, and z axis along the symmetry axis combining two hydrogen atoms.

three bands at 1474, 1436 and 1319 cm^{-1} of $C_6H_2Cl_4$ correspond to the three bands at 1345, 1392 and 1297 cm^{-1} of $C_6D_2Cl_4$ respectively, and assigned the first pair of bands to the ring stretching vibration of species B_{2u}, the second to the ring stretching vibration of species B_{1u} and the third to the ring in-plane deformation vibration of species B_{2u}.

It appeared somewhat curious that in the region between 1200 and 1000 cm^{-1} we found two bands of $C_6H_2Cl_4$ at 1116 and 1060 cm^{-1}, but only one band of $C_6D_2Cl_4$ at 1051 cm^{-1} corresponding to them. The intensities of both of the two bands of $C_6H_2Cl_4$ were too remarkable to be considered as overtone or combination bands. On closer examination of the shape of the band at 1051 cm^{-1} of $C_6D_2Cl_4$, we found the two absorption maxima at 1054 and 1047 cm^{-1} which were not known to be the branches of a single band or to be the peaks of two independent bands. Badger and Zumwalt[3] gave the band envelopes of several types of unsymmetrical rotator molecules. The ρ[*1] and S values of the molecule of $C_6D_2Cl_4$ are 1.8 and −0.7 respectively for which the band envelope is not given in their paper. But the estimation from the different band envelopes described in their paper told us that the splitting of the two maxima would not be greater than 3 cm^{-1}.

Dennison[4] also showed that the diagrams of the fine structure of the band, but it was difficult to estimate the splitting of the two absorption maxima from these diagrams. If one approximates the molecule of 1, 2, 4, 5-tetrachlorobenzene by a symmetric rotator[*2], the approximate value of the splitting can be found to be about 5 cm^{-1} [*3]. Actually this splitting distance was found to be about 7 cm^{-1}, a little larger than the above-mentioned estimated and calculated values. But such an amount of discrepancy between the observed and calculated (or estimated) values is not enough to favor the supposition that these two absorption maxima would be caused by the two independent bands. However, we shall take this supposing at present, for it appears to explain more easily the correspondence between the absorption bands of each substance. Thus we assigned the band at 1116 and 1060 cm^{-1} of $C_6H_2Cl_4$ to the C–H in-plane bending vibration of species B_{2u} and to the ring deformation vibration of species B_{1u} respectively, and for their corresponding bands of $C_6D_2Cl_4$ we considered that the band at 1047 cm^{-1} of $C_6D_2Cl_4$ corresponds to the former band and the band at 1054 cm^{-1} of $C_6D_2Cl_4$ to the latter.

In the region below 1000 cm^{-1} were found four remarkable bands of each substance, that is, 880, 820, 645 and 509 cm^{-1} for $C_6H_2Cl_4$, and 874, 725, 617 and 504 cm^{-1} for $C_6D_2Cl_4$. Kakiuchi[5] assigned the band at 867 cm^{-1} of $C_6H_2Cl_4$ to the out-of-plane C–H bending vibration. It is evident that this is the band which was observed at 880 cm^{-1} in our experiments[*4]. But we found in the spectrum of $C_6D_2Cl_4$ a remarkable band at 874 cm^{-1} which evidently corresponds to the band at 880 cm^{-1}. It means that the frequency shift caused by the replacement of hydrogen atoms by deuterium atoms is only 6 cm^{-1}. This frequency shift is too small for a vibration mainly concerned with the C–H bond. Thus we assigned the band at 820 cm^{-1} to the out-of-plane C–H vibration, for its corresponding band of $C_6D_2Cl_4$ was found at 725 cm^{-1}, showing a great frequency shift. But the intensities of these bands appear to be too weak for the out-of-plane C–H and C–D vibrations, and we have not found a plausible explanation for this fact. As for the above-mentioned band at 880 cm^{-1} (874 cm^{-1} for $C_6D_2H_2$) we assigned it to the C–Cl stretching vibration of species B_{1u}. And to the other C–Cl stretching vibration which belongs to species B_{2u}, we assigned the band at 645 cm^{-1} (617 cm^{-1} for $C_6D_2Cl_4$). The last pair of bands which were found at 509 cm^{-1} (for $C_6H_2Cl_4$) and at 504 cm^{-1} (for $C_6D_2Cl_4$) were assigned to the out-of-plane deformation vibration of the ring. The assignment given above is shown in Table III.

It should be mentioned here that the assignment shown in Table III based on the assumption that the band at 1051 cm^{-1} of $C_6D_2Cl_4$ is composed of two closely positioned independent bands. If not, the assignment should be quite changed as follows.

We regarded the absorption maxima at 1054 and 1047 cm^{-1} observed in the spectrum of $C_6D_2Cl_4$ as the branches of one band which corresponds to the band at 1116 or at 1060 cm^{-1} of $C_6H_2Cl_4$. Then one of these two bands has no corresponding band of $C_6D_2Cl_4$ except the band at 874 cm^{-1}. If we consider the band

3) R. M. Badger and L. R. Zumwalt, *J. Chem. Phys.*, **6**, 711 (1938).

*1 Badger and Zumwalt defined $\rho = (a-c)/b$, where a, b and c are the reciprocals of three principal moments of inertia, I_A, I_B and I_C respectively.

4) D. M. Dennison, *Rev. Mod. Phys.*, **33**, 280 (1931).

*2 For this molecule three principal moments of inertia were calculated as $I_A = 688 \times 10^{-40}$, $I_B = 1752 \times 10^{-40}$ and $I_C = 2440 \times 10^{-40}$. Thus the approximation by the symmetric rotator is not very bold.

*3 In this calculation we assumed that $I_B = 2000 \times 10^{-40}$. This is the approximate mean value of the real I_B and I_C values.

5) Y. Kakiuchi, *J. Chem. Soc. Japan, Pure Chem. Sec.* (*Nippon Kagaku Zasshi*), **80**, 356 (1959).

*4 He used the frequencies observed by Plyler and his collaborators[21]. Those frequencies were observed in the liquid state, so it is quite natural that there are small discrepancies between their frequencies and our frequencies observed in the vapor state.

TABLE III. ASSIGNMENT I

Species	$C_6H_2Cl_4$	$C_6D_2Cl_4$	Mode
B_{1u}	3094	2300	C–H or C–D stretching
	1436	1392	Ring stretching
	1060	1054	Ring deformation
	880	874	C–Cl stretching
	—	—	C–Cl bending
B_{2u}	1474	1345	Ring stretching
	1319	1297	Ring deformation
	1116	1047	C–H or C–D bending
	645	617	C–Cl stretching
	—	—	C–Cl bending
B_{3u}	820	725	C–H or C–D bending
	509	504	Ring deformation
	—	—	C–Cl bending

at 874 cm^{-1} of $C_6D_2Cl_4$ as corresponding to the band at 1116 or at 1060 cm^{-1}, this great frequency shift suggests that the pair is to be assigned to the C–H (C–D) in-plane bending vibration of species B_{2u}. Then there are two possible assignments of the other pair (the band at 1060 or at 1116 cm^{-1} of $C_6H_2Cl_4$ and the band at 1051 cm^{-1} of $C_6D_2Cl_4$), that is, an assignment to the ring deformation vibration and an assignment to the C–Cl stretching vibration of species B_{1u}. In the case of this molecule the frequency of the ring deformation vibration of species B_{1u} might be rather low, for it could occur without coupling with a stretching mode of the ring. The frequency of a C–Cl stretching vibration which is generally expected at about 700 cm^{-1} might easily couple with the vibrations of other modes in this case, and its frequency might change over a wide region. From these considerations we concluded that the pair of bands in question is to be assigned to the C–Cl stretching vibration of species B_{1u}. Concerning the question as to which of the above-mentioned two bands at 1116 cm^{-1} and at 1060 cm^{-1} of $C_6H_2Cl_4$ is to be assigned to C–H in-plane bending vibration of species B_{2u}, we decided to assign the former band to this normal vibration from the consideration of the product rule.

As for the other fundamental bands, we assigned the pair of bands at 509 cm^{-1} ($C_6H_2Cl_4$) and 504 cm^{-1} ($C_6D_2Cl_4$) to the ring in-plane deformation vibration of species B_{1u} and the pair of bands at 645 cm^{-1} ($C_6H_2Cl_4$) and 617 cm^{-1} ($C_6D_2Cl_4$) to the C–Cl stretching vibration of species B_{2u}. In addition to the above-mentioned change in the assignment, the correspondence of three pairs of ring stretching vibrations (in the region 1300~1500 cm^{-1}) is also changes from the consideration of the product rule as is shown in Table IV.

This is the second assignment which seems to us to be as plausible as the former one. This assignment is shown in Table IV.

TABLE IV. ASSIGNMENT II

Species	$C_6H_2Cl_4$	$C_6D_2Cl_4$	Mode
B_{1u}	3094	2300	C–H or C–D stretching
	1474	1392	Ring stretching
	1060	1047	Ring deformation
	509	504	C–Cl stretching
	—	—	C–Cl bending
B_{2u}	1436	1345	Ring stretching
	1319	1297	Ring deformation
	1116	874	C–H or C–D bending
	645	617	C–Cl stretching
	—	—	C–Cl bending
B_{3u}	880	725	C–H or C–D bending
	—	—	Ring deformation
	—	—	C–Cl bending

Discussion

According to the product rule the theoretical value of the ratio of products of the frequencies is 1.407 for all three species (B_{1u}, B_{2u} and B_{3u}) in the case of this molecule. As we could not observe all of the fundamental frequencies under our experimental conditions, it was not possible to apply the product rule to the results obtained perfectly, but it was possible to ascertain whether the ratio of products calculated from the observed frequencies alone exceeds the theoretical value or not. We carried out this calculation for every species of both of the above-mentioned assignments. The results are shown in Table V.

TABLE V. CALCULATED RATIOS OF THE PRODUCTS OF OBSERVED FREQUENCIES

	Species	Calculated ratio	Number of observed frequency
Assignment I	B_{1u}	1.405	4 of 5
	B_{2u}	1.242	4 of 5
	B_{3u}	1.142	2 of 3
Assignment II	B_{1u}	1.456	4 of 5
	B_{2u}	1.449	4 of 5
	B_{3u}	1.214	1 of 3

None of the calculated ratios of assignment I exceeded the theoretical value 1.407, while two of the three calculated ratios of assignment II exceed the theoretical values. From the theoretical point of view assignment I shows no contradiction. But on closer examination one will find some points of discussion. In the first place the value of the ratio for species B_{1u} of assignment I is almost equal

to the theoretical value, so the ratio of the unobserved fifth frequencies must be nearly 1. As the fifth frequency is that of the C–Cl bending vibration (or skeletal vibration), this requirement will probably be fulfilled. In the second place those ratios for the species B_{2u} and B_{3u} of the assignment I are so small that the ratios of the last unobserved frequency of these species must be considerably great, that is, 1.144 and 1.232 for the species B_{2u} and B_{3u} respectively. Considering the fact that both of these values are ratios of the frequencies of C–Cl bending vibrations, they are evidently too great to attribute to the single ratios of frequencies. This appears to be an absolute defect of assignment I as well as of the above-mentioned ambiguity in the explanation of the band at 1051 cm^{-1} of $C_6D_2Cl_4$.

As for assignment II, as we mentioned previously, there are two ratios exceeding the theoretical values. However, a discrepancy of a few per cent must be expected between the observed and theoretical ratios, as there are various factors which cause the deviation, such as small mechanical errors of the spectrometer, the unharmonicity of the vibrations, Fermi resonance, etc. Therefore, provided that the ratios of C–Cl bending frequencies are nearly 1, the discrepancies found for species B_{1u} and B_{2u} might not absolutely deny assignment II.

In the case of species B_{3u}, since only one of the three frequencies was observed, the application of the product rule was quite impossible. But the ratio of 1.214 obtained for the first pair of frequencies of this species seems to be perfectly plausible for the C–H (or C–D) out-of-plane bending vibration, and this assignment appears to be strongly preferable to that for species B_{3u} of assignment I.

After all, although we could not find an adequate difference between two assignments shown in Table V to draw out any unambiguous conclusion, assignment II seems to us a little more plausible than the other. In order to remove this ambiguity it may be necessary to carry out the measurement of the spectra of these substances in the far infrared region or to observe the precise shape of each fundamental band or to find out the exact force constants which will allow us to calculate the normal frequencies of these molecules with sufficient accuracy.

Summary

The infrared absorption spectra of ordinary and deuterated 1, 2, 4, 5-tetrachlorobenzenes were measured in the vapor state using the high temperature cell. For the results obtained by the measurements we proposed two possible assignments of the fundamental infrared bands, and made the discussion comparing these two tentative assignments. However, at present we have no experimental base upon which we can decide the superiority of one to the other. In order to solve this difficulty we are going to make an investigation of the spectra of these molecules in the far infrared region as well as the calculation of the exact force constants of the chlorobenzenes.

This work was done at the laboratory of Professor J. Lecomte of the Laboratoire des Recherches Physiques, Faculté des Sciences de Paris. The author acknowledges greatefully Professor Lecomte's encouragement and advice. He also wishes to thank Dr. Leitch of the National Research Council at Ottawa for kindly sending deuterated 1, 2, 4, 5-tetrachlorobenzene prepared by him.

Laboratoire des Recherches Physiques
Faculté des Sciences de Paris

π Electronic Structure of Cinnamaldehyde

By Kōzō Inuzuka

(Received March 6, 1961)

In two previous papers[1,2] we studied the electronic structure of the acrolein molecule. This molecule has an intense absorption band of (π, π^*) type in the region near 2000 Å, which was assigned to an intramolecular charge transfer band by Nagakura[3]. Cinnamaldehyde is regarded as a derivative of acrolein, in which a hydrogen atom is substituted by a phenyl group. From this point of view the comparison of the spectra of acrolein and cinnamaldehyde may be interesting.

The absorption spectrum of cinnamaldehyde was measured in *n*-hexane solution in the 2000~3000 Å region. Molecular orbital calculation was made for the π electronic structure of the cinnamaldehyde molecule with a view to understanding its absorption band, as there has scarcely been any theoretical work done on the electronic structure of this molecule.

Ultraviolet Absorption Spectra

The ultraviolet absorption spectra of cinnamaldehyde and acrolein are shown in Fig. 1.

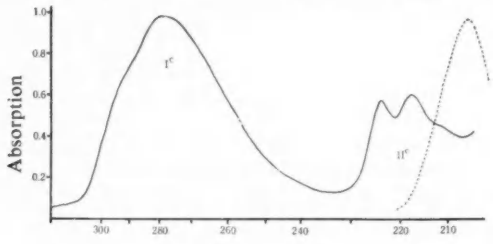

Fig. 1. Ultraviolet absorption spectra of cinnamaldehyde and acrolein.
Solid line: cinnamaldehyde in *n*-hexane
Broken line: acrolein in *n*-hexane

The spectra of these molecules were measured with a Hitachi self-recording quartz spectrophotometer of type E. P. S. The solvent was *n*-hexane carefully purified by the method of Weissberger and Proskauer[4]. It appears that the cinnamaldehyde band is displaced to the red with respect to the acrolein band, owing to the extension of conjugation within the molecule. In order to ascertain that the transition in cinnamaldehyde corresponding to the absorption in the 2000 Å region is of the $\pi-\pi^*$ type, the effect on the spectrum of changing the solvent from *n*-hexane to ethanol was also studied.

Calculation of Energy Levels

Although the methods of Pariser and Parr[5] and others simplify the calculation of molecular energy levels in very ingenious ways, it is still not easy to apply the theory to a molecule such as cinnamaldehyde. In the present calculation the MO's of cinnamaldehyde were obtained by the simple LCAO-MO method and we took account of the interaction of electrons by including configuration interaction to some extent[6]. As the molecular dimension of cinnamaldehyde is not known, we relied on the structure inferred from the result of the electric dipole moment value by Bently et al.[7] The molecular structure is shown in Fig. 2,

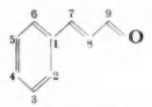

Fig. 2. Cinnamaldehyde.

but in our calculation a somewhat more simplified model was used. Actually cinnamaldehyde has not C_{2v} symmetry, but the orbitals obtained in our approximation are what would be found if C_1-C_7=C_8-C_9-O was linear. Thus the cinnamaldehyde MO's may be said to resemble those with C_{2v} symmetry. The MO's of cinnamaldehyde were obtained by the simple LCAO-MO method with neglect of overlap integrals. The Coulomb integral α_o and the resonance integral β_{co} are expressed as

$$\alpha_o = \alpha + \delta_o\beta$$

$$\beta_{co} = \rho_{co}\beta$$

1) K. Inuzuka, This Bulletin, **34**, 6 (1961).
2) K. Inuzuka, ibid., **34**, 729 (1961).
3) S. Nagakura, *Mol. Phys.*, **3**, 105 (1960).
4) A. Weissberger and E. S. Proskauer, "Organic Solvents", Interscience Publishers, Inc., New York, N. Y. (1955).
5) R. Pariser and R. G. Parr, *J. Chem. Phys.*, **21**, 466, 767 (1953).
6) H. Baba and S. Suzuki, ibid., **32**, 1706 (1960).
7) J. B. Bentley, K. B. Everard, R. J. B. Marsden and L. E. Sutton, *J. Chem. Soc.*, **1947**, 2957.

Table I. Orbital energies and orbitals for cinnamaldehyde

i	Symmetry	Orbital energy $(\varepsilon_i-\alpha)/\beta$	Orbital ϕ_i
1	b_1	2.481	$0.0956\chi_1+0.0508(\chi_2+\chi_6)+0.0303(\chi_3+\chi_5)+0.0245\chi_4+0.1544\chi_7+0.2644\chi_8+0.5374\chi_9-0.7751\chi_o$
2	b_1	2.100	$0.4826\chi_1+0.3928(\chi_2+\chi_6)+0.3423(\chi_3+\chi_5)+0.3260\chi_4+0.2593\chi_7+0.1065\chi_8-0.0775\chi_9-0.1825\chi_o$
3	b_1	1.429	$0.3051\chi_1-0.0094(\chi_2+\chi_6)-0.3185(\chi_3+\chi_5)-0.4458\chi_4+0.5174\chi_7+0.4171\chi_8+0.0126\chi_9-0.2515\chi_o$
4	a_2	1.000	$1/2(\chi_2+\chi_3-\chi_5-\chi_6)$
5	b_1	0.815	$0.4091\chi_1+0.2871(\chi_2+\chi_6)-0.1752(\chi_3+\chi_5)-0.4298\chi_4-0.2739\chi_7-0.5158\chi_8-0.1237\chi_9+0.2555\chi_o$
6	b_1	−0.429	$0.1751\chi_1-0.2630(\chi_2+\chi_6)-0.0622(\chi_3+\chi_5)+0.2897\chi_4+0.5130\chi_7-0.3310\chi_8-0.4883\chi_9+0.3580\chi_o$
7	a_2	−1.000	$1/2(-\chi_2+\chi_3-\chi_5+\chi_6)$
8	b_1	−1.117	$0.4721\chi_1-0.1815(\chi_2+\chi_6)-0.2694(\chi_3+\chi_5)+0.4824\chi_4-0.1870\chi_7-0.1824\chi_8+0.4632\chi_9-0.2248\chi_o$
9	b_1	−1.650	$0.0747\chi_1+0.1169(\chi_2+\chi_6)-0.2675(\chi_3+\chi_5)+0.3243\chi_4-0.4061\chi_7+0.5347\chi_8-0.4723\chi_9+0.2121\chi_o$
10	b_1	−2.129	$0.4909\chi_1-0.3811(\chi_2+\chi_6)+0.3204(\chi_3+\chi_5)-0.3010\chi_4-0.3218\chi_7+0.2245\chi_8-0.1275\chi_9+0.0497\chi_o$

Table II. Energies and wave functions for lower excited states of cinnamaldehyde

Symmetry	Excitation energy, eV.		Wave function	Oscillator strength
	calcd.	obs.		
B_2^-	4.10		$0.946V_{46}-0.326V_{57}$	0.000
A_1	4.11	4.41	V_{56}	0.806
B_2^+	5.50	5.53	$0.326V_{46}+0.946V_{57}$	0.337

where $\alpha=\alpha_c$ and $\beta=\beta_{cc}$. We adopted the values of the parameters $\delta_o=1.5$ and $\rho_{co}=2^{1/2}$ as given by Baba et al.[6] Other Coulomb integrals were assumed to be equal to α. The resonance integrals except those of the benzene ring and carbonyl group, were calculated by the approximation generally adopted

$$\beta_{rs}=(S_{rs}/S)\beta$$

were S_{rs} is the overlap integral between neighboring atom r and s, and S the overlap integral for benzene. In Table I the MO energies and orbitals of cinnamaldehyde are given. For the resonance integral values which are necessary for determining the energies of configurations the values given by Goodman and others[8,9]

$$\beta(B_2)=2.98\text{ eV.}$$

$$\beta(A_1)=3.30\text{ eV.}$$

were used. The configuration interaction was considered between those configurations with lower energy and belonging to the same symmetry. The matrix element of the total Hamiltonian $\mathbf{H}$ between the configurations V_{ik} and V_{jl} is given by

$$\int V_{ik}^*\mathbf{H}V_{jl}\,d\nu=2[ki|jl]-[kl|ji] \qquad (i\neq j,\ k\neq l)$$

where

$$[ij|kl]=\int\phi_i^*(1)\phi_k^*(2)(e^2/r_{12})\phi_j(1)\phi_l(2)d\nu$$

MO's ϕ_i are obtained by the simple LCAO procedure neglecting differential overlap. The integral $[ij|kl]$ can be expressed in terms of atomic orbitals as

$$[pp|qq]=\int\chi_p^*(1)\chi_q^*(2)(e^2/r_{12})\chi_p(1)\chi_q(2)d\nu$$

For the integrals of this type we employed Pariser and Parr's results[5]. To avoid difficult calculation only the interaction between V_{46} and V_{57} belonging to the same symmetry is considered. In this way the value of the matrix element

$$\int V_{46}^*\mathbf{H}V_{57}\,d\nu=0.449\text{ eV.}$$

is obtained. If we assume that there is approximately no interaction between V_{56} and other configurations, the energy of the state represented by V_{56} is calculated directly. The energies of the states resulting from the interaction of V_{46} and V_{57} were obtained including the

8) L. Goodman and H. Shull, *J. Chem. Phys.*, **27**, 1388 (1957).
9) E. G. McRae and L. Goodman, *J. Mol. Spectroscopy*, **2**, 464 (1958).

configuration interaction energy between them as given above. The oscillator strength, f, is calculated by the method described by Mulliken and Rieke[10],

$$f = 1.085 \times 10^{11} \times \omega \sum_r Q_r^2 \quad (r = x, y, z)$$

where ω is the frequency of the transition in cm^{-1} and Q_r is the transition moment defined by

$$Q_r = \int \Psi_i^* \, r \, \Psi_j \, d\tau$$

Ψ_i is a state wave function. The results are shown in Table II.

Discussion

The electronic spectrum of cinnamaldehyde in *n*-hexane solution has three absorption peaks at about 280, 224 and 218 mμ (Fig. 1). Among these three peaks the one at 280 mμ is the strongest, having two weak shoulders near 293 and 300 mμ. In Fig. 3 the orbital energy level

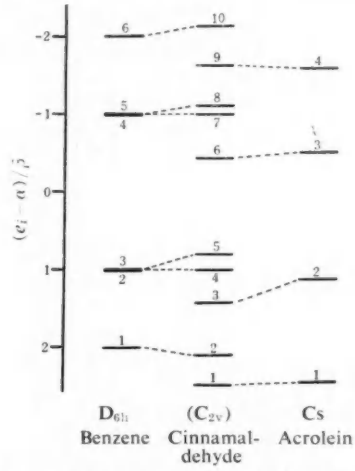

Fig. 3. Orbital energy level diagram.

diagram of cinnamaldehyde is given with those of benzene and acrolein. From this figure the occupied levels 4, 5 and the vacant levels 7, 8 of cinnamaldehyde may be assigned to the degenerate levels 2, 3 and 4, 5 of benzene. The levels 3 and 6 of cinnamaldehyde may be assigned to the levels 2 and 3 of acrolein in ground and upper states, respectively. We assigned the band at 280 mμ (4.41 eV.) to the calculated value 4.11 eV. (A_1), because the value of calculated oscillator strength of A_1 state is much greater than that of B_2^- state. Therefore, the band at 280 mμ corresponds to the transition from ϕ_5 to ϕ_6. In our experiment no band corresponding to the calculated value 4.10 eV. (B_2^-) was found. The reason why we could not find the band (B_2^-) may be explained by the interpretation that the band (A_1) of cinnamaldehyde is displaced to the longer wavelength side by the greater extension of conjugation and covers the band (B_2^-). This interpretation conforms with the result of our calculation and with the work of Thomas et al.[11]

It should be mentioned here about the electron distribution associated with ϕ_3, ϕ_5 and ϕ_6 of cinnamaldehyde. Table III shows the

Table III. Distribution of an electron in MO's ϕ_3, ϕ_5 and ϕ_6

	ϕ_3	ϕ_5	ϕ_6
C_1^2	0.0931	0.1674	0.0307
C_2^2	0.0001	0.0824	0.0692
C_3^2	0.1015	0.0307	0.0039
C_4^2	0.1987	0.1848	0.0839
C_7^2	0.2677	0.0750	0.2631
C_8^2	0.1739	0.2660	0.1096
C_9^2	0.0002	0.0153	0.2385
C_0^2	0.0632	0.0651	0.1281

distribution of an electron occupying the MO's ϕ_3, ϕ_5 and ϕ_6 in terms of squares of coefficients of atomic orbitals. It seems that the excitation of an electron from ϕ_5 to ϕ_6 transfers the electronic charge from the benzene ring to the acrolein group. This suggests that the transition from ϕ_5 to ϕ_6 corresponds to an intramolecular charge transfer band. In the region of the band II[c] there are two peaks at 224 and 218 mμ. Of these the 218 mμ peak is higher than the 224 mμ peak. There may arise a question as to whether or not the two main peaks constituting the band II[c] reveal the vibrational structure of an electronic transition, or represent two different transitions. The frequency separation between them is 1230 in *n*-hexane and 1030 cm^{-1} in ethanol solutions, respectively, at room temperature. The change of 200 cm^{-1} is too great. It may be reasonable to interpret the two peaks as two different transitions. The band at 224 mμ (5.53 eV.) may be assigned to the calculated excitation energy 5.56 eV. (B_2^+), and may correspond to the A_{1g}-B_{2u} transition in benzene.

On the other hand, from the energy level diagram Fig. 3, we tentatively assign the band at 218 mμ (5.69 eV.) to a transition V_{36} which has the lowest energy among the transitions V_{36}, V_{58}, V_{47} and V_{48}. The transition energies for them are directly obtained from the

10) R. S. Mulliken and C. A. Rieke, *Rep. Progr. Phys.*, 8, 231 (1941).

11) J. F. Thomas and G. Branch, *J. Am. Chem. Soc.*, 75, 4793 (1953).

orbital energies in Table I, this is, 1.858β, 1.932β, 2.000β, 2.117β. Since cinnamaldehyde has in reality no C_{2v} symmetry and the energies of these configurations are close to each other, the configuration interaction between them must be taken into consideration in order to ascertain the above assignment for V_{36}. For simplicity only the interaction is here considered between configurations of apparently the same symmetry type. Accordingly, the interaction between V_{36}, V_{58} and V_{47} is taken into consideration. The state energies for them were calculated including configration interaction. The results of the calculation are shown in Table IV. The calculated value for V_{36} is

TABLE IV. EXCITATION ENERGIES FOR LOWER EXCITED STATES OF CINNAMALDEHYDE

	$(m_i-m_j)\beta$ eV.	Including C. I.	Obs.
V_{36}	6.13	5.53	5.69
V_{58}	6.38	6.22	
V_{47}	6.60	7.37	

in good agreement with the observed value within present approximation. The calculated value 5.53 eV. for V_{36} conforms rather with the band at 224 mμ (5.53 eV.), but we may tentatively assign the transition from ϕ_3 to ϕ_6 to the band at 218mμ within the present approximation. Since the orbitals ϕ_3 and ϕ_6 of cinnamaldehyde correspond to the orbitals ϕ_2 and ϕ_3 of acrolein in Fig. 3, it may be said that the 218 mμ band corresponds to the transition in the substituent group.

Summary

State energies of the cinnamaldehyde molecule are calculated by the simple LCAO-MO method, including configuration interaction and assuming the C_{2v} symmetry. The results of the calculation conform well with the observed absorption bands lying in the 2000~3000 Å region. In cinnamaldehyde the 280 mμ band is assigned to the intramolecular charge transfer band. The B_2^- band which we could not find in spectrum of cinnamaldehyde may be covered under the charge transfer band which is greatly shifted toward the red as the result of extension of conjugation. In the region of the band II^c two peaks at 224 and 218 mμ represent two different transitions, respectively. The former is assigned to the B_2^+ type transition and the latter to the transition in the acrolein group.

The author expresses his sincere thanks to Professor Sunao Imanishi and Dr. Yoshiya Kanda for their encouragement throughout this work. He thanks also Dr. Rhōichi Shimada and Mr. Akira Sadō for their kind advice.

Department of Chemistry
Faculty of Science
Kyushu University
Hakozaki, Fukuoka

The Diamagnetic Susceptibility of Benzoate, Salicylate, Propionate, Butyrate and Succinate Ions

By S. SRIRAMAN and S. THIRUVENGADATHAN

(Received February 9, 1961)

Magnetic susceptibilities of simple ions were evaluated by a number of workers. The importance of such a study was clearly brought out by the work of Hoare and Brindley[1], Varadachari[2] and Subramaniam[3]. In the present investigation a few alkali and alkaline earth compounds containing benzoate, salicylate, propionate, butyrate and succinate radicals have been studied in the solid state and the susceptibilities of the anions calculated assuming the previously accepted values for the cations.

1) F. E. Hoare and G. W. Brindley, *Proc. Roy. Soc.*, **147A**, 88 (1934).
2) P. S. Varadachari, *Proc. Ind. Acad. Sci.*, **2A**, 16 (1935).
3) K. C. Subramaniam, ibid., **4A**, 404 (1936).

Experimental

The substances used were mostly either Merck's G. R. or B. D. H., A. R. and a few whose purity was not definite were recrystallized befor use. The salts were all found to be free from ferromagnetic impurities. Great care was taken to prevent the solids from absorbing atmospheric moisture and where this tendency existed the salts were analyzed for the moisture content by gravimetric methods and kept in vacuum desiccator before use.

Measurements of the susceptibilities of the acids

and their salts were made with a Curie balance. The retorsion method[4] was employed. A correction for the displaced air was applied for every bulb. For every salt and acid more than half a dozen bulbs containing different masses of the salts were examined at three field currents, viz. 4, 5 and 6 amp. Benzene (B. D. H., A. R. grade) was used as the standard and its specific susceptibility was taken as 0.702*. The susceptibilities of the salts were calculated from the usual formula.

$$\frac{\theta_S}{\theta_B} = \frac{m_S\chi_S - K_a v_S}{m_B\chi_B - K_a v_B}$$

Here θ_S, θ_B and m_S, m_B represent the deflections for and the masses of, the substance and benzene respectively; v_S and v_B represent the volume of the air displaced by the substance and benzene respectively. K_a refers to the paramagnetic susceptibility of air at the room temperature. Its value at N. T. P. is 0.029×10^{-6} (I. C. T. 6, 354, 1929) and its value at the room temperature (30°C) was found from the relation K_a/T^2 is constant where K_a is the susceptibility of air at absolute temperature T°K.

Results

The susceptibilities obtained for the acids and their salts are recorded in Table I. For the evaluation of ionic susceptibilities of the anions under investigation, Flordal and Frivold's[5] values derived from salts in dissolved

TABLE I. SUSCEPTIBILITY VALUES FOR THE ACIDS AND THEIR SALTS

No.	Substance	Mol. wt.	χ_S	χ_M	χ_{Ma}*	χ_{Ma} (others)
1	Benzoic acid, C_6H_5COOH	122.20	0.5832	71.27	71.27	67.78[6] 70.29[7] 70.28[8] 70.62[9]
2	$NaC_7H_5O_2$	144.11	0.5350	77.10	77.10	77.60[10]
3	$KC_7H_5O_2$	160.25	0.5332	85.45	85.45	82.62[10]
4	$Ca(C_7H_5O_2)_2\cdot3H_2O$	336.15	0.5575	187.40	148.52	151.00[10]
5	$Sr(C_7H_5O_2)_2$	311.63	0.4912	153.07	153.07	166.70[10]
6	$Ba(C_7H_5O_2)_2\cdot2H_2O$	415.16	0.4589	190.52	164.60	177.30[10]
7	Salicylic acid, HOC_6H_4COOH	137.12	0.5367	73.59	73.59	72.23[9]
8	$NaC_7H_5O_3$	160.11	0.5138	82.26	82.26	85.70[10]
9	$KC_7H_5O_3$	176.21	0.5146	90.68	90.68	93.70[10]
10	$Ca(C_7H_5O_3)_2$	314.33	0.5050	158.74	158.74	162.00[10]
11	$Sr(C_7H_5O_3)_2$	361.88	0.4700	170.08	170.08	176.10[10]
12	$Ba(C_7H_5O_3)_2$	411.60	0.4305	177.19	177.19	188.00[10]
13	Propionic acid, CH_3CH_2COOH	74.04	0.5898	43.67	43.67	43.60[11]
14	$NaC_3H_5O_2$	96.07	0.5308	50.99	50.99	48.90[10]
15	$KC_3H_5O_2$	112.18	0.5347	59.98	59.98	57.20[10]
16	$Ca(C_3H_5O_2)_2$	186.24	0.5475	101.97	101.97	100.40[10]
17	$Sr(C_3H_5O_2)_2$	234.00	0.4423	103.50	103.50	107.90[10]
18	$Ba(C_3H_5O_2)_2$	283.52	0.4118	116.75	116.75	123.50[10]
19	Butyric acid, $CH_3CH_2CH_2COOH$	88.10	0.6146	54.15	54.15	55.70[12]
20	$NaC_4H_7O_2$	110.09	0.5391	59.35	59.35	61.60[10]
21	$KC_4H_7O_2$	126.10	0.5220	65.82	65.82	70.00[10]
22	$Ca(C_4H_7O_2)_2$	214.29	0.4988	106.89	106.89	119.50[10]
23	$Sr(C_4H_7O_2)_2$	261.81	0.4400	115.20	115.20	129.60[10]
24	$Ba(C_4H_7O_2)_2$	311.59	0.4018	125.20	125.20	145.60[10]
25	Succinic acid, $COOH(CH_2)_2COOH$	118.09	0.4804	56.73	56.73	57.10[13]
26	$Na_2C_4H_4O_4$	162.16	0.4159	67.44	67.44	76.82[10]
27	$K_2C_4H_4O_4$	194.31	0.4480	87.05	87.05	89.22[10]
28	$CaC_4H_4O_4$	156.20	0.4245	66.31	66.31	54.84[10]
29	$SrC_4H_4O_4$	203.75	0.3584	73.02	73.02	71.50[10]
30	$BaC_4H_4O_4$	253.43	0.3345	84.77	84.77	97.60[10]

* χ_{Ma}=Anhydrous molar susceptibility.

* All susceptibility values given in this paper indicate the diamagnetic susceptibilities in 10^{-6} c. g. s. unit.

4) S. R. Rao, ibid., **1**, 123 (1934).
5) V. M. Flordal and D. E. Frivold, *Ann. Physik*, **23**, 425 (1935).
6) F. M. Gray and W. M. Birse, *J. Chem. Soc.*, **105**, 2715 (1914).
7) K. Kido, *Sci. Rep. Tohoku, Imp. Univ.*, **24**, 701 (1936).
8) C. M. French, *Trans. Faraday. Soc.*, **50**, 1321 (1954).
9) K. Venkateswarlu and S. Sriraman., ibid., **53**, 438 (1957).
10) Mata Prasad et al., (a) *Proc. Ind. Acad. Sci.*, **16A**, 307 (1942); (b) ibid., **20A**, 224 (1944); (c) *J. Chem. Phys.*, **17**, 819 (1949); (d) ibid., **18**, 936 (1950); (e) ibid., **18**, 941 (1950); (f) ibid., **20**, 129 (1952).
11) P. Pascal, (a) *Compt. rend.*, **149**, 342 (1909); (b) ibid., **158**, 158 (1914); (c) ibid., **159**, 429 (1914); (d) ibid., **173**, 144 (1921).
12) K. Kido, *Sci. Rep. Tohoku. Imp. Univ.*, **21**, 869 (1932); ibid., **22**, 835 (1933).
13) B. K. Singh, *Proc. Ind. Acad. Sci.*, **22A**, 163 (1945).

TABLE II. SUSCEPTIBILITIES OF THE CATIONS

Ion	Na^+	K^+	Ca^{2+}	Sr^{2+}	Ba^{2+}
χ_{ion}	6.90	15.00	8.80	18.30	29.30

state for Na^+, K^+, Ca^{2+}, Sr^{2+} and Ba^{2+} are used and these are given in Table II for ready reference.

The susceptibilities of the anions are evaluated using Pascal's law. Also the acid values were taken to represent the value of the corresponding ion on the assumption that H^+ does not contribute anything[14]. The mean values obtained for the anions under study are given in Table III.

TABLE III. IONIC SUSCEPTIBILITIES

Ion	Mean value from salts	χ_{ion} from acid	Mean
Benzoate $C_7H_5O_2^-$	69.11	71.27	70.19
Salicylate $C_7H_5O_3^-$	75.17	73.59	74.38
Propionate $C_3H_5O_2^-$	44.39	43.67	44.03
Butyrate $C_4H_7O_2^-$	49.74	54.15	51.95
Succinate $C_4H_4O_4^{2-}$	55.68	56.73	56.21

Discussion

The general method adopted for the evaluation of the ionic susceptibilities is on the basis that the molar susceptibility of a heteropolar salt is the sum of the constituent ions. The data available on the subject show that in the case of several ions, the values given by different authors differ sometimes by large amounts. Bhatnagar and co-workers[15] and Mata Prasad and co-workers[10] have followed a statistical method in which they subtracted all the known values of the susceptibilities of anions from the molar susceptibilities of a number of salts of a cation and took the arithmetical mean of the values thus obtained as the correct value for the cation. Kido[12], Joos[16] and Ikenmeyer[17] have observed that a linear relation exists between the susceptibilities of ions of chemically related elements belonging to the same group of the periodic table and their atomic numbers. This method of evaluation of the ionic susceptibilities has been questioned by Trew[18] and Selwood[19] on the ground that it is open to theoretical objection. Mata Prasad and co-workers[10] have followed Kido's[12] suggestion. Their results show that the susceptibility values of the anions deduced from the salts of Li, Na, K etc., are distinctly different from those deduced from the salts of Ca, Sr and Ba. This difference is large in some cases and small in others. If the linear relation is assumed then the assignment of ionic value could be done by measuring the molar susceptibilities of only two salts containing the cations of the same column of the periodic table.

When two ions combine there is every likelihood of a deformation taking place in both the ions. It is quite possible that the degree of deformations in ions may be different for the different groups of cations. To what extent this will affect the susceptibility of the anions is a question which is worth considering. On the basis of Pascal's additive law[11] the χ of anions can be calculated assuming the values of alkali and alkaline earth metallic ions. In Table IV this calculation has been made with the values obtained by Mata Prasad and co-workers[10], Rao and Sriraman[20] and Venkateswarlu and Sriraman[9] for formate, acetate and oxalate ions.

The anion values given in Table IV show definitely that they do not change abruptly as we pass from one group of metallic ions to another. All the values are of the same order subject to the error in the measurements of the susceptibility of the salts.

It is interesting to compare these values for a few typical ions with the values (Table V) obtained by Prasad and others by graphical method on the basis of linearity. For four ions the values from alkali salts are larger than from alkaline earth salts, for the last two ions the change is the other way about and for the oxalate ion no change is observed. If the values of the various ions are calculated from their own measurements on the basis of additivity, such marked variations are not found. Considering the graphical method adopted, Trew[18] has definitely pointed out that the graphs do not show linearity and the points do not lie on a single straight line. Our results in the present investigation also confirm this point. The linearity may be approximately true in a very few cases as Kido[12] found but it is certainly not applicable in all cases. The large amount of literatures available on the subject and the convincing facts brought out by Trew[18] show that the additivity method

14) K. Reichender, *Ann. Physik*, **1**, 169 (1929).
15) S. S. Bhatnagar et al., *Phil. Mag.*, **18**, 449 (1934).
16) V. G. Joos, *Z. Physik*, **19**, 347 (1923).
17) K. Ikenmeyer, *Ann. Physik*, **1**, 169 (1929).
18) V. C. G. Trew, *Trans. Faraday, Soc.*, **37**, 476 (1941).
19) P. W. Selwood, "Magnetochemistry", Interscience Publishers Inc., New York (1952).
20) S. R. Rao and S. Sriraman, *Phil. Mag.*, **24**, 1025 (1937).

TABLE IV

Substance	Prasad and co-workers		Rao and Sriraman	
	χ_{Ma}	χ_{Anion}	χ_{Ma}	χ_{Anion}
Sodium formate, NaHCOO	24.50	17.60	24.80	17.90
Calcium formate, $Ca(HCOO)_2$	45.30	18.30	39.50	15.35
Barium formate, $Ba(HCOO)_2$	73.70	22.20	66.60	18.65
Sodium acetate, $NaCH_3COO$	39.22	32.22	37.60	30.70
Barium acetate, $Ba(CH_3COO)_2$	99.49	35.10	88.04	29.37
			Venkateswarlu and Sriraman	
Sodium oxalate, $Na_2C_2O_4$	51.20	37.40	47.74	33.94
Potassium oxalate, $K_2C_2O_4$	65.64	35.64	64.89	34.89
Calcium oxalate, CaC_2O_4	44.30	35.50	42.08	33.28
Strontium oxalate, SrC_2O_4	54.64	36.34	51.20	32.90
Barium oxalate, BaC_2O_4	64.80	35.50	63.10	33.80

TABLE V

Anion	χ_{anion}, graphical		χ_{anion} additive
	Li, K, Na	Ca, Sr, Ba	
Formate	20.50	15.00	17.30[20]
Acetate	34.00	25.00	29.80[20]
Oxalate	34.40	34.00	33.86[9]
Succinate	58.80	36.00	55.67[21]
Salicylate	81.00	74.50	74.62[21]
Malonate	45.00	53.00	—
Stearate	206.00	212.00	—

21) S. Sriraman and S. Thiruvengadathan, This paper.

of evaluating the ionic value is more reliable subject to the accuracy of the measurements and the small error involved in the assumption of the cation values.

The authors wish to express their grateful thanks to Dr. K. Venkateswarlu for his keen and continued interest throughout this investigation.

Department of Physics
Annamalai University
Annamalainagar, South India

Refractometric Study of Some Cyano and Oxalato Complex Anions

By Yoshio MATSUNAGA*

(Received February 20, 1961)

The molar refraction of simple salts, particularly in the dissolved state, has been studied extensively by Fajans and others; however, little attention has been paid to that of complex salts. It seemed of great interest to examine the following two effects based on this physical quantity;

(1) polarization effect; the decrease of mobility of electrons in ligands due to the field of a central metal ion, and

(2) delocalization effect; the increase of mobility of electrons by the formation of π-bonds.

The former effect is expected to contribute to the decrease of molar refraction and the latter to the increase. With this hope we studied the molar refraction of some cyano and oxalato complex salts. Because of the high polarizability and the great ability for π-bond formation of ligand, cyano complex anions of the inner orbital type were chosen to demonstrate the above-mentioned two effects. On the other hand, oxalato complex anions are of the outer orbital type and the interaction between the constituents may not be very strong.

Experimental

Materials.—They were prepared by the methods described in the references cited. $K_3Cu(CN)_4$, prepared from cupric sulfate and potassium cyanide, and dried at 150°C[1]. $K_2Zn(CN)_4$, prepared from zinc sulfate and potassium cyanide, and dried at

* Present address: Cyanamid European Research Institute, Cologny, Geneva, Switzerland.

1) W. Biltz, *Z. anorg. u. allgem. Chem.*, **170**, 161 (1928).

105°C[2]. $K_2Cd(CN)_4$, prepared from cadmium sulfate and potassium cyanide, and dried at 105°C[1]. $K_2Hg(CN)_4$, prepared from mercuric cyanide and potassium cyanide, and dried at 80°C[1]. $K_3Cr(CN)_6$, prepared from potassium dichromate and potassium cyanide, and dried at 100°C[3]. $K_3Mn(CN)_6$, prepared from potassium cyanide and manganese(III) phosphate[3]. $K_3Fe(CN)_6$ and $K_4Fe(CN)_6$, Dog brand guaranteed reagents supplied by Koso Chemical Co., Ltd. Tokyo. $K_3Co(CN)_6$, prepared from cobalt chloride and potassium cyanide[3]. $K_2Ni(CN)_4$, prepared from nickel sulfate and potassium cyanide, and dried at 105°C[3]. $K_3Al(C_2O_4)_3 \cdot 3H_2O$, prepared from aluminum sulfate, potassium oxalate and oxalic acid[4]. $K_3Fe(C_2O_4)_3 \cdot 3H_2O$, prepared from ferric sulfate, barium oxalate, and potassium oxalate[4]. $K_2C_2O_4 \cdot H_2O$, prepared from oxalic acid and potassium carbonate.

Measurements.—The refractive index n of aqueous solutions was measured with a Pulfrich refractometer using the NaD line. The density d of the same solution was determined with Ostwald's pycnometers of about 10 cc. Most salts involved in this study are easily soluble in water, so that a concentration higher than three per cent by weight was applied. The specific refraction r of the respective solution was calculated from these data using the Lorentz-Lorenz formula,

$$r = (n^2-1)/(n^2+2) \times 1/d$$

The molar refraction R of the dissolved salt was derived from this specific refraction by the application of the additivity rule,

$$R = MW[r(\text{soln.}) - (100-w) \times r(\text{water})]/w$$

where w is the concentration of salt and MW is the molecular weight. The value R was found to be independent of concentration in the measured range.

TABLE I. MOLAR REFRACTION OF COMPLEX SALTS

	Molar refraction, cc.		
	Solution		Crystal[c]
Salt	Obs.	Lit.	
$K_3Cu(CN)_4$	46.8	—	44.9[d]
$K_2Zn(CN)_4$	37.8	—	37.5
$K_2Cd(CN)_4$	39.9	—	40.5
$K_2Hg(CN)_4$	43.1	—	43.2
$K_3Cr(CN)_6$	55.5	—	56.2
$K_3Mn(CN)_6$	61.0	—	—
$K_3Fe(CN)_6$	61.2	61.44[a], 60.91[b]	58.4
$K_4Fe(CN)_6$	67.4	67.8[a], 69.06[b]	—
$K_3Co(CN)_6$	59.2	—	—
$K_2Ni(CN)_4$	42.1	—	—
$K_2Al(C_2O_4)_3$	59.5	—	—
$K_2Fe(C_2O_4)_3$	66.4	—	—
$K_2C_2O_4$	22.5	—	—

a See Ref. 5.
b See Ref. 6.
c The values of density were taken from Ref. 1, and those of refractive index from Ref. 7 except that for $K_3Cu(CN)_4$.
d Refractive indices were taken from Ref. 8.

Results and Discussion

In Table I are presented our observed values of molar refraction of the complex salts in the dissolved state together with a few recorded values and also some estimated values for the crystalline salts. The molar refraction of aqueous complex anion was estimated, assuming that the contributions of cation and anion are additive. The value for aqueous K^+ ion was taken as 2.255 cc.[9] The molar refraction of aqueous ions is generally smaller than that of gaseous ions. For example the values: 0.20, 0.50 and 0.28 cc. were given by Fajans and Joos for gaseous Li^+, Na^+ and Mg^{2+} ions, respectively[10]. On the other hand, they gave −0.42, +0.200 and −1.57 cc. for the abovementioned ions in the dissolved state. The difference between the values in the two states can be ascribed to the polarization, or the decrease of mobility of electrons in water molecules by the electrostatic force due to the cation concerned. Great polarizing power is expected from small ions of high valency. The negative values assigned to aqueous Li^+ and Mg^{2+} ions arise from the large polarization effect on the water molecules in the hydration sphere. However, the magnitude of this effect in hydrated ions seems to be too small and inaccurate to be discussed quantitatively. The size of complex anions is much larger than that of simple ions, therefore we may consider that the molar refraction of aqueous complex anion is approximately equal to that of gaseous complex anion.

We assume that the molar refraction of complex anions is given by the sum of the following three terms:

(1) The sum of the molar refractions of the constituents in the gaseous state. The term A in Table II gives the molar refraction of the imaginary complex anion in which there is neither metal-ligand nor ligand-ligand interaction.

2) G. Bauer, "Handbuch der Präparativen Anorgachen Chemie", F. Enke, Stuttgart (1954), pp. 807, 819.
3) W. C. Fernelius, "Inorganic Syntheses", vol. 2, McGraw-Hill Book Co., New York (1946), pp. 203, 213, 225, 227.
4) H. S. Booth, ibid., Vol. I., Mc Graw-Hill Book Co., New York (1939), p. 35.
5) A. Heydweiller, *Physik. Z.*, **26**, 526 (1925).
6) M. T. Rogers and J. G. Malik, *J. Am. Chem. Soc.*, **77**, 6515 (1955).
7) A. N. Winchell and R. C. Emmons, "The Microscopic Characters of Artificial Inorganic Solid Substances or Artificial Minerals", John Wiley & Sons, Inc., New York (1931), pp. 173, 177, 178.
8) E. G. Cox, W. Wardlaw and K. C. Webster, *J. Chem. Soc.*, **1936**, 775.
9) K. Fajans and R. Lühdemann, *Z. physik. Chem.*, **B29**, 150 (1935).
10) K. Fajans and G. Joos, *Z. Physik*, **23**, 1 (1924).

(2) The contribution of polarization of ligands: the term *P* in Table II. The ligand-ligand interaction may be ignored because of the rather large size of cyanide and oxalate ions. Therefore, the magnitude of this term may be assumed to be proportional to the polarizing power of central metal ion; namely to the valency of metal ion and to the reciprocal of the square of metal-ligand distance.

(3) The contribution of delocalization of electrons by the formation of π-bonds: the term *D* in Table II. The magnitude of this term may depend on the configuration of complex ion and the number of available electrons.

Table II. Molar refraction of complex anions

Anion	*R* for anion cc.	*A*, cc. (additive)	*P*, cc. (polarization)	*D*, cc. (delocalization)
$Cu(CN)_4^{3-}$	40.1	34.7	− 6.4	11.8
$Zn(CN)_4^{2-}$	33.3	34.3	−12.8	11.8
$Cd(CN)_4^{2-}$	35.4	36.3	−12.8	11.9
$Hg(CN)_4^{2-}$	38.6	36.7	−12.8	14.7
$Cr(CN)_6^{3-}$	48.8	50.9	−16.5	15.4
$Mn(CN)_6^{3-}$	54.3	50.9	−16.5	20.9
$Fe(CN)_6^{3-}$	54.4	50.9	−16.5	21.0
$Fe(CN)_6^{4-}$	58.2	51.1	−11.0	19.1
$Co(CN)_6^{3-}$	52.5	50.9	−16.5	19.1
$Ni(CN)_4^{2-}$	37.6	34.3	− 8.7	(12)
$Al(C_2O_4)_3^{3-}$	52.8	54.1	− 1.3	0
$Fe(C_2O_4)_3^{3-}$	59.7	54.5	− 1.3	6.5

The molar refraction of gaseous cyanide ion was estimated to be 8.40 cc. based on the value observed for potassium cyanide in the dissolved state[11] and that of gaseous oxalate ion 18.0 cc. similarly. Pauling has given the following values for gaseous cations; Cu^+ 1.08, Zn^{2+} 0.72, Cd^{2+} 2.74, Hg^{2+} 3.14 and Al^{3+} 0.136 cc.[12] We assumed 0.7 cc. for Ni^{2+} and Fe^{2+} ions and 0.5 cc. for trivalent ions of the first transition metals. The terms *A* given in Table II were calculated using these values. It must be noted that the values of tetrahedral complex anions are in good agreement with the observed molar refractions except in the case of $Cu(CN)_4^{3-}$ ion, However, as is shown in the following paragraph, this agreement arises from the compensation between the terms *P* and *D*.

For the estimation of the term *P* we must know the distance between ligand and central metal ion. Only the following values are available; Zn–CN (center) 2.61, Cd–CN 2.67 and Hg–CN 2.65 Å[13]. We may assume that the required distances are the same in the series of tetrahedral cyano complex anions including $Cu(CN)_4^{3-}$. The maximum error arising from this assumption may not be more than 10 per cent of the term *P* or about 1 cc., as seen in Table II. The positive charge on central metal ion is mostly neutralized as a result of polarization of ligands. The magnitude of the term *D* for the isoelectronic $Cu(CN)_4^{3-}$ and $Zn(CN)_4^{2-}$ ions may be assumed to be roughly the same. Therefore, the chief difference between the two is that of the valency of the central metal ions, and the term *P* for $Cu(CN)_4^{3-}$ ion may be about one half of that for $Zn(CN)_4^{2-}$ ion. Consequently the difference between $(A-R)$ for $Zn(CN)_4^{2-}$ ion and that for $Cu(CN)_4^{3-}$ ion gives the magnitude of the term *P* for the latter. The term *P* estimated for $Zn(CN)_4^{2-}$ ion was assumed to be applicable to the other two tetrahedral complex anions. The $Cu(CN)_4^{3-}$ ion has been known to dissociate appreciably in dilute solution[14]. However, we ignored this fact in our treatment of molar refraction because rather concentrated solutions were used for our measurements.

For octahedral cyano complex anions the isoelectronic ions $Fe(CN)_6^{4-}$ and $Co(CN)_6^{3-}$ were used for the basis of discussion. We assumed again that the distance between metal ion and ligand is nearly constant in these five complex anions, therefore the term *P* for $Fe(CN)_6^{4-}$ ion may be about two thirds of that for $Co(CN)_6^{3-}$ ion and the term *D* for this pair may be roughly the same. The term *P* estimated for $Co(CN)_6^{3-}$ ion was applied to the other trivalent cyano complex anions.

The contribution of polarization effect on a cyanide ion was found to be about 1.6 cc. per unit charge on central metal ion for tetrahedral anions and about 0.9 cc. per unit charge for octahedral ones. The similar polarization found in the reaction,

$$H^+ + CN^- \rightarrow \text{gaseous HCN} \quad (6.47\,\text{cc.})^{15}$$

1.93 cc. may be compared with the above two estimations. As the mutual repulsion of cyanide ions in a complex anion must be weaker in a tetrahedral configuration than in an octahedral one, the cyanide ions in the former are closer to the central metal ion than those in the latter. Therefore, the observed order of polarization of a cyanide ion; HCN > tetrahedral complex anion > octahedral complex anion seems to be reasonable. The contribution of electron-delocalization to molar refraction was estimated to be around 3 cc. per cyanide ion for both tetrahedral and octahedral complex

11) M. Le Blanc and P. Rohland, *Z. physik. Chem.*, **19**, 261 (1896).
12) L. Pauling, *Proc. Roy. Soc.*, **A114**, 181 (1927).
13) R. G. Dickinson, *J. Am. Chem. Soc.*, **44**, 774 (1922).
14) J. H. Baxendale and D. T. Westcott, *J. Chem. Soc.*, **1959**, 2347.
15) K. Fajans, *Z. physik. Chem.*, **B24**, 103 (1934).

anions. The term P for the square planar $Ni(CN)_4^{2-}$ ion was obtained using a value of 4×3 cc. for its term D, and the polarization of a cyanide in per unit charge in this anion seems to be nearly the same as that for octahedral complex anions.

In the case of oxalato complex anions, the observed molar refraction of $Al(C_2O_4)_3^{3-}$ ion, in which the aluminum ion has no d-electron for π-bonding, is only slightly smaller than its term A or we may say in agreement with its term A within the limit of estimations. This agreement suggests that the polarization of the oxalate ions by the field of the aluminum ion is very small. The term D for $Fe(C_2O_4)_3^{3-}$ ion was found to be about 6.5 cc. This value is much less than that for cyano complex anions of the inner orbital type.

TABLE III. COMPARISON BETWEEN MOLAR REFRACTION AND MOLAR VOLUME OF CYANO COMPLEX ANIONS

Anion	Molar refraction cc.	Molar volume[a] cc.
$Cu(CN)_4^{3-}$	40.1	93
$Zn(CN)_4^{2-}$	33.3	118
$Cd(CN)_4^{2-}$	35.4	128
$Hg(CN)_4^{2-}$	38.6	126
$Cr(CN)_6^{3-}$	48.8	135
$Mn(CN)_6^{3-}$	54.3	—
$Fe(CN)_6^{3-}$	54.4	129
$Fe(CN)_6^{4-}$	58.2	126
$Co(CN)_6^{3-}$	52.5	129
$Ni(CN)_4^{2-}$	37.6	98

a These values were taken from Ref. 1.

Recently Hieber and his collaborators have discussed the molar volumes of some complex cyano anions[16,17]. They have observed the following series of molar volumes for the isoelectronic anions with the configuration of rare gas type,

$$Zn(CN)_4^{2-} > Cu(CN)_4^{3-} > Ni(CN)_4^{4-}$$

and $$Co(CN)_6^{3-} > Fe(CN)_6^{4-} > Mn(CN)_6^{5-}$$

and concluded that the decrease of molar volume can be correlated with the increasing double bond character of metal-carbon bonds. The importance of polar structures as the determining factor was also pointed out for the molar volume of anions of non-rare gas type. Although molar refraction is a measure of size of complex anion, these two physical quantities have no simple correlation as seen in Table III. For the pairs of isoelectronic complex anions; $Cu(CN)_4^{3-}$ and $Zn(CN)_4^{2-}$, and $Fe(CN)_6^{4-}$ and $Co(CN)_6^{3-}$, the molar refractions were found in the reverse order to the molar volumes.

16) W. Hieber, R. Nast and J. G. Floss, *Z. anorg. u. allgem. Chem.*, **283**, 188 (1956).
17) W. Hieber and O. Vohler, ibid., **294**, 219 (1958).

Summary

The molar refractions of ten cyano and two oxalato complex salts were measured in the dissolved state using the NaD line. The molar refractions of complex anions were assumed to be given by the sum of (1) the molar refractions of the ligands and the central metal ion in the gaseous state, (2) the polarization of the ligands due to the field of the central metal ion, and (3) the delocalization of electrons by the metal-ligand π-bonding. The estimation of each term was attempted on the assumption that the chief difference between isoelectronic anions, for example $Cu(CN)_4^{3-}$ and $Zn(CN)_4^{2-}$, is that of the valency of the central metal ions and the contribution of delocalization is roughly the same in such a pair. The polarization of a cyanide ion was found to be about 1.6 cc. per unit charge of metal ion for tetrahedral anions and about 0.9 cc. for octahedral ones. The contribution of π-bonding was estimated to be around 3 cc. per metal-ligand bond for both of the above-mentioned cyano complex anions. The small polarization and delocalization effects were observed in the case of oxalato complex anions.

The author wishes to express his hearty thanks to Professors Eiichi Minami and Shizuo Fujiwara for their interest and encouragement.

Department of Chemistry
Faculty of Science
The University of Tokyo
Hongo, Tokyo

The Preparation of cis- and trans-4-tert-Butylcyclohexyl-1-carbinols

By Nobuo MORI

(Received March 18, 1961)

In the course of the investigation[1] concerning the conformation of a toluenesulfoxymethyl group directly bound to a cyclohexane ring, it was found to be desirable to study *cis*- and *trans*-4-*tert*-butylcyclohexyl-1-carbinyl *p*-toluenesulfonates.

The present work relates to a process for the preparation of the hitherto unknown *cis*- and *trans*-4-*tert*-butylcyclohexyl-1-carbinols and their *p*-toluenesulfonates.

The *cis*- and *trans*-carbinols have now been prepared from 4-*tert*-butylbenzoic acid by hydrogenating them over platinum oxide in acetic acid and over Raney nickel in neutral aqueous medium, respectively. The resulting *cis*- and *trans*-4-*tert*-butylhexahydrobenzoic acids were converted into their ethyl esters which were treated with lithium aluminum hydride to give the *cis*- and *trans*-carbinols respectively, and they were converted into the *p*-toluenesulfonates. The process carried out is shown in the following scheme.

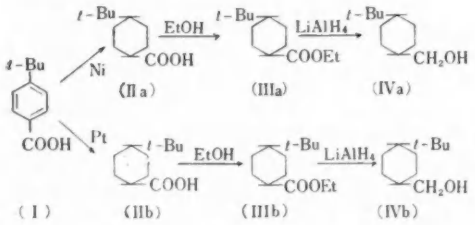

tert-Butylbenzoic acid (I) used as starting material was obtained by reacting dry benzene with *tert*-butyl alcohol over aluminum chloride[2], brominating the resulting *tert*-butylbenzene with bromine over iron powder[3] and treating a Grignard reagent of the 4-*tert*-butylbromobenzene with carbon dioxide according to the method[4] for the conversion of *tert*-butyl chloride into *tert*-butylacetic acid.

The hydrogenation of substituted benzene compounds in neutral medium with Raney nickel generally gives thermodynamically stable hydrogenated benzene compounds as main products and on the contrary in acetic acid with platinum oxide less stable stereoisomers. For example, the hydrogenation[1,5] of 4-methyl- or isopropylbenzoic acid over Raney nickel gives mainly the corresponding *trans*-hexahydrobenzoic acid melting at a higher temperature and over platinum oxide the corresponding cis-isomer melting at a lower temperature. The hydrogenation of the 4-isopropylbenzoic acid by either of the above methods does not proceed so readily as with the 4-methylbenzoic acid. The 4-methylbenzoic acid is completely hydrogenated with Raney nickel under an initial pressure of 90 atm. at 180～200°C in 2 hr. to give the hexahydrobenzoic acid, while the hydrogenation of the isopropylbenzoic acid[5] is effected under 150～200 atm. 200°C for 4～5 hr. On the other hand, the hydrogenation[1,5] of the methyl- and isopropylbenzoic acids with platinum oxide is completed under atmospheric pressure in 2～4.5 and 6 hr., respectively.

In the present work, the butylbenzoic acid (I) was hydrogenated in a neutral aqueous solution with Raney nickel under an initial pressure of 90 atm. 250～260°C in 5 hr., although the uptake of hydrogen was not complete and this reaction was probably accompanied by hydrogenolysis, and the *trans*-hexahydrobenzoic acid melting at 175～176°C after recrystallization was obtained in a 40% yield. On the other hand, the butylbenzoic acid (I) was not hydrogenated in acetic acid with platinum oxide within 4 hr. at 60～70°C under atmospheric pressure, but the uptake of hydrogen was very readily and completely effected under an initial pressure of 60 atm. at about 100°C in 1 hr. and the *cis*-hexahyrobenzoic acid (IIb) was obtained as scales, m. p. 115～117°C after recrystallization, in a good yield. The difficulty in hydrogenation of these 4-alkylbenzoic acids increases as the alkyl group goes from methyl to *tert*-butyl. These acids were converted into their anilides by the method without the danger of isomerization.

The above acids were converted into their ethyl esters by refluxing in ethyl alcohol with a small amount of sulfuric acid in a short

1) N. Mori, This Bulletin, **34**, 1299 (1961).
2) C. S. Marvel et al., *J. Am. Chem. Soc.*, **66**, 914 (1944).
3) R. C. Huston, W. B. Fox and M. N. Binder, *J. Org. Chem.*, **3**, 251 (1938).
4) H. Gilman and R. H. Kirby, "Organic Syntheses", Coll. Vol. I, Second edition (1941), p. 361.
5) R. G. Cooke and A. K. Macbeth, *J. Chem. Soc.*, 1939, 1245.

period. The refractive index and the density of the cis-ester (IIIb) are higher than those of the trans-ester (IIIa). In Table I, the physical constants of the *cis*- and *trans*-4-*tert*-butylhexahydrobenzoic acids and their derivatives obtained in the present work are shown with those of 4-methyl and isopropylhexahydrobenzoic acids and their derivatives for comparison.

Table I. Physical constants of isomeric 4-alkyl-hexahydrobenzoic acids and their derivatives

4-Alkyl	Free acid M. p., °C	Anilide M. p., °C	Ethyl ester n_D^{20}	Ethyl ester d_4^{20}
trans-tert-Bu	175~176	139.5	1.4515	0.9282
cis-tert-Bu	115~117	191	1.4593	0.9400
trans-isoPr[5]	94	—	—	—
cis-isoPr[5]	liq.	—	1.4491	—
trans-Me[6]	111	—	1.4392	0.9361
cis-Me[6]	13	—	1.4425	0.9448

These trans- and cis-esters IIIa and IIIb were converted into the corresponding carbinols IVa and IVb by treatment with lithium aluminum hydride, according to the method[1] for the conversion of the isomeric 4-methylhexahydrobenzoic acid ethyl esters into their carbinols. It is well known that hydrogenolysis of esters with lithium aluminum hydride proceeds with complete retention of configuration while that with sodium in alcohol and over copper chromite catalyst proceeds with some isomerization. The purified *cis*-carbinol is in needles melting at 56~57°C and the trans-isomer is in needles of m. p. 25~27°C. The refractive index and the density of the *cis*-carbinol which was in a super-cooled liquid form before purification are higher than those of the super-cooled *trans*-carbinol, as shown in Table II, which also includes those of 4-methyl- and isopropyl-cyclohexyl-1-carbinols for comparison, and this fact is in accordance with the Auwers-Skita rule[7].

Table II. Physical constants of isomeric 4-alkylcyclohexyl-1-carbinols and their tosylates

4-Alkyl	Carbinol n_D^{20}	Carbinol d_4^{20}	Tosylate M. p., °C
trans-tert-Bu	1.4683	0.9092	83 ~84
cis-tert-Bu	1.4781	0.9243	95 ~95.5
trans-isoPr[5]	1.4661*	0.9007*	—
cis-isoPr[5]	1.4682*	0.9051*	—
trans-Me[5]	1.4578*	0.8962*	44.5~44.7[8]
cis-Me[5]	1.4617*	0.9074*	30.5~31.0[8]

* Values at 30°C.

6) G. H. Keats, ibid., **1937**, 2003.
7) K. von Auwers, *Ann.*, **420**, 84 (1920); A. Skita, *Ber.*, **53**, 1792 (1920); A. Skita and W. Faust, ibid., **64**, 2878 (1931).

Experimental

4-*tert*-Butylbenzoic Acid (I).—A Grignard reagent solution was prepared in the usual way by adding dropwise 4-*tert*-butyl-bromobenzene (70 g.) in dry ether (200 cc.) to magnesium strips (8 g.) covered with ether (50 cc.) while warming on steam bath and stirring. The solution was cooled to −15~−10°C in an ice-salt bath and then treated with a stream of dry carbon dioxide until the temperature rose no more. The reaction mixture was decomposed with dilute sulfuric acid and the ethereal layer was washed with aqueous sodium hydroxide solution. The aqueous layer separated was acidified with concentrated hydrochloric acid to give an acid product which melted at 163~164.4°C (lit.[2] 164°C) after one recrystallization from aqueous methanol.

***trans-tert*-Butylhexahydrobenzoic Acid (IIa).**—A solution (pH=8.0) of the butylbenzoic acid (12 g.) in 7% sodium hydroxide solution was hydrogenated in the presence of Raney nickel (6 g.) under an initial pressure of 90 atm. at 250~260°C. The reaction was stopped after 5 hr. although the uptake of hydrogen was not complete. After removal of the catalyst, the solution was acidified with concentrated hydrochloric acid and the precipitated material (10 g.) was repeatedly recrystallized from aqueous methanol to give the pure *trans*-hexahydrobenzoic acid (3 g.) as plates, m. p. 175~176°C (lit.[5] 174°C).

Found: C, 71.8; H, 10.9. Calcd. for $C_{11}H_{20}O_2$: C, 71.7; H, 10.9%.

A part of the acid was converted into an anilide by refluxing for 10 min. with one equivalent each of thionyl chloride and pyridine in dry benzene and then for 2 min. with two equivalents of aniline. Recrystallization of the anilide from aqueous ethanol readily gave fine plates, m. p. 139.5°C.

Found: N, 5.6. Calcd. for $C_{17}H_{25}ON$: N, 5.4%.

***cis-tert*-Butylhexahydrobenzoic Acid (IIb).**—A solution of the butylbenzoic acid (10 g.) in purified glacial acetic acid (60 cc.) was hydrogenated with platinum oxide (0.5 g.) under an initial pressure of 60 atm. at 90~100°C until no more hydrogen was absorbed. After removal of the catalyst and the solvent, the crystalline residue was taken up in a small volume (about 20 cc.) of petroleum ether and the undissolved parts were filtered off. The filtrate was concentrated and cooled. The separated plates were filtered off and recrystallized repeatedly from aqueous methanol to give the pure *cis*-hexahydrobenzoic acid (6 g.) as scales, m. p. 115~117°C (lit.[5] 116°C).

Found: C, 71.7; H, 10.6. Calcd. for $C_{11}H_{20}O_2$: C, 71.7; H, 10.9%.

The anilide of the cis-acid was obtained by the method used for the trans-acid as long needles from aqueous methanol and ligroin, m. p. 191°C which was depressed to 124~127°C on admixture with the trans-anilide.

Found: N, 5.6. Calcd. for $C_{17}H_{25}ON$: N, 5.4%.

8) Eliel and Acharya reported that the acids were first obtained by Stolow, but the details of preparation are not described. See E. L. Eliel and R. V. Acharya, *J. Org. Chem.*, **24**, 151 (1959).

Ethyl *trans*-*tert*-Butylhexahydrobenzoate (IIIa).—The trans- acid (3 g.) was refluxed in ethanol (30 cc.) with concentrated sulfuric acid (0.5 cc.) for 2 hr. After concentration of the reaction mixture, the residue was taken up in ether, washed with water, 10% sodium carbonate solution and then water, dried with sodium sulfate and concentrated. The residue was distilled under reduced pressure to give the ethyl ester (3 g.) which boiled at 125~137°C (mainly 135~136°C)/25 mmHg and had n_D^{20} 1.4522. Redistillation gave the pure ester which had b. p. 146~148°C/29 mmHg, n_D^{20} 1.4515 d_4^{20} 0.9282 and MR_D 61.70 (Calcd. 61.69).

Ethyl *cis-tert*-Butylhexahydrobenzoate (IIIb).—The cis- acid (3.5 g.) gave similarly the cis-ethyl ester (3.5 g.) which, after redistillation, had b. p. 134~137°C/28 mmHg, n_D^{20} 1.4593, d_4^{20} 0.9400 and MR_D 61.74 (Calcd. 61.69).

***trans-tert*-Butylcyclohexylcarbinol (IVa).**—The trans-ester (2.5 g.) in dry ether (30 cc.) was added dropwise to a suspension of lithium aluminum hydride (1.0 g.) in dry ether (60 cc.) at 0~5°C and the reaction mixture was stirred for another hour. This mixture was then treated with a small amount of cold dilute sulfuric acid until the ether layer was clear and then filtered. The filtrate and washings of the filter cake were combined, dried with potassium carbonate and concentrated. The residue was distilled to give the carbinol (1.8 g.) as a viscous oil which had b. p. 140~140.5°C/28.5 mmHg, n_D^{20} 1.4683, d_4^{20} 0.9092, MR_D 52.13 (Calcd. 52.32), which solidified in a refrigerator and melted at 25~27°C.

Found: C, 77.5; H, 12.9. Calcd. for $C_{11}H_{22}O$: C, 77.6; H, 13.0%.

The carbinol (1.1 g.) was treated with *p*-toluenesulfonyl chloride (1.5 g.) in dry pyridine (5 cc.) by the usual way[1] at 0~5°C and allowed to stand overnight in a refrigerator with occasional shaking. The mixture was poured into a mixture of ice and concentrated hydrochloric acid. The separated crystalline solid was filtered off and recrystallized twice from aqueous ethanol to give the *trans-p*-toluenesulfonate (1.4 g.) as needles, m. p. 83~84°C.

Found: C, 66.8; H, 8.6. Calcd. for $C_{18}H_{28}O_3S$: C, 66.6; H, 8.66%.

***cis-tert*-Butylcyclohexylcarbinol (IVb).**—A similar treatment of the cis-ester (3.0 g.) with lithium aluminum hydride (1.2 g.) gave the *cis*-carbinol (1.4 g.) as a viscous oil, b. p. 133~136°C/27 mmHg, n_D^{20} 1.4781, d_4^{20} 0.9243 and MR_D 52.16 (Calcd. 52.32), which soon partially solidified on being allowed to stand in a refrigerator. The semi-solid mass was pressed on a porous tile and recrystallized from aqueous ethanol to give the pure *cis*-carbinol as long needles, m. p. 56~57°C.

Found: C, 78.2; H, 12.8. Calcd. for $C_{11}H_{22}O$: C, 77.6; H, 13.0%.

The pure carbinol was treated by the method used for the *trans*-carbinol with *p*-toluenesulfonyl chloride to give the *cis-p*-toluenesulfonate. Recrystallization from methanol gave needles, m. p. 95~95.5°C.

Found: C, 66.7; H, 8.8. Calcd. for $C_{18}H_{28}O_3S$: C, 66.6; H, 8.66%.

Tokyo College of Science
Shinjuku-ku, Tokyo

Semiconductivity and Absorption Spectrum of Perylene Single Crystal

By Mizuka Sano and Hideo Akamatu

(Received March 6, 1961)

Concerning the electronic conduction in organic solids, most of which are aromatic compounds, the investigation on single crystals is of special interest. For instance, it is desirable to determine the anisotropy of the electrical conductivity. If it is presumed that the conduction takes place in association with the overlapping of π-electron orbitals, the resistivity should be the lowest in such a direction where the overlapping is the largest. Mette and Pick[1] have observed such an anisotropy in the anthracene single crystal. We have found a similar anisotropy of thin evaporated films of perylene, coronene and violanthrene in which minute crystals are in alignment along the textured structure[2]. In this note, the investigation on the perylene single crystal is presented. It contributes to the above argument and suggests the correlation between the conduction level and the electronic absorption band in the molecular crystal.

Perylene, which was synthetized from naphthalene following Scholl[3], was recrystallized from the benzene solution and the gracial acetic acid solution successively, then sublimed in vacuo. However, these procedures could not

1) H. Mette and H. Pick, *Z. Phys.*, **134**, 566 (1953).

2) H. Inokuchi, H. Kuroda and H. Akamatu, This Bulletin, **34**, 749 (1961).

3) R. Scholl, *Ber.*, **43**, 2202 (1910).

eliminate a trace of reddish substance, terrylene ($C_{30}H_{16}$). Finally, the chromatographic technique with alumina was applied to its benzene solution in the dark. Subsequent sublimation yielded a faint yellow product.

Thin perfect single crystals were obtained when the sublimation procedure was carefully controlled and made to be slow. In a favorable condition, flake-like crystals were produced on the glass wall, which possessed the area of about 4×6 mm^2 with the thickness of 60~280 μ. It was proved by means of the X-ray diffraction that the surface plane of the flake-like crystal is the (001) plane.

The electrical resistivity was measured by applying the voltage perpendicularly to the (001) plane, or in parallel to the plane. Aquadag was employed as the electrodes. The voltage source was a battery of dry elements with a voltage up to 450 V. The measurement was carried out, with the aid of direct current amplifier, in vacuo (10^{-3} mmHg) over a temperature range from 40 to 110°C.

No departure from Ohm's law was observed in the voltage region employed (up to 1.6×10^3 V./cm.). The resistivity decreased with increasing temperature and a good linear realationship was obtained between the logarithm of the resistivity (ρ) and the reciprocal of the temperature, (Fig. 1), which indicates the applicability of the following formula.

$$\rho=\rho_0\exp(\varepsilon/2kT)$$

where ε is the energy gap.

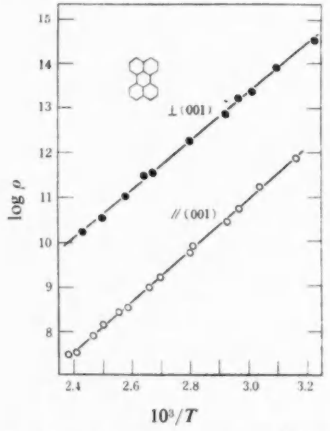

Fig. 1. The relation between resistivity and temperature for perylene single crystal.

It was found that the resistivity is isotropic in the (001) plane. But in the direction perpendicular to this plane, the resistivity is higher by a factor of 10^2 than that in the (001) plane, (Table I).

TABLE I. THE VALUES OF ε AND $\rho_{15°C}$ AND THE ABSORPTION SPECTRUM OF PERYLENE CRYSTAL

	ε eV.	$\rho_{15°C}$ Ω·cm.
$\perp$ (001)	2.1	6.5×10^{15}
$\parallel$ (001)	2.2	4.1×10^{13}
Film*		
from the sandwich-type cell	2.0	$10^{15}\sim10^{19}$
from the surface-type cell	2.2	10^{13}
Absorption spectrum		
the peak of the p-band	2.67	
the onset of the p-band	2.26	

* after Inokuchi, Kuroda and Akamatu[2]

The absorption spectra of the perylene crystal and its solution in ethyl alcohol were recorded by the spectrophotometer (Cary model 11). The spectrum of the single crystal resembles closely that of the solution, excepting some broadening and a small shift toward the long wavelength side. In consequence, according to Clar's classification[4], the absorption bands of the crystal can be assigned to the p-, α- and β-band respectively, referring to the absorption bands of the solution.

In the neighborhood of the absorption edge, it is rather difficult to decide precisely the threshold value. However, the onset of the p-band is found in the vicinity of 466 mμ for the solution and 550 mμ for the crystal. The value of light quantum for the latter is in agreement with the observed value of ε, (Table I).

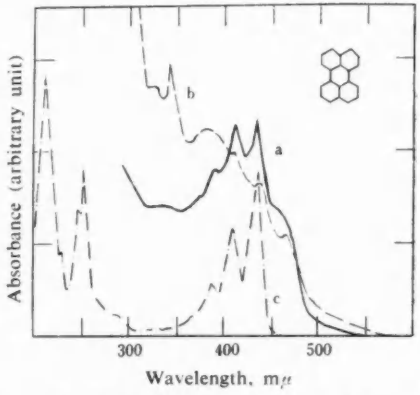

Fig. 2. Absorption spectra of perylene. (a) Single crystal, (b) Evaporated film, (c) Solution in ethyl alcohol

The anisotropy was found in regard to the conductivity, but not to the value of the energy gap. The same result has been obtained for

4) E. Clar, "Aromatische Kohlenwasserstoffe", Springer Verlag, Berlin (1952).

the evaporated film of perylene[2]. It can be concluded that the anisotropy arises due to the difference in the mobility of free carriers which is dependent on the direction of drift, but not due to the difference in the number of carriers which are in thermal equilibrium.

The direction of π-bond orbitals in each molecule extends perpendicularly from the molecular plane, and molecules are arranged in the crystal in such a way that the molecular planes are parallel with each other with a distance of 3.47 Å and nearly perpendicular to the (001) plane[5]. Therefore, the direction of the lowest resistivity is coincident with the direction of the extending of π-bond orbitals of molecules in the crystal. The maximum overlapping of the orbitals is expected to be between neighboring molecules in this direction.

If a conduction level could be assumed in the molecular crystal, the observed value of the energy gap implies that it lies in the neighborhood of the onset of the *p*-absorption band. No theory has yet explained the reason why the lowest excited state contributes to the conduction, but it is likely that the excitation of π-electrons to the lowest excited singlet state is the first process of electronic conduction in the perylene crystal.

Department of Chemistry
Faculty of Science
The University of Tokyo
Hongo, Tokyo

5) D. M. Donaldson, J. M. Robertson and J. G. White, *Proc. Roy. Soc.*, **A220**, 311 (1953).

Syntheses of γ-Ionone Analogues. I–II.

By Atsuaki Arai and Iwao Ichikizaki

(Received March 18, 1961)

I. Several Asymmetric Bifunctional Dienophiles and their Diels-Alder Adducts with 2, 3-Dimethyl-1, 3-butadiene

Tetrolaldehydes or crotonaldehydes containing an adequate functional substituent in the γ-position seem to be suitable as the dienophiles for the preparation of the Diels-Alder adducts which can be used as the key intermediates for a certain synthetical project concerning γ-ionone analogues. In spite of their apparently simple structure, such compounds and their Diels-Alder adducts have hitherto scarcely been reported.

One of the present authors and his co-workers[1] synthesized the diethylacetals of γ-hydroxytetrolaldehyde (I), γ-dialkylaminotetrolaldehyde (II) and of γ-dialkylaminocrotonaldehyde (III), and then explained that all these acetals could neither give the free parent aldehydes nor behave as a dienophile, while they reported that γ-methoxycrotonaldehyde (XIa) was proved to be a dienophile. In this paper the authors wish to describe the preparation of several dienophiles in such series and the Diels-Alder reactions of them with a typical symmetric diene, 2, 3-dimethyl-1, 3-butadiene.

Five dienophiles — γ-methoxy-, γ-benzyloxy- and γ-tetrahydropyran-2-yloxytetrolaldehyde (VIIIa, VIIIb and VIIIc), γ-methoxy- and γ-benzyloxycrotonaldehyde (XIa and XIb) — were prepared successfully by the manganese dioxide oxidation of the corresponding carbinols (VIIa, VIIb, VIIc, Xa and Xb) as shown by the following scheme:

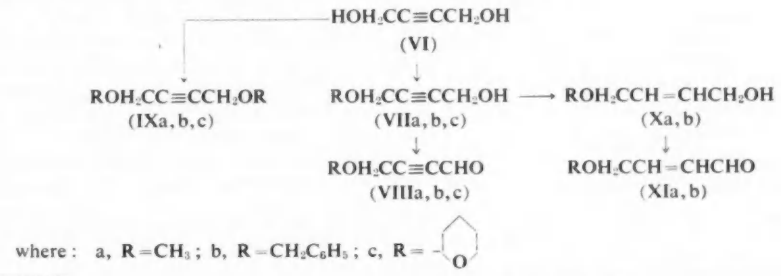

where: a, $R=CH_3$; b, $R=CH_2C_6H_5$; c, R =

1) I. Ichikizaki, Ching-Chung Yao, Y. Fujita and Y. Hasebe, This Bulletin, **28**, 80 (1955).

4-Methoxy-2-butyn-1-ol (VIIa) was prepared in 43% yield through a partial methylation of 2-butyn-1,4-diol (VI) with dimethyl sulfate in an aqueous alkali. A modified procedure was applied for the preparation of 4-benzyloxy-2-butyn-1-ol (VIIb) by adding benzyl chloride at 110~115°C into a xylene suspension of monosodium butyndiolate prepared beforehand from a large excess of VI with sodamide in liquid ammonia. In both cases appreciable amounts of 1,4-dialkoxy-2-butynes (IXa and IXb) were isolated.

Catalytic hydrogenation of the acetylenic carbinols, VIIa and VIIb, in the presence of a palladium-calcium carbonate catalyst in ethyl acetate gave the corresponding ethylenic carbinols, Xa and Xb, in good yields.

An attempted preparation of 4-tetrahydropyran-2′-yloxy-2-butyn-1-ol (VIIc) directly from VI and dihydropyran was proved to be unsatisfactory, since it was extremely difficult to separate the pure product from the reaction mixture containing 1,4-bistetrahydropyran-2′-yloxy-2-butyne (IXc), unchanged VI besides VIIc. IXc was, therefore, prepared at first by heating VI with two moles of dihydropyran in the presence of a catalytic amount of concentrated hydrochloric acid or *p*-toluenesulfonic

TABLE I. 4-ALKOXY-2-BUTYN-1-ALS AND 4-ALKOXY-2-BUTEN-1-ALS
$ROCH_2C{\equiv}CCHO$ (VIII), $ROCH_2CH{=}CHCHO$ (XI)

Compound Number	R	B. p. °C/mmHg	n_D^T	Yield, % based on the parent carbinol	Molecular formula	Analysis, % Found C	Calcd. C	Found H	Calcd. H
VIIIa	$-CH_3$	68~69/25	1.4504^{20}	41	$C_5H_6O_2$	59.99	61.21	6.58	6.16
VIIIb	$-CH_2C_6H_5$	116~117/1.0 111~112/0.7	1.5383^{21}	55	$C_{11}H_{10}O_2$	75.58	75.84	5.93	5.79
VIIIc[a]		83~84/0.8	1.4902^{16}	68	$C_9H_{12}O_3$	64.55	64.27	7.54	7.19
XIa	$-CH_3$	73~74/27		45	$C_5H_8O_2$	59.76	59.98	8.15	8.05
XIb	$-CH_2C_6H_5$	111~113/1.0	$1.5310^{15.5}$	52	$C_{11}H_{12}O_2$	74.92	74.97	6.88	6.86

a) ν_{max}(liquid film) 2245, 2200 (C≡C); 1670 (C=O, conj.); 1185, 1125, 1083, 1060, 1031, 967, 944, 904, 874 cm^{-1} (C-O-C); no absorption band of hydroxyl group is observed.
$\lambda_{max}^{n\text{-hexane}}$ 221 mμ (ε 26400)

TABLE II. SOLID DERIVATIVES OF 4-ALKOXY-2-BUTYN-1-ALS AND 4-ALKOXY-2-BUTEN-1-ALS
$ROCH_2C{\equiv}CCHO$ (VIII), $ROCH_2CH{=}CHCHO$ (XI)

Parent aldehyde Number	R	Semicarbazone Appearance	M. p. °C	λ_{max}^{EtOH} mμ (ε)	Molecular formula	Analysis, % Found N	Calcd. N	2,4-Dinitrophenylhydrazone Appearance	M. p. °C	Molecular formula	Analysis, % Found N	Calcd. N
VIIIa	$-CH_3$							Orange-yellow needles	111~112.2	$C_{11}H_{10}O_5N_4$	19.90	20.14
VIIIb	$-CH_2Ph$	Slightly yellow needles	138.5~139[a]	236 (33700) 281 (41500)	$C_{19}H_{17}O_2N_3$	13.47	13.67	Yellow needles	121~122	$C_{17}H_{14}O_5N_4$	15.89	15.81
VIIIc								Yellow needles	120~120.5[b]	$C_{10}H_8O_5N_4$	21.13	21.21
XIa	$-CH_3$							Red-orange needles	140~141	$C_{11}H_{12}O_5N_4$	19.83	19.99
XIb	$-CH_2Ph$	Needles	148~149	264 (34500)	$C_{12}H_{15}O_2N_3$	18.27	18.02	Orange silk-like needles	166.5	$C_{17}H_{16}O_5N_4$	15.68	15.72

a) Phenylsemicarbazone
b) This 2,4-dinitrophenylhydrazone was identical with that of 4-hydroxy-2-butyn-1-al (I).

TABLE III. DIELS-ALDER ADDUCTS OF γ-SUBSTITUTED TETROL- AND CROTONALDEHYDES WITH 2,3-DIMETHYL-1,3-BUTADIENE

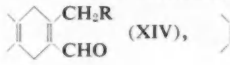
(XIV),
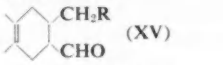
(XV)

Dienophiles Number	Condition of D-A reaction Temp. °C	Time hr.	Adduct Number	R	Yield %	B. p. °C/mmHg	n_D^T	Molecular formula	Analysis, % Found Calcd. C	H
VIIIa	140~150	13	XIVa	$-OCH_3$	84.3	113~117 /3	1.5161^{18}	$C_{11}H_{16}O_2$	71.68 73.30	8.93 8.95
VIIIb	145~153	14	XIVb	$-OCH_2Ph$	81.6	141~145 /0.03	1.5554^{20}	$C_{17}H_{20}O_2$	79.37 79.65	7.83 7.86
VIIIc	120~130	21	XIVc[a]		72	146~147 /0.75	1.5221^{20}	$C_{15}H_{22}O_3$	71.60 71.97	8.80 8.86
XIa	125~135	13	XVa	$-OCH_3$	73	82~84[b] /2.5		$C_{11}H_{18}O_2$	72.58 72.49	9.81 9.96
XIb	125~135	13	XVb	$-OCH_2Ph$	71.5	130~135 /0.01		$C_{17}H_{22}O_2$	79.12 79.03	8.49 8.58
Croton-aldehyde	140~150	9	XVI	$-H$	72.4	98/18[c]	1.4731^{20}	$C_{10}H_{16}O$	78.70 78.89	10.68 10.59

a) λ_{max}^{EtOH} 235 mμ (ε 7600); ν_{max} (liquid film) 1675 (C=O); 1198, 1181, 1118, 1078, 1057, 1028, 973, 907, 873 cm^{-1} (C-O-C-O)

b) Ref. 1, b. $p._{2.5}$ 82~84°C.

c) O. Diels and K. Alder, *Ann.*, **470**, 62 (1929), reported b. $p._{12}$ 89°C.

acid in tetrahydrofuran, then it was similarly treated with one equivalent of VI to afford pure VIIc in a good yield. The tetrahydropyranyl ether thus prepared was fairly soluble in water and afforded the 2,4-dinitrophenylhydrazone of 5-hydroxypentanal (XII) in quantitative yield by the Brady reagent.

So far as the authors were aware, none of the acetylenic primary carbinols had ever been reported to be oxidized into the aldehydes by the technique after Attenburrow[2], however, all of the 4-alkoxy-2-butyn-1-ols (VIIa, VIIb and VIIc) and the 4-alkoxy-2-buten-1-ols (Xa and Xb) were successfully oxidized by the usual method with active manganese dioxide to yield the corresponding aldehydes (VIIIa, VIIIb, VIIIc, XIa and XIb), which were all proved to be the dienophiles of moderate activity as described later. Their properties and analytical data are shown in Table I and their solid derivatives are summarized in Table II.

It is worth noticing in this connection that the same oxidation technique seems not to be applicable to γ, γ-dialkoxyacetylenic carbinol, because 4,4-diethoxy-2-butyn-1-ol (XIII)[1,3] was recovered unchanged on treatment with active manganese dioxide under more vigorous conditions than that generally adopted[2,4,5].

Treatment of 4-tetrahydropyran-2′-yloxy-2-butyn-1-al (VIIIc) with the Brady reagent afforded in an excellent yield 2,4-dinitrophenylhydrazones of 5-hydroxypentanal (XII) and that of 4-hydroxy-2-butyn-1-al (I), while the latter was also obtained in a good yield by similar treatment of 4,4-diethoxy-2-butyn-1-ol (XIII). This means that VIIIc is readily hydrolyzed and quantitatively affords the above two aldehydes, namely XII and I.

The condensation between each of the aldehydes (VIIIa, VIIIb, VIIIc, XIa and XIb) and 2,3-dimethyl-1,3-butadiene under the conditions as listed in Table III essentially afforded only a sole adduct. Some chemical evidences, which will be described in the following paper, of the adducts and the ultraviolet absorption data of their semicarbazones listed in Table IV demonstrate that they all have normal structures as expected.

On the Diels-Alder reaction involving α, β-acetylenic carbonyl compound, only a few examples which have resulted in the formation of an inhomogeneous product owing to the migration of the double bonds or the partial aromaticization have been reported[6,7]. It

2) J. Attenburrow, A. F. B. Cameron, I. H. Chapman R. M. Evans, B. A. Hem, A. B. A. Jansen and T. Walker, *J. Chem. Soc.*, **1952**, 1094.

3) R. G. Jones and M. G. Main, *J. Am. Chem. Soc.*, **75**, 4048 (1953).

4) M. Harfenist and A. Bavley, *J. Org. Chem.*, **19**, 1608 (1954).

5) B. C. L. Weedon et al., *J. Chem. Soc.*, **1953**, 1578, 3286.

6) J. C. Lunt and F. Sondheimer, ibid., **1950**, 3361.

7) E. A. Braude, E. R. H. Jones, F. Sondheimer and J. B. Toogood, ibid., **1949**, 607.

TABLE IV. SOLID DERIVATIVES OF THE DIELS-ALDER ADDUCTS

Adduct		2,4-Dinitrophenylhydrazone				Semicarbazone				
Number	R	Appearance	M. p. °C	Molecular formula	Analysis, % Found Calcd. N	Appearance	M. p. °C	λ_{max}^{EtOH} mμ (ε)	Molecular formula	Analysis, % Found Calcd. N
XIVa	$-OCH_3$	Red-orange needles	203～204	$C_{17}H_{20}O_5N_4$	15.93 15.55	Needles	218.5～219.5 (decomp.)	272.5 (23400)	$C_{12}H_{19}O_2N_3$	17.89 17.71
						Prisms	175～177	273 (28100)	$C_{15}H_{23}O_2N_3$	13.55 13.41
XIVb	$O-CH_2Ph$	Red-orange needles	203	$C_{23}H_{24}O_5N_4$	12.86 12.84	Needles	179～180[b]	237 (11700) 284 (32900)	$C_{24}H_{27}O_2N_3$	11.07 10.79
XIVc		Dark-red needles	209～210[a]	$C_{21}H_{26}O_6N_4$	13.60 13.02	Needles	187～188	272 (28300)	$C_{16}H_{25}O_3N_3$	13.50 13.67
XVa	$-OCH_3$	Yellow needles	159～160	$C_{17}H_{22}O_5N_4$	15.54 15.46	Needles	152～153[c]	232.5 (12400) 269 (33700)	$C_{12}H_{21}ON_3S$	16.40 16.46
XVb	$O-CH_2Ph$	Yellow needles	134.5～135	$C_{23}H_{26}O_5N_4$	12.41 12.78	Plates	143[b]	248 (27100)	$C_{24}H_{29}O_2N_3$	10.64 10.73
XVI	$-H$	Bright yellow needles	193～194	$C_{16}H_{20}O_4N_4$	16.64 16.86					

a) Found: C, 58.38; H, 6.02. Calcd. C, 58.59; H, 6.09%; $\lambda_{max}^{CHCl_3}$ 234 mμ (ε 25300), 259 (15100), 378 (31400)
b) Phenylsemicarbazone
c) Thiosemicarbazone, Ref. 1, m.p. 152°C

should be noted, therefore, that when the condensation between VIIIc and 2, 3-dimethyl-1, 3-butadiene was carried out at 140°C the expected adduct (XIVc) was obtained in only 24% yield and the principal product was colorless crystals, m.p. 60°C, formulated as $C_{10}H_{12}O$, which could also be obtained in 34% yield by heating XIVc with *p*-toluenesulfonic acid in tetrahydrofuran. This crystalline product has a strong menthol-like odor and becomes gradually a dark-brown resinous matter on exposure to air and light. By considering the fact that its properties and the infrared spectrum closely resemble those of phthalane[8] the authors estimated its structure as 5, 6-dimethyl-1, 3-dihydroisobenzofuran (XVII). The nuclear magnetic resonance spectrum[9] of this compound, obtained at 56.4 mc., was in complete accord with the structure XVII. The spectrum of XVII displayed three singlet peaks at −2.53, 1.55 and 2.84 p.p.m. whose area varied in a ratio of approximately 1 : 2 : 3, respectively. The resonance of −2.53 p.p.m. can be assigned to the aromatic hydrogens, while that of 2.84 p.p.m. is definitely associated with the hydrogens of methyl groups. The methylene groups linked with oxygen atom satisfactorily were accounted for by the peak of 1.55 p.p.m.

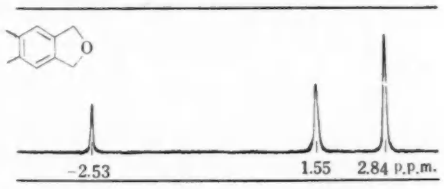

Fig. 1. NMR spectrum of 5,6-dimethyl-1,3-dihydroisobenzofuran.

II. Synthesis of 2-Methylene-4, 5-dimethylcyclohexylmethanol and Related Compounds

In this paper the authors wish to describe the preliminary work which has been carried out in the course of study for the preparation of an analogue of γ-cyclogeraniol and related compounds by employing the Diels-Alder adducts reported in the preceding paper.

An attempt was made at first to synthesize 4-(2′-methylene-4, 5-dimethyl-4′-cyclohexenyl)-but-3-en-2-one by employing 3, 4-dimethyl-6-methoxymethyl-3-cyclohexenylmethanal (XVa) as the starting substance. Condensation of XVa with acetone in the presence of barium hydroxide afforded in 69% yield 4-(3′, 4′-dimethyl-6′-methoxymethyl-3′-cyclohexenyl) -but-3-en-2-one (XVIII) which on heating with hydrogen bromide at 130°C gave a crude oil, from which a considerable amount of only one orange 2, 4 dinitrophenylhydrazone was obtained. Since the infrared spectrum of the hydrazone did not exhibit a characteristic absorption band of exocyclic methylene group, its parent aldehyde was considered to be a triply unsaturated ketone as represented by XIX which resulted from XVIII after elimination of methyl alcohol. Consequently the use of such a methoxymethyl compound as XVIII for the preparation of γ-ionone analogue was regarded as being practically unsuitable.

In order to hydrogenate a double bond in the ring of XVa a carbonyl group was once protected as the acetal. By the method of Salmi[10] XVa was converted into the corresponding ethylendioxy compound XX in 79% yield, which was hydrogenated over a palladium-charcoal catalyst in ethanol to give the saturated acetal XXI. The XXI was readily hydrolyzed, when heated under reflux in tetrahydrofuran with 2 N aqueous sulfuric acid, to yield the free aldehyde XXII which was condensed with acetone in the usual method giving 4-(4′, 5′-dimethyl-2′-methoxymethylcyclohexyl)-but-3-en-2-one (XXIII).

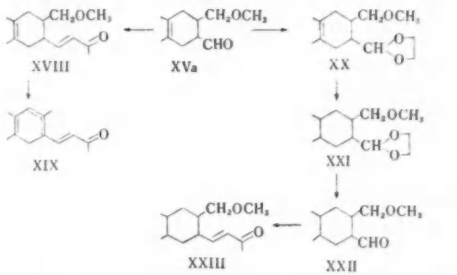

Since the conversion of a side methoxymethyl group into an exocyclic methylene had failed, a formyl group that is another functional group of such an adduct as XVa was investigated for the same purpose by employing 3, 4, 6-trimethyl-3-cyclohexenylmethanal (XVI) as a simple model.

In an autoclave XVI was hydrogenated in the presence of Raney nickel catalyst and anhydrous dimethylamine to afford in 80% yield *N*, *N*-dimethyl-2, 4, 5-trimethylcyclohexylmethylamine (XXV), together with an appreciable amount of 2, 4, 5-trimethylcyclohexylmethanol (XXIV). Though it is well known[11]

8) J. Entel, C. H. Ruof and H. C. Howard, *J. Am. Chem. Soc.*, 74, 441 (1952).

9) The NMR spectra were determined on a Varian Associates V-4300C high resolution NMR spectrometer with ca. 10% solution in CCl_4 with water as an external reference standard.

10) E. I. Salmi, *Ber.*, 71, 1803 (1938).

11) W. S. Emerson, "Organic Reactions", Vol. IV, (1948), pp. 174—255.

that primary and secondary amines are generally converted into tertiary amines by reductive condensation with various carbonyl compounds, no case with alicyclic aldehyde has been reported until the above preparation was completed[12].

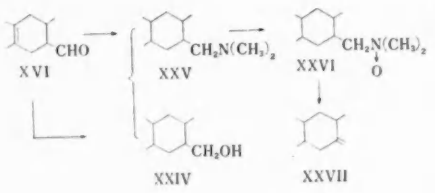

Oxidation of the tertiary amine XXV with 30% aqueous hydrogen peroxide gave in 82% yield an amine oxide XXVI as a colorless syrup which was characterized as crystalline picrate. The amine oxide XXVI was pyrolyzed in the manner described by Cope and his co-workers[13]. The decomposition proceeded smoothly at 120 ~130°/2.5 mmHg under nitrogen, and gave in yield of 61% based on XXV, a colorless mobile liquid, $C_{10}H_{18}$, which showed b.p. 59~59.2°/16.2 mmHg, n_D^{20} 1.4601 and was proved to be homogeneous by vapor phase chromatography. From the infrared absorption bands at 3077, 1648 and 885 cm^{-1} indicative of exocyclic methylene group, 1-methylene-2, 4, 5-trimethylcyclohexane (XXVII) was assigned for the hydrocarbon. The above result demonstrates that the thermal decomposition of XXVI gave exclusively the expected unsaturated hydrocarbon and also provided a further example in support of the specific formation of methylene cycloalkanes previously reported by Cope and his co-investigator[14,15].

Since three of the new Diels-Alder adducts —XIVb, XIVc and XVb— have all a functional group readily convertible to a hydroxyl group, an attempt was made to prepare from them 2-methylene-4, 5-dimethylcyclohexylmethanol (XXXVIII) which can be regarded as an analogue of γ-cyclogeraniol.

In order to isolate XIVb of high purity the phenylsemicarbazone obtainable in yield of 96% from the original adduct was hydrolyzed on steam distillation in the presence of concentrated sulfuric acid and *o*-phthalic acid, whereas 2, 4, 5-trimethylbenzaldehyde (XXVIII), m. p. 43°C (lit.[16] m. p. 42°C), was obtained in 60% yield with benzyl alcohol. The compound XXVIII was also formed in 20% yield by heating XIVb under reflux in xylene with a catalytic amount of *p*-toluenesulfonic acid, and it was characterized as the semicarbazone and 2, 4-dinitrophenylhydrazone, both of which were identical with those of an authentic sample prepared by the sulfur dehydrogenation of 3, 4, 6-trimethyl-3-cyclohexenylmethanal (XVI). On condensation with acetone, the aldehyde XXVIII afforded 4-(2′, 4′, 5′-trimethylphenyl)-but-3-en-2-one (XXIX) which showed m. p. 49.5°C (semicarbazone, m. p. 223~224°C; 2, 4-dinitrophenylhydrazone, m. p. 247~249°C).

An attempted acid-catalyzed reaction of XIVb with ethylene glycol following the method of Salmi[10] gave in only 33.5% yield an acetal which was probably XXX[17], while a considerable amount of XXVIII was yielded from

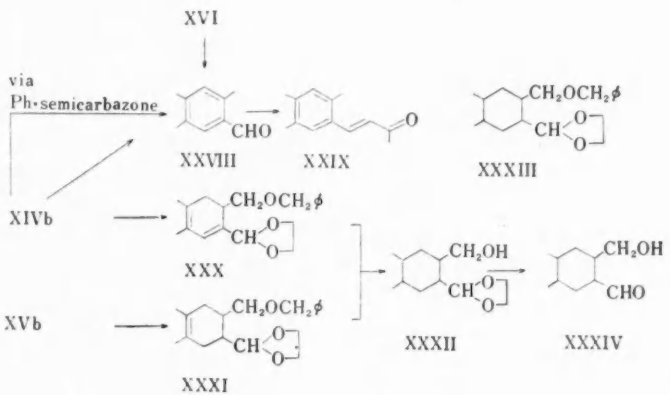

12) The 12th Annual Meeting of the Chemical Society of Japan, Kyoto, April, 1959.
13) A. C. Cope, R. A. Pike and C. F. Spencer, *J. Am. Chem. Soc.*, 75, 3212 (1953).
14) A. C. Cope, C. L. Bumgardner and E. E. Schweizer, ibid., 79, 4729 (1957).
15) A. C. Cope, E. Ciganek, C. F. Howell and E. E. Schweizer, ibid., 82, 4663 (1960).
16) L. Gattermann, *Ann.*, 347, 347 (1906).
17) Such migration of double bonds in the presence of acid will be discussed in the following paper, Part III.

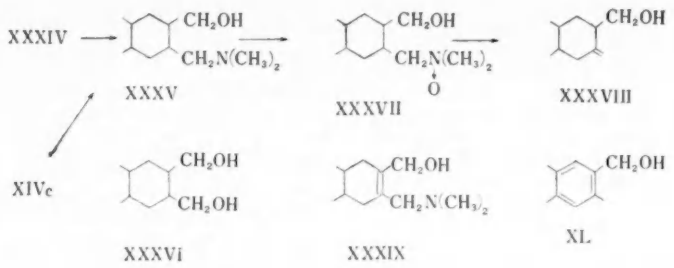

the elimination of benzyl alcohol. However, 6-benzyloxymethyl-3,4-dimethyl-3-cyclohexenylmethanal (XVb) could be converted into the corresponding acetal XXXI in a good yield without the elimination of benzyl alcohol.

XXX as well as XXXI usually afforded XXXII on hydrogenation over a palladium-charcoal catalyst; however, they occasionally afforded an appreciable amount of 2-benzyloxymethyl-4, 5-dimethylcyclohexylmethanal ethylene acetal (XXXIII), when hydrogenated with a catalyst prepared from less active charcoal. This result suggests that the hydrogenation of double bonds proceeded more rapidly than the hydrogenolysis of the benzyloxy group. On hydrolysis with diluted aqueous sulfuric acid in tetrahydrofuran the acetal XXXII was readily converted into the hydroxy aldehyde XXXIV.

On catalytic hydrogenation with dimethylamine over Raney nickel catalyst, XXXIV afforded in 60% yield *N, N*-dimethyl-4, 5-dimethyl-2-hydroxymethylcyclohexylmethylamine (XXXV) and simultaneously a considerable amount of 1, 2-bishydroxymethyl-4, 5-dimethylcyclohexane (XXXVI), m. p. 113~115°C. XXXV was successively oxidized with 30% hydrogen peroxide in the usual method to the *N*-oxide XXXVII, which was decomposed at 120~130°C to exclusively yield 2-methylene-4, 5-dimethylcyclohexylmethanol (XXXVIII), b. p. 94~97°C/17.5 mmHg, n_D^{27} 1.4729, as shown by its infrared absorption bands at 3058, 1642 and 884 cm^{-1}.

In another attempt to prepare the hydroxy amine XXXV directly from XIVc by similar reductive alkylation of dimethylamine with the aldehyde XXXIV as described above, XXXV was obtained in yield of 43.5% and it was usually contaminated with a base which was assumed from the methiodide to be the unsaturated aminoalcohol XXXIX. In this reduction a neutral compound, $C_{10}H_{14}O$, which shows m.p. 84.5°C; λ_{max}^{EtOH} 217 mμ (ε 175), 267 (338) and 274 (322), was also isolated in 32% yield. The infrared spectrum exhibited the presence of hydroxyl group (~3360, 1038) as well as of 1, 2, 4, 5-tetra-substituted aromatic group (879 cm^{-1}), and clearly suggested that this compound was to be 2, 4, 5-trimethylbenzyl alcohol (XL) which had been reported elsewhere to show m. p. 168°C[18]. The NMR spectrum provided an independent confirmation of its structure. The spectrum[9] consisted of five peaks at −2.23, −2.10, 0.30, 2.25 and 2.50 p. p. m. the chemical shifts of which permit the unequivocal assignment. The two non-equivalent hydrogens on the ring are accounted for by the peaks of −2.23 and −2.10 p. p. m. The three methyl groups were found at 2.50 p. p. m. as a singlet peak, while the methylene group with hydroxyl group was found at a lower magnetic field (0.30 p. p. m.). The resonance at 2.25 p. p. m. can be assigned to the proton of hydroxyl group.

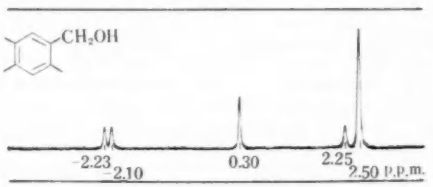

Fig. 2. NMR spectrum of 2,4,5-trimethylbenzyl alcohol.

Experimental[19]

4-Methoxy-2-butyn-1-ol (VIIa) and 4-Methoxy-2-buten-1-ol (Xa).—These compounds were prepared by the method of Ichikizaki et al[1]. 4-Methoxy-2-butyn-1-ol (VIIa), b. p. 105.5~106°C/20.5 mmHg, n_D^{20} 1.4595, was obtained in 43% yield. In addition to VIIa, 1, 4-dimethoxy-2-butyne (IXa), b.p. 63~65°C/20 mmHg, was obtained in 9% yield as a by-product. 4-Methoxy-2-buten-1-ol (Xa), b.p. 88~89°C/20 mmHg, n_D^{12} 1.4490, was obtained by hydrogenation of VIIa with a palladium-calcium carbonate catalyst (5% Pd) in 89% yield.

18) W. J. Hickinbottom, "Chemistry of Carbon Compounds", Vol. III-A, Ed. by E. H. Rodd, Elsevier Pub. Co. (1954), p 499.

19) All melting points were determined on the Kofler block and are uncorrected. The ultraviolet spectra were determined with a Hitachi EPU-2A spectrophotometer and the infrared spectra were obtained with a Perkin-Elmer model 112, a Kôken model DS-301, and a Nippon Bunkô model IR-S recording spectrophotometers with sodium chloride optics.

4-Benzyloxy-2-butyn-1-ol (VIIb). — 2-Butyne-1, 4-diol (VI) (200 g.) was added portionwise to a solution of sodamide (prepared from 35 g. of sodium) in liquid ammonia (1 l.) under vigorous stirring at −45∼−50°C over a period of 10 min. After being stirred for additional 2 hr. under cooling, the reaction mixture was diluted with xylene (800 ml.) and then set aside overnight to evaporate ammonia. The residual suspension was heated gradually to 100°C under stirring to remove the remaining ammonia as completely as possible. To it benzyl chloride (200 g.) was added dropwise over a period of 30 min. under vigorous stirring at 110∼115°C and the mixture was stirred for an additional hour. After being cooled, the reaction mixture was poured into cold water (500 ml.) and the xylene layer separated was washed with 10% sulfuric acid and water and dried over sodium sulfate. Distillation gave two fractions, 198 g. (69.2%), b. p. 142∼147°C/4 mmHg and 9 g., b. p. 170∼175°C/2 mmHg. Upon redistillation the lower boiling fraction afforded pure 4-benzyloxy-2-butyn-1-ol (VIIb), b. p. 143∼146°C/2.5 mmHg, n_D^{25} 1.5379.

Found: C, 73.76; H, 7.07. Calcd. for $C_{11}H_{12}O_2$: C, 74.97; H, 6.86%.

Upon redistillation the higher boiling fraction afforded pure 1, 4-dibenzyloxy-2-butyne (IXb), b. p. 169∼170°/1.5 mmHg, $n_D^{13.5}$ 1.5590.

Found: C, 81.20; H, 6.71. Calcd. for $C_{18}H_{18}O_2$: C, 81.17; H, 6.81%.

4-Benzyloxy-2-buten-1-ol (Xb).—A solution of 4-benzyloxy-2-butyn-1-ol (VIIb) (100 g.) in ethyl acetate (140 ml.) was hydrogenated with a palladium-barium carbonate catalyst (2.5% Pd, 1.5 g.) at 22°C until 14515 ml. of hydrogen (1.05 equiv.) had been absorbed. After removal of the catalyst and solvent the residue was distilled to afford 4-benzyloxy-2-buten-1-ol (Xb) (83 g., 82%), b. p. 125∼127.5°C/2 mmHg, n_D^{25} 1.5267.

Found: C, 74.08; H, 7.88. Calcd. for $C_{11}H_{14}O_2$: C, 74.13; H, 7.92%.

1, 4-Bistetrahydropyran-2′-yloxy-2-butyne (IXc). —A solution of dihydropyran (18.5 g., 0.22 mol.) in tetrahydrofuran (20 ml.) was added dropwise to a solution of VI (8.6 g., 0.1 mol.) in tetrahydrofuran (20 ml.) containing 2 drops of concentrated hydrochloric acid with stirring at 60°C over a period of 30 min. and the resulting mixture was gently refluxed for additional 3 hr. After being cooled, the reaction mixture was made alkaline with a cold 5% aqueuos sodium carbonate solution and extracted with three 80 ml. portions of ether. The combined extracts were washed 4 times with a saturated aqueous sodium chloride solution, dried over potassium carbonate and evaporated. Distillation of the residue under nitrogen gave the bis-ether IXc (17 g., 67%), b. p. 144∼146°C/1.0 mmHg, n_D^{16} 1.4913; ν_{max}^{film} 2226 (C≡C), 1186, 1120, 1081, 1056, 1022, 973, 946, 905 and 872 cm^{-1} (C–O–C–O).

Found: C, 65.66; H, 8.70. Calcd. for $C_{14}H_{22}O_4$: C, 66.11; H, 8.72%.

4-Tetrahydropyran-2′-yloxy-2-butyn-1-ol (VIIc). —A solution of the bis-ether IXc (25.4 g., 0.1 mol.) in tetrahydrofuran (10 ml.) was added dropwise to a solution of VI (8.6 g., 0.1 mol.) in tetrahydrofuran (30 ml.) containing 3 drops of concentrated hydrochloric acid under gentle reflux and then boiled for 3 hr. The resultant reaction mixture was worked up as described in the preceding section to leave a pale yellow oil which was distilled through a 8 cm. Vigreux column to yield VIIc (23.0 g., 68%), b. p. 122∼124°C/0.8 mmHg, n_D^{19} 1.4913; ν_{max}^{film} 3470∼3450 (OH) and 2220 cm^{-1} (C≡C). The characteristic absorption bands in its finger-print region were almost superimposable on those of the bis-ether IXc.

Found: C, 63.27; H, 8.46. Calcd. for $C_{11}H_{14}O_3$: C, 63.51; H, 8.29%

Upon treatment with the Brady reagent, this compound yielded 2, 4-dinitrophenylhydrazone of 5-hydroxypentanal which was crystallized from aqueous methanol and showed m. p. 115°C, undepressed on admixture with the authentic sample.

4, 4-Diethoxy-2-butyn-1-ol (XIII).—This compound was obtained in 57.7% by the method of Ichikizaki et al.[1], and had b. p. 118∼119°C/3 mmHg and n_D^{26} 1.4335 (lit.[1] b. p. 88°C/0.5 mmHg, n_D^{25} 1.4493).

The 2, 4-dinitrophenylhydrazone crystallized from 50% methanol in yellow needles, m. p. 120∼120.5°C (lit.[1] m. p. 119°C).

Found: N, 21.13. Calcd. for $C_{10}H_{9}O_5N_4$: N, 21.21%.

General Procedure for Oxidation of Carbinols (VII and X) with Manganese Dioxide.—A solution of the carbinol (5 g.) obtained above in benzene (5 ml.) was added dropwise to a suspension of manganese dioxide (50 g.) prepared by the method of Attenburrow et al.[2] in the same solvent (350 ml.) over a period of 5∼15 min. under vigorous stirring at room temperature and the resultant mixture was stirred for additional 3∼5 hr. During this period the initial temperature increased 10∼12°C. The reaction mixture was filtered and the precipitate was washed with petroleum ether. The washing was combined with the filtrate and evaporated in a nitrogen atmosphere under reduced pressure. Fractionation of the residue afforded the desired aldehydes whose properties and elemental analyses are listed in Table I. The solid derivatives prepared from these aldehydes are summarized in Table II.

Attempted Oxidation of 4, 4-Diethoxy-2-butyn-1-ol (XIII) with Manganese Dioxide. — XIII was treated with manganese dioxide according to the general procedure described above. Distillation afforded a trace of fore-run and unchanged starting material (76%). Although XIII was treated with a large excess of the oxidizing agent in boiling benzene for 10 hr., the unchanged starting material was recovered (78%), and the desired aldehyde could not be obtained.

Reaction of 4-Tetrahydropyran-2′-yloxy-2-butyn-1-al (VIIIc) with the Brady Reagent.—VIIIc was treated with the Brady reagent in the usual manner giving a mixture of two 2,4-dinitrophenylhydrazones. Recrystallization from aqueous methanol yielded 2, 4-dinitrophenylhydrazone of 4-hydroxy-2-butyn-1-al in yellow needles, m. p. 120∼120.5°C, undepressed on admixture with a sample prepared from XIII.

On addition of water the mother liquor afforded

2, 4-dinitrophenylhydrazone of 5-hydroxypentanal in orange-yellow leaflets, m. p. 115°C, undepressed on admixture with the authentic sample prepared as described below.

5-Hydroxypentanal (XII).—This compound was prepared in 65% yield by the method of Schniepp et al.[20] and showed b. p. 61~61.5°C/5 mmHg and n_D^{17} 1.4510 (lit. b. p.5 4~55°C/3 mmHg, n_D^{25} 1.4514[20]; b. p. 80°C/12 mmHg, n_D^{20} 1.4510[21]).

The 2, 4-dinitrophenylhydrazone crystallized from 50% methanol in orange-yellow leaflets, m. p. 115~116°C (lit. m. p. 109°C[22]; m. p. 107~109°C[23]).

Found: N, 20.19. Calcd. for $C_{11}H_{14}O_5N_4$: N, 19.85%.

General Procedure for Diels-Alder Addition of 2, 3-Dimethyl-1, 3-butadiene to γ-Alkoxytetrolaldehydes VIII and γ-Alkoxycrotonaldehydes XI.—A solution of freshly distilled aldehyde (1 equiv.), 2, 3-dimethyl-1, 3-butadiene (1.05 equiv.) and a trace of quinol in an appropriate solvent was taken in a 50~100 ml. glass bomb and was heated under nitrogen in an oil bath under the conditions described in Table III. After removal of the solvent the residue was distilled under reduced pressure to afford a crude product which was purified by redistillation through a short Vigreux column to give a pure adduct.

Some physical properties and sold derivatives of the adducts thus obtained are summarized in Tables III and IV.

Phenylsemicarbazone of 2-Benzyloxymethyl-4, 5-dimethylcyclohexa-1, 4-dienylmethanal (XIVb).—A solution of the aldehyde XIVb (4.0 g.) in ethanol (20 ml.) and phenylsemicarbazide (3.8 g.) in the same solvent (12 ml.) were refluxed for 5 min. The cooled reaction mixture was diluted with water and allowed to stand overnight at room temperature. A white precipitate which had been separated was collected and crystallized from ethanol-ethyl acetate to afford phenylsemicarbazone of XIVb (5.8 g., 96%) in needles, m. p. 179~180°C.

The elemental analysis and the ultraviolet absorption data are listed in Table IV.

5, 6-Dimethyl-1, 3-dihydroisobenzofuran (XVII).—*a) From 4-Tetrahydropyran-2'-yloxy-2-butyn-1-al (VIIIc) and 2, 3-Dimethyl-1, 3-butadiene.*—A solution of the aldehyde VIIIc (3.06 g.) in benzene (10 ml.) was treated with 2, 3-dimethyl-1, 3-butadiene (1.8 g.) in the presence of a trace of quinol at 140°C for 10 hr. by the general procedure described above. Distillation afforded two fractions: b. p. 90~110°/1.5 mmHg (1.5 g., 55.5%) and b. p. 133~135°C/0.55 mmHg (1.1 g., 24.1%).

The lower boiling fraction of colorless oil solidified immediately after distillation and crystallized from aqueous methanol in colorless fine plates which melted at 60°C and had a characteristic menthol-like odor. The infrared spectrum (KBr disk) showed absorption bands at 1606 (w), 1543 (m), 1495 (m), 1440 (s), 1418 (m), 1389 (s), 1320 (m), 1214 (m), 1127 (m), 1086 (m), 1028 (s), 890 (s) and 768 cm^{-1} (s), and also indicated the absence of the carbonyl group.

Found: C, 80.82; H, 8.40. Calcd. for $C_{10}H_{12}O$: C, 81.04; H, 8.16%.

Upon treatment with the Brady reagent this compound yielded red 2, 4-dinitrophenylhydrazone which crystallized from ethanol-ethyl acetate in red needles, m. p. 208~209°C.

Found: C, 55.11; H, 5.62; N, 15.74. Calcd. for $C_{16}H_{16}O_5N_4$: C, 55.48; H, 5.24; N, 16.18%.

An attempt to prepare the semicarbazone of this product in the usual manner was unsuccessful.

These evidences, therefore, strongly suggest that the lower boiling product is probably 5, 6-dimethyl-1, 3-dihydroisobenzofuran (XVII).

The higher boiling fraction of a pale yellow viscous oil was an expected adduct which was proved to be identical with XIVc (Tables III and IV) by mixed melting point determination of their 2, 4-dinitrophenylhydrazones and by infrared comparison.

b)—From 4, 5-Dimethyl-2-tetrahydropyran-2'-yloxymethylcyclohexa-1, 4-dienylmethanal (XIVc).—A solution of the aldehyde XIVc (0.5 g.) in tetrahydrofuran (20 ml.) was heated with *p*-toluenesulfonic acid (0.1 g.) under reflux for 3 hr. After removal of the solvent the residue was taken in ether and the ethereal solution was washed with a 2% aqueous sodium carbonate solution and water, dried and evaporated. Distillation of the residue afforded an oil which boiled at 130°C (bath temperature)/15 mmHg and solidified rapidly. Recrystallization from petroleum ether yielded colorless plates which melted at 60°C and proved to be identical with XVII obtained from a) by mixed melting point determination and infrared comparison.

The compound XVII was unstable and on exposure to air or light furnished a dark-brown resinous material.

3, 4-Dimethyl-6-methoxymethyl-3-cyclohexenylmethanal Ethylene Acetal (XX).—A mixture of the aldehyde XVa (6.6 g.), ethylene glycol (4.0 g.), *p*-toluenesulfonic acid (20 mg.) and benzene (30 ml.) was taken in a flask provided with an azeotropic water separator and heated under reflux in an oil bath (120~130°C) until no more aqueous phase has been separated from an azeotropic distillate (for ca. 4 hr.). The solvent was removed under reduced pressure and the residual brown oil was thoroughly extracted with ether. The combined ethereal extracts were washed with a 10% aqueous sodium carbonate solution and with water, dried over sodium sulfate and evaporated under reduced pressure. Distillation of the residue afforded the acetal XX (6.5 g., 79.3%) as a colorless liquid, b. p. 105~106°C/2.0 mmHg, n_D^{25} 1.4868.

Found: C, 68.90; H, 9.97. Calcd. for $C_{13}H_{22}O_3$: C, 68.99; H, 9.80%.

This compound afforded 2, 4-dinitrophenylhydrazone, m. p. 160°C, undepessed on admixture with that of XVa.

4, 5-Dimethyl-2-methoxymethylcyclohexylmethanal Ethylene Acetal (XXI).—The acetal XX (6.5 g.) in absolute ethanol (40 ml.) was hydrogenated in the presence of 5% palladium-on-charcoal (0.2 g.) at 100°C and a pressure of 120 kg./cm^2 for 2 hr.

20) L. E. Schniepp and H. H. Geller, *J. Am. Chem. Soc.*, **68**, 1646 (1946).
21) C. D. Hurd and W. H. Saunders Jr., ibid., **74**, 5326 (1952).
22) G. F. Woods and H. Sanders, ibid., **68**, 2111 (1946).
23) G. F. Woods and D. N. Kramer, ibid., **69**, 2246 (1947).

The catalyst was removed by filtration and the filtrate was evaporated under reduced pressure. Distillation of the residue yielded the saturated acetal XXI (5.0 g., 77%), b.p. 103~105°C/2.5 mmHg, n_D^{25} 1.4659.

Found: C, 68.44; H, 10.48. Calcd. for $C_{13}H_{24}O_3$: C, 68.38; H, 10.59%.

The 2, 4-dinitrophenylhydrazone crystallized from ethanol in yellow plates, m. p. 129~130°C.

Found: N, 15.40. Calcd. for $C_{17}H_{24}O_5N_4$: N, 15.38%.

4, 5-Dimethyl-2-methoxymethylcyclohexylmethanal (XXII).—A mixture of the acetal XXI (1.8 g.), tetrahydrofuran (30 ml.) and 2 N sulfuric acid (30 ml.) was heated under reflux for 24 hr. The cooled reaction mixture was made slightly alkaline with a 10% sodium carbonate solution, concentrated under reduced pressure and then extracted with ether. The ethereal extract was washed with water, dried and evaporated. Distillation of the residue afforded the aldehyde XXII (1.0 g., 69%), b.p. 93~95°C/1.0 mmHg, n_D^{17} 1.4710; ν_{max}^{liquid} 1730 cm^{-1} (C=O), $\nu_{max}^{CCl_4}$ 1725.2 cm^{-1} (C=O); λ_{max} 226 mμ (ε 499), 294 (59) in 75% aqueous dioxane.

Found: C, 71.58; H, 10.67. Calcd. for $C_{11}H_{20}O_2$: C, 71.69; H, 10.94%.

The 2, 4-dinitrophenylhydrazone showed m. p. 130°C, undepressed on admixture with that of XXI.

4-(3', 4'-Dimethyl-6'-methoxymethyl-3'-cyclohexenyl)-but-3-en-2-one (XVIII).—The aldehyde XVa (3.6 g.) was added dropwise to a boiling solution of barium hydroxide (0.7 g.) in 90% aqueous acetone (20 ml.) and the resultant mixture was refluxed for 7.5 hr. The cooled reaction mixture was neutralized with 1 N hydrochloric acid, concentrated under reduced pressure and then extracted with ether. The dried ethereal solution was fractionated to yield the unsaturated ketone XVIII (3.0 g., 68.5%), b. p. 122~123°C/3 mmHg, $n_D^{22.5}$ 1.5000; ν_{max}^{liquid} 1680 (C=O), 1624 (C=C), 1115 (C-O-C) and 983 cm^{-1} (trans-CH=CH-).

Found: C, 75.42; H, 10.10. Calcd. for $C_{14}H_{22}O_2$: C, 75.63; H, 9.97%.

The 2, 4-dinitrophenylhydrazone crystallized from ethanol in red prisms, m. p. 155~156°C.

Found: N, 14.05. Calcd. for $C_{20}H_{26}O_5N_4$: N, 13.92%.

4-(4', 5'-Dimethyl-2'-methoxymethylcyclohexyl)-but-3-en-2-one (XXIII).—The aldehyde XXII (1.7g.) was added dropwise to a boiling solution of barium hydroxide (0.3 g.) in 90% aqueous acetone (10 ml.) and the resultant mixture was refluxed for 10 hr., and was then treated in the same manner as that described above to yield the ketone XXIII (1.2 g., 58%), b. p. 120~122°C/2 mmHg, n_D^{32} 1.4781.

Found: C, 74.34; H, 10.65. Calcd. for $C_{14}H_{24}O_2$: C, 74.95; H, 10.78%.

The 2, 4-dinitrophenylhydrazone crystallized from ethanol in red-orange plates, m. p. 127~129°C.

Found: N, 14.06. Calcd. for $C_{20}H_{28}O_5N_4$: N, 13.85%.

Reaction of 4-(3', 4'-Dimethyl-6'-methoxymethyl-3'-cyclohexenyl)-but-3-en-2-one (XVIII) with Hydrobromic Acid.—A mixture of the unsaturated ketone XVIII (0.3 g.) and a constant boiling hydrobromic acid (b. p. 123°C, 12 ml.) was heated in a 50 ml. glass bomb at 130°C for 4 hr. The black tarry oil formed was poured into an ice-cooled 10% aqueous sodium carbonate solution and extracted with ether. The ethereal extract was washed, dried and evaporated. Distillation of the residue afforded a colorless oil (0.11 g.), b. p. 90~100°C/0.8 mmHg, $n_D^{24.5}$ 1.5241. This oily product gave a positive Beilstein test and a 2, 4-dinitrophenylhydrazone which contained no bromine atom and crystallized from ethanol in orange needles, m. p. 174~175°C.

Found: C, 61.15; H, 6.13. Calcd. for $C_{19}H_{22}O_4N_4$: C, 61.61; H, 5.99%.

Although the position of the double bonds on the ring could not be confirmed, the derivative obtained above was seen clearly to be 2, 4-dinitrophenylhydrazone of 4-(2', 4', 5'-trimethylcyclohexadienyl)-but-3-en-2-one, since elemental analysis was very satisfactory and the infrared spectrum exhibited no absorption band attributable to the exocyclic methylene group.

2, 4, 5-Trimethylcyclohexylmethanol (XXIV).—3, 4, 6-Trimethyl-3-cyclohexenylmethanal (XVI) (3.04 g.) in ethanol (30 ml.) was hydrogenated over a Raney nickel catalyst (1.5 g.) in a 100 ml. stainless-steel autoclave at 192°C and a pressure of 192 kg./cm² for 1 hr. The catalyst was removed by filtration and the filtrate was evaporated. Distillation of the residue afforded XXIV (2.9 g., 93%) as a colorless oil, b. p. 110°C/16 mmHg, n_D^{17} 1.4700.

Found: C, 76.62; H, 13.02. Calcd. for $C_{10}H_{20}O$: C, 76.86; H, 12.90%.

***N, N*-Dimethyl-2, 4, 5-trimethylcyclohexylmethylamine (XXV).**—A mixture of XVI (7.4 g.), anhydrous dimethylamine (2.9 g.), a Raney nickel catalyst (1.2 g.) and ethanol (50 ml.) was shaken with hydrogen at 180~220°C and a pressure of 121 kg./cm² for 4 hr., after which time a pressure of 58 kg./cm² of hydrogen was absorbed. The catalyst was removed by filtration and the filtrate was evaporated under reduced pressure. Distillation of the residue afforded a crude product (7.9 g.) b. p. 100~105°C/16 mmHg, n_D^{21} 1.4622~1.4658. This oil was taken up in ether and extracted with diluted hydrochloric acid. The aqueous extracts were combined, neutralized with aqueous sodium hydroxide and then extracted with ether. The dried ethereal solution was distilled under reduced pressure to yield a pure amine XXV (6.6 g., 80%), b. p. 98~99°C/15 mmHg, $n_D^{17.5}$ 1.4607.

Found: C, 78.77; H, 13.52. Calcd. for $C_{12}H_{25}N$: C, 78.61; H, 13.75%.

The methiodide crystallized from ethanol in leaflets, m. p. 262°C (decomp.).

Found: C, 48.19; H, 8.83; N, 4.18; I, 38.5. Calcd. for $C_{13}H_{28}NI$: C, 48.0; H, 8.6; N, 4.3; I, 39.0%.

The picrate was obtained as a yellow oil which could not be induced to crystallize.

The ethereal solution which had been shaken with acid was dried and then distilled under reduced pressure to yield a neutral compound (0.8 g., 10.8%), b. p. 114~116°C/17 mmHg, $n_D^{20.5}$ 1.4668. This compound was proved to be identical with

XXIV obtained above by comparison of their infrared spectra.

***N, N*-Dimethyl-2, 4, 5-trimethylcyclohexylmethylamine Oxide (XXVI).**—To a solution of the amine XXV (6.11 g., 1/30 mol.) in methanol (5 ml.) was added dropwise 30% aqueous hydrogen peroxide (13 g., 1/10 mol.) under vigorous stirring at 0°C and the resultant mixture was allowed to warm to room temperature. The mixture was stirred for 11.5 hr. and set aside overnight, after which time all of the reaction mixture was homogeneous. The excess of hydrogen peroxide was then decomposed with platinum foil (0.3 g.) under stirring for 35 hr. at room temperature. After removal of the platinum foil the solution was evaporated under reduced pressure (15~17 mmHg) at below 35°C to leave a syrupy residue which was taken up in absolute ethanol (10 ml.). The solution was evaporated through a 25 cm. Vigreux column under reduced pressure. This work-up was repeated 4 times to remove the last traces of water and afforded the amine oxide XXVI as a very viscous colorless liquid. The product thus obtained was used in the next preparation without further purification, since its practical purity was indicated by the determination of an amine oxide prepared in another run described below.

When an excess of picric acid in aqueous ethanol was mixed with an aqueous ethanolic solution of a crude amine oxide prepared from the amine XXV (0.46 g.) in the manner described above, there was obtained a picrate which crystallized from absolute ethanol in yellow plates, m. p. 165~166.5°C. The yield was 0.82 g. (82%).

Found: C, 50.36; H, 6.80; N, 12.69. Calcd. for $C_{18}H_{29}O_8N_4$: C, 50.46; H, 6.59; N, 13.08%.

1-Methylene-2, 4, 5-trimethylcyclohexane (XXVII).—The amine oxide XXVI obtained above was taken in a 100 ml. flask fitted with a 15 cm. Vigreux column and heated to 110°C, at this temperature decomposition of the amine oxide occurred. After 30 min. the distillation became slower and the bath was heated to 180°C. The pyrolysis products, which distilled mainly at 120~130°C (bath temperature), were swept with nitrogen through a trap cooled with a freezing mixture and then through a liquid nitrogen cooled trap. The products were combined and taken up in ether. The ethereal solution was washed twice with 10% hydrochloric acid and 3 times with water, dried over magnesium sulfate and then in the presence of a small amount of quinol concentrated under a 25 cm. Vigreux column at atmospheric pressure. The residue was distilled under nitrogen to yield the hydrocarbon XXVII (2.8 g., 61.0% based on XXV), b. p. 59~59.2°C/16.2 mmHg, n_D^{20} 1.4601. This hydrocarbon decolorized rapidly a dilute solution of bromine in carbon tetrachloride and readily consumed potassium permanganate in acetone solution. ν_{max}^{liquid} 3077, 1648, 885 (>C=CH$_2$); 1464, 1384 (-CH$_2$- and CH$_3$) and 1770 cm^{-1} (over-tone of δ CH).

Found: C, 87.12; H, 12.63. Calcd. for $C_{10}H_{18}$: C, 86.88; H, 13.12%.

The aqueous washings were combined and concentrated under reduced pressure to leave a crystalline residue, which was taken up in absolute ethanol. The solution was evaporated to dryness yielding a crude *N, N*-dimethylhydroxylamine hydrochloride (2.0 g., 61.5%), m. p. 103~105°C. A sample recrystallized from absolute ethanol in needles, m. p. 105~106.5°C (lit. m. p. 104.5~106.5°C[18] and m. p. 106.5~109°C[24]).

2-Benzyloxymethyl-4, 5-dimethylcyclohexa-4, 6-(or -1, 4-) dienylmethanal Ethylene Acetal (XXX).—A mixture of the aldehyde XIVb (47.2 g.), *p*-toluenesulfonic acid (0.05 g.), ethylene glycol (26.2 g.) and benzene (250 ml.) was taken in a flask provided with an azeotropic water separator and heated under reflux at 120°C for 4 hr. The water was drawn off from time to time. After the excess of benzene was removed under reduced pressure the residue was extracted with ether. The ethereal solution was washed with a 10% aqueous sodium carbonate solution and with water, dried over sodium sulfate and then evaporated. Distillation of the residue afforded a lower boiling fraction (5.8 g.), b. p. 52~80°C/0.001 mmHg, and an acetal XXX (18.5 g., 33.5%) as a pale yellow viscous oil, b. p. 144~148°C/0.001 mmHg, n_D^{26} 1.5429.

Found: C, 75.73; H, 8.21. Calcd. for $C_{19}H_{24}O_3$: C, 75.97; H, 8.05%.

The lower boiling fraction on treatment with the Brady reagent yielded a 2, 4-dinitrophenylhydrazone. Recrystallization from ethanol-ethyl acetate gave a pure sample, m. p. 226°C, undepressed on admixture with the 2, 4-dinitrophenylhydrazone of 2, 4, 5-trimethylbenzaldehyde.

6-Benzyloxymethyl-3, 4-dimethyl-3-cyclohexenylmethanal Ethylene Acetal (XXXI).—A mixture of the aldehyde XVb (8.3 g.), ethylene glycol (9.0 g.), *p*-toluenesulfonic acid (0.05 g.) and benzene (40 ml.) was refluxed at 130~135°C for 4 hr. The reaction mixture was worked up in the manner described above to yield the acetal XXXI (7.2 g., 74.2%), b. p. 150~155°C/0.017 mmHg.

Found: C, 73.98; H, 8.55. Calcd. for $C_{19}H_{28}O_3$: C, 75.46; 8.67%.

4, 5-Dimethyl-2-hydroxymethylcyclohexylmethanal Ethylene Acetal (XXXII).—*a) From XXX.*—The acetal XXX (16.5 g.) in ethanol (40 ml.) was hydrogenated over a 5% palladium-on-charcoal catalyst (1.0 g.) in a stainless-steel autoclave at 120°C and a pressure of 120 kg./cm^2 for 8 hr. The catalyst was filtered off and the filtrate was evaporated. Distillation of the residue afforded a saturated acetal XXXII (3.9 g., 33%) as a viscous oil, b. p. 112~120°C/1.3 mmHg, $n_D^{25.5}$ 1.4786.

Found: C, 66.90; H, 10.62. Calcd. for $C_{12}H_{22}O_3$: C, 67.25; H, 10.35%.

The 2, 4-dinitrophenylhydrazone crystallized from methanol-light petroleum in orange-yellow leaflets, m. p. 194~196°C.

Found: N, 16.19. Calcd. for $C_{16}H_{22}O_5N_4$: N, 15.99%.

Further distillation afforded a higher boiling viscous oil (6.7 g.), which boiled at 120~125°C/0.001 mmHg and was thought probably to be 2-benzyloxymethyl-4, 5-dimethylcyclohexylmethanal ethylene acetal (XXXIII), since it afforded readily

24) A. C. Cope, N. A. LeBel, H. H. Lee and W. R. Moore, ibid., 79, 4720 (1957).

XXXII on hydrogenolysis under the same conditions as those described above.

b) From XXXI.—The acetal XXXI (11.4 g.) in ethanol (50 ml.) was hydrogenated over 5% palladium-on-charcoal (1.0 g.) for 5 hr. in the manner described above to yield XXXII (6.2 g., 77.5%), b. p. 131~134°C/3.0 mmHg.

The 2, 4-dinitrophenylhydrazone prepared from this liquid showed m. p. 195~196°C, undepressed on admixture with a sample obtained in a).

The 3, 5-dinitrobenzoate crystallized from benzene-petroleum ether in plates, m. p. 110~111°C.

Found: C, 55.47; H, 5.96; N, 7.01. Calcd. for $C_{19}H_{24}O_8N_2$: C, 55.87; H, 5.92; N, 6.86%.

4,5-Dimethyl-2-hydroxymethylcyclohexylmethanal (XXXIV).—A mixture of the acetal XXXII (3.1 g.), tetrahydrofuran (16 ml.) and 2 N sulfuric acid (16 ml.) was refluxed for 2.5 hr. The cooled reaction mixture was neutralized with a 30% aqueous sodium carbonate solution and extracted with ether. The ethereal solution was washed with a saturated sodium chloride solution, dried over sodium sulfate and then evaporated. Distillation of the residue under nitrogen afforded the hydroxyaldehyde XXXIV (1.9 g., 77.3%), which boiled at 99~105°C/2.0 mmHg and solidified rapidly. Recrystallization from methanol-light petroleum yielded colorless plates, m. p. 84°C; ν_{max}^{KBr} 3333, 1724, 1456, 1124, 1087, 1047, 971, 899 and 877 cm^{-1}; λ_{max} 225 mμ (ε 37.3), 294 (29.1) in 75% aqueous dioxane.

Found: C, 70.81; H, 10.62. Calcd. for $C_{10}H_{19}O_2$: C, 70.54; H, 10.66%.

The 2, 4-dinitrophenylhydrazone crystallized from methanol in orange-yellow leaflets, m. p. 194~195°C, undepressed on admixture with that of XXXII.

***N*, *N*-Dimethyl-4,5-dimethyl-2-hydroxymethylcyclohexylmethylamine (XXXV).**—*a) From XXXIV.*—A mixture of the aldehyde XXXIV (1.2 g.), anhydrous dimethylamine (0.8 g.), Raney nickel catalyst (1.2 g.) and absolute ethanol (30 ml.) was shaken with hydrogen in a 100 ml. autoclave at 180~190°C and a pressure of 118 kg./cm² for 1.6 hr. The catalyst was filtered off and the solution was evaporated to leave an oil, which was taken up in ether and extracted twice with 2 N hydrochloric acid. The aqueous extracts were combined, made alkaline with a 10% sodium hydroxide solution and then extracted with ether. The dried ethereal solution on distillation afforded the aminoalcohol XXXV (0.8 g., 57%), b. p. 100~105°C/2.0 mmHg, $n_D^{19.5}$ 1.4666.

Found: C, 71.73; H, 12.40. Calcd. for $C_{12}H_{25}ON$: C, 72.30; H, 12.64%.

The methiodide crystallized from ethanol-ethyl acetate in prisms, m. p. 221°C.

Found: C, 45.40; H, 8.33. Calcd. for $C_{13}H_{28}ONI$: C, 45.87; H, 8.28%.

The ethereal solution which had been shaken with hydrochloric acid was distilled to yield an oil (0.15 g., 12%), which boiled at 115~121°C/2.0 mmHg and solidified on being set aside for a short time. Recrystallization from light petroleum afforded colorless plates, m. p. 113~115°C.

Found: C, 69.01; H, 11.23. Calcd. for $C_{10}H_{20}O_2$: C, 69.72; H, 11.70%.

This compound is thought probably to be 1, 2-bishydroxymethyl-4, 5-dimethylcyclohexane (XXXVI), since the elemental analysis is very satisfactory and the infrared spectrum exhibits strong absorption bands of the hydroxyl group at 3310 and 1045 cm^{-1} but no band attributable to an aldehyde group.

b) From XIVc.—A mixture of the aldehyde XIVc (2.9 g.), anhydrous dimethylamine (2.0 g.), Raney nickel (2.0 g.) and ethanol (40 ml.) was shaken with hydrogen at 200~220°C and a pressure of 197 kg./cm² for 3 hr. When the resultant reaction mixture was worked up as in the case of XXXIV, there were obtained a crude amino compound (1.2 g., 43.5%) and a neutral one (0.8 g., 31.6%).

The amino compound boiled at 80°C/0.55 mmHg, n_D^{15} 1.4755, and the infrared spectrum exhibited strong absorption bands of hydroxyl group at 3370 and 1066 cm^{-1} and characteristic bands attributable to the *tert*-amino group at 2838, 2800 and 2742 cm^{-1}.

Found: C, 72.53; H, 12.80; N, 7.10. Calcd. for $C_{12}H_{25}ON$: C, 72.30; H, 12.64; N, 7.03%.

The methiodide crystallized from methanol-ethyl acetate in leaflets, m. p. 221°C, undepressed on admixture with that of XXXV obtained in a).

From the crude methiodide, there was obtained a small amount of crystals which were slightly soluble in methanol-ethyl acetate. Recrystallization afforded a pure sample, m. p. 271~272°C.

Found: C, 46.30; H, 7.93. Calcd. for $C_{13}H_{26}ONI$: C, 46.00; H, 7.73%.

The elemental analysis indicates that the methiodide is probably that of *N*, *N*-dimethyl-4, 5-dimethyl-2-hydroxymethyl-1-cyclohexenylmethylamine (XXXIX).

The neutral product of colorless liquid obtained above boiled at 95~105°C/0.6 mmHg and solidified rapidly. Recrystallization from petroleum ether yielded 2,4, 5-trimethylbenzyl alcohol (XL) in needles, m. p. 84.5°C.

The infrared spectrum (KBr disk) exhibited strong absorption bands of hydroxyl group at 3360 and 1038 cm^{-1} and other principal bands at 1621 (w), 1513 (m), 1450 (s), 1078 (s), 1009 (s), 996 (s), 899 (m), 888 (m), and 877 cm^{-1} (s). λ_{max}^{EtOH} 217 mμ (ε 175), 265 (338) and 274 (322).

Found: C, 80.02; H, 9.51. Calcd. for $C_{10}H_{14}O$: C, 79.95; H, 9.39%.

***N*, *N*-Dimethyl-4, 5-dimethyl-2-hydroxymethylcyclohexylmethylamine Oxide (XXXVII).**—To a solution of the amine XXXV (0.6 g.) in methanol (3.6 ml.) was added 30% aqueous hydrogen peroxide (1.5 g.) and the resultant mixture was stirred at 30°C for 50 hr., after which time the reaction mixture gave no color with phenolphthalein. The excess of hydrogen peroxide was then decomposed with a small amount of platinum foil and the solution was worked up as in the case of XXVI to yield the amine oxide XXXVII (0.55 g., 84.6%) as a colorless glass, which was characterized as the picrate which could not be induced to crystallize. The product thus obtained was used in the next pyrolysis without further purification.

4, 5-Dimethyl-2-methylenecyclohexylmethanol (XXXVIII).—The amine oxide XXXVII (0.4 g.) obtained above was pyrolysed as in the case of XXVII to yield a neutral XXXVIII (0.12 g., 42%),

b. p. 94～97°C/17.5 mmHg, n_D^{22} 1.4729. The infrared spectrum (liquid film) exhibited absorption bands of hydroxyl group at 3385 and 1053 cm^{-1}, the bands attributable to exocyclic double bond at 3058, 1642 and 884 cm^{-1} and other principal bands at 1765, 1459 and 1384 cm^{-1}.

Found: C, 77.79; H, 11.85. Calcd. for $C_{10}H_{18}O$: C, 77.86; H, 11.76%.

2, 4, 5-Trimethylbenzaldehyde (XXVIII).—*a) By Sulfur Dehydrogenation of 3, 4, 6-Trimethyl-3-cyclohexenylmethanal (XVI).*—The aldehyde XVI (2.3 g.) was heated under reflux with sulfur (1.2 g.) at 220～230°C in an oil bath until the evolution of hydrogen sulfide ceased (for ca. 40 min.). The resultant yellowish dark-brown mixture was distilled to yield a yellow oil (0.45 g.), b. p. 128～130°C/18 mmHg, n_D^{20} 1.5591 (lit.[25] b. p. 55～60°C/5～10 mmHg).

The 2, 4-dinitrophenylhydrazone crystallized from ethanol-ethyl acetate in red needles, m. p. 223～224.5°C.

Found: C, 58.40; H, 5.07. Calcd. for $C_{16}H_{16}O_4N_4$: C, 58.53; 4.91%.

The semicarbazone crystallized from ethanol-ethyl acetate in needles, m. p. 239°C; λ_{max}^{EtOH} 226 mμ (ε 16500), 285 (23400),

Found: C, 64.36; H, 7.35. Calcd. for $C_{11}H_{15}ON_3$: C, 64.36; H, 7.37%.

b) By the Action of p-Toluenesulfonic Acid on 2-Benzyloxymethyl-4, 5-dimethylcyclohexa-1, 4-dienylmethanal (XIVb).—A mixture of the unsaturated aldehyde XIVb (1.0 g.), *p*-toluenesulfonic acid (0.3 g.) and xylene (10 ml.) was heated under reflux for 4 hr. The cooled reaction mixture was neutralized with a 10% aqueous sodium carbonate solution and extracted with ether. The ethereal solution was washed with water, dried over sodium sulfate and then evaporated. Distillation of the residue afforded a colorless oil (0.2 g., 35%), b. p. 80～90°C/0.6～0.8 mmHg.

The 2, 4-dinitrophenylhydrazone crystallized from ethanol-ethyl acetate in bright red prisms, m. p. 225～226.5°C, undepressed on admixture with that of XXVIII obtained in a).

c) By Hydrolysis of Phenylsemicarbazone of 2-Benzyloxymethyl-4, 5-dimethylcyclohexa-1, 4-dienyl methanal (XIVb).—Steam distillation of the phenylsemicarbazone (4.5 g.) of XIVb from a mixture of *o*-phthalic acid (4.5 g.), ethylene glycol (40 ml.), concentrated sulfuric acid (14.0 g.) and water (40 ml.) afforded benzyl alcohol (0.3 g.) and the aldehyde XXVIII (1.3 g., 60%) as a colorless liquid after the usual workup. The regenerated aldehyde was distilled to yield a pure compound, which boiled at 87°C/1.0 mmHg and was crystallized upon treatment with petroleum ether. Recrystallization from methanol-petroleum ether afforded colorless plates, m. p. 43°C (lit.[16] m. p. 42°C); λ_{max}^{EtOH} 215 mμ (ε 22400), 261 (14700), 298 (2400). The infrared spectrum (KBr disk) exhibited a strong absorption band of carbonyl group at 1686 cm^{-1}, and other principal bands at 3000 (m, sh), 2934 (m), 2856 (m), 2742(m), 1608 (s), 1551 (s), 1501 (m), 1454 (s), 1386 (m), 1255 (m), 1187 (s), 1082 (m), 887 (m) and 775 cm^{-1} (s).

Found: C, 80.95; H, 8.21. Calcd. for $C_{10}H_{12}O$: C, 81.04; H, 8.16%.

The 2, 4-dinitrophenylhydrazone crystallized from ethyl acetate in bright red needles, m. p. 226～227°C.

The semicarbazone crystallized from chloroform-ethyl acetate in fine needles, m. p. 239～240°C.

The melting points of mixtures of the above derivatives with samples obtained in a) showed no depression.

4-(2', 4', 5'-Trimethylphenyl)-but-3-en-2-one (XXIX).—A solution of the aldehyde XXVIII (0.4 g.) obtained in c) in acetone (5 ml.) was added dropwise to a boiling mixture of barium hydroxide (0.2 g.), acetone (8 ml.) and water (2 ml.) and the resulting mixture was heated under reflux for 18.5 hr. The cooled reaction mixture was acidified with 1 N hydrochloric acid, concentrated under reduced pressure and then extracted with ether. The ethereal extracts were combined, washed and dried. Distillation of the residue afforded a colorless oil (0.2 g., 40%), which boiled at 120～140°C (bath temperature)/3.0 mmHg and solidified on standing. Recrystallization from petroleum ether yielded XXIX in colorless prisms, m. p. 49.5～50°C (lit.[26] m. p. 51°C); λ_{max}^{EtOH} 216.5 mμ (ε 12600), 233 (10700), 305 (21900); ν_{max}^{KBr} 1683 (conjugated C=O), 1660 (conjugated C=C), 978 (trans -CH=CH-) and 869 cm^{-1}.

The 2, 4-dinitrophenylhydrazone crystallized from methanol-chloroform in dark-red needles, m. p. 247～249°C.

Found: N, 15.29. Calcd. for $C_{19}H_{20}O_4N_4$: N, 15.21%.

The semicarbazone crystallized from ethanol-ethyl acetate in leaflets, m. p. 223～224°C; λ_{max}^{EtOH} 237 mμ (ε 18600), 307 (42600).

Found: N, 17.20. Calcd. for $C_{14}H_{19}ON_3$: N, 17.13%.

We wish to thank Dr. Asaji Kondo of the Tokyo Institute of Technology for the microanalyses; Drs. Tadashi Sato of Waseda University and Kenji Kuratani of the Aeronautical Research Institute, the University of Tokyo, for the infrared spectra; and Dr. Ichiro Yamaguchi of the Japan Atomic Energy Research Institute for the nuclear magnetic resonance spectra.

Laboratory of Organic Chemistry
Kobayasi Institute of
Physical Research
Kokubunji, Tokyo

25) C. D. Shacklett and H. A. Smith, ibid., **75**, 2654 (1953).
26) W. John et al., *Z. Physiolo. Chem.*, **268**, 104 (1941).

Thermodynamical Studies on Binary Systems Consisting of Polar and Non-polar Liquids. IV. Estimation of the Electrostatic Part of the Excess Enthalpy from the Observed Values aud Comparison with the Calculated Values

By Kazuo AMAYA

(Received March 13, 1961)

In a previous paper[1], the author calculated the electrostatic part of the excess enthalpy of binary systems composed of polar and non-polar liquids according to Onsager's model. In this paper the observed values of these quantities have been derived under reasonable assumptions and are compared with the calculated values.

The Principle of the Estimation of the Electrostatic Part of the Excess Enthalpy from the Experimental Results

In order to derive the electrostatic part of the excess enthalpy due only to the permanent dipole of the polar molecule from the experimental result of the heat of mixing, the non-electrostatic part of the excess enthalpy must be estimated under reasonable assumptions and subtracted from the experimental value, since the observed excess enthalpy contains not only the electrostatic but also the non-electrostatic part.

As a first approximation, it may be assumed that the intermolecular interaction enery of polar molecules is the sum of the non-electrostatic part of the energy due to dispersion forces and the electrostatic one due to dipoles if higher multipoles are neglected.

From this assumption the cohesive energy for 1 mol. of pure polar liquid, ΔU_2, may be given by

$$\Delta U_2 = \Delta U_2^{el} + \Delta U_2^{n-el} \tag{1}$$

where ΔU_2^{el} and ΔU_2^{n-el} are the electrostatic and the non-electrostatic part of cohesive energy respectively.

Since the electrostatic intermolecular energy is absent in non-polar liquids, the cohesive energy for non-polar liquid ΔU_1 is given by the non-electrostatic intermolecular energy due to dispersion forces of non-polar molecules:

$$\Delta U_1 = \Delta U_1^{n-el} \tag{2}$$

Further, if the non-electrostatic part of the energy due to dispersion forces is assumed to be the sum of the energy due to dispersion forces of the nearest neighbor pairs, then for 1 mol. of polar liquid ΔU_2^{n-el} is given by

$$\Delta U_2^{n-el} = 1/2 \cdot N_A z \omega_{22} \tag{3}$$

and similarly for 1 mol. of non-polar liquid,

$$\Delta U_1^{n-el} = 1/2 \cdot N_A z \omega_{11} \tag{4}$$

where N_A is Avogadro's number, z is the number of the nearest neighbors and ω_{22} and ω_{11} are the non-electrostatic part of interaction energy due to dispersion forces of the nearest neighbor pairs of polar and non-polar molecules respectively.

When 1 mol. of the solution is formed from x_2 mole of polar liquid and $(1-x_2)$ mol. of non-polar liquid, both liquids being composed of molecules of similar size, the total energy of the system ΔU_{12} is given by

$$\Delta U_{12} = \frac{1}{2} x_2^2 N_A z \omega_{22} + x_2(1-x_2) N_A z \omega_{12} + \frac{1}{2}(1-x_2)^2 N_A z \omega_{11} + \Delta U_{12}^{el} \tag{5}$$

where ω_{12} is the non-electrostatic part of the nearest neighbor pair interaction energy of the pair consisting of polar and non-polar molecules and ΔU_{12}^{el} is the electrostatic part of the energy due to dipoles for 1 mol. of the solution. Thus the excess energy U^E is given by

$$U^E = x_2(1-x_2) N_A z \omega + \Delta U_{12}^{el} - x_2 \Delta U_2^{el} \tag{6}$$

where ω is the part of interchange energy due to dispersion forces given by

$$2\omega = 2\omega_{12} - \omega_{22} - \omega_{11} \tag{7}$$

In a similar way the electrostatic part of the excess energy due to dipole-dipole interaction as well as the non-electrostatic contribution due to dispersion forces may be expressed as a function of volume fraction v_2 of the polar liquid:

$$U^E = V\alpha^{n-el} v_2(1-v_2) + \Delta U_{12}^{el}(v_2) - v_2 \cdot \Delta U_2^{el} \tag{8}$$

where V is the volume of 1 mol. of the solution.

1) K. Amaya, This Bulletin, **34**, 1349 (1961).

TABLE I. VALUES OF $\alpha^{el}_{obs}(0)$, $\alpha^{el}_{obs}(1)$, $\Delta\alpha^{el}_{obs}$ AND $\alpha^{el}_{obs}(0)/\alpha^{el}_{obs}(1)$ FOR THE SYSTEMS IN WHICH NON-POLAR COMPONENTS ARE NON-AROMATIC

System	$\alpha^{el}_{obs}(0)$ joul./cc.	$\alpha^{el}_{obs}(1)$ joul./cc.	$\Delta\alpha^{el}_{obs}$ joul./cc.	$\alpha^{el}_{obs}(0)/\alpha^{el}_{obs}(1)$
Chlorobenzene—Cyclohexane	12.5	4.9	7.6	2.54
Bromobenzene—Cyclohexane	15.7	6.1	9.6	2.58
Benzonitrile—Cyclohexane	65.6	25.0	40.6	2.62
Nitrobenzene—Cyclohexane	75	37	38	2.03
Cyclohexanone—Cyclohexane	54.9	31.8	23.1	1.73
Diethylketone—Cyclohexane	54.4	28.9	25.5	1.89
Methylpropylketone—Cyclohexane	56.9	32.5	24.4	1.75
n-Butylchloride—Cyclohexane	21.8	11.2	10.6	1.95
n-Butylcyanide—Cyclohexane	59.2	33.9	25.3	1.75
Chlorocyclohexane—Methylcyclohexane	16.0	9.95	6.0$_5$	1.61
Bromocyclohexane—Methylcyclohexane	17.5	11.3	6.2	1.55
cis-Dichloroethylene—*trans*-Dichloroethylen	10.4	5.4	5.0	1.95
Pyridine—1,4-Dioxane	4.7	<1.9	>2.8	2.24

It may be assumed that α^{n-el}, the contribution of dispersion forces to the van Laar coefficient is constant over the whole concentration range, because the coefficients α for binary systems of non-polar liquids are nearly constant. In addition it is also assumed that there is no volume change on mixing. Then U^E is equal to H^E:

$$U^E = H^E = V\alpha^{n-el}v_2(1-v_2) + H^{E-el} \quad (9)$$

$$U^{E-el} = H^{E-el} = U^{E-el} - \Delta U_{12}{}^{el}(v_2) - v_2 \cdot \Delta U_2{}^{el} \quad (10)$$

Further, if the electrostatic part is expressed in the form

$$H^{E-el} = V\alpha^{el}v_2(1-v_2) \quad (11)$$

then

$$H^E = V(\alpha^{n-el} + \alpha^{el})v_2(1-v_2) \quad (12)$$

where α^{el} is the electrostatic contribution to α.

The Estimation of α^{n-el}, Non-electrostatic Part of α

The values of α^{el} can be obtained if the values of α^{n-el} are estimated under reasonable assumptions. And for estimating the non-electrostatic part of the heat of mixing, the following procedures are employed:

(1) The Systems of Cyclohexane—Aliphatic Polar Molecule. — For cyclohexane—*n*-hexane system the heat of mixing per mole of cyclohexane at the extreme dilution is about 573 joul./mol.[2] corresponding to the value of 5.3 joul./cc. for α. Since for non-polar liquid systems the values of α do not vary with concentration, it may be reasonable to use the above value over all the concentration range. Even for the binary systems of cyclohexane and polar aliphatic hydrocarbon derivatives, it may be permissible, as an approximation, to take the value of 5.3 joul./cc. non-electrostatic part of α, neglecting the difference for between CH_3, CH_2 and the polar groups.

(2) The Systems of Cyclohexane—Benzene Derivative.—In (1) the observed values of the electrostatic part of α at the two extreme concentrations of $v_2=1$ and 0, $\alpha^{el}_{obs}(1)$ and $\alpha^{el}_{obs}(0)$, are obtained by subtracting the value of 5.3 joul./cc. from the observed values at the corresponding concentrations. If the ratios, $\alpha^{el}_{obs}(0)/\alpha^{el}_{obs}(1)$, are calculated, they are found to lie between 2.0 and 1.5 as shown in Table I. Accordingly, if may be permissible to approximate the corresponding ratio in the cyclohexane—toluene system to be 2. Then, by empolying the observed value of $\alpha_{obs}(0) = 24.78$ joul./cc., $\alpha_{obs}(1) = 20.81$ joul./cc. for this system, the non-electrostatic part of α of 17.0 joul./cc. is obtained. As an approximation, neglecting the difference between CH_3 group of toluene and polar groups in other benzene derivatives, it may be plausible to assume the value of 17.0 joul./cc. as the non-electrostatic part of α for cyclohexane—benzene derivative systems.

The ratios of $\alpha^{el}_{obs}(0)/\alpha^{el}_{obs}(1)$ for the systems in which the non-polar components are non aromatic are shown in Table I.

It is seen from the table that the values of the ratio $\alpha^{el}_{obs}(0)/\alpha^{el}_{obs}(1)$ for the aromatic polar molecules are nearly equal to about 2, but slightly larger than those for non-aromatic molecules.

(3) The Systems of Cyclohexane—Cyclohexanone, Methylcyclohexane — Harocyclohexane and *cis*- and *trans*-Dichloroethylene Systems.—It is assumed that the non-electrostatic part of α is equal to zero because of the similarity of the two components.

2) Landolt-Bernstein, Physikalische-Chemiche Tabellen, III. Erg., p. 2826.

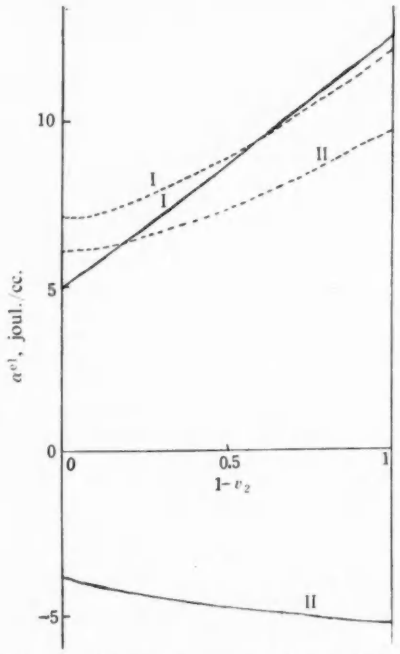

Fig. 1.1. Chlorobenzene—cyclohexane (I) and chlorobenzene—toluene (II) systems.

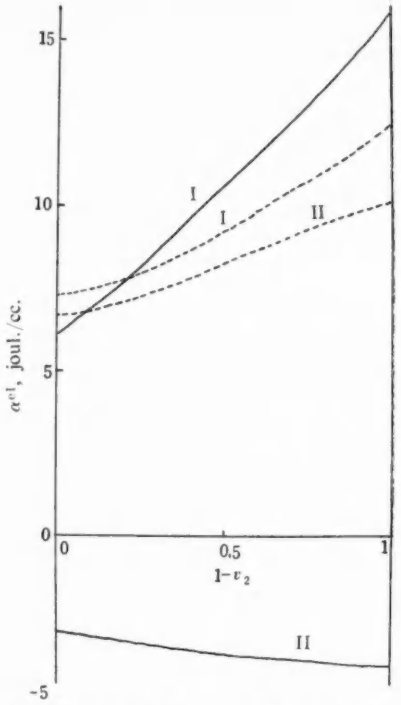

Fig. 1.2. Bromobenzene—cyclohexane (I) and bromobenzene—toluene (II) systems.

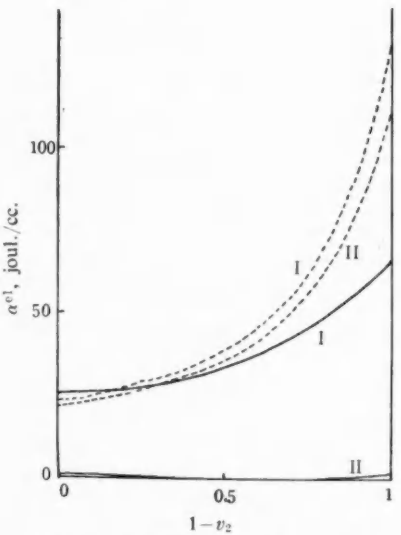

Fig. 1.3. Benzonitrile — cyclohexane (I) and benzonitrile—toluene (II) systems.

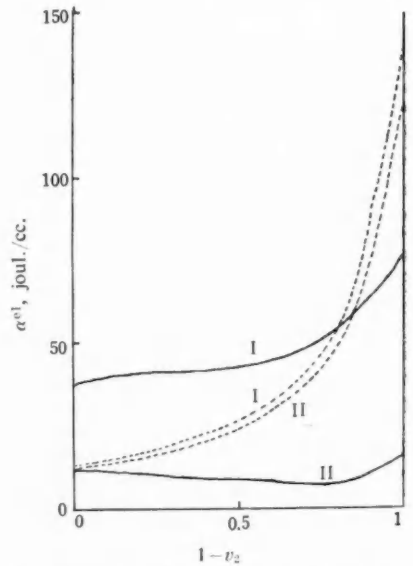

Fig. 1.4. Nitrobenzene — cyclohexane (I) and nitrobenzene—toluene (II) systems.

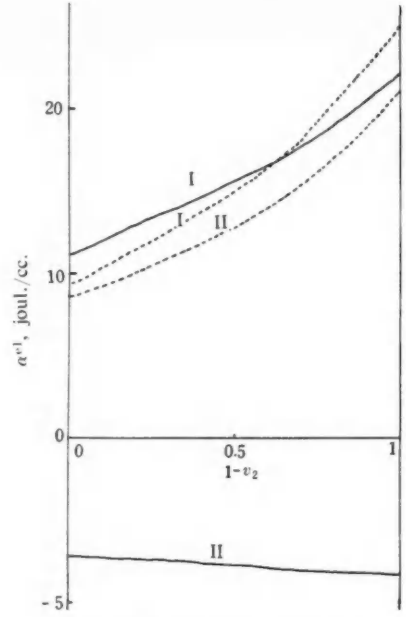

Fig. 1.5. Butylchloride — cyclohexane (I) and butylchloride—toluene (II) systems.

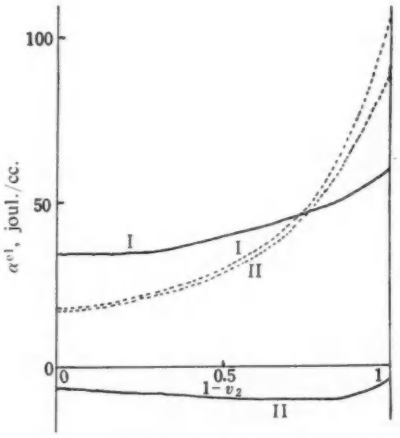

Fig. 1.6. Butylcyanide — cyclohexane (I) and butylcyanide—toluene (II) systems.

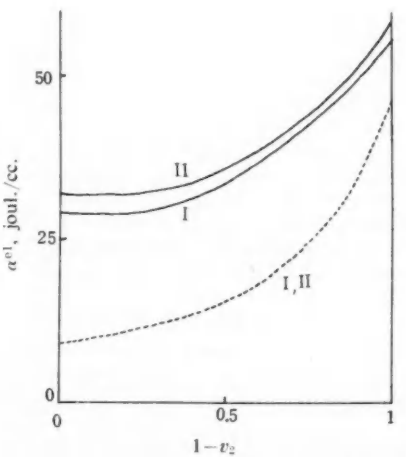

Fig. 1.7. Diethylketone — cyclohexane (I) and methylpropylketone — cyclohexane (II) systems.

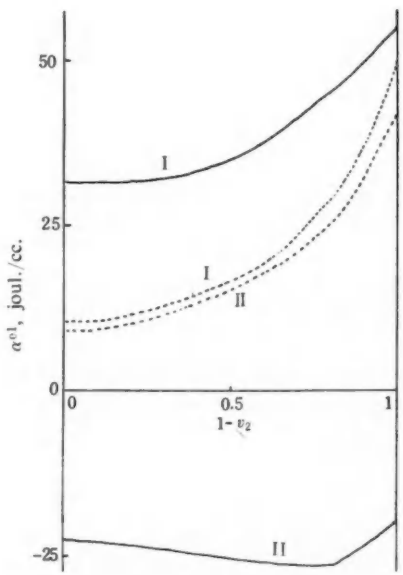

Fig. 1.8. Cyclohexanone—cyclohexane (I) and cyclohexanone—toluene (II) systems.

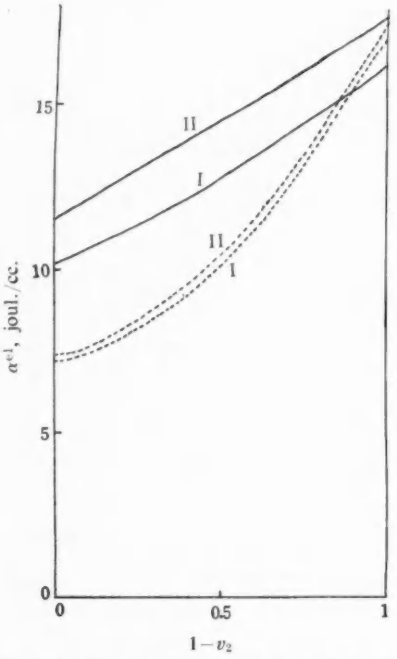

Fig. 1.9. Chlorocyclohexane—methylcyclohexane (I) and bromocyclohexane—methylcyclohexane (II) systems.

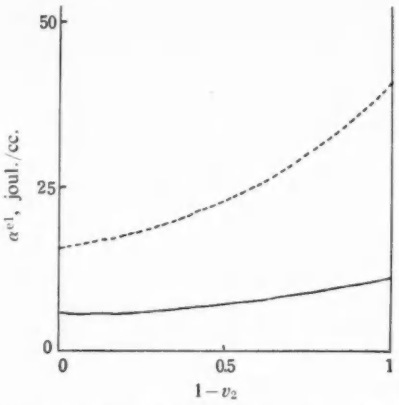

Fig. 1.10. *cis*-Dichloroethylene—*trans*-dichloroethylene system.

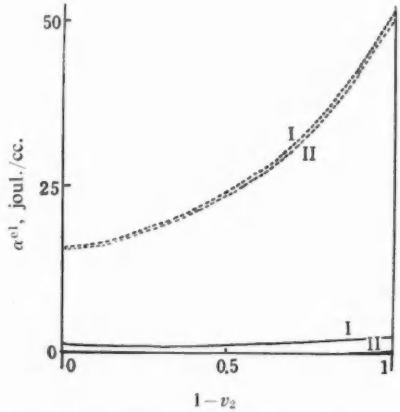

Fig. 1.11. Pyridine—1,4-dioxane (I) and pyridine—benzene (II) systems.

Fig. 1.1—1.11. The observed and the calculated values of electrostatic part of van Laar coefficient α^{el} plotted against volume fraction.
—— Observed ---- Calculated

For the systems in which non-polar components are aromatic such as toluene or benzene, α^{n-el}, the non-electrostatic part of α, is estimated as follows.

(4) The Systems of Toluene—Aromatic Polar Molecule.—For the systems of toluene—benzene derivatives and of benzene—pyridine, the α^{n-el} are assumed to be zero for their structural similarity.

(5) The Systems of Toluene—Aliphatic Polar Molecule.—For butylchloride—toluene, and butylcyanide—toluene systems, the values of α^{n-el} are estimated from the data of heat of mixing for the toluene—*n*-heptane system[3], by neglecting the differences between the polar group and CH_3 or CH_2 groups as before. For the present cases the value of α for *n*-heptane (1.5 joul./cc.) are assumed to be α^{n-el}.

For the cyclohexanone-toluene system α^{n-el} is assumed to be 17.0 joul./cc. as before.

3) Landolt-Bernstein, Physikalische-Chemische Tabellen, H. W. II, p. 1567.

Results and Discussion

The values of the electrostatic part of the van Laar coefficient α^{el}_{obs} were plotted against volume fraction with solid lines in Figs. 1.1—1.11.

Before comparing them with the calculated values, it will be examined whether there exist any regularity between these values and dielectric constants of the polar component or not.

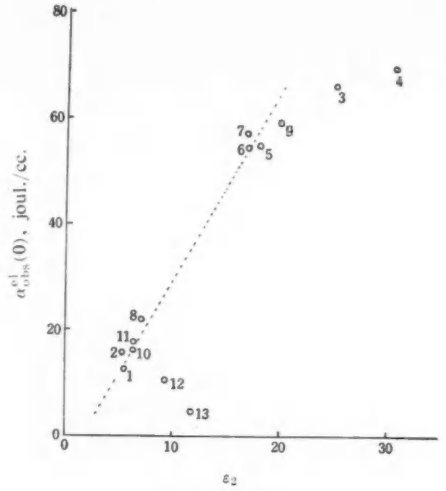

Fig. 2.

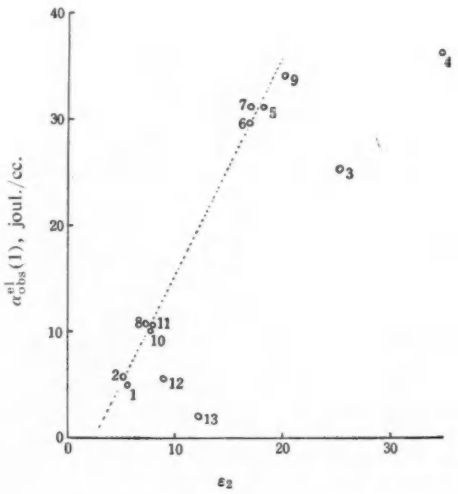

Fig. 3.

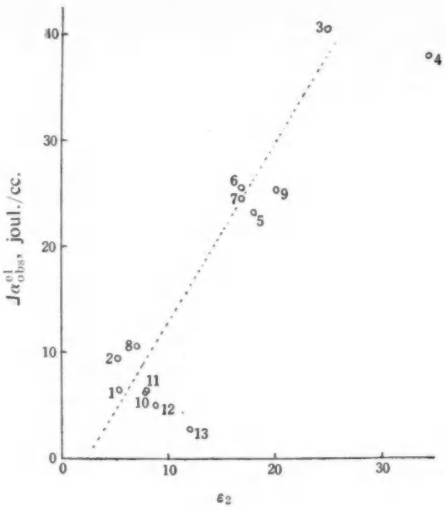

Fig. 4.

Figs. 2, 3 and 4. The plots of observed values of electrostatic part of van Laar coefficients at concentration $v_2=0$ and $v_2=1$ and their difference, $\alpha^{el}_{obs}(0)$, $\alpha^{el}_{obs}(1)$ and $\Delta\alpha^{el}_{obs}$ respectively vs. dielectric constant of polar components ε_2 for systems with non-aromatic non-polar components.

1. Chlorobenzene—Cyclohexane
2. Bromobenzene—Cyclohexane
3. Benzonitrile—Cyclohexane
4. Nitrobenzene—Cyclohexane
5. Cyclohexanone—Cyclohexane
6. Diethylketone—Cyclohexane
7. Methylpropylketone—Cyclohexane
8. *n*-Butylchloride—Cyclohexane
9. *n*-Butylcyanide—Cyclohexane
10. Chlorocyclohexane—Methylcyclohexane
11. Bromocyclohexane—Methylcyclohexane
12. *cis*-Dichloroethylene—*trans*-Dichloroethylene
13. Pyridine—1,4-Dioxane

For systems in which non-polar components are non-aromatic such as cyclohexane and methyl cyclohexane etc., the values of α^{el}_{obs} at $v_2=1$ and $v_2=0$, $\alpha^{el}_{obs}(1)$ and $\alpha^{el}_{obc}(0)$ respectively, are shown in Table I.

The difference of $\alpha^{el}_{obs}(0)$ and $\alpha^{el}_{obs}(1)$, $\Delta\alpha^{el}_{obs}$, for the above systems are also shown in Table I.

The values of $\alpha^{el}_{obs}(0)$, $\alpha^{el}_{obs}(1)$ and $\Delta\alpha^{bl}_{obs}$ are plotted against the dielectric constants ε_2 of the polar components, in Figs. 2—4.

As is seen from the above figures, it is likely that $\alpha^{el}_{obs}(1)$, $\alpha^{el}_{obs}(0)$ and $\Delta\alpha^{el}_{obs}$ have a kind of correlation to the dielectric constants of the polar components, that is, each plot gives approximately a straight line which intersects the abscissa at about $\varepsilon_2=2$. It should be noted, however, that a slight deviation is observed for butylcyanide and nitrobenzene which have much larger dipole moments than the others. The fact that the straight line intersects the absissa at about $\varepsilon_2=2$, which is neary equal to the dielectric constant of the non-polar components shows that on mixing these non-polar liquids with liquids having a dielectric constant of about 2, which might be non-polar, the electrostatic part of the heat of mixing vanishes.

This indicates that the estimation of α^{n-el} mensioned above was not so inappropriate.

For *cis*-dichloroethylene—*trans*-dichloroethylene and pyridine—dioxane systems the plots

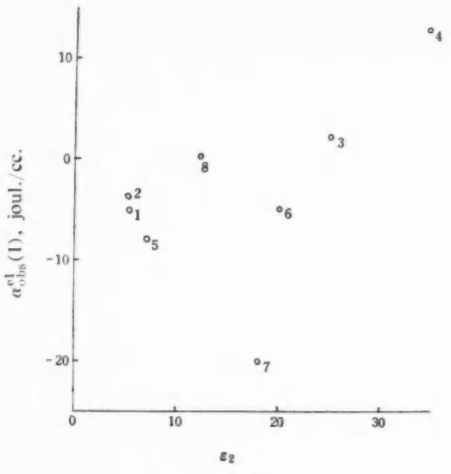

Fig. 5.

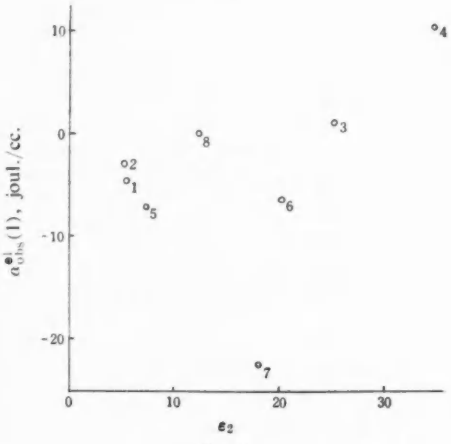

Fig. 6.

of $\alpha^{el}_{obs}(1)$, $\alpha^{el}_{obs}(0)$ and $\Delta\alpha^{el}_{obs}$ versus ε_2 deviate largely from the other systems. This might be due to the quadrupole moment of the non-polar component molecules. These non-polar molecules behave apparently as non-polar so far as the dielectric constant is concerned, but energetically not. The contribution from the local dipoles of these molecules which is not considered here, should be introduced, in systems containing molecules with quadrupole moment. The assumption of a single point dipole is drastic for the *cis*-dichloroethylene molecule, which has two large bond dipoles at a finite distance, and this may also be one of the reasons of the deviations for the system of *cis*- and *trans*-dichloroethylenes. For the pyridine—dioxane system the deviation is much greater than the above system, and this may

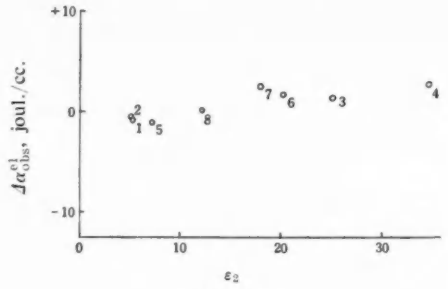

Fig. 7.

Figs. 5, 6, 7. The plots of observed values of electrostatic part of van Laar cofficients at concentrations $v_2=0$ and $v_2=1$ and their difference, $\alpha^{el}_{obs}(0)$, $\alpha^{el}_{obs}(1)$ and $\Delta\alpha^{el}_{obs}$ respectively vs. dielectric constant of polar components ε_2 for systems with aromatic non-polar components.

1. Chlorobenzene—Toluene
2. Bromobenzene—Toluene
3. Benzonitrile—Toluene
4. Nitrobenzene—Toluene
5. *n*-Butylchloride—Toluene
6. *n*-Butylcyanide—Toluene
7. Cyclohexanone—Toluene
8. Pyridine—Benzene

be attributed to the large quadrupole moments of dioxane or the special interaction between pyridine and dioxane.

For the nitrobenzene—cyclohexane system, the plot of α^{el}_{obs} versus v_2 has a peculiar shape compared with the remaining systems of this group. This may be attributed to the antiparallel orientation of nitrobenzene molecules in pure liquid and its concentrated solution, which is evidenced by the increase of the dielectric constant on application of a strong electric field[4]. This antiparallel orientation exists only at a concentration higher than about 80 mol. %, and at a lower concentration antiparallel orientation vanishes. As the antiparallel orientation of dipoles in pure liquid and concentrated solution is stable, the vanishing of the antiparallel orientation requires some energy and this contributes to make the values of α^{el} increase. This effect is important in a concentration higher than 80 mol. %, and in the actual system the values of α are rather shifted in the positive direction in this concentration range compared with the other systems.

For systems in which non-polar components are aromatic such as toluene and benzene, the values of $\alpha^{el}_{obs}(1)$ and $\alpha^{el}_{obs}(0)$ and their differences $\Delta\alpha^{el}_{obs}$ are obtained by graphical extrapolation, and are shown in Table II.

4) A. Piekara, Achelekowski, *J. Chem. Phys.*, **25**, 794 (1956).

TABLE II. VALUES OF $\alpha^{el}_{obs}(0)$, $\alpha^{el}_{obs}(1)$ AND $\Delta\alpha^{el}_{obs}$ IN joul./cc. FOR THE SYSTEMS IN WHICH NON-POLAR COMPONENTS ARE AROMATIC

System	$\alpha^{el}_{obs}(0)$	$\alpha^{el}_{obs}(1)$	$\Delta\alpha^{el}_{obs}$
Chlorobenzene—Toluene	−5.1	−4.3	−0.8
Bromobenzene—Toluene	−3.7	−3.1	−0.6
Benzonitrile—Toluene	2.5	1.1	1.4
Nitrobenzene—Toluene	13.2	10.5	2.7
n-Butylchloride—Toluene	−8.1	−7.2	−0.9
n-Butylcyanide—Toluene	−4.7	−6.5	1.8
Cyclohexanone—Toluene	−20.0	−22.5	2.5
Pyridine—Benzene	0.3	0	0.3

The values of $\alpha^{el}_{obs}(1)$, $\alpha^{el}_{obs}(0)$ and $\Delta\alpha^{el}_{obs} = \alpha^{el}_{obs}(0) - \alpha^{el}_{obs}(1)$ are plotted against the dielectric constant of the polar components and are shown in Figs. 5—7.

It is seen from the figures that no regulality is observed for $\alpha^{el}_{obs}(1)$ and $\alpha^{el}_{obs}(0)$ but for $\Delta\alpha^{el}_{obs}$ and they are nearly independent of the dielectric constants of the polar component. These are not on a line intersecting the abscissa at about $\varepsilon_2 = 2$.

Now the observed value will be compared with the calculated value. In Figs. 1.1—1.11, the values of α^{el}_{calcd} together with α^{el}_{obs} are plotted against the volume fractions of the polar component for the 21 binary systems of polar and non-polar liquids.

It is seen from the figures that for the systems in which non-polar components are non-aromatic both α^{el}_{obs} and α^{el}_{calcd} are positive and increase as the volume fraction of the polar component v_2 decreases. This confirms the fact that the variations of α with concentration are essentially due to the dipole of the polar component. However, quantitative agreements are poor for some of systems. For those in which non-polar components are aromatic, then differ in the manner of the change of α with concentration and sometimes even in their signs giving no qualitative agreement. This also confirms the fact that for the latter group of the systems, some kind of effect coherent to the aromaticity of the non-polar component which is not taken into consideration in the assumption of the derivation of the theory, occurs in the actual cases, and this may be the reason for the qualitative disagreement.

Further, quantitative comparison of α^{el}_{obs} and α^{el}_{obs} for the systems in which non-polar components are non-aromatic are made for the former group of the systems whose α^{el} may be considered to be explained principally by dipolar forces. The ratios of the calculated value to the experimental one, $\alpha^{el}_{calcd}/\alpha^{el}_{obs}$ are calculated for those systems at five values of concentration $v_2 = 1.00$, 0.75, 0.50, 0.25 and 0. The values of these ratios are plotted against the volume fraction in Fig. 8.

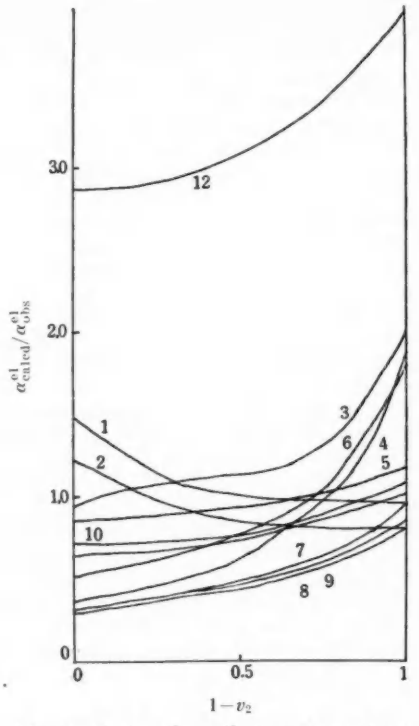

Fig. 8. Ratio $\alpha^{el}_{calcd}/\alpha^{el}_{obs}$ vs. volume fraction.

1. Chlorobenzene—Cyclohexane
2. Bromobenzene—Cyclohexane
3. Benzonitrile—Cyclohexane
4. Nitrobenzene—Cyclohexane
5. *n*-Butylchloride—Cyclohexane
6. *n*-Butylcyanide—Cyclohexane
7. Cyclohexanone—Cyclohexane
8. Diethylketone—Cyclohexane
9. Methylpropylketone—Cyclohexane
10. Chlorocyclohexane—Methylcyclohexane
11. Bromocyclohexane—Methylcyclohexane
12. *cis*-Dichloroethylene—*trans*-Dichloroethylene

It is seen from the result that most of the values of $\alpha^{el}_{calcd}/\alpha^{el}_{obs}$ are less than 2, whereas for the two systems, namely, of *cis*- and *trans*-dichloroethylene and of pyridine—dioxane, they differ considerably from the rest. Especially for the latter, it is too large to show in the figure. This indicates that the contribution due to the effect which cannot be explained merely with dipolar forces, presumably due to the quadrupole of the constituent molecules, is contained in the above two systems.

It indicates that in calculating electrostatic energy, contributions from multipoles higher than dipole such as quadrupole etc. must be taken into account for such systems.

It also indicates that for the rest of the group of the systems except the system containing the component molecules with larger dipole moments, such as nitrobenzene, benzonitrile and butylcyanide, the heats of mixing at infinite dilution of polar liquid in non-polar liquid are rather in good agreement with the theory despite of its rough assumptions. Rather good agreement obtained in a very dilute region for the systems with polar molecules of moderate magnitude of dipole moment, may be evidence that in these dilute regions, the assumptions made in the theory are not far from the actual circumstances.

Disagreement in the concentrated region may principally be due to the roughness of the theory such as the neglect of the short range interaction.

For systems containing polar molecules of large dipole moment the calculated values differ greatly from the experimental values.

This suggests that the larger the dipole moments is, the less satisfied is the condition of the assumption made in the theory in the actual circumstances.

Summary

The electrostatic part of the van Laar coefficients were derived from the observed value of heats of mixing and some regularity was found between these values and the dielectric constant of polar components if non-polar components are non-aromatic (group I). However, no regularity exists between them if non-polar components are aromatic (group II). These values were also compared with the calculated values. For group I, qualitative agreements were obtained and this confirms the fact that the variation of α with concentration is due to dipolar interaction of the polar components. The agreement is poor for systems containing a polar component with large dipole moments or for one containing a non-polar component with quadrupole moment. For group II, no qualitative agreement was obtained.

The author wishes to express his thanks to Professor Ryoichi Fujishiro of Osaka City University and to Professor Yonezo Morino of the University of Tokyo for their constant encouragement and discussions.

Government Chemical Industrial Research Institute
Shibuya-ku, Tokyo

Thermodynamical Studies on Binary Systems Consisting of Polar and Non-polar Liquids. V. The Anomalies in the Binary Systems of Polar Liquid with Aromatic Non-polar Liquid

By Kazuo AMAYA

(Received March 30, 1961)

In a previous paper it has been shown that an anomalous stabilization effect exists in those systems consisting of polar and aromatic non-polar components. To elucidate the cause of these phenomena, plausible explanations are proposed from the molecular view point.

Experimental Evaluation of the Anomalous Stabilization Effect

As is stated above, the binary systems containing the aromatic non-polar molecule and polar molecule show anomalous behavior in the heats of mixing.

First the decrease of the van Laar coefficient α due to the anomalous effect which was observed in aromatic non-polar solvents but not in non-aromatic solvents, will be estimated on reasonable assumptions.

Consider an imaginary non-polar liquid which is normal in nature such as cyclohexane, and its dielectric constant is the same as that of toluene. It may be reasonable to assume that the electrostatic part of the imaginary heat of mixing of the above imaginary non-polar liquid with polar liquids, if observed, would deviate from the theoretical values calculated for systems containing toluene in a previous paper, to the same extent as that of the deviation of the experimental value from the calculated one in the corresponding systems consisting of the same polar liquid and cyclohexane, because the dielectric constant of

toluene and cyclohexane differs only slightly. Then the van Laar coefficient due to the electrostatic part of imaginary heat of mixing may be estimated according to the following expression by the use of $\alpha^{el}_{c,obs}$ and $\alpha^{el}_{c,calcd}$ for the cyclohexane-polar liquid system and the $\alpha^{el}_{t,calcd}$ for the toluene-polar liquid system.

$$\alpha^{el}_{i,obs}=\alpha^{el}_{c,obs}\cdot\alpha^{el}_{t,calcd}/\alpha^{el}_{c,calcd} \quad (1)$$

where $\alpha^{el}_{i,obs}$ is the van Laar coefficient for an imaginary binary system mentioned above. The results obtained are shown in Table I.

TABLE I. VAN LAAR COEFFICIENT DUE TO STABILIZATION ENERGY α_{stab} AND THE VALUES OF STABILIZATION ENERGY ΔE_{stab} IN THE SYSTEMS COMPOSED OF POLAR LIQUID AND TOLUENE

System	v_2	α^{el}_1 joul./cc.	$\alpha_{stab}=\alpha^{el}_{obs}-\alpha^{el}_1$ joul./cc.	ΔE_{stab} joul./mol.
	1.0	4.16	− 8.5	0
Chlorobenzene	0.75	5.76	−10.1	196
—Toluene	0.50	7.18	−12.1	319
	0.25	8.57	−13.6	269
	0	10.07	−15.2	0
	1.0	5.54	− 8.6	0
Bromobenzene	0.75	7.73	−11.0	218
—Toluene	0.50	9.59	−13.1	348
	0.25	11.37	−15.0	299
	0	12.28	−16.0	0
	1.0	23.07	−22.0	0
Benzonitrile	0.75	24.44	−23.9	467
—Toluene	0.50	30.88	−30.9	812
	0.25	42.52	−42.3	840
	0	55.87	−53.4	0
	1.0	33.60	−23.1	0
Nitrobenzene	0.75	37.00	−27.4	533
—Toluene	0.50	37.63	−29.1	762
	0.25	44.13	−36.2	718
	0	64.95	−51.8	0
	1.0	9.95	−17.3	0
n-Butylchloride	0.75	11.60	−19.4	384
—Toluene	0.50	13.64	−21.3	565
	0.25	15.75	−24.5	488
	0	18.20	−26.9	0
	1.0	32.29	−38.8	0
n-Butylcyanide	0.75	33.45	−40.6	808
—Toluene	0.50	37.54	−45.5	1210
	0.25	45.25	−53.4	1067
	0	50.26	−55.0	0
	1.0	28.92	−51.4	0
Cyclohexanone	0.75	28.48	−51.0	1003
—Toluene	0.50	32.34	−55.2	1456
	0.25	41.15	−64.6	1286
	0	46.61	−66.6	0

These values would be the corresponding electrostatic part of the van Laar coefficient for heats of mixing of toluene and the polar liquids if toluene were normal in nature as cyclohexane is, and do not show any anomalous behavior. The difference between such apparent values and the observed values may be considered to be the contribution from the anomalous effect. The part of the contribution of the anomalous effect to the van Laar coefficient α_{stab} thus obtained are also shown in the same table together with the stabilization energy per mole of the solution. It is seen that α_{stab} is dependent on the concentration.

The Origin of the Anomalous Stabilization Effect

The Anisotropy of the Aromatic Non-polar Molecules.—If an anisotropic non-polar molecule is placed in an electric field, it tends to orient its most polarizable axis to be parallel to the direction of the electric field. In a region near the polar molecule, a strong electric field is produced arouud it and hence aromatic molecules in this region would tend to orient their most polarizable axis along the direction of the electric field. Then the effective dielectric constant of this region increases somewhat more than the original macroscopic value, the extent of which depends on the anisotropy of the non-polar molecule and the magnitude of the dipole moment of the polar molecule.

The increase of the dielectric constant of the non-polar liquid makes the calculated values of the van Laar coefficient decrease as is seen from the above results that the calculated values of the electrostatic part of the van Laar coefficient α^{el}_{calcd} for tolune-polar liquid system is an amount of 80~90% of those for the corresponding system of cyclohexane-polar liquid. Anisotropy constants for benzene and toluene are reproduced for reference from the literature:

$$\text{for benzene}\begin{cases}\alpha_1=123.1\\ \alpha_2=123.1\\ \alpha_3=\ 63.5\end{cases}\quad\begin{matrix}\bar{\alpha}=103.2\\ \alpha_1/\bar{\alpha}=1.193\end{matrix}$$

$$\text{for toluene}\begin{cases}\alpha_1=156.4\\ \alpha_2=136.6\\ \alpha_3=\ 74.8\end{cases}\quad\begin{matrix}\bar{\alpha}=122.6\\ \alpha_1/\bar{\alpha}=1.276\end{matrix}$$

If we suppose that the non-polar molecules given above orient their most polarizable axis completely along the direction of the electric field produced by the polar molecule, the effective dielectric constant may be increased from 2.366 of toluene to about 3.

The values calculated with the values of 3

for the dielectric constant of non-polar liquid indicate the maximum contribution of this effect. In actual cases, however, the orientation of the non-polar molecule along the direction of the electric field is disturbed by thermal agitation and the effective dielectric constant may be less than 3.

The orientational effect in the solution consisting of anisotropic non-polar molecules accompanying the increase of effective dielectric constant in the region of small x_2 would make the values of α^{el}_{calcd} smaller than before.

But with this consideration alone it is impossible to make the values of α^{el} negative and also to explain the concentration dependence of α_{stab}.

The Addition Stabilizing Effect due to Orientation of Anisotropic Non-polar Molecules in an Electric Field.—The molecules of toluene and benzene are somewhat anisotropic, and when they are placed in a strong electric field, they tend to orient their most polarizable axis in the direction of the applied electric field. In the gaseous state this effect results in the increase of polarizability, and hence somewhat stabilizes the molecules. But this effect makes little contribution as was explained above.

In the liquid state, however, molecules interact with each other, and if we are admitted to assume the orientation of these molecules increases the intermolecular interaction energy, these stabilizing effects may be explained consistently.

Anisotropic non-polar molecules near a polar molecule are in a more ordered state than those far from the polar molecule because of the strong dipolar field of the latter. It may be reasonable to assume that in a region near the dipolar molecule, anisotropic non-polar molecules stick together more or less as they do in their solid state and the degree or the extent of the orientation depends on the magnitude of the dipolar field.

Let us consider an anisotropic non-polar molecule whose polarizabilities along three principal axes x, y and z are α_x, α_y and α_z respectively.

When this molecule is placed in an electric field F, then the electrostatic energy of the molecule, E is expressed as

$$E=-\frac{1}{2}(\alpha_x\cos^2\theta_{\mu x}+\alpha_y\cos^2\theta_{\mu y}+\alpha_z\cos^2\theta_{\mu z})F^2 \tag{2}$$

where $\theta_{\mu x}$, $\theta_{\mu y}$ and $\theta_{\mu z}$ denote the angles between the direction of the electric field and each principal x, y and z axis respectively.

For simplicity, assuming that

$$\alpha_x=\alpha_y \tag{3}$$

the electrostatic energy E is given by

$$E=-\frac{1}{2}(\alpha_z\cos^2\theta_{\mu z}+\alpha_x\sin^2\theta_{\mu z})F^2$$
$$=-\frac{1}{2}\{(\alpha_z-\alpha_x)\cos^2\theta_{\mu z}+\alpha_x\}F^2 \tag{4}$$

then

$$\overline{\cos^2\theta_{\mu z}}=\frac{2\int_{\pi/2}^{0}\int_{0}^{2\pi}\cos^2\theta_{\mu z}\cdot\exp\left[\frac{1}{2}\{(\alpha_z-\alpha_x)\cos^2\theta_{\mu z}+\alpha_x\}\times(F^2/\boldsymbol{kT})\right]\cdot\sin\theta_{\mu z}\mathrm{d}\theta_{\mu z}\mathrm{d}\varphi}{\int_{\pi/2}^{0}\int_{0}^{2\pi}\exp\left[\frac{1}{2}\{(\alpha_z-\alpha_x)\cos^2\theta_{\mu z}+\alpha_x\}\times(F^2/\boldsymbol{kT})\right]\cdot\sin\theta_{\mu z}\mathrm{d}\theta_{\mu z}\mathrm{d}\varphi}$$
$$=\frac{\int_{\pi/2}^{0}\cos^2\theta_{\mu z}\exp\left[\frac{1}{2}(\alpha_z-\alpha_x)(F^2\cos^2\theta_{\mu z}/\boldsymbol{kT})\right]\times\sin\theta_{\mu z}\mathrm{d}\theta_{\mu z}}{\int_{\pi/2}^{0}\exp\left[\frac{1}{2}(\alpha_z-\alpha_x)F^2\cos^2\theta_{\mu z}/\boldsymbol{kT}\right]\cdot\sin\theta_{\mu z}\mathrm{d}\theta_{\mu z}} \tag{5}$$

Putting $\cos^2\theta_{\mu z}=x$, and $1/2\cdot(\alpha_z-\alpha_x)F^2/\boldsymbol{kT}=a$, then the above expression becomes

$$\overline{x^2}=\frac{\int_0^1 x^2\mathrm{e}^{ax^2}\mathrm{d}x}{\int_0^1\mathrm{e}^{ax^2}\mathrm{d}x}=\frac{\left[\frac{x}{2a}\mathrm{e}^{ax^2}\right]_0^1}{\int_0^1\mathrm{e}^{ax^2}\mathrm{d}x}-\frac{1}{2a} \tag{6}$$

As the integration in the denominater, $\int\mathrm{e}^{ax^2}\mathrm{d}x$ can not be expressed in a simple formula, the integrand is expanded in a power series, and is integrated, and then the following expression is obtained

$$\int\mathrm{e}^{ax^2}\mathrm{d}x=\int\left(1+ax^2+\frac{a^2x^4}{2!}+\frac{a^3x^6}{3!}+\cdots\right)\mathrm{d}x$$
$$=x+\frac{a}{3}x^3+\frac{a^2x^5}{5\cdot2!}+\frac{a^3x^7}{7\cdot3!}+\cdots \tag{7}$$

For extreme cases of $a\ll1$ and $a\gg1$, the following approximate formula are obtained.

For $a\ll1$

$$\int_0^1\mathrm{e}^{ax^2}\mathrm{d}x=1+\frac{a}{3}+\frac{a^2}{10}+\cdots \tag{8}$$

$$\left[\frac{x}{2a}\mathrm{e}^{ax^2}\right]_0^1=\frac{1}{2a}+\frac{1}{2}+\frac{a}{4}+\cdots \tag{9}$$

then

$$\frac{\left[\frac{x}{2a}\mathrm{e}^{ax^2}\right]_0^1}{\int_0^1\mathrm{e}^{ax^2}\mathrm{d}x}=\left(\frac{1}{2a}+\frac{1}{2}+\frac{a}{4}+\cdots\right)\times\left(1+\frac{a}{3}+\frac{a^2}{10}+\cdots\right)^{-1}$$
$$=\frac{1}{2a}+\frac{1}{3}+\frac{7}{90}a+\cdots \tag{10}$$

Then

$$\overline{\cos^2\theta_{\mu z}}=\frac{1}{3}+\frac{7}{90}a+\cdots \tag{11}$$

For $a \gg 1$, $\overline{\cos^2\theta_{\mu z}}$ tend to unity.

For the molecule with $\alpha_z > \alpha_x = \alpha_y$, $\overline{\cos^2\theta_{\mu z}}$ tends to 1/3 as a approaches to zero, and to 1 as it approaches to infinite. For the molecule $\alpha_z < \alpha_y = \alpha_y$, $\overline{\cos^2\theta_{\mu z}}$ tends to 1/3 as a approaches to zero and to 0 as it approaches to infinite.

As the value of $\overline{\cos^2\theta_{\mu z}}$ varies with the order of the molecular arrangement, it may be reasonable to define an order parameter as

$$s = (\overline{\cos^2\theta_{\mu z}} - 1/3)/(1-1/3) \quad \text{for } \alpha_z > \alpha_x \quad (12)$$

and

$$s = (1/3 - \overline{\cos^2\theta_{\mu z}})/1/3 \quad \text{for } \alpha_z < \alpha_x \quad (13)$$

s is proportional to a for small values of a and tends to approach to 1 for large values of a like the Langevin function. It may reasonably be assumed that the stabilization energy due to orientation of the anisotropic non-polar molecules is proportional to s and as a result it may be saturated in a strong electric field corresponding to a great value of a.

Now, the order of magnitude of a for actual cases will be considered. For the values of $(\alpha_z - \alpha_x)$ the value $\approx 60 \times 10^{-25}$ cc. per molecule of toluene is taken, and for F, if the values of an electric field at a distance of 3Å from a point dipole of 1D is taken, the value of F is 3.7×10^4 e. s. u., there a for $T = 300°$K becomes 0.05 for 1D, and 0.82 for 4D. For chlorobenzene a is about 0.15 and for nitrobenzene this value is about 0.8.

Now, let us consider the order of magnitude of this effect. Since this effect is cooperative with respect to an aromatic non-polar molecule, it is natural that the contribution from this effect vanishes in a limit at zero concentration of aromatic non-polar component. Then it may be resonable to attribute the concentration dependent part of α_{stab} to this effect.

At infinite dilution of polar liquids, this stabilization energy per mole of polar liquid is from about 700 to 3200 joul.

On the other hand, heats of fusion, which may be considered to be a measure of orientational energy for benzene and toluene are about 9840 joul. and 6620 joul. per mole, respectively. As one polar molecule is surrounded by several of the nearest neighboring non-polar molecules at infinite dilution, a slight extent of ordered state in the group of molecules is possible to introduce considerable stabilization energy to their systems. Therefore, the magnitude of the above values of stabilizing energy seems to be not unreasonable as the contribution from this effect.

The stabilization energy of toluene at an infinite dilution of the polar molecule caused by 1 mol. of polar molecule is plotted against μ^2 in Fig. 1.

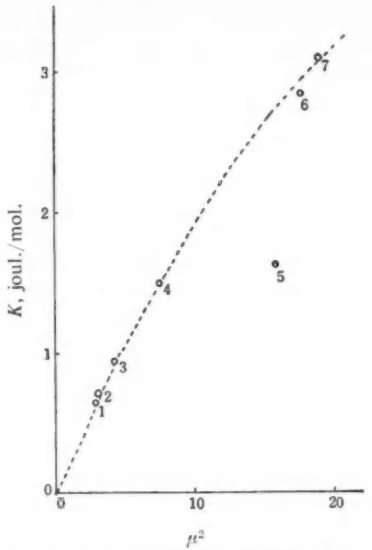

Fig. 1. Concentration dependent part of stabilization energy per mole of polar components at infinite dilution in toluene plotted against square of dipole moment of the polar molecules.

1. Chlorobenzene
2. Bromobenzene
3. *n*-Butylchloride
4. Cyclohexanone
5. *n*-Butylcyanide
6. Nitrobenzene
7. Benzonitrile

It is seen from the figure that the saturation effect is only slightly observed as the theory predicts. This fact makes the above explanation plausible. As for a concentration independent part of α_{stab}, further investigations will be necessary.

Summary

The anomalous stabilization energy for the systems containing polar and aromatic non-polar liquids was evaluated on reasonable assumptions. The van Laar coefficient due to this stabilizing effect was found to be dependent on the concentration. The stabilization effect corresponding to the concentration dependent part of the van Laar coefficient was explained by the cooperative orientation of aromatic non-polar molecules around the polar molecules.

The author wishes to express his thanks to Professor Ryoichi Fujishiro of Osaka City University and to Professor Yonezo Morino of the University of Tokyo for their constant encouragement and discussions.

Government Chemical Industrial Research Institute
Shibuya-ku, Tokyo

Mass-spectrometric Study on Ionization and Dissociation of Diethyl Ether by Electron Impact

By Ichiro KANOMATA

(Received March 28, 1961)

Since 1930 many studies on ionization and dissociation of organic molecules by electron impact have been made by means of a mass-spectrometer. The reason for using a mass-spectrometer for these kinds of studies is to obtain the information on the decomposition processes through determination of M/e values and of the appearance potentials of ions formed by electron impact.

The study on the processes of ionized decomposition by electron impact is not only fundamental for the radiation chemistry of organic compounds but also helpful for the researches on molecular structures and chemical reactions.

The author previously reported the mass-spectrometric study on ionization and dissociation of the ethyl alcohol molecule by electron impact[1,2]. The present report relates to the decomposition of the diethyl ether molecule which has one oxygen atom, and the ionization of the molecule is thought to "cause the removal" of one of the lone pair 2 p electrons of this oxygen atom as well as in the case of ethyl alcohol in the previous study.

Experimental

The mass spectrometer[3] used for this study was a 90° sector type ($R=12$ cm.), and the appearance potentials (AP) of ions were determined by the extrapolated difference method[4]. The ionization potential of the molecule was calibrated with the ionization potential of argon (15.76 eV.) and the appearance potentials of fragment ions were determined by referring to the ionization potential of the molecule. The sample was chemically pure and was not particularly refined.

Results

The appearance ratios of ions produced from the molecule by 75 eV. electron impact are shown in Table I. From the table it is obviously recognized that the M/e=31 ion (CH_2OH^+ or CH_3O^+) is the most abundant, and the M/e=29, 59, 45 and 74 ions are also abundant. The appearance potentials of these five species of ions obtained are tabulated in Table II.

Table I. Appearance ratios

M/e	Ion	Appearance ratio
75	Isotope peak	0.3
74	$(C_2H_5)_2O^+$	25.7
60	$(CH_3)(C_2H_5)O^+$, isotope peak	2.1
59	$(CH_2)(C_2H_5)O^+$	46.0
46	$C_2H_5OH^+$, isotope	0.4
45	$(C_2H_5)O^+$	31.3
44	$C_2H_4O^+$	3.1_5
43	$C_2H_3O^+$	12.7_5
42	$C_2H_2O^+$	3.0
41	C_2HO^+	6.0
31	CH_2OH^+ or CH_3O^+	100.0
30	CH_2O^+	3.1_5
29	CHO^+ or $C_2H_5^+$	63.5
28	CO^+ or $C_2H_4^+$	10.2
27	$C_2H_3^+$	37.1
26	$C_2H_2^+$	8.0
15	CH_3^+	14.3
14	CH_2^+	2.7

Table II. Appearance potentials (eV.)

M/e	Ion	Appearance potential
74	$(CH_3CH_2)O^+(CH_2CH_3)$	9.55 ± 0.02
59	$CH_2O^+CH_2CH_3$	10.80 ± 0.08
45	$CH_3CH_2O^+$	13.23 ± 0.04
31	CH_2O^+H or CH_3O^+	$12.3_5\pm0.1$
29	$C_2H_5^+$ or CHO^+	14.0 ± 0.2

Discussion

When a molecule R_1R_2 is composed of R_1 and R_2 atoms (or radicals), the appearance potential of R_1^+ ions is given by

$$A(R_1^+)=I(R_1R_2)+D(R_1^+-R_2) \quad (1)$$

$$=I(R_1)+D(R_1-R_2) \quad (2)$$

Here, $I(R)$ is the ionization potential of atom (radical) R, and $D(R_1-R_2)$ is the bond dissociation energy between R_1 and R_2. Of course, radicals or atoms produced may generally have some excitational or kinetic energy. In case the molecule consists of many atoms as organic compounds, however, the potential

1) T. Kambara and I. Kanomata, *Buturi* **4**, 71 (1949).
2) T. Kambara and I. Kanomata, *Hitachi Hyoron Rombunshu*, No. 7, 15 (1949).
3) I. Kanomata, Y. Kaneko and T. Oguri, *Mass Spectroscopy*, No. 3, 12 (1954).
4) J. W. Warren, *Nature*, **165**, 811 (1950).

surfaces that give the binding energies between atoms approach each other, and therefore the excess energy may be small as reported by some authors[5,6]. From this point of view the neglect of this excess energy will not be serious in the course of this discussion.

The processes of production of ions are as follows:

$$M/e=74 \quad (C_2H_5)_2O^+, \quad AP\ 9.55\ eV.$$

This ion is the parent ion and the appearance potential is the ionization potential of diethyl ether molecule. This value was obtained by Morrison[7] as 9.72 eV. by critical slope method and by Price[8] spectroscopically as 10.2 eV. These results are largely different from each other beyond their errors of measurement, though the reason can not be explained.

It must be considered what kind of electron in the molecule is concerned with its ionization. Mulliken[9] reported that the lone pair electrons of the oxygen atom in the molecules, such as water and alcohol, have the lowest ionization potential by charge transfer effect. Hence the ionization occurs at first by the removal of one of these electrons. The fact that the ionization potentials decrease in the order of H–O–H (12.76 eV.), CH_3–O–H (10.95 eV.), CH_3–O–CH_3 (10.5 eV.) and C_2H_5–O–C_2H_5 (9.55 eV.) can be explained by this charge transfer effect. This postulate was also used when the present author and Kambara studied the ionization and dissociation of ethyl alcohol[1,2], propyl alcohol[10,11], acetone and acetic acid[12] molecules by electron impact, and will be required to discuss the dissociation process for the production of M/e=59 ion from diethyl ether. From these facts, the ionization potential 9.55 eV. is thought to be that of the oxygen atom in the molecule.

$$M/e=59 \quad (CH_2{=}O{-}C_2H_5)^+, \quad AP\ 10.80\ eV.$$

Equation 1, in this case, leads to $A(R_{59}^+)=I(R_{74})+D(R_{59}^+-R_{15})$. Inserting the observed values, $D(R_{59}^+-R_{15})=10.80-9.55=1.25$ eV. is obtained. This dissociation energy of the ionic state should correspond to the dissociation energy of the C–C bond of the neutral molecule. The reason why the dissociation energy for such an ionized molecule is apparently low may be elucidated as follows.

If one of the lone pair electrons of the oxygen atom in the molecule is removed by ionization in accordance with Mulliken's postulate, the other electron left in the atom may have new binding activity, that is, the trivalency of the O^+ ion. Therefore, when the structure of M/e=59 ion is assumed as $\begin{matrix}H\\H\end{matrix}\!\!>\!C{=}O^+{-}C_2H_5$, this ion should be more stabilized, by the energy of formation of trivalent structure, than the structure of $\begin{matrix}H\\ \cdot C{-}O^+{-}C_2H_5\\H\end{matrix}$ which is yielded by only removing a CH_3 radical from the parent ion.

In order to estimate this stabilization energy of formation of trivalent bond, it is assumed that the dissociation energy of the C–C bond of the diethyl ether molecule is equal to that of ethane.

$$D(R_{59}-R_{15})=D(CH_3-CH_3)=80\pm6\ \text{kcal.}^{13}$$
$$=83.3\pm1\ \text{kcal.}^{14}$$
$$=3.6\ \text{eV.}$$

Then the stabilization energy becomes 3.6−1.25 =2.35 eV.=54 kcal./mol. Consequently, under the assumption of the additivity of bond energy, the total binding energy of trivalent bond of O^+ in this case is obtained as (3.26 eV. ×2+2.35 eV.=8.87 eV.=)204 kcal./mol., where 3.26 eV. is the value of D(C–O).

It may be recognized that in this ion resonance occurs as in carbon monoxide molecule, causing the stabilization near 58 kcal. of resonance energy of carbon monoxide[15].

$$M/e=45 \quad (C_2H_5{-}O)^+, \quad AP\ 13.23\ eV.$$

This ion is thought to be produced by the removal of a C_2H_5 radical from the parent ion. Therefore the relation $A(C_2H_5-O\cdot^+)=I(C_2H_5-O\cdot)+D(R_{45}-R_{29})$ exists. According to Syrkin and Dyatkina's data[16] on heat of dissociation, D(C–O) for diethyl ether is 75 kcal./mol. (3.26 eV.), hence from the above equation $I(C_2H_5-O^+\cdot)=10.0$ eV. is obtained. This value is somewhat greater than the ionization potential of the parent molecule (9.55 eV.). This seems to be due to the charge transfer effect which is adopted to explain the low value of the ionization potential of the parent molecule. As regards this ion, of course, the stabilization due to trivalency of O^+ can not take place.

5) F. H. Field and J. L. Franklin, "Electron Impact Phenomena", Academic Press Inc. Publishers, New York (1957).
6) C. E. Berry, *Phys. Rev.*, **78**, 597 (1950).
7) J. D. Morrison and A. J. C. Nicholson, *J. Chem. Phys.*, **20**, 1021 (1951).
8) T. M. Sugden, A. D. Walsh and W. C. Price, *Nature*, **148**, 373 (1941).
9) R. S. Mulliken, *J. Chem. Phys.*, **3**, 506 (1935).
10) T. Kambara, *J. Phys. Soc. Japan*, **5**, 31 (1950).
11) T. Kambara, ibid., **5**, 36 (1950).
12) T. Kambara, ibid., **5**, 84 (1950).
13) M. Szwarc, *Chem. Revs.*, **47**, 75 (1950).
14) J. S. Roberts and H. A. Skinner, *Trans. Faraday Soc.*, **45**, 339 (1949).
15) L. Pauling, "The Nature of the Chemical Bond", Cornell University Press, Ithaca (1939).
16) Y. U. Syrkin and M. E. Dyatkina, "Structure of Molecules and Chemical Bond", Interscience Publishers, Inc., New York (1950).

M/e=31 $(CH_3\text{-}O\text{-}H)^+$, AP 12.3$_5$ eV.

The structure of this ion may be thought to be either CH_3O^+ or CH_2OH^+. Though this ion is the most abundant among those produced by 75 eV. electron impact, it can not be produced through a simple process, as the rupture of only one bond in the cases of M/e =59 and 45. Thus, in this dissociation process, rearrangement of atoms in the molecule is necessary.

The following dissociation process is energetically reasonable.

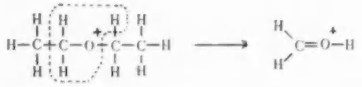

That is, it is thought that with the ionization of the oxygen atom, the rupture of bonds and the formation of O-H bond take place simultaneously. Assuming the bond energy additivity, the energy necessary for this process will be calculated as follow:

ionization of oxygen atom	9.55 eV.
rupture of C-C bond	3.6 eV.
rupture of C-O bond	3.26 eV.
rupture of C-H bond[17]	2.9 eV.
formation of O-H bond	−4.8 eV.
formation of $>C=O^+-$ structure	−2.35 eV.

The sum of these energies is 12.16 eV. in total and agrees well with the appearance potential obtained.

On the contrary, if this ion is assumed to have the structure of CH_3O^+, the energy necessary for the reaction becomes more than 16 eV. Therefore the structure of M/e =31 ion is concluded to be $H_2C=O^+-H$.

M/e=29 $C_2H_5^+$ or CHO^+, AP 14.0 eV.

If the M/e=29 ion is $C_2H_5^+$, Eq. 2 leads

$$A(C_2H_5^+) = I(C_2H_5) + D(C_2H_5\text{-}OC_2H_5)$$

Then $I(C_2H_5) = 14.0 - 3.26 = 10.74$ eV.

The ionization potential of C_2H_5 radical can be estimated from various data. For example, Bleakney gave a rather high value of 9.8 eV. from the decomposition of ethyl alcohol, and the mean value of the data given from various ionized decompositions of organic compounds is 8.75 eV.[5] Moreover, the energy for direct ionization of C_2H_5 radical has the rather low value of 8.60 eV.[18] Therefore, this ion should not be $C_2H_5^+$ ion, but CHO^+.

If it is assumed that radicals of H, CH_3 and C_2H_5 are produced in the course of the formation of CHO^+, the heat of reaction can be calculated from the thermochemical data as follows.

$$A(CHO^+) = \Delta H_f(CH_3) + \Delta H_f(C_2H_5) + \Delta H_f(H) + \Delta H_f(CHO^+) - \Delta H_f(C_2H_5OC_2H_5) = 14.3 \text{ eV}.$$

The calculated value agrees well with the experimental result.

From the standpoint of bond energy additivity, and the assumed reaction of

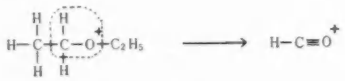

as in the case of M/e=31 ion, the energy necessary for the reaction will be calculated as follows.

ionization of the molecule	9.55 eV.
rupture of C-C bond	3.6 eV.
rupture of C-O bond	3.26 eV.
rupture of C-H bond	2.9 eV.
$H\text{-}C\text{-}O^+ \rightarrow H\text{-}C\equiv O^+$	-2.35×2 eV.

The sum of these energies is 14.6 eV. The difference between this value and the measured appearance potential is somewhat great, but this is unavoidable under such a loose assumption and rough calculation.

The total bond energy of O^+ ion in the case of CHO^+ is also calculated as in the case of M/e=59 ion. That is to say, provided that the energy of the C-O bond 3.26 eV. is conserved in one of the triple bond of CHO^+ ion, the total energy of O^+ is calculated as

$$3.26 + 2.35\times2 = 7.96 \text{ eV.} = 182 \text{ kcal./mol.}$$

This value is rather small compared with that of M/e=59 ion.

The reason why the stabilization is smaller in this case than in the case of M/e=59 ion is thought to be due to the existence of fewer resonance structures.

Summary

A mass spectrometric study on ionization and dissociation of diethyl ether has been carried out.

The M/e=31 ion is the most abundant among the ions produced by 75 eV. electron impact and the M/e=29, 59, 45 and 74 ions are abundant in this order next to M/e=31 ion.

The appearance potential measurement of these ions leads to the following conclusion. The ions are formed by the removal of one of the lone pair electrons of the oxygen atom in the molecule.

17) C. E. Cumming and M. E. Bleakney, *Phys. Rev.*, **58** 787 (1940).
18) J. A. Hipple and D. P. Stevenson, ibid., **63**, 121 (1943).

By considering the trivalent structure of O^+ and by applying the bond energy additivity, which is adequate for hydrocarbons, to such an ionized dissociation process the producing processes of such ions can be satisfactorily revealed.

The stabilization energy for the formation of $\rangle C=O^+-$ structure is obtained as 54 kcal./mol. by such a calculation.

The author would like to express his deep appreciation to Professor K. Kido and Professor T. Titani for their kind guidance and to Mr. Y. Kaneko and Mr. T. Oguri for their earnest coorporation.

Department of Physics
Tokyo Metropolitan University
Setagaya-ku, Tokyo

Proton Magnetic Resonance Spectra of Methylthiophenesulfonylchlorides

By Kensuke Takahashi, Yasuo Matsuki, Yoshiteru Miyake and Genjiro Hazato

(Received March 31, 1961)

In the previous communication[1], the relative magnitude of the coupling constants for the ring protons in thiophene derivatives was assumed to be $J_{23}>J_{34}>J_{25}>J_{24}$, in which the values for J_{25} and J_{24} could not be determined experimentally. This assumption is in accordance with the recent experimental works by Gronowitz and Hoffman[2]. In this note, the experimental results of the proton magnetic resonance spectra for the six isomers of methylthiophenesulfonylchloride are presented. Those results complement the previous communication on the substituted thiophenes. The observed values of J_{25} and J_{24} and some experimental coupling constants for the methyl group and the ring proton are also presented. Some qualitative results of the solvent effect on the chemical shifts of these isomers are also presented.

Experimental

The apparatus and procedure were similar to those previously described[1], and cyclohexane was used as an internal reference. The compounds used in the present observations were synthesized by Matsuki and his collaborators. Details of the preparation of these new compounds will be given later in Journal of the Chemical Society of Japan, Ind. Chem. Sec. The boiling points and the measured conditions of the samples are given in Table I; with respect to these six isomers, 2-methyl-5-thiophenesulfonylchloride is the only one which is reported in the literature[3], as far as we know.

Table I

Substituent	B. p. °C/mmHg	Measured condition wt. % Sample	CCl_4	C_6H_{12}
2-CH_3, 3-SO_2Cl	91~93/3	77.9		22.1
2-CH_3, 4-SO_2Cl	92~94/3	56.9	30.7	12.4
2-CH_3, 5-SO_2Cl	96~98/3	81.9		18.1
3-CH_3, 2-SO_2Cl	98~100/2.5	83.2		16.8
3-CH_3, 4-SO_2Cl	96.2~97/3	82.7		17.3
3-CH_3, 5-SO_2Cl	100~101/3	78.9		21.1

Results and Discussion

The chemical shifts for the ring protons and for the methyl protons are given in Table II, in c. p. s. at 40 Mc./sec. The values given here are reproducible within the deviation of about 1 c.p.s. Each of the two substituents, methyl and chlorosulfonyl groups, as previously

Table II. The proton magnetic resonance data in methylthiophenesulfonylchlorides, referred to cyclohexane in c. p. s. at 40 Mc./sec.

Substituent	Assignment 2-H	3-H	4-H	5-H	CH_3
2-CH_3, 3-SO_2Cl	—	—	234	226	52
2-CH_3, 4-SO_2Cl	—	226	—	257	44
2-CH_3, 5-SO_2Cl	—	216	247	—	46
3-CH_3, 2-SO_2Cl	—	—	223	250	47
3-CH_3, 4-SO_2Cl	228	—	—	270	44
3-CH_3, 5-SO_2Cl	239	—	247	—	36

1) K. Takahashi, Y. Matsuki, T. Mashiko and G. Hazato, This Bulletin, **32**, 156 (1959).

2) S. Gronowitz and R. A. Hoffman, (a) *Arkiv för Kemi*, **13**, 279 (1958); (b) ibid., **15**, 45 (1959); (c) ibid., **16**, 501 (1960); (d) ibid., **16**, 515 (1960); (e) idid., **16**, 539 (1960); (f) ibid., **16**, 563 (1960); (g) *Acta Chem. Scand.*, **13**, 1687 (1959).

3) W. E. Truce and M. F. Amos, *J. Am. Chem. Soc.*, **73**, 3013 (1951).

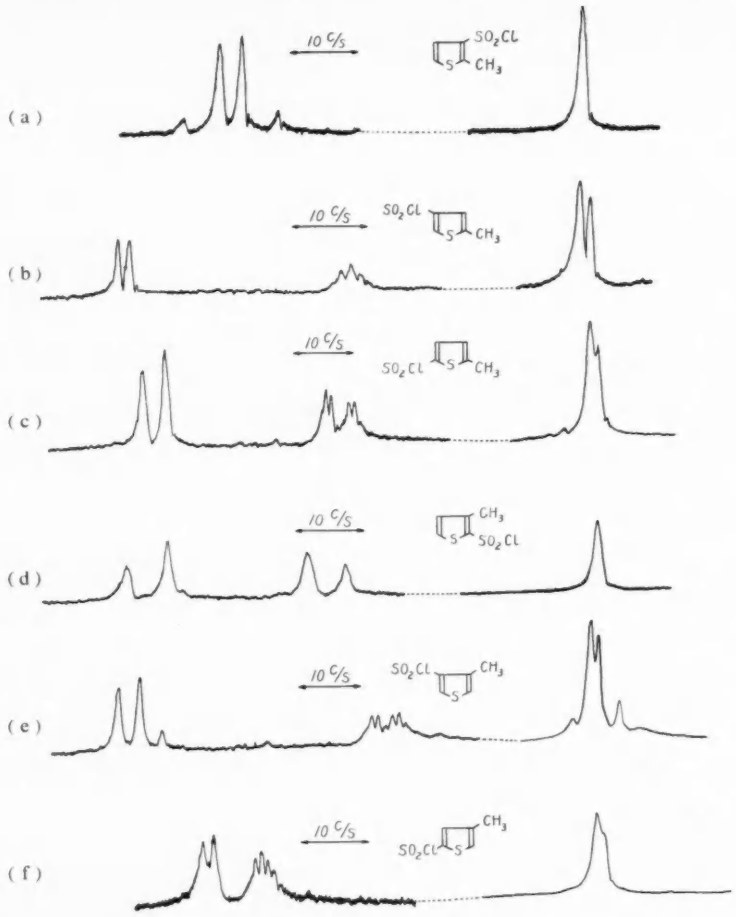

Fig. 1. The proton magnetic resonance spectra at 40 Mc./sec., showing
(a) 2-methyl-3-thiophenesulfonylchloride
(b) 2-methyl-4-thiophenesulfonylchloride
(c) 2-methyl-5-thiophenesulfonylchloride
(d) 3-methyl-2-thiophenesulfonylchloride
(e) 3-methyl-4-thiophenesulfonylchloride
(f) 3-methyl-5-thiophenesulfonylchloride.
Applied magnetic field increases from left to right in all figures. Some extra peaks probably due to the presence of the small isomeric impurities are observed in c, e and f.

reported[1], gives the reverse effect on the chemical shift, so that all spectra here observed can be assigned easily from the standpoint of the chemical shift. In a case where the signal is split by the indirect spin-spin interaction, the shift given in Table II is that for the center of the resonance pattern, so that the difference of the values given for two ring protons in a compound (for example, in 2-methyl-3-thiophenesulfonylchloride, 234 minus 226 equals to 8 c.p.s.) does not equal the true chemical shift for those ring protons, but equals $(J^2+\delta^2)^{1/2}$. The analysis of the two-proton system was reported very early by Hahn and Maxwell[4], and later by Bannerjee, Das and Saha[5]. In this system, the spectrum consists of two

4) E. L. Hahn and D. E. Maxwell, *Phys. Rev.*, **88**, 1070 (1952).
5) M. K. Bannerjee, T. P. Das and A. K. Saha, *Proc. Roy. Soc.*, **A226**, 490 (1954).

doublets; the separation in each doublet just gives the coupling constant between two protons. The disubstituted thiophenes are also the typical model of the two-proton system in which the analysis of the spectrum can be done very easily. But sometimes, as in the case of some methylthiophenesulfonylchlorides, the spectra are somewhat complicated owing to the small interaction between the ring protons and the substituents. The magnitude of the coupling constant for the ring proton and its neighboring methyl protons, as previously reported[1], has the order of about 1.0 c.p.s.; however, the chemical shift between them is more than 170 c.p.s. at 40 Mc./sec. The chemical shifts are here so large compared with the coupling constants ($J/\delta < 0.006$) that the spectra can be analyzed by the simple method of the two-proton system. The results of the simple treatment are given in Table III.

Table III. The coupling constants (J) and the chemical shifts (δ) of two ring protons in methylthiophenesulfonylchlorides in c. p. s. at 40 Mc./sec. Measured conditions are summarized in Table I

Substituent	J	δ
2-CH_3, 3-SO_2Cl	5.3±0.1	6.6±0.1
2-CH_3, 4-SO_2Cl	1.5±0.1	29.5±0.6
2-CH_3, 5-SO_2Cl	4.1±0.1	30.6±0.1
3-CH_3, 2-SO_2Cl	5.2±0.1	26.2±0.1
3-CH_3, 4-SO_2Cl	3.5±0.1	40.2±0.3
3-CH_3, 5-SO_2Cl	1.8±0.1	7.5±0.1

The proton magnetic resonance spectra of the six isomers studied are reproduced in Fig. 1, in which the ring proton spectra are shown at the left-hand side and the methyl proton spectra at the right-hand side. With respect to the ring proton spectra, a and d in Fig. 1 show the typical type of two-proton system; on the other hand, the other figures in Fig. 1 show some small splittings caused by methyl protons. For 2-methyl-3-thiophenesulfonylchloride, each of the two ring proton spectra is a little asymmetric as shown in a of Fig. 1. The doublet at the low field side is somewhat broader than the doublet at the high field side. Similar broadening is observed also in the doublet at the high field side, the 4-proton spectrum in 3-methy-2-thiophenesulfonylchloride, as shown in d of Fig. 1. For 2-methyl-4-, 2-methyl-5-, 3-methyl-4- and 3-methyl-5-thiophenesulfonylchloride, as shown in b, c, e and f in Fig. 1*, the ring proton spectra consist of two doublets. The one at the low field side has a simple structure and the other doublet at the high field side shows the fine structure caused by the interaction with methyl protons. The methyl proton spectra at the higher field side show also a doublet. In these four isomers, the 2-methyl group couples to 3-proton with a coupling constant of 1.1 c. p. s. However, the 3-methyl group couples to 2-proton with the same value but does not couple to 4-proton with the same order of coupling constant. This trend was also obseved in the spectrum of 3-methyl-2-thiophenesulfonylchloride, as shown in d of Fig. 1., in which no resolved fine structure was observed. The interaction between 4-proton and the adjacent methyl group is small. But the spectra of 4-proton are somewhat broader than those of 5-proton in 2-methyl-3- and 3-methyl-2-thiophenesulfonylchloride, as shown in a and d of Fig. 1. Consequently, it can be assumed that 2-methyl or 3-methyl group couples to 4-proton with a small coupling constant but couples to 5-proton with no appreciable constant. Similar results on the long range coupling in thiophene derivatives also have been obtained by others[2f,2g,6].

The coupling constants between two ring protons in the six isomers studied are 5.3 and 5.2 c.p.s. for J_{23}, 4.1 c.p.s. for J_{34}, 3.5 c.p.s. for J_{25}, and, 1.5 and 1.8 c.p.s. for J_{24}, as shown in Table III. The previous assumption[1] that the coupling constants between the ring protons for thiophene derivatives are $J_{23} > J_{34} > J_{25} > J_{24}$, is also consistent with the present observed values. It is very interesting to note that the observed coupling constant between the two protons by way of the sulfur atom (J_{25}) are relatively large, as compared with the meta-coupling constants for the benzene derivatives[7]; this trend is also obtained in thiophene which was analyzed recently by several authors[2b,8,9].

Chemical shifts depend upon the nature and the concentration of the solvents, so that the observation of the solvent effects on the chemical shift in the present compounds has also been made. The measured conditions and the results are summarized in Table IV. Three typical solvents were used, cyclohexane and carbon tetrachloride as nonpolar solvents, and acetone as a polar solvent. The experiment was carried out with the definite dilute solution of the compounds in each solvent, because of the limited amount of the synthesized material

* In c, e and f in Fig. 1, some extra peaks probably due to the presence of small isomeric impurities are observed.

6) P. L. Corio and I. Weinberg, *J. Chem. Phys.*, **31**, 569 (1959).
7) H. S. Gutowsky, C. H. Holm, A. Saika and G. A. Williams, *J. Am. Chem. Soc.*, **79**, 4596 (1957).
8) T. Isobe, *Bull.Chem. Res. Inst. Non-Aqueous Solutions, Tohoku Univ.*, **9**, 115 (1960).
9) R. J. Abraham and H. J. Bernstein, *Can. J. Chem.*, **37**, 2095 (1959).

TABLE IV. DISPLACEMENTS OF THE PROTON RESONANCES WHEN THE SAMPLES ARE DILUTED WITH CYCLOHEXANE, CARBON TETRACHLORIDE AND ACETONE, IN C. P. S. AT 40 Mc./sec., REFERRED TO THE VALUES GIVEN IN TABLE II, MINUS SIGN SHOWING THE DISPLACEMENT TO THE HIGHER FIELD

Substituent	Measured Solution, wt. %				Displacement, c. p. s.				
	Sample	C_6H_{12}	CCl_4	$(CH_3)_2CO$	2-H	3-H	4-H	5-H	CH_3
2-CH_3, 3-SO_2Cl	10.6	89.4			—	—	−1.5	−6.5	−0.5
2-CH_3, 4-SO_2Cl	10.6	83.7	5.7		—	−2.0	—	−5.5	−2.5
2-CH_3, 5-SO_2Cl	8.0	92.0			—	−8.0	−6.0	—	−3.5
3-CH_3, 2-SO_2Cl	11.5	88.5			—	—	−7.5	−10.0	−2.0
3-CH_3, 4-SO_2Cl	12.4	87.6			−8.5	—	—	−7.5	−1.5
3-CH_3, 5-SO_2Cl	11.3	88.7			−9.0	—	−5.0	—	−2.5
2-CH_3, 3-SO_2Cl	6.7	1.9	91.4		—	—	+1.0	−1.5	+2.5
2-CH_3, 4-SO_2Cl	5.0	1.1	93.9		—	0.0	—	−1.5	+1.0
2-CH_3, 5-SO_2Cl	4.4	1.0	94.6		—	−3.0	−1.5	—	+0.5
3-CH_3, 2-SO_2Cl	6.4	1.3	92.3		—	—	−4.0	−5.0	0.0
3-CH_3, 4-SO_2Cl	7.2	3.7	89.2		−5.0	—	—	−3.5	0.0
3-CH_3, 5-SO_2Cl	8.2	2.2	89.6		−3.5	—	−1.5	—	+1.0
2-CH_3, 3-SO_2Cl	14.6	15.4		70.0	—	—	+4.5	+13.5	+3.0
2-CH_3, 4-SO_2Cl	9.1	13.6	5.0	72.3	—	+7.5	—	+16.0	+2.5
2-CH_3, 5-SO_2Cl	12.8	14.5		72.7	—	+8.0	+8.0	—	+4.0
3-CH_3, 2-SO_2Cl	13.2	14.3		72.5	—	—	+7.5	+14.5	+1.5
3-CH_3, 4-SO_2Cl	15.3	14.4		70.3	+13.0	—	—	+12.0	+0.5
3-CH_3, 5-SO_2Cl	14.0	15.1		70.9	+16.0	—	+8.0	—	+2.0

at hand, and a small amount of cyclohexane was used also as an internal reference. One of our aims in this experiment was to find a key for the assignment of the chemical structure by the NMR spectrum. As shown in Table IV, it is clear that, in the six compounds studied, all α-protons are sensitive to the polarity of the solvents as compared with β-protons, notably in the case of the solution in acetone. It should be kept in mind that the self-polarizabilities given by de Heer[10] for α- and β-carbon atoms in thiophene are qualitatively in argreement with the present results of the solvent effect.

The Chemical Institute of
Non-Aqueous Solution
Tohoku University
Katahira-cho, Sendai

10) J. de Heer, *J. Am. Chem. Soc.*, **76**, 4802 (1954).

Proton Magnetic Resonanace Spectra of p-Cresol

By Ichiro YAMAGUCHI

(Received March 28, 1961)

Schaefer and Schneider[1] investigated the ring proton resonance spectra of the *p*-substituted toluene derivatives and obtained many fruitful results concerning the interaction between ring protons and solvent molecules. The present author previously reported an NMR study of several hydrogen-bonded systems[2-5]. In these reports, explanations of the NMR behavior of the ring protons were made when the protons are affected by a change in the hydrogen-bonding situation in the molecule. In the present work, the NMR spectra of *p*-cresol, which gives rather a simple spectrum for the ring protons, were measured in various solutions and the NMR behaviors of methyl, hydroxyl and ring protons were interpreted in terms of hydrogen bond formation.

1) T, Schaefer and W. G. Schneider, *J. Chem. Phys.*, **32**, 1218 (1960).

2) I. Yamaguchi, This Bulletin, **34**, 353 (1961).
3) I. Yamaguchi, ibid., **34**, 744 (1961).
4) I. Yamaguchi, ibid., **34**, 451 (1961).
5) I. Yamaguchi, to be published.

Experimental

The NMR measurements were made with a Varian NMR spectrometer at a resonance frequency of 56.4 Mc./sec. and at a temperature of 20°C. Chemical shifts of methyl, hydroxyl and ring protons from an external reference of water proton were determined by the side band technique and the susceptibility corrections were applied. *p*-Cresol was a guaranteed grade reagent and was purified by distillation. The solvents used were benzene, chloroform, carbon tetrachloride, dioxane, acetone and pyridine. These were purified with a Podobielniak distillator. Solutions with concentrations between 0.02 and 1 mol. fractions were prepared for each solvent.

Results and Discussion

Figure 1 shows the concentration dependence of the chemical shifts of the methyl, hydroxyl and ring protons in carbon tetrachloride solutions. The hydroxyl proton resonance curves show characteristic behavior of each solution as shown in Fig. 2. On the other hand, the methyl and ring proton resonance curves show slight dependence on the solvent. Generally, the resonance fields of the methyl and ring protons decrease on dilution. The greater part of the causes of this inclination can be ascribed to the diamagnetic anisotropy effect of aromatic rings in the solution[6]. The resonance in the ring protons shows an interesting concentration dependence: Pure cresol liquid gives a single line spectrum while it gives a spectrum with a structure in dilute solution, arising from the proton pairs being chemically different from each other.

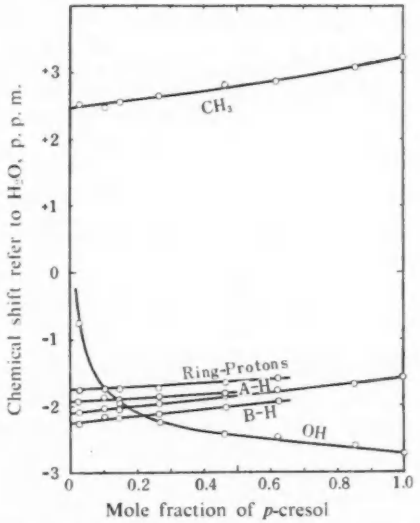

Fig. 1. Concentration dependence of chemical shift for *p*-cresol in CCl_4 solution.

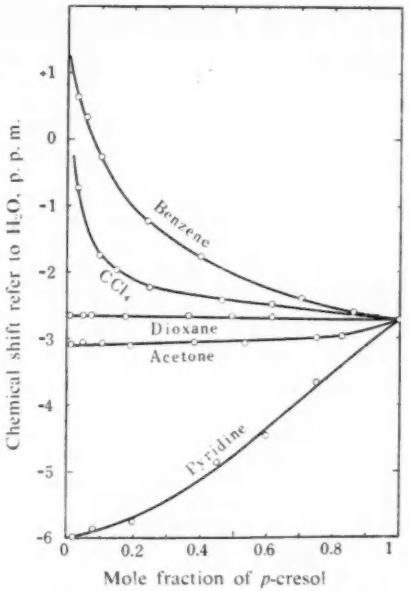

Fig. 2. Concentration dependence of OH proton chemical shift for *p*-cresol in various solutions.

Methyl Proton. — The chemical shift of the methyl protons for benzene and pyridine solutions is apparently independent of the concentration because the net content of aromatic rings in the solutions is almost invariable. Those for the other solutions show the concentration dependence which is characteristic of the anisotropic effect of benzene rings of the solute in these solvents. The dilution shifts are almost the same as those for ring protons in benzene[6]* for the same solutions. The slope of the curve for the acetone solution is smaller than the others and this finding is parallel to the case of the ring protons in benzene. There seemed to be no notable effect of the hydrogen bonding on the methyl proton resonance.

Hydroxyl Proton. — Pure *p*-cresol gives a hydroxyl proton resonance line at slightly lower field than that in pure phenol[7]. This may be caused by the strengthening of the hydrogen bond by the hyperconjugation effect of the *p*-methyl group, although the hydrogen bond energies for the two compounds are comparable

* The curves appeared in Ref. 6 were corrected for the susceptibility of the solutions.

6) A. A. Bothner-By and R. E. Glick, *J. Chem. Phys.*, 26, 1651 (1957).

7) R. L. Batdorf, Ph. D. Thesis, Univ. of Minnesota, 1955.

to each other[8]. The solvent and concentration dependences of the hydroxyl proton resonance are shown in Fig. 2. The curves for benzene, chloroform and carbon tetrachloride solutions show the dissociation process of the hydrogen bond between the solute molecules on dilution. The curves for dioxane, acetone and pyridine solutions suggest new hydrogen bond forms between the solute and the solvents on dilution.

The curves for the carbon tetrachloride solution are as similar as those for phenol in carbon tetrachloride solution[9], exhibiting a representative NMR behavior of the dissociation process of a hydrogen bond system. The curve for the concentration above the concentration of about 0.3 mol. fraction is considered to correspond to the dissociation process of polymer species. In the range below about 0.05 mol. fraction the dissociation of dimer molecules is considered to be dominant. The resonance field for the benzene solution increases simply on dilution. This behavior of the curve is caused by several factors; the dissociation of the associated molecules, the ring current effect of benzene and the hydrogen bond formation with the π-electron system of the solvent molecule. The last may cause the rapid increase of the resonance field on dilution.

In dioxane and acetone solutions, the solute is considered to form a new hydrogen bond with the solvent molecules on dilution while the associated *p*-cresol molecules dissociate. The new hydrogen bonds are probably weaker ones than the intermolecular hydrogen bond of *p*-cresol. This is because the resonances at the infinite dilution are due to a more shielded proton than that in the intermolecular hydrogen bond of *p*-cresol. Pyridine, a strong proton acceptor, appeared to form a strong hydrogen bond with *p*-cresol as suggested by the curve. Pyridine seems to destroy the hydrogen-bonded association or chelation[2] of a compound by its strong proton accepting power.

Ring Proton.—The ring proton resonance in solutions appears at a slightly higher field than those for benzene in respectively the same solvents. This is due to the electron-releasing substituents of methyl and hydroxyl groups in *p*-cresol. *p*-Cresol liquid gives a single resonance line for the ring protons while diluted *p*-cresol with any solvent gives a spectrum with a characteristic structure of the A_2B_2 system[10] as shown in Fig. 1. The slope of the concentration-dependence curves for ring protons is due mainly to the anisotropic effect of the aromatic rings in the solutions. The slope of the curves for B-protons (ortho to methyl group) in chloroform, carbon tetrachloride, dioxane and acetone solutions are slightly gentler than those for benzene in respectively the same solutions[6]. This easier characteristic of the slope may be ascribed to the bulkier molecular size of *p*-cresol compared to that of benzene[11]. Therefore the B-protons can plausibly be assumed to be scarcely affected by the varying situations of the hydrogen bonding but to some effect proper to the proton in an aromatic ring. The slope for A-protons (ortho to hydroxyl group) is much easier than that for the B-protons.

If the effect of the ring current is removed for simplicity's sake from considerations of NMR behavior of the ring protons, the B-proton resonance is nearly independent of the concentration of the solutions, while the A-proton resonance is displaced to a higher field on dilution. The cause of this inclination for the A-protons may be ascribed to some changes in the following effects affected by the hydrogen bond formation; (i) the inductive and mesomeric effects of the hydroxyl group, (ii) the electrostatic field which originated from the hydroxyl bond moment, (iii) effect of magnetic anisotropy of the solvent molecule in the proximity of A-proton, (iv) preferential hydrogen bond formation between A-proton and solvent molecule, and (v) dispersion effect of solvent molecule on the A-proton. The effects (i) and (ii) have their origin in the molecule itself while (iii), (iv) and (v) come from the interaction with the solvent. Since the behavior for the A-proton is common to all solutions, the effects (iii) and (iv) are ruled out. It is difficult to consider a preferential dispersion effect on the A-proton, and the effect (v) is also ruled out. On hydrogen bond formation, the length and the polarization of the O–H bond may increase[12] and hence the electrostatic field at the A-protons originating from the bond moment may be altered. This electric field might cause the displacement of the A-proton resonance. However, the direction of the displacement is to a higher field with increasing bond moment. Therefore, the contribution of the effect (ii) should be small. For this reason, the effect (i) is considered to be dominant to cause the displacement of the resonance in A-proton. With the effect (i), this inclination for the A-protons

8) G. C. Pimentel and A. L. McClellan, "The Hydrogen Bond", Freeman, San Francisco (1960), Appendix B.
9) C. M. Huggins, G. C. Pimentet and J. N. Shoolery, *J. Phys. Chem.*, **60**, 1311 (1956).
10) H. J. Bernstein, J. A. Pople and W. G. Schneider, *Can. J. Chem.*, **35**, 65 (1957); R. E. Richards and T. P. Schaefer, *J. Mol. Spectroscopy*, **2**, 1280 (1958).
11) J. A. Pople, W. G. Schneider and H. J. Bernstein, "High Resolution Nuclear Magnetic Resonance, "McGraw-Hill, New York (1959), p. 426.
12) See for example: A. Burawoy, "Hydrogen Bondnig", Ed. by D. Hadzi, Pergamon Press, New York (1959), p. 259.

TABLE I. CHEMICAL SHIFTS, DILUTION SHIFT, COUPLING CONSTANT AND COALESCENT CONCENTRATION OF RING PROTON SPECTRUM IN *p*-CRESOL

Solvent	δ_{ring} (p. p. m.) conc.=1	conc.=0	Dilution shift (p. p. m.) $\delta_1-\delta_0$	δ_{AB} (c./sec.)	J_{AB} (c./sec.)	Coalese. conc. (mol. fraction)
Benzene	−1.56	−1.46	+0.10	18.6	8.5	~0.2
$CHCl_3$	〃	−2.03	−0.47	16.6	〃	~0.6
CCl_4	〃	−2.03	−0.47	15.3	〃	~0.7
Dioxane	〃	−1.97	−0.41	20.3	〃	~0.8
Acetone	〃	−1.89	−0.33	14.7	〃	~0.6

may be interpreted as follows: On formation of a strong intermolecular hydrogen bond between *p*-cresol molecules, the electron density on the oxygen atom should increase. This dense distribution of the negative charge is supplied from the ring, especially from the ortho-positions by inductive and mesomeric mechanisms. Thus the chemical shift of the A-proton is displaced to a lower field in the concentrated range. This qualitative explanation is plausible for the systems of hydroxyl hydrogen bond so far investigated by the present author[2,3].

Table I gives the chemical shift of the ring proton systems (δ_{ring}) at the concentrations of zero and 1 mol. fractions, the dilution shift ($\delta_1-\delta_0$), the relative chemical shift and the spin coupling constant between A and B protons at infinite dilution, and the concentration where the lines of the spectrum coalesce. Figure 3 shows the position of the spectra of the ring protons schematically for the solutions investigated. The spectrum for benzene solution is displaced to a considerably high field compared to those for the other solutions. This is due to the anisotropic effect of benzene. The B-proton resonance at the infinite dilution for chloroform, carbon tetrachloride and dioxane solutions occur at about the same field in relation to one another, whereas the A-proton resonance for them occurs at fields different from one another. This fact also supports the inactiveness of the B-protons against the change in the environments. The B-proton resonance for acetone solution is the only exception: The resonance occurs at a slightly higher field than for the other solutions mentioned above. The same is observed for the ring protons of benzene in acetone solution[6]. Therefore, the preferential hydrogen bond interaction of an acetone molecule with the B-proton as suggested by Schneider and Schaefer[1] is denied in this case. This discrepancy may partly be attributed to the large dielectric constant of acetone[1].

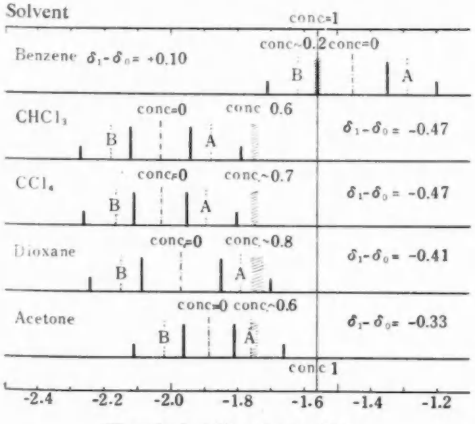

Chemical shift refer to H_2O

Fig. 3. Ring proton spectra for *p*-cresol in various solutions.

In Fig. 3, the field where the resonance lines coalesce to a single line is indicated by a shaded range. It is surprising that the fields are almost the same for all solutions (about −1.74 p.p.m.) except benzene solution although the concentrations are different from one another. The coincidence of the field may have some meaning concerning the structure of the solutions or may rather be an accident. However, in this work, this phenomenon could not be well interpreted with the anisotropic effect of the aromatic rings in the solutions at the coalescent concentration. The single coalesced line in the concentrated range may suggest that only the same species of associated polymers as in pure *p*-cresol exists in this range. In benzene solution, the coalescence occurs at an exceptionally low concentration. This may be ascribed to the poor ability of the benzene molecule to disrupt the hydrogen bonds due to the geometrical similarity of the flat molecular shape of benzene and *p*-cresol.

It may be noted that the resonance fields of the methyl protons at the coalescent concentration for the four solutions are approximately +2.95 p. p. m., and this value is also nearly independent of the solvent. Accompanying the ring proton resonance data, this fact may also supply some information about the structure of the solutions.

Summary

The proton magnetic resonance spectra of *p*-cresol in several solutions were measured. The concentration dependence of the resonance in methyl protons suggests no remarkable effect of the hydrogen bonding on methyl protons. The resonance in the hydroxyl proton shows characteristic concentration dependences which are ascribed to the dissociation of the associated molecule in benzene, chloroform and carbon tetrachloride solutions and to the formation of new hydrogen bonds with solvent in acetone, dioxane and pyridine solutions. The ring proton resonance spectrum is a single line in concentrated range whereas it is an A_2B_2 type spectrum in dilute range. The splitting of the spectrum in dilute solutions is ascribed to the change in the screening of the proton ortho to the hydroxyl group affected by the change in the intermolecular hydrogen-bonding situation. The shielding of the proton ortho to the methyl group appeared to be unaffected by the same change.

Japan Atomic Energy Research Institute
Division of Radiation Applications
Tokai, Ibaraki-ken

Nuclear Magnetic Resonance in Amino-group of Aniline Derivatives

By Ichiro YAMAGUCHI

(Received March 28, 1961)

The association of aniline molecules by their weak hydrogen bonds was suggested by several authors[1,2]. However, the association is still not well ascertained. Nuclear magnetic resonance measurements of aniline derivatives have not yet been made and are expected to give valuable information about the intermolecular hydrogen bond of these compounds and, in connection with the work on dimethyl phenols[3], about the effects of the ortho-methyl group on the proton resonance chemical shift of the amino-group. Thus this paper presents the study of the hydrogen bond of the amino-group by NMR measurements.

Experimental

All the NMR measurements were carried out with a Varian NMR spectrometer at a radio frequency of 56.4 Mc./sec. and at a temperature of 20°C. The compounds investigated were aniline, *o*-, *m*- and *p*-toluidines and 2, 3-, 2, 4-, 2, 5-, 2, 6- and 3, 4-dimethylanilines. These were all guaranteed grade reagents and purified by distillation immediately before making solutions. The solvents used were carbon tetrachloride and acetone. These were purified with a Podobielniak fractional distillator. Solutions with concentrations of between 0.01 and 1 mol. fractions were made for all liquid aniline derivatives. 3, 4-Dimethyl aniline is solid and the concentrations of the solutions measured were up to saturated solution. The chemical shifts from water as an external reference were determined by the side band technique. Corrections for bulk diamagnetic susceptibility of the solutions were made. The values of the volume susceptibility were obtained by applying Pascal's rule and appropriate extrapolations. Their values were 0.676 for aniline, 0.70 for all toluidine isomers and 0.68 for all dimethyl aniline isomers.

Results and Discussion

The concentration dependence of the amino proton resonance for carbon tetrachloride solutions are shown in Fig. 1a and those for acetone solutions in Fig. 1b. Pure aniline derivatives investigated give amino proton resonance at $+1.7 \sim +1.9$ p. p. m. The resonance fields are remarkably higher than those of hydroxyl proton resonance in phenols. Figure 2 shows an example of the concentration dependence of the chemical shifts for dimethyl aniline isomers. The resonance of the amino protons in carbon tetrachloride solutions was a sharp single absorption while that in acetone solutions was generally broad, especially in dilute solutions.

In Fig. 1, curves for the amino protons in various aniline derivatives investigated are observed to fall in a rather narrow field range and apparently there is no notable feature connecting the relative position of the methyl group to the amino group. This fact is remarkably in contrast with the hydroxyl proton resonance of dimethyl phenol isomers[3]. In

1) E. Fischer, *Z. Naturforsch.*, **9a**, 90 (1954); A. E. Lutskii, *Zhur. Obshchei. Khim.*, **26**, 2299 (1956).
2) J. C. Dearden and W. F. Forbes, *Can. J. Chem.*, **38**, 896 (1960).
3) I. Yamaguchi, This Bulletin, **34**, 774 (1961).

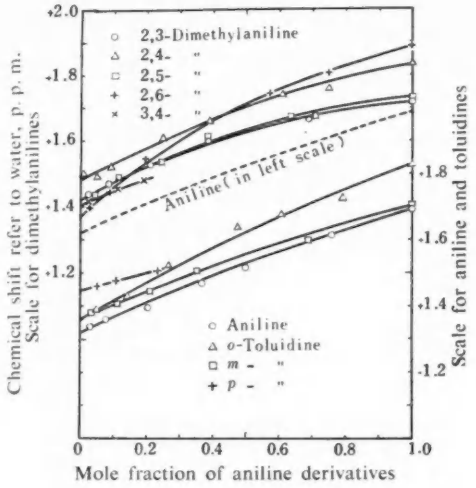

Fig. 1a. Concentration dependence of amino proton chemical shift for aniline derivatives in carbon tetrachloride solution.

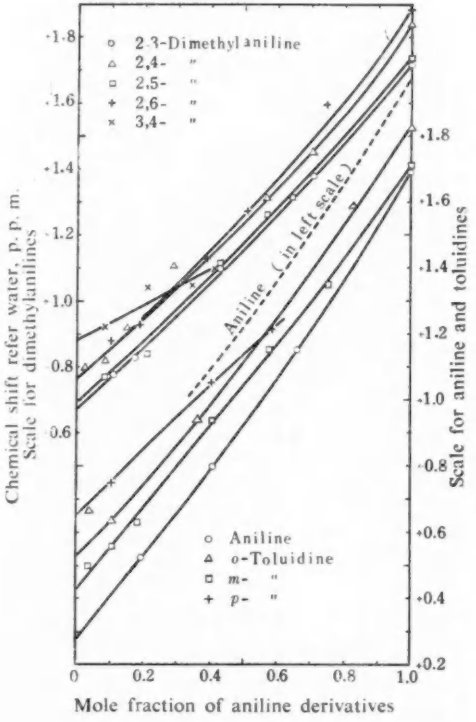

Fig. 1b. Concentration dependence of amino proton chemical shift for aniline derivatives in acetone solution.

this narrow range, the curves for dimethyl aniline isomers appear at the highest field side, those for toluidine isomers at the middle and that for aniline at the lowest side. This order seems to correspond exactly to the order of the base strength of these compounds. The cause of this arrangement of the shifts would mainly be the inductive effect of the methyl groups. In each group of the isomers, the curves for compounds with ortho- or para-methyl group appear at a higher field than those with the meta-methyl group. This result suggests that the mesomeric effect of the methyl group also has an important role to the chemical shift of the amino protons.

Dodd and Stephenson[4] showed a correlation between the basicity of amines and the NH frequency shift in the infrared absorption spectrum caused by hydrogen bond formation between amines and acetone or pyridine. Thus it seems to be natural to expect some correlations between basicity and hydrogen bond shift of proton resonance spectrum of an aniline. Several authors[5,6] pointed out that the basicity of aniline derivatives is strongly dependent on the position and the inductive and mesomeric effects of a substituent in the ring. For example, among *m*- and *p*-toluidines and aniline the base strength of *p*-toluidine is the strongest and that of aniline is the weakest, and this fact was ascribed to the inductive and mesomeric effects of the methyl group. However, the effect of an ortho-substituent on the basicity is not simple because of the additional specific ortho effect[7].

The base strengths of aniline derivatives were reported by several authors[5,7]. Although the pK_a value of a compound reported in one paper is slightly different from that in another, due partly to the solvent and concentration used, the order of the magnitude of the pK_a values is almost the same. The following is the increasing sequence of the pK_a values of aniline derivatives: 3, 4-diMe-, *p*-Me-, 2, 4-diMe-, 3, 5-diMe-, *m*-Me-, 2, 3-diMe-anilines, aniline, 2, 5-diMe-, *o*-Me- and 2, 6-diMe-anilines. The order of the values of the chemical shift in carbon tetrachloride solutions seems to correlate approximately with that of the base strengths of the compounds although some lack of accordance between the two orders is observed. Qualitatively, the factor which

4) R. E. Dodd and G. W. Stephenson, "Hydrogen Bonding", Ed. by Hadzi, Pergamon Press, New York (1959), p. 177.
5) R. N. Beale, *J. Chem. Soc.*, **1954**, 4494.
6) M. Gillois and P. Rumph, *Bull. soc. chim. France*, **1954**, 112.
7) N. F. Hall and M. R. Sprinkle, *J. Am. Chem. Soc.*, **54**, 3469 (1932); G. Thomson, *J. Chem. Soc.*, **1946**, 1113; van Helden et al., *Rec. trav. chim.*, **73**, 39 (1954); B. M. Wepster, ibid., **76**, 357 (1957).

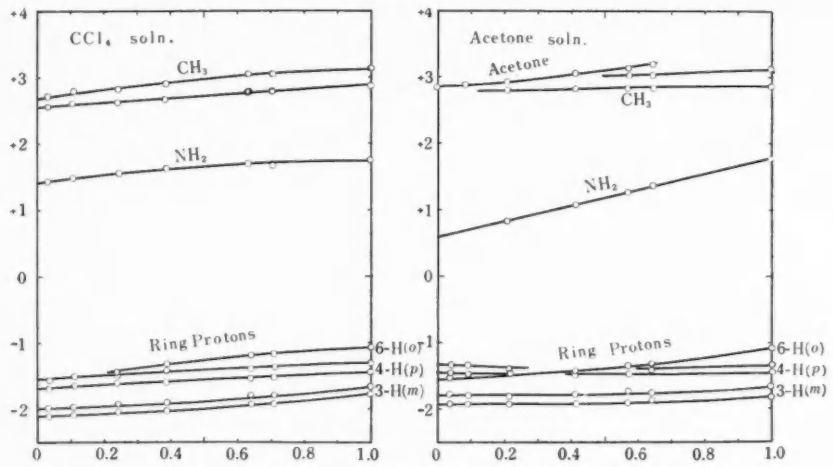

Fig. 2. Concentration dependence of chemical shift for 2,5-dimethyl aniline in carbon tetrachloride and acetone solutions.

determines the base strength of an amine is the charge density on the nitrogen atom[8] and not that on the proton in the amino group. The effective charge density on the nitrogen atom, which has lone pair electrons as well as valence electrons, may be affected in a complicated way rather by changes in the structural and chemical circumstances of the amino-group than by the electronic effect of substituents. Therefore the slight lack of accordance between the order of the proton resonance chemical shifts and that of the base strengths may be observed.

For carbon tetrachloride solutions, the slope of the concentration dependence curve for the amino protons is considerably small and is nearly the same as, but slightly smaller than, that for methyl protons in toluidine and dimethylaniline isomers. The positive slope of the curves is caused by the magnetic anisotropy effect of the aromatic rings in the solutions[9]. If the slope of the curves for methyl protons is assumed to arise merely from the anisotropic effect and if the amino protons are assumed to be affected by the same anisotropic field as that for methyl protons, the curves for the amine protons which are subtracted by the anisotropic effect can be obtained. These curves have a negative slope which might be an indication of a dissociation process of hydrogen bonds on dilution. The association of aniline molecules by intermolecular hydrogen bonds is not well ascertained, although it is, with less confidence, pointed out by several authors with physicochemical measurements[1] and infrared studies[2]. If a hydrogen bond with the same order of strength as an OH hydrogen bond exists between solute molecules, the slope would be more concentration dependent. The slopes which were observed are much smaller than those of dissociation processes of the OH hydrogen-bonded systems. This difference in the NMR behavior between the system might be partly due to the difference between the effective charge in the electronic shielding of the OH group and that of the amino group on formation of hydrogen bonds. It is unfortunate that the data available for estimation of bond energies of the N–H···N hydrogen-bonded systems as well as NMR data for amino protons are very scarce, and at the present stage, no decisive conclusion on the extent of the hydrogen bonding for aniline derivatives can be drawn from the NMR shift data. However, from the knowledge of the NMR measurements so far made with the OH hydrogen-bonded systems, it may be said that the hydrogen-bonded association of aniline derivatives occurs and the strength of it is fairly weak.

For acetone solutions, the effect of the hydrogen bond formation between the solute and the solvent is remarkable and the dilution shifts are large compared with those for carbon tetrachloride solutions. The order of the magnitude of the chemical shifts of the amino protons in acetone solutions is almost the same as that for carbon tetrachloride solutions.

A measure for the ability of the hydrogen

8) See for example: G. W. Wheland, "Resonance in Organic Chemistry", John & Wiley, New York (1955).
9) A. A. Bothner-By and R. E. Glick, *J. Chem. Phys.*, **26**, 1651 (1957).

Table I. Chemical shifts, dilution shifts and Δ value of NH_2 proton in aniline derivatives (in p. p. m.)

Compound	Pure *p*-cresol	CCl_4 soln.		Acetone soln.		Δ
		Concn.=0	$\delta_1-\delta_0$	Concn.=0	$\delta_1-\delta_0$	
Aniline	+1.69	+1.33	0.36	+0.28	1.41	1.05
o-Toluidine	+1.82	+1.37	0.45	+0.53	1.29	0.84
m-Toluidine	+1.71	+1.37	0.34	+0.44	1.27	0.93
p-Toluidine	—	+1.44	—	+0.66	—	0.78
2,3-Dimethyl aniline	+1.72	+1.42	0.30	+0.67	1.05	0.75
2,4-Dimethyl aniline	+1.84	+1.48	0.36	+0.78	1.06	0.70
2,5-Dimethyl aniline	+1.73	+1.43	0.30	+0.68	1.05	0.75
2,6-Dimethyl aniline	+1.88	+1.38	0.50	+0.76	1.08	0.62
3,4-Dimethyl aniline	—	+1.5	—	+0.9	—	0.6

bond formation of a compound, Δ value*, proposed by the present author[10] is listed in Table I for the aniline derivatives investigated. The values of the chemical shift and the dilution shifts for the amino protons in carbon tetrachloride and acetone solutions are also listed in Table I. The magnitudes of the Δ value are about 1 and this value suggests the weakness in the ability of hydrogen bond formation of the compounds. This value nearly corresponds to the ability of 2,6-di-*tert*-butyl-*p*-cresol[10]. The Δ values for aniline and *m*-toluidine are large while that of 2,6-dimethyl aniline is remarkably small. With the data of the dilution shift for carbon tetrachloride solutions, the extent of the hydrogen bond formation of the aniline derivatives is clearly dependent on the existence of the ortho-methyl group.

Among the curves of the amino proton resonance for carbon tetrachloride solutions the behavior of the curves for 2,*x*-dimethyl anilines ($x=3, 4$ and 5) are peculiar as indicated by their small dilution shifts compared with that of 2,6-dimethyl aniline. The value is even smaller than that of *o*-toluidine. Considering the behavior of the curves by subtracting the anisotropic effect of the rings in the solution medium, this peculiarity apparently means that 2,*x*-dimethylanilines ($x=3, 4$ and 5) associate to a higher extent than *o*-toluidine does. However, this intrerpetation can not be accepted from the standpoint of the Δ values of these compounds. This discrepancy may possibly be caused by an additional effect of the *x*-(meta- or para-) methyl group on the amino proton resonance and this effect counterbalances the effect of the ortho-methyl group.

The ring proton spectra for dimethyl aniline isomers show slight concentration dependence. The displacement of the ortho-proton resonance line to a lower field on dilution is observed. The displacement is more remarkable for acetone solutions than for carbon tetrachloride solutions. This inclination is opposed to the behavior of the ortho-proton curves for phenol derivatives[3,11]. On association of aniline derivatives, the charge migration from the ring to the amino group would not be so much as for phenol derivatives because, possibly, the hydrogen bonding is very weak. However, the proton in the amino group is attracted by the proton-accepting group and this results the change in the electrostatic field at the ortho-proton[12]. In this way, the association would cause the displacement of the resonance field of the ortho-proton to a higher field. In acetone solutions, a weak hydrogen bond between the acetone and the ortho-proton would form and the displacement of the ortho-proton resonance to a lower field on dilution is observed as in the case of dimethyl phenols in acetone solution[3].

Summary

Concentration dependenec of the chemical shift of amino protons in aniline derivatives in carban tetrachloride and acetone solutions were measured. The chemical shift of the amino proton in aniline derivatives is revealed to be clearly dependent on the existence of the ortho-methyl group. In carbon tetrachloride solutions, the concentration dependence of the resonance lines is slight, suggesting that the association of the solute molecules by hydrogen bonding is very weak. In acetone solutions, the dependence suggests hydrogen bond formation between solute and acetone. The base strength of aniline derivatives appeared to have no direct correlation with the

10) I. Yamaguchi, This Bulletin, **34**, 451 (1961).

* Δ is defined as the difference between the chemical shift of a hydnogen-bonded proton at infinite dilution for carbon tetrachloride solution and that for an acetone solution.

11) I. Yamaguchi, This Bulletin, **34**, 353 (1961).

magnitude of the chemical shift of amino proton in these compounds. The ring proton spectra of dimethyl aniline are slightly concentration dependent. The resonance in the ortho-protons appears to be displaced to a lower field on dilution and this tendency was ascribed to the change in the electrostatic field at the proton arising from the N–H bond moment change by hydrogen bond formation.

Japan Atomic Energy Research Institute
Division of Radiation Applications
Tokai, Ibaraki-ken

Synthesis and Reactions of Cyano- and Carboxytropones

By Katsuo KIKUCHI

(Received March 20, 1961)

It has been reported that several kinds of cyanotropolones[1-4] can be obtained by the reaction of bromotropolones with cuprous cyanide or with potassium cyanide. In the case of cyanotropone, however, only the synthesis of 2-cyanotropone from 2-bromotropone and cuprous cyanide has been reported.[5]

In the present paper it is shown that several kinds of Grignard reagents react with 3-cyanotropolone (I)[1-4] to give corresponding 2-aryl- or 2-alkyl-7-cyanotropones. In this respect it is interesting to note that the cyano group of I is rather inactive to the Grignard reagents used and that the expected 3-aroyl- or 3-acyltropolones are not obtained.

The reaction of phenylmagnesium bromide and I afforded 7-cyano-2-phenyltropone (IIa) as yellow plates. Proof of the structure of IIa was obtained both by decarboxylation and by decarboxylative bromination of 2-phenyltropone-7-carboxylic acid (VIa) from IIa to yield 2-phenyltropone[6-9] and 7-bromo-2-phenyltropone[8,10], respectively.

Similarly, the reaction of I with α- and β-naphthylmagnesium bromide each afforded 7-cyano-2-α-naphthyltropone (IIb) as yellow needles and 7-cyano-2-β-naphthyltropone (IIc) as yellow plates. A similar reaction of I with methylmagnesium iodide afforded 7-cyano-2-methyltropone (IId) as colorless needles in rather poor yield. The treatment of I with benzylmagnesium chloride, however, resulted in the formation of 2-benzyl-7-cyanotropone (IIe) as yellow needles of m. p. 102°C and yellow prisms (III) of m. p. 145°C, with the latter predominating. The ultraviolet absorption spectra of IIa—IIe are shown in Fig. 1.

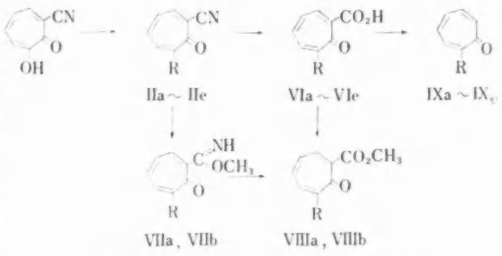

R a, C_6H_5; b, α-$C_{10}H_7$; c, β-$C_{10}H_7$; d, CH_3; e, $C_6H_5CH_2$

III was easily reacted both with concentrated hydrochloric acid and with ethanolic hydrogen chloride to give colorless needles (IV) and colorless prisms (V), respectively. Detailed studies on the structures of III, IV and V are now under way.

The cyanotropones (IIa–IIe) obtained above were easily hydrolyzed with sulfuric acid to give corresponding tropone carboxylic acids. Thus, 2-phenyltropone-7-carboxylic acid (VIa), 2-α-naphthyltropone-7-carboxylic acid (VIb), 2-β-naphthyltropone-7-carboxylic acid (VIc), 2-methyltropone-7-carboxylic acid (VId) and

1) B. J. Abadir, J. W. Cook, J. D. Loudon and D. K. V. Steel, *J. Chem. Soc.*, **1952**, 2350.
2) T. Nozoe, Y. Kitahara and S. Masamune, *Proc. Japan Acad.*, **29**, 17 (1953).
3) T. Nozoe and Y. Kitahara, ibid., **30**, 204 (1954).
4) Y. Kitahara, *Sci. Repts. Tohoku Univ., Ser. I*, **40**, 74 (1956).
5) T. Nozoe, S. Seto and S. Matsumura, *Proc. Japan Acad.*, **28**, 483 (1952).
6) T. Nozoe, T. Mukai and J. Minegishi, ibid., **27**, 419 (1951).
7) W. E. Doering and C. F. Hiskey, *J. Am. Chem. Soc.*, **74**, 5688 (1952).
8) W. E. Doering and J. R. Mayer, ibid., **75**, 2387 (1953).
9) T. Nozoe, T. Mukai, J. Minegishi and T. Fujisawa, *Sci. Repts. Tohoku Univ., Ser. I*, **37** 388 (1953).
10) T. Mukai, ibid., **38**, 280 (1954).

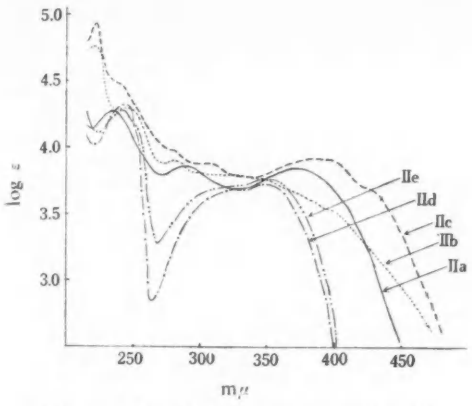

Fig. 1. Ultraviolet absorption spectra of IIa—IIe in methanol.

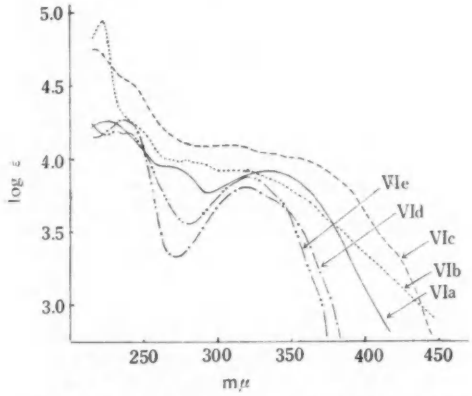

Fig. 2. Ultraviolet absorption spectra of VIa—VIe in methanol.

2-benzyltropone-7-carboxylic acid (VIe) were obtained. The ultraviolet absorption spectra of VIa–VIe are shown in Fig. 2.

When treated with methanolic hydrogen chloride, 7-cyano-2-phenyltropone (IIa) afforded methyl 2-phenyltropone-7-carboximidate (VIIa) as pale yellow needles, the structure of which was ascertained by the hydrolysis of VIIa with dilute hydrochloric acid to give methyl 2-phenyltropone-7-carboxylate (VIIIa). Similar treatment of 7-cyano-2-α-naphthyltropone (IIb) afforded methyl 2-α-naphthyltropone-7-carboximidate (VIIb) as an oil, the hydrolysis of which afforded methyl 2-α-naphthyltropone-7-carboxylate (VIIIb).

Attempted synthesis of formyltropones by Stephen's method did not succeed.

When heated to reflux in acetic anhydride, VIa, VIb and VIc were easily decarboxylated to give 2-phenyltropone (IXa), 2-α-naphthyltropone (IXb)[11] and 2-β-naphthyltropone (IXc)[11] respectively.

The treatment of VIa with 2 mol. equivalents of bromine in acetic acid afforded an acid (X) accompanied with 7-bromo-2-phenyltropone (XI) or with 5, 7-dibromo-2-phenyltropone (XII)[12]. The structures of the latter two compounds were identified by respective admixture with authentic samples.

When heated to its decomposition points, X was submitted to decarboxylation to give yellow needles (XIII). Both X and XIII were converted by bromine in acetic acid to 5, 7-dibromo-2-phenyltropone (XII). This fact indicates that X and XIII are 5-bromo-2-phenyltropone-7-carboxylic acid and 5-bromo-2-phenyltropone, respectively.

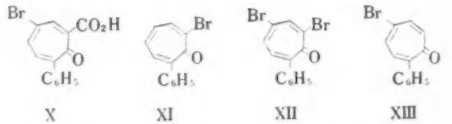

X XI XII XIII

The action of bromine on IIb and IIc gave no satisfactory results.

The action of alkali on 2-phenyltropone-7-carboxylic acid (VIa) was next examined. It was already reported that the action of sodium hydroxide solution on tropone-4-carboxylic acid[12] gave terephthalic acid. The behavior of VIa to alkali, however, was somewhat different. VIa, when heated with dilute sodium hydroxide solution, was easily submitted to rearrangement to form a dibasic acid XIVa of m. p. 217~218°C (decomp.), in good yield. Analysis of XIVa and its dimethyl ester XIVb are in agreement with the formulae $C_{11}H_{12}O_4$ and $C_{16}H_{16}O_4$ respectively. XIVa reduces Fehling's solution and ammoniacal silver nitrate solution. Mild oxidation of XIVa with alkaline-ammoniacal silver nitrate solution gave colorless crystals (XV) which were identified as *o*-biphenylcarboxylic acid. The treatment of XV with concentrated sulfuric acid yielded fluorenone (XVI), which was also obtained directly from XIVa by the action of the same acid under evolution of gas.

XIVa absorbed one mole of hydrogen on palladium-charcoal and on Adam's catalyst to give colorless needles (XVIIa), m. p. 223~225°C (decomp.); dimethyl ester (XVIIb) of XVIIa, m. p. 81~82°C. Analysis of XVIIa and XVIIb are in agreement with the formulae $C_{11}H_{14}O_4$ and $C_{16}H_{18}O_4$, respectively. XVVIIa, when

11) K. Kikuchi, *J. Chem. Soc. Japan, Pure Chem. Sec.* (*Nippon Kagaku Zasshi*), **77** 1439 (1956).
12) J. R. Bartels-Keith, A. W. Johnson and A. Langemann, *J. Chem. Soc.*, **1952**, 4461.

heated above its melting point, gave an anhydride (XVIII) of m. p. 125~127°C, which gave the original acid by sodium carbonate solution. The uptake of two moles of hydrogen by XIVa was difficult, but on one occasion, it was reduced on palladium-charcoal to give a small yield of colorless crystals, m. p. 160~170°C which without further purification, was converted to its dimethyl ester (XIX), m. p. 77~78°C. The analysis of XIX is in agreement with the formula $C_{16}H_{20}O_4$.

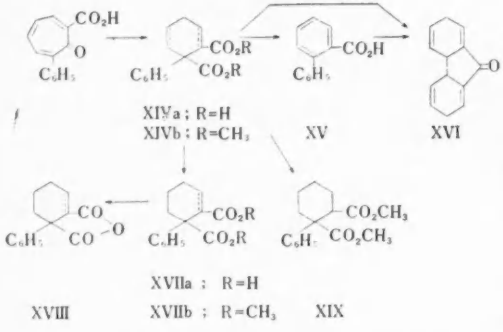

XIVa; R=H
XIVb; R=CH$_3$

XVIIa; R=H
XVIIb; R=CH$_3$

From these facts, it seems almost certain that XIVa is 1-phenylcyclohexadiene-1, 2-dicarboxylic acid but the exact location of double bonds in the cyclohexadiene ring is not clarified yet.

Similar treatment of 2-α-naphthyltropone-7-carboxylic acid (VIb) with dilute sodium hydroxide gave a dicarboxylic acid (XX)($C_{18}H_{14}O_4$) of m. p. 237~238°C (decomp.), which was converted to benzanthrone (XXI) with concentrated sulfuric acid. XX is considered to be 1-α-naphthylcyclohexadiene-1, 2-dicarboxylic acid formed in a manner similar to that in the case of XIVa.

The reaction of 5-bromo-2-phenyltropone-7-carboxylic acid (X) with dilute alkali, however, gave *o*-biphenylcarboxylic acid (XV). The mechanism of its formation is tentatively assumed as follows.

Recently it was reported[13] that the reaction of 4-bromo-2-phenyltropone and 4-mercapto-2-phenyltropone with alkali gave the same *o*-biphenylcarboxylic acid (XV). It seems interesting that the rearrangement of troponoid compounds is accompanied with the formation of hydroaromatic compounds or with the elimination of substituents other than in 2-(i. e. 7-) position.

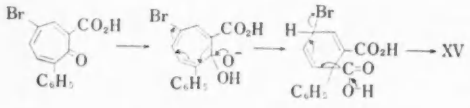

13) T. Muroi, *J. Chem. Soc. Japan, Pure Chem. Sec.* (*Nippon Kagaku Zasshi*), **80**, 303 (1959).

Experimental

7-Cyano-2-phenyltropone (IIa).—To a solution of phenylmagnesium bromide, prepared from 9.6 g. of bromobenzene, 1.7 g. of magnesium and 30 cc. of absolute ether, and subsequently diluted with 40 cc. of anhydrous tetrahydrofuran, was added 3.0 g. of powdered 3-cyanotropolone (I) during 10 min. with stirring. The resulting clear solution was stirred for 2.5 hr. at 45~55°C, decomposed with dilute sulfuric acid and extracted with chloroform. The chloroform solution was washed with water, dried and the solvent was removed by distillation. The yellow crystals thereby obtained were recrystallized from a mixture of benzene and petroleum ether to give yellow plates (IIa), m. p. 134~135°C. Yield, 2.22 g.

Found: C, 80.69; H, 3.89; N, 7.04. Calcd. for $C_{14}H_9ON$: C, 81.14; H, 4.38; N, 6.76%.

7-Cyano-2-α-naphthyltropone (IIb).—To a solution of α-naphthylmagnesium bromide, prepared from 2.8 g. of α-bromonaphthalene, 0.34 g. of magnesium and 5 cc. of absolute ether, was added a solution of 0.5 g. of I dissolved in dehydrated dioxane and was stirred for 7 hr. at 75~80°C. After being left overnight, the reaction mixture was decomposed with dilute sulfuric acid and extracted with chloroform. The chloroform extract was washed with water, dried and the solvent was removed. The residual oil provided 0.34 g. of IIb, m. p. 160~162°C. Recrystallization from benzene gave yellow needles, m. p. 163~164°C.

Found: C, 84.52; H, 4.18; N, 5.78. Calcd. for $C_{18}H_{11}ON$: C, 84.03; H, 4.31; N, 5.44%.

7-Cyano-2-β-naphthyltropone (IIc).—To a solution of β-naphthylmagnesium bromide, prepared from 2.8 g. of β-bromonaphthalene, 0.34 g. of magnesium, a small amount of iodine and 5 cc. of absolute ether, was added a solution of 0.5 g. of I dissolved in dehydrated dioxane, and the reaction mixture was treated as in the case of IIb. The residual oil provided 0.42 g. of IIc, m. p. 177~180°C. Recrystallization from dioxane gave yellow plates, m. p. 180~181°C.

Found: C, 84.51; H, 4.01; N, 5.56. Calcd. for $C_{18}H_{11}ON$: C, 84.03; H, 4.31; N, 5.44%.

7-Cyano-2-methyltropone (IId).—To a solution of methylmagnesium iodide, prepared from 2.56 g. of methyl iodide, 0.5 g. of magnesium and absolute ether and subsequently diluted with dehydrated tetrahydrofuran, was added 0.8 g. of powdered I with stirring. After being stirred for another 4 hr. at 45~50°C, the mixture was treated as in the case of IIa to give 0.12 g. of IId. Recrystallization from ethanol gave colorless needles, m. p. 119~120°C.

Found: C, 74.41; H, 4.66; N, 9.72. Calcd. for C_9H_7ON: C, 74.47; H, 4.86; N, 9.65%.

Reaction of 3-Cyanotropolone (I) and Benzylmagnesium Chloride.—To a solution of Grignard reagent prepared from 3.78 g. of benzyl chloride, 0.75 g. of magnesium and 15 cc. of absolute ether

and diluted with 15 cc. of dehydrated tetrahydrofuran, was added 1.5 g. of I with stirring. The mixture was stirred for another 2 hr. at 45~50°C, decomposed with dilute sulfuric acid and extracted with chloroform. The chloroform extract was washed with water, the solvent was removed under reduced pressure, and 530 mg. of yellow crystals (III) thereby obtained, were collected by filtration. Chromatographic separation of the filtrate over silica gel gave 40 mg. of III and 120 mg. of 2-benzyl-7-cyanotropone (IIe).

IIe was recrystallized from ethanol to give pale yellow prisms, m. p. 101~102°C.

Found: C, 81.16; H, 4.72; N, 6.51. Calcd. for $C_{15}H_{11}ON$: C, 81.43; H, 5.01; N, 6.33%.

III was recrystallized from ethanol to give yellow prisms, m. p. 144~145°C.

Found: C, 79.81; H, 6.22; N, 4.51. Calcd. for $C_{22}H_{19}O_2N$: C, 80.22; H, 5.81; N, 4.25%.

Reaction of Compound (III) and Concentrated Hydrochloric Acid.—The addition of 0.5 cc. of concentrated hydrochloric acid to 100 mg. of III at room temperature gave viscous syrup which soon solidified to colorless crystals. They were collected by filtration and recrystallized from a large amount of *n*-butanol to give colorless microneedles (IV), m. p. 225°C (decomp.).

Found: C, 76.04; H, 6.62; N, 4.24. Calcd. for $C_{22}H_{21}O_3N$: C, 76.06; H, 6.09; N, 4.03%.

Reaction of Compound (III) and Ethanolic Hydrogen Chloride.—The addition of 0.5 cc. of ethanol, saturated with hydrogen chloride, to 100 mg. of III at room temperature yielded a clear solution. After being left for 10 min., the solvent was removed and the crystals that were obtained were recrystallized from ethanol to give colorless prisms (V), m. p. 173~174°C.

Found: C, 76.25; H, 6.98; Calcd. for $C_{24}H_{23}O_3 \cdot N$: C, 76.77; H, 6.71%.

2-Phenyltropone-7-carboxylic Acid (VIa).—A mixture of 1.7 g. of IIa and 17 cc. of 75% sulfuric acid was heated at 140~150°C for one hour and the mixture was poured onto ice. The crystals that separated out were recrystallized from ethanol to give yellow plates, m. p. 107~108°C. Yield, 1.6 g.

Found: C, 74.18; H, 4.47. Calcd. for $C_{14}H_{10}O_3$: C, 74.33; H, 4.46%.

Methyl Ester (*VIIIa*).—Obtained by the reaction of VIa and ethereal diazomethane. Recrystallization from methanol gave yellow needles, m. p. 99~100°C.

Found: C, 74.88; H, 4.87. Calcd. for $C_{15}H_{12}O_3$: C, 74.99, H, 5.03%.

p-Toluidide.—Obtained by the usual method. Recrystallization from ethanol gave orange-yellow crystals, m. p. 121~122°C.

Found: N, 4.56. Calcd. for $C_{21}H_{17}O_2N$: N, 4.44%.

2-α-Naphthyltropone-7-carboxylic Acid (VIb).—Obtained by heating a mixture of 100 mg. of IIb, 1 cc. of 50% sulfuric acid and 1 cc. of glacial acetic acid at 150~160°C for one hour. Recrystallization from ethanol gave orange yellow prisms, m. p. 139~140°C. Yield, 80 mg.

Found: C, 78.01; H, 4.51. Calcd. for $C_{18}H_{12}O_3$: C, 78.25; H, 4.38%.

Methyl Ester (*VIIIb*).—Yellow prisms of m. p. 105~106°C.

Found: C, 78.17; H, 4.72. Calcd. for $C_{19}H_{14}O_3$: C, 78.60; H, 4.85%.

2-β-Naphthyltropone-7-carboxylic Acid (VIc).—Obtained as in the case of VIb. Recrystallization from *n*-butanol gave reddish orange microcrystals, m. p. 189~190°C.

Found: C, 78.17; H, 4.38. Calcd. for $C_{18}H_{12}O_3$: C, 78.25; H, 4.38%.

Methyl Ester.—Yellow plates, m. p. 81~82°C.

Found: C, 78.53; H, 5.07. Calcd. for $C_{19}H_{14}O_3$: C, 78.60; H, 4.85%.

2-Methyltropone-7-carboxylic Acid (VId).—Obtained as in the case of VIa. Recrystallization from ethanol gave colorless plates, m. p. 146~147°C.

Found: C, 65.75; H, 4.72. Calcd. for $C_9H_8O_3$: C, 65.85; H, 4.91%.

2-Benzyltropone-7-carboxylic Acid (VIe).—Obtained as in the case of VIa. Pale yellow needles of m. p. 128~129°C.

Found: C, 74.76; H, 4.75. Calcd. for $C_{15}H_{12}O_3$: C, 74.99; H, 5.03%.

Methyl 2-Phenyltropone-7-carboximidate (VIIa).—A mixture of 100 mg. of IIa and 2 cc. of absolute methanol was saturated with dry hydrogen chloride under ice-chilling, and the resulting clear red solution was left overnight at 0°C. Benzene and water were added successively to the solution, and the aqueous layer was neutralized cautiously with cold dilute aqueous solution of sodium carbonate. The crystals that separated out were collected by filtration, yield 70 mg. Recrystallization from ether gave pale yellow needles (VIIa) m. p. 85~86°C.

Found: N, 6.04. Calcd. for $C_{15}H_{13}O_2N$: N, 5.85%.

Picrate.—Reddish orange prisms, m. p. 141~142°C.

Found: N, 12.03. Calcd. for $C_{21}H_{16}O_9N_4$: N, 11.96%.

Acid Hydrolysis of VIIa.—A solution of 30 mg. of VIIa in 2 N hydrochloric acid was warmed on a water bath for 10 min. and cooled. The crystals that separated out were collected by filtration and recrystallized from methanol to give yellow crystals, m. p. 98~100°C. These crystals showed no depression of melting point on admixture with VIIIa.

Methyl 2-α-Naphthyltropone-7-carboximidate (VIIb).—Similar treatment of IIb as in the case of IIa provided VIIb as an oil which could not be solidified. This oil was subjected to acid hydrolysis with 2 N hydrochloric acid by which yellow crystals, m. p. 105~106°C were obtained. These crystals showed no depression of melting point on admixture with VIIIb.

Decarboxylation of 2-Phenyltropone-7-carboxylic Acid (VIa).—A solution of 50 mg. of VIa in 0.5 cc. of acetic anhydride was heated to reflux for 1.5 hr., shaken with water to decompose the acetic anhydride and extracted with benzene. The benzene extract was washed with 2 N sodium carbonate and water, dried and the solvent was evaporated. The pale yellow crystals (IXa) m. p. 82~83°C thereby obtained showed no depression of melting point on admixture with 2-phenyltropone.

Decarboxylation of 2-α-Naphthyltropone-7-carboxylic Acid (VIb).—Treatment of VIb similar to that in the case of VIa yielded pale yellow crystals m. p. 110°C which showed no depression of melting point on admixture with an authentic sample of 2-α-naphthyltropone (IXb).

Decarboxylation of 2-β-Naphtyltropone-7-carboxylic Acid (VIc).—Treatment of VIc similar to that in the case of VIa yielded pale yellow crystals of m. p. 132~134°C, undepressed on admixture with an authentic sample of 2-β-naphthyltropone (IXc).

Bromination of VIa.—a) To a solution of 50 mg. of VIa in 0.5 cc. of acetic acid was added 70 mg. of bromine. After standing for 5 hr. the whole was heated for 10 min. on a water bath, diluted with water and extracted with benzene. The benzene extract was washed with dilute sodium carbonate solution and the aqueous layer was acidified with dilute hydrochloric acid by which 30 mg. of 5-bromo-2-phenyltropone-7-carboxylic acid (X) was obtained as yellow needles. Recrystallization from ethanol raised the melting point to 174~175°C (decomp.).

Found: C, 55.10; H, 3.11. Calcd. for $C_{14}H_9O_3Br$: C, 55.11; H, 2.96%.

The benzene layer was washed with water, dried and the solvent was evaporated. Residual oil provided some crystals on standing which were recrystallized from cyclohexane to give pale yellow plates (XI), m. p. 78~80°C. These crystals showed no depression of melting point on admixture with 7-bromo-2-phenyltropone.

b) Similar treatment of 50 mg. of VIa with 70 mg. of bromine, except when heating was prolonged to one hour, afforded 20 mg. of X and several milligrams of pale yellow needles (XII) m. p. 131~132°C, which showed no depression of melting point on admixture with 5, 7-dibromo-2-phenyltropone.

Decarboxylation of X.—Acid (X), when heated to its melting point and subsequently sublimed under reduced pressure, was easily decarboxylated to give 5-bromo-2-phenyltropone (XIII). Recrystallization from ethanol gave pale yellow needles, m. p. 130~131°C.

Found: C, 59.34; H, 3.17. Calcd. for $C_{13}H_9OBr$: C, 59.79; H, 3.47%.

Bromination of X.—To a solution of 40 mg. of X in acetic acid was added 40 mg. of bromine and the mixture, after standing for one hour, was heated on a water bath for one hour, diluted with water and extracted with benzene. The benzene extract was washed successively with water, 2 N sodium carbonate and water, and the solvent was removed. The crystals thereby obtained were recrystallized from ethanol to give yellow needles (XII), m. p. 130~131°C, with undepressed melting point on admixture with 5, 7-dibromo-2-phenyltropone (XII).

Bromination of XIII.—To a solution of 30 mg. of XIII dissolved in 0.5 cc. of acetic acid was added 50 mg. of bromine and the mixture was allowed to stand for two days. The mixture was then diluted with water, extracted with benzene and the benzene solution was washed successively with water, 2 N sodium carbonate and water. The residual oil, obtained upon removal of the solvent, was heated on a water bath for 30 min. and cooled. The crystals thereby obtained were repeatedly recrystallized from ethanol to give yellow crystals (XII) m. p. 127~130°C, with undepressed melting point on admixture with 5, 7-dibromo-2-phenyltropone.

Reaction of VIa and Alkali.—A solution of 100 mg. of VIa dissolved in 1 cc. of 1 N sodium hydroxide was heated on a water bath for an hour, treated with active charcoal and then acidified with 2 N hydrochloric acid by which 80 mg. of 1-phenylcyclohexadiene-1, 2-dicarboxylic acid (XIVa) was obtained. Recrystallization from dilute ethanol gave colorless prisms, m. p. 216~217°C (decomp.).

Found: C, 68.60; H, 4.96. Calcd. for $C_{14}H_{12}O_4$: C, 68.84; H, 4.95%. Neutral equivalent as a dibasic acid, 122; Found. 126.

These crystals gradually reduced Fehling's solution and the ammonical silver nitrate solution.

Dimethyl Ester (XIVb).—Obtained by the reaction of XIVa and ethereal diazomethane. Recrystallization from methanol gave colorless prisms, m. p. 95~96°C.

Found: C, 70.41; H, 5.64. Calcd. for $C_{16}H_{16}O_4$; C, 70.57; H, 5.92%.

Oxidation of XIVa.—A solution of 50 mg. of XIVa dissolved in 1.5 cc. of alkaline-ammoniacal silver nitrate solution (prepared by dissolving 0.3 g. of silver nitrate in 3 cc. each of concentrated aqueous ammonia and 10% sodium hydroxide solution) was heated on a water bath for 30 min. After removal of the precipitate that formed, the filtrate was acidified and the crystals that separated out were collected by filtration. Recrystallization from dilute ethanol gave colorless prisms (XV), m. p. 108~109°C. Treatment of XV with concentrated sulfuric acid at room temperature yielded crystals (XVI), m. p. 80~82°C. XV and XVI were identified as *o*-biphenylcarboxylic acid and fluorenone, respectively, by the mixture melting point determination.

Action of Concentrated Sulfuric Acid on XIVa.—Addition of 0.3 cc. of concentrated sulfuric acid to 30 mg. of XIVa at room temperature resulted in deep reddish purple solution under evolution of gas. After being warmed slightly on a water bath, the reaction mixture was poured onto crushed ice. The crystals that separated out were collected by filtration and recrystallized from dilute ethanol to give yellow prisms (XVI), m. p. 80~82°C, with undepressed melting point on admixture with fluorenone.

Catalytic Reduction of XIVa.—a) A solution of 250 mg. of XIVa dissolved in 10 cc. of methanol was catalytically reduced at ordinary temperature and pressure, with the addition of 30 mg. of Adam's catalyst. Absorption of hydrogen was 35 cc. After removal of the catalyst by filtration, methanol was removed, and the crystalline residue was recrystallized from methanol to give colorless needles (XVIIa) of m. p. 223~224°C (decomp.). Yield, 100 mg.

Found: C, 67.77; H, 5.53. Calcd. for $C_{14}H_{14}O_4$; C, 68.28; H, 5.73%.

Dimethyl Ester (XVIIb).—Colorless needles, m. p. 81~82°C.

Found: C, 69.68; H, 6.25. Calcd. for $C_{16}H_{18}O_4$: C, 70.05; H, 6.61%.

Anhydride (XVIII).—Acid (XVIIa) was heated above its melting point for one minute and cooled. The crystalline mass was recrystallized from methanol to give colorless needles of m. p. 125~127°C.

Found: C, 72.71; H, 5.17. Calcd. for $C_{14}H_{12}O_3$: C, 73.67; H, 5.30%.

b) A solution of 150 mg. of XIVa dissolved in 5 cc. of methanol was catalytically reduced at ordinary temperature and pressure, with the addition of 100 mg. of palladium-charcoal (5%). The absorption of hydrogen was about 30 cc. After removal of the catalyst by filtration, methanol was removed, and the crystalline residue was washed with a small amount of ether. These crystals of m. p. 160~170°C were, without further purification, converted to their dimethyl ester (XIX) by the action of ethereal diazomethane. Recrystallization from methanol gave colorless prisms, m. p. 77~78°C. These crystals showed depression of the melting point on admixture with XVIIb.

Found: C, 69.88; H, 7.13. Calcd. for $C_{16}H_{20}O_4$: C, 69.54; H, 7.30%.

Reaction of 2-α-Naphthyltropone-7-carboxylic Acid (VIb) and Alkali.—Similar treatment of VIb as in the case of VIa gave 1-α-naphthylcyclohexadiene-1, 2-dicarboxylic acid (XX) as colorless prisms, m. p. 237~238°C (decomp.).

Found: C, 73.68; H, 5.00. Calcd. for $C_{18}H_{14}O_4$: C, 73.46; H, 4.80%.

Action of Sulfuric Acid on XX.—Similar treatment of XX with concentrated sulfuric acid as in the case of XIVa gave yellow needles (XXI), m. p. 169~170°C, with undepressed melting point on admixture with benzanthrone.

Reaction of 5-Bromo-2-phenyltropone-7-carboxylic Acid (X) and Alkali.—A solution of 20 mg. of X dissolved in 0.4 cc. of 1 N sodium hydroxide was heated for one hour on a water bath and acidified with dilute hydrochloric acid. The crystals thereby obtained were collected by filtration and recrystallized from ethanol to give colorless crystals (XV), m. p. 105~108°C, with undepressed melting point on admixture with *o*-biphenylcarboxylic acid. By treatment with concentrated sulfuric acid, XV was converted to fluorenone (XVI) and identified by mixture melting point determination.

The author wishes to express his sincere thanks to Professor Tetsuo Nozoe of Tohoku University for his guidance and encouragement throughout this work, as well as to Professor Shuichi Seto, Professor Yoshio Kitahara and Assistant Professor Toshio Mukai of Tohoku University for their kind advice and suggestions. He is also grateful to Mrs. Kuniko Kodaira for the measurements of ultraviolet absorption spectra and to Mr. Shinichi Ohyama and Miss Ayako Iwanaga for the elemental analyses.

Department of Chemistry
Faculty of Liberal Arts and Science
Yamagata University
Yamagata

Infrared and Raman Spectra of Dialkoxymethanes in Various Phases and the Assignment of Spectra of Methoxyethoxymethane

By Kenkichi NUKADA

(Received March 23, 1961)

The study of internal rotation around the C–C bond has been carried out in great detail by several authors[1], but detailed discussion of that arround the C–O bond has not been carried out so far.

In this paper, the rotational isomerism of compounds containing two C–O bonds such as dialkoxymethanes ($R_1OCH_2OR_2$) is discussed from the spectroscopical point of view. Infrared spectra of vapor, liquid and solid phases and Raman spectra of liquid phase were obtained, and the possible interpretation of these results was given by referring to other available data such as dipole moment.

With the conclusion thus obtained, the assignments of vibrational frequencies of dimethoxymethane and diethoxymethane are reported in the other papers[2,3], and that of methoxyethoxymethane is presented in this paper.

Experimental

The samples used were dimethoxymethane (DMM, $CH_3OCH_2OCH_3$), methoxyethoxymethane

1) S. Mizushima, "Structure of Molecules and Internal Rotation", Academic Press, New York (1954).

2) K. Nukada, *Spectrochim. Acta*, to be published.

3) K. Nukada, This Bulletin, to be published.

(MEM, $CH_3OCH_2OC_2H_5$), diethoxymethane (DEM, $C_2H_5OCH_2OC_2H_5$) and diisopropoxymethane (DPM, $(CH_3)_2CHOCH_2OCH(CH_3)_2$). All the compounds were synthesized in our laboratory and their purity was checked by gas chromatography[4,5].

Infrared spectra of vapor and liquid phases were obtained by means of Perkin Elmer 21 spectrophotometer and those of solid phase were obtained by means of Perkin Elmer 12C spectrophotometer, both equipped with a sodium chloride prism. Infrared spectra at an elevated temperature were obtained with a gas celll designed and constructed by Mr. H. Tomita of our laboratory[6]. Because dialkoxymethanes are rapidly decomposed at high temperature by oxygen in air, care should be taken to remove oxygen as completely as possible from a gas cell in a high temperature experiment. Solid infrared spectra were obtained with a low temperature cell designed by us[7].

Raman spectra were taken by means of Cary 81 spectrophotometer. The degree of depolarization was measured by wrapping two types of polaroids around a Raman tube.

Results and Discussion

Infrared Spectra of Dimethoxymethane in Various Phases. — The spectra of vapor and liquid phases are shown in Fig. 1a.

The intensity of vapor bands at 1235 and 1110 cm^{-1} shows an appreciable decrease as compared with that of liquid bands. Of these, the liquid band at 1110 cm^{-1} is known as a branch of "methylal's doublet", and it is a remarkable fact that in vapor phase a branch of the doublet turns to be a shoulder. As will be described in the following section and in the other paper[8], in other dialkoxymethanes and in ethylidene dialkyl ethers ($R_1OCH(CH_3)OR$) the smae behavior of spectra were also observed.

The low temperature infrared spectra are shown in Fig. 1b. It was found that two types of spectra are obtained at low temperature below melting point. It is dependent upon

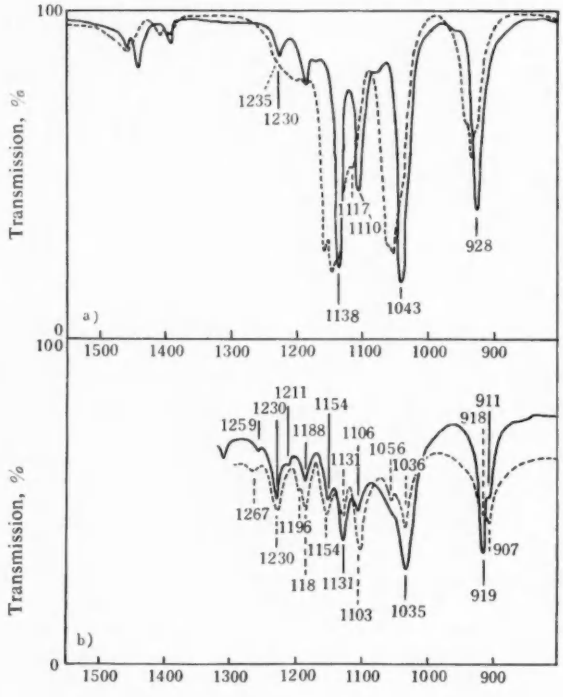

Fig. 1. Infrared spectra of dimethoxymethane ($CH_3OCH_2OCH_3$).

a) Solid line, CCl_4 solution, cell thickness: 0.15 mm., 1.5%. Dashed line, vapor
b) Solid line, Type A spectrum of solid phase. Dashed line, Type B spectrum of solid phase

4) K. Nukada, *Reports Govn. Chem. Ind. Research Inst. Tokyo*, 55, 92 (1960).
5) K. Nukada, ibid., to be published.
6) H. Tomita, unpublished.
7) K. Nukada, *J. Chem. Soc. Japan, Pure Chem. Sec.* (*Nippon Kagaku Zasshi*), 80, 218 (1959).
8) K. Nukada, This Bulletin, to be published.

the critical condition of freezing the material. An example of freezing procedure is as follows: After cooling gradually, spectrum A (solid line in Fig. 1b) was obtained at −150°C, then after once melting and cooling again, spectrum B (dashed line in Fig. 1b) was obtained at −134°C. The last procedure was repeated and spectrum B was obtained again. After once melting and cooling again, spectrum A was obtained at −135°C. Lastly, on raising the temperature, spectrum B was obtained at −110°C. It is not clear at present that the difference of these spectra is due either to the difference of crystallized states between two types of solid phase, or is due to the fact that one of them is in a super-cooled state. Spectrum A is more similar to that of the solution except for the band at 1230 cm^{-1}, the relative intensity of which is greater than that of liquid phase spectrum, and for new bands at 1259, 1211, 1051 and 911 cm^{-1}, appearing as shoulders. Spectrum B is, on the other hand, quite different from that of the solution, that is, the intensity ratio of the band at 1131 cm^{-1} to one at 1103 cm^{-1} changes appreciably.

From these results the following assumption seems to be possible. In DMM, two rotational isomers exist, namely α and β forms. The bands at 1138 1043 and 928 cm^{-1} are due to vibrations belonging to the α form, and the bands at 1230 and 1110 cm^{-1} are due to vibrations belonging to the β form. If this assumption is true, both forms are mixed moderately in liquid phase and the α form exists predominatingly in vapor phase. In solid phase, both forms are still mixed but the abundance ratio of the two forms changes as compared with that in the case of the liquid phase, that is, the β form is more predominant. The possible forms may be gauche-gauche form (or less polar form), two methyl groups of which rotate about 120° from the central OCO plane in an anticlockwise sence, and trans-trans form (or more polar form), the COCOC skeleton of which is planar.

If this assumption is ture,

1) The dipole moment of vapor and liquid phase should be considerably different at room temperature,

2) Some solvent effect is expected since the dipole moments of two isomers are considerably different, and

3) The appearance of the vapor spectrum should change to some extent with increasing temperature.

In the following description, the abovementioned assumption is examined by checking these three items in detail.

1) In his prewar paper, Kubo illustrated the diagram showing the correlation between dipole moment and azimuthal angles of rotation of methyl groups in DMM[9]. From this diagram together with the observed value of dipole moment, Kubo has concluded that in the vapor phase DMM has one stable configuration, in which two methyl groups rotate to the opposite sides of central OCO plane (gauche-gauche form). Recently, Uchida et al. measured the dipole moment of DMM in liquid phase at 25°C (0.67D) and found that it is in good agreement with the value of vapor extrapolated to 25°C (0.69D)[10]. Uchida et al. has concluded that DMM is a mixture of rotational isomers, most of which is helical or almost helical in structure (gauche-gauche form). These results lead to a definite conclusion that at least at room temperature, the abundance ratio of isomers are, if they exist, almost equal in vapor and liquid phases.

Therefore, the cause of appreciable change between infrared spectra of vapor and condensed phases is not due to the change of abundance ratio of isomers between two phases, but due to some other kind of effect such as the change of intermolecular interaction between two phases.

2) In Fig. 2, the infrared spectrum of acetonitrile solution of DMM is shown. As acetonitrile is a very polar solvent (dielectric constant of which is 38), there must be some systematic change of spectra between acetonitrile solution and non-polar solvent solution, if the rotational isomerism actually exists in solution. From Fig. 2, the ratio of absorbance of the band at 1140 cm^{-1} to that of the band at 1111 cm^{-1} (K_{1140}/K_{1111}) is calculated to be 0.374.

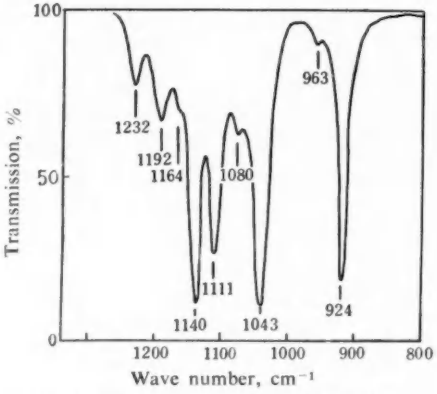

Fig. 2. Infrared spectrum of dimethoxymethane ($CH_3OCH_2OCH_3$). Acetonitrile solution, cell thickness: 0.015 mm., 20%.

9) M. Kubo, *Sci. Papers Inst. Phys. Chem. Research*, **29**, 179 (1936).

10) J. Uchida, Y. Kurita and M. Kubo, *J. Polymer Sci.*, **19**, 365 (1956).

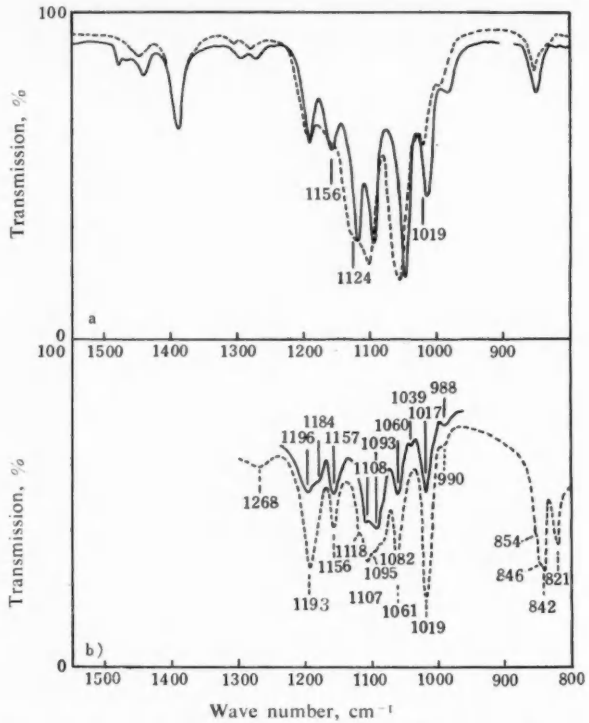

Fig. 3. Infrared spectra of diethoxymethane ($C_2H_5OCH_2OC_2H_5$).

a) Solid line, CCl_4 and CS_2 solutions, cell thickness: 0.15 mm., 2%. Dashed line, vapor.
b) Solid phase spectra, solid line, cell thickness: 0.015 mm. Dashed line, cell thickness: 0.05 mm.

The ratio is also calculated to be 0.331 in the case of carbon tetrachloride solution. Though it is impossible to obtain such a ratio in the case of vapor (Fig. 1a), it is clear that is has a very high value. Hence if these two bands belong to another type of rotational isomers, a more polar form must be predominant in the vapor phase, but this is inconsistent with the measurement of dipole moment[9]. From these considerations, it is reasonable to assume that these two bands belong to the same type of isomers.

3) Vapor spectra of DMM were taken at the temperature range between 24 and 100°C. No change in the appearance of the spectra was observed. The dipole moment of the vapor varies with the temperature as mentioned by Uchida et al., and they have explained this as the change of abundance ratio between isomers with temperature variation[10]. The present observation seems to be inconsistent with the conclusion of them. The most reasonable interpretation to make a compromise between the results of infrared spectra and those of dipole moment is as follows. This molecule has one form (gauche-gauche form) below 100°C, both in the vapor and liquid phases. The variation of dipole moment with temperature is due to the increase of amplitude of torsional oscillation, while the change of appearance of spectra among three phases is due to the change of intermolecular interaction.

As will be described in detail in the other papers[2,3], the change of band intensity among different phases is sometimes a useful measure in assigning spectra. One example is as follows. If an infrared band is strong in the liquid phase but weak in the vapor phase and the corresponding Raman band is strong and polarized, this band is safely assigned to a totally symmetrical vibration. The change of band intensity between vapor and liquid phases is also observed in the case of DMM-d_2 ($CH_3 \cdot OCD_2OCH_3$), DMM-d_6 ($CD_3OCH_2OCD_3$), DMM-d_8 ($CD_3OCD_2OCD_3$), DEM and DEM-d_2 ($C_2H_5OCD_2OC_2H_5$). The author has found that in all cases the above-mentioned rule can be used in the assignment of spectra.

Infrared and Raman Spectra of Diethoxymethane in Various Phases. — Since DEM has four internal rotational axes, a possible number of rotational isomers may be larger than that of DMM. But from the spectroscopical point of view, isomers concerning C–ethoxy axes are important and those concerning C–C axes are less important.

In Fig. 3a, infrared spectra of vapor and liquid phases of DEM are shown. As in the case of DMM, the appearance of spectra is rather different between two phases, that is, the intensity of vapor bands at 1156, 1124 and 1019 cm^{-1} shows an appreciable decrease as compared with those of liquid phase spectra.

Solid infrared spectra of DEM are shown in Fig. 3b. Just as in the case of DMM, two types of spectra, namely A and B, are observed according to the slight change of the critical condition of freezing the material. In the type A spectrum, the intensity of the bands at 1193, 1019, 842 and 821 cm^{-1} shows an appreciable increase and that of the band at 1095 cm^{-1} shows a decrease as compared with those of carbon tetrachloride solution. The appearance of the type B spectrum is similar to that of the carbon tetrachloride solution, except for the doublet at 1100 cm^{-1}.

In Fig. 4, the infrared spectrum of acetonitrile solution is shown. There exists no difference between the spectra of carbon tetrachloride and of acetonitrile solutions.

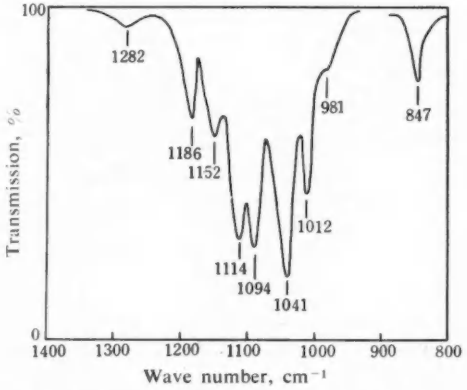

Fig. 4. Infrared spectrum of diethoxymethane ($C_2H_5OCH_2OC_2H_5$). Acetonitrile solution.

In Fig. 5, Raman spectra of carbon tetrachloride and acetonitrile solutions of DEM are shown. The intensity of the band at 1047 cm^{-1} increases and that at 1187 cm^{-1} decreases in acetonitrile solution. There is, however, no other experimental evidence that the former band belongs to the more polar form and the latter to the less polar form, hence the intensity change is probably due to simple solvent effect, that is, is due to the difference of intermolecular interaction between two kinds of solutions.

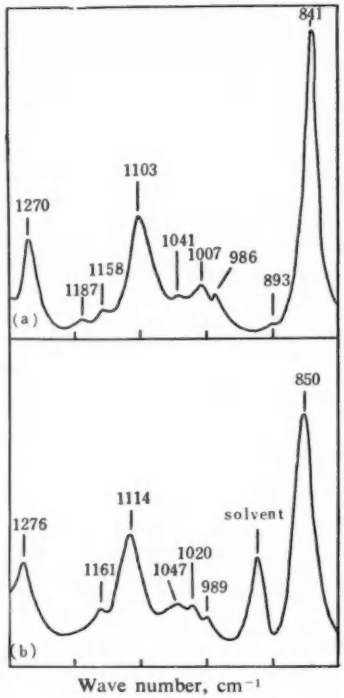

Fig. 5. Raman spectra of diethoxymethane ($C_2H_5OCH_2OC_2H_5$).

a) Pure liquid.
b) Acetonitrile solution (60%).

Vapor spectra of DEM were taken at the temperature range between 24 and 100°C. As no change was observed in the appearance of spectra within the temperature range, DEM has almost one and the same form in vapor phase below 100°C.

According to the measurement of Kubo, dipole moment of DEM is, in vapor phase, 1.22D at 56°C and slightly increases with rising temperature (1.26D at 203°C). Kubo has concluded that this molecule has one stationary form in vapor and that the difference of dipole moment between DMM and DEM (0.5D) is due to the difference of azimuthal angles of alkyl groups from the central OCO plane[11]. Since there is no dipole measurement on liquid phase the molecular structure of DEM of liquid phase is not clear, but from the analogy

11) M. Kubo, *Sci. Papers Inst. Phys. Chem. Research*, **30**, 169 (1936).

with DMM one could assume that the molecular form is the same both in vapor and liquid phases (nearly gauche-gauche form, but that the azimuthal angles of ethyl groups from central OCO plane are smaller than those of methyl groups in DMM), and that the change of appearance of spectra among different phases is dependent on the difference of intermolecular interaction. The detail of assignment will be reported elsewhere[3].

Infrared Spectra of Methoxyethoxymethane in Various Phases.—In Figs. 6 and 7, infrared spectra of vapor, liquid and solid phases of MEM are shown.

The vapor bands at 1131 and 926 cm^{-1} become weaker as compared with the liquid bands, and the doublet at 1112 cm^{-1} (and 1096 cm^{-1}) in the liquid phase is distorted in the vapor phase,that is, it becomes singlet in the vapor phase. The solid bands at 1218 cm^{-1} and 1013 cm^{-1} become much stronger and one at 1135 cm^{-1} becomes weaker as compared with the liquid bands.

It is quite hard, as in the case of DMM and DEM, to interpret such a complicated change of spectra among various phases as the change of abundance ratio of the rotational isomers. It is better to assume that from the analogy of

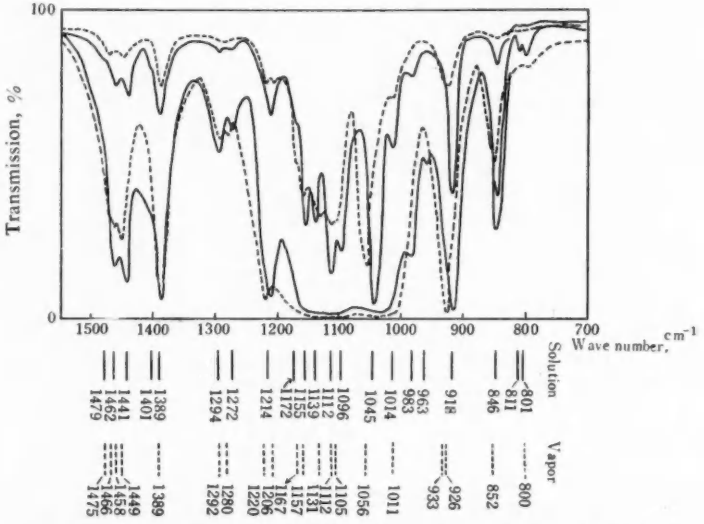

Fig. 6. Infrared spectra of methoxyethoxymethane ($CH_3OCH_2OC_2H_5$).
Solid line, CCl_4 and CS_2 solutions, cell thickness: 0.15 mm., 20% and 2%. Dashed line, vapor.

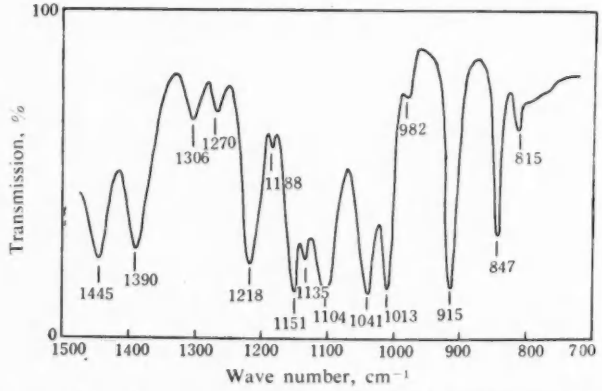

Fig. 7. Infrared spectrum of methoxyethoxymethane ($CH_3OCH_2OC_2H_5$).
Solid, cell thickness: 0.015 mm.

DMM, MEM has also one form in the liquid and vapor phases at least near room temperature. If the dipole moment of the vapor and liquid phases are observed, one can establish the validity of the above-mentioned assumtion.

Assignment of Infrared and Raman Spectra of Methoxyethoxymethane. — In this section the assignment of the infrared and Raman spectra (Fig. 8) of MEM is given by assuming that this molecule has only one form in its vapor and liquid phases.

The assignment of bands at 3000 cm^{-1} has

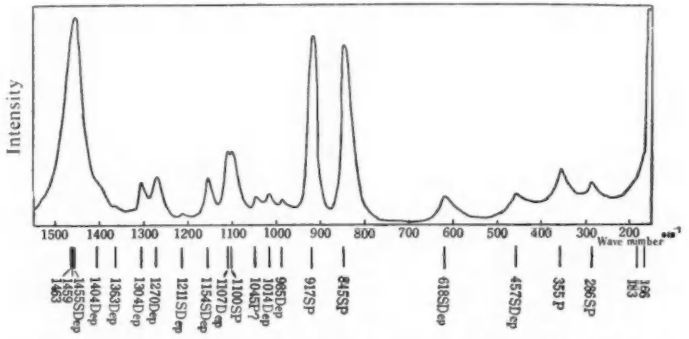

Fig. 8. Raman spectrum of methoxy ethoxy methane ($CH_3OCH_2OC_2H_5$).

TABLE I. VIBRATIONAL FREQUENCIES OF METHOXYETHOXYMETHANE

Infrared		Raman	Assignment
Vapor	Liq.		
1475 (vw)	1479 (w)		CH_2 scissoring (MeO and EtO)
1466} 1458} (m)	1462 (m)	1463 (m, sh)	sym. CH_3 deformation (MeO)
		1459 (m, sh)	
1449 (m)	1441 (m)	1455 (s) S. Dep.	asym. CH_3 deformation (MeO and and EtO)
	1401 (w)		
1389 (m)	1389 (m)	1404 (w) Dep.	sym. CH_3 deformation (EtO)
		1363 (w) Dep.	CH_2 wagging (OCH_2O) ?
1292 (vw)	1294 (w)	1304 (m) S. Dep.}	CH_2 rocking (EtO)
1280 (w)	1272 (w)	1270 (m) S. Dep.}	CH_2 twisting (OCH_2O and EtO)
1220} 1206} (w)	1214 (m)	1211 (w) S. Dep.	CH_3 rocking (MeO)
1167 (w)	1172 (w)		
1157 (m)	1155 (s)	1154 (m) S. Dep.	
1131 (sb)	1139 (s)		asym. COCOC stretching
1112} 1105} (s)	1112 (s)	1107 (s) Dep. ?	CC stretching CH_2 rocking (EtO)
1011 (w)	1014 (m)	1014 (w) Dep.	CH_3 rocking (EtO)
	983 (w)	985 (w) Dep.	
	963 (vw)		
	1096 (s)	1100 (s) S. P.	sym. COCOC stretching
1056 (s)	1045 (s)	1045 (w) P. ?	asym. COCOC stretching
933} 926} (m)	918 (s)	917 (s) S. P.	CH_3 rocking (MeO)
852 (w)	846 (m)	845 (s) S. P.	sym. COCOC stretching
	811 (w)		
800 (vw)	801 (w)		
		618 (m) S. Dep.	asym. COCOC deformation
		457 (m) S. Dep.	sym. COCOC deformation
		355 (m) P.	sym. COCOC deformation
		286 (m) S. P.	CCO deformation
		183 (sh)} 166 (sh)}	torsional vibration ?

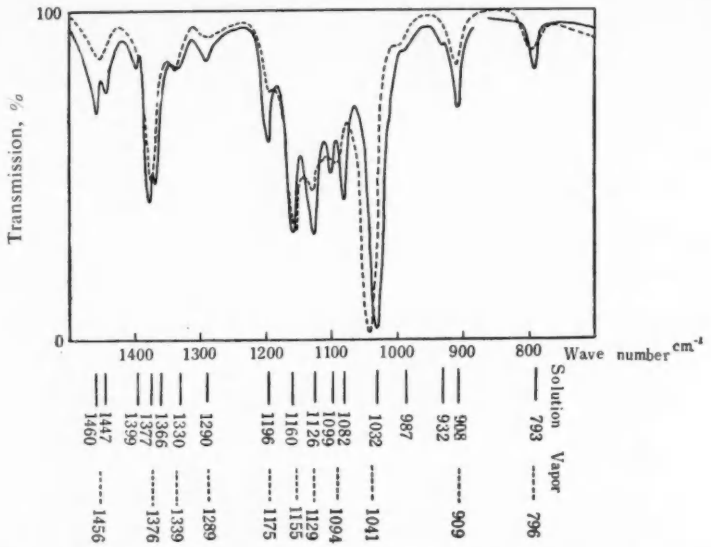

Fig. 9. Infrared spectra of diisopropoxymethane ($(CH_3)_2CHOCH_2OCH(CH_3)_2$).
Solid line, CCl_4 and CS_2 solutions, cell thickness: 0.15 mm., 2%. Dashed line, vapor.

already been given by the same author[12].

The appearance of infrared spectra between 1500 and 1250 cm^{-1} is quite similar to that of DEM and DEM-d_2, except for the lack of a very weak band a 1360 cm^{-1}. It means that the absorbance of bands in the ethoxyl group is greater than that of the methoxyl group. The appearance of Raman bands is, on the other hand, slightly different from that of DEM and DEM-d_2, that is, the intensity of the band at 1404 cm^{-1} decreases and that at 1304 cm^{-1} increases.

As the interaction between methoxyl and ethoxyl groups may be weak, the spectra of MEM within this region may be reasonably explained by assuming the simple superimposition of spectra, of methoxyl and ethoxyl compounds as shown in Table I.

A medium infrared band at 1214 cm^{-1} (having a corresponding weak Raman band) is assigned to the methyl rocking of methoxyl group. This is consistent with the fact that at this frequency many compounds containing methoxyl group have a medium infrared band and that the homologues of these compounds having no methoxyl group have no infrared band[2,3,13,14].

Spectra between 1150 and 800 cm^{-1} are very complicated not only in this molecule but in many other molecules containing oxygen atoms such as ethers, other dialkoxymethanes, ethylidene alkyl ethers, 2, 2-dialkoxypropane and orthoaliphatic acid esters. The skeletal COCOC stretching should clearly exist within this region. As shown in the discussion of DMM and its deuterated compounds[2], DEM and DEM-d_2[3] and dimethyl ether and dimethyl ether-d_6[15,16], skeletal stretchings are mixed with CH deformation vibrations to some extent, and from inspection without exact calculation it is quite hard to give a rigorous assignment. Nevertheless, some bands could be assigned reasonably from the strong similarity of spectra among homologues.

The strong liquid infrared band at 1096 cm^{-1} (having no vapor infrared band and a strong and strongly polarized Raman band) is assigned to the symmetrical COCOC stretching. In DMM and DEM, liquid infrared bands around 1100 cm^{-1} have a corresponding very weak vapor infrared band and a medium or strong and strongly polarized Raman band. They have been assigned to the symmetrical COCOC stretching in good agreement with the present assignment.

The strongest infrared band at 1045 cm^{-1} (having a corresponding weak Raman band) is assigned to the asymmetrical COCOC stretching by the analogy with DMM.

Two very strong and strongly polarized

12) K. Nukada, *J. Chem. Soc. Japan, Pure Chem. Sec.* (*Nippon Kagaku Zasshi*), **80**, 976 (1959).
13) K. Nukada, ibid., **80**, 1112 (1959).
14) K. Nukada, ibid., **81**, 1028 (1960).
15) Y. Kanazawa and K. Nukada, This Bulletin, to be published.
16) Y. Kanazawa and S. Saeki, ibid., to be published.

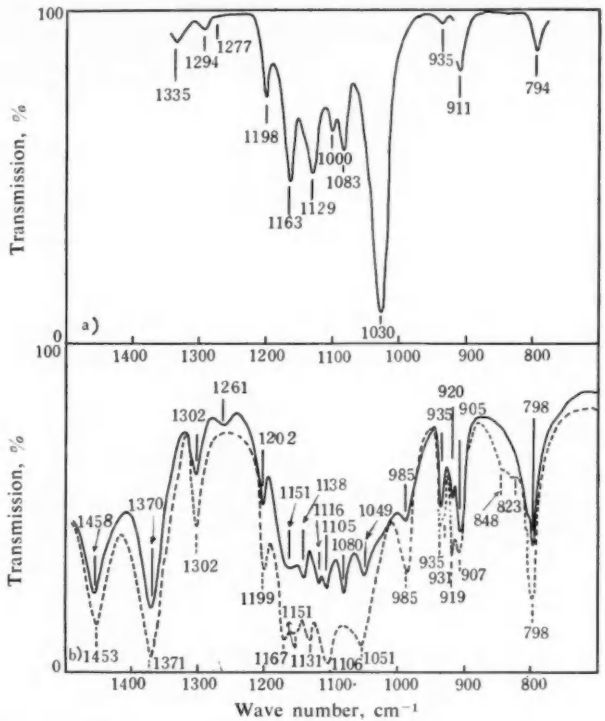

Fig. 10. Infrared spectra of diisopropoxymethane $(CH_3)_2CHOCH_2OCH(CH_3)_2$.

a) Acetonitrile solution, cell thickness: 0.015 mm., 20%

b) Solid, solid line, cell thickness: 0.015 mm. Dashed line, cell thickness: 0.05 mm.

Raman bands at 917 and 845 cm^{-1} (having corresponding strong and weak infrared bands, respectively) are assigned to the methyl rocking of the methoxy group and the symmetrical COCOC stretching, respectively. The basis of the assignment will be described in other papers[2,3].

The assignment of the remaining bands between 1150 and 800 cm^{-1} is very difficult only from the comparison of the spectra of homologues. They may be mixtures of asymmetrical COCOC stretchings, CC stretching, methylene rocking of ethoxyl group, and methyl rocking of methoxyl and ethoxyl groups.

The bands below 700 cm^{-1} are due to the skeletal deformation and torsional vibrations.

In DMM, DMM-d_2, DMM-d_6, DMM-d_8[2], DEM and DEM-d_2[3], three medium Raman bands appear at 640~560 cm^{-1} (depolarized), 450~370 cm^{-1} (depolarized) and at 325~295 cm^{-1} (polarized). The present data of MEM are completely consistent with these results. Therefore, they could be assigned to the asymmetrical, symmetrical (central angle OCO and two terminal angles COC vibrate in the opposite phases) and symmetrical (all angles vibrate in the same phase) COCOC skeletal deformations, respectively, from the analogy with the case above mentioned. In DEM and DEM-d_2, an additional strongly polarized Raman band appears at 240 cm^{-1}. In MEM, the band at 286 cm^{-1} is strongly polarized and the origin of this band is probably like that of the band at 240 cm^{-1} in DEM and DEM-d_2, hence this band is assigned to OCC deformation as in the case of DEM and DEM-d_2.

Torsional vibrations are expected to exist below 250 cm^{-1}, and Raman bands at 183 and 166 cm^{-1} may be assigned to these vibrations, although the assignment is somewhat doubtful as these bands are very weak and appear as a shoulder of very strong exciting line.

Infrared Spectra of Diisopropoxymethane in Various Phases.—Infrared spectra of DPM in vapor and liquid phases are shown in Fig. 9. As in the case of other dialkoxymethanes, the intensity of some bands (1175, 1129 and 1094 cm^{-1}) become smaller in the vapor phase.

No appreciable difference is found between the spectra of carbon tetrachloride and acetonitrile solutions (Fig. 10a).

Solid infrared bands have at least two different shapes, which are dependent on the critical condition of freezing the material, as shown in Fig. 10b.

The vapor spectra were taken at the temperature range between 24 and 106°C, but no change was observed.

The results are thus very similar to those in the case of DMM, DEM and MEM. Therefore, the same assumption as the above-mentioned one may also be held in this case. Because DPM has great bulk at the terminals (isopropyl groups) and the steric repulsion between isopropyl groups and the central methylene group is expected to be very large, this molecule may take a nearly planar zig-zag form.

Summary

The rotational isomerism of dialkoxymethanes ($CH_3OCH_2OCH_3$, $CH_3OCH_2OC_2H_5$, $C_2H_5OCH_2OC_2H_5$ and $(CH_3)_2CHOCH_2OCH(CH_3)_2$) is discussed from the spectroscopical point of view. The experimental results are as follows.

1) The appearance of infrared spectra is appreciably different among the vapor, liquid and solid phases. Of these, the solid spectrum gives the most complicated figure.

2) No solvent effect is obtained in acetonitrile solution.

3) No change is observed in the vapor infrared spectrum between room temperature and 100°C.

It is concluded from these results and data of dipole moment that dimethoxymethane exists as one configuration in the liquid and vapor phases, the terminal methyl groups of which are rotating about 120° anticlockwise sense from the central OCO plane.

The configuration of other dialkoxymethanes are assumed to be of one form by the analogy of experimental results.

Finally, the assignment of vibrational spectra of methoxyethoxymethane is presented.

The author wishes to express his sincere thanks to Dr. Y. Mashiko for his valuable discussion.

Government Chemical Industrial Research Institute of Tokyo
Shibuya-ku, Tokyo

Infrared and Raman Spectra of Diethoxymethane and Diethoxymethane-d_2

By Kenkichi NUKADA

(Received March 30, 1961)

In previous papers, the author has reported the characteristic vibrations of infrared spectra of dialkoxymethanes[1] and ethylidene dialkyl ethers[2], and more recently the assignment of vibrational spectra of dimethoxymethane ($CH_3OCH_2OCH_3$) and its deuterated compounds[3].

In this paper, infrared and Raman spectra of diethoxymethane (DEM, $C_2H_5OCH_2OC_2H_5$) and diethoxy methane-d_2 (DEM-d_2, $C_2H_5OCD_2OC_2H_5$) are presented and the assignment of spectra are given by referring to the above-mentioned results[1-3].

DEM has four internal rotational axes and there is a possibility of more than two rotational isomers existing in it. The author has examined the rotational isomerism of dialkoxymethanes and concluded that dimethoxymethane, the simplest homologue of DEM, takes one form in vapor and liquid phases near room temperature. He did not obtain such a definite conclusion in the case of DEM, but from the similarity of the change of infrared spectra among various phases between dimethoxymethane and DEM, he suggested that DEM also takes one and the same form in vapor and liquid phases (two ethoxyl groups rotate about 120° in an anticlockwise sense from the central OCO plane) near room temperature[4]. In this paper, the assignment is given with the assumption mentioned above.

1) K. Nukada, *J. Chem. Soc. Japan, Pure Chem. Sec.* (*Nippon Kagaku Zasshi*), **80**, 1112 (1959).
2) K. Nukada, ibid., **80**, 976 (1959).
3) K. Nukada, *Spectrochim. Acta*, to be published.
4) K. Nukada, This Bulletin, to be published.

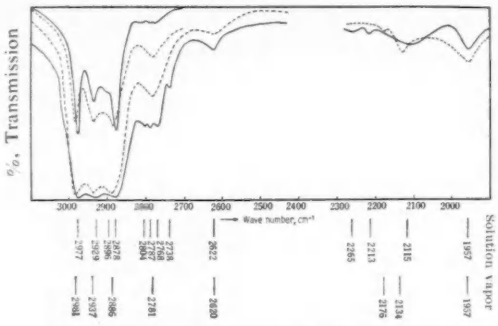

Fig. 1a. Infrared spectra of DEM (C–H and C–D stretching region).

Solid line, CCl_4 solution (25 and 5 vol. %, 0.15 mm.) Dashed line, vapor

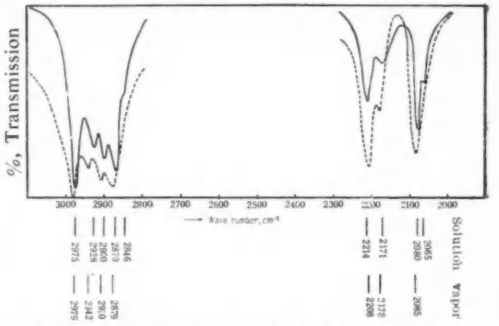

Fig. 1c. Infrared spectra of DEM-d_2 (C–H and C–D stretching region).

Solid line, CCl_4 solution, (10 vol.%, 0.15 mm.) Dashed line, vapor

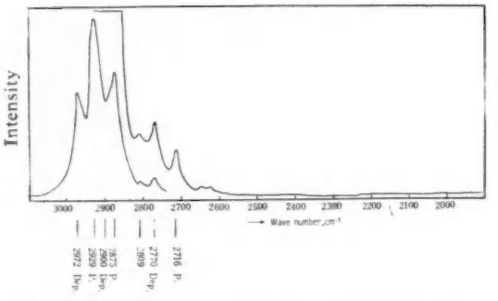

Fig. 1b. Raman spectra of DEM (C–H and C–D stretching region).

Pure liquid

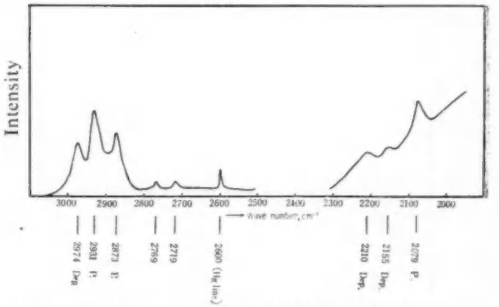

Fig. 1d. Raman spectra of DEM-d_2 (C–H and C–D stretching region).

Pure liquid

Experimental

DEM and DEM-d_2 were prepared from ethanol and formaldehyde, and from ethanol and formaldehyde-d_2, respectivity. The detailed description of the prepatation will be reported elsewhere[5].

Infrared spectra were obtained by means of a Perkin Elmer 12C spectrophotometer equipped with a lithium fluoride prism and a 21 spectrophotometer equipped with a sodium chloride or a cesium bromide prism.

Raman spectra were obtained by means of a Cary 81 spectrophotometer. In the case of DEM-d_2, a capillary tube, the capacity of which is 0.2 cc. was used. The degree of depolarization was measured by wrapping two kinds of polaroids around a Raman tube.

The spectra thus obtained are illustrated in Figs. 1—3.

Results and Discussion

C–H and C–D Stretching Vibrations. — The features of the Raman spectra of DEM and DEM-d_2 are quite similar in the 3000 cm^{-1} region. They have two strongly polarized bands at 2929～2931 cm^{-1} and at 2873～2875 cm^{-1}, and one depolarized band at 2972～2974 cm^{-1}. The features of the infrared spectra are, on the other hand, slightly different from each other. Thus, the intensity ratios of the bands at 2928～2929 cm^{-1} to those at 2896～2900 cm^{-1} are different in these two compounds.

The strongest infrared bands at 2977～2975 cm^{-1} in DEM and DEM-d_2 (the corresponding Raman bands being strongly depolarized) are assigned to the asymmetrical methyl stretching of the ethoxyl group[2].

The strong infrared bands at 2870～2878 cm^{-1}, having corresponding strongly polarized Raman bands, in DEM and DEM-d_2 are assigned to the symmetrical methyl stretching[1].

In dimethoxymethane-d_6 ($CD_3OCH_2OCD_3$), bands at 2932 and 2887 cm^{-1} are assigned respectively to the asymmetrical and the symmetrical methylene stretchings of OCH_2O group[3]. The corresponding CD_2 stretchings

5) K. Nukada, *Reports Gov. Chem. Ind. Research Inst. Tokyo*, to be published.

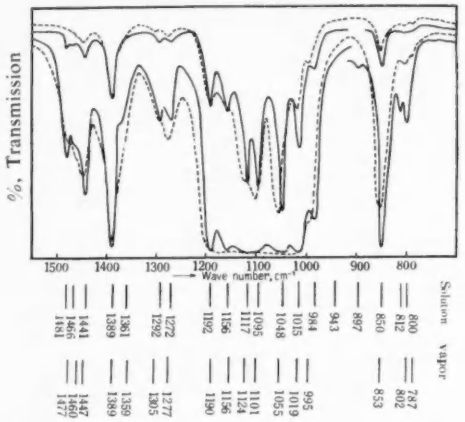

Fig. 2a. Infrared spectra of DEM (finger print region).

Solid line, CCl_4 and CS_2 solution (0.15 mm., 20 and 3 vol.%), dashed line, vapor

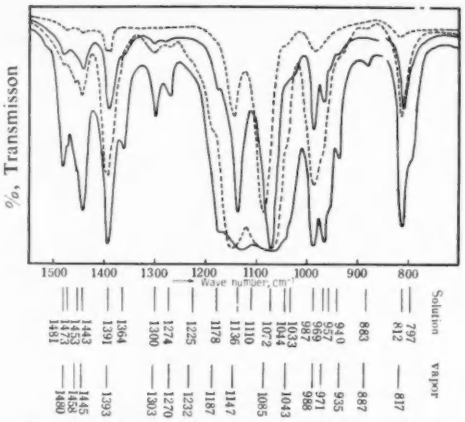

Fig. 2c. Infrared spectra of DEM-d_2 (finger print region).

Solid line, CCl_4 and CS_2 solution, (0.15 mm., 20 and 3 vol.%), dashed line, vapor

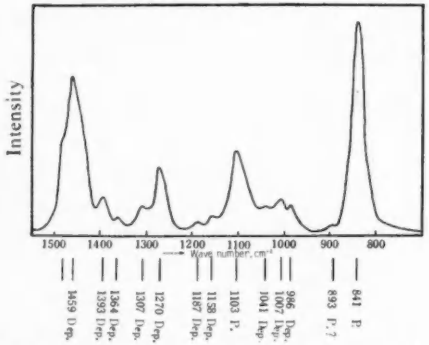

Fig. 2b. Raman spectrum of DEM (finger print region).

Pure liquid

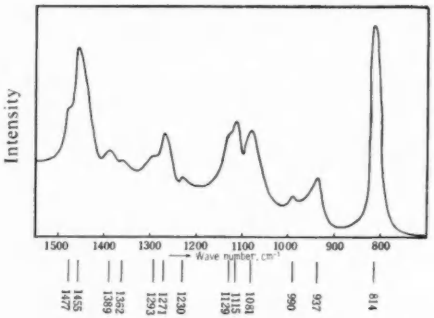

Fig. 2d. Raman Spectrum of DEM-d_2 (finger print region).

Pure liquid

are found in dimethoxymethane-d_2 ($CH_3OCD_2 \cdot OCH_3$) to be at 2188 (strongly depolarized in Raman) and at 2080 cm^{-1} (strongly polarized in Raman), respectively. In DEM-d_2, two strong infrared bands appear at 2214 (the corresponding Raman band being strongly depolarized) and at 2080 cm^{-1} (the corresponding Raman band being strongly polarized); hence they are assigned to the asymmetrical and the symmetrical CD_2 stretchings of the OCD_2O group, respectivery, on the analogy of the above mentioned results. The asymmetrical and symmetrical methylene stretchings of the OCH_2O group in DEM are then expected to appear near 2930 and 2890 cm^{-1}, respectively. The relative intensity of the infrared band at 2928~2929 cm^{-1} becomes lower in DEM-d_2 as compared with the one in DEM, while that at 2870~2878 cm^{-1} does not chow an appreciable change between DEM and DEM-d_2. Then it is certain that the asymmetrical methylene stretching of the OCH_2O group exists at 2930 cm^{-1} in DEM, and that it is probably overlapped by the other type of vibration. The overlapping band is presumably the asymmetrical methylene stretching of ethoxy group[2]. The bands at 2870~2878 cm^{-1} in DEM and DEM-d_2 are assigned to the symmetrical methylene stretching of the ethoxyl group, overlapped by the symmetrical methylene stretching of the OCH_2O group, as described above, and also by the symmetrical methyl stretching of the ethoxyl group. Since the intensity of these bands does not alter appreciably between DEM DEM-d_2, the absorbance of the symmetrical methylene stretching

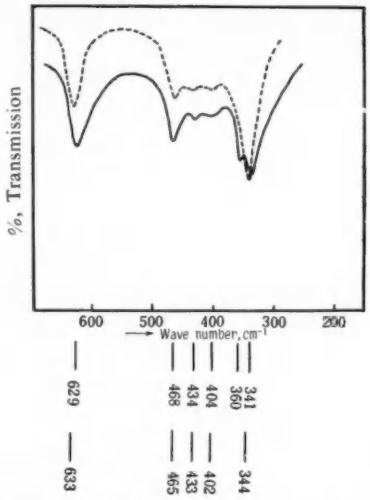

Fig. 3a. Infrared spectra of DEM (skeletal deformation region).

Solid line, pure liquid (0.2 mm.), dashed line vapor

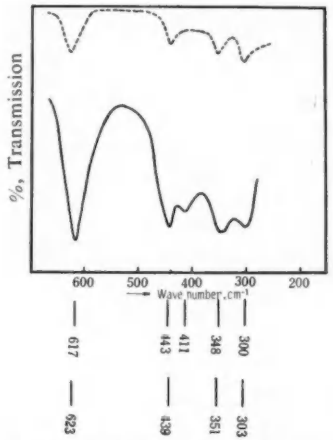

Fig. 3c. Infrared spectra of DEM-d_2 (skeletal deformation region).

Pure liquid (0.2 mm.)

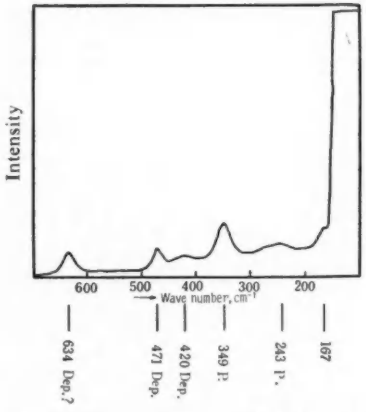

Fig. 3b. Raman spectrum of DEM (skeletal deformation region).

Pure liquid

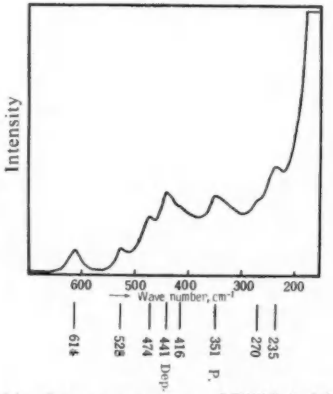

Fig. 3d. Raman spectrum of DEM-d_2 (skeletal deformation region).

Pure liquid

of the OCH_2O group is concluded to be small.

The possibility of the Fermi resonance occurring between two types of methylene groups may be small, because the interaction between them is believed to be negligible.

The remaining weak bands may be overtone and/or combination.

Skeletal Stretching and C–H and C–D Deformation Vibrations. — The appearance of the spectra of DEM and DEM-d_2 is quite similar in the range between 1480 and 1270 cm^{-1} both in infrared and Raman. Therefore, the absorbance of the ethoxyl group is more predominant than that of the OCH_2O group in this frequency region.

Medium infrared and Raman bands appear at 1477~1481 cm^{-1} both in DEM and DEM-d_2. In ethylidene diethyl ether ($C_2H_5OCH(CH_3)\cdot OC_2H_5$), ethylidene methyl ethyl ether ($CH_3OCH(CH_3)OC_2H_5$), 2, 2-diethoxypropane ($C_2H_5OC(CH_3)_2OC_2H_5$)[6], triethyl orthoformate ($HC(OC_2H_5)_3$) and in triethyl orthopropionate

6) K. Nukada, ibid., to be published.

TABLE I. VIBRATIONAL FREQUENCIES OF DIETHOXYMETHANE AND DIETHOXYMETHANE-d_2*

DEM			DEM-d_2			
IR		Raman	IR		Raman	Assignment
Vapor	Liq.		Vapor	Liq.		
2981(s)	2977(s)	2972(s) Dep.	2979(s)	2975(s)	2974(s) Dep.	asym. CH_3 stretching
2937(m)	2929(m)	2929(s) S. P.	2942(m)	2928(m)	2931(s) S. P.	asym. CH_2 stretching (OCH_2O, EtO)
	2896(w)		2910(m)	2900(m)		combination or overtone
2886(m)	2878(s)	2875(s) S. P.	2879(s)	2870(s)	2873(s) S. P.	{sym. CH_3 stretching {sym. CH_2 stretching (OCH_2O, EtO)
			2208(s)	2214(s)	2210(w) Dep.	asym. CD_2 stretching
			2178(m)	2171(m)	2155(w) Dep.	CD_2, combination or overtone
			2085(s)	2080(s)	2079(m) S. P.	sym. CD_2 stretching
			2063(sh)	2065(sh)		CD_2, combination or overtone
1477(vw)	1481(m)	1481(m, sh)	1480(vw)	1481(m) 1473(vw)	1477(m, sh)	CH_2 scissoring (OCH_2O, EtO)
1460(vw)	1466(vw)	1459(s) S. Dep.	1458(vw)	1453(vw)	1455(s) S. Dep.	asym. CH_3 deformation
1447(w)	1441(vw)		1445(w)	1443(m)		EtO, combination or overtone (COCOC)
1389(m)	1389(m)	1393(m) Dep.	1393(m)	1391(m)	1389(m)	{sym. CH_3 deformation {CH_2 wagging (OCH_2O)
1359(vw)	1361(vw)	1364(w) Dep.		1364(vw)	1362(w)	CH_2 wagging (EtO)
1305(w)	1292(w)	1307(w) Dep.	1303(vw)	1300(w)	1293(w)	CH_2 rocking (EtO)
1277(w)	1272(w)	1270(s) Dep.	1270(vw)	1274(w)	1272(s) Dep.	CH_2 twisting (EtO)
			1232(vw)	1255(w)	1230(w) P. ?	CD_2 scissoring or twisting+COCOC stretching
1190(m)	1192(m)	1187(w) Dep.				CH_2 twisting or wagging (OCH_2O)
1156(w)	1156(m)	1158(w) Dep.				CH_2 rocking (OCH_2O)
1124(m)	1117(s)		1147(s)	1136(s)	1129(w)	asym. COCOC streching
				1110(vvw)	1115(s) P.	CD_2 scissoring or twisting
1101(s)	1095(s)	1103(s) P.	1085(s)	1072(s)	1081(s)	sym. COCOC stretching
1055(s)	1048(s)	1041(w) Dep.	988(m)	987(s)	990(m)	asym. COCOC stretching
1019(m)	1015(s)	1007(m) Dep.	935(vw)	940(w)	937(m) Dep.	sym. CC stretching
995(w)	984(w)	986(w) Dep.	971(w)	969(m)		asym. CC stretching
853(m)	850(m)	841(s) S. P.	817(w)	812(s)	814(s) S. P.	sym. COCOC stretching
	943(vw)					
	897(vw)	893(w) P. ?	887(vw)	883(vw)		
802(vw)	812(vw)					
787(vw)	800(vw)			797(vw)		
633(s)	629(s)	634(m) Dep. ?	623(s)	617(s)	614(m)	asym. COCOC deformation
					528(w)	
					474(w)	
465(m)	468(s)	471(m) Dep.	439(s)	443(s)	441(m) Dep.	sym. COCOC deformation
433(w)	434(m)	420(w) Dep.		411(m)	416(w)	
402(w)	404(m)					
	360(w)					
344(s)	341(s)	349(m) S. P.	351(s)	348(s)	351(m) P.	sym. COCOC deformation
			303(m)	300(m)		
					270(vw)	
		243(w) S. P.			235(w)	sym. OCC deformation
		167(w)				

* P. and Dep. mean "polarized" and "depolarized", and S. means "strongly".

$(C_2H_5C(OC_2H_5)_3)$[7], a weak or medium infrared band is observed in this region. But in diisopropoxymethane $((CH_3)_2CHOCH_2OCH\cdot(CH_3)_2)$[8], ethylidene dimethyl ether $(CH_3\cdot OCH(CH_3)OCH_3)$, trimethyl orthoformate $(HC(OCH_3)_3)$, trimethyl orthoacetate $(CH_3C\cdot(OCH_3)_3)$ and in trimethyl ortho-*n*-valerate $(CH_3(CH_2)_3C(OCH_3)_3)$[7], no band exists in this region. Hence the bands at 1477～1481 cm^{-1} are assigned to the methylene vibration of the ethoxyl group, certainly the scissoring vibration. The methylene scissoring of the OCH_2O group can also exist at this frequency[3], but the absorbance of the latter may probably smaller than that of the former and it is hard to observe it.

All compounds containing oxygen atoms which the author has studied[1-4,6-8] have weak infrared and strong and depolarized Raman bands around 1460 cm^{-1} except for dimethoxymethane and dimethoxymethane-d_8 $(CD_3\cdot OCD_2OCD_3)$. The last two compounds contain no methyl group, thus the bands in this region should be due to the methyl group. Therefore the bands at 1455～1466 cm^{-1} (very weak in infrared and strong and depolarized in Raman) in DEM and DEM-d_2 are assigned to the asymmetrical methyl deformation of the ethoxyl group.

The origin of infrared bands at 1440～1443 cm^{-1} both in DEM and DEM-d_2 is not clear, but they must be due to the vibration of the ethoxyl group, or the combination or overtone of skeletal vibrations.

The medium infrared and polarized Raman bands at 1389～1393 cm^{-1} both in DEM and DEM-d_2 are assigned to the symmetrical methyl deformation of the ethoxyl group. From the result on dimethoxymethane and its deuterated compounds[3] the methylene wagging of the OCH_2O group could exist in this region. So in DEM, these two bands may probably overlap.

The very weak infrared and weak Raman bands at 1359～1362 cm^{-1} in DEM and DEM-d_2 are assigned to the methylene wagging of the ethoxyl group.

The features of doublet at 1292～1307 cm^{-1} and 1270～1274 cm^{-1} do not alter strongly between DEM and DEM-d_2, thus these bands are also due to the ethoxyl group. Of these, the former bands are assigned to the methylene rocking and the latter to the methylene twisting, because the Raman intensity of the latter is greater than that of the former and it is expected that the twisting vibration, the species of which is A, should give a stronger band.

In conclusion, it becomes clear that bands due to the ethoxy group are at 1477～1481, 1455～1466, 1441～1443, 1389～1393, 1361～1364, 1292～1307 and at 1270～1274 cm^{-1} (all the values are those of liquid phase). The skeletal vibrations may not appear in such a high frequency region.

The weak Raman band at 1230 cm^{-1} (having a corresponding very weak infrared band) in DEM-d_2 may be due to CD_2 vibration coupled with the COCOC skeletal vibration. Since the Raman band is polarized, it is assigned to the CD_2 scissoring or twisting, being coupled with an A type skeletal stretching, to some extent.

The medium bands at 1187～1192 cm^{-1} both in infrared and Raman in DEM disappear in DEM-d_2 (in which a very weak infrared band appears at 1178 cm^{-1}, though the origin of this band may be different as the intensity is too low). Hence these bands are due to the methylene vibration of the OCH_2O group, probably the twisting or wagging.

The bands at 1156～1158 cm^{-1} in DEM both in infrared and Raman disappear in DEM-d_2. In dimethoxymethane and dimethoxymethane-d_6, weak infrared bands at this freqencey are assigned to the methylene rocking of the OCH_2O group[3]. According to these results, these bands are assigned to the methylene rocking of the OCH_2O group.

From the study on dimethoxymethane and its deuterated compounds, the skeletal COCOC stretching should exist between 1150～800 cm^{-1}[3]. In DEM and DEM-d_2, the additional skeletal stretchings due to CC bonds could exist in this region. But the absorbance of the latter ones may be smaller than that of the former, hence the features of the spectra of DEM and DEM-d_2 are actually similar to those fo dimethoxymethane at this frequency region.

The infrared bands at 1117 and at 1136 cm^{-1} in DEM and DEM-d_2 are the next strongest bands in the liquid phase, and the corresponding Raman bands are very weak. In dimethoxymethane and its deuterated compounds, the strong infrared bands around 1140 cm^{-1}, the corresponding Raman bands of which are extremely weak, are assigned to the asymmetrical skeletal stretching[3]. These bands are then assigned to one of the asymmetrical COCOC stretchings.

The Raman band at 1115 cm^{-1} in DEM-d_2 is due to the OCD_2O methylene vibration. As it is strongly polarized, it may be assigned to the scissoring or twisting being coupled with the symmetrical skeletal stretching to some extent.

The strong infrared band at 1095 cm^{-1} in

7) K. Nukada, *J. Chem. Soc. Japan, Pure Chem. Sec.* (*Nippon Kagaku Zasshi*), **81**, 1028 (1960).
8) K. Nukada, This Bulletin, to be published.

DEM corresponds to the band at 1072 cm^{-1} in DEM-d_2. As the corresponding Raman bands are strong and strongly polarized (in DEM), these bands are assigned to one of the symmetrical COCOC stretchings.

The strong infrared band appears at 1048 cm^{-1} in DEM, but no corresponding band exists in DEM-d_2 near that frequency. In DEM-d_2, the remaining band, the intensity of which is rather high, is the band at 987 cm^{-1}. Furthermore the intensity of the corresponding Raman bands is not so high in both cases, thus it is reasonable to correlate the two bands as the same type of skeletal vibration. The remaining modes are one symmetrical and one asymmetrical vibration, but as described in detail later the symmetrical one should appear at 800~850 cm^{-1} both in DEM and DEM-d_2. Accordingly these bands are assigned to the asymmetrical COCOC stretching.

The bands at 1015 and 984 cm^{-1} in DEM and those at 940 and 969 cm^{-1} in DEM-d_2, may be due to CC stretchings. The former ones are assigned to the symmetrical mode and the latter to the asymmetrical one, respectively, since the intensity of the corresponding Raman bands of the former is higher than that of the latter.

The strongest and strongly polarized Raman bands exist at 841 and 814 cm^{-1} in DEM and DEM-d_2, respectively. In dimethoxymethane, its deuterated compounds[3], methoxyethoxymethane and in diisopropoxymethane[9], there appear the strongest and strongly polarized Raman bands, being assigned to the symmetrical skeletal stretching, between 900 and 800 cm^{-1}. Thus these bands are also definitely assigned to the symmetrical COCOC stretching. Just as in the case of dimethoxymethane and its deuterated compounds[3], the corresponding infrared bands are not so strong, and in the vapor phase its intensity becomes lower than that of the liquid phase. As already mentioned in the study of dimethoxymethane, the mode of this vibration is such that two terminal ethoxyl groups vibrate symmetrically and the central OCO group does not move much.

Skeletal Deformation Vibrations. — It is expected that five skeletal angle deformations appear over 200 cm^{-1} and six torsional vibrations below 250 cm^{-1}. At the present, no infrared band below 280 cm^{-1} is obtained because of the experimental limitation and Raman band below 200 cm^{-1} is hardly observable since the strong exiting line disturbs the observation of weak Raman band. All the skeletal deformations could then be observed either in infrared or in Raman, while the torsional vibrations are hardly observable.

There are three pairs of strong Raman bands in DEM and DEM-d_2, namely at 634 and 614, 471 and 441, and 349 and 351 cm^{-1}. In dimethoxymethane, its deuterated compounds[3] and in methoxyethoxymethane[4], there appear such pairs of Raman bands. The appearance of infrared spectra is also quite similar between DEM and DEM-d_2, that is, three pairs of strong infrared bands appear at the same frequency regions. Hence they are certainly due to the skeletal deformations

Of these, the bands at 349~351 cm^{-1} are strongly polarized in Raman, so they are assigned to the symmetrical COCOC deformation. As in the case of dimethoxymethane and its deuterated compounds, these are the vibrations all skeletal angles of which move in the same phase.

The degree of depolarization of the remaining two bands is not clear, but on the analogy of dimethoxymethane the bands at 614~634 cm^{-1} in DEM and DEM-d_2 are assigned to the asymmetrical deformation and the last bands at 441~470 cm^{-1} to the other symmetrical one, two COC angles and the OCO angle of which vibrate in the opposite phases.

As the Raman bands at 235~243 cm^{-1} in DEM and DEM-d_2 are strongly polarized, they are assigned to the symmetrical OCC deformation. The assignment of the asymmetrical one is not clear.

The remaining weak bands may be overtone and/or combination of torsional vibrations.

Summary

Infrared spectra between 3000 and 280 cm^{-1} (vapor and liquid phases) and Raman spectra (liquid phase) of diethoxymethane ($C_2H_5 \cdot OCH_2OC_2H_5$) and of diethoxymethane-d_2 ($C_2H_5OCD_2OC_2H_5$) were observed and the assignment of the spectra is presented with the assumption that these molecules take one form both in the vapor and liquid phases. In the assignment, that of the homologues such as dimethoxymethane, its deuterated compounds, methoxyethoxymethane and diisopropoxymethane, are taken into consideration.

The author wishes to express his sincere thanks to Dr. Y. Mashiko for his valuable discussions.

Government Chemical Industrial Research Institute of Tokyo
Shibuya-ku, Tokyo

9) K. Nukada, ibid., to be published.

Structure of Enteromycin. III. Structure of Demethoxyenteromycin*

By Kōmei MIZUNO

(Received April 4, 1961)

The present work was initiated with a view to knowing the structure of dehydroxydihydrodemethoxyenteromycin (XXII)[1] and establishing the structure of demethoxyenteromycin (XII) by making clear the partial structures of *O*-acetyldemethoxyenteromycin (XVIII), *N*-methyldemethoxyenteromycin methyl ester (XIX), and *O*-methyldemethoxyenteromycin methyl ester (XX).

XXII has a molecular formula having one mole less hydrogen than dehydroxytetrahydrodemethoxyenteromycin (XV), namely glycyl-β-alanine, and its hydrolysis with hydrochloric acid gives glycine, acetaldehyde and others. The infrared spectum (Report II, Fig. 6) of this compound shows the absorption of C=C and the ultraviolet spectrum (Report II, Fig. 7) inhibits an adsorption similar to that of α,β-unsaturated carboxylic acids. Further the infrared spectra (Report II, Figs. 2 and 4) of XVIII and XX reveals the clear absorption of NH. From these facts it is reasonable to assign the structure of *N*-glycyl-3-aminoacrylic acid to XXII. Accordingly, of the presumptive formulas, D

$$NH_2CH_2CONHCH=CHCOOH \qquad (XXII)$$

and C, for enteromycin and demethoxyenteromycin described in Report II, the α,β-unsaturated ones would be preferential.

Catalytic reduction of XVIII on Adams platinum oxide yielded acetic acid (XXVII) and glycyl-β-alanine, and this fact ascertained the presence of $\rangle$NOAc in XVIII. On the other hand, the position of the $\rangle$NOH group in XII was clarified to be at the terminal N in the formula C. Catalytic reduction of XIX and hydrolysis of the resulting viscous substance (ester) (XX) yielded sarcosine (XXIX) and β-alanine. The same treatment of XX gave glycine and β-alanine. From these results, it is proper to think that the remaining hand of the hydroxyimino group (HO–N$\langle$C) in XII is not used for a N–N combination (the infrared spectra of XVIII and XX reveal the absorption of NH) or for a N–C combination (in a N–C combination is present, it must be split off by catalytic reduction before the formation of XXII which is a readily saturable unsaturated compound). In other words, the terminal N of XII ought to participate in aldoxime. Since thus XII is a strongly phenolic aldoxime compound, it gives two methyl derivatives (CH_3–$\overset{O}{\overset{\uparrow}{N}}$=CH– and H_3CO·N=CH–) as Fuson[2] pointed out, and XIX is understood as the *N*-methyl derivative taking

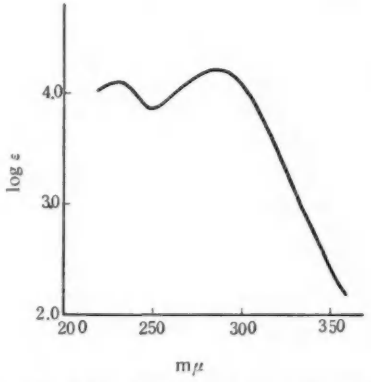

Fig. 1. Ultraviolet absorption spectrum of *O*-methyldemethoxyenteromycin methyl ester (XX) in methanol.

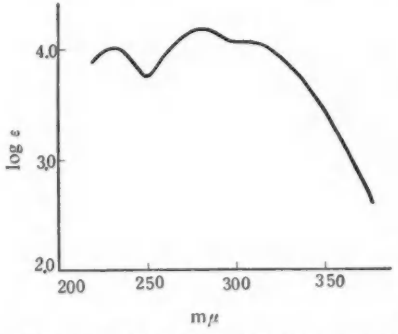

Fig. 2. Ultraviolet absorption spectrum of *N*-methyldemethoxyenteromycin methyl ester (XIX) in methanol.

* This constitutes Part XXXVII of a series entitled "Studies on Antibiotics" by S. Tatsuoka, and was reported at the forum on Natural Organic Compounds, October 1960.

1) K. Mizuno, This Bulletin, **34**, 1425 (1961).

2) R. C. Fuson, "Advanced Organic Chemistry" (1950), p. 515.

oxide-form, and XX as the *O*-methyl derivative taking ether-form. The ultraviolet spectrum (Fig. 1) of XX, like that of XVIII, showed such strong absorptions at λ 225 mμ and 280 mμ as those of diketone[3] compounds, whereas the ultraviolet spectrum (Fig. 2) of XIX exhibited such a strong absorption at λ 295 mμ as the conjugate nitrone-form[4] may show. These facts seem to be in good accord with the above-mentioned structures.

Namely, the structure of XII must be *N*-(hydroxyiminoacetyl)-3-aminoacrylic acid,

$$HON{=}CHCONHCH{=}CHCOOH \quad (XII)$$

and consequently the structure of methyl *N*-(*N*-oxy-methyliminoacetyl)-3-aminoacrylate

$$H_3\overset{\overset{O}{\uparrow}}{C}N{=}CHCONHCH{=}CHCOOCH_3 \quad (XIX)$$

is presumed for XIX, and the structure of methyl *N*-(*O*-methylhydroxyiminoacetyl)-3-aminoacrylate

$$H_3CON{=}CHCONHCH{=}CHCOOCH_3 \quad (XX)$$

for XX.

Experimental

Acid Decomposition of Dehydroxydihydrodemethoxyenteromycin.—A solution of 30 mg. of dehydroxydihydrodemethoxyenteromycin (XXII) in 3 cc. of 6 N hydrochloric acid was heated at 100°C for 6 hr. in a sealed tube, the air of which was replaced with nitrogen. One half of the reaction mixture was allowed to react with 2, 4-dinitrophenylhydrazine dissolved in hydrochloric acid, and the product was subjected to paper chromatography to detect the spot of the 2, 4-DNPH of acetaldehyde at R_f 0.35. The remaining half was evaporated to dryness and the residue was chromatographed, finding a single spot of glycine at R_f 0.40.

Catalytic Reduction of *O*-Acetyldemethoxyenteromycin.—A solution of 30 mg. of *O*-acetyldemethoxyenteromycin in 50 cc. of pure methanol was reduced in the presence of 20 mg. of Adams platinum oxide. The reaction mixture was diluted with 20 cc. of pure water and filtered, and 10 cc. of the filtrate was passed through a column of Amberlite IR-120 (H-form). The effluent, after addition of aqueous ammonia, was concentrated under diminished pressure and the residue was chromatographed by the method of Kennedy et al[5]. (solvent system: 95% ethanol containing ammonia. Detective reagent: a solution of B.P.B. in 70% ethanol, made acid with citric acid) to detect a blue spot, which was identified as ammonium acetate, and hence the presence of acetic acid in the reaction mixture was confirmed. It is evident that the spot is not formic acid because it does not reduce the ammoniacal silver nitrate solution of Brown et al.[6] The remaining filtrate (60 cc.) was concentrated under reduced pressure, giving 10 mg. of crystals, m.p. 225°C (decomp.), the infrared spectrum and R_f value in paper chromatography of which were in complete accord with those of glycyl-β-alanine.

Catalytic Reduction of *N*-Methyldemethoxyenteromycin Methyl Ester and Hydrolysis of the Product.—A solution of 30 mg. of *N*-methyldemethoxyenteromycin methyl ester in 10 cc. of pure methanol was reduced on 20 mg. of Adams platinum oxide. The reaction mixture was filtered and concentrated under reduced pressure, leaving a small amount of a very viscous substance (XXVIII). The infrared spectrum of the substance showed the absorption of COOR, but its ultraviolet spectrum revealed no specific absorption in the long wave region beyond λ 220 mμ. Part of the substance was hydrolyzed with 6 N hydrochloric acid and the resulting free amino acid was investigated by the ninhydrin reaction and paper chromatography, whereupon a blue spot was detected at R_f 0.65 and a pink spot at R_f 0.73. The former spot was identified as β-alanine and the latter as sarcosine. The substance, after dinitrophenylation, gave three yellow spots; i.e. a spot at R_f 0.37 in the first development, at R_f 0.30 in the second development, a spot at R_f 0.52 in the first development, at R_f 0.28 in the second development, and a spot at R_f 0.40 in the first development, at R_f 0.43 in the second development, and they were identified as DNP-alanine, 2, 4-dinitrophenol, and DNP-sarcosine, respectively. The spots of DNP-β-alanine and DNP-sarcosine were extracted with hot water, and from the absorptions of the extracts the two compounds were found to be contained in equimolecular amounts.

The rest of the substance (XXVIII) was dinitrophenylated and the ether soluble portion of the product was hydrolyzed with hydrochloric acid and chromatographed, when no spot of DNP-sarcosine was detected, and the presence of only free β-alanine was confirmed.

Catalytic Reduction of *O*-Methyldemethoxyenteromycin Methyl Ester and Hydrolysis of the Product.—A solution of 30 mg. of *O*-methyldemethoxyenteromycin methyl ester in 10 cc. of pure methanol was reduced on 20 mg. of Adams platinum oxide. The reaction mixture was filtered and concentrated under reduced pressure to give a viscous substance. The product was hydrolyzed with hydrochloric acid and chromatographed as before, detecting glycine and β-alanine.

Summary

The structure of dehydroxydihydrodemethoxyenteromycin was assumed to be *N*-glycyl-3-aminoacrylic acid. From the fact that catalytic reduction of *O*-acetyldemethoxyenteromycin afforded acetic acid and glycyl-β-alanine, and that *N*-methyl- and *O*-methyldemethoxyenteromycin methyl ester have the partial structures of *N*-(*N*-oxy-methyliminoacetyl)- and *N*-(*O*-

3) L. Dorfmann, *Chem. Revs.*, **1953**, 80.
4) W. D. Emmons, *J. Am. Chem. Soc.*, **79**, 5739 (1957); **78**, 6208 (1956).
5) E. P. Kennedy and H. A. Barker, *Anal. Chem.*, **23**, 1033 (1951).
6) F. Brawn and C. P. Hall, *Nature*, **166**, 66 (1950).

methylhydroxyiminoacetyl)-, respectively, it was made clear that demethoxyenteromycin is an aldoxime having the structure of *N*-(hydroxyiminoacetyl)-3-aminoacrylic acid.

Research Laboratories
Takeda Chemical Industries, Ltd.
Higashiyodogawa-ku, Osaka

*Structure of Enteromycin. IV**

By Kōmei MIZUNO

(Received April 4, 1961)

As reported in the previous papers[1-3], enteromycin (I) differs from demethoxyenteromycin (XII) in molecular formula only by CH_2O, but they are greatly different in property. From the fact that enteromycin is demethoxylated by heating under evolution of formaldehyde, and from the results of the decomposition of I and XII, enteromycin seems to have a specific functional group containing a methoxyl group. Therefore, the clarification of the functional group was considered to be the most important problem for establishing the structure of I. So the course of the conversion of I to XII by catalytic reduction was restudied first of all. On the other hand, attempts were made to know the position of the functional group by clarifying the structure of the amido compounds, XIV[1] and XXI[2], of I and XII.

Enteromycin methyl ester[1] (II) is soluble in many solvents and its catalytic reduction gives prisms (XXX) [m. p. 196°C (decomp.), $C_6H_8O_4N_2$], which are positive to the reaction of Barton et al.[1] The product has a methoxyl group, and though its infrared spectrum (Fig. 1) shows no absorption of $COOCH_3$ (1710 cm^{-1}), its ultraviolet spectrum exhibits two absorption maxima at λ 225 mμ (ε 11000) and 280 mμ (ε 16000). However, as the product was positive to the Barton reaction, it was assumed to be demethoxyenteromycin methyl ester and the assumption was confirmed by the following experiments. Acetylation of XXX with acetic anhydride in warm water afforded prisms (XXXI) [m. p. 127°C, $C_8H_{10}O_5N_2$] negative to the Barton reaction. As the infrared spectrum (Fig. 2) of this product showed a clear absorption of $=NOCOCH_3$ (1775 cm^{-1}), it was assumed to be *O*-acetyldemethoxyenteromycin methyl ester, and the assumption was confirmed by the formation of the same compound by methylation of *O*-acetyldemethoxyenteromycin (XVIII) with diazomethane. From the above fact, it was found that II is demethoxylated only by catalytic reduction without heating, and that such a phenomenon seems to be due to the specific position of the methoxyl group in the functional group in I and II.

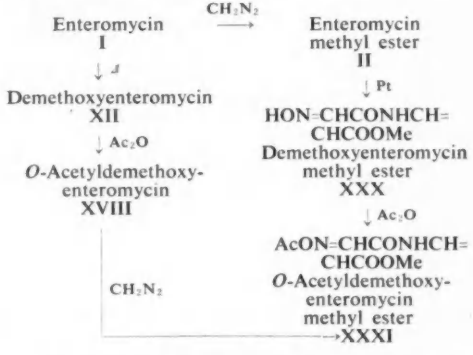

Catalytic reduction of enteromycin amide (XIV) on palladium-carbon yielded prisms (XXXII) [m. p. 179°C (decomp.), $C_5H_9O_4N_3$] and the product was called dihydroenteromycin amide. It was positive to the Barton reaction but negative to the ninhydrin reaction and the reaction of the hydrazino group[4], and though its ultraviolet spectrum (Fig. 3) showed an absorption maximum at λ 250 mμ (ε 5100), its infrared spectrum (Fig. 4) exhibited no absorption of C=C. Hydrolysis of the product with hydrochloric acid afforded β-alanine but neither glyoxylic acid nor acetaldehyde, and alkaline

* This constitutes Part XXXVIII of a series entitled "Studies on Antibiotics" by S. Tatsuoka, and was reported at the forum on Natural Organic Compounds, October 1960.

1) K. Mizuno, This Bulletin, **34**, 1419 (1961).
2) K. Mizuno, ibid., **34**, 1425 (1961).
3) K. Mizuno, ibid., **34**, 1631 (1961).
4) F. H. Pollard and A. J. Banister, *Anal. Chim. Acta*, **14**, 70 (1956).

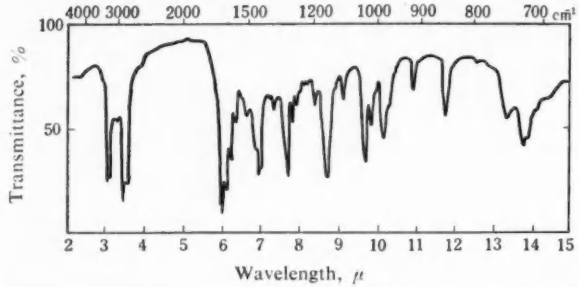

Fig. 1. Infrared absorption spectrum of demethoxyenteromycin methyl ester (XXX).

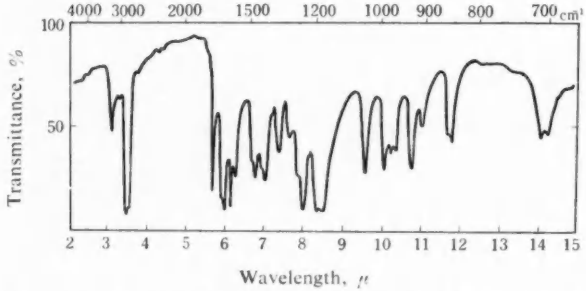

Fig. 2. Infrared absorption spectrum of *O*-acetyl demethoxyenteromycin methyl ester (XXXI).

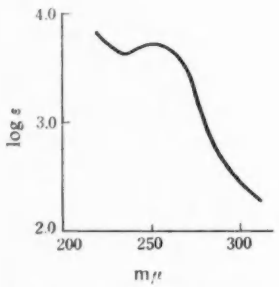

Fig. 3. Ultraviolet absorption spectrum of dihydroenteromycin amide (XXXII) in methanol.

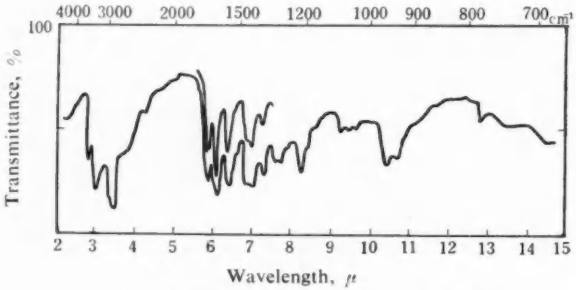

Fig. 4. Infrared absorption spectrum of XXXII.

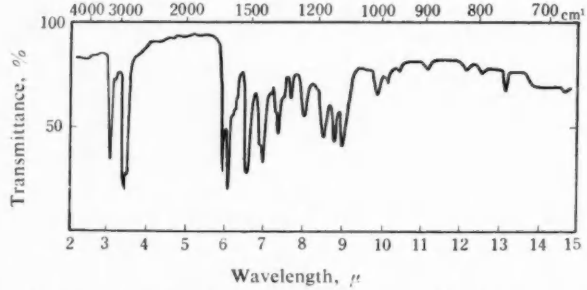

Fig. 5. Infrared absorption spectrum of a pyrazoline derivative (III) of enteromycin methyl ester.

hydrolysis of the product furnished β-alanine and oxalic acid under evolution of a basic gas.

Catalytic reduction of XXXII for a long time in the presence of palladium-carbon gave a light pink product readily soluble in water (XXXIII) [m. p. 213°C (decomp.), $C_5H_9O_3N_3$], which was negative to the Barton reaction but positive to the ninhydrin reaction. The product was hydrolyzed with alkali, and in the reaction mixture were detected β-alanine, ammonia and oxalic acid, by paper chromatography. Further reduction of the above product on Adams platinum oxide produced ammonia and glycyl-β-alanine. From these results, amidinocarbonyl-β-alanine was assigned as the structure of XXXIII.

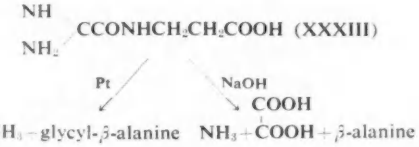

Accordingly, XXXII was considered to have the structure of *N*-(hydroxyamidinocarbonyl)-β-alanine (XXXII-i) and XIV the structure of *N*-(hydroxyamidinocarbonyl)-3-aminoacrylic acid (XIV-i) among the four formulas shown below:

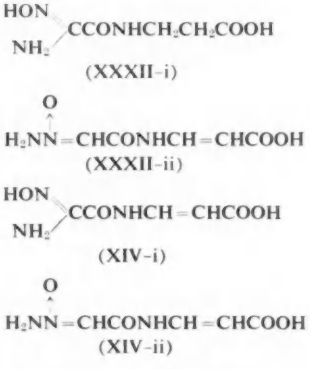

An aqueous solution of the product (XXXIV) obtained by catalytic reduction of demethoxy-enteromycin amide (XXI) on palladium-carbon showed no specific absorption in the long wave region beyond λ 220 mμ, and hydrolysis of the product with hydrochloric acid produced acetaldehyde, ammonia and glycine. On the other hand, XXI furnished acetaldehyde and glyoxylic acid when hydrolyzed with hydrochloric acid, and its infrared spectrum (Report II, Fig. 5) exhibited no absorption of C=C. From this fact, XXI was presumed to be 3-amino *N*-(hydroxyiminoacetyl)-β-alanine.

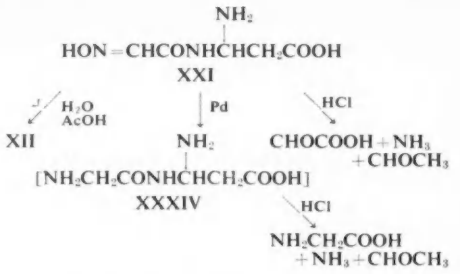

The amidation product of XII has not the same structure as that (XIV-i) of enteromycin amide. Judging from the structure of XIV-i, it is evident that the $-OCH_3$ group of the functional group characteristic of I is situated on the HO-N=CH-CO- side of XII and its position seems to be the nitrogen of the oxime or the α-carbon atom.

To make clear that enteromycin also has a 3-amino acrylic acid portion, the structure of the diazomethane addition product[1] (III) of enteromycin methyl ester was investigated. Catalytic reduction of III on Adams platinum oxide and hydrolysis of the product with hydrochloric acid yielded glycine but not β-alanine. The infrared spectrum (Fig. 5) of III exhibited no absorption of C=C. From these results the addition product was considered to be a pyrazoline[5] derivative formed by addition of diazomethane to the α, β-double bond. This suggested that II also has such a double bond.

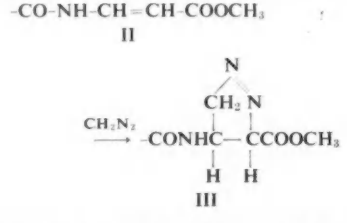

Namely, enteromycin also contains a 3-amino-acrylic acid portion.

From these results and considerations, the following two formulas were presumed as the structure of enteromycin.

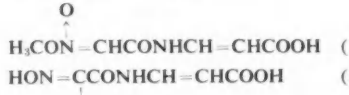

Of the two formulas, (I-i) was preferred from the following experimental data.

i) Glyoxylic acid was produced by acid hydrolysis.

5) K. V. Auwers and O. Ungemach, *Ber.*, **66**, 1205 (1933)

ii) Methylation with diazomethane gave not *N*- or *O*-methyl compound but a pyrazoline derivative.

iii) The products obtained in various stages of catalytic reduction had no methoxy group[6].

iv) Ultraviolet Spectrum showed at λ 298 mμ a strong absorption suspected to be due to conjugated nitrone.

v) To be negative to the reaction of Barton et al. for the phenolic hydroxyl group.

vi) Infrared spectra of I and II exhibited no absorption of –OH.

vii) Only one acidic group was observed.

Arndt et al.[7] once synthesized *O*-methyl-*aci*-nitroacetate and found that this compound was converted by heating into the corresponding oxime under evolution of formaldehyde. Gilman[8] explained the mechanism as this; a proton of the methoxyl is attracted by the coordinating oxygen and as a result the methoxyl converts into formaldehyde, while the corresponding oxime is formed. The formula I–i, having such a functional group, well explains the mechanism of the demethoxylation of enteromycin by heating. Since formation of formaldehyde from a methoxyl group may not be possible in any other group than the functional group, the formula I–i seems to be conclusively right from this point alone.

The problem still to be solved is whether or not amidation of a compound having such a specific structure as I–i furnishes a substance similar to XIV–i.

To clarify this point, ethyl *O*-methyl-*aci*-nitroacetate $C_5H_9O_4N$; $H_3CON{=}CHCOOC_2H_5$ (O above N) synthesized by the method of Arndt et al. was amidated under the same conditions as in I and detailed investigation was made on the product (XXXV) [m. p. 171°C (decomp.), $C_2H_5O_2N_3$]. The product was positive to the Barton reaction and its ultraviolet spectrum (Fig. 6) showed an absorption at λ 250 mμ (ε 5100), which was in accord with that of dihydroenteromycin amide (XXXII). Alkaline hydrolysis of XXXV evolved a basic gas and produced oxalic acid, and acetylation of it with acetic anhydride in warm water gave an *O*-acetyl compound [m. p. 168°C (decomp.), $C_4H_7O_3N_3$], which was negative to the Barton reaction and the infrared spectrum of which showed the absorption of AcON = (1755 cm^{-1}).

Next, XXXV was reduced for a long time in the presence of palladium-carbon, and the light pink product (XXXVI) yielded ammonia

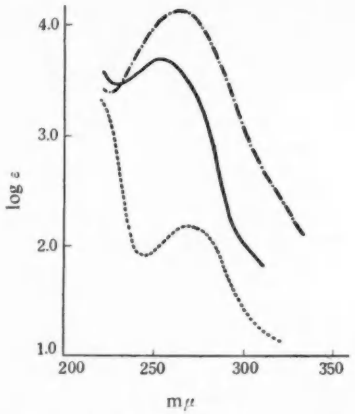

Fig. 6. Ultraviolet absorption spectra of ethyl *O*-methyl *aci*-nitroacetate (-·-·-), oxamide monoxime (XXXV) (——), and ethyl nitroacetate (----) in methanol.

and oxalic acid when hydrolyzed with alkali, and oxamide (XXXVII) when treated with hot water. Since, however, XXXVI was not isolated, the following experiments were carried out. XXXV was reduced on Adams platinum oxide and the product was hydrolyzed with hydrochloric acid, giving glycine. Catalytic reduction of the *O*-acetyl derivative of XXXV with palladium-carbon in acetic anhydride yielded a light pink product assumed to be *N*, *N'*-diacetyldiaminoacetamide [m. p. 257°C (decomp.), $C_6H_{11}O_3N_3$], and the structure was confirmed from the formation of glyoxylic acid by the hydrolysis of the product with hydrochloric acid.

From these results, XXXV is represented by the formula below and may be called oxamide monoxime. Thus XXXV was found to have a structure similar to XIV–i.

Thus, conversion of I–i to XIV–i was considered possible, and hence the plane structure of enteromycin was established as *N*-(*O*-methyl-*aci*-nitroacetyl)-3-aminoacrylic acid (I–i).

The steric configuration of I was investigated next. The infrared spectra of III, XXI, XXXII and XXXIII, which are considered to be saturated in the 3-aminoacrylic acid portion, scarcely showed the absorption of trans[9] C=C (960~990 cm^{-1}), whereas I, II, XII, XIV, XVIII, XIX, XX, XXII, XXX and XXXI, which are considered to be unsaturated in the portion, exhibited the absorption without exception, and therefore the configuration of the portion is assumed to be trans.

6) K. Johnson and E. F. Degering, *J. Am. Chem. Soc.*, 61, 3194 (1939).
7) F. Arndt and J. D. Rose, *J. Chem. Soc.*, 1935, 7.
8) H. Gilman, "Organic Chemistry Advanced Treatise I", 1st. ed. (1938), p. 627.
9) L. J. Bellamy, "The Infrared Spectra of Complex Molecules", Methuen & Co., Ltd., London, John Wiley & Sons, Inc., New York (1954), p. 40.

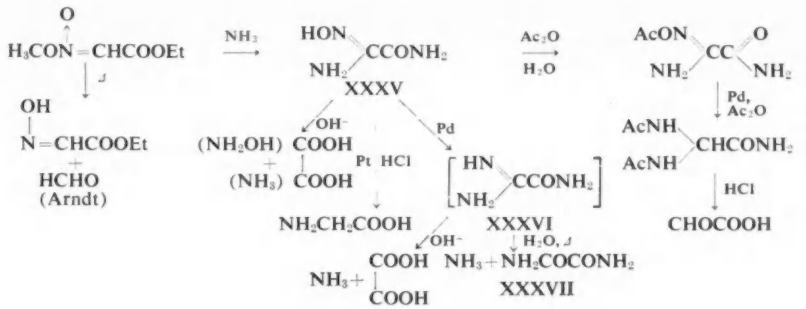

XII is an aldoxim and takes two crystal forms, but its *O*-acetyl derivative (XVIII) takes only one crystal form. Treatment of XVIII with alkali carbonate afforded XIIa but not the corresponding nitrile.

According to the rule proposed by Hantzsch et al.[10] and corrected by Brady et al.[11,12] and Meisenheimer et al.[13,14], and if all the compounds of the present work follow the rule, the configuration of the hydroxyiminoacetyl group of XII is assumed to be *syn*, and the hydrogen attached to the α-carbon atom is on the same side of the double bond as the coordinating oxygen in the *aci*-nitroacetyl group of I-i, and therefore** XXXVIII and XXXIX may be assigned to enteromycin and demethoxyenteromycin, respectively.

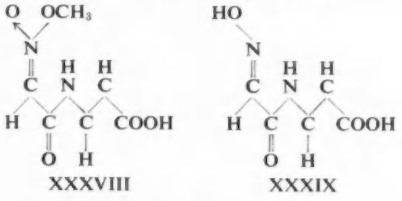

XXXVIII XXXIX

Experimental

Demethoxyenteromycin Methyl Ester (XXX).—A solution of 200 mg. of enteromycin methyl ester (II) in 40 cc. of pure methanol was reduced on 80 mg. of Adams platinum oxide until 0.8~0.9 mol. of hydrogen was absorbed. The catalyst was filtered off and the filtrate was evaporated at low temperature under reduced pressure, leaving about 150 mg. of crystals, m. p. 178°C (decomp.), which were recrystallized from methanol to give ca. 70 mg. of needles, m. p. 196°C (decomp.). The product is positive to the ferric chloride-potassium ferricyanide reaction.

Found: C, 42.00; H, 4.87; N, 15.86; O-CH_3, 18.29. Calcd. for $C_6H_8O_4N_2$: C, 41.86; H, 4.68; N, 16.28; O-CH_3, 18.03%.

***O*-Acetyldemethoxyenteromycin Methyl Ester (XXXI).**—a) To a solution of 50 mg. of XXX in 3 cc. of hot water was added several drops of acetic anhydride and the mixture, after standing for 10 min., was adjusted to pH 6.0 with sodium hydrogen carbonate and extracted with ethyl acetate. The extract was washed with water and evaporated at low temperature under reduced pressure, and the residual prisms, m. p. 116°C (ca. 20 mg.) were recrystallized from acetone. The product melted at 127°C.

b) A suspension of 300 mg. of *O*-acetyldemethoxyenteromycin (XVIII) in 7 cc. of ethyl acetate was allowed to react with a solution of diazomethan (produced from 1 g. of nitrosomethylurea) in 20 cc. of ether for 30 min. and the colorless reaction mixture was evaporated at low temperature under reduced pressure to leave a syrupy substance. The syrupy substance was left standing with a little ether and the resulting crystals (ca. 250 mg.) were recrystallized from acetone in prisms, m. p. 127°C. The product and that in a) gave the same infrared spectrum and their mixed melting point showed no depression.

Found: C, 45.16; H, 4.86; N, 12.76; O-CH_3, 13.96. Calcd. for $C_8H_{10}O_5N_2$: C, 44.86; H, 4.71; N, 13.08; O-CH_3, 14.36%.

Dihydroenteromycin Amide (XXXII).—A solution of 500 mg. of enteromycin amide (XIV) in 400 cc. of hot pure methanol was cooled and reduced on 150 mg. of palladium-carbon (1:10) until about one mole of hydrogen was absorbed (ca. 90 min.). The reaction mixture was evaporated at low temperature under reduced pressure, the syrupy residue was dissolved in 10 cc. of methanol, and ether was added to the filtered solution to deposit light pink crystals. The crystals were filtered off, the filtrate was concentrated, and ether was added to the syrupy residue, separating about 380 mg. of crystals, m. p. 176°C (decomp.), which were recrystallized

10) A. Hantzsch and A. Werner, *Ber.*, **23**, 11 (1890); **24**, 13 (1891).
11) D. L. Brady and G. Bischop, *J. Chem. Soc.*, **127**, 1357 (1925).
12) G. W. Wheland, "Advanced Organic Chemistry", (1949), p. 338.
13) J. Meisenheimer et al., *Ann.*, **495**, 249 (1932).
14) H. Gilman, "Organic Chemistry Advanced Treatise 1", 2nd ed., (1948) p. 467.
** Recently, Nishikawa et al.[15] conducted infrared spectroscopic analysis on the compounds of the present work and on their deuterium-substituted derivatives and reported that the intramolecular hydrogen bond observed between NH and coordinating oxygen in enteromycin methyl ester (II) could be explained only by its *anti*-configuration. If their assumption is right, the configuration of enteromycin is in reverse with that of XXXVIII and does not apply to the rule of Hautzsch et al.
15) M. Nishikawa et al., *J. Pharm. Soc. Japan* (*Yakugaku Zasshi*), in press.

from methanol in white plates, m.p. 179°C (decomp.) (250 mg.). The product is positive to the ferric chloride-potassium ferricyanide reaction, gives yellowish brown color with ninhydrin, and furnishes a spot at R_f 0.55 on Consden's paper chromatography described in Report I.

Found: C, 34.56; H, 5.49; N, 24.18. Calcd. for $C_5H_9O_4N_3$: C, 34.28; H, 5.18; N, 23.99%.

Decomposition of Dihydroenteromycin with Hydrochloric Acid.—A solution of 10 mg. of XXXII in 1 cc. of 6 N hydrochloric acid was heated under reflux at 100°C for one hour. In one half of the reaction mixture 5 mg. of 2,4-dinitrophenylhydrazine was dissolved and the solution was investigated by paper chromatography to detect no 2,4-DNPH of acetaldehyde or of glyoxylic acid. The remaining half of the reaction mixture was evaporated to dryness and the residue was chromatographed, giving the spot of β-alanine at R_f 0.65.

Decomposition of Dihydroenteromycin with Alkali.—A solution of 10 mg. of XXXII in 1 cc. of 1 N sodium hydroxide was refluxed for one hour, when a basic gas evolved copiously. The reaction mixture was passed through a column of Amberlite IR-120 (H-form) and the effluent was subjected to paper chromatography, detecting the spot of oxalic acid at R_f 0.20. The substance adsorbed on Amberlite IR-120 was eluted with 1 N ammonium hydroxide and the solution was chromatographed as above to give a spot of β-alanine.

Dehyroxydihydroenteromycin Amide (XXXIII).—A solution of 700 mg. of XXXII in 40 cc. of acetic acid was catalytically reduced for about 40 hr. in the presence of 200 mg. of palladium-carbon and the reaction mixture was concentrated at low temperature under reduced pressure in the atmosphere of nitrogen, leaving crystals, which, after washing first with ether and then with methanol, afforded about 350 mg. of light pink crystals, m.p. 205°C (decomp.). The product is positive to the ninhydrin reaction (light blue color) and gives a spot at R_f 0.77 on paper chromatography (Consden's method).

Found: C, 38.02; H, 6.00; N, 26.86. Calcd. for $C_5H_9O_3N_3$: C, 37.73; H, 5.70; N, 26.41%.

Addition of 1 cc. of 1 N sodium hydroxide to 20 mg. of the product evolved a gas, which was basic to pH test paper and reddened the Nessler's reagent, suggesting that it is ammonia. The mixture was boiled for one hour under reflux and subjected to paper chromatography, detecting oxalic acid and β-alanine.

Desaminodehydroxytetrahydroenteromycin [Glycyl-β-alanine] (XV).—A solution of 30 mg. of XXXIII in 5 cc. of 70% methanol was reduced on 20 mg. of Adams platinum oxide and the reaction mixture, after being filtered, was concentrated, leaving about 13 mg. of glycyl-β-alanine.

Catalytic Reduction of Demethoxyenteromycin Amide and Hydrolysis of the Product.—A solution of 30 mg. of demethoxyenteromycin amide (XXI) in 10 cc. of pure methanol was reduced on 15 mg. of palladium-carbon. The reaction mixture was neutral and evolved no ammonia, and it exhibited no specific absorption in the long wave region beyond 220 mμ. The reaction mixture was diluted with 3 cc. of water, the catalyst was filtered off, and the filtrate was concentrated at low temperature under reduced pressure, leaving a white residue, which was hydrolyzed by heating with 4 cc. of 3 N hydrochloric acid at 100°C for 2 hr. A 2 cc. portion of the reaction mixture was allowed to react with 2,4-dinitrophenylhydrazine and the resulting 2,4-DNPH was chromatographed to find the spot of the 2,4-DNPH of acetaldehyde at R_f 0.36. The rest of the reaction mixture was evaporated to dryness under diminished pressure and the residue was also chromatographed, detecting a large amount of glycine and traces of β-alanine.

Ethyl *O*-Methyl-*aci*-nitroacetate.—An amount of 2.7 g. of ethyl nitroacetate (K_p 79~81°C) prepared from ethyl acetoacetate by the method of Arndt et al.[5] was dissolved in 10 cc. of ether, and the solution was left standing with 40 cc. of an ether solution of diazomethane produced from 5 g. of nitrosomethylurea. The reaction mixture was evaporated at low temperature under reduced pressure, leaving an oily substance showing an absorption maximum (ε 13500) at λ 262 mμ.

Found: C, 41.05; H, 6.45; N, 9.02. Calcd. for $C_5H_9O_4N$ (ethyl *O*-methyl-*aci*-nitroacetate): C, 40.81; H, 6.17; N, 9.52%.

Oxamide Monoxime (XXXV).—To a solution of 1.5 g. of ethyl *O*-methyl-*aci*-nitroacetate in 10 cc. of methanol was added 50 cc. of methanol saturated with ammonia, and the yellowish orange-colored mixture, after standing at room temperature overnight, was concentrated at low temperature under reduced pressure, giving 1 g. of light yellow crystals, m.p. 165°C (decomp.). The crystals were dissolved in hot methanol, decolorized with carbon, and the solution was cooled to furnish about 600 mg. of colorless prisms, m.p. 171°C (decomp.), positive to the ferric chloride-potassium ferricyanide reaction but negative to the ninhydrin reaction.

Found: C, 23.58; H, 4.83; N, 40.27. Calcd. for $C_2H_5O_2N_3$: C, 23.30; H, 4.89; N, 40.77%.

An amount of 20 mg. of the product was boiled with 2 cc. of 1 N sodium hydroxide for one hour, when a basic gas evolved copiously. The reaction mixture was passed through a column of Amberlite IR-120 (H-form) and the effluent was chromatographed, giving the spot of oxamide at R_f 0.20.

***O*-Acetyloxamide Monoxime.**—To a solution of 2.5 g. of oxamide monoxime (XXXV) in 7 cc. of hot water was added dropwise 2 cc. of acetic anhydride at 60°C with vigorous stirring. After about 20 min. the reaction mixture was concentrated at low temperature under reduced pressure and the separated crystals were recrystallized from acetone in prisms, m.p. 168°C (decomp.).

The product was negative to the ferric chloride-potassium ferricyanide reaction and showed the infrared spectrum characteristic of =NOCOR (1755 cm^{-1}).

Found: C, 33.32; H, 4.83; N, 29.04. Calcd. for $C_4H_7O_3N_3$ (*O*-acetyloxamide monoxime; $CH_3COON{=}C(NH_2)CONH_2$: C, 33.10; H, 4.86; N, 28.96%.

***N*, *N'*-Diacetyldiaminoacetamide.**—A solution of 1 g. of *O*-acetyloxamide monoxime $AcON{=}C(NH_2)\text{-}CONH_2$ in a mixture of 20 cc. of glacial acetic acid and 7 cc. of acetic anhydride was reduced on 500 mg.

of palladium-carbon (1 : 10) for about 6 hr. The reaction mixture, after addition of water, was concentrated under reduced pressure, and the part sparingly soluble in hot acetone of the product was recrystallized from water to give about 800 mg. of light pink crystals, m. p. 257°C (decomp.).

Found: C, 41.51; H, 6.49; N, 24.41. Calcd. for $C_6H_{11}O_5N_3$ *N*,*N'*-diacetyldiaminoacetamide, $(CH_3CO\cdot NH)_2CHCONH_2$: C, 41.61; H, 6.60; N, 24.27%.

A solution of 50 mg. of the product in about 1 cc. of water was heated with a solution of 2,4-dinitrophenylhydrazine in hydrochloric acid for about 2 hr. to hydrolyze and at the same time to produce the 2,4-DNPH derivative. The reaction mixture was extracted with ethyl acetate and the extract was shaken with a sodium hydrogen carbonate solution. The alkaline solution was made acidic and extracted again with ethyl acetate, and the extract, after washing with water and drying, was evaporated at low temperature under reduced pressure, giving yellowish white needles, m. p. 192°C. The infrared spectrum of the product was in accord with that of the 2,4-DNPH of glyoxylic acid and the product showed the same color reaction (orange-brown with alkali) and the same R_f value (0.40) in paper chromatography as the 2,4-DNPH of glyoxylic acid.

Oxamide (XXXVII).—Catalytic reduction of a solution of 700 mg. of XXXV in a mixture of 10 cc. of methanol and 10 cc. of glacial acetic acid absorbed one mole of hydrogen in about 30 min. The reaction mixture had not the absorption maximum at λ 250 mμ and gave a light blue color with ninhydrin. The reaction mixture was concentrated at low temperature under reduced pressure and the syrupy residue was crystallized by addition of ether. The product was washed with ether, treated with cold water and warm water successively, and recrystallized from hot water to give about 200 mg. of crystals, m. p. above 300°C, negative to the ninhydrin reaction.

Found: C, 27.27; H, 4.76; N, 31.84. Calcd. for $C_2H_4O_2N_2$ (oxamide): C, 27.27; H, 4.58; N, 31.81%.

The ninhydrin positive substance (XXXVI) detected immediately after the reduction could not be isolated.

Catalytic Reduction of Oxamide Monoxime.—A solution of 10 mg. of XXXV in 10 cc. of glacial acetic acid was reduced to 20 mg. of Adams platinum oxide for about 2 hr. The reaction mixture was concentrated under reduced pressure and hydrolyzed by heating with 3 cc. of 6 N hydrochloric acid at 100°C for about one hour. Paper chromatography of the white residue of the hydrolysis mixture gave a spot of glycine.

Decomposition of *O*-Acetyldemethoxyenteromycin with Sodium Carbonate.—A mixture of 100 mg. of *O*-acetyldemethoxyenteromycin (XVIII) and 4 cc. of 5% sodium carbonate solution was allowed to stand at room temperature for 70 min. The reaction mixture was neutralized with acetic acid and extracted with ethyl acetate. The plates, m. p. 175°C (decomp.) (70 mg.) obtained from the extract were positive to the ferric chloride-potassium ferricyanide reaction and exhibited the same infrared spectrum as demethoxyenteromycin (XII).

Found: C, 38.12; H, 3.77; N, 17.52. Calcd. for $C_3H_6O_4N_2$: C, 37.98; H, 3.83; N, 17.02%.

Summary

Catalytic reduction of enteromycin methyl ester afforded demethoxyenteromycin methyl ester. Since demethoxyenteromycin amide was presumed to be 3-amino-*N*-(hydroxyiminoacetyl)-β-alanine, while enteromycin amide was considered to be *N*-(hydroxyamidinocarbonyl)-3-aminoacrylic acid, the two presumptive formulas, I-i and I-ii, were proposed for enteromycin. As the amido compound prepared by amidation of synthetic ethyl *O*-methyl-*aci*-nitroacetate was assumed to have the structure of hydroxyamido carbonyl amide (oxamide monoxime) and as enteromycin was demethoxylated by heating under evolution of formaldehyde, the formula I-i was found to be preferential, considering together other properties of the compound, and therefore the plane structure of enteromycin was established to be *N*-(*O*-methyl-*aci*-nitroacetyl)-3-aminoacrylic acid. The steric configuration of the 3-amino acrylic acid seems to be trans and that of the *O*-methyl *aci*-nitroacetyl group (the configuration of the hydrogen attached to the α-carbon atom and of the coordinating oxygen) to be syn.

The author is grateful to Dr. S. Kuwada, Director of the Laboratories for his kindness to give the chance to conduct the present work and for his encouragement throughout the work. Thanks are to Drs. K. Tanaka, A. Miyake, M. Miyamoto, Y. Ueno, J. Ueyanagi and T. Kanzawa for their kind advice. The author is also indebted to Messrs. Y. Kawamatsu, T. Yoshikawa for their kind assistance, to Dr. K. Nakazawa, Messrs. M. Shibata, M. Inowe and their coworkers who gave the starting material, to Messrs. M. Nishikawa, H. Nakamachi for their infrared spectroscopic analyses, to Dr. Y. Asahi for his measurement of dissociation constants, to Messrs. M. Kan, H. Kashiwagi and Mrs. Y. Tsukamoto, Misses F. Suzuki, M. Ueda, and H. Nabekura for their elementary analyses and Mr. T. Nakata for his azotometric determination.

Research Laboratories
Takeda Chemical Industries, Ltd.
Higashiyodogawa-ku, Osaka

Oxidation of Ferrous Ions in Aqueous Solutions by Cobalt-60 Gamma Rays. II[1]*. Effect of Anions at High Dose*

By Hiroshi HOTTA and Shin-ichi OHNO

(Received April 18, 1961)

It is well-known that the Fricke dosimeter ($G(Fe^{3+})=15.6$) is the best secondary standard dosimeter, but it has the upper limit of applicable doses due to the solubility of oxygen in the solution. The air-free system may also be applicable up to higher doses as a good dosimeter ($G(Fe^{3+})=8.2$) for the same kind of radiations with the Fricke dosimeter, if the procedure of degassing oxygen is not minded. For this purpose, the property at high dose was examined.

The reaction scheme for the air-free system is usually assumed as follows:

$$Fe^{2+}+OH=Fe^{3+}+OH^- \quad (1)$$

$$Fe^{2+}+H_2O_2=Fe^{3+}+OH^-+OH \quad (2)$$

$$Fe^{2+}+H+H^+=Fe^{3+}+H_2 \quad (3)$$

As the dose increases, $G(Fe^{3+})$ decreases gradually above a certain dose due to re-reduction of ferric ion produced, by the reaction

$$Fe^{3+}+H=Fe^{2+}+H^+ \quad (4)$$

competing with reaction 3. However, this reaction may not be so simple, for ferric ion is usually associated with anions in the solution, as discussed later.

On the other hand, sodium chloride is usually added by 0.001 M as a stabilizer for the Fricke dosimeter to suppress the effect of organic impurities, for chloride ion scavenges OH radical, which reacts with the impurities, like

$$Cl^-+OH+H^+=Cl+H_2O \quad (5)$$

and this reaction does not affect the $G(Fe^{2+})$ due to the following reaction[2]

$$Fe^{2+}+Cl=Fe^{3+}+Cl^- \quad (6)$$

The effect of anions, especially halide ions, on the radiolysis of ferrous solutions at high dose was investigated in the present study to obtain the detailed information of reaction 4.

Experimental

The preparation of solutions and the irradiation method by 10 kc. cobalt-60 gamma rays were the usual ones as was mentioned in Part I[1]. The composition of the solutions used is listed in Table I. All the solutions containing halide salts were dissolved in the "standard solution", which contained 0.04 M ferrous ammonium sulfate in 0.8 N sulfuric acid.

The concentration of ferric ion was usually measured by a Shimadzu spectrophotometer. The molar extinction coefficient of ferric ion at 304 mμ, which was 2150 cm^{-1} at 24°C, was constant between 0.2 N and 1.2 N sulfuric acid, but increased by 0.8% for

TABLE I. COMPOSITION OF SOLUTIONS USED IN M AND THEIR k_4/k_3 IN Eq. iii

Run	$FeSO_4(NH_4)_2SO_4$	H_2SO_4	Na_2SO_4	NaCl	KBr	KF	O_2	k_4/k_3
a	0.5	0.4	—	—	—	—	Free	9.77
b	0.5	1.4	—	—	—	—	Free	0.85
c	0.5	2.4	—	—	—	—	Free	0.80
d	0.5	4.0	—	—	—	—	Free	0.63
e	0.5	0.4	1.0	—	—	—	Free	2.7
f	0.04	0.4	—	0.001	—	—	Free	0.77
g	0.04	0.4	—	0.01	—	—	Free	2.1
h	0.04	0.4	—	0.1	—	—	Free	14
i	0.04	0.4	—	0.5	—	—	Free	54
j	0.04	0.4	—	0.001	—	—	Satur.	—
k	0.04	0.4	—	0.01	—	—	Satur.	—
l	0.04	0.4	—	0.1	—	—	Satur.	—
m	0.04	0.4	—	—	0.1	—	Free	2.1
n	0.04	0.4	—	—	—	0.1	Free	0.14
p	0.04	0.4	—	—	—	—	Free	0.67

1) Part I: H. Hotta, A. Terakawa and S. Ohno, This Bulletin, 33, 442 (1960).

2) H. A. Dewhurst, *Trans. Faraday Soc.*, 48, 965 (1952).

the rise of one degree centigrade between 13 and and 38°C. However, this was measured by the titration method of potassium permanganate for solutions containing fluoride ion or a large amount of ferric ion.

Results

Dependence of the Concentration of Ferrous and Sulfate Ions.—The oxidation of ferrous ion in the nitrogen-saturated solution of 0.5 M ferrous ammonium sulfate in 0.8 N sulfuric acid is shown as "a" in Fig. 1. The $G(Fe^{3+})$ was initially 8.2, and gradually decreased above 7×10^{6}r (0.05 M in ferric ion). The result for the 0.1 M ferrous solution, measured up to 0.09 M in ferrous ion, was almost the same as solution a. The $G(Fe^{3+})$ for the 0.04 M ferrous solution began to come down at 4×10^{6} r (0.03 M in ferric ion). The decrease of $G(Fe^{3+})$ at high dose is due to reaction 4 as mentioned in the "Introduction". On the other hand, the reaction

$$OH + H_2 = H + H_2O \qquad (7)$$

may promote reaction 4 at high dose, at which hydrogen molecules are accumulated in the closed medium. The conversion ratio of ferric ion to initial ferrous ion at the bending point of the (Fe^{3+})-dose curve is different between the above solutions.

The effect of sulfate concentration on $G(Fe^{3+})$ at high dose in nitrogen-saturated 0.5 M ferrous ammonium sulfate solutions is shown in Fig. 1, that is, solutions b, c and d were dissolved in 2.8, 4.8 and 8 N sulfuric acid, respectively, and solution f contained 1 M sodium sulfate in 0.8 N sulfuric acid. The decrease of $G(Fe^{3+})$ is considerably suppressed by 2.8 N sulfuric acid, but this effect does not increase much by the more concentrated sulfuric acid. Sulfuric acid is more effective than sodium sulfate as compared between solutions b and e which contained the same amount of sulfate group (1.4 M).

Effect of Halide Ions.—The oxidation of ferrous ion in the nitrogen-saturated standard solutions containing f 0.001 M, g 0.01 M, h 0.1 M and i 0.5 M sodium chloride, respectively, is shown in Fig. 2. As the concentration of of sodium chloride increases, the observed points depart at the lower dose from the straight line of solution f, and the $G(Fe^{3+})$ decreases with the increase of the dose.

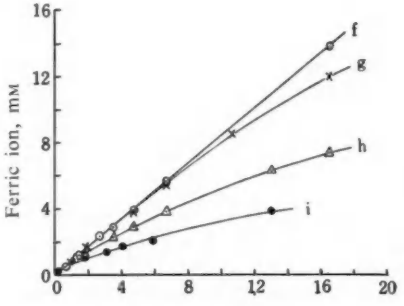

Fig. 2. Oxidation of ferrous ion in the nitrogen-saturated solutions f (⊙), g (×), h (△) and i (●).

On the other hand, the oxidation of ferrous ion in the oxygen-saturated standard solutions containing j 0.001 M, k 0.01 M, and l 0.1 M sodium chloride, respectively, is shown in Fig. 3. The thermal air oxidation of ferrous ion catalyzed by chloride ion, corrected in Fig. 3, were $(2.5\pm0.5)\times10^{-4}$ M in these solutions. The effect of chloride ion as seen in Fig. 2 does not appear even in solution l till oxygen is consumed.

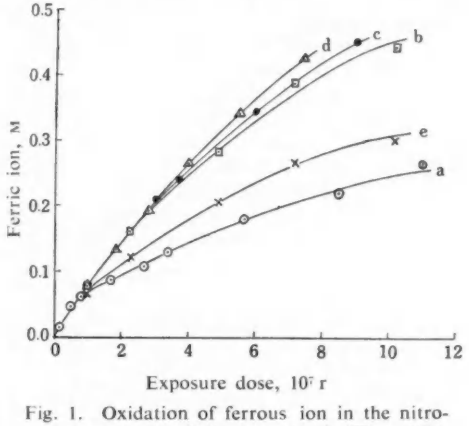

Fig. 1. Oxidation of ferrous ion in the nitrogen-saturated solutions a (⊙), b (⊡), c (●), d (△) and e (×).

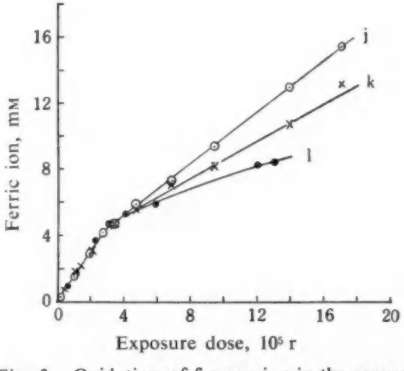

Fig. 3. Oxidation of ferrous ion in the oxygen-saturated solutions j (⊙), k (×) and l (●).

Table II. Concentration of complexes in M

Run	X	Fe^{III}	Fe^{3+}	$FeSO_4^+$	$Fe(SO_4)_2^-$	FeX^{2+}	FeX_2^+	FeX_3	X^-
h	Cl	0.01	9.1×10^{-5}	2.6×10^{-3}	7.3×10^{-3}	3.8×10^{-5}	4.9×10^{-6}	2.0×10^{-9}	0.1
i	Cl	0.01	9.0×10^{-5}	2.55×10^{-3}	7.2×10^{-3}	1.9×10^{-4}	1.2×10^{-4}	2.5×10^{-6}	0.5
m	Br	0.01	9.2×10^{-5}	2.6×10^{-3}	7.4×10^{-3}	4.6×10^{-6}	?	?	0.1
n	F*	0.01	5.3×10^{-5}	1.5×10^{-3}	4.2×10^{-3}	1.3×10^{-3}	2.6×10^{-3}	1.6×10^{-4}	1.55×10^{-4}
p	None	0.01	9.2×10^{-5}	2.6×10^{-3}	7.4×10^{-3}	—	—	—	—

Note: * On assumption that $\frac{(H^+)(F^-)}{(HF)}=1.17\times10^{-3}$ ($\mu=0.5$)[4].

Table III. Association constant of ferric complexes at 25°C

Ligand	K_1	K_2	K_3	Ionic strength	Reference
SO_4	95	9.4	—	1.0	5
F	1.62×10^5	8.9×10^3	500	0.5	4
Cl	4.2 ±0.2	1.3±0.4	0.04±0.02	1.0	6
Br	0.5	—	—	1.0	6

Note: $K_n=\frac{(FeX_n^{n-3})}{(FeX_{n-1}^{n-4})(X^-)}$

Furthermore, the effect of 0.1 M various halide ions, namely, h sodium chloride, m potassium bromide n potasium fluoride, and p nothing, in the nitrogen-saturated standard solution, was studied as shown in Fig. 4. The effectiveness on the $G(Fe^{3+})$ is in the order of

$$Cl^- > Br^- > SO_4^{2-} > F^- \qquad (i)$$

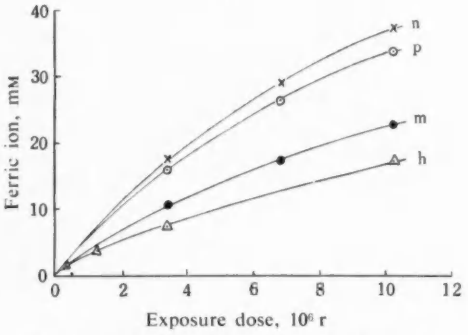

Fig. 4. Oxidation of ferrous ion in the oxygen-saturated solutions h (△), m (●), n (×) and p (⊙).

Discussion

If chloride ion is only a scavenger for OH radicals as mentioned in the "Introduction", the $G(Fe^{3+})$ should not be affected by the excess of chloride ion. However, the $G(Fe^{3+})$ in the air-free systems decreases at high dose with increase of chloride ion in Figs. 2 and 3. On the other hand, as mentioned already, ferric ions are more or less associated with anions; for example, as $FeCl^{2+}$, $FeCl_2^+$, $FeCl_3$ etc., and even if bare, hydrated with water molecules. Therefore, it is supposed that the reduction rate is different between those ferric complexes.

When the present hypothesis is correct, the observed series i for the effectiveness of various anions on the reduction of ferric ion might be understood by the properties and concentration of the complexes in the solutions. The concentrations of respective complexes in the irradiated standard solutions containing 0.1 M halide salt and 0.01 M ferric species are estimated in Table II without correction of activity on the asumption that ferrous and ammonium ions do not associate with any ion. The concentration of SO_4^{2-} is assumed to be 0.30 M in those solutions from Kerker's result[3]. Furthermore, the association constants of respective complexes in Table III[4-6] are used directly in the evaluation, for the association constant is usually not so changed between 0.5 and 1.0 of ionic strength expected from the above estimation for sulfuric acid.

Ferrous ion is considered to be also associated with hydrogen ion in the acidic solution through the oxygen atom of a water molecule like

$$Fe^{2+}\cdots O\begin{matrix}H\\ \cdots H^+\cdots H\end{matrix} \qquad (ii)$$

3) M. Kerker, *J. Am. Chem. Soc.*, **79**, 3664 (1957).
4) J. Hudis and A. C. Wahl, ibid., **75**, 4153 (1953).
5) R. A. Whiteker and N. Davidson, ibid., **75**, 3081 (1953).
6) E. Rabinowitch and W. A. Stockmayer, ibid., **64**, 335 (1942).

and the approach of a hydrogen atom to the hydrogen ion is assumed to be the rate-determining step of reaction 3. Therefore, if the effect of reaction 7 is ignored, the reaction scheme in the "Introduction" leads to the equation for the rate of oxidation in the mixture of ferric and ferrous ions[7].

$$\frac{d(Fe^{III})}{d(Dose)} = 2G(H_2) + \frac{2G(H)}{1+\frac{k_4(Fe^{III})}{k_3(Fe^{II})}} \quad \text{(iii)}$$

where k_3 and k_4 are the rate constants of reactions 3 and 4, respectively, and (Fe^{III}) and (Fe^{II}) are the concentration of ferric and ferrous species obtained by chemical analysis, respectively. Then, the appearent ratios, k_4/k_3, without considering complex formation, are obtained as listed in Table I as the measure of relative reduction rates. The larger value is more reliable.

Exactly speaking, since (Fe^{III}) and (Fe^{II}) do not always mean their free ion concentration (Fe^{3+}) and (Fe^{2+}), due to complex formation or imperfect dissociation, the apparent ratio should be rewritten as

$$\frac{k_4(Fe^{III})}{k_3(Fe^{II})} = \frac{1}{k_3(Fe^{2+})}\sum(c_i)k_4^i \quad \text{(iv)}$$

where c_1 and k_4^i are the concentration and rate constant of reduction reaction in reference to the i'th ferric complex, respectively, as

$$FeX^{2+} + H = Fe^{2+} + X^- + H^+ \quad (8)$$

instead of reaction 4. If the difference between (Fe^{II}) and (Fe^{2+}) is ignored, the relative rate constant to reaction 3, the k_4^i/k_3, for respective ferric complexes are obtained in Table IV

Table IV. Relative reduction rate and standard oxidation-reduction potential of ligand

Ligand	k_4^i/k_3 in Eq. iv	Standard oxidation-reduction potential V.
Br	3000	1.065
Cl	3400 ± 300	1.385
H_2O	20~70	1.77
SO_4	<2	1.98
F	≈0	2.85

from the estimation in Table II. The contribution except for Fe^{3+}, $FeSO_4^+$, FeX^{2+} is also ignored in the evaluation, for the concentration or reaction rate of ignored complexes is small in comparison with those species. The value for $FeCl^{2+}$ is obtained from k_4/k_3 of solutions g, h and i. The value of hydrated ferric ion corresponds to free ferric ion in Table II. The assumption for the concentration of SO_4^{2-} is effective for the values in Table IV, but not effective for the ratio between them. It is concluded from Table IV that the reduction rate of ferric chloride and bromide complexes by hydrogen atom is more than fifty times as great as hydrated ferric ions. Also that ferric sulfate complexes are much less reductive than hydrated ferric ion, and ferric fluoride complexes are scarcely reductive at all. It is also understood by the lower reductivity of ferric sulfate complexes why the dose-yield curve is straight ($G(Fe^{3+}) = 8.2$) up to high dose in spite of the production of ferric ion.

The quantitative analysis is impossible for the result of the concentrated solutions as shown in Fig. 1 for the lack of fundamental constants. However, since the k_4/k_3 of sulfuric acid solution is approximately proportional to the ratio of concentration, $(Fe^{3+})/(Fe^{III})$ from Eq. iv, this ratio can give some information for those systems. That is, the ratio, $(Fe^{3+})/(Fe^{III})$, is a function of the concentration of sulfate ion, which suppresses the concentration of free ferric ion by the formation of ferric sulfate complexes as less-reductive species, including the dependence of association constant on ionic strength[5,8]. It is concluded from the ratios in Table I that the concentration of free ferric ion in the solutions decreases and that of free sulfate ion increases with increase of sulfuric acid up to 1 M, but neither concentration changes so much in the more concentrated sulfuric acid solution. The fact is confirmed by the study of the dissociation of sulfuric acid[3,9]. Sodium sulfate is not so effective as sulfuric acid for the suppresion of the reduction reaction in comparison between solutions b and e containing the same amount of sulfate group, for the dissociation of sulfuric acid is suppressed by sodium sulfate. The difference of k_4/k_3 between solutions a and p containing the same amount of sulfuric acid may be due to the effect of direct reaction with thermerized electron as suggested by Weiss[10] or other reactions in a hot track in the concentrated solution.

On the other hand, in Fig. 3, the $G(Fe^{3+})$ in the presence of oxygen is not affected by chloride ion even in solution till oxygen is consumed. It is because all hydrogen atoms from the radiolysis of water associate rapidly with oxygen as HO_2 which is an oxydizing reagent. According to Rothschild and Allen, the association rate is more than one hundred times as fast as the rate of reaction 3[7].

7) W. G. Rothschild and A. O. Allen, *Radiation Research*, **8**, 101 (1958).

8) B. N. Mattoo, *Z. phys. Chem.*, **19**, 156 (1959).

9) T. F. Young and L. A. Blatz, *Chem. Revs.*, **44**, 93 (1949).

10) J. Weiss, *Nature*, **186**, 751 (1960).

Silverman and Dodson reported that the rate of electron exchange reaction between ferric chloride complex and ferrous ion is about ten times as fast as that between free ferric and ferrous ions[11]. For such a case, the ligand atom gives a chance for multi-charged ions to anchor easily at the same site, and also serves as the bridge of electron transfer. Brown[12] suggested that the effectiveness may be a function of the electronegativity and polarizability[13]. Since the reactivity of the hydrogen atom for the present reaction is not due to electrostatic force but due to unpaired electron, some difference is expected between the two cases. In fact, the electron exchange reaction between Tl^+ and Tl^{3+} is promoted in sulfuric acid[14], but ferric sulfate complex is less reductive for hydrogen atom than hydrated ferric ion as shown in Table IV. Anyhow, it is necessary for the reaction

$$Fe^{3+}-X^- + H \longrightarrow Fe^{2+} + XH \qquad (9)$$

even if XH is dissociated afterwards, that the ligand X loss one electron. The standard oxidation-reduction potential of the ligand to do so, ΔE, which may be a function of electronegativity and polarizability, corresponds to the reductivity of complexes in Table IV. The discrepancy for the order of bromide complex may be due to the uncertainty of its association constant. When the reduction rate of complexes might be expressed as

$$k = A \exp\left(-\frac{\Delta E}{RT}\right) \qquad (v)$$

the k_4'/k_3 of fluoride complex is expected to be the order of 0.01.

11) J. Silverman and R. W. Dodson, *J. Phys. Chem.*, **56**, 846 (1952).
12) Discussion in Ref. 11.
13) J. R. Tessman, A. H. Kahn and Wm. Shockley, *Phys. Rev.*, **92**, 890 (1953).
14) C. H. Brubaker, Jr., K. O. Groves, J. P. Mickel and C. P. Knop, *J. Am. Chem. Soc.*, **79**, 4641 (1957).

Summary

The $G(Fe^{3+})$ of air-free acidic ferrous sulfate solutions decreases gradually with the increase of dose due to the re-reduction of ferric ion produced. The decrement depends on the property of anion as well as sulfuric acid in the solution in the order of

$$Cl^- > Br^- > SO_4^{2-} > F^-$$

The relative reduction rate of ferric complexes is obtained in Table IV as a result of the estimation of respective complexes in the solution; that is, ferric chloride and bromide complexes promote the reduction of ferric ion, and ferric sulfate and fluoride complexes suppress it.

Japan Atomic Energy Research Institute
Tokai, Ibaraki-ken

15) L. Pauling, "General Chemistry", Chap. 32, W. H. Freeman & Co., (1953).

*Synthesis of Several Tertiary Alcohols from Propanol-2 and Ethylene by Gamma-ray Irradiation**

By Kozo Hirota and Motoyoshi Hatada

(Received April 22, 1961)

In previous reports[1,2], it was found that several higher ketones can be synthesized by a chain telomerization from acetaldehyde and terminal olefins by γ-ray irradiation with high G values. Similar telomerization may also occur with a high yield in the system of propanol-2 and ethylene, considering Urry's research[3] on the peroxide- and light-induced additions of several alcohols to olefins. The chain-carrying radical of this system, however, is $(CH_3)_2\dot{C}OH$ instead of $CH_3\dot{C}O$ in the systems of acetaldehyde and olefins, as will be shown as follows:

Initiating step:

$$(CH_3)_2CHOH \rightsquigarrow (CH_3)_2\dot{C}OH + H$$

Propagating step:

* Chain Telomerization Induced by Gamma-rays. II.
1) K. Hirota and M. Hatada, This Bulletin, **33**, 1682 (1960).
2) K. Hirota, S. Iizuka and M. Hatada, Abstract Papers of the 13th Annual Meeting of the Chemical Society of Japan (1960).
3) W. H. Urry et al., *J. Am. Chem. Soc.*, **76**, 450 (1954).

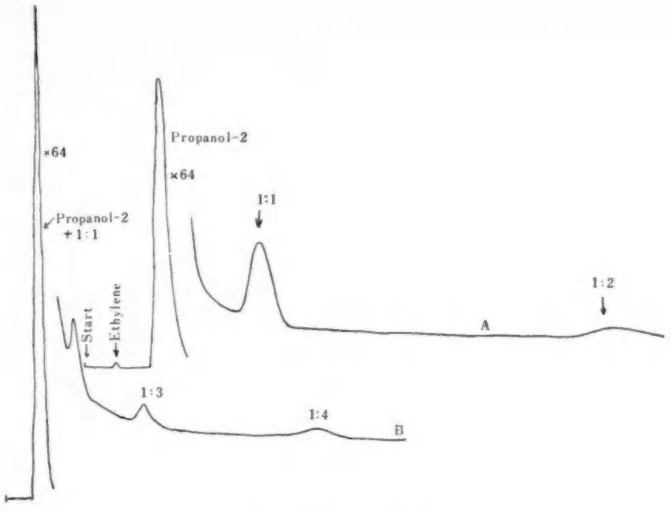

Fig. 1. Gaschromatograms of the samples after irradiation.
Curve A was obtained by using D. O. P. 3 m. column at 107°C.
Curve B was obtained by using H. V. O. 6 m. column at 180°C.

$$(CH_3)_2\dot{C}OH + C_2H_4 \xrightarrow{k_{p1}} (CH_3)_2C(OH)CH_2\dot{C}H_2$$

$$(CH_3)_2C(OH)CH_2\dot{C}H_2 \xrightarrow{+C_2H_4,\,k_{p1}} \xrightarrow{+(CH_3)_2CHOH,\ k_{d1}} (CH_3)_2C(OH)(CH_2)_2\dot{C}H_2$$

$$(CH_3)_2(C_2H_5)COH + (CH_3)_2\dot{C}OH$$

By a similar scheme $(CH_3)_2C(OH)(CH_2)_3\dot{C}H_2$ will produce $(CH_3)_2C(OH)(CH_2)_3$ and $(CH_3)_2C(OH)(CH_2)_3CH_2CH_2\dot{C}H_2$ with velocity constants k_{d2} and k_{p2}, respectively, etc.

It is the object of the present paper to report that the expected telomerization proceeds even at room temperature.

Experimental

Commercial pure propanol-2 was used after distillation, while commercial ethylene (research grade) was used without further purification. No impurity was found in the gases by either gaschromatographical or mass-spectral analyses.

Every sample for irradiation was degassed and distillated into glass tubes (1.2 cm. in diameter; ca. 20 cm. in length), equipped with a breakable joints. After the tubes were sealed, they were irradiated by γ-rays from the Co-60 source (700 c) installed in this laboratory. Dosimetry was based on a ferrous oxidation yield of 15.5. After the irradiation, the samples were taken out through the breakable joint and were put through gaschromatographic analysis (Apparatus; Shimadzu GC1A type).

The initial ratios of propanol to ethylene in the sample were about ten if otherwise not described. These ratios will be denoted as R hereafter, which, however, is not necessarily equal to that in solution, because ethylene is hardly soluble.

Results

In the sample irradiated, *tert*-amyl alcohol (1 : 1 telomer) and *tert*-heptyl alcohol (1 : 2 telomer) were identified by the use of a 3.0 m. column of dioctyl phthalate, while *tert*-nonyl alcohol (1 : 3 telomer) and *tert*-undecyl alcohol (1 : 4 telomer) were also detected by the use of a 6.0 m. column of high vacuum-oil (Fig. 1). However, the existence of higher telomers will be estimated, especially when R is large, as is done in the discussions.

In Fig. 2, the amount of the 1 : 1 telomer produced is plotted against the irradiated time. After an induction period is observed in the initial part of the curve, a linear increase is found in the amount. It is interesting to note that a similar induction period was also observed[4] in the gamma-ray-induced telomerization of acetaldehyde and ethylene. Such an effect may be due to the presence of some undetectable impurities, e. g. oxygen or other radical-scavengers. The G value calculated from the linear part of the curve is ca. 1.2×

4) Cf. K. Hirota, H. Ochi and M. Hatada, *Isotopes and Radiation (Tokyo)*, 3, No. 6 (1960). (Short communication).

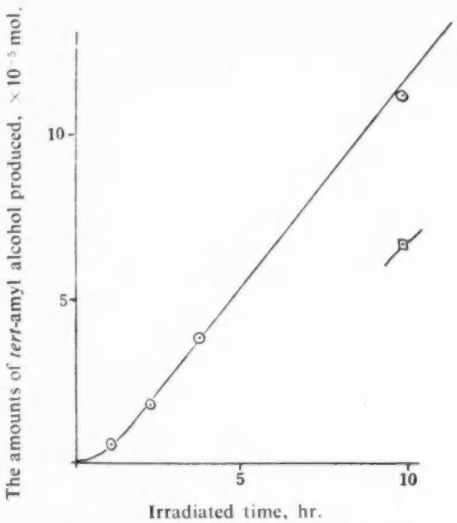

Fig. 2. The amounts of *tert*-amyl alcohol vs. irradiation time.
Dose rate, 5.7×10^{4} r/hr.
$(CH_3)_2CHOH/C_2H_4(=R)$ in mole, 1 : 10
Irradiation temperature, 6°C

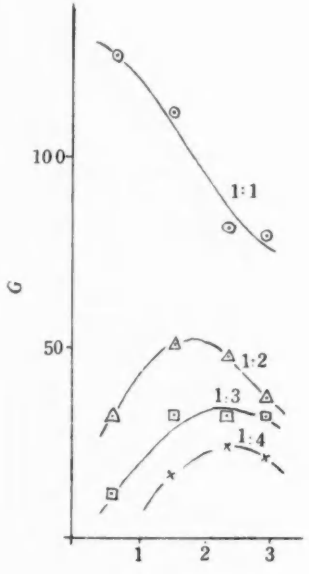

Fig. 3. *tert*-Alcohols produced vs. the amount of ethylene in the system.
Dose rate, 5.7×10^{4} r/hr.
Energy absorbed, 8.5×10^{19} eV.
Irradiation temp., 9°C

10^2, suggesting that this reaction proceeds by a chain mechanism. Figure 3 shows the relation between R and G values of the product at 9°C, where other variables are kept constant. By use of the data of Fig. 3 molar fraction F_i of the $1:i$ telomers to the total telomers is plotted in Fig. 4, making R as the ordinate. The full curves in the figure will be explained in the discussion.

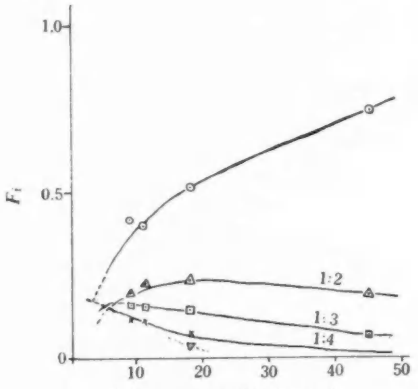

Fig. 4. Distribution of the telomers corresponding to the data of Fig. 3.
—— Calculated by

$$F_i=\frac{C_iR}{\prod_{i=1}^{n}(C_iR+1)}$$

▽ Assumed value for 1 : 5 telomer

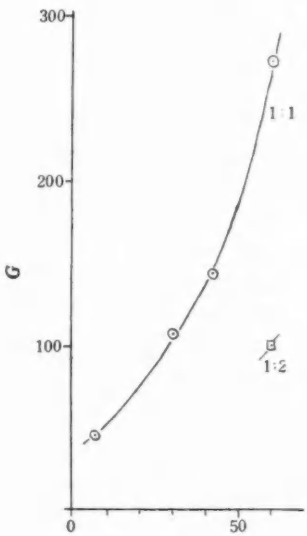

Fig. 5. *tert*-Amyl alcohols vs. irradiation temp.

Temperature dependency of G values on the amount of the products is shown in Fig. 5. It is clear that the higher is the reaction temperature, the more *tert*-amyl alcohol is produced and G value reaches about 300 at 60°C. Plots of logarithms of the G values vs. $1/T$°K give a straight line as shown in Fig. 6, by which an activation energy of 6.3 kcal./mol. can be determined. This value, however, is not necessarily that of the reaction, but is of complex nature, because the solubility of ethylene into alcohol changes when the reaction temperature is changed as is seen in our experiment.

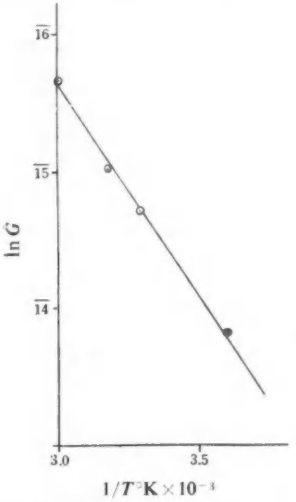

Fig. 6. ln G(*tert*-amyl alcohol) vs. $1/T$°K. E_A=6.3 kcal./mol.

Discussion

If the telomerization proceeds by the reaction scheme shown in the introduction, the distribution of the telomers produced will be given as molar fractions F_i by the theoretical relation[5]:

$$F_i = \frac{C_i R}{\prod_{i=1}^{n}(C_i R+1)}$$

where C_n's=k_{dn}/k_{pn} are transfer constants. Assuming that the molar ratio of alcohol to ethylene in the solution is the same as that (R) of the starting material and that higher telomers are produced though small in amount, chain transfer constants C_i's were calculated from the observed F_i's in the sample of R=18, and were found to be 0.062, 0.056, 0.073 and 0.12 for i=1, 2, 3 and 4, respectively, if G value of 1 : 5 telomer is assumed to be 8. The mean value of C_1, C_2 and C_3, i.e. 0.062, resembles Urry's average transfer constant, 0.057[3], obtained at 115~130°C, using di-*tert*-butyl peroxide as initiator. This means that the chain-propagating step of the radiation-induced reaction is similar to that of the reactions induced by chemical initiators, although the reaction temperatures, pressure and R values are different in the two reactions.

However, exactly speaking, plots of F_i determined from the observed data vs. R do not lie on the full curves calculated from the above C_i's so completely as shown in Fig. 4. Similar comparison of the theory and experiment was better in the systems of acetaldehyde and propylene[1] or isobutylene[2]. The discrepancy in this system may be brought about by the assumptions adopted in the calculation i.e., G value of 1 : 5 telomer and neglect of the change of solubility of ethylene to propanol-2 with pressure. Though a better coincidence may be obtained by the introduction of solubility data, this correction could not be carried on, because of the absence of such data. On the other hand, production of higher alcohols, corresponding to 1 : i telomer ($i \geq 5$), ought to be considered, as assumed to some extent in the calculation, because if they are completely neglected, the coincidence became more than that shown in Fig. 4.

The overall activation energy obtained above (6.3 kcal./mol.) nearly equals that of the abstraction reaction of hydrogen atom from α-carbon of propanol-2, i.e., 7.3 kcal./mol.[6] Considering the ambiguity included in the former value, such a degree of coincidence indicates that the step which produces the chain-carrying radical may be regarded as being the rate-determining one in the above mechanism.

In the irradiated samples containing a small amount of iodine (10^{-3} mol. in propanol-2), not even a trace of telomers was found, probably due to the radical-scavenging action of iodine. This finding may serve as an evidence of the radical mechanism as assumed by us. However, since formation of CH_nI^+ and CH_4OI^+ was recently observed mass spectrometrically by the ion-molecule reactions[7];

$$CH_n^+ + I_2 \rightarrow CH_nI^+ + I$$
$$\text{or} \quad CH_n^+ + I_2 \rightarrow CH_{n-1}I^+ + HI$$
$$CH_3OH^+ + I_2 \rightarrow CH_4OI^+ + I$$

an ion-scavenging action of iodine can be taken into account. It is possible therefore that some ion or ions also play some role in the

5) Cf. C. Walling, "Free Radicals in Solution", John Wiley & Sons, New York (1957), p. 245.

6) A. F. Trotman-Dickenson and E. W. R. Steacie, *J. Chem. Phys.*, **19**, 329 (1951); *Quart. Rev.*, **7**, 198 (1953).

7) A. Henglein, *Z. Elektrochem.*, **64**, 1015 (1960).

present reaction, but probably in some intermediate step which preceeds the production of $(CH_3)_2\dot{C}OH$. Then the initiating step above the mechanism will be composed of several elementary ones.

Though the *G* value of this telomerization is of the same order of magnitude as the system of acetaldehyde and propylene or isobutylene, it is smaller by one or two orders of magnitude at the same temperature than that of the system where acetaldehyde was used instead of propanol-2[4]. This may be attributed to the difference in nature between the chain-carrying radicals, i.e., acetyl radical and isopropyl radical in both systems.

Summary

Tertiary amyl and higher tertiary alcohols have been synthetized at 6~60°C by irradiating gamma-rays on mixture of propanol-2 and ethylene enclosed in glass vessels. It has been found that as the irradiation temperature the *G* value of these telomers increases markedly, e.g. up to ca. 300 at 60°C. It has been concluded from the distribution of the telomers produced that this reaction proceeds by a chain mechanism, making isopropyl radical $(CH_3)_2\dot{C}OH$ as the chain-carrying radical. It has been estimated that the characteristic of gamma-rays will be found in the step prior to the production of the isopropyl radical. If the rays can play some role in this reaction.

The authors wish to express their sincere thanks to Mr. Hiroshi Ochi for his help in performing the present research.

Osaka Laboratories
Japanese Association for Radiation Research on Polymers
Neyagawa, Osaka (M. H. & K. H.)
Department of Chemistry
Faculty of Science
Osaka University
Nakanoshima, Osaka (K. H.)

Syntheses and Ultraviolet Spectra of Aromatic Azo Compounds. I. Bromo-methylazobenzenes

By Yujiro NOMURA

(Received April 22, 1961)

The reaction of Grignard reagents with aromatic diazonium salts was first investigated by Hodgson and Marsden[1], who found that the addition of the zinc chloride double salts of several diazonium chlorides to arylmagnesium bromides in refluxing dry ether gave azo compounds in low yields.

Oda and Nakano[2], on the other hand, reported that the zinc chloride double salt of benzenediazonium chloride reacted with alkyl- or arylmagnesium bromides in ether at 0°C to give 6~34% of the theoretical amount of alkyl- or arylbenzenes.

Curtin and Ursprung[3] reinvestigated these reactions following the procedure of Oda et al. and observed that azo compounds were formed in 2~35% yields and no significant amounts of biaryls, reported by Oda et al. to be products of these reactions, could be obtained. They postulated that small amounts of metal impurities might be contained in magnesium employed by Oda et al. which catalyzed the reaction in an abnormal way.

The formation of biarly or azo compound in the reaction of Grignard reagent with diazonium ion may be represented by the following equations:

$$R-\overset{\oplus}{N}\equiv N: \longleftrightarrow R-N=\overset{\oplus}{N}: + R'MgX \rightarrow R-R' + N_2 + MgX^{\oplus} \quad (1)$$

$$R-N=\overset{\oplus}{N}: + R'MgX \rightarrow R-N=N-R' + MgX^{\oplus} \quad (2)$$

If the reaction proceeded according to 1, the same mole of nitrogen as biaryl R-R′ should be evolved. But no significant amounts of nitrogen have been observed to evolve in these reactions in accordance with the observations of Curtin et al. Since azobenzenes initially formed by the reaction 2 might react further

1) H. H. Hodgson and E. Marsden, *J. Chem. Soc.*, **1945**, 274.
2) R. Oda and K. Nakano, *Repts. Inst. Chem. Res., Kyoto Univ.*, **19**, 91 (1949); R. Oda, *Mem. Fac. Eng. Kyoto Univ.*, **14**, 195 (1952).
3) D. Y. Curtin and J. A. Ursprung, *J. Org. Chem.*, **21**, 1221 (1956).

TABLE I. BROMO-METHYLAZOBENZENES

No.	Compound	M.p., °C	Color	Found N, % (Calcd. for $C_{13}H_{11}BrN_2$: N, 10.18%)	Yield*
I	2-Bromo-2'-methyl	88~89[a]	Red	10.10	64
II	2-Bromo-3'-methyl	44.5~45.5[b]	Orange red	9.99	40
III	2-Bromo-4'-methyl	60.5~61.5[c]	Red orange	10.03	60
IV	3-Bromo-2'-methyl	49[c]	Red orange	10.24	61
V	3-Bromo-3'-methyl	79~79.5[c]	Orange	10.23	52
VI	3-Bromo-4'-methyl	119.5[d]	Orange yellow	10.08	65
VII	4-Bromo-2'-methyl	53.5~54[c]	Red orange	10.14	42
VIII	4-Bromo-3'-methyl	81.5[c]	Orange	10.19	68
IX	4-Bromo-4'-methyl	153[a]	Brown orange	10.03	68
X	4-Bromo-2-methyl	73~73.5[b]	Red orange	9.97	73
XI	4-Bromo-3-methyl	68.5[b]	Yellow orange	10.35	74
XII	2-Bromo-4-methyl	43.5~44[c]	Red orange	10.20	65.6

a) Recrystallized from ethanol.
b) Distilled in vacuo and then recrystallized from methanol.
c) Distilled in vacuo and then recrystallized from dilute ethanol.
d) Recrystallized from ethanol containing a small amount of benzene.
* Based on bromocompound used.

with excess Grignard reagent to yield hydrazobenzenes[4] and their derivatives[5], it was suspected that the attack of Grignard reagents on azobenzenes might be responsible for the rather poor yields of azo compounds.

The present study was carried out for the purpose of applying the reactions of Grignard reagents with diazonium salts to the preparations of various azo compounds and always the excess of diazonium salts over Grignard reagents were used expecting better yields of azo compounds.

General Procedure.—The ethereal solution of tolylmagnesium bromide prepared from 1 mol. of bromotoluene and the excess of magnesium was added slowly with vigorous stirring to the suspension of 1.3~1.5 mol. of the zinc chloride double salt of bromobenzenediazonium chloride at a rate necessary to maintain refluxing. The resulting dark red mixture was stirred for an additional 60 min. at room temperature and then poured onto ice-cold dilute hydrochloric acid. The ether layer was separated and washed with water and dried. Evaporation of the ether gave a solid or oil, which crystallized upon standing. The crude bromo-methylazobenzenes thus obtained were recrystallized from alcohol or distilled in vacuo, followed by recrystallization from alcohol.

In the syntheses of 4-bromo-2-methylazobenzene (X), 4-bromo-3-methylazobenzene (XI) and 2-bromo-4-methylazobenzene (XII), phenyl magnesium bromide and the excess of the zinc chloride double salts of bromotoluene-diazonium chlorides were used.

4) H. Franzen and W. Deibel, *Ber.*, **38**, 2716 (1905).
5) E. Bamberger and M. Tichvinsky, ibid., **35**, 4179 (1902).

The bromo-methylazobenzenes prepared by this method were shown in Table I. They are all new compounds except 4-bromo-4'-methylazobenzene (IX)[6] and 4-bromo-3-methylazobenzene (XI)[7], which showed no depression of their melting points on admixture with a respective authentic specimen prepared according to the literature.

Electronic absorption spectra were measured in an alcoholic solution. The maxima of the absorption spectra of bromo-methylazobenzenes were listed in Table II. It can be seen that the *K*-bands of bromo-methylazobenzenes shift

TABLE II. WAVELENGTHS AND INTENSITIES OF ELECTRONIC ABSORPTION MAXIMA (IN ETHANOL)

	K-band		*R*-band	
	λ, mμ	ε_{max}	λ, mμ	ε_{max}
I	329	14400	465	420
II	324	15700	455	430
III	333	19550	456	460
IV	327	18700	454	510
V	321	19900	446	670
VI	329	22300	442	570
VII	332	22800	456	590
VIII	328	24600	446	460
IX	333	26100	441	570
X	333	26600	457	610
XI	327	25600	445	530
XII	331	18900	456	450

6) 4-Bromo-4'-methylazobenzene was synthesized by D. Bigiavi et al., *Gazz. chim. ital.*, **57**, 557 (1927), by the condensation of *p*-nitroso-toluene and *p*-bromoaniline.
7) 4-Bromo-3-methylazobenzene was prepared by the bromination of 3-methylazobenzene or by the condensation of 5-amino-2-bromotoluene and nitrosobenzene. J. Burns et al., *J. Chem. Soc.*, **1928**, 2932.

towards a longer wavelength than unsubstituted azobenzene (λ_{max} 318 mμ, ε_{max}=20900 in alcohol) especially when methyl or bromine is in ortho or para positions. On the other hand, the molecular extinction coefficients (ε_{max}) became larger when methyl or/and bromine was situated in ortho, meta and para positions, in this order.

Experimental

Ultraviolet absorption spectra were measured by a Hitachi EPU 2 type spectrophotometer using a 1 cm. quartz cell.

Preparation of the Zinc Chloride Double Salt of Diazonium Chloride.—The mixture of 1 mol. of amine and 3~4 mol. of hydrochloric acid (1 : 1) was diazotized at 0°C with sodium nitrite dissolved in a small amount of water. To the resulting solution of diazonium chloride was added a cold saturated solution of zinc chloride (200 cc.) with stirring, when the zinc chloride double salt of diazonium chloride was separated out. After being allowed to stand in ice water for some time with occasional stirring, the double salt was filtered by suction and washed several times with a little ice-cold alcohol and then with ether. The double salt was spread in air and then dried in vacuum desiccator. The yield was excellent in most cases.

A few examples of the preparation of the zinc chloride double salt of diazonium chloride was shown below.

Thirty two grams of 2-amino-5-bromotoluene were added to 100 cc. of dilute hydrochloric acid (1 : 1), and the resulting suspension of the amine hydrochloride was diazotized at 0°C. A saturated solution of zinc chloride (about 40 cc.) was added to the diazotized solution with stirring. The yield of the double salt was 40 g. or 98% of the theoretical. In the same manner, from 17.2 g. of *p*-bromoaniline was obtained 28.0 g. (95% yield) of the double salt, and from 17.2 g. of *m*-bromoaniline was obtained 28.3 g. of the double salt.

Preparations of Bromo-methylazobenzenes.—Twelve bromo-methylazobenzenes were prepared following the general procedure described above. An example is given below in the preparation of 2-bromo-2'-methylazobenzene (I).

Seventeen grams of the zinc chloride double salt of *o*-bromobenzenediazonium chloride and 150 cc. of dry ether were put in a 300 cc. flask equipped with an efficient stirrer, a reflux condenser and a dropping funnel. A Grignard solution prepared from 7 g. of *o*-bromotoluene and 1.3 g. of magnesium in ether and diluted to about 40 cc. with dry ether was introduced from the dropping funnel to the suspension of the diazonium salt with vigorous stirring over a period of 15 min. without external cooling. Exothermic reaction occurred and gentle reflux continued for some time after all the Grignard solution was added. The mixture was diluted to double its volume with ether and shaken with cold dilute hydrochloric acid and then with water, dried over calcium chloride and evaporated to give the red crystals, which were recrystallized from ethanol with a small amount of decolorizing charcoal. The yield of 2-bromo-2'-methylazobenzene was 7 g. or 64% of the theoretical amount based on *o*-bromotoluene.

Summary

1) Twelve bromo-methylazobenzenes have been synthesized by the reactions of Grignard reagents with zinc chloride double salts of diazonium compounds. Ten of them are new compounds.

2) The ultraviolet absorption spectra of bromo-methylazobenzenes have been measured and some regularities of the absorption maxima have been observed in them.

The author is indebted to Dr. Nozomu Ebara for the determination of the ultraviolet absorption spectra.

Department of Chemistry
College of General Education
The University of Tokyo
Meguro-ku, Tokyo

Photoreduction of Methylene Blue by the Visible Light in the Aqueous Solution Containing Certain Kinds of Inorganic Salts. III. Kinetic Treatment of the Reaction

By Yoshiharu Usui and Masao Koizumi

(Received April 13, 1961)

It has been established in the previous papers[1] that upon irradiation of the aqueous solution of methylene blue containing various kinds of salts by visible light, the formation of leuco dye takes place accompanied by demethylation and the irreversible decomposition of dye; and in particular its rate is quite high in the presence of phosphate, sodium hydroxide and borate. Leuco formation and demethylation proceed as simultaneous reactions and in most cases the rate of the former is higher than that of the latter, which can be suppressed almost completely under suitable conditions.

Now it is very remarkable that the leuco-formation can occur without any reducing agents in the ordinary sense, and how this occurs still awaits further studies and is a very important problem to be solved. In the previous paper two possibilities were suggested for the primary process, i.e., the reaction of the excited dye and that of the ground state on one hand and the reaction between the excited dye and hydroxide ion on the other. Of course the problem must be attacked from various standpoints, and the present paper is chiefly concerned with the investigation from the reaction kinetics.

Kinetic Treatment

The present reaction as a whole is too complicated to be treated exactly, but it is desirable to get an approximate rate formula which can reproduce the experimental results, as a means for studying further the reaction scheme. Now the most reliable data supplied by the experiments are the decline of the main absorption band of the dye. But as already stated, the formation of leuco dye is accompanied with demethylation which causes the shift of the maximum toward the shorter wavelength. Therefore, by applying the minimum ratio method of Blaisdell[2] to the absorption spectra of the irradiated solution, the one due to the remaining methylene blue was evaluated and its analysis was undertaken. The decrease in dye concentration obtained from the above treatment is, of course the sum due to leuco-formation, demethylation and irreversible decomposition, but in view of the fact that these reactions take place with about the same ratio for a particular system during the most part of one run, the rate derived therefrom may well correspond to that of leuco-formation. It is necessary however, to pay due attention to this point when the rates for different systems are compared; for example, in case of phosphate the rate of demethylation is of about the same order of that of leuco-formation, while in case of sodium hydroxide the former is quite a good deal smaller than the latter.

In Fig. 1 plots of ε_{max} against time are given for the typical results so far obtained, in which ε_{max} pertains to the maximum of the absorption spectra of methylene blue after

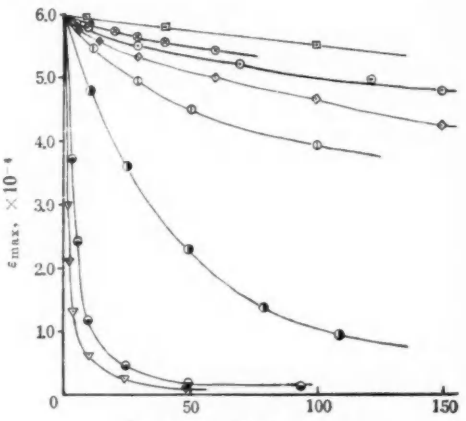

Fig. 1. Photobleaching of methylene blue in deaerated solutions containing various inorganic compounds.

◉ HCl(1×10^{-3} M), ◗ NaOH(1×10^{-3} M),
◯ Na_2SO_4, ⊗ NaCl, • NaI,
⊙ Without any salt, ◗ Borate buffer,
▽ Phosphate buffer

1) Y. Usui, H. Obata and M. Koizumi, This Bulletin, 34, 1049 (1961); H. Obata, ibid., 34, 1057 (1961).
2) B. E. Blaisdell, *J. Soc. Dyers. & Colorists*, 65, 619 (1949).

Blaisdell's treatment*. It is seen that broadly speaking, they are classified into three groups on the grounds of the magnitude of bleaching. The first group with a very small rate contains sodium sulfate, sodium iodide, sodium chloride and the pure aqueous solution. The second group with a medium rate contains only borate buffer, and the third one with the largest rate are phosphate buffer and sodium hydroxide solution. As stated below the first and the second groups have the rate formula which is approximately of the first order in respect to dye while for the third group the second order rate formula fits the experimental data quite satisfactorily. Hence the first and second group may be lumped together. In the following the rate for borate buffer and that for phosphate buffer will be separately discussed, each as a representative of the two groups.

Borate Buffer Solution.—Approximately, the rate is represented as of the first order with respect to dye, but as the reaction proceeds it becomes progressively smaller than that calculated from the simple first order rate formula. The cause for this retardation may supposedly be due to the interference of a certain reaction product; for example, such a product as hydrogen peroxide and this was really confirmed by the following experiment. Thus into the solution of methylene blue of which 80~90% had previously been photobleached, a suitable quantity of dye was newly dissolved in vacuo to make the concentration about equal to that of the previous one. Using such a solution the photoreaction was once more repeated and its rate was compared with that of the previous experiment.

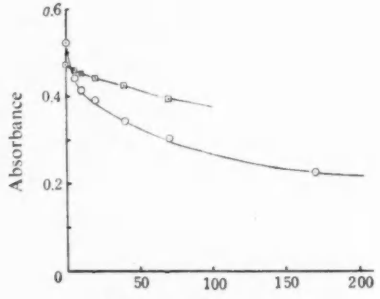

Fig. 2. Retardation by reaction product(s) in borate buffer at 30°C.
(● : 1st run, ◉ : 2nd run)

* Since the optical density of the solution during the course of the reaction is relatively small, the inner filter effect of the demethylated dye need not be taken into account.

As shown in Fig. 2, the rate in the second run is much smaller than that in the first one. On the basis of this result we now propose the following scheme as a tentative one.

$$\begin{array}{ccccccccc} \mathrm{MB} & \xrightarrow{h\nu} & \mathrm{MB^*} & \rightarrow & \mathrm{MB^t} & \cdots\cdots & \xrightarrow{a} \mathrm{X} & \xrightarrow{k_1} & \mathrm{P} \\ & & \downarrow & & \downarrow & & \downarrow k_d \quad \searrow^{k_2} & & +\mathrm{P} \\ & & \mathrm{MB} & & \mathrm{MB} & & \mathrm{MB} & & \mathrm{MB} \end{array} \qquad \text{(A)}$$

In this scheme it is assumed that the dye molecule goes via the triplet state to a certain intermediate X, and a is a fraction of excited dye which attains to X. X then is assumed to react in three different ways, i.e., the product-forming reaction of the (apparent) first order (rate constant; k_1) the usual deactivation process (rate constant; k_d) and a process of particular deactivation caused by the attack of some reaction product (rate; $k_2[\mathrm{P}][\mathrm{X}]$). In fact it is entirely unknown how the reaction product may interfere with the reaction, but here the above scheme may conventionally be adopted rather as a trial one, partially because of the simplicity of the formula obtained therefrom.

If the reaction proceeds in a steady state according to the above scheme, the rate formula may be expressed as follows;

$$-\frac{\mathrm{d}[\mathrm{MB}]}{\mathrm{d}t} = k_1[\mathrm{X}] = \frac{ak_1C}{k_1+k_d+k_2(C_0-C)} \qquad (1)$$

in which C_0 is the initial concentration of dye. In the absence of the retarding effect of the product, this equation is reduced to the following,

$$-\frac{\mathrm{d}[\mathrm{MB}]}{\mathrm{d}t} = \frac{ak_1C}{k_1+k_d}$$

Here it is to be added that the absorption of light is assumed to be approximately proportional to the dye concentration C.

Below it will be shown that the above trial formula is satisfactory to some extent.

Integration of 1 leads to

$$\frac{\ln C_0-\ln C}{C_0-C} = \frac{k_2}{k_1+k_d+k_2C_0} + \frac{ak_1}{k_1+k_d+k_2C_0}\,\frac{t}{C_0-C} \qquad (2)$$

This equation requires a linear relation between $(\ln C_0-\ln C)/(C_0-C)$ and $t/(C_0-C)$, which in fact is well satisfied by most of the experimental results within the experimental error. This is shown in Fig. 3.

It is also evident from the figure that Eq. 2 does not hold in the case of phosphate buffer. The values for intercept, $S=k_2/(k_1+k_d+k_2C_0)$, inclination, $\alpha=ak_1/(k_1+k_d+k_2C_0)$ and the ratio of the latter to the former, $ak_1/k_2(=\alpha/S)$,

TABLE I. RESULTS OF KINETIC TREATMENT

Condition of soln, M	pH	Concn. of dye*, M	$S\times10^{-5}$	$\alpha\times10^{6}$	α/S, mol. $l^{-1}\cdot sec^{-1}$
a) Na_2SO_4 ; 1.0×10^{-2}	6.10	1.2×10^{-5}	0.968	1.63	1.7×10^{-9}
b) NaI ; 1.0×10^{-2}	6.10	1.2×10^{-5}	0.640	0.32	5.0×10^{-10}
c) NaCl ; 1.0×10^{-2}	6.18	2.0×10^{-5}	0.676	0.69	1.0×10^{-9}
d) Plain aq. soln.	6.22	1.6×10^{-5}	0.566	0.71	1.3×10^{-9}
e) Na-Borate ; 7.8×10^{-3} HCl ; 1.6×10^{-2}	7.50	4.0×10^{-6}	6.96	17.7	2.5×10^{-9}
f) Na-Borate ; 7.8×10^{-3} HCl ; 1.6×10^{-2}	7.50	8.0×10^{-6}	2.46	4.84	2.0×10^{-9}
g) Na-Borate ; 7.8×10^{-3} HCl ; 1.6×10^{-2}	7.50	1.2×10^{-5}	1.34	3.10	2.3×10^{-9}
h) Na-Borate ; 7.8×10^{-3} HCl ; 1.6×10^{-2}	7.55	1.6×10^{-5}	1.16	3.68	3.2×10^{-9}
i) Na-Borate ; 7.8×10^{-3} HCl ; 0	9.15	1.2×10^{-5}	0.103	54.3	5.3×10^{-7}
j) Na-Borate ; 7.8×10^{-3} HCl ; 1.2×10^{-2}	8.30	1.2×10^{-5}	0.103	10.8	1.1×10^{-7}
k) Na-Barate ; 7.8×10^{-3} HCl ; 1.4×10^{-2}	7.85	1.2×10^{-5}	0.108	4.97	4.6×10^{-9}
l) Na-Borate ; 7.8×10^{-3} HCl ; 1.7×10^{-2} NaCl ; 1.0×10^{-1}	7.61	1.2×10^{-5}	1.01	9.30	9.3×10^{-9}

* Analytical concentration of the initial solution.

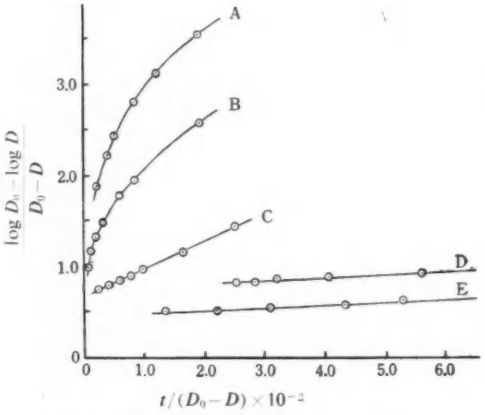

Fig. 3. Application of Eq. 2 for various salt solutions.
A. Phosphate buffer
B. NaOH aq. soln.
C. Borate buffer
D. Na_2SO_4 aq. soln.
E. aq. soln.

are summarised in Table I except for phosphate and sodium hydroxide for which Eq. 2 does not hold.

For the further support of Eq. 2, the effect of the initial concentration on the rate was examined in case of borate buffer. From Eq. 2 the reciprocal of the intercept ($=1/S$) should satisfy the following equation,

$$\frac{1}{S}=\frac{k_1+k_d}{k_2}+C_0 \qquad (3)$$

hence the plot of $1/S$ against C_0 should be a straight line of slope 1. The slope experimentally obtained is about 0.91 as shown in Fig. 4.

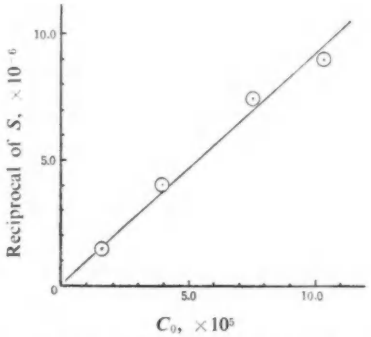

Fig. 4. Plot of $1/S$ against initial concn. C_0.

Further, the reciprocal of inclination of Eq. 2 being represented as follows,

$$\frac{1}{\alpha}=\frac{k_1+k_d}{ak_1}+\frac{k_2}{ak_1}C_0 \qquad (4)$$

the plot of $1/\alpha$ against C_0 should be linear with the inclination of k_2/ak_1. This was in fact satisfied by the experimental data, the value obtained being 4.4×10^5 (mol^{-1} l. sec.)

which agrees approximately with the mean value of (e)—(h) in Table I ($S/\alpha=4.0\times10^{8}$).

Thus the reliability of Eq. 2 was substantiated to some extent, and so the effect of pH on the rate, which was examined in the region of pH, 7.40~9.15 keeping the concentration of borate ion constant, was analyzed by Eq. 2. The values of $\log \alpha/S(\alpha/S=ak_1/k_2)$ for the various pH values are shown in Table II.

Table II

pH	$\log[OH^-]$	$\log \alpha/S$
9.15	−4.85	−7.28(−7.69)
8.30	−5.70	−7.97
7.85	−6.15	−8.32
7.55	−6.45	−8.63
7.40	−6.60	−8.48

It is apparent that the value of α/S increases approximately proportionally to the concentration of $[OH^-]$.

Phosphate Buffer Solution. — It is assumed that the essential difference against the case of borate lies only in the bimolecular reaction of X and MB, which leads to the production of leuco dye, all the other steps being quite similar as in the previous one. Thus

$$MB \xrightarrow{h\nu} MB^* \rightarrow MB^{\dagger} \cdots\cdots \xrightarrow{a} X \xrightarrow[k_1']{MB} P$$

$$\downarrow \qquad \downarrow \qquad\qquad \downarrow k_d' \quad \downarrow k_2' \quad \searrow$$

$$MB \qquad MB \qquad\qquad MB \quad MB \qquad P$$

whence the rate is expressed as follows,

$$-\frac{d[MB]}{dt}=\frac{2ak_1'C^2}{k_1'C+k_d'+k_2'(C_0-C)}=\frac{2ak_1'C^2}{k_d'+(k_1'-k_2')C+k_2'C_0} \qquad (5)$$

In view of the fact that the experimental data can quite satisfactorily be reproduced by the second order rate formula, it may be permissible to put $k_1'=k_2'$. Then,

$$-\frac{d[MB]}{dt}=\frac{2ak_1'C^2}{k_d'+k_2'C_0}=2kC^2 \qquad (6)$$

where

$$k=\frac{ak_1'}{k_d'+k_2'C_0}$$

Some examples for the relation $1/C\sim t$ are shown in Fig. 5. Most of the experimental results satisfy the linear relation. (Table III).

When the initial concentration is varied, the following relation should hold between the reciprocal of k and C_0

$$\frac{1}{k}=\frac{k_d'}{ak_1'}+\frac{k_2'}{ak_1'}C_0 \qquad (7)$$

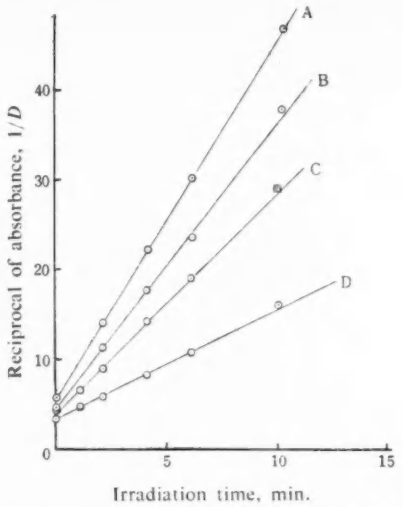

Fig. 5. Plot of the reciprocal of absorbance (D) against the irradiation time at constant pH.
Initial concn. of dye; A····· 4×10^{-6} M
B····· 8×10^{-6} M
C·····1.2×10^{-5} M
D·····1.6×10^{-5} M

Table III. Kinetic data and condition of the solution
(Concn. of total phosphate=6.7×10^{-2} M)

Concn. of dye, M	pH	k, mol^{-1} l. sec^{-1}
4×10^{-6}	7.56	2.00×10^{3}
8×10^{-6}	7.58	1.09×10^{3}
1.2×10^{-5}	7.54	1.03×10^{3}
1.6×10^{-5}	7.58	0.67×10^{3}
1.2×10^{-5}	6.94	0.94×10^{3}
1.2×10^{-5}	7.71	1.16×10^{3}
1.2×10^{-5}	8.07	1.30×10^{3}
1.2×10^{-5}	8.81	1.48×10^{3}

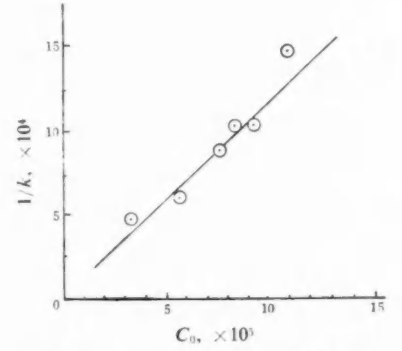

Fig. 6. Plot of $1/k$ against initial concn. C_0 for Eq. 7.

It was confirmed that the experimental results approximately satisfy the above relation. This is shown in Fig. 6.

The effect of pH on the rate was examined and the results are shown in Table IV.

TABLE IV

pH	log[OH⁻]	log k
8.81	−5.19	3.17
8.07	−5.93	3.11
7.71	−6.29	3.06
7.52	−6.48	3.02
6.94	−7.06	2.97

In contradistinction to the case of borate buffer, the rate is scarcely affected by the variation of pH.

The Effect of Some Added Substances

The Behavior when Ferric Chloride and *o*-Phenanthroline are Added. — In the previous paper it was reported that when these substances are added to the borate buffer solution of methylene blue and irradiated, the complex between Fe^{2+} and *o*-phenanthroline is formed, the quantity of which attains to more than ten times that of the dye. Thus, it was concluded from the above result, that no impurity contained in dye participates essentially in the reaction. In addition to this conclution, the investigation of this system is important with regard to the quantitative relation between the leuco-formation and the irreversible photodecomposition. So further description will be given below.

A typical result is shown in Fig. 7, in which the absorption band of 510 mμ is due to trisphenanthroline iron(II) complex. In this experiment the concentration of the complex produced by 2 min. irradiation is about fourteen times that of the decrease in dye concentration. This decrease is due to the irreversible bleaching, the solution not being decolorized by aeration. Thus it may be judged that if the formation of leuco dye takes place only by the accompanying irreversible decomposition of dye, then one molecule of dye decomposed ought to be able to produce more than ten molecules of leuco dye. This makes the above view highly improbable.

It is to be added that when the irradiation is continued after all the Fe^{3+} has been consumed to produce trisphenanthroline iron(II) complex, the bleached dye partially recovers its color upon the introduction of air. Therefore it is certain that as long as Fe^{3+} exists the produced leuco dye reduces Fe^{3+}, but after the disappearance of Fe^{3+} the existence of the reduced dye persists.

It is regrettable that no such experiment can be performed for the phosphate solution on account of the small solubility of Fe^{3+} salt.

The Effect of the Addition of Pyruvate. — It was reported in the previous paper that a small quantity of hydrogen peroxide was detected in case of borate buffer but not in phosphate buffer. Now it is well known that in general hydrogen peroxide is rapidly decomposed by the addition of pyruvate, and it is interesting to investigate the effect of the addition of pyruvate upon the rate and to compare the two cases when the phosphate or borate buffer is used. The concentrations of pyruvate (C_{py}) added to the borate buffer are 1.2×10^{-4}, 2.2×10^{-4}, and 2.4×10^{-4} M. The results are shown in Fig. 8.

It is apparent from the figure that the slope becomes steeper with the increase of the concentration of pyruvate. Further, when α/S-values for the two cases, one with pyruvate and the other without it but otherwise in the similar conditions are compared, the value for the former is definitely larger; thus from Fig. 8 for $C_{py}=2.2\times10^{-4}$ M, $\alpha/S=7.57\times10^{-3}$ and for $C_{py}=0$, $\alpha/S=2.97\times10^{-3}$ (mol. l^{-1} sec^{-1}). The above results are well comprehended if the k_2-value in the second term on the right side of Eq. 2 gets smaller with the addition of pyruvate. Although the possibility for other steps to be affected might not be neglected, it seems most plausible that the

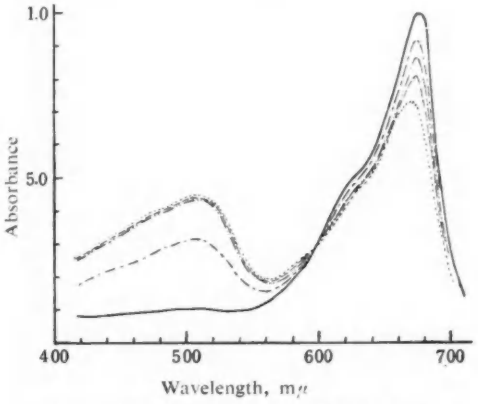

Fig. 7. The spectral change of the mixture of methylene blue-borate buffer, *o*-phenanthroline and ferric chloride solution when irradiated.
—— initial
—— 2 min.-irradiation
—— 5 min.-irradiation
—— 20 min.-irradiation
····· 50 min.-irradiation

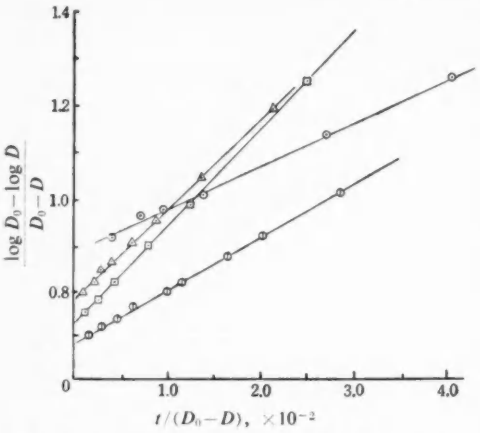

Fig. 8. The effect of the addition of pyruvate on Eq. 2 (D……optical density).
- ⊙ [Pyr] = 0
- ① [Pyr] = 1.2×10^{-4} M
- △ [Pyr] = 2.2×10^{-4} M
- ● [Pyr] = 2.4×10^{-4} M

addition of pyruvate chiefly affects the k_2-value in view of the result obtained for phosphate buffer (described below).

When ten times as much pyruvate as the concentration of methylene blue was added to phosphate buffer, the rate was also represented as of the second order with respect to dye and the k value of Eq. 6 was evaluated to be 5.3×10^{2} (mol^{-1} l. sec^{-1}). This is slightly smaller than 6.2×10^{2}, which is the k-value in the absence of pyruvate but otherwise having similar conditions. It is evident that the addition of pyruvate to the phosphate buffer scarcely affects the rate.

Thus the effect of pyruvate-addition is quite different in the case of phosphate and borate, and this is just what is expected from the results already obtained.

The Effect of the Addition of Quinone. — It was reported in the previous paper that in the case of phosphate buffer, neither hydrogen peroxide nor oxygen was detected. But it is premature to deny the formation of oxygen only on the basis of this analysis, because the produced oxygen may be consumed in the irreversible photodecomposition of dye. In order to detect the oxygen formed, it seems rather essential to make the experiment under conditions such that the oxygen which might be produced, be accumulated so rapidly that it is scarcely consumed in the photooxidation of dye.

With this view in mind and from the analogy of the Hill reaction in photosynthesis, the addition of quinone was tested. Thus if the quinone does not attack the excited dye but only oxidizes the leuco dye produced as in the case of the Hill reaction, the oxygen is expected to be accumulated.

Preliminary tests demonstrated, however, that the addition of quinone, the quantity being up to several times (in mole) that of the dye induces a quite complicated spectral change of methylene blue when the evacuated solution is irradiated. In addition, spectra of methylene blue in the above solution were found to change even in the dark though the rate was much slower.

Thus there is no doubt that the direct photoreaction does take place between dye and quinone. This reaction seems to be interesting from a different point of view, but it is clear that quinone is too reactive to be used for the above object. Hence further studies have been abandoned. Other kinds of quinones or other types of oxidants more mild in character should be searched.

Quantum Yield

In both buffer solutions, the quantum yield (γ) for the initial stage was evaluated by using the inclination of the curve of optical density against time, and the number of photons (I_{abs}) absorbed by the solution, both in the initial stage. The latter quantity was measured with the combination of the thermopile (Moll and Burger standard thermopile) and White single potentiometer (Leeds and Northrup).

The following table shows the results obtained for borate and phosphate buffer solutions.

Table V. Quantum yield

Condition		I_{abs} (photons. sec^{-1} cc^{-1})	$\Delta D/\Delta t$ (D, min^{-1})	γ
a)	Phosphate	7.2×10^{15}	0.089	9.2×10^{-4}
	buffer	6.9×10^{16}	0.029	7.1×10^{-4}
b)	Borate	3.5×10^{15}	0.006	3.0×10^{-4}
	buffer	8.7×10^{15}	0.010	2.2×10^{-4}

Discussion

It was found in the previous paper that the general feature of the reaction is somewhat different in borate and phosphate buffer. Now in the present paper additional differences were found from the kinetic standpoint. Thus the rate in borate buffer is approximately of the first order in dye while that of the phosphate buffer, is of the second order, and moreover the pH effect is quite different in two cases. Therefore, two cases will be separately discussed, anticipating the essential difference in mechanism.

In case of borate the rate being of the first order in dye, the interaction of two dye molecules of which one acts as an electron-donor and the other as an acceptor can safely be neglected. The result of the experiment pertaining to the formation of trisphenanthroline iron(II) chloride also denies such an interaction. Thus one cannot but consider that in this case the oxidation of water is taking place under some cooperative action of the salt. In fact, as reported in the previous paper, a small quantity of hydrogen peroxide was detected.

As regards the photofission of water by visible light, Yamafuji reported a long time ago[3] that hydrogen peroxide was produced when the solution of eosine or chlorophyll was irradiated by the solar light. Their experiments, however, were criticized by Rabinowitch[4] and at present their results seem to be judged to be doubtful.

Indeed the decomposition of water by the visible light by virtue of the following scheme

$$H_2O \rightarrow H + OH$$

or

$$HO^- \rightarrow e + OH \qquad (6)$$

must be almost impossible from the energetic reason, except for the case in which the absorption of more than two photons takes part in one act. However, if the reaction in the following molecular mechanism occurs,

$$D^+ + 2OH^- \rightarrow DH + HO^-_2 \qquad (7)$$

the free enthalpy change is not so great. It is ca. $\Delta G^\circ_{298} = 49.65$ kcal./mol. so that with an efficient use of the energy of photon absorbed, ca. 43.0 kcal., only 6.6 kcal. needs to be provided for the reaction 7 to occur. If borate ion can afford a certain amount of free enthalpy in some way, then the quantum yield experimentally obtained would be attained by the process 7.

In connection with this it is tempting to recall that borate is an electron deficient substance and to suppose that some of the borate ions may be in a certain energy-rich state combining with hydroxide ion. Alternatively there might be a possibility that a certain species of dye such as $(D\cdots OH)H^+$ which Lewis[5] proposed, takes part in the reaction to make it energetically feasible. The result that the rate is approximately of the first order in $[OH^-]$ in spite of the second order for the stoichiometric equation, might be related with this.

Next the case of phosphate will be discussed. In this case neither hydrogen peroxide nor oxygen was detected and the reaction proceeds in the second order with regards to dye. These facts seem at first strongly to suggest that the initial process is the interaction of the excited dye with the ground-state-dye molecule, the electron transfer taking place between them according to

$$D^* + D \rightarrow D^- + D^+ \qquad (8)$$

and resulting in the leuco-formation from one dye molecule and the irreversible decomposition of another. But judging from the result that 70~80% of the bleached dye is recolorized by the introduction of air, it seems necessary that one molecule of dye decomposed ought to be able to reduce about three dye molecules and that the reducing power of the substances produced by dye-decomposition should be much larger; otherwise the quantity of reduced dye would be much less. Hence the above scheme would not be accepted unless it is confirmed experimentally that the above requirements are really satisfied. At the present stage it seems rather improbable that the leuco-formation only occurs through 8 though it may contribute to some extent.

On the other hand, the reaction

$$2D^+ + 2OH^- \rightarrow 2DH + O_2 \qquad (9)$$

seems not entirely impossible from the energetic view point. Thus its ΔG°_{298} is 55.93 kcal. and taking the energy of photon, 43.0 kcal. into account, the free enthalpy is evaluated to be about 6.4 kcal. for one dye molecule. Should the phosphate ion be able to provied energy in some way, reaction 9 would be realized just as reaction 7.

The role of phosphate ion must be clarified irrespective of wether the reaction goes via 8 or 9.

The photoreduction which has been confirmed in this series of investigation would be expected to occur in other thiazine dyes and this has really been ascertained in the case of thionine. Since the demethylation need not be taken into account for thionine, the quantitative study would be more feasible particularly as regards the interrelation between leuco-formation and irreversible decomposition. These are now in course of study.

Summary

Kinetic treatment was undertaken for the photobleaching of the aqueous solution of methylene blue containing various inorganic salts.

If a certain kind of inhibiting action due to

3) K. Yamafuji et al., *Biochem. Z.*, **301**, 404 (1939).
4) E. I. Rabinowitch, "Photosynthesis and Related Processes", Vol. I, Interscience Publishers, Inc., New York (1956), p. 78.
5) G. N. Lewis et al., *J. Am. Chem. Soc.*, **65**, 1150 (1943).

some reaction product(s) is taken into consideration, the rate for borate buffer is satisfactorily reproduced as the first order of excited dye, while for phosphate buffer it is second order with regard to dye. It was further found from this analysis that the rate of the essential step (or steps) of the reaction for the case of borate is approximately proportional to the concentration of OH^-, while for the case of phosphate it is almost independent of pH.

The quantity of irreversible decomposition of dye in case of borate buffer was estimated to be very small against that of the reversible bleaching, the former being a few tenths of the latter from the experimental results obtained when ferric chloride and *o*-phenanthroline were added to the borate buffer solution.

Judging from the results hitherto obtained, it is most plausible that the photoreduction of methylene blue in case of borate takes place through the decomposition of water. But in case of phosphate, there still remains some possibility that the reaction commences by the interaction of excited dye and ground state dye, electron transfer taking place between them.

The quantum yield of the bleaching reaction was measured and found to be $(2\sim3)\times10^{-4}$ for borate buffer and $(7\sim9)\times10^{-4}$ for phosphate buffer.

Thanks are due to Dr. Shunji Kato and Mr. Hiroshi Obata for helpful discussions.

Department of Chemistry
Faculty of Science
Tohoku University
Katahira-cho, Sendai

Raman Spectra of p-Dichlorobenzene and p-Dichlorobenzene-d_4

By Shinnosuke SAËKI

(Received April 3, 1961)

The molecular spectra of *p*-dichlorobenzene have been studied by many investigators, and the author has reported on the infrared absorption spectra of ordinary and deuterated *p*-dichlorobenzene previously[1]. In this paper, the Raman spectra of the same substances will be reported upon, for it is essential for the assignment of the molecular vibration to study the Raman spectra as well as the infrared spectra.

As the molecule of *p*-dichlorobenzene has the center of symmetry, the thirty normal vibrations are divided into two groups according to the rule of mutual exclusion. Consequently, fifteen vibrations are active in Raman effect and eleven vibrations are active in infrared absorption spectrum. Though this fact does much to simplify the molecular spectra of this substance, the Raman spectrum of this substance is still rather complicated with the appearence of the overtone lines, combination lines and lines due to the Fermi resonance in addition to the above-mentioned eleven fundamental lines.

Concerning the Raman spectrum of *p*-dichlorobenzene, a number of papers have been published since many years ago[2-4]. In these papers, the assignment of the lines was carried out inductively, comparing the spectrum with those of other benzene derivatives of the same type and observing a frequency change between them for each corresponding band or line. Since the number and the variety of the treated substance were extensive, and since the conclusions were made after prudent examinations, one can put much confidence in most of the results obtained by this method. However, since in a different molecule the strength to the interatomic bonds (force constants) changes as well as the masses of atoms, a slight ambiguity appears to be left in the assignment which resulted from such inductive studies. Actually the proposed assignments of some Raman lines of *p*-dichlorobenzene seemed to be somewhat indefinite and arbitrary.

In the study reported here, as the Raman spectra were observed for completely deuterated *p*-dichlorobenzene as well as for the ordinary one, the product rule could be applied in order

1) S. Saëki, This Bulletin, 33, 1021 (1960).

2) A. Stojiljković and D. H. Whiffen, *Spectrochim. Acta*, 12, 47 (1958).

3) D. H. Whiffen, ibid., 7, 253 (1955).

4) C. Garrigon-Lagrange, J-M. Lebas and M-L. Josien, ibid., 12, 305 (1958).

to verify the assignment proposed. In addition to the frequencies, the qualitative depolarization ratio of each line was also observed by the two exposure method using the polaroid cylinders in order to obtain more definite assignments than previous ones.

Experimental

Ordinary *p*-dichlorobenzene of extra pure grade on the market was recrystallized three times from the ethanol solution, and then sublimed before being used for the measurement of the Raman spectra. The melting point of the obtained substance was 53°C.

The deuterated one was prepared and purified as follows. Ordinary *p*-dichlorobenzene was stirred at 105°C for six hours in heavy sulfuric acid. The reaction mixture was poured on ice and the precipitate filtered off and washed with water and dried. The exchange with heavy sulfuric acid was repeated until the strongest band of $C_6HD_3Cl_2$ could hardly be observed in the infrared absorption spectrum of the substance. It was necessary to repeat the exchange reaction two or three times in order to attain such purity. Then the obtained substance was further purified in the same way as that for ordinary *p*-dichlorobenzene, but because of the smallness of the quantity, the purification could not be carried out so thouroughly as in the case of ordinary *p*-dichlorobenzene. The deuterated substance was probably a little less pure than the ordinary one.

The Cary model 81 automatic recording Raman spectrophotometer was used for the measurements, of which the source was the mercury arc lamp of Toronto type, and the dispersion of the grating was 4 Å/mm. at 5000 Å.

The spectra were measured in the solution of 1 g. *p*-dichlorobenzene in 5 ml. carbon tetrachloride. The qualitative depolarization ratios were measured by placing the polaroid cylinder around the Raman tube and by polarizing the exciting light to the directions parallel or perpendicular to the axis of the tube.

Results

The observed Raman spectra are shown in Figs. 1—4. As are shown in Figs. 3 and 4, the base lines of the spectra of deuterated *p*-dichlorobenzene rose gradually towards the higher frequency ends of the spectra, showing remarkable backgrounds. It might probably be caused by the slight resinous impurity, which could not be removed completely by the purification because of the small quantity of deuterated substance available, as we mentioned previously.

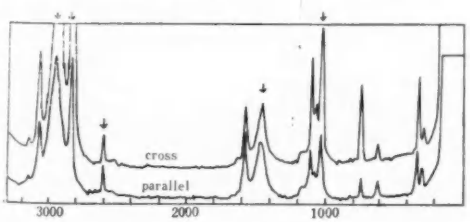

Fig. 1. Raman spectra of *p*-dichlorobenzene (1 g. in 5 ml. methanol).

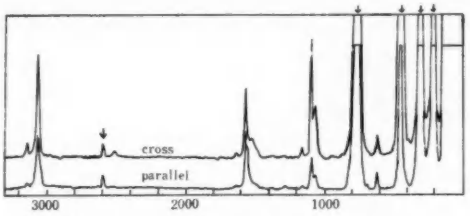

Fig. 2. Raman spectra of *p*-dichlorobenzene (1 g. in 5 ml. carbon tetrachloride).

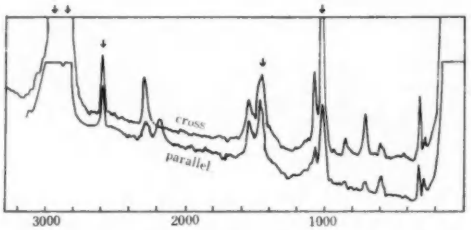

Fig. 3. Raman spectra of *p*-dichlorobenzene-d_4 (1 g. in 5 ml. methanol).

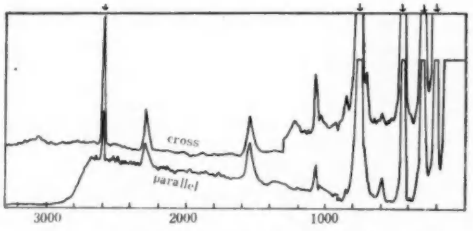

Fig. 4. Raman spectra of *p*-dichlorobenzene-d_4 (1 g. in 5 ml. carbon tetrachloride).

The observed frequencies and intensities of Raman lines are listed in Tables I and II. The intensities are described by the heights of lines measured on the chart. The notation "masked" means that the line could not be observed, due to the masking effect of a strong Raman line of the solvent in the spectra of that solution while it was observed in the other solution. Though the Raman spectra of the substances were observed in the solution in methanol or in carbon tetrachloride, there is no possibility that a Raman line is masked in both methanol and carbon tetrachloride solutions, for there is no frequency region

TABLE I. RAMAN SPECTRA OF *p*-DICHLOROBENZENE

Methanol soln.			Carbon tetrachloride soln.			Depolarization ratio
$\tilde{\nu}$	Intensity		$\tilde{\nu}$	Intensity		
	Cross	Parallel		Cross	Parallel	
295	14	17		Masked		dep.
329	54	27		Masked		p.
349	sh.	1		Masked		?
	Unobserved		400	4	2	?
623	13	14	625	16	16	dep.
744	56	16		Masked		p.
1067	19		1067	16	5	p.
1077	sh.	10	1080	25	5	p.
1103	80	35	1103	83	25	p.
1177	6	3	1163	8	3	p.
	Unobserved		1285	2	3	dep.
	Unobserved		1378	2	0	?
	Masked		1531	12b	sh.	p.
1571	38	39	1572	48	51	dep.
	Unobserved		1630	4	3	dep.
2520	4	0	2523	5	1	p.
3071	66	33	3071	75	39	p.
3147	8	5	3147	11	4	?

TABLE II. RAMAN SPECTRA OF *p*-DICHLOROBENZENE-d_4

Methanol soln.			Carbon tetrachloride soln.			Depolarization ratio
$\tilde{\nu}$	Intensity		$\tilde{\nu}$	Intensity		
	Cross	Parallel		Cross	Parallel	
288	11	12		Masked		dep.
324	42	27		Masked		p.
607	12	14	606	11	17	dep.
708	30	9	710	sh.	sh.	p.
863	14	6	861	13	5	p.
937	?					
1078	54	28	1078	39	18	p.
ca. 1520	2	3	ca. 1520	sh.	0	p.
1553	24	22	1553	28	30	dep.
2285			2285	8?	12?	dep.
2301	36	15	2301	31	19	p.

where both methanol and carbon tetrachloride have a strong Raman line. The only exception is the region between a line at 1460 cm^{-1} of methanol and a line at 1530 cm^{-1} of carbon tetrachloride. But fortunately, as neither of these lines was very strong, there was little possibility that a line would escape observation even in this region, so long as its intensity is not extremely weak.

The notation "unobserved" in the tables means that the line was not observed in one of the solutions while it was observed in the other solution. As all of these lines had very small intensities, it was not unreasonable that they were unobservable in one of the solutions. However, they could still not be adopted uncritically as the Raman lines of solute.

The notation "sh." means a line observed as a shoulder of a strong Raman line of the solute itself or the solvent, and "p." and "dep." represent a line which apparently changed and apparently did not change its intensity when excited by incident light polarized parallel and perpendicular to the axis of the Raman tube, respectively.

Discussion

The molecule of *p*-dichlorobenzene belongs to a point group V_h, and its fifteen Raman active normal vibrations are factored into six of the species A_g (in-plane), five of the species B_{3g} (in-plane), one of the species B_{1g} (out-of-plane) and three of the species B_{2g} (out-of-plane). Therefore six polarized (and probably strong) lines and nine depolarized lines were expected to be observed in the Raman spectrum. The modes of these normal vibrations are shown in Table III.

TABLE III. THE MODES OF THE NORMAL VIBRATIONS OF *p*-DICHLOROBENZENE

Species	No.*	Mode
A_g	ν_1	C-H or C-D stretching
	ν_2	Ring stretching
	ν_3	C-H or C-D in-plane bending
	ν_4	Ring stretching
	ν_5	C-Cl stretching
	ν_6	Ring in-plane deformation
B_{1g}	ν_9	C-H or C-D out-of-plane bending
B_{2g}	ν_{15}	C-H or C-D out-of-plane bending
	ν_{16}	Ring out-of-plane deformation
	ν_{17}	C-Cl out-of-plane bending
B_{3g}	ν_{23}	C-H or C-D stretching
	ν_{24}	Ring stretching
	ν_{25}	C-H or C-D in-plane bending
	ν_{26}	Ring in-plane deformation
	ν_{27}	C-Cl in-plane bending

* The normal vibrations were numbered after Herzberg.

p-Dichlorobenzene. — Seventeen Raman lines are observed in the spectrum of this substance. Therefore the number of observed lines exceedes the number of Raman active normal vibrations. However, since there were several lines which were apparently considered to be overtones or combinations, this fact does not mean that all of the Raman active normal vibrations have been observed.

As we mentioned previously, six polarized lines were expected to be observed, but actually nine polarized lines were found in the observed spectrum, as is shown in Table I. Considering its frequency value, one of these polarized lines observed at 2522 cm^{-1} *1 must be explained as an overtone or a combination. The number of remaining observed lines was still more than the number of expected lines. Considering the vibrational modes shown in Table III, these six lines belonging to the species A_g, one was expected to appear near 3000 cm^{-1}, one at about 1500 cm^{-1}, and two between 1300 and 1000 cm^{-1}. Though the vibrational mode of ν_4 was described as the ring stretching, it proved to be the "breathing" vibration of the benzene ring on closer examination. Therefore its frequency might be relatively low and expected to appear in this region, and two below 1000 cm^{-1}. Accordingly it was clear that the line at 3071 cm^{-1} had to be assigned to C–H stretching vibration, the line at 1531 cm^{-1} to the ring stretching vibration, the line at 774 cm^{-1} to the C–Cl stretching vibration, and the line at 331 cm^{-1} to the ring in-plane deformation vibration.

Concerning the assignment of the lines observed in the region 1000~1300 cm^{-1}, there were some points of discussion. While only two of the totally symmetric normal vibrations were expected to appear in this region, four polarized Raman lines were actually observed at 1067, 1080, 1103 and 1163 cm^{-1} *2. As the line at 1103 cm^{-1} had much greater intensity than the other three, this line may the most plausibly be assigned to the breathing vibration of the ring. From the facts that the line at 1067 cm^{-1} was very close to the line at 1080 cm^{-1}, and that these two lines were hardly resolved in the spectrum of the methanol solution, these two lines might be considered to be brought out by a Fermi resonance between a fundamental and an overtone or a combination vibration (for example 545(b_{1u})[12] ×2=1090 (A_g), 744 (a_g)+331 (a_g)=1075 (A_g)). Then the frequency of the in-plane bending vibration of C–H bonds was estimated to be about 1075 cm^{-1}, the mean value of these two frequencies. Provided that the two normal vibrations were assigned in such a way, the line at 1163 cm^{-1} had to be considered as an overtone or a combination, or a fundamental which belongs to a species other than A_g. However it was also possible to take the line at 1163 cm^{-1} for the in-plane bending vibration of C–H bonds, and to take the lines at 1067 and 1080 cm^{-1} for the above-mentioned combination and overtone respectively. This alternative assignment seems to be somewhat unreasonable taking into account their relative intensities, nevertheless this could not be considered to be absolutely impossible. The superiority of one to the other will be revealed later by the application of the product rule.

The next step is to assign the other lines to the normal vibrations which belong to species other than A_g. These normal vibrations consist of four out-of-plane vibrations which belong to the species B_{1g} or B_{2g}, and five in-plane vibrations which belong to the species B_{2g}. As is shown in Table II, two of the four out-of-plane vibrations are those of C–H bonds, and their frequencies must be higher than 819 cm^{-1}, which is the frequency of the infrared active out-of-plane vibration of C–H bonds (species B_{2u}[12]) in which the four C–H bonds vibrate from the plane of the molecule up and down in the same phase. Though the frequencies of these vibrations were estimated to be between 819 and 1100 cm^{-1}, no depolarized line was observed in this region. Since naturally too much confidence should not be put in the observed degrees of depolarization, it would not be impossible to assign the lines at 1067 and 1080 cm^{-1} to these out-of-plane vibrations. However, since these lines had been well explained as a combination and as an overtone, as was mentioned above, and since the observed degrees of depolarization were not consistent with the above assignments, it appears better to consider that the normal vibrations in question were not observed and to assign the above lines to a combination and an overtone than to make a strained assignment. Further discussion concerning these lines will be seen later.

The other two out-of-plane vibrations are those of the ring and of the C–Cl bonds. Since the frequency of the former was expected to be about 400 cm^{-1}, the line observed at 400 cm^{-1} in the solution of carbon tetrachloride was assigned to it. But it should be mentioned here that there remained a little ambiguity in this assignment, since the intensity of the line was so weak that it was not observed in the solution of methanol. As the out-of-plane bending vibrations of C–Cl bonds were expected to be observed in lower frequency region —probably in the vicinity of 300 cm^{-1}, the line at 294 cm^{-1} was assigned to this vibration.

*1 As a slight discrepancy was generally seen between the frequency observed in methanol solution and that oserved in carbon tetrachloride solution, the mean value of these two was used in this paper as a rule. However, in the case that an apparent difference existed between the accuracies of two observed frequencies, the more accurate one was used.

*2 Since the second and the fourth lines were observed much more clearly in carbon tetrachloride than in methanol as is seen in Figs. 1 and 2, the frequencies observed in carbon tetrachloride solution were adopted as is mentioned in the last foot-note.

The last five normal vibrations to be assigned are those which belong to the species B_{3g}. The frequency of the stretching vibration of C–H bonds was naturally a little higher than 3000 cm^{-1}, and in the observed spectra a weak line was found at 3147 cm^{-1} in addition to the strong line at 3071 cm^{-1} which was already assigned to the vibration of the species A_g. The observation of the qualitative depolarization ratio showed that this weak line was considerably polarized. In addition to this fact, the frequency 3147 cm^{-1} appeared to be too high even for an aromatic C–H stretching vibration. Therefore this line had to be assigned not to the C–H stretching vibration, but to the overtone of the ring stretching vibration of 1572 cm^{-1} which will be discussed below. The C–H stretching vibration of the species B_{3g} should be considered to overlap with that of the species A_g at 3071 cm^{-1}.

Three of the remaining normal vibrations are the stretching vibration of the ring, the in-plane deformation vibration of the ring and the in-plane bending vibration of C–H bonds. There might be no objection to assigning three depolarized lines observed at 1572, 1285 and 623 cm^{-1} to them respectively. As for the last remaining normal vibration, that is, the C–Cl in-plane bending vibration, there was no observed line except a very weak line at 349 cm^{-1} to be assigned to it. Though the intensity of this line was very low, this line had been observed also by Whiffen et al.[2] And since there were no lines observed in the spectra to be assigned to the C–Cl bending vibrations except the two lines observed at 349 and at 294 cm^{-1}, it appeared to be quite plausible to assign the former line to the in-plane, and the latter line to the out-of-plane bending vibration of C–Cl bonds respectively.

A brief discussion should be given here concerning the lines which had not yet been treated above that is, the weak lines at 2520, 1630 and 1378 cm^{-1}, of which the degrees of depolarization could not be measured with adequate certainty. The line at 2520 cm^{-1}, though observed to be polarized, could not be explained as a line belonging to the species A_g. This line might probably be a combination line of the species B_{3g}, that is, 1405 (b_{2u}) + 1091 (b_{1u}). The line at 1630 cm^{-1} was measured as a depolarized line, and explained as being 1091 (b_{1u}) + 545 ($_{1u}$). The line at 1378 cm^{-1} was easily explained as 819(b_{3u}) + 544(b_{3u}).

Deuterated *p*-Dichlorobenzene. — The Raman lines observed for deuterated *p*-dichlorobenzene was not so many as for an ordinary one. The observed eleven lines were shown in Table II. According to the measurement of the qualitative polarization ratios, six of these lines were polarized. But the result obtained for the line at about 1520 cm^{-1} was a little ambiguous, because its intensity was so weak that the observation of the depolarization ratio was very difficult even qualitatively. However, these six polarized lines were unambiguously assigned to the six normal vibrations of the species A_g, as is shown in Table IV. The comparison of this assignment with that for ordinary *p*-dichlorobenzene will be given later.

The remaining five observed lines are to be assigned to the remaining nine normal vibrations, of which four out-of-plane vibrations belong to the species B_{1g} or B_{2g}, and five in-plane vibrations belong to the species B_{3g}. It might be apparent that two of the out-of-plane vibrations concerning C–D bonds have frequencies higher than 695 cm^{-1}, the frequency of the C–D out-of-plane vibration of the species B_{3u} observed in the infrared absorption spectrum[1]. However no corresponding line was observed in such a region of frequency, so it had to be concluded that these vibrations had too low intensities to be observed. The other two out-of-plane vibrations were expected to appear from 350 to 400 cm^{-1} and at about 250 cm^{-1} respectively, considering their vibrational modes (Table III). But there was no line to correspond to the former vibration. The line corresponding to the latter vibration was observed at 288 cm^{-1} with remarkable intensity, but it was difficult to determine whether this line was to be assigned to the out-of-plane or in-plane vibration of C–Cl bonds.

Concerning the in-plane normal vibrations belonging to the species B_{3g}, there might be no difficulty in assigning the line at 2285 cm^{-1} to the C–D stretching vibration and the line at 1553 cm^{-1} to the ring stretching vibration. As for the in-plane bending vibration of C–D bonds, since the corresponding vibration of ordinary *p*-dichlorobenzene was observed at 1285 cm^{-1} with relatively low intensity, the frequency was expected to be a little lower than 1000 cm^{-1} in the case of a deuterated one. No distinct line was observed in this frequency region at first sight, but the closer examination of the spectra revealed a very weak line at 937 cm^{-1}, the intensity of which was so weak that the line could hardly be distinguished from the noises. It might be a little questionable to consider it as a real Raman line, but if we remember that the line at 1285 cm^{-1} of ordinary *p*-dichlorobenzene was also very weak and that the corresponding line of deuterated *p*-dichlorobenzene has to appear in the region of 900~1000 cm^{-1}, this line could be assigned to the C–D in-plane bending vibration.

The line at 607 cm^{-1} was easily assigned to

the ring in-plane deformation vibration.

To the C–Cl in-plane bending vibration, it is possible to assign the line at 288 cm^{-1}, but, as is mentioned above, it might also be possible to assign it to the in-plane bending vibration of C–Cl bonds. As in the case of ordinary *p*-dichlorobenzene, the decision of the assignment for these vibrations appear to be impossible at this point.

The Product Rule.—According to the Teller-Radlich product rule, the theoretical ratios of the products of the frequencies for each substance are 1.998 for the species A_g, 1.249 for the species B_{1g}, 1.408 for the species B_{2g} and 1.969 for the species B_{3g}, where the calculations were carried out using the following values for molecular constants:

$m_H = 1.0081$ (in physical atomic weight)
$m_D = 2.0147$ (in physical atomic weight)
$m_C = 12.0038$ (in physical atomic weight)
$m_{Cl} = 34.9801$ (in physical atomic weight)
$r_{C-H} = 1.08$ (Å)
$r_{C-Cl} = 1.68$ (Å)
$r_{C-C} = 1.39$ (Å)

and 120° for all of the bond angles.

The assignments for the six normal vibrations of the species A_g were unambiguously determined in the case of ordinary *p*-dichlorobenzene, but in the case of a deuterated substance there remained a question which of the two lines at 1163 cm^{-1} and 1075 cm^{-1} was to be assigned to the in-plane vibration of C–H bonds. If the ratio of the products of the frequencies was calculated assuming the latter assignment, the result was 1.825, a little less than the theoretical value 1.998. On the contrary, if the former assignment was assumed, the ratio became 1.991, in good accordance with the theoretical value. This result led us to the conclution that it was the line at 1163 cm^{-1} to be assigned to the C–H bending vibration of the species A_g.

Here, in connection with this assignment a comment should be mentioned about the exchange of the vibrational modes. As was stated above, according to this assignment, ν_3's were 1163 and 1078 cm^{-1} for ordinary and deuterated *p*-dichlorobenzene respectively, and ν_4's were 1103 and 863 cm^{-1} for ordinary and deuterated ones respectively. The fact that the line at 1103 cm^{-1} was much more intense than the line at 1163 cm^{-1} in the spectra of ordinary *p*-dichlorobenzene suggests to us that the mode of the former is the breathing of the benzene ring and that of the latter is the C–H in-plane bending vibration. However, in the case of a deuterated substance, it was clear from the consideration of the frequency that

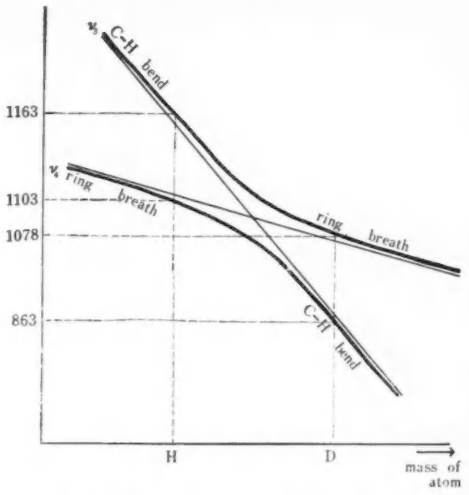

Fig. 5. The variation of vibrational mode with atomic mass.

the line at 1078 cm^{-1} was the breathing of the benzene ring and that the line at 863 cm^{-1} was the C–D in-plane bending vibration. Thus the exchange of the vibrational modes shown in Fig. 5 took place in the case of these molecules. This consideration suggested that the breathing vibration of the benzene ring strongly couples with the C–H or C–D in-plane bending vibration in these molecules, and that the modes of these vibrations are by no means simple, but rather complicated combinations of some simple modes.

It was impossible to apply the product rule to the species B_{1g} and B_{2g} because of the insufficient number of the observed lines. As was already stated above, only one normal vibration—the C–H or C–D out-of-plane vibration—belongs to the species B_{1g}. Therefore, provided that the line at 1067 or 1080 cm^{-1} of ordinary *p*-dichlorobenzene corresponds to this vibration, the frequency of the corresponding vibration of deuterated substance could be estimated at about 850 cm^{-1} by utilizing the product rule. As is shown in Table II, a remarkable line was indeed observed at 863 cm^{-1} in the spectra of deuterated substance, but it was already assigned to a vibration of the species A_g, because the measurement of the depolarization ratio showed it to be polarized. In addition to such a lack of a corresponding line, both lines at 1067 and 1080 cm^{-1} of the ordinary substance were themselves polarized, and so it seemed to be unreasonable to assign either of them to the vibration of the species B_{1g}.

As the C–Cl in-plane bending vibration of

TABLE IV. ASSIGNMENTS OF RAMAN LINES OF ORDINARY AND DEUTERATED *p*-DICHLOROBENZENES

Species	No.	$\tilde{\nu}$ $C_6H_4Cl_2$	$\tilde{\nu}$ $C_6D_4Cl_2$	Mode
A_g	ν_1	3071	2301	C–H or C–D stretching
	ν_2	1531	ca. 1520	Ring stretching
	ν_3	1163	1078	C–H in-plane bending Ring breathing
	ν_4	1103	863	Ring breathing C–D in-plane bending
	ν_5	744	708	C–Cl stretching
	ν_6	329	324	Ring in-plane deformation
B_{1g}	ν_9	—	—	C–H or C–D out-of-plane bending
B_{2g}	ν_{15}	—	—	C–H or C–D out-of-plane bending
	ν_{16}	400?	—	Ring out-of-plane deformation
	ν_{17}	295	288	C–Cl out-of-plane bending
B_{3g}	ν_{23}	3071	2285	C–H or C–D stretching
	ν_{24}	1572	1553	Ring stretching
	ν_{25}	1285	937?	C–H or C–D in-plane bending
	ν_{26}	623	607	Ring in-plane deformation
	ν_{27}	349	—	C–Cl in-plane bending

deuterated *p*-dichlorobenzene, which corresponds to the line at 349 cm^{-1} of the ordinary substance, was not observed, the exact application of the product rule was impossible for the species B_{3g} also. However, the ratio of products of the frequencies calculated from four pairs of observed frequencies alone was 1.963, which was very near to the theoretical value 1.969 irrespective of the omission of the fifth pair. Generally speaking, a vibration directly concerned with C–H bonds naturally shows the sensitive frequency shift with the substitution of the hydrogen atoms by deuterium atoms. The other vibrations—especially when their frequencies are very different from the frequency of C–H vibration—show little frequency shift. Therefore the C–Cl bending vibration of deuterated *p*-dichlorobenzene was expected to have a frequency nearly equal to that of the corresponding vibration of ordinary *p*-dichlorobenzene, 349 cm^{-1}. This means that the ratio of the frequencies for the fifth vibration of the species B_{3g} is probably little larger than 1, and therefore, if the above-mentioned calculation had been carried out taking account of this pair of frequencies, the result would be still in good accordance with the theoretical value. This consideration means that the application of the product rule could prove the correctness of the assignment for the species B_{3g} too.

The assignment which was determined above is shown in Table IV.

Summary

The Raman spectra of ordinary and deuterated *p*-dichlorobenzene were measured in solutions. The qualitative depolarization ratios of observed Raman lines were also measured by the two exposure method using the polaroid cylinders. On the basis of these results, the assignments of normal vibrations for these substances were determined. The assignments for the in-plane normal vibrations (species A_g and B_{3g}) were verified applying the product rule.

The author gratefully acknowledges the encouragement and advice given him by Dr. Y. Mashiko.

Government Chemical Industrial Research Institute of Tokyo
Shibuya-ku, Tokyo

Decomposition of Mono- and Diethanolamine Carbamate in Glycerol Solution

By Mamoru MATSUDA

(Received May 4, 1961)

Monoethanolamine (MEA) and diethanolamine (DEA) provide excellent methods to remove acidic gases from natural and refinery gases. At normal temperatures these amines have strong affinity for the gases, while at higher temperatures these amines are recovered by expulsion of the acidic gases.

Many papers have been published on the absorption reaction of carbon dioxide with MEA or DEA[1-5], and a few on the reverse reaction[6,7]. However, no kinetic study of the decomposition of the MEA and DEA carbamate or carbonate has hitherto been carried out.

The present paper reports the activation energies for decomposition and absorption obtained from the rate of decomposition, and the heats of formation, together with equilibrium constants, over the temperature range of 110 to 140°C.

Experimental

Chemicals. — MEA, DEA and glycerol were of reagent grade and fractionally distilled in vacuo. Solvents such as xylene, *n*-butyl acetate, *n*-butyl alcohol, acetic acid, and toluene were also of reagent grade. Carbon dioxide from a steel cylinder was purified by passing through concentrated sulfuric acid and anhydrous calcium chloride.

Preparation of Samples. — MEA (1 part) was dissolved in glycerol (2 parts). The reaction between the solution, n_D^{20} 1.4680, d_{20}^{20} 1.187, and carbon dioxide took place by bubbling the latter through the former gently for 3 hr. The sample thus obtained had carbon dioxide 0.06385 g./g. sample (0.334 mol. CO_2/mol. MEA), n_D^{20} 1.4803, d_{20}^{20} 1.250. The DEA glycerol solution (1 : 2 by vol.), n_D^{20} 1.4729, d_{20}^{20} 1.211, was treated with the same procedure as above; 0.02485 g. CO_2/g. sample (0.220 mol. CO_2/mol. DEA), n_D^{20} 1.4779, d_{20}^{20} 1.228.

Apparatus and Technique. — The apparatus for the decomposition of the sample was as shown in Fig. 1. The reaction tube R was a 50 ml. test tube, 2.5 cm. in diameter, charged with glass rods, 0.4 cm. $\phi \times 1.0$ cm. The manometer M was provided with an entraining liquid, a saturated aqueous solution of sodium chloride acidified with sulfuric acid containing a few drops of methyl orange. The cooling zone N was an effective, comparatively large, about 100 ml., heat exchanger, and the temperature of it was maintained constant by circulating water at 20°C. The graduated glass tube G, 3 mm. in diameter, lying horizontally, was calibrated exactly by measuring the length of mercury of known weight.

The experiment was carried out as follows: the apparatus consisting of R, M, N and G, was filled with pure carbon dioxide. About 9 g. of mercury was employed to stop the open end of the graduated glass G. The reaction temperature was maintained within ±0.2°C by the vapor of the boiling solvent which was heated by an oil-bath thermostat O regulated to ±1°C. When the system reached an equilibrium, as shown by a steady state of the colored solution inside the U-tube M and the mercury plug P, all the variables—barometric pressure, temperatures of cooling water T_5, of the room T_3, of the reaction tube T_2, and of the solvent vapor T_1—were recorded. Then the plug was set to zero

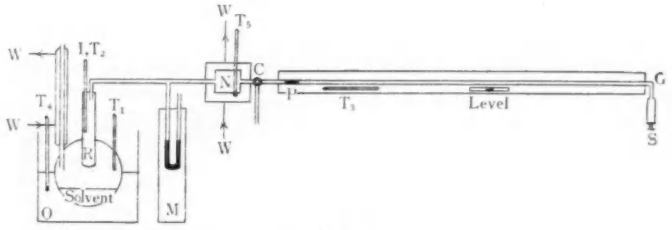

Fig. 1

1) J. W. Mason and B. F. Dodge, *Trans. Am. Inst. Chem. Engrs.*, **32**, 27 (1936).
2) D. S. Cryder and J. O. Maloney, ibid., **37**, 827 (1941).
3) A. L. Shneerson and A. G. Leibush, *J. Appl. Chem., (U. S. S. R.)*, **19**, 867 (1946); *Chem. Abstr.*, **41**, 4340 (1947).
4) D. W. Van Krevelen and P. J. Hoftijzer, *Chem. Eng. Prog.*, **44**, 529 (1948).
5) F. Goodridge, *Trans. Faraday Soc.*, **49**, 1324 (1953); **51**, 1703 (1955).
6) R. M. Reed and W. R. Wood, *Trans. Am. Inst. Chem. Engrs.*, **37**, 363 (1941).
7) H. C. Paulsen et al., U. S. Pat. 2701750 (1955).

by means of a two way cock C and a syringe S. A weighed sample was poured from 2 ml. syringe into the reaction tube through an open glass tube I. The glass tube was closed with a rubber plug. It took less than 3 seconds. The temperature in the tube did not substantially decrease. The sample began to evolve carbon dioxide pushing the mercury plug. The syringe S was operated manually to maintain the inside and outside pressures equal at all times by reading the manometer M. The position of the mercury plug, time, and other variables were recorded at short intervals. The experiment was repeated two or three times at the same temperature.

Gravimetric analyses of carbon dioxide of the fresh and the heated samples which still retained carbon dioxide were carried out. The apparatus and technique were the same as those of Knorr's method[8].

Results and Discussion

Figures 2 and 3 are graphs of the increase in volume of the gases formed as a function of time due to the decomposition of the samples over the temperature range of about 110 to 140°C. It can not be assumed that the increase in volume was due only to the evolution of carbon dioxide. Vapor of the amines and the solvent, the change of atmospheric pressure and room temperature may affect the measurements. The temperature and the pressure were substantially constant during the experiments. As to the vapor of the amines and the solvent, a blank test showed that the vapor increased the volume by about 0.3 ml./g. sample at 136°C for the initial period of the reaction, in about half a minute. After that period the reaction system reached an equilibrium.

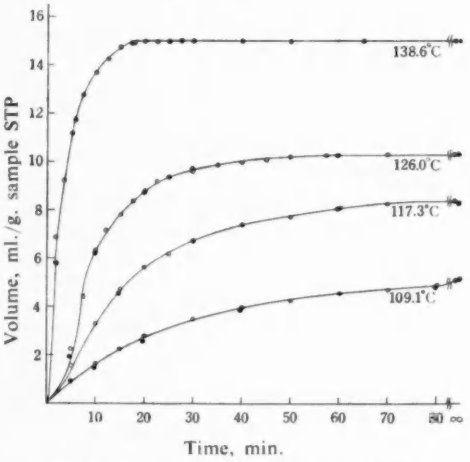

Fig. 2. Rate of decomposition of MEA carbamate in glycerol solution at constant pressure.
● Theoretical
○ Experimental

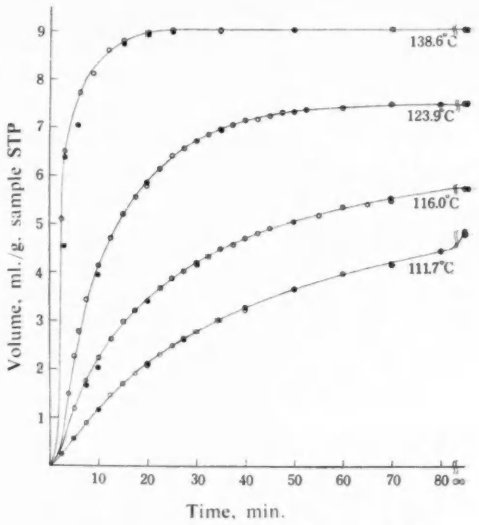

Fig. 3. Rate of decomposition of DEA carbamate in glycerol solution at constant pressure.
● Theoretical
○ Experimental

The results of gravimetric and volumetric analyses at equilibrium were listed in Table I.

TABLE I. THE AMOUNT OF CARBON DIOXIDE, EVOLVED AND RESIDUAL (ml. CO_2/g. sample STP)

	Temp., °C	Vol. of evolved gas, u_0 (volumetric)	Vol. of residual CO_2 (gravimetric)
MEA	138.6	15.0±0.5	17.3 ±0.2
	126.0	10.3±0.4	22.0 ±0.1
	117.3	8.4±0.2	23.8 ±0.1
	109.1	5.1±0.2	27.2 ±0.1
	At room temp.	—	32.27±0.05
DEA	138.6	9.1±0.3	3.5 ±0.1
	123.9	7.5±0.2	5.1 ±0.1
	116.0	5.8±0.1	6.8 ±0.1
	111.7	4.9±0.2	7.7 ±0.1
	At room temp.	—	12.58±0.05

Concerning the reaction mechanism of the amines and carbon dioxide, Van Krevelen and Hoftijzer suggested that in aqueous solution the complete reaction took place in two steps, the first being a dissociation of the amine and the second the combination of the fragments, and the reaction was a third order[1]. As to

8) W. W. Scott, "Scott's Standard Method of Chemical Analysis", D. Van Nostrand Co., Inc., New York (1939), p. 235.

the reaction order a similar conclusion was reached by Cryder and Maloney[2], and Smola[9]. The work of Mason and Dodge[1], and of Shneerson and Leibush[3], showed that the concentration of carbon dioxide in aqueous solution of the amine at equilibrium varied about 0.5 to 0.9 mol. per amine as the temperature decreased from about 75 to 0°C, and the absorption would take place as follows:

$$2RR'NH + H_2O + CO_2 \rightleftarrows (RR'NH_2)_2CO_3$$

$$(RR'NH_2)_2CO_3 + CO_2 + H_2O \rightleftarrows 2RR'NH_2HCO_3$$

$$R = HOCH_2CH_2;\ R' = R \text{ or } H$$

Goodridge interpreted the reaction in terms of zero order as tentative, and presented the following mechanism in the absence of water[5]:

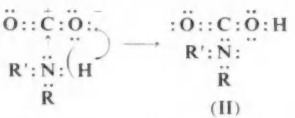

(II)

The amine carbamates in glycerol solution were decomposed, according to the following reactions:

$$RR'NCOONH_2RR' \underset{k_2}{\overset{k_1}{\rightleftarrows}} 2RR'NH + CO_2 \quad (1)$$

MEA $R = HOCH_2CH_2,\ R' = H$

DEA $R = R' = HOCH_2CH_2$

The partial pressure of carbon dioxide was constant at 1 atmospheric pressure. The reaction was reversible as the formula 1, and the following differential equation will be valid:

$$du/dt = k_1(a_0 - u) - k_2(a_0' + 2u)^2 p_{CO_2} \quad (2)$$

$$= k_1(a_0 - u) - k_2'(a_0' + 2u)^2 \quad (3)$$

where

a_0 = initial concentration of MEA or DEA carbamate, mol./g. sample,

a_0' = initial concentration of MEA or DEA, mol./g. sample,

k_1 = rate constant of decomposition of the carbamate,

k_2 = rate constant of absorption of the MEA or DEA,

u = moles of the decomposed carbamate at the time t, and

p_{CO_2} = partial pressure of carbon dioxide.

When $u = 0$ at $t = 0$ and $u = u_e$ at $t = \infty$, the solution of the Eq. 3 is:

$$(Ka_0 - a_0'^2)/u = (\sqrt{K^2 + 8K(2a_0 + a_0')}/2) \cdot \coth(k_2' t \sqrt{K^2 + 8K(2a_0 + a_0')}/2) + (K + 4a_0')/2 \quad (4)$$

where $K = k_1/k_2' = (a_0' + 2u_e)^2/(a_0 - u_e)$ (5)

$$k_2' = k_2 p_{CO_2} \quad (6)$$

A relation between rate constants, k_1 and k_2', and equilibrium constant K, should be expressed as $k_1/k_2' = K^{1/\nu(r)}$, where $\nu(r)$ = the number of occurrence of a rate determining step necessary to complete an overall reaction formula[10]. At present, however, $\nu(r) = 1$, as will be explained.

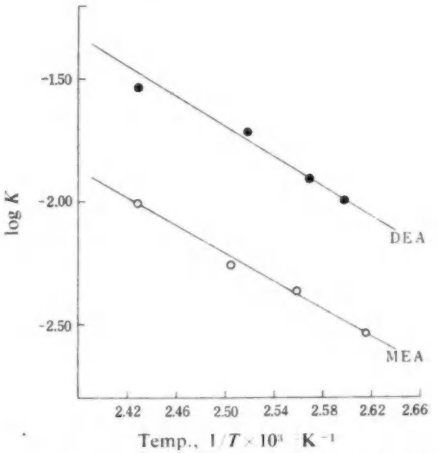

Fig. 4. Temperature dependence of equilibrium constant K; $\log K$ vs. $1/T$ ($\times 10^{-3}$).

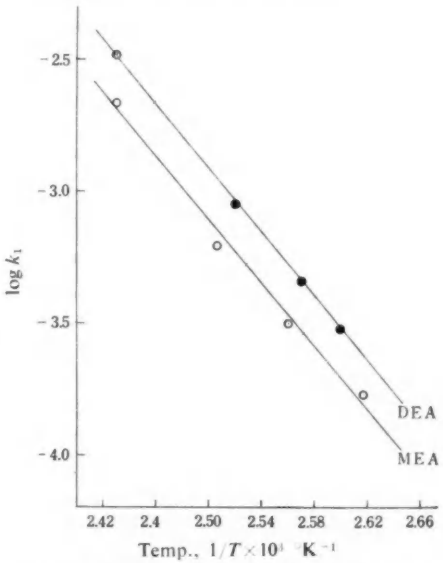

Fig. 5. Temperature dependence of rate constant k_1; $\log k_1$ vs. $1/T$ ($\times 10^{-3}$).

9) A. Smola, *Mitt. chem. Forsch.*, **2**, 38 (1948); **2**, 43 (1948).

10) J. Horiuti, *Chem. & Chem. Ind. (Kagaku to Kogyo)* **9**, 355 (1956).

On the basis of the amount of carbon dioxide at equilibrium, equilibrium constants were calculated. The temperature dependence of the equilibrium constants was shown in Fig. 4. From the slopes of the lines the heats of the reaction were calculated by the van't Hoff's equation, and were found to be 12.9 and 13.4 kcal./mol. CO_2 for MEA system and DEA system, respectively. Since a_0, a', K, t and u were known by the experiment, the rate constants, k_1 and k_2', at each temperature, were calculated. After the initial period the values of the rate constants became equal within the limits of experimental error. The calculated values of u obtained from Eq. 4, using these rate constants and the others, were plotted against the time. The agreement with the experimental values supports the validity of Eqs. 1 to 6. The values of $\log k_1$ and $\log k_2'$ were plotted against the reciprocals of corresponding absolute temperatures, as shown in Figs. 5 and 6, and the Arrhenius' energies of activation of the decomposition and the absorption were calculated over the temperature range of 110 to 140°C, and were found to be 27.5 and 14.4 kcal./mol. for the MEA system, 27.8 and 13.6 kcal./mol. for DEA system, respectively.

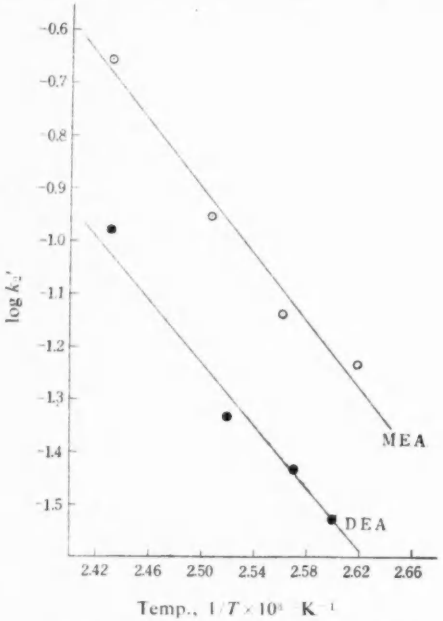

Fig. 6. Temperature dependence of rate constant k_2'; $\log k_2'$ vs. $1/T$ ($\times 10^{-3}$).

As to the samples, the reaction products should have the formula RR'NCOONH$_2$RR' (I), since the solution had still excess amine which would eventually change the products of the type RR'NCOOH (II), if present, to the type (I).

The author wishes to express his sincere thanks to Mr. Shûzô Kishida for his encouragement. This paper is published by the permission of the Technical Research and Development Institute, Defense Agency.

2nd R & D Center
Technical Research
and Development Institute
Defense Agency Japan
Setagaya-ku, Tokyo

Photoconductivity of Polycyclic Aromatic Compounds

By Mizuka SANO

(Received May 10, 1961)

Since Akamatu and Inokuchi reported the photoconductivity of violanthrone[1], a number of investigations have been made on the photoconductive phenomena in aromatic compounds[2-7]. These investigations, however, have been concentrated mainly on compounds consisting of a small number of rings, such as anthracene and pyrene, which possess resistivities as high as 10^{21} ohm. cm. at room temperature[8]; hence, they may be classified as insulation photoconductors rather than semiconductors. Recently Kallmann and Pope[8] showed

1) H. Akamatu and H. Inokuchi, *J. Chem. Phys.*, **20**, 1481 (1952).
2) H. Inokuchi, This Bulletin, **27**, 22 (1954).
3) H. Inokuchi, ibid., **29**, 131 (1956).
4) D. M. J. Compton, T. C. Waddington and W. G. Schneider, *J. Chem. Phys.*, **27**, 160 (1957).
5) L. E. Lyons and G. C. Morris, *J. Chem. Soc.*, **1957**, 3648.
6) B. Rosenberg, *J. Chem. Phys.*, **29**, 1108 (1958).
7) D. C. Northrop and O. Simpson, *Proc. Roy. Soc.*, **A 244**, 377 (1958).
8) H. Kallmann and M. Pope, *J. Chem. Phys.*, **32**, 300 (1960).

that the injected holes from an electrode contributed to the major conduction in anthracene, and Moore and Silver[9] concluded that anthracene is an extrinsic photoconductor rather than the intrinsic one.

On the other hand, relatively little work has been done on the photoconductive behaviors in multi-ring compounds, though it is known that the semiconductive properties are enhanced with the increase of the number of rings.

Experimental

Materials.—Most of the materials were synthetized by Drs. Handa and Aoki in our laboratory. All of them were carefully purified by recrystallization from solutions. To the final process of the purification the vacuum sublimation method was applied repeatedly.

Procedures.—Two types of photocells, i.e., the surface-type cell and the sandwich-type cell, were employed for the investigation of photoconduction. The surface-type cell consisted of a uniform film of aromatic compound with a thickness of about one micron and an area of 15×15 mm^2. The film was deposited on a pyrex glass plate (the dimension of which was 20 mm. $\times$ 25 mm.) by slow sublimation in vacuo. Colloidal graphite, "Aquadag", was applied on the film to serve as the electrodes, which were 1 cm. in length and about 3 mm. in width, with a gap of 1 mm. between them. The sandwich-type cell was formed by sublimation of the compound onto a pyrex plate on which a transparent aluminum conducting film had been previously deposited. The second aluminum film, lying entirely on the organic film, completed a photocell with an area of 10×5 mm^2 and a thickness of a few microns.

The sublimation of organic compounds was carried out in vacuo (10^{-3} mmHg) without decomposition over temperatures ranging from 80 to 380 °C. The growth of a film was followed by observing the color of reflected light, and in this way the thickness could be estimated accurately enough to prepare an appropriate film for photoconduction.

Most of the aromatics employed absorb the light intensely in the spectrum region extending from near ultraviolet to near infrared, so that a tungsten lamp is one of the most convenient light sources. The Mazda 750-watt projector lamp was used, being associated with second-order interference filters to isolate narrow particular wavelength regions. The maximum transmissive wavelengths of the regions, which were 9~16 mμ in half band width, ranged from 392 to 1324 mμ, with an interval of 50~100 mμ.

Absolute measurements of intensity of incident light on an organic photocell were made with the Nihonbunko vacuum thermopile which was placed at the position of the photocell. The sensitivity of the thermopile was 5.6 microvolts per one microwatt with the time constant of 33 milliseconds and the resistance of 4.2 ohm. A germanium phototransistor and a PbS photocell were used as auxiliary instruments for the measurement of light intensity, because these detectors endure a higher intensity of light better than the thermopile. The maximum intensity, 6×10^{15} photons/sec·cm^2, was obtained for the light which was isolated by the 1324 mμ filter.

Measurements of electric current were made with association of the Takeda Model V-1M dc amplifier. The ampplifier has the input resistance ranging from 4.5×10^5 to 4.4×10^{11} ohm. The voltage source applying to an organic photocell was a battery of dry elements with voltage of up to 700 V.

The apparatus, as illustrated in Fig. 1, consisted of five parts; the outer glass cylinder, the liquid nitrogen container with the photocell holder, the radiation shield, the optical windows and four conducting leads. The photocell was mounted on the holder by being pressed with a polystyrene plate and nuts.

Measurements of temperature were made with the germanium resistor which had been calibrated with a pentane direct-readings thermometer. The resistance of the resistor changed from 27 to 10 ohm. following the temperature change from +15 to −196 °C. The complete evacuation and the heat radiation shield prevented condensation of moisture on the surface of optical window. The apparatus was placed in a metal box, which served for shutting out the photocell from light and also for preventing electrical disturbance.

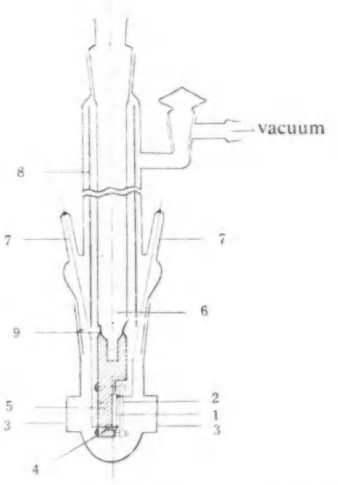

Fig. 1. The apparatus for conductivity measurement.

1 Photocell
2 Polystyrene plate
3 Optical windows
4 Germanium-registor thermometer
5 Specimen holder
6 Liquid nitrogen container
7 Conducting leads
8 Radiation shield
9 Copper-soft glass joint

9) W. Moore and M. Silver, ibid., 33, 1671 (1960).

Results

Change in Photocurrent with Electric Potential. —The electric current was measured as a function of applied potential under the illumination of monochromatic light. Most of the observations were made with surface-type photocells in vacuo, to avoid the effects of space charge which were occasionally observed with sandwich-type photocells.

The current responded to potential variation instantaneously and then remained constant with time. The potential dependence of photocurrent was reproducible, as in the case of dark current similarly. When the logarithm of the current i was plotted against the logarithm of the applied potential V, a linear relationship was obtained. This is illustrated in Fig. 2 for pyranthrene. From this, the potential-current relation could be expressed by the following formula,

$$i \propto V^{\alpha}$$

The values of α for pyranthrene, violanthrene and perylene are shown in Table I. In this table, it is seen that α is approximately unity, under different conditions of illumination with regard to wavelength and intensity of light. Hence, it can be concluded that the photocurrent obeys Ohm's law over the range of potential applied up to 7×10^{3} V./cm.

Change in Photocurrent with Light Intensity. —The photocurrent in surface-type photocells was observed as a function of light intensity. The relation between photocurrent and light intensity yielded two regions generally, as illustrated in Figs. 3 and 4. In each region, the relationship between the photocurrent i_p and the light intensity L could be expressed by the formula,

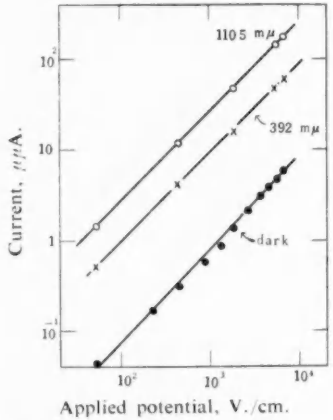

Fig. 2. The relation between current and applied potential for pyranthrene.

TABLE I. THE α-VALUE FOR SURFACE-TYPE PHOTOCELLS

	Illumination: Wavelength mμ	Illumination: Intensity photons/sec. cm²	α-Value
Pyranthrene (film)	Dark	—	1.05
	392	10^{15}	1.01
	529	10^{13}	1.14
	1055	10^{15}	1.10
	1105	10^{17}	1.00
Violanthrene (film)	Dark	—	1.11
	557	10^{13}	1.15
Perylene (film)	470	10^{13}	1.20
Perylene (single crystal)	392	10^{16}	1.17
	403	10^{16}	1.15
	502	10^{16}	1.17
	502	10^{17}	1.19

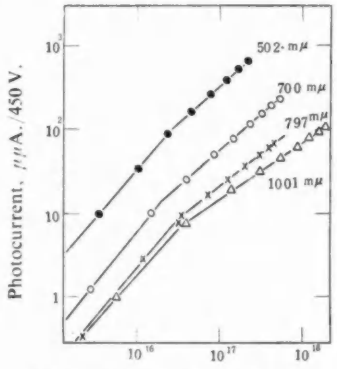

Fig. 3. The relation between photocurrent and light intensity for pyranthrene (surface-type photocell).

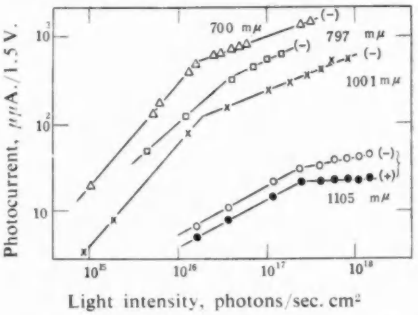

Fig. 4. The relation between photocurrent and light intensity for pyranthrene (sandwich-type photocell).

Illuminated electrode was biased positively, (+) and negatively (−).

$$i_p \propto L^n$$

In the region of low light intensity, usually not much exceeding 10^{16} photons/sec. cm^2, the photocurrent changed approximately in linearity with the light intensity, i. e., the exponent n was nearly unity. This relation was seemingly independent of the wavelength of incident light, the atmosphere, the applied potential and the temperature.

While in the region of high light intensity, n possessed a smaller value than unity, and was dependent on the wavelength of illumination. Nevertheless, no appreciable difference of n-value was noted according to the variation of temperature, potential, or atmosphere. The n-values are summarized in Table II.

No indication of saturation was observed with surface-type photocells even in the region of the highest light intensity, around 10^{18} photons/sec. cm^2. However, sandwich-type photocells showed the saturation of photocurrent at the light intensity of 2×10^{17} photons/sec. cm^2, as illustrated in Fig. 4.

TABLE II. THE n-VALUE FOR PYRANTHRENE AND PERYLENE SURFACE-TYPE PHOTOCELLS IN THE REGION OF HIGH LIGHT INTENSITY

Wavelength of illumination mμ	Pyranthrene film			Perylene single crystal	
	In vacuo*		In dry air	In vacuo*	In dry air
	290°K	185°K	290°K	290°K	290°K
403	0.86			0.98	0.87
450	0.84			0.95	0.87
502	0.95		1.06	1.12	1.15
552	1.00	1.03		1.10	1.02
599	0.89			0.86	0.82
655	0.82			0.79	0.68
700	0.85	0.81	0.87		
747	0.77				
797	0.77		0.74		
853	0.61				
901	0.62				
945	0.73				
1001	0.67		0.63	0.78	
1105	0.76	0.78		0.79	
1195	0.78			0.78	
1324	0.92	0.91	0.88		

* 10^{-3} mmHg after being flushed with argon gas.

Change in Photocurrent with Temperature.—The temperature dependence for photocurrent was measured over the range from 173 to 290°K. The surface-type photocell was employed with association of the apparatus which is shown in Fig. 1. The photocurrent increased with an increase in the temperature. Plots of the logarithm of photocurrent i_p against the reciprocal of temperature gave a straight line

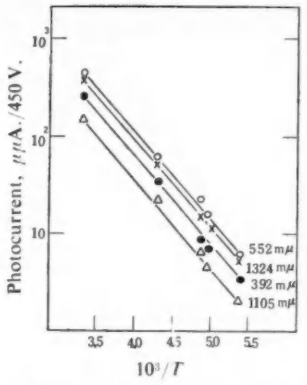

Fig. 5. The photocurrent vs. temperature for pyranthrene (surface-type photocell).

(Fig. 5), and the relation follows the equation,

$$i_p = i_0 \exp(-E/kT)$$

where E is the activation energy of photocurrent.

It is of interest that the activation energy, e. g., 0.18 eV. for pyranthrene, was found to be independent of the intensity and the wavelength of incident light over the range from 392 to 1324 mμ employed.

Generation of Charge Carriers.—An attempt was made to measure the photocurrent which was produced by the illumination onto a limited area of the aromatic film between the electrodes of surface-type photocell. Aquadag electrodes were painted on the pyranthrene film with a gap of 7 mm. between them. When the whole area between the electrodes was illuminated, the maximum photocurrent, of the value of 12×10^{-12} A./450 V., was observed. When the illumination was made onto the half part of the area between the electrodes by masking the other half, the magnitude of photocurrent was smaller than that expected if the photons in the same number had been uniformly distributed over the whole area. When the illumination was focused onto one of the electrodes alone, the increase of current was hardly observed. In addition, when the light fell onto a small limited area of the film, the magnitude of photocurrent assigned per unit area was nearly equal to that of the photocurrent produced by the illumination on the half area. Consequently it might be concluded that the charge carriers are not produced in a particular portion such as the Aquadag electrode or the contact area, but in the area between both elctrodes. Nevertheless, there is no explanation for the fact that the maximum photocurrent was produced by the illumination on the whole area. Probably the difference is

related to the decay pocess of charge carriers.

The photocurrent produced by an asymmetric illumination with respect to the polarity of ppalied potential was also measured. Onto a pyranthrene surface-type cell an image of slit of monochromatic light was collimated so that the illuminated strip lay parallel to the electrodes. Keeping the applied potential ($2.25\times\times10^{2}$ V./cm.) and light intensity (2.8×10^{17} photons/sec.cm^{2} for 552 mμ illumination) constant, the photocurrent was measured as the image was moved from one electrode to the other. The photocurrent was always greater when the illuminated portion was located close to the negatively biased electrode. In this case, the photoelectromotive force due to the asymmetric illumination was undetectable, even under the illumination of the highest light intensity.

Also, a sandwich-type photocell possesses the asymmetry in itself, because the light intensity of illumination is diminished successively along the electric potential. The photocurrent of a pyranthrene film (about 10 μ in thickness), which was sandwiched between two evaporated aluminum films, was 1.5 times greater when the illuminated side was negatively biased than when it was positively biased at the applied potential of 1.5×10^{3} V./cm.

The thermoelectromotive force, which was observed with compressed powder of isoviolanthrone, was of the order of 10^{-4} V./deg., indicating conduction predominantly by electrons.

Discussion

The semiconductive behaviors of polycyclic aromatic compounds have been fairly extensively studied, but the theoretical interpretation of their electronic conduction has not been completed, because the intermolecular interactions in the solid state are scarcely known. However, a significant part of the behavior of organic semiconductors can be discussed, for convenience, in terms of the band model. It may be postulated that the empty band and the full band are formed from the energy levels of the excited states and the ground state of π-electrons of the molecule respectively. In this case, the band widths might be narrow; especially the width of the full band is so narrow because of poor overlapping of the wave functions for the ground state, that the full band may be regarded as a series of discrete levels. Consequently it is quite probable that the holes are almost confined to the particular molecules in which they are generated, and most of the electric current is conducted by electrons through the crystal. The model was supported by the signs of the thermoelectromotive force and the polarity for the maximum photocurrent which was produced by an asymmetric illumination. In addition, as the ohmic nature of photocurrent as well as the experiment on the limited-area illumination indicated, the generation of charge carriers took place in the bulk of aromatic film, neither from the electrode nor the electrode-film contact. Hence, the multi-ring compounds are seemingly intrinsic photoconductors. The light intensity dependence for photocurrent has been usually accounted for by the concept of the trapping process of charge carriers. For instance, Rose[10] explained the variation of the exponent n from 1 to 0.5 by the population of the effective trapping centers which varies depending on the intensity of illumination. Our result showed that n possesses unity at a low light intensity and possesses a smaller value than unity at a high light intensity. This result is coincident qualitatively with that shown by Rose. The temperature dependence for photocurrent can not be easily interpreted because more than one parameter can change with temperature. However, the activation energy of photocurrent was independent on the wavelength of light. This result seems to indicate that the activation energy is not associated with the formation of charge carriers, such as the dissociation of electron-hole pairs, but with the transport process of carriers. If the trapping centers are assumed to be of the same depth below the empty band, and the temperature dependence could be ascribed to the variation of the mobility of carriers, the activation energy indicates the depth of trapping center. However, the nature of the centers has not been established. As suggested by Nelson[11] for the case of cationic dyestuff, every molecule might be regarded as a trapping center in the polycyclic aromatic compounds.

Summary

The voltage, light intensity, and temperature dependences for photocurrent in multi-ring compounds were studied as well as the photocurrent produced by the limited-area illumination. The photocurrent was found to be ohmic over the range of voltage employed. The photocurrent increased linearly with the intensity of light in the region of low light intensity, while it increased as the fractional power of the light intensity in the region of high intensity. The photocurrent increased with an increase of the temperature, and the activation energy of the photocurrent was found to be independent of the wavelength and the intensity of illumination.

10) A. Rose, *RCA Review*, **12**, 362 (1951).
11) R. C. Nelson, *J. Chem. Phys.*, **30**, 406 (1959).

The signs of the thermoelectric power as well as the polarity for the maximum photocurrent, and the experiment on the limited-area illumination indicated that the conduction in polycyclic aromatic compounds was due predominantly to electrons which were generated in the bulk of aromatic film.

The author expresses his hearty thanks to Professor Hideo Akamatu for his kind direction and advice, and also to Dr. Hiroo Inokuchi for his continuous advice in this work. The cost of this research has been defrayed from the Scientific Research Encouragement Grant from the Ministry of Education to which the author's thanks are due.

Department of Chemistry
Faculty of Science
The University of Tokyo
Hongo, Tokyo

---

*Stereoregular Polymers. IX. Polymerization of Optically Active α-Olefins**

By Shun'ichi NOZAKURA, Shigeru TAKEUCHI, Heimei YUKI and Shunsuke MURAHASHI

(Received April 18, 1961)

In their previous work[1], the authors polymerized styrene with anionic catalysts containing the optically active alkyl group such as optically active amylsodium or triamylaluminum combined with titanium trichloride. The purpose was to obtain optically active polystyrene, in which one helical configuration (either right- or left-handed screw helix) presumably induced by the active group might be predominantly present. However, the attempt was not successful.

X-Ray analyses of various isotactic polymers have shown that the crystalline structure of the polymer, and accordingly the crystallinity and the melting temperature are largely dependent on the side group of the chain[2]. In other words, the type of helix, i.e. the number of monomeric units or of turns in the identity period, may be decided definitely by the shape and size of the substituent group of the chain.

The present work was carried out as one of the programs of attempting to regulate the direction of helical configuration of polymer chain in its screw sense. Two optically active α-olefins, *l*-4-methyl-1-hexene and *d*-3-methyl-1-pentene, were polymerized by the Ziegler catalyst and the nature of the polymer was examined in anticipation that the asymmetric substituent might induce the helical configuration, which exists with only one (right- or left-handed) screw sense, in the polymer chain.

Experimental

Preparation of Monomers.—*l-2-Methyl-1-butanol.*—Commercial fusel oil was fractionally distilled by Stedman type column (about seventy theoretical plates) repeatedly. *l*-2-Methyl-1-butanol thus obtained showed b. p. 128 °C and α_D^{25} −9.36° (*l*=20 cm.) (optical purity 98.7%)[3].

d-1-Chloro-2-methylbutane.—The alcohol was converted to the chloride by thionyl chloride. Yield 78.7%, b. p. 99 °C, $[\alpha]_D^{20}$ +1.63° (optical purity 97%)[4].

Optically Active 1-Bromo-2-ethoxy-4-methylhexane.—2-Methylbutylmagnesium chloride derived from optically active *d*-1-chloro-2-mehthylbutane was made to react with α, β-dibromo ethyl ether[5] to give 1-bromo-2-ethoxy-4-methylhexane[6]. Yield 60.3%, b. p. 91~93 °C/15 mmHg.

l-4-Methyl-1-hexene[7].—The ethoxyheptyl bromide gave *l*-4-methylhexene in 61% yield by refluxing an alcoholic solution with zinc powder for 10 hr.

* This paper is based upon a portion of a thesis submitted by S. Takeuchi in partial fulfillment of the requirements for the Degree of Master of Science in Osaka University, March, 1960.

1) S. Murahashi, S. Nozakura and S. Takeuchi, This Bulletin, **33**, 658 (1960).

2) G. Natta, *Angew. Chem.*, **68**, 393 (1956).

3) R. M. Ideda, R. E. Kepner and A. D. Webb, *Anal. Chem.*, **28**, 1335 (1956).

4) A. Mackenzie and G. W. Clough, *J. Chem. Soc.*, **103**, 698 (1913).

5) L. S. Swallen and C. E. Boord, *J. Am. Chem. Soc.*, **52**, 651 (1930); H. B. Dykstra, J. F. Lewis and C. E. Boord, ibid., **52**, 3396 (1930).

6) D. C. Rowland, K. W. Greenlee, J. M. Derfer and C. E. Boord, *J. Org. Chem.*, **17**, 807 (1952).

7) F. J. Soday and C. E. Boord, *J. Am. Chem. Soc.*, **55**, 3293 (1933).

TABLE I

	Polymerization[a]				Polymer			
	Monomer g.	$AlEt_3$ g.	$TiCl_4$ g.	Yield %	M. p. °C	$[\alpha]_D$(in toluene)	$[\eta]^b$	d_4^{13}
l-4-Methyl-1-hexene	3.6	0.56	0.38	19	180~182	+251°(27.5°)	0.86	0.862[c]
〃	5.7	0.75	0.50	7	171~174	+249 (21)	0.79	0.86
5-Methyl-1-hexene	3.1	0.38	0.25	25	112~114	+ 54 (22)	—	—[d]
〃	2.1	0.38	0.25	58	102~104	+ 52 (22)	—	—
〃	1.6	0.38	0.25	46	96	+ 54 (22)	—	—
d-3-Methyl-1-pentene	4.4	0.75	0.50	20	260~264	+255 (24)[g]	—	0.831[e]
dl-3-Methyl-1-pentene	1.3	0.38	0.25	8	200~205	— —	—	0.832[f]

a, Solvent: 20 ml. *n*-heptane. b, Toluene solution at 29.9°. c, Found: C, 84.94; H, 14.29. d, Found: C, 85.26; H, 14.10; Ash, 0.26. e, Found: C, 84.60; H, 14.09; Ash, 0.89. f, Unfractionated. Found: C, 85.38; H, 14.12; Ash, trace. All the samples contained traces of ash. Calcd. for $[C_8H_{2n}]_p$: C, 85.63; H, 14.37%. g, in petrolatum liquid.

B. p. 87~88°C, $[\alpha]_D^{31}$ −2.50° (optical purity 94%)[8] n_D^{31} 1.3970, d_4^{31} 0.692.

5-Methyl-1-hexene.—It was synthesized similarly from commercial isoamyl alcohol via isoamyl chloride in 16% yield based on the chloride. B. p. 83~85°C. The isoamyl chloride showed an optical activity ($[\alpha]_D^{32}$ +0.33°), which corresponded to that calculated for a mixture of 81% pure isoamyl chloride and 19% *d*-1-chloro-2-methylbutane[9].

d-3-Methyl-1-pentanol.—Optically active 3-methyl-1-pentanol was synthesized from formaldehyde and 2-methylbutylmagnesium chloride derived from *d*-1-chloro-2-methylbutane (b. p. 99~100°C, $[\alpha]_D^{19}$ +1.71°, optical purity ca. 100%), which was obtained from optically pure *l*-2-methyl-1-butanol, b. p. 127.5~128.5°C, $[\alpha]_D^{11}$ −9.55° (*l*=20 cm.). Gaseous formaldehyde was bubbled through the ethereal solution of the Grignard reagent with dry nitrogen. The subsequent decomposition and steam-distillation of the product gave *d*-3-methyl-1-pentanol in 38.3% yield, b. p. 147~149°, $[\alpha]_D^{19}$ −8.41° (literature[8]: $[\alpha]_D^{19.5}$ −8.53°).

d-3-Methylpentyl Acetate.—The acetate was obtained from the alcohol by using *p*-toluenesulfonic acid as a condensing catalyst, yield 69%, b.p. 156~158°C, $[\alpha]_D^{8}$ +8.53° (literature[8]: $[\alpha]_D^{19}$ −8.30°).

d-3-Methyl-1-pentene.—The methylpentyl acetate was dropped with a stream of nitrogen through a quartz tube packed with glass pieces at 500°C. The pyrolysis gave *d*-3-methyl-1-pentene in 36% yield. b. p. 54~55°C, $[\alpha]_D^{17}$ +32.95° (literature[8]: $[\alpha]_D^{17}$ +32.86°).

dl-3-Methyl-1-pentanol.—Ethylene oxide was bubbled through an ethereal solution of *sec*-butylmagnesium chloride using nitrogen as a carrier gas. The product was decomposed by saturated aqueous ammonium chloride and steam-distilled to give *dl*-3-methyl-1-pentanol. Yield 52%, b. p. 148~150°C.

dl-3-Methyl-1-pentene.—The racemic 3-methyl-1-pentene was obtained from the racemic methylpentanol via its acetate similarly as described on the optically active methylpentene. Yield 35% based on the alcohol, b. p. 54~56°C.

Polymerization.—The heptene monomers, *l*-4-methyl-1-hexene and 5-methyl-1-hexene, were polymerized in a five-necked flask described previously[10]. The vessel was flushed with dry nitrogen, and charged with *n*-heptane, titanium tetrachloride and aluminum triethyl (*n*-heptane solution), and the monomer was injected by a hypodermic syringe through a rubber cap fitted on the vessel. The mixture was heated for 10 hr. at 70°C. All procedures were done in a stream of dry nitrogen. The reaction mixture was then poured into a large volume of methanol containing a small amount of hydrochloric acid to decompose the catalyst. After being allowed to stand overnight the precipitated polymer was collected by centrifugation, washed with methanol, and dried.

The hexene monomers, *d*- and *dl*-3-methyl-1-pentene, were polymerized by analogous procedures but using a sealed tube as the reaction vessel and at 50°C for longer periods, 40 hr. for racemic and 144 hr. for *d*-monomer.

The results of polymerization were summarized in Table I.

The polyheptenes were soluble in chloroform, carbon tetrachloride, toluene, benzene, decalin, carbon disulfide, and hot *n*-heptane, and insoluble in ether, alcohol and acetone.

Poly-*d*-3-methyl-1-pentene was almost insoluble in usual organic solvents. This was slightly soluble above its melting point in petrolatum liquid, dibutyl phthalate and dioctyl phthalate. The solution in petrolatum liquid was maintained clear and stable even after it had cooled to room temperature, but the polymer precipitated from the phthalate solutions below about 290°C and no appreciable amount of polymer appeared from the liquid phases by adding methanol.

On the other hand, the polymeric product of *dl*-3-methyl-1-pentene was found to be largely contaminated with polyethylene produced from the Ziegler catalyst itself and was fractionated successively by boiling toluene and by boiling decalin. The toluene-soluble fraction (68%) containing a considerable amount of polyethylene melted between 130 and 190°C. The decalin-soluble fraction (17%) and the remaining insoluble fraction (15%) melted at 225~226°C and 245~247°C, respectively. The solubility of decalin-insoluble fraction seemed

8) P. Pino and L. Lardicci, *Chem. & Ind.*, **1959**, 483.
9) F. C. Witmore and J. H. Olewine, *J. Am. Chem. Soc.*, **60**, 2570 (1938).
10) S. Murahashi, S. Nozakura, M. Sumi and K. Hatada, This Bulletin, **32**, 1094 (1959).

to be slightly greater than that of poly-*d*-3-methyl-1-pentene but was about the same.

Optical Rotation.—For the determinations of optical rotatory dispersion and optical purity a Rudolph high-precision photoelectric spectropolarimeter model 200S-80 was used.

The observed optical rotation of a solution of poly-*d*-3-methyl-1-pentene in petrolatum liquid was α_D^{24} +4.68° (l=20 cm.) at c=0.0745. The petrolatum liquid, however, had an optical rotation α_D^{24} +2.15° (l=10 cm.), and the specific rotation of the polymer, $[\alpha]_D^{24}$ +255°, was calculated from the difference of rotations of the solution and the solvent.

Density.—Determination of polymer density was carried out by a density gradient tube using methanol and water as media.

Melting Point.—The polymer sample was placed on a metal block under the microscope. The metal block was heated by a hot plate and the melting point of the sample was measured.

Results

The dependence of the optical rotation on the concentration of poly-*l*-4-methyl-1-hexene was examined in four solvents, toluene, decalin, carbon tetrachloride and carbon disulfide. The results are shown in Fig. 1. The linear ralationships between the rotation and the polymer concentration were obtained in each solvent. These led to the values of specific rotation $[\alpha]_D^{27.5}$ +251° (toluene), $[\alpha]_D^{24}$ +268° (decalin), $[\alpha]_D^{25}$ +236° (carbon tetrachloride) and $[\alpha]_D^{13}$ +290° (carbon disufide).

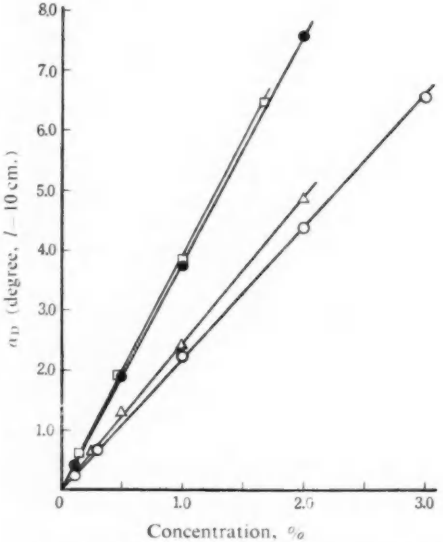

Fig. 1. Optical rotation vs. concentration of poly-*l*-4-methyl-1-hexene in various solvents: ○ in toluene at 27.5°C; △ in decalin at 24°C; □ in carbon tetrachloride at 25°C; ● in carbon disulfide at 13°C.

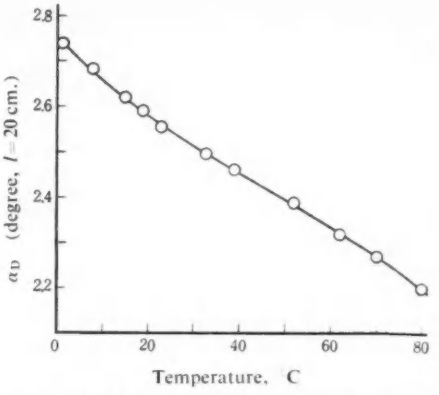

Fig. 2. Temperature dependence of optical rotation of 0.5% poly-*l*-4-methyl-1-hexene solution in decalin.

The plots of the optical rotation of 0.5% poly-*l*-4-methyl-1-hexene solution in decalin vs. temperature are shown in Fig. 2. The rotation decreased almost linearly with the elevation of temperature from 2 to 80°C.

To the toluene solution of the polymer (concentration 1.05%) *n*-heptane, a poor solvent for the polymer, was added successively and the change of optical rotation of the solution was followed. Similarly *n*-butanol, a precipitant against the polymer, was added in another series of this experiment. The results showed that the rotation was rather strictly linear to the concentration of the polymer alone (Fig. 3). In these experiments the ageing of the

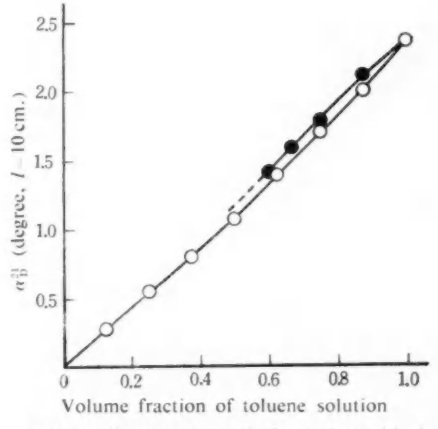

Fig. 3. Changes in optical rotation with the addition of *n*-heptane (○) and *n*-butanol (●) to 1.05% solution of poly-*l*-4-methyl-1-hexene in toluene. Dotted line, precipitation occurred.

solution caused no change in the optical rotation after adding the poor or the bad solvent.

The optical rotatory dispersion was measured with the polymer in two solvents, decalin (c= 0.4%, l=10 cm.) and toluene-*n*-heptane mixture (1 : 1 vol./vol., c=0.6%, l=10 cm.). The results are shown in Figs. 4 and 5. The plots $\alpha_\lambda\lambda^2$ vs. α_λ, where α_λ is the optical rotation at a wavelength λ, were linear as shown in Fig. 5, and no abnormal dispersion was observed.

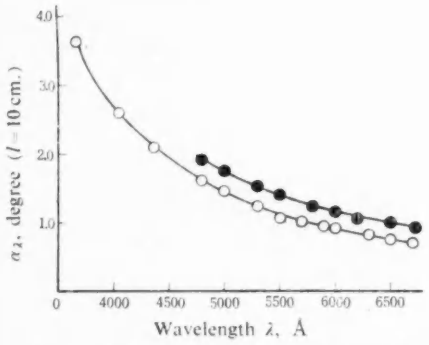

Fig. 4. Optical rotatory dispersion of poly-*l*-4-methyl-1-hexene: ○ in decalin (c=0.4) at 21°C; ● in toluene-*n*-heptane mixture (1 : 1 vol./vol., c=0.6) at 19°C.

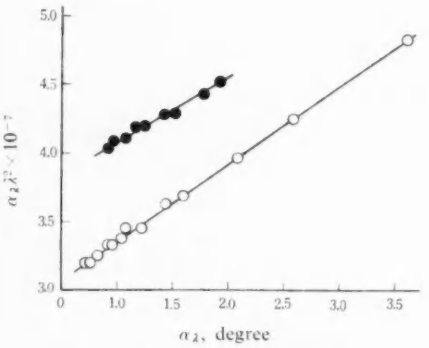

Fig. 5. $\alpha_\lambda\lambda^2$ vs. α_λ in the optical rotatory dispersion of poly-*l*-4-methyl-1-hexene: ○ in decalin; ● in toluene-*n*-heptane mixture.

All the polymers obtained here gave sharp crystalline X-ray patterns except the toluene-soluble fraction of poly-*dl*-3-methyl-1-pentene. The patterns given by poly-*d*-3-methyl-1-pentene and the decalin-insoluble fraction of poly-*dl*-3-methyl-1-pentene were completely different. The spacings obtained from the powder X-ray diagrams are summarized in Table II.

TABLE II. SPACINGS FOR POLY-*d*-3-METHYL-1-PENTENE AND POLY-*dl*-3-METHYL-1-PENTENE

Poly-*d*-3-methyl-1-pentene	Poly-*dl*-3-methyl-1-pentene[a]
9.60 Å (vs)	9.26 (s)
6.92 (vw)	8.65 (s)
6.18 (m)	5.38 (s)
5.55 (vw)	4.74 (mw)
5.09 (vw)	4.20 (m)
4.66 (s)	3.91 (m)
4.23 (vw)	
4.05 (w)	
3.26 (w)	
3.07 (vw)	
2.75 (vw broad)	
2.53 (vw)	
2.39 (vw)	

a Decalin-insoluble fraction.

Discussion

Both of the optically active polymers, poly-*l*-4-methyl-1-hexene and poly-*d*-3-methyl-1-pentene, showed enormously large optical rotations compared with those of the monomers. The large optical rotations seemed to be contributed not only by the neighboring groups around the asymmetric carbon atom of the side group but also by the molecular asymmetry of the helical configuration of the main chain, more practically by a predominant concentration of either right- or left-handed helix in the solution.

It is doubtful that the isotactic polymer such as poly-α-olefin still maintains its helical structure in the solution. However, Takeda and his collaborators[11] recently stated from their infrared absorption study that in carbon disulfide isotactic polystyrene retained its helical structure[12] even in the solution state. This encouraged us to investigate the optical rotation of poly-*l*-4-methyl-1-hexene in solution by varying the conditions in order to learn its exact nature.

The concentration of the helix might vary with the concentration of the polymer, if it remained in the solution in any extent. The temperature might also affect the concentration of the helix. The concentration of the helix would be considered to be related to the interaction between the molecules of polymer and solvent. A good solvent may release the helical configuration of the polymer to transform it into a randomly coiled structure and, on the other hand, poor solvent might probably coil up the chain to a helix as shown by

11) M. Takeda, K. Iimura, A. Yamada and Y. Imamura, ibid., 32, 1150 (1959).
12) H. Tadokoro et al., ibid., 32, 313, 534 (1959); *J. Polymer Sci.*, 36, 553 (1959).

Doty and his coworkers[13] for poly(γ-benzyl L-glutamate).

However, the concentration, the temperature and the addition of bad solvent gave no distinct change in the specific rotation of the polymer in solution, compared with the large change observed in the helix-coil transformation of poly (γ-benzyl L-glutamate). In addition, the plots of optical rotatory dispersion fitted the equation $\alpha_\lambda\lambda^2=\lambda_c^2\alpha_\lambda+A'$[13] derived from the simple one-term Drude equation $[\alpha_\lambda]=A/(\lambda^2-\lambda_c^2)$, where λ_c, A and A' are the constants, respectively, and no complex dispersion was found. These facts strongly suggest that the optical rotation of this polymer is attributed to only one species, the asymmetric carbon atom of the substituent group, at least in solution.

The polymer formed from the 5-methyl-1-hexene monomer had a specific rotation $[\alpha]_D^{22}$ +54° in toluene. Obviously this was caused by *l*-4-methyl-1-hexene units in the polymer which had been contained in the monomer used. Reding[14] has reported that the polymer produced from a mixture of 4-methyl-1-pentene and 3-methyl-1-butene was a copolymer but not a mixture of the homopolymers of each monomer. Therefore, it may be preferable to consider the polymer obtained here as being also the copolymer of 5-methyl-1-hexene and *l*-4-methyl-1-hexene. It must be noted that the specific rotation of this polymer was about 20% of that of poly-*l*-4-methyl-1-hexene and the percentage was coincident with the content of *d*-1-chloro-2-methylbutane in amyl chloride mixture used as the starting material of the monomer, although many steps had been taken in the way from the chloride to the polymer.

The optical rotatory behavior of poly-*l*-4-methyl-1-hexene gave no positive evidence either for the existence of helical configuration in solution or, if any, for a predominant existence of right- or left-handed helices. This might be caused by the absence of strong intramolecular attraction such as hydrogen bond to coil up the chain to a helix in solution. Even if the helix was maintained in solution, the one carbon atom inserted between the main chain and the asymmetric carbon atom would weaken the steric influence of the neighboring groups around the asymmetric carbon atom. This might result in no regulation of the direction of helical configuration in a single screw sense.

The density of poly-*l*-4-methyl-1-hexene was coincident with the value reported for poly-*dl*-4-methyl-1-hexene by Natta[2]. The melting point was also approximately the same as those observed by Natta (188°C)[2] and Campbell (157~160°C)[15] with the polymer formed from the racemic monomer. These facts seem to suggest that there is almost no difference in the crystalline structure of either the optically active or the racemic polymer even in the solid state.

On the contrary, the melting point of poly-*d*-3-methyl-1-pentene is distinctly higher than that of the decalin-insoluble fraction of poly-*dl*-3-methyl-1-pentene, which seemed to have almost the same crystallinity and stereoregularity as those of the former polymer from its solubility behavior. Furthermore, the X-ray diffraction patterns of these two polymers are so different that the polymers appeared to be constituted with completely different monomeric units from each other.

The low conversion and also the very low stereospecificity in the polymerization of *dl*-3-methyl-1-pentene suggest the difficulty of isotactic propagation of this monomer. This may be caused by the copolymerization of the *d*- and *l*-monomers, in which the asymmetric tertiary carbon atoms are adjacent to the vinyl groups.

. In the polymerization of racemic monomer three types are probable in the formation of its polymer: a mixture of homopolymers of *d*- and *l*-monomer each, a random copolymer and a block-copolymer of these. Furthermore, each type of these is able to form isotactic, atactic and stereo-block polymers in regard to the main chain of the polymer.

For the polymer of *dl*-3-methyl-1-pentene the authors obtained three fractions according to the solubility difference. The problem as to which of the above mentioned types correspond to the respective fractions is very interesting, although this is not certain at the present stage of this work.

In poly-3-methyl-1-pentene the asymmetric carbon atom of side chain is adjacent and so close to the main chain of the polymer that it may affect the configuration of the chain, contrary to the case of poly-4-methyl-1-hexene. Therefore, the predominant or exclusive formation of either the right- or left-handed helix may be expected in much more probability for poly-*d*-3-methyl-1-pentene than for poly-*l*-4-methyl-1-hexene. Unfortunately, the detailed investigation on the optical rotation of poly-*d*-3-methyl-1-pentene could not be done due to the extremely low solubility of the polymer, although the polymer showed a

13) P. Doty and J. T. Yang, *J. Am. Chem. Soc.*, **78**, 498 (1956); **79**, 761 (1957).
14) F. P. Reding, *J. Polymer Sci.*, **37**, 555 (1959).
15) T. W. Campbell and A. C. Haven, Jr., *J. Appl. Polymer Sci.*, **1**, 73 (1959).

very large specific rotation, $[\alpha]_D^{24}$ +255°, in petrolatum liquid.

After the completion of this work, papers by Pino and Lorenzi[16], and Bailey and Yates[17] appeared, which described the same subject independently. Bailey and Yates reported that the specific rotation of poly-*d*-3-methyl-1-pentene $[\alpha]_D^{25}$ was −257° in 1,1-ditolylethane. The present sample of the same polymer showed distinctly dextro rotation also in 1,1-ditolylethane, but the exact value could not be obtained, because the concentration of the solution was too small to be measured, due to the extremely low solubility of the polymer in 1,1-ditolylethane at room temperature. Pino and Lorenzi reported that the various soluble fractions of poly-*d*-3-methyl-1-pentene, which seemed to be atactic or stereoblock, had dextro rotations.

Pino and Lorenzi concluded in their paper that in dilute solution and in the molten state the isotactic and stereo-block polymers of optically active α-olefins may be at least in part spiralized and that helices of a single screw sense may largely prevail, because of the remarkable dependence of the optical rotation on stereoregularity and temperature. However, the temperature coefficient of optical rotation must also be dependent on the magnitude of specific rotation itself and in this respect the temperature coefficients of the optical rotation of optically active poly-α-olefins may be considered to be not so large. Other considerations seem to be necessary to explain the large optical rotations of these isotactic polymers formed from optically active α-olefins.

The authors wish to thank Dr. Yōzō Chatani for his help in the X-ray investigation.

Department of Polymer Science
Faculty of Science
Osaka University
Nakanoshima, Osaka

16) P. Pino and G. P. Lorenzi, *J. Am. Chem. Soc.*, **82**, 4745 (1960).
17) W. J. Bailey and E. T. Yates, *J. Org. Chem.*, **25**, 1800 (1960).

Studies on Phenolic Resins. IV. Physical and Chemical Properties of Coating Films of Japanese Lac (Urushi) (Rigidity Modulus-Temperature Relations Measured by Torsional Pendulum Method)

By Tsutomu KUWATA, Jū KUMANOTANI and Seiji KAZAMA

(Received April 17, 1961)

Japanese lac (*urushi*) has been used as a natural coating material for more than two thousand years in Japan and China. It has been recognized that the coating film prepared from Japanese lac has many excellent properties and utility. The decorative coating film for artificial and wooden articles has a beautiful color tone and as the protective coating film, it is known by experience to have outstanding physical and chemical properties, compared with the films of the usual paints or varnishes. Traditional wooden crafts coated with *urushi* are very famous and used with appreciation all over the world, but our country imports a large quantity of raw Japanese lac from other Asian countries, because it produces only five per cent of the demand. Therefore, it has been hoped to make up industrial processes to synthesize some substance that can be used in place of natural Japanese lac, or some kind of compounding component or filler for it. There were two ways of attempting this aim.

One attempt was to synthesize the compouds chemically identical with the natural substance. The substance which is usually called Japanese lac is a sap of Rhus vernicifera D. C., produced in Japan and China. Chemical identification of urushiol, the principal component and polymerization unit of Japanese lac, was carried out by Majima[1] and Dawson[2] and the latter established that urushiol was composed of four

1) R. Majima, "Untersuchungen über den Japanlack", (1924).
2) S. V. Sunthankar and C. R. Dawson, *J. Am. Chem. Soc.*, **76**, 5070 (1954).

derivatives of catechol, substituted at 3-position with paraffinic, olefinic, diolefinic, and triolefinic straight chains of 15 carbons, and the average number of double bonds in the mixture were about two for one molecule. Some of these compounds were synthesized by Dawson[3] and Yukawa[4] but their processes cannot be applied to industrial production. Many chemically analogous compounds were synthesized in the past but they could not be used practically.

Another attempt was made in the industrial field for the purpose of obtaining substitutes or fillers for Japanese lac, and several kinds of coating materials, which formed a film apparrently similar to that of Japanese lac, were prepared and commercialized as "synthetic Japanese lac". But the interesting and important feature of Japanese lac, which must be taken into account, is that it contains an oxidation-reduction enzyme, laccase, and air-drying of Japanese lac proceeds through a characteristic oxidation-polymerization of urushiol with oxygen in the air, catalyzed with laccase[5]; also that the characteristic reaction is thought to be one of the factors that give good properties to the film. Though the molecular structure and reaction mechanism of laccase are not yet known, it was proved to act only on *ortho*- or *para*-polyhydroxy or polyamino aromatic compounds[5]. Therefore commercialized so-called "synthetic Japanese lacs", which are oil varnishes, are not affected by laccase, and they degrade the mechanical properties of the film when used as fillers for Japanese lac.

In another paper the authors studied the preparative method of compounds capable of polymerizing at room temperature together with urushiol, affected with laccase equally to it, when added to natural Japanese lac as fillers[6].

Evaluation of those compounds should be carried out in respect of the physical and mechanical properties of the coating films formed from the mixtures of them and Japanese lac, as compared with the properties of Japanese lac film.

Although it is well known by experience that the coating films of Japanese lac have ideal physical and mechanical properties, scientific studies have been limited to the subjects of resistance to chemical reagents and electrical insulation, and no data were available about the mechanical properties.

In this paper the authors first studied, by means of the torsional pendulum method, the mechanical properties of coating films, prepared through various processes from Japanese lac. This method had been developed to study the visco-elastic behavior of polymers, and in spite of its being a simple operation, it presented useful data such as rigidity modulus and decrement of oscillation at any temperature, and glass transition temperature of the film.

As the results of the observation of the mechanical properties of the coating films which were the oxidation polymerization products of urushiol under the action of laccase or heat, it was revealed that the Japanese lac films had excellent, characteristic properties, never found in other kinds of coating films.

Then the authors determined the mechanical data of three coating film samples each prepared from the mixtures of 10 parts of Japanese lac and 6 parts of the synthetic compound. These three compounds were chosen from a series of catechol derivatives, which had been synthesized by the authors for the purpose of obtaining a good filler for Japanese lac. It was evidently approved by the properties of the film samples that those compounds were excellent fillers for Japanese lac and able to be used in place of urushiol.

Experimental by Torsional Pendulum Method

The torsional pendulum method developed by Inoue[7] to investigate the mechanical characteristics of polymer films is simple in operation, and gives reliable data. Torsional pendulum apparatus has as the main part an inertia bar attached at its center to the lower end of a pending sample film strip, and a mirror is set below the center. The period and the amplitudes of damping oscillation of the bar are measured by the lamp-and-scale system. Rigidity modulus (G) and logarithmic decrement (λ) are calculated from these data.

Procedure.—Torsional pendulum apparatus with sample film was set in a low temperature thermostat, slowly heated up to 40°C and kept at this temperature for 40 min. This duration was necessary for the internal structure of the sample to reach equilibrium at this temperature. Then the temperature was cotinuously dropped at the rate of 1°C/2 min. down to −60°C, while measuring the amplitudes and the period of 3~6 oscillation cycles every 5 or 10°C. The temperature was slowly raised to room temperature, and the apparatus with sample was kept there overnight. Next day it was set in an electric heating thermostat, and the temperature was continuously raised at the rate of 1°C/2 min. to about 150°C and the measurement was carried out every 5 or 10°C.

The rigidity modulus (G) of the sample film was calculated from the period, and the logarithmic

3) B. Love and C. R. Dawson, ibid., **78**, 4083 (1956).
4) T. Yukawa, Presented at the 13th Annual Meeting of Chem. Soc. Japan, Tokyo, April, 1960.
5) G. Bertrand, *Compt. rend.*, **124**, 1032, 1355 (1897).
6) T. Kuwata, J. Kumanotani and S. Kazama, *J. Chem. Soc. Japan, Ind. Chem. Sec.* (*Kogyo Kagaku Zasshi*), **64**, 1629 (1961).
7) Y. Inoue, ibid., **55**, 262 (1952).

decrement (λ) was calculated from the amplitude change.

G and λ were plotted against temperature, and the temperature where λ was maximum was glass transition temperature (T_g) of the sample film.

TABLE I. LIST OF SAMPLES

No.	Sample film
1	Air-dried film of kiurushi
2	Baked film of kiurushi
3	Air-dried film of sugurome urushi
4	Baked film of sugurome urushi
5	Air-dried film of sugurome urushi
6	Tested strip of sample No. 5, heated at 100°C for 2 hr. after measurement up to 110°C
7	Sample No. 5, kept in air for 25 days
8	Sample No. 1, kept in air for 30 months
9	Tested strip of sample No. 8, kept in air overnight after measurement up to 150°C
10	Sample No. 2, kept in air for 30 months
11	Sample No. 3, kept in air for 30 months
12	Tested strip of sample No. 11, kept in air overnight after measurement up to 150°C
13	Sample No. 5, kept in air for 30 months
14	Air-dried film of Thailand-sugurome urushi, kept in air for 30 months
15	Air-dried film of sugurome processed mixture of kiurushi and distilled urushiol (1 : 1 part) kept in air for 7 months
16	Air-dried film of sugurome-processed mixture of kiurushi (10 parts) and linseed oil (3 parts)
17	Air-dried film of sugurome-processed mixture of kiurushi (10 parts) and linseed oil (6 parts)
18	Sample No. 16, kept in air for 30 months
19	Air-dried film of sugurome-processed mixtre of kiurushi (10 parts), linseed oil (2 parts) and ester gum (1 part)
20	Baked film of sugurome-processed mixture of kiurushi (10 parts), linseed oil (2 parts) and ester gum (1 part)
21	Sample No. 20, kept in air for 30 months
22	Air-dried film of sugurome-processed mixture of kiurushi (10 parts) and catechol derivative A (6 parts)
23	Air-dried film of sugurome-processed mixture of kiurushi (10 parts) and catechol derivative B (6 parts)
24	Air-dried film of sugurome-processed mixture of kiurushi (10 parts) and catechol derivative C (6 parts)
25	Air-dried film of oil varnish of reactive *o*-cresol resin
26	Air-dried film of oil varnish of nonreactive *o*-cresol resin

The inertia bar used in the experiment was made of aluminum, the length being 20.64 cm., weight 34.01 g. moment of inertia 1210 g. cm^2. The periods measured were 3~15 sec. It had been reported that in order to obtain reliable data the periods should lie in the range from 2 to 17 sec.[5]

Sample Films.—The sample films are listed in Table I. The meanings of several terms which are unique to Japanese lac are as follows.

Kiurushi (raw Japanese lac); this is the sap of the plant.

Sugurome process; this is a unique process in the preparation of usual commercial coating material of Japanese lac in Japan. Raw Japanese lac, alone or with other substances, is stirred in a wooden vessel for a time, then heated at about 38°C for about 7 hr. under stirring. During the process dehydration and partial oxidation of the lac take place.

Sugurome urushi; *sugurome-processed* Japanese lac. The raw Japanese lac of Samples Nos. 1—4, 8—12, 15—24, was taken from a lot produced in Moppo, China. The Samples Nos. 5, 6, 7, 13, were taken from another lot. Sample No. 14 was the film formed from Thailand lac, the main component of which is not urushiol but thithiol.

Sugurome-proscess in the preparation of Sample No. 5, was a little different from that of Sample No. 3, but details were not ascertained.

The torsional pendulum method required the sample film strip, of which the breadth b was about 1 cm. and the thickness h was more than 0.02 cm. because b/h ratio should be 10~50 in order to obtain reliable data. But the thickness of the uniform film formed by one coating was 0.002~0.004 cm. The authors prepared the sample coating films by coating the sample lacs on tin plates (25 cm. × 15 cm.), repeating the coating and drying to touch-free state five to ten times until the films formed became thick enough.

Air-drying was carried out in a wet atmosphere in order to activate laccase. In case of baking, every coat was heated by an infrared lamp (40~60°C) to give a touch-free surface, and finally the film was heated at 100°C for 1 hr. in an electric drier.

The sample film thus formed on the tin plate was cut into strips, about 1 cm. broad, and these strips were torn off after amalgamation of the tin surface. The dimensions of the test strips we used were 13~15 cm. in length and 30~60 in b/h.

Samples Nos. 22—24 were the air-dried films of *sugurome-processed* mixtures of *kiurushi* (10 parts) and catechol derivatives (6 parts). Catechol derivative A was the ester of homoprotocatechuic acid and linseed oil alcohol; B, mixed glyceride of protocatechuic acid and linseed oil fatty acid (1 : 2); C, allyl ester of addition product of catechol and linseed oil fatty acid.

Samples Nos. 25 and 26 were the films of varnishes of phenolic resins, observed in comparison with Japanese lac.

All sample films except those of which the duration of exposure to air are noted in Table I were examined within 10 days after preparation.

8) J. Furuichi, *J. Appl. Phys., Japan*, **27**, 720 (1958).

Table II. Physical properties of Japanese lac coating films

Sample No.	T_g, °C	G_g, dyn./cm²	G_r, dyn./cm²	G_h, dyn./cm²	λ_{max}
1	70	1.1×10^9	5.2×10^9	4.8×10^5	0.33
2	85	2.2×10^9	7.1×10^9	1.4×10^9	0.19
3	30	7.3×10^5	1.2×10^9	2.4×10^5	0.31
4	45	1.3×10^9	2.7×10^9	3.9×10^5	0.22
5	45	2.4×10^9	5.0×10^9	5.6×10^5	0.21
6	58	4.1×10^9	7.9×10^9	1.3×10^9	0.21
7	63	1.9×10^9	5.8×10^9	6.6×10^5	0.23
8	100	2.1×10^9	7.7×10^9	1.1×10^9	0.27
9	115	2.5×10^9	7.7×10^9	1.3×10^9	0.18
10	130	2.5×10^9	9.7×10^9	1.8×10^9	0.18
11	83	7.9×10^5	5.4×10^9	2.5×10^5	0.49
12	93	1.2×10^9	7.2×10^9	3.5×10^5	0.30
13	95	2.2×10^9	6.8×10^9	7.4×10^5	0.23
14	77	8.4×10^5	3.5×10^9	1.8×10^5	0.29
15	90	2.0×10^9	6.0×10^9	7.9×10^5	0.21
16	10	2.0×10^9	1.4×10^9	3.9×10^5	0.20
17	−45	3.9×10^9	4.5×10^5	2.2×10^5	0.17
18	81	1.3×10^9	6.2×10^9	3.6×10^5	0.28
19	20	1.3×10^9	1.3×10^9	1.4×10^5	0.33
20	35	2.4×10^9	3.6×10^9	7.3×10^5	0.22
21	86	2.4×10^9	8.3×10^9	8.0×10^5	0.27
22	10	1.8×10^9	1.2×10^9	2.6×10^5	0.22
23	0	1.4×10^9	6.4×10^5	2.5×10^5	0.21
24	0	1.7×10^9	8.2×10^5	3.2×10^5	0.20
25	17	1.6×10^9	9.8×10^5	1.8×10^5	0.44
26	8	2.2×10^9	5.2×10^5	—	0.30

Results and Discussion

The results of the experiments are shown in Table II and Figs. 1—5. The following abbreviations are used: T, temperature in °C; G, rigidity modulus in dyn./cm²; λ, logarithmic decrement; T_g, glass transition temperasure; G_g, rigidity modulus at glass transition temperature; G_r, rigidity modulus at 20°C; G_h, high temperature rigidity modulus or the minimum rigidity modulus above T_g; λ_{max}, the maximum logarithmic decrement shown at T_g. (T_g was defined as the temperature at which λ reached the maximum)

Characteristic *G-T* Relations of Coating Films of Japanese Lac.—All kinds of coating films formed from synthetic resins show glass transition phenomena. Not to mention the films of thermoplastic resins[9], those of cross-linked polymers, such as epoxy[10], alkyd[11] and phenolic resin varnish[12] change markedly in physical and mechanical properties as the temperature changes through T_g, over a relatively narrow temperature range. Below T_g they are in the glassy state, being rigid and a little brittle, and values of G are about 10^{10} dyn./cm². Above T_g they are in the rubbery state, being soft and flexible, and values of G range between 10^7 and 10^8 dyn./cm², so they lack in mechanical strength. The abrupt change in properties depending upon temperature is undesirable for practical use and, therefore, each kind of coating film can be used in a limited range of temperature.

But it is revealed by the authors' experiment that the coating films of Japanese lac were quite different from and superior to those from usual synthetic resins in their properties.

As shown in Fig. 1, in temperature range around T_g, temperature dependence of G of air-dried and baked films of *kiurushi* and *sugurome-urushi* was less than that of Samples Nos. 25 and 26, which were air-dried films of oil varnishes of *o*-cresol resins presented as examples of phenolic resin. G of Japanese lac films changed so mildly with temperature from lower to higher temperature ranges, as T_g could not be determined distinctly from *G-T* curve. T_g was determined from the λ-*T* relation and the λ-*T* curve, too, was smooth compared with that of the synthetic resin film.

At room temperature, three coating films, except the baked film of *kiurushi*, had ample flexibility in spite of their great rigidity modulus, compared with synthetic resin films.

9) Y. Inoue, *J. Chem. Soc. Japan, Ind. Chem. Sec.* (*Kogyo Kagaku Zasshi*), **63**, 1427 (1960).
10) K. Ueki, ibid., **64**, 1425 (1951).
11) L. W. Chen, unpublished.
12) J. Kumanotani, unpublished.

Among them the air-dried film of *sugurome-urushi* was the most rigid but as flexible as samples Nos. 25 and 26, which were in the rubbery state and had smaller values of G_r. Values of G_h of Japanese lac films were, generally, larger than those of synthetic resin films, in which case it was reported that films with G_h greater than 10^9 dyn./cm^2 were insufficient in flexibility[13]. These data of mechanical properties of Japanese lac films showed that the films had an excellent tolerance to temperature change and good adaptability as protective coating films over a wide temperature range.

By G-T and λ-T relations, G_h and T_g, we are able to know the deformation behavior of a polymer substance when loaded by mechanical force, and assume the internal polymeric structure of the polymers. T_g increases with the increase of intermolecular forces caused by the polar group, and of the density of the cross-link of polymer molecules. This is because T_g shows the temperature at which thermal energy becomes sufficient to allow segments of polymers to move beyond energy barriers of environments. G_h increases with increase of density of cross-link, the deformation of polymer substance being restricted only by cross-links of molecules at the temperatures enough above T_g.

Japanese lac films are cross linked polymers formed by oxidation-polymerization of urushiol, activated with laccase or heat. The cross-linking points are catechol nucleus and double bonds of side chains of urushiol molecules. Therefore the films are considered to have some complicated three dimensional structure. In case of air-drying, the action of laccase contributes to the formation of this characteristic structure. The films are in transitional state, some parts being in the glassy state and the others in the rubbery state over a wide range of temperature and they do not show sharp glass transition. Also the rubber parts increase with the rise of temperature, G and λ changing smoothly.

The ideal combination of rigidity and flexibility of the films is also considered to be owing to the characteristic polymer structure of polymerized urushiol with rigid benzene ring and flexible long side chain.

The large values of G_h of Japanese lac films suggested high density of cross-link, but it must be noted that the density of cross-link at high temperature was higher than that at room temperature, because thermal cross-linking reaction took place during the measurement up to the temperature at which G_h was given. This fact was pointed out from comparison of T_g and G_h between Samples No. 8 and No. 9, and between No. 11 and No. 12. And it may be mentioned that the increase of G with temperature above the temperature at which G_h was given was due to both entropy elasticity effect and the increasing density of cross-link.

The above mentioned two characteristics in physical properties of Japanese lac films (1. They do not show sharp glass transition phenomenon. 2. They have ideally combined flexibility and rigidity.) are unique to them.

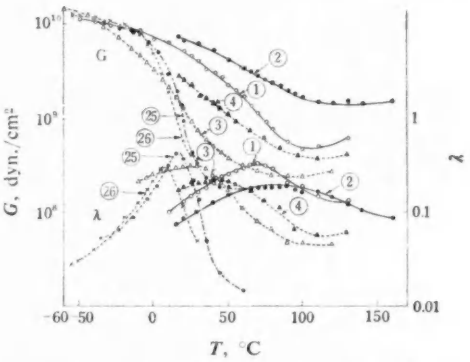

Fig. 1. Rigidity modulus-temperature relations.

① Air-dried film of kiurushi
② Baked film of kiurushi
③ Air-dried film of sugurome urushi
④ Baked film of sugurome urushi
㉕ Air-dried film of oil varnish of reactive *o*-cresol resin
㉖ Air-dried film of oil varnish of nonreactive *o*-cresol resin

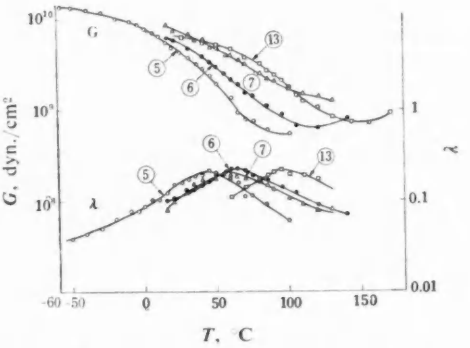

Fig. 2. Rigidity modulus-temperature relations.

⑤ Air-dried film of sugurome urushi
⑥ Tested strip of ⑤, heated at 100°C for 2 hr. after measurement
⑦ Sample ⑤, kept in air for 25 days
⑬ Sample ⑤, kept in air for 30 months

13) Y. Inoue, "Kōgyōkagaku Zensho", Vol. 30, Nikkan Kogyo Shimbunsha, Tokyo (1960), p. 120.

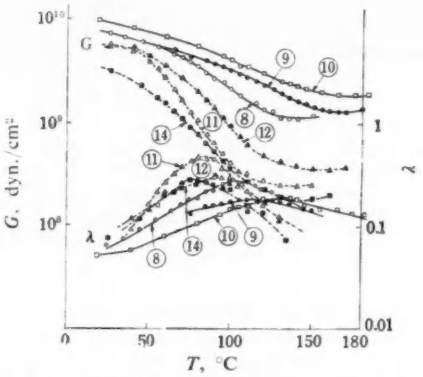

Fig. 3 Rigidity modulus-temperature relations.

⑧ Sample ①, kept in air for 30 months
⑨ Tested strip of ⑧, kept in air overnight after measurement
⑩ Sample ②, kept in air for 30 months
⑪ Sample ③, kept in air for 30 months
⑫ Tested strip of ⑪, kept in air overnight after measurement
⑭ Air-dried film of thailand-sugurome urushi, kept in air for 30 months

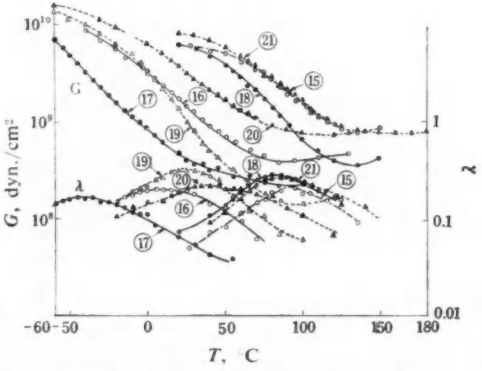

Fig. 4 Rigidity modulus-temperature relations.

⑮ Air-dried film of sugurome processed mixture of kiurushi and distilled urushiol (1 : 1 part), kept in air for 7 months
⑯ Air-dried film of sugurome processed mixture of kiurushi (10 parts) and linseed oil (3 parts)
⑰ Air-dried film of sugurome processed mixture of kiurushi (10 parts) and linseed oil (6 parts)
⑱ Sample ⑯, kept in air for 30 months
⑲ Air-dried film of sugurome processed mixture of kiurushi (10 parts), linseed oil (2 parts) and ester gum (1 part)
⑳ Baked film of sugurome processed mixture of kiurushi (10 parts), linseed oil (2 parts) and ester gum (1 part)
㉑ Sample ⑳, kept in air for 30 months

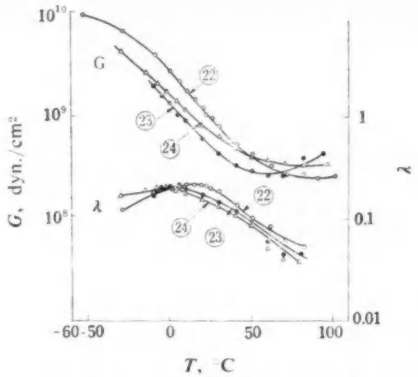

Fig. 5 Rigidity modulus-temperature relations.

㉒ Air-dried film of sugurome processed mixture of kiurushi (10 parts) and catechol derivative A (6 parts)
㉓ Air-dried film of sugurome processed mixture of kiurushi (10 parts) and catechol derivative B (6 parts)
㉔ Air-dried film of sugurome processed mixture of kiurushi (10 parts) and catechol derivative C (6 parts)

The films from synthetic Japanese lac may be necessary to be characterized by these points in order to exceed films from other synthetic resins. These characteristics were retained in Samples Nos. 5—21, which are used in practice as Japanese lac films.

Effect of *Sugurome-process* on Physical and Chemical Properties of Coating Films.— Coating films from *sugurome-urushi* (Samples Nos. 3, 4, 5, 11, 13) were more fiexible and had lower values of T_g, G_r and G_h than films from *kiurushi* (Samples Nos. 1, 2, 8 and 10). The differences in those physical properties were remarkable between them either in case of air-dried films (between No. 1 and No. 3) or baked (between No. 2 and No. 4), or after they were kept in air for 30 months (between No. 8 and No. 11). T_g of baked film from *kiurushi* was valued at 85°C and it lacked in flexibility at room temperature. The cause of the difference is not clear but it may be due to the characteristic unit of polymerization induced by laccase-oxygen(air)-polymerization. Further investigation is needed about the chemical change during the *sugurome-process*. But this traditinal process proved to be very advantageous in preparing qualified coating material of Japanese lac to form air-dried film with a large value of G_r and ample flexibility (Sample No. 3).

Sample No. 5 was also air-dried film of *sugurome-urushi*, but it differed from Sample

No. 3 in physical properties, because the lot of *kiurushi* and conditions of *sugurome-process* and drying process were respective for each. The properties of Sample No. 5 lay between those of Sample No. 1 (from *kiurushi*) and No. 3, and this relationship was retained after time elapsed (Samples Nos. 8, 11 and 13). The quality of Japanese lac may be modified to various extents by changing the condition of the *sugurome-process*.

Effect of Fillers. Linseed oil is used today commonly as a filler for Japanese lac. A mixture of *kiurushi* and linseed oil is *sugurome-processed* and commercialized. Sample No. 16 which was air-dried film of *sugurome-processed* mixture of *kiurushi* (10 parts) and linseed oil (3 parts), had a lower value of T_g, about the same value of G_r and a higher value of G_h than Sample No. 3 (from *sugurome-urushi*). No considerable difference was found between *G-T* curves of the two (Figs. 1 and 4), and they were almost identical in mechanical properties. The decrease of T_g was due to the decrease of intermolecular force caused by the addition of the drying oil, and the increase of G_h was due to the increase of cross-link density induced by the reaction of the double bonds.

But in the case of Sample No. 17 (*kiurushi* 10 parts, linseed oil 6 parts), T_g was much depressed to -45°C and values of G_r and G_h also depressed. At high temperatures the oil oozed out of the film. The small values of λ_{max} of these samples were due to their plasticity. Those facts indicate that if a large amount of linseed oil is added to Japanese lac, its plasticizing effect deteriorates the physical properties of the film.

Sugurome-processed mixture of *kiurushi*, linseed oil and ester gum is called "*shuai-urushi*" and is of general use. Owing to the polar group and polycondensed ring of ester gum, the T_g of air-dried film of *shuai-urushi* (sample No. 19) was rather high but the small value of G_h indicated the small density of cross-link. In baked film (Sample No. 20) values of G_r and G_h were greater than those of baked film from *sugurome-urushi*.

Sample No. 15 was air-dried film from *sugurome processed* mixture of 10 parts of *kiurushi* and 10 parts of urushiol isolated by molecular distillation of alcohol extract from kiurushi, and kept in air for 7 months. The content of laccase of the mixture equalled a half of that of No. 3 (*sugurome-urushi*). The film had a strong esthetic appeal and excellent flexibility, and what is more, values of T_g, G_r and G_h were higher than those of Sample No. 11 (Sample No. 3, kept in air for 30 months). Contrary to the case of linseed oil, laccase acted on urushiol very effectively, and it is concluded that if any compound similar to urushiol is obtained, a great amount can be added to Japanese lac.

The principal component of Thailand lac is not urushiol but thithiol, a mixture of 4-heptadecenylcatechols with 1.5~2 double bonds in average. It contains laccase but the content is less than in Japanese lac, and 4-substituted catechol seems to be inferior to 3-substituted catechol in chemical reactivity. Therefore its film formation takes a long time and it is used as a filler for Japanese lac. Sample No. 14 was air-dried film of *sugurome-processed* Thailand lac, kept in air for 30 months. The film was bad in its physical properties and color. Compared with No. 11 (*sugurome-urushi* of Japanese lac), values of T_g, G_r and G_h were lower, showing low density of cross-link.

Effect of Heat and Exposure to Air. There are two ways of drying, namely, air-drying and baking. In most cases *sugurome-urushi* is air-dried on articles. Samples Nos. 2, 4 and 20 were baked films of *kiurushi*, *sugurome-urushi* and *shuai-urushi* respectively. Compared with Samples Nos. 1, 3 and 19 (air-dried films), baked films had higher values of T_g, G_r and G_h, lower value of λ_{max} and were less flexible and less glossy than the corresponding air-dried films. These differences in properties between them were also found in the case of No. 8 and No. 10 (after 30 months). The reaction mechanism in film formation is considered to be respective for each drying process.

Samples Nos. 1, 2, 3, 5, 16 and 20 were kept in air for 30 months to investigate changes in physical and chemical properties with time. They were Samples Nos. 8, 10, 11, 13, 18 and 21 respectively. As shown in Table II, changes of values of T_g and G_r for each were as follows:

Sample	T_g, °C	$G_r \times 10^{-9}$, dyn. cm^2
Air-dried film of kiurushi	70→100	5.2→7.7
Baked film of kiurushi	85→130	7.1→9.7
Air-dried film of sugurome-urushi (No. 3)	30→ 83	1.2→5.4
Air-dried film of sugurome-urushi (No. 5)	45→ 95	5.0→6.8
Air-dried film of sugurome-processed mixture of kiurushi (10 parts) and linseed oil (3 parts)	10→ 81	1.4→6.2
Air-dried film of shuai-urushi	35→ 86	3.6→8.3

But concerning the values of G_h of these samples, they were almost unchanged except in the case of air-dried film of *kiurushi* whose G_h changed from 4.8×10^8 to 1.1×10^9 dyn./cm^2.

These facts indicated that the films were oxidized in air, polar groups being formed in polymer molecules. On account of the increase of intermolecular forces caused by the polar groups, the films became rigid at room temperature and values of T_g rose. However, cross-liking did not take place during the exposure except in air-dried film of *kiurushi*. This phenomenon may be associated with the effect of heating or sugurome-process when the film was formed.

Even in the films kept in air for 30 months, thermal cross-linking occurred during the measurement up to 150°C, and as shown in Fig. 3, values of T_g, G_r and G_h increaed. (No. 8→No.9, No. 11→No. 12)

Evaluation of Synthetic Catechol Derivatives as Fillers.—As reported in another paper[6], the authors synthesized a series of catechol derivatives for the purpose of obtaining good fillers for Japanese lac. From them the next three compounds were chosen;

A. Ester of homoprotocatechuic acid and linseed oil alcohol
B. Glyceride prepared from 1 mol. of protocatechuic acid, 2 mol. of linseed oil fatty acid and 1 mol. of glycerine.
C. Allyl ester of addition product of catechol and linseed oil fatty acid.

Mixtures of 10 parts of *kiurushi* and 6 parts of catechol derivatives were *sugurome-processed*, and air-dried films shown in Table I were formed, namely, Samples Nos. 22, 23 and 24 respectively. Velocity of the drying was not slow.

Physical data of these samples mesured by the torsional pendulum method are given in Table II and Fig. 5.

Values of T_g of these samples ranged from 0~10°C, closing that of Sample No. 16 (*kiurushi* 10 parts and linseed oil 3 parts) and far above that of No. 17 (*kiurushi* 10 parts and linseed oil 6 parts, T_g; −45°C). Therefore it was evidently approved that these catechol derivatives were much more advantageous than linseed oil as fillers for Japanese lac. Especially the $G-T$ curve of Sample No. 22 was almost identical with that of Sample No. 3 (*sugurome-urushi*). It is considered that catechol derivative A polymerizes together with urushiol under the action of laccase, to form a film almost identical with the film of pure Japanese lac in physical properties.

Summary

As to Japanese lac some reports are found in literature concerning chemical identification of the lac component, or electrical insulation and resistance of the film to chemical reagents, but no physical and chemical properties related to internal polymer structure of the film had ever been investigated. In this paper the authors studied the physical and chemical properties of the film of Japanese lac by means of the torsional pendulum method.

As the results of the experiment, the following characteristics of the films prepared by various processes from Japanese lac were revealed:

1. The films do not show sharp glass transition phenomenon and are durable as a protective coating over a wide range of temperature.
2. The films from *sugurome-processed* Japanese lac have ample flexibility and considerable rigidity, ideally combined.
3. During exposure to air, the films are oxidized with formation of polar group in polymer molecules. But cross-linking does not take place except in air-dried film of raw Japanese lac.

The above mentioned physical and chemical properties of the film account for the characteristic, complicated three dimensional polymer structure caused by action of laccase and chemical structure of urushiol, and such excellent properties can not be found in any other films from synthetic resins. The results obtained are of practical use and they should be taken into consideration in the study of preparation of fillers or substitutes for Japanese lac.

Catechol derivatives synthesized by the authors were confirmed to be fairly good fillers.

The authors wish to thank Professor Y. Inoue of the Tokyo Institute of Technology for his valuable advice. They are also indebted to the Saitō Shōten, Ltd. for the preparation of the sample films.

Department of Applied Chemistry
Faculty of Engineering
The University of Tokyo
Hongo, Tokyo

Non-Empirical Calculation of the π-Electronic Structure of Cyclobutadiene Molecule by Valence Bond Method

By Shozaburo TAKEKIYO

(Received October 21, 1960)

Non-empirical calculation of the energy levels of the cyclobutadiene molecule was first made by Craig[1] from the point of view of molecular orbital method and later a calculation by valence bond method was performed, by McWeeny[2-4] using orthogonalized atomic orbitals[5].

In the calculation by Craig a complete basis of antisymmetric molecular orbital configurations was taken into considerations and, on the other hand, in the working of McWeeny a complete set of canonical structures was included. Energy levels in both of the methods, therefore, should arrive at a complete agreement theoretically*. But it was pointed out by Shida and Kuri[6] that the numerical value 11.1289 eV. of molecular integral γ_{22} in the paper of Craig should be corrected to 10.5586 eV. The difference between these two values may have some effects on the energy levels.

In this paper, therefore, the calculation of the π-electronic energy levels and the wave functions of the molecule is made by valence bond method, including the complete set of canonical structures and considering all kinds of overlap, single exchange, and multiple exchange integrals. The results are compared with those due to ASMO CI calculation.

Calculations are also made in the way of the orthogonalization of atomic orbitals, and Slater functions, and thus the magnitude of the ionic character of the molecule is found. The results are discussed in comparison with those due to the non-orthogonal orbitals.

Calculation

Cyclobutadiene was assumed to be a square molecule in which the bond distance between two neighboring carbon atoms is 1.40 Å. Slater $2p_\pi$-orbitals were used for the atomic orbitals of the four carbon atoms, with the screening constant $Z_C = 3.18$. π-Electron repulsive integrals were taken from Craig[1] and penetration and core integrals were calculated directly by the present author according to the method of Parr and Mulliken[7]. The canonical structures and the corresponding energies are shown in Fig. 1.

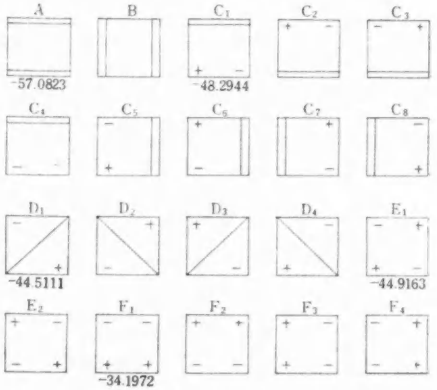

Fig. 1. Canonical structures and the energy values for the structures. (Energies are in electron volts and are relative to $4W_{2p}$, where W_{2p} is the energy of a $2p_\pi$-electron of a carbon atom in its valence state.)

Bases Ψ_i's for irreducible representations of the group, to which the molecule belongs, are given in Table I, where N_i is the normalization constant and Ψ_K is the normalized bond eigenfunction for structure K.

In our approximation the Hamiltonian operator H is expressed in the form

$$H = \sum_i H_{\text{core}}(i) + (1/2)\sum_{\substack{i,\ j \\ i \neq j}} (e^2/r_{ij})$$

where

$$H_{\text{core}}(i) = T(i) + U_{\text{core}}(i)$$

$T(i)$ is the kinetic energy operator for electron i and $U_{\text{core}}(i)$ is the potential energy operator for this electron in the field of the core.

Calculated wave functions Φ_i's for the molecule and the corresponding energy values E_i's

1) D. P. Craig, *Proc. Roy. Soc.*, **A202**, 498 (1950).
2) R. McWeeny, ibid., **A223**, 63 (1954).
3) R. McWeeny, ibid., **A223**, 306 (1954).
4) R. McWeeny, ibid., **A227**, 288 (1955).
5) P.-O. Löwdin, *J. Chem. Phys.*, **18**, 365 (1951); P.-O. Löwdin, ibid., **21**, 496 (1953).
* Agreement of the results in both of the methods has been reported by McWeeny[4].
6) S. Shida and Z. Kuri, *J. Chem. Soc. Japan, Pure Chem. Soc.* (*Nippon Kagaku Zasshi*), **76**, 322 (1955).
7) R. G. Parr and R. S. Mulliken, *J. Chem. Phys.*, **18**, 1338 (1950).

TABLE I. RELATIONS BETWEEN BOND EIGENFUNCTIONS AND BASES

$$
\begin{aligned}
&\Psi_1 = (1/N_1)(\Psi_A + \Psi_B)\\
&\Psi_2 = (1/N_2)(\Psi_{C1} + \Psi_{C2} + \Psi_{C3} + \Psi_{C4} + \Psi_{C5} + \Psi_{C6} + \Psi_{C7} + \Psi_{C8})\\
{}^1A_{1g}\quad &\Psi_3 = (1/N_3)(\Psi_{D1} + \Psi_{D2} + \Psi_{D3} + \Psi_{D4})\\
&\Psi_4 = (1/N_4)(\Psi_{E1} + \Psi_{E2})\\
&\Psi_5 = (1/N_5)(\Psi_{F1} + \Psi_{F2} + \Psi_{F3} + \Psi_{F4})
\end{aligned}
$$

$$
{}^1B_{1g}\quad \begin{cases}
\Psi_6 = (1/N_6)(\Psi_{C1} - \Psi_{C2} + \Psi_{C3} - \Psi_{C4} + \Psi_{C5} - \Psi_{C6} + \Psi_{C7} - \Psi_{C8})\\
\Psi_7 = (1/N_7)(\Psi_{D1} - \Psi_{D2} + \Psi_{D3} - \Psi_{D4})\\
\Psi_8 = (1/N_8)(\Psi_{E1} - \Psi_{E2})
\end{cases}
$$

$$
{}^1B_{2g}\quad \begin{cases}
\Psi_9 = (1/N_9)(\Psi_A - \Psi_B)\\
\Psi_{10} = (1/N_{10})(\Psi_{C1} + \Psi_{C2} + \Psi_{C3} + \Psi_{C4} - \Psi_{C5} - \Psi_{C6} - \Psi_{C7} - \Psi_{C8})\\
\Psi_{11} = (1/N_{11})(\Psi_{F1} + \Psi_{F2} - \Psi_{F3} - \Psi_{F4})
\end{cases}
$$

TABLE II. WAVE FUNCTIONS FOR THE MOLECULE AND THE CORRESPONDING ENERGY VALUES

Based on non-orthogonal atomic orbitals

$$
\begin{aligned}
&\Phi_1({}^1B_{2g}) = 0.80023\Psi_9 + 0.26085\Psi_{10} - 0.01111\Psi_{11} && E_1 = 4W_{2p} - 58.3517\ \text{eV}.\\
&\Phi_2({}^1A_{1g}) = 0.75393\Psi_1 + 0.32697\Psi_2 - 0.11784\Psi_3 + 0.09264\Psi_4 - 0.00386\Psi_5 && E_2 = 4W_{2p} - 56.3627\ \text{eV}.\\
&\Phi_3({}^1B_{1g}) = 0.68396\Psi_6 + 0.24527\Psi_7 + 0.21925\Psi_8 && E_3 = 4W_{2p} - 52.6519\ \text{eV}.
\end{aligned}
$$

Based on orthogonalized atomic orbitals

$$
\begin{aligned}
&\bar{\Phi}_1({}^1B_{2g}) = 0.82284\bar{\Psi}_9 + 0.55729\bar{\Psi}_{10} - 0.11117\bar{\Psi}_{11} && \bar{E}_1 = 4\bar{\alpha} + 41.8774\ \text{eV}.\\
&\bar{\Phi}_2({}^1A_{1g}) = 0.78562\bar{\Psi}_1 + 0.55233\bar{\Psi}_2 - 0.01629\bar{\Psi}_3 + 0.25304\bar{\Psi}_4 + 0.11591\bar{\Psi}_5 && \bar{E}_2 = 4\bar{\alpha} + 44.0248\ \text{eV}.\\
&\bar{\Phi}_3({}^1B_{1g}) = 0.75721\bar{\Psi}_6 + 0.49877\bar{\Psi}_7 + 0.42174\bar{\Psi}_8 && \bar{E}_3 = 4\bar{\alpha} + 46.9387\ \text{eV}.
\end{aligned}
$$

are given in Table II. In the table, $\bar{\Phi}_i$'s are the wave functions for the molecule, obtained in the way of the orthogonalization of the atomic orbitals, $\bar{E}_i$'s are the corresponding energy values, and $\bar{\alpha}$ is as follows:

$$\bar{\alpha} = \int \bar{k}(i) H_{\text{core}}(i) \bar{k}(i) \mathrm{d}v_i$$

where $\bar{k}(i)$ is the orthogonalized expression of atomic orbital $k(i)$ of electron i on atom k and $\mathrm{d}v_i$ is the volume element of this electron.

Ionic Character

Now, ionic characters, evaluated on the basis of non-orthogonal atomic orbitals are generally different from the values, obtained in their orthogonalized representation[5],*1.

Probabilities P_K's of structure K's in both of the ground ${}^1B_{2g}$ state and the first excited ${}^1A_{1g}$ state were calculated from the following expression and the results are shown in Table III.

$$P_K = C_K \sum_L C_L \int \Psi_K \Psi_L \, \mathrm{d}\tau$$

where C_K is the coefficient of normalized bond eigenfunction Ψ_K in $\Phi_1({}^1B_{2g})$ or $\Phi_2({}^1A_{1g})$ and $\mathrm{d}\tau$ is the product of the volume element for all the π-electrons.

*1 It does not appear that considerations of such discrepancies for π-electronic systems have been made.

TABLE III. PROBABILITIES OF STRUCTURES

Based on non-orthogonal atomic orbitals

$A=B$	C_i	D_i	E_i	F_i
Ground ${}^1B_{2g}$-state				
0.3924	0.0265	0.0008	0	0
First excite ${}^1A_{1g}$-state				
0.3503	0.0300	0.0054	0.0194	−0.0002

Based on orthogonalized atomic orbital

$A=B$	C_i	D_i	E_i	F_i
Ground ${}^1B_{2g}$-states				
0.3385	0.0388	0.00309	0	0
First excited ${}^1A_{1g}$-state				
0.3086	0.0381	0.0001	0.0320	0.0034

From these results, ionic characters are

$$
\begin{aligned}
{}^1B_{2g}\ \text{state} &\begin{cases} 21.517\% & \text{based on } k(i)\\ 32.293\% & \text{based on } \bar{k}(i)\end{cases}\\
{}^1A_{1g}\ \text{state} &\begin{cases} 29.946\% & \text{based on } k(i)\\ 38.280\% & \text{based on } \bar{k}(i)\end{cases}
\end{aligned}
$$

In the ${}^1B_{2g}$ and ${}^1A_{1g}$ states the ionic characters based on $\bar{k}(i)$ are larger than on $k(i)$ by 10.776% and 8.334%, respectively.

Bond orders B_{ij}'s between neighboring two carbon atoms i and j were evaluated by formula

$$B_{ij} = \sum_K P_K (n_{ij}^K + 1)$$

where n_{ij}^K is the number of the π-electronic

covalent bonds between carbon atoms i and j in structure K. The results are

$^1B_{1g}$ state $\begin{cases} 1.445 & \text{based on } k(i) \\ 1.416 & \text{based on } k(i) \end{cases}$

$^1A_{1g}$ state $\begin{cases} 1.410 & \text{based on } k(i) \\ 1.385 & \text{based on } k(i) \end{cases}$

Double bond characters based on $k(i)$ are larger by 2.92% and 2.52% than these based on $\bar{k}(i)$ the $^1B_{1g}$ and $^1A_{1g}$ states, respectively.

Discussion

Energy levels of the molecule, calculated by various methods, are shown diagrammatically in Fig. 2.

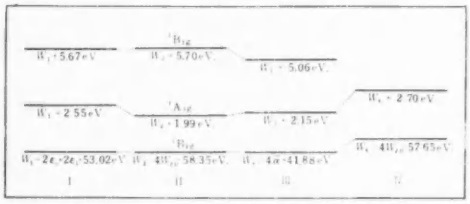

Fig. 2. Comparison of energy levels.

I. ASMOCI method[1]. II. VB method (based on non-orthogonal atomic orbitals). III. VB method (based on orthogonalized atomic orbitals). IV. Heitler-London method.

The $^1A_{1g}$ level evaluated by the present author (II) is lower by 0.56 eV. relatively than that of Craig. But influences of the difference in the values of the molecular integral on the other levels hardly appear at all[*2].

One of the causes for the discrepancies of the ionic characters in the two ways is that, in the cases of the use of the orthogonalized atomic orbitals, exchange integrals which appear in the interactions of covalent structures give generally repulsive forces.

Actually, in the case of an exchange integral J,

$$J = \int\cdots\cdots\bar{a}(1)b(2)\bar{c}(3)\bar{d}(4)\cdots\cdots H \cdots\cdots\bar{a}(1)\bar{c}(2)b(3)\bar{d}(4)\cdots\cdots d\tau$$

is expanded as follows and J is, therefore, equal to $(\bar{b}\bar{c}|\bar{b}\bar{c})$.

$$J = \sum_{\substack{k \\ k\neq b,\ c}} \bar{\alpha}_k S_{bc}^2 + 2\bar{\beta}_{bc}\bar{S}_{bc} + (1/2)\sum_{\substack{k,\ l \\ k\neq b,\ c \\ l\neq b,\ c,\ k}} (\bar{k}\bar{k}|\bar{l}\bar{l})\bar{S}_{bc}^2 + 2\sum_{\substack{k \\ k\neq b,\ c}} (\bar{k}\bar{k}|\bar{b}\bar{c})\bar{S}_{bc} + (\bar{b}\bar{c}|\bar{b}\bar{c})$$

where

$$\bar{\alpha}_k = \int k(i)H_{\mathrm{core}}(i)\bar{k}(i)dv_i^{*3}$$

$$\bar{\beta}_{kl} = \int k(i)H_{\mathrm{core}}(i)\bar{l}(i)dv_i$$

$$\bar{S}_{kl} = \int k(i)\bar{l}(i)dv_i$$

$$(\bar{k}\bar{l}|\bar{p}\bar{q}) = e^2\int(1/r_{ij})\bar{k}(i)\bar{l}(i)\bar{p}(j)\bar{q}(j)dv_i\,dv_j$$

From similar analyses multiple exchange integrals lead to zeros. In the use of the orthogonalized atomic orbitals, therefore, the weight of the covalent structures appears generally smaller than in the use of the non-orthogonal orbitals.

Accordingly, when π-electron densities or bond orders etc. are considered as the measure of chemical reactivities, it will be necessary for attention to be given to the discrepancies of these values in the two ways.

Summary

π-Electronic energy levels, probalities of the resonance structures, and bond orders of cyclobutdiene molecule have been calculated by the valence bond method on the bases of two ways, one is based on non-orthogonal atomic orbitals and the other on their orthogonalization. Calculated ionic characters are 21.517% (ground $^1B_{1g}$ state), 29.946% (first excited $^1A_{1g}$ state) in the former and 32.293%, 38.280% in the latter. Bond orders between neighboring carbon atoms are 1.445, 1.410 and 1.416, 1.385 respectively.

The author wishes to express his hearty thanks to Professor Kyosuke Omori, Kyushu University, for his kind guidance and encouragement throughout this study.

Thanks are also due to Professor Saburo Nagakura, the University of Tokyo, for his valuable advice.

Faculty of Liberal Arts
Nagasaki University
Ohashi, Nagasaki

*2 Relative differences of levels between II and III in Fig. 2 seem to be due to the approximate orthogonalization of atomic orbitals[4,5].

*3 Since atoms except carbon are generally included in π-electronic system, α_k is here to be distinguished from α in the previous paragraph.

Statistical Thermodynamics of Solutions of Optically Active Substances. I. Excess Free Energy of Binary Solution of d- and l-Isomers

By Kazuo AMAYA

(Received March 1, 1961)

In recent years considerable progress has been made in the field of the theory of solutions and the fundamental features of various types of binary solutions such as polymer solutions, and associated solutions, etc. were explained theoretically. However, there seem to be no papers which treat the problem of of the solutions containing optical isomers. In this paper the idea of interaction of surface points in groups will be introduced to elucidate the fundamental features of the solution consisting of optical isomers.

The Model of the Solutions of Optical Isomers

In the statistical mechanical lattice theory of solutions of anisotropic molecules, the model usually adopted is that the surface of the molecule is cevided into a definite number of contact points and each contact point is grouped into an energetically equivalent element and the number of contact points belonging to each group has a definite value. The configurational energy of the system is a sum of interaction energies of the pairs of each contact point. In such a model, however, the mutual configuration of different kinds of elements in one and the same molecule is not taken into account.

According to the above model, the molecules of *d*- and *l*-optical isomers have the same number of contact points of the same kind of elements, so that these two kinds of molecules cannot be distinguished. In order to distinguish one isomer from the other, mutual configuration of contact points of different kinds in one and the same molecule must be introduced into the above model, and at least three contact points of different kinds of elements must interact in groups at a time.

To meet the above requirement the following model is proposed.

(1) The molecule is a regular polyhedron composed of z planes of which one consists of *a*-element and the remaining $z-1$ ones are consist of *b*-elements, and further, the *a*-element is composed of three sub-elements 1, 2, 3, the arrangement of these three elements, viewed toward the plane from the outside of the molecule along the direction normal to it, is in the order, 1, 2, 3 clockwise for *d*-isomers and 1, 3, 2 for *l*-isomers, the mirror image of *d*-isomers.

(2) Each molecule occupies one site of the quasi-crystalline lattice of z nearest neighbors, and the molecular axis which passes the center of the molecule and the *a*-plane composed of *a*-element can take z directions. When the direction is specified, it can take 3 further different arrangements by the rotation around the axis and thus the molecule at one site can have $3z$ orientational freedom in all*.

(3) The molecules contact with plane to plane and the total configurational energy of the system is the sum of the interaction energy of pairs of planes, the kind of pair of planes is $a-a$, $a-b$ and $b-b$ and the $a-a$ pair contains 6 kinds of sub pairs, 11, 22, 33, 12, 13 and 23 and ab pair 3 kinds of sub pairs, $b1$, $b2$ and $b3$. If *a*-elements of *l*-isomers and *d*-isomers are denoted by a_l and a_d respectively, the a_l-a_l pair can take 3 configurations $\begin{pmatrix}1&2&3\\1&3&2\end{pmatrix}$, $\begin{pmatrix}1&2&3\\2&1&3\end{pmatrix}$ and $\begin{pmatrix}1&2&3\\3&2&1\end{pmatrix}$ with interaction energy $\omega_{11}+2\omega_{23}$, $2\omega_{12}+\omega_{33}$ and $2\omega_{13}+\omega_{22}$ respectively, where ω_{ij} denotes the interaction energy of a pair of i and j element.

For a_d-a_d pair the same value of interaction energy is obtained for each configuration. For a_l-a_d pair, three configurations are represeted $\begin{pmatrix}1&2&3\\1&2&3\end{pmatrix}$, $\begin{pmatrix}1&2&3\\3&1&2\end{pmatrix}$ and $\begin{pmatrix}1&2&3\\2&3&1\end{pmatrix}$ with interaction energy $\omega_{11}+\omega_{22}+\omega_{33}$, $\omega_{12}+\omega_{13}+\omega_{23}$ and $\omega_{12}+\omega_{13}+\omega_{23}$ respectively, can take place.

$\begin{pmatrix}1&2&3\\1&2&3\end{pmatrix}$ means the configuration in which sub elements 1, 2 and 3 of a_d plane of *d*-isomers interact with sub element of 1, 2 and 3 of a_l plane of *l*-isomers forming sub pairs 11, 22 and 33. Generally, distinguishable pairs are obtained by cycling the lower row of numbers without permutation.

The Configurational Partition Function and the Excess Free Energy

Using the above model, the configurational partition functions and the excess free energy

* Strictly speaking the regular polyhedron must have a symmetry of C_{3h} around all of z axes passing through the center of the molecule and that of each of z planes.

of the binary system of *d*- and *l*-optical isomers were derived based on the method of expansion of Kirkwood[1].

Generally configurational partition function Ω is, by definition, expressed as

$$\Omega = \sum e^{-E/kT} \tag{1}$$

where E denotes the potential energy of a system for a particular configuration and summation is carried out over all configurations.

For the system of pure *l*-isomers, its configurational partition function Ω_l is represented

$$\Omega_l = \sum e^{-E_l/kT} = e^{-\bar{E}_l/kT}\left(\sum e^{-(E_l-\bar{E}_l)/kT}\right) = e^{-\bar{E}_l/kT}\left(\sum e^{-W_l/kT}\right) \tag{2}$$

where E_l denotes the potential energy of the system of pure *l*-isomers and $\bar{E}_l$ denotes the unweighted average of E_l over all configurations and W_l denotes $E_l-\bar{E}_l$. If g_l denotes the number of distinguishable configurations of the system consisting of N_l molecules of *l*-isomer, then the configurational partition function of the system is expressed, following Kirkwood[1], as

$$\ln \Omega_l - \ln g_l - \frac{N_l\chi_l}{kT} = \sum \ln \frac{1}{g_l} \sum e^{-W_l(N_l)/kT} \tag{3}$$

where $N_l\chi_l = \bar{E}_l$ and g_l according to the above model, is equal to $(3z)^{N_l}$.

By the use of an auxiliary quantity h_l defined by

$$h_l = 1 - \frac{1}{g_l} \sum e^{-W_l(N_l)/kT} \tag{4}$$

Eq. 3 can be rewritten as

$$\ln \Omega_l - N_l \ln 3z - \frac{N_l\chi_l}{kT} = \ln(1-h_l) = -h_l - \frac{1}{2}h_l^2 - \frac{1}{3}h_l^3 - \frac{1}{4}h_l^4 - \cdots\cdots \tag{5}$$

If the h_l in Eq. 4 is expanded in powers of $W_l(N_l)/kT$, the following formula is obtained.

$$h_l = \frac{\langle W_l(N_l)\rangle_{Av.}}{kT} - \frac{\langle W_l^2(N_l)\rangle_{Av.}}{2!\,(kT)} + \frac{\langle W_l^3(N_l)\rangle_{Av.}}{3!\,(kT)^3} - \cdots\cdots \tag{6}$$

where $\langle W_l(N_l)\rangle_{Av.}$ denotes the unweighted average of $W_l(N_l)$ over all configurations, and similarly $\langle W_l^t(N_l)\rangle_{Av.}$ denotes the unweighted average of the t th power of $W_l(N_l)$ over all configurations. Substituting 6 into 5 the following expression is obtained.

$$\ln \Omega_l - N_l \ln 3z - \frac{N_l\chi_l}{kT} = -\frac{\langle W_l(N_l)\rangle_{Av.}}{kT} - \{\langle W_l(N_l)\rangle^2_{Av.} - \langle W_l^2(N_l)\rangle_{Av.}\}/2!\,(kT)^2 - \{\langle W_l^3(N_l)\rangle_{Av.} - 3\langle W_l(N_l)\rangle_{Av.}\langle W_l(N_l)\rangle_{Av.}\}/3!\,(kT)^3 - \{2\langle W_l(N_l)\rangle^3_{Av.}\}/3!\,(kT)^3 - \cdots\cdots \tag{7}$$

As $\bar{E}_l$ is the unweighted average of E_l, it follows that

$$\langle W_l(N_l)\rangle_{Av.} = \overline{(E_l-\bar{E}_l)} = \bar{E}_l - \bar{E}_l = 0 \tag{8}$$

Then Eq. 7 is rewritten as

$$\ln \Omega_l - N_l \ln 3z - \frac{N_l\chi_l}{kT} = \frac{\langle W_l^2(N_l)\rangle_{Av.}}{2!\,(kT)^2} - \frac{\langle W_l^3(N_l)\rangle_{Av.}}{3!\,(kT)^3} - \cdots\cdots \tag{9}$$

Similarly, for the system of N_d *d*-isomers, the following expression is obtained.

$$\ln \Omega_d - N_d \ln 3z - \frac{N_d\chi_d}{kT} = \frac{\langle W_d^2(N_d)\rangle_{Av.}}{2!\,(kT)^2} - \frac{\langle W_d^3(N_d)\rangle_{Av.}}{3!\,(kT)^3} - \cdots\cdots \tag{10}$$

In the following, it will be shown that χ_l is equal to χ_d. As χ_l is the unweighted average of E_l over all configurations, χ_l is proportional to

$$\bar{\omega}_{a_l-a_l} + 2(z-1)\bar{\omega}_{a_l-b} + (z-1)^2\bar{\omega}_{b-b} \tag{11}$$

and similarly χ_d is proportional to

$$\bar{\omega}_{a_d-a_l} + 2(z-1)\bar{\omega}_{a_d-b} + (z-1)^2\bar{\omega}_{b-b} \tag{12}$$

where $-$ denotes the unweighted average and $\omega_{a_l-a_l}$, $\omega_{a_l-a_d}$, ω_{a_l-b}, ω_{a_d-b} and ω_{b-b} denote the interaction energy of a_l-a_l, a_l-a_d, a_l-b, a_d-b and $b-b$ plane pairs respectively.

Further, according to the assumption made above, the following relation is obtained.

$$\bar{\omega}_{a_l-a_l} = \frac{1}{3}\{\omega_{11}+\omega_{22}+\omega_{33}+2(\omega_{12}+\omega_{23}+\omega_{31})\} = \bar{\omega}_{a_d-a_d} \tag{13}$$

Thus each of three different configurations of a_l-a_l a_d-a_d pair of plane have the same interaction energy. Further

$$\bar{\omega}_{a_l-b} = \omega_{1b}+\omega_{2b}+\omega_{3b} = \bar{\omega}_{a_d-b} \tag{14}$$

From 11, 12, 13 and 14, we obtain

$$\chi_l = \chi_d = \chi_0 \tag{15}$$

As is stated above, the interaction energy of the pairs of planes in *l*-isomers $\omega_{a_l-a_l}$, ω_{a_l-b} and ω_{b-b} and in *d*-isomers $\omega_{a_d-a_d}$, ω_{a_d-b} and ω_{b-b} have the same value, and the total energy E is the sum of such interaction energies of pairs of planes. Further for one specified configuration in the system consisting of N_0 molecules of *l*-isomers, with a specified number of pairs of a_l-a_l, a_l-b and $b-b$ plane contacts,

1) J. G. Kirkwood, *J. Chem. Phys.*, **6**, 70 (1938).

there exists the corrsponding configuration in the system contisting of N_0 molecules of *d*-isomers, for, one to one correspondence exists between both isomers.

Then the total configurational energy for one specified configuration for *l*-isomers is equal to that of the corresponding configuration in α-isomers, that is

$$E_l = E_d \tag{16}$$

and hence

$$W_l(N_0) = W_d(N_0) = W_0(N_0) \tag{17}$$

For $d-l$ mixtures consisting of N_l *l*-isomers and N_d *d*-isomers, the configurational partition function Ω_{dl} is expressed as

$$\begin{aligned}\ln \Omega_{dl} = & N \ln 3z - \ln \frac{N!}{(Nx)!\,\{N(1-x)\}!} \\ & - N \cdot \chi_{ld}(x)/\boldsymbol{kT} = -\langle W_{dl}(N,x)\rangle_{Av.}/\boldsymbol{kT} \\ & - \{\langle W_{dl}(N,x)\rangle^2_{Av.} \\ & - \langle W^2_{dl}(N,x)\rangle_{Av.}\}/2!\,(\boldsymbol{kT})^2 \\ & - \{\langle W^3_{dl}(N,x)\rangle_{Av.} - 3\langle W^2_{dl}(N,x)\rangle_{Av.} \\ & \cdot \langle W_{dl}(N,x)\rangle_{Av.}\}/3!\,(\boldsymbol{kT})^3 \\ & - 2\langle W_{dl}(N,x)\rangle^3_{Av.}/3!\,(\boldsymbol{kT})^3 \end{aligned} \tag{18}$$

where $N = N_l + N_d$ and $N \cdot \chi_{dl}(x)$ is the unweighted mean of interaction energy of the system and $x = N_l/N$. Since $\chi_{dl}(x)$ is proportional to

$$\begin{aligned} & x^2\{\bar{\omega}_{al-al} + 2(z-1)\bar{\omega}_{al-b} + (z-1)^2\omega_{b-b}\} \\ & + 2(1-x)x\{\omega_{al-ad} + (z-1)(\omega_{al-b} + \omega_{ad-b}) \\ & + (z-1)^2\omega_{b-b}\} + (1-x)^2 \\ & \{\omega_{ad-ad} - 2(z-1)\bar{\omega}_{ad-b} + (z-1)^2\omega_{b-b}\} \end{aligned} \tag{19}$$

$\bar{\omega}_{al-ad}$ is the mean of three interaction energies

$$\omega_{11}+\omega_{22}+\omega_{33},\ \omega_{12}+\omega_{23}+\omega_{31},\ \omega_{12}+\omega_{23}+\omega_{31}$$

Each term differs from that of ω_{al-al} or ω_{ad-ad} but the unweighted mean over these three configurations, becomes the same value as follows:

$$\begin{aligned} \bar{\omega}_{ad-al} &= \frac{1}{3}(\omega_{11}+\omega_{22}+\omega_{33}+\omega_{12}+\omega_{23}+\omega_{31} \\ &\quad +\omega_{12}+\omega_{23}+\omega_{31}) \\ &= \frac{1}{3}\{\omega_{11}+\omega_{22}+\omega_{33}+2(\omega_{12}+\omega_{23}+\omega_{31})\} \\ &= \omega_{al-al} = \omega_{ad-ad} \end{aligned} \tag{20}$$

Hence, from 19, 20, 11 and 12, we have

$$\chi_{dl}(x) = \chi_l = \chi_d = \chi_0 \tag{21}$$

$$\langle W_{dl}(N,x)\rangle_{Av.} = \overline{(E_{dl} - \bar{E}_{dl})} = \bar{E}_{dl} - E_{dl} = 0 \tag{22}$$

For the system consisting of N *d*-isomers or N *l*-isomers, free energy is expressed as

$$\begin{aligned} F_d = F_l &= -\boldsymbol{kT}\ln\Omega_0 = \boldsymbol{NkT}\ln 3z + N\chi_0 \\ &\quad + \frac{\langle W^2_0(N)\rangle_{Av.}}{2!\,(\boldsymbol{kT})} - \frac{\langle W^3_0(N)\rangle_{Av.}}{3!\,(\boldsymbol{kT})^2} + \cdots\cdots \end{aligned} \tag{23}$$

For $d-l$ mixtures consisting of $N_l\,(=Nx)$ molecules of *l*-isomer and $N_d\ (=N(1-x))$ molecules of *d*-isomer, we obtain

$$\begin{aligned} F_{dl} &= -\boldsymbol{kT}\ln\Omega_{dl} = \boldsymbol{NkT}\ln 3z + N\chi_0 \\ &\quad + \boldsymbol{NkT}\{x\ln x + (1-x)\ln(1-x)\} \\ &\quad + \frac{\langle W^2_{dl}(N,x)\rangle_{Av.}}{2(\boldsymbol{kT})} - \frac{\langle W^3_{dl}(N,x)\rangle_{Av.}}{3!\,(\boldsymbol{kT})^2} \\ &\quad + \cdots\cdots \end{aligned} \tag{24}$$

As each configuration has a different energy, that is $W_{dl}(N,x) \neq W_0(N)$, then the free energy of mixing ΔF_m is represented as

$$\begin{aligned} \Delta F_m &= \boldsymbol{NkT}\{x\ln x + (1-x)\ln(1-x)\} \\ &\quad + \frac{1}{2(\boldsymbol{kT})}\{\langle W^2_{dl}(N,x)\rangle_{Av.} - \langle W^2_0(N_l)\rangle_{Av.} \\ &\quad - \langle W^2_0(N_d)\rangle_{Av.}\} - \frac{1}{3!\,(\boldsymbol{kT})^2} \\ &\quad \times\{\langle W^3_{dl}(N,x)\rangle_{Av.} - \langle W^3_0(N_l)\rangle_{Av.} \\ &\quad - \langle W^3_0(N_d)\rangle_{Av.}\} + \cdots\cdots \end{aligned} \tag{25}$$

Then the problem is reduced to a calculation of second and heigher powers of $W_{dl}(N,x)$, $W_0(N_l)$ and $W_0(N_d)$. Now $\langle W^2_0(N_l)\rangle$, $\langle W^2_0(N_d)\rangle$ and $W^2_{dl}(N)$ will be considered.

According to the model mentioned above, potential energy E of the system consisting of N molecules of *l*- or *d*-isomers with the particular configuration having N_{bb} *bb* pairs, N_{ab} *ab* pairs, N_{aa_1} aa_1 pairs, N_{aa_2} aa_2 pairs and N_{aa_3} aa_3 pairs, where aa_1, aa_2 and aa_3 denote three kinds of *aa* contact, is expressed as

$$\begin{aligned} E &= N_{bb}\omega_{bb} + N_{ab}\omega_{ab} + N_{aa_1}\omega^0_{aa_1} + N_{aa_2}\omega^0_{aa_2} \\ &\quad + N_{aa_3}\omega^0_{aa_3} \end{aligned} \tag{26}$$

where $\omega^0_{aa_1}$, $\omega^0_{aa_2}$ and $\omega^0_{aa_3}$ denote those interaction energies corresponding to aa_1, aa_2 and aa_3 pairs respectively and these values are $\omega_{11}+2\omega_{23}$, $\omega_{22}+2\omega_{13}$ and $\omega_{33}+2\omega_{12}$ respectively. Then the average value E becomes

$$\begin{aligned} E &= \bar{N}_{bb}\omega_{bb} + \bar{N}_{ab}\omega_{ab} + \bar{N}_{aa_1}\omega_{aa_1} \\ &\quad + \bar{N}_{aa_2}\omega_{aa_2} + \bar{N}_{aa_3}\omega_{aa_3} \\ &= \frac{1}{2}zN\left\{\frac{(z-1)^2}{z^2}\omega_{bb} + \frac{2(z-1)}{z^2}\omega_{ab}\right. \\ &\quad \left. + \frac{1}{z^2}\cdot\frac{1}{3}(\omega_{aa_1}+\omega_{aa_2}+\omega_{aa_3})\right\} \end{aligned} \tag{27}$$

As $W_0(N)$ means the difference between the

potential energy of the system of particular configuration and that averaged over all configurations, $W_0(N)$ for the particular configuration mentioned above becomes

$$W_0(N)=E-\bar{E}=\left\{N_{bb}-\frac{1}{2}N\frac{(z-1)^2}{z}\right\}\omega_{bb}+\left\{N_{ab}-\frac{N(z-1)}{z}\right\}\omega_{ab}+N_{aa_1}\omega^0_{aa_2}+N_{aa_2}\omega^0_{aa_3}+N_{aa_3}\omega^0_{aa_1}-\frac{1}{6}\frac{N}{z}(\omega^0_{aa_1}+\omega^0_{aa_2}+\omega^0_{aa_3}) \quad (28)$$

In calculating $\langle W_0^2(N)\rangle_{Av.}$, we must strictly take the average over all possible configurations. However, since of all configurations the configurations with $N_{bb}=\bar{N}_{bb}$, $N_{ab}=\bar{N}_{ab}$ and $\sum_{i=1}^{3}N_{aa_i}=N_{aa}$ occupy the predominant part, and the average over these configurations, may differ very little from that over all configurations, we approximately take the former average in place of the latter. Then

$$W_0(N)=\sum_{i=1}^{3}{}'N_{aa_i}\omega^0_{aa_i}-\frac{1}{6}\frac{N}{z}\left(\sum_{i=1}^{3}\omega^0_{aa_i}\right) \quad (29)$$

where $\sum'$ donates the summation under the restriction that $\sum_{i=1}^{3}N_{aa_i}=1/2\cdot N/z$ and $\langle W_0^2(N)\rangle_{Av.}$ becomes

$$\langle W_0^2(N)\rangle=\left(\sum_{i=1}^{3}{}'N_{aa_i}\omega^0_{aa_i}\right)^2-2\sum_{i=1}^{3}{}'N_{aa_i}\omega^0_{aa_i}\times\frac{1}{6}\frac{N}{Z}\left(\sum_{i=1}^{3}\omega^0_{aa_i}\right)+\left(\frac{1}{6}\frac{N}{z}\sum_{i=1}^{3}\omega^0_{aa_i}\right)^2=\left(\sum_{i=1}^{3}{}'N_{aa_i}\omega^0_{aa_i}\right)^2-\left(\frac{1}{6}\frac{N}{z}\sum_{i=1}^{3}\omega^0_{aa_i}\right)^2 \quad (30)$$

As all configurations of *aa* pair can take place with equal probability the first term of 30 becomes

$$\left(\sum_{i=1}^{3}{}'N_{aa_i}\omega^0_{aa_i}\right)^2=\left(\frac{1}{2}\frac{N}{z}\right)^2\int_0^1\int_0^y[\{\omega^0_{aa_1}x+\omega^0_{aa_2}(y-x)\}+\omega^0_{aa_3}(1-y)]^2dxdy=\left(\frac{1}{2}\frac{N}{z}\right)^2\frac{1}{6}(\omega^{0^2}_{aa_1}+\omega^{0^2}_{aa_2}+\omega^{0^2}_{aa_3}+\omega^0_{aa_1}\omega^0_{aa_2}+\omega^0_{aa_2}\omega^0_{aa_3}+\omega^0_{aa}\omega_{aa_1}) \quad (31)$$

Substituting 31 into 30 the following formula is obtained:

$$\langle W_0^2(N)\rangle_{Av}=\left(\frac{1}{2}\frac{N}{z}\right)^2\cdot\frac{1}{36}\{(\omega^0_{aa_1}-\omega^0_{aa_2})^2+(\omega^0_{aa_2}-\omega^0_{aa_3})^2+(\omega^0_{aa_3}-\omega^0_{aa_1})^2\} \quad (32)$$

For the system consisting of N_l molecules of *l*-isomers and N_d molecules of *d*-isomer, $\langle W_{dl}^2(Nx)\rangle$, where $N=N_l+N_d$ and $x=N_l/(N_l+N_d)$, can be obtained in a similar way. In this case the average may be taken over the configurations in which $N^{ll}_{aa}=N^{ll}_{\bar{a}\bar{a}}=Nx^2/2z$, $N^{dl}_{aa}=N^{dl}_{\bar{a}\bar{a}}=Nx(1-x)/z$ and $N^{dd}_{aa}=N^{ll}_{bb}=N(1-x)^2/2z$ where N^{ll}_{aa}, N^{dl}_{ab} and N^{dd}_{aa} are the number of pairs of a_l-a_l, a_l-a_d and a_d-a_d respectively. The a_l-a_d pair can have three different configuration with corresponding interaction energies $\omega^{ld}_{aa_1}$, $\omega^{ld}_{aa_2}$ and $\omega^{ld}_{aa_3}$. As mentioned above $\omega^{ld}_{aa_1}=\omega_{11}+\omega_{22}+\omega_{33}$, $\omega^{ld}_{aa_2}=\omega^{ld}_{aa_3}=\omega_{12}+\omega_{13}+\omega_{23}$, then

$$\sum_{i=1}^{3}\omega^{ld}_{aa_i}=\omega_{11}+\omega_{22}+\omega_{33}+2(\omega_{12}+\omega_{13}+\omega_{23})=\sum_{i=1}^{3}\omega^{ll}_{aa_i}=\sum_{i=1}^{3}\omega^{dd}_{aa_i}=\sum_{i=1}^{3}\omega^0_{aa_i} \quad (33)$$

From 33 the following expressions are obtained.

$$W_{dl}(N,x)=\sum_{i=1}^{3}{}'(N^{ll}_{aa_i}\omega^{ll}_{aa_i}+N^{ll}_{aa_i}\omega^{ld}_{aa_i}+N^{dd}_{aa_i}\omega^{ld}_{aa_i}-\frac{1}{6}\frac{N}{z}\sum_{i=1}^{3}\omega^0_{aa_i})=\sum_{i=1}^{3}{}'\left\{N^{ll}_{aa_i}\omega^{ll}_{aa_i}-\frac{Nx^2}{2z}\left(\frac{1}{3}\sum_{i=1}^{3}\omega^{ll}_{aa_i}\right)\right\}+\sum_{i=1}^{3}{}'\left\{N^{ld}_{aa_i}\omega^{ld}_{aa_i}-\frac{Nx(x-1)}{z}\left(\frac{1}{3}\sum_{i=1}^{3}\omega^{dl}_{aa_i}\right)\right\}+\sum_{i=1}^{3}{}'\left\{N^{dd}_{aa_i}\omega^{dd}_{aa_i}-\frac{N(1-x)^2}{2z}\left(\frac{1}{3}\sum_{i=1}^{3}\omega^{dd}_{aa_i}\right)\right\} \quad (34)$$

where $\sum'$ denotes the summation under the restrictions that $\sum_{i=1}^{3}N^{ll}_{aa_i}=Nx^2/2Z$, $\sum_{i=1}^{3}N^{dl}_{aa_i}=Nx(1-x)/z$ and $\sum_{i=1}^{3}N^{dd}_{aa_i}=(1-x)^2/2z$. Since the mean values in $\{\ \}$ of 34 become zero, then

$$\langle W^2_{dl}(N,x)\rangle_{Av}=\left(\frac{1}{2}\frac{N}{z}x^2\right)^2\cdot\frac{1}{36}\{(\omega^{ll}_{aa_1}-\omega^{ll}_{aa_2})^2+(\omega^{ll}_{aa_2}-\omega^{ll}_{aa_3})^2+(\omega^{ll}_{aa_3}-\omega^{ll}_{aa_1})^2\}+\left\{\frac{Nx(1-x)}{z}\right\}^2\cdot\frac{1}{36}\{(\omega^{dl}_{aa_1}-\omega^{dl}_{aa_2})^2+(\omega^{dl}_{aa_2}-\omega^{dl}_{aa_3})^2+(\omega^{dl}_{aa_3}-\omega^{dl}_{aa_1})^2\}+\left\{\frac{1}{2}\frac{N}{z}(1-x)^2\right\}^2\cdot\frac{1}{36}\{(\omega^{dd}_{aa_1}-\omega^{dd}_{aa_2})^2+(\omega^{dd}_{aa_2}-\omega^{dd}_{aa_3})^2+(\omega^{dd}_{aa_3}-\omega^{dd}_{aa_1})^2\}=\left(\frac{1}{2}\frac{N}{z}\right)^2\{x^4+(1-x)^4\}\cdot\frac{1}{36}\times\{(\omega^0_{aa_1}-\omega^0_{aa_2})^2+(\omega^0_{aa_2}-\omega^0_{aa_3})^2+(\omega^0_{aa_3}-\omega^0_{aa_1})^2\}+\left(\frac{N}{z}\right)x^2(1-x)^2\times\frac{1}{36}\{(\omega^{dl}_{aa_1}-\omega^{dl}_{aa_2})^2+(\omega^{dl}_{aa_2}-\omega^{dl}_{aa_3})^2+(\omega^{dl}_{aa_3}-\omega^{dl}_{aa_1})^2\} \quad (35)$$

If the terms higher than second power of W in 25 are neglected, free energy of mixing $\Delta_m F$ or excess free energy F^E may be expressed as

$$\Delta_m F - NkT\{x \ln x + (1-x) \ln (1-x)\} = F^E$$
$$= -\frac{1}{2kT}\left[\left(\frac{1}{2}-\frac{N}{z}\right)^2\{x^4+(1-x)^4 - x^2-(1-x)^2\}\times\frac{1}{36}\{(\omega^0_{a\,a_1}-\omega^0_{a\,a_2})^2 + (\omega^0_{a\,a_2}-\omega^0_{a\,a_3})^2+(\omega^0_{a\,a_3}-\omega^0_{a\,a_1})\}\right.$$
$$\left.+\left(\frac{N}{z}\right)^2 x^2(1-x)^2\times\frac{1}{36}\{(\omega^{d\,l}_{a\,a_1}-\omega^{d\,l}_{a\,a_2})^2 + (\omega^{d\,l}_{a\,a_2}-\omega^{d\,l}_{a\,a_3})^2+(\omega^{d\,l}_{a\,a_3}-\omega^{d\,l}_{a\,a_1})^2\}\right] \qquad (36)$$

Discussions

As is seen from the above result the principal term of excess free energy F^E is inversely proportional to absolute temperature. This is due to the fact that the optical *d*- and *l*-isomers are energetically identical in random mixture (see Eqs. 21 and 22), so that the first order terms are dropped in the expansion. It is in remarkable contrast to that of the usual binary solutions where the principal terms of F^E are independent of temperature.

Dependency of the term on mole fraction x of one component is complicated and is higher than quadratic in x. This is another feature of the system of optically active substances.

The term is usually very small and is quite negligible.

However, if the difference $|\omega^0_{a\,a_i}-\omega^0_{a\,a_j}|$ or $|\omega^{d\,l}_{a\,a_i}-\omega^{d\,l}_{a\,a_j}|$ happens to be great, the contribution from these terms may become appreciable. For instance consider an optical active molecule whose sub elements 1, 2 and 3 are $-NH_2$, $-C{=}O$ and $-OH$ group respectively. Then hydrogen bonding is formed between the pairs 1−2, 1−3, 2−3 and 3−3 but is not formed between pairs 1−1 and 2−2.

If we assume that interaction energies of these pairs which form hydrogen bonding are all equal and 5 kcal./mol. and those of the pairs which do not form hydrogen bonding are neglected, then F^E becomes according to 36.

$$F^E \approx \frac{1.45}{(2z)^2} \text{ kcal./mol.}$$

at $T=300°K$ and $x=0.5$

If we assume that $Z=4$, F^E becomes $F^E \approx 22$ cal./mol. Although the value 22 cal./mol. obtained above is quite approximate because of the neglect of higher orders than the second, the order of magnitude of the value may not differ from that obtained by rigorous calculation.

Summary

A statistical mechanical theory of solutions consisting of *d*- and *l*-optical isomers is developed based on a new model of optically active molecules, and the excess free energy of the system is also derived and the order of magnitude of this quantity is examined.

The auther wishes to express his hearty thanks to Peofessor Yonezo Morino of the University of Tokyo for his helpful discussions.

Government Chemical Industrial Research Institute
Shibuya-ku, Tokyo

Forschung über die katalytische Entwässerung des Isoamylalkohols. III. Prüfung über die Bestandteile der durch Zinksulfat-Katalysator-Entwässerung entstehenden Produkten

Von Akira MITSUTOMI

(Eingegangen am 8. April, 1961)

Die im vorangehenden Bericht[1] beschriebenen Versuche zeigten klar, dass der Zinksulfat-Katalysator der Beste ist, wenn aus Isoamylalkohol die hauptsächlich aus Trimethyläthylen bestehenden Olefinen hergestellt werden sollen. Dass diese unter Anwendung des genannten Katalysators aus Isoamylalkohol hergestellten Olefine ein Gemisch aus Trimethyläthylen, Isopropyläthylen und Methyläthyläthylen darstellen, ist allerdings nach ihrem Siedepunkt und weiteren physikalischen Konstanten anzunehmen, ist aber keineswegs nach exakter Prüfung der Bestandteile bestätigt.

Der Verfasser schreibt im folgenden die

1) A. Mitsutomi, Dieses Bulletin, 34, 1525 (1961).

Ergebnisse der Forschung zur Bestimmung der Bestandteile nieder.

Beschreibung der Versuche

Als Katalysatoren wurde nach den Versuchsergebnissen bis zu der II. Mitteilungen das Gemisch aus 330 g Zinksulfat ($ZnSO_4 \cdot 7H_2O$) und 770 g japanischer Säureerde mit Zusatz 100 ccm 28% Ammoniak eingesetzt, danach noch in Kugelformen verarbeitet, zuerst bei 60°C 2 Std, dann bei 120°C 5 Std erhitzt und aufgetrocknet, anschliessend ins Reaktionsrohr eingefüllt und bei 500°C 8 Std aktiviert.

TABELLE I. ERGEBNISSE DER FEINDESTILLATION VON DEN REAKTIONSPRODUKTEN

Nummerierung der Fraktion	Destillationstemp. (Korr.) °C	Prozentuales Destillationsverhältnis, %	n_D^{20}
1	21.7~30.8	14.4	1.3708
2	30.8~33.8	5.0	1.3852
3	33.8~35.8	6.6	1.3880
4	35.8	13.0	1.3880
5	35.8~42.8	5.0	1.3970
	Rückstand	32.0	1.4028

Probe $n_D^{20}=1.4059$

Ganz gleichartige, aber verkleinerte Versuchsanlage, wie sie im vorangehenden mitteilung beschrieben ist, wurde herangezogen und die Reaktionstemperatur auf 350~400°C eingestellt.

Zuerst wurden flüssige Reaktionspodukte der Feindestillation unterworfen, wodurch fünf Fraktionen erhalten wurden. Sie sind in Tabelle I aufgestellt.

Prüfung der ersten Fraktion.—Das Infrarotspektrum der ersten Fraktion ist in Abb. 1 gezeigt.

Es sind die für Isopropyl-Gruppe charakteristischen Gerüstschwingungen 6.9 μ und 7.27 μ, die intensiv erscheinen. Ferner sind 10.1 μ, 11.03 μ, 11.32 μ usw. für spezifisch bemerkbar.

Diese Umstände unterstreichen das Vorhandensein des Isopropyläthylens.

Ferner ist die Absorption 12.53 μ für 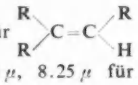 festzustellen, ausserdem sind 9.33 μ, 8.25 μ für Trimethyläthylen schwach dargestellt.

Diese Umstände lassen beurteilen, dass diese Fraktion neben viel Mengen Isopropyläthylen das Mitvorhandensein geringer Menge Trimethyläthylen zulässt.

Prüfung von Fraktion Nr. 2.—Das Infrarotspektrum von Fraktion Nr. 2 ist in Abb. 2 gezeigt.

Die Besichtigung dieses Infrarotspektrums lässt

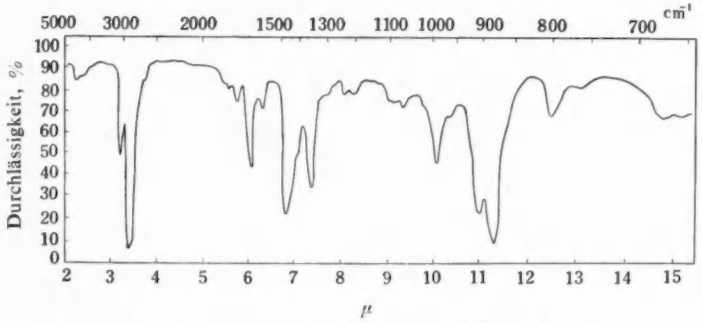

Abb. 1. Infrarotspektrum von Fraktion Nr. 1.

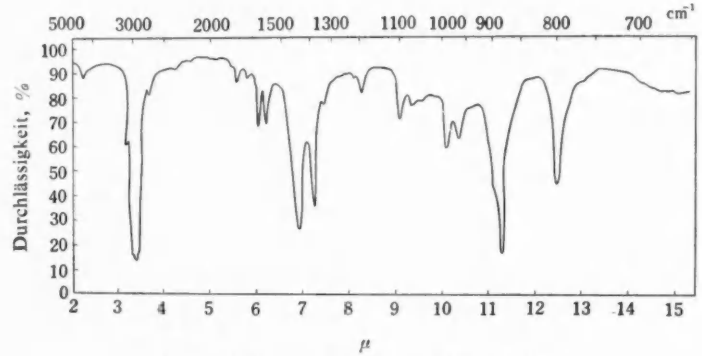

Abb. 2. Infrarotspecktrum von Fraktion Nr. 2.

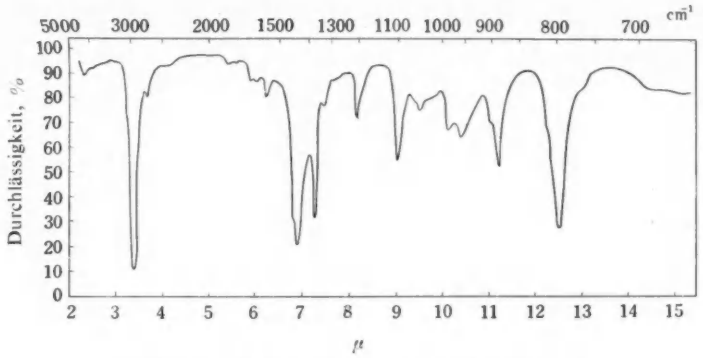

Abb. 3. Infrarotspektrum von Fraktion Nr. 3.

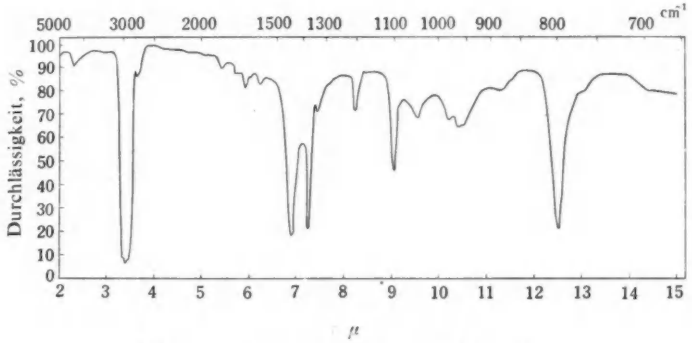

Abb. 4. Infrarotspectrum von Fraktion Nr. 4.

wissen, dass ausser der für 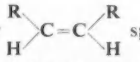 spezifischen 12.50 μ Wellenlänge die bei den obengenannten und unterstrichenen Wellenlängen mit den charakteristischen Gerüstschwingungen bei Trimethyläthylen gut übereinstimmen.

Ferner zu beachten ist die Absorption von 11.28 μ, die als charakteristische Gerüstschwingung für Bindung von 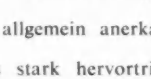 allgemein anerkannt ist. Der Umstand, dass dies stark hervortritt, lässt wissen, dass die Fraktion Nr. 2 das Gemisch aus Trimethyläthylen und Methyläthyläthylen fast in gleichen Anteilen darstellt.

Prüfung von Fraktion Nr. 3.—Das Infrarotspektrum diesser Fraktion (Abb. 3) zeigt gute Übereinstimmung der Absorptionsstellungen mit denen in Abb. 2, nur dass die 12.50 μ stärker ist als bei Abb. 2, während die 11.28 μ schwächer ist, woraus mit Recht zu schliessen ist, dass diese Fraktion das Gemisch aus vielen Mengen Trimethyläthylen und geringer Menge Methyläthyläthylen darstellt.

Prüfung von Fraktion Nr. 4.—Der Brechungsindizes $n_D^{20}=1.3880$ dieser Fraktion ist fast mit den Literaturangaben von Trimethyläthylen $n_D^{20}=1.3874$, identisch, was annehmen lässt, dass es sich hierbei doch um reines Trimethyläthylen handelt. Bei ihrem Ultrarotspektrum (abb. 4) sind ausser der charakteristischen Gerüstgchwingungen für 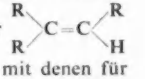 die Gesamtkurvenverzeichnungen fast mit denen für Trimethläthylene übereinstimmend. Kein Vorhandensein anderer Verbindungen ist anzunehmen.

Bestandteilmässige Untersuchung des Destillationsrückstandes.—Wenn Reaktionstemperaturen der Entwässerung von Isoamylalkohol variieren und dabei die flüssigen Produkte (Rückstand von der Tabelle I) hinsichtlich ihres Brechungsindies miteinander verglichen werden, so lassen sich annähernd ein konstanten Wert finden (Tabelle II), dieser zeigt dass die Produkte bestandteilmässig keinerlei grössere unterschiede aufweisen.

Tabelle II. Zusammenhang der Reaktionstemperaturen mit den Brechungsindizien der Reactionsprodukte

Reaktionstemperatur, °C	375～425	350～400	325～375
n_D^{20}	1.4050	1.4059	1.4048

Da ihre bestandteilmässige Untersuchung tatsächlich keine grösseren Unterschiede voneinander ergab,

TABELLE III. DESTILLATIONSERGEBNISSE VON DESTILLATIONSRÜCKSTANDGEMISCH

Fraktion-nummern	Destillations-temperatur °C/mmHg	Destillate-menge ccm	n_D^{20}	Anmerkung
1	92～94/760	5	1.3961	farblos, klar, stechendes Geruch
2	94～96/760	7.5	1.3961	ditto
3	96～102/760	3.5	1.3993	ditto
4	50～72/46	3	1.4292	hellgelb, aromatisches Geruch
5	72～80/46	3.5	1.4326	ditto
6	931～15/7	1.5	1.4648	gelbbraun, aromatisches Geruch
	Rückstand	6		pechartig, dickklebrig

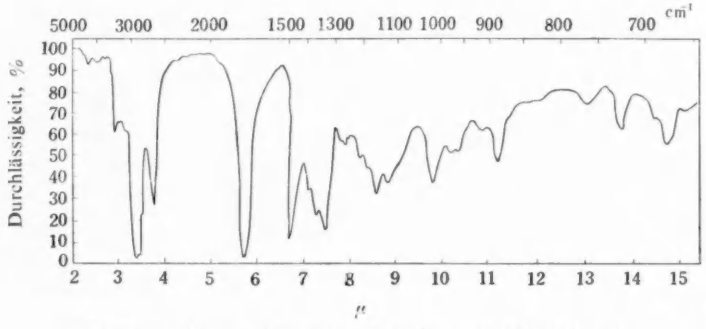

Abb. 5. Infrarotspektrum von Fraktion Nr. 2 (Tabelle III).

wurden diese drei Reaktionsprodukte voneinander abgesondert destilliert und die jeweiligen Destillate wurden zusammengebracht und dieses Rückstandsgemisch wieder der destillation unterzogen. Die Ergebnisse sind in Tabelle III aufgestellt.

Die Fluoreszenz-Indikator-Adsorptionsanalyse an der Fraction Nr. 2 hiervon ergab, dass das Gemisch aus Olefin 3.7%, aromatischartige Verbindungen 2.9% und gleich wie Alkohol polarisierte Substanzen 93.4% besteht.

Aus dem Infrarotspektrum der Fraktion Nr. 2 (Abb. 5) ist zu sehen, dass die für Aldehyde bzw. Keton-Radikal charakteristische Gerüstschwingungen

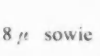

3.7 μ und 5.8 μ sowie die für C—C— Radikal spezifischen 7.25 μ und 7.3 μ alle ausdrucksvoll in Erscheinung treten, das weist klar auf, dass Isovaleraldehyde in vielen Mengen enthalten sind. Die Absorption 2.9 μ zeigt das Vorhandensein des OH Radikals auf, während die 3.4 μ und 3.5 μ für Alkyl-Radikal klarsichtlich auftreten. Die Zusammenfassung dieser Tatsachen lässt beurteilen, dass diese Fraktion das Gemisch aus Isovaleraldehyde in vielen Mengen und unverwandte Isoamylalkohol in geringer Menge darstellt.

Ferner wurde nach chemischer Untersuchung erkannt, dass die Fraktionen von Nr. 1 bis 3, welche vollkommen gleiches stechendes Geruch besitzen, bestandteilmässig vollständig gleich sind wie die Fraktion Nr. 2. Wie aus Tabelle III ersichtlich, sind die Brechungsindizien miteinander fast identisch. Erst bei der Fraktion Nr. 4 steigt der Indizies etwas an und zwar immer höher mit den erhöhten Siedepunkten. Das Geruch geht von dem Stechenden nebenbei zum Aromatischen über. Hieraus ist das Vorhandensein der Polymere anzunehmen. Hinsichtlich der Tatsache, dass bei qualitativer Analyse des Schwefels mittels Nitroprussidnatrium und der Doktor-Lösung die Fraktionen Nr. 5, 6 und der Rückstand positiv sind, wurden die ebengenannten Nr. 5 und 6 gründlich gewaschen. Nämlich, bei der Fraktion Nr. 5 wurden 110 ccm Doktor-Lösung auf 3.1 ccm Proben in mehr als 10 Portionen eingeteilt angewandt und gewaschen. Die öligen Schichten blieben aber trotz des Waschens immer noch gelblich oder hellbraunlich, wurden nicht farblos.

Nun wurde 15 ccm der Fraktion Nr. 5 mit 500 ccm Doktor-Lösung in 20 Portionen gewaschen, aber die Farbtönung blieb immer noch unverändert. Der Brechungsindizies war $n_D^{20}=1.4550$ und die qualitative Analyse des Schwefels zeigte sich als positiv.

TABELLE IV. DESTILLATIONSERGEBNISSE DES GEWASCHENEN ÖLS (FRAKTION NR. 5 DER TABELLE III)

Fraktionen	Destillations-temperatur °C/10 mmHg	n_D^{20}	Schwefel-versuche	Anmerkung
1	46～ 67	1.4420	±	Gelb
2	67～ 85	1.4392	+	〃
3	112～135	1.4443	+	〃
	Rückstand		+	Schwarz-braunlich, dickkle-brig

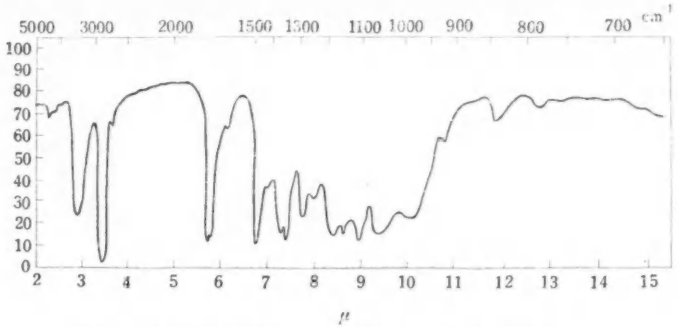

Abb. 6. Infrarotspektrum von Fraktion Nr. 3. (Tabelle IV)

Das gewaschene Öl wurde unterm verminderten Druck destlliert. Die Ergebnisse sind in Tabelle IV verzeichnet.

Bei infrarotspectraler Untersuchung (Abb. 6) der Fraktion Nr. 3 der Tabelle IV erwiesen sich die für Aldehyd oder Keton spezifischen Absorption 3.42 μ und 5.8 μ intensiv, während im Übrigen die weiteren Absorptionen mit denen als Isovaleraldehyde im grossen und ganzen übereinstimmten. Die Feststellbarkeit der Absorptionswellenlänge 2.9 μ für OH Radikal und der Absorption für Isopropyl-Radical ist klarer Nachweis für Isoamylalkohol. Es ist daher anzunehmen, dass es sich bei diesen öligen Substanzen um ein Gemisch aus Isovaleraldehyd und Isoamylalkohol handelt.

Die obigen Ergebnisse lassen für den Destillationsrückstand auf das Folgende schliessen.

Die Fluoreszenz-Indikator-Adsoptionsanalyse an dem ungewaschen Rückstand ergab, dass die jeglichen Fraktionen fast gleiche Zusammensetzung haben, wie die Tabelle V zeigt. Die Untersuchungsergebnisse bei der Fraktion Nr. 2 können ruhig für die übrigen Fraktionen als gültig betrachtet werden. Damit könnte eine jeweilige untersuchung erübrigt sein.

Tabelle V. Aufstellung der Ergebnisse bei Fluoreszenz-Indikator-Adsorptionsanalyse von dem ungewaschnen Rückstand der Tabelle IV

Frak-tions-nummern	Olefine %	Schwefel-verbindungen %	Gemisch von Isovaleral-dehyde und Isoamyl-alkohol, %
1	7.8	2.8	89.4
2	3.7	2.9	93.4
3	3.9	4.7	91.4
4	5.7	0.3	94.0

Ferner bei dem gewaschenen Rückstand ist zu finden, dass ausser Isovaleraldehyd und Isoamylalkohol etwa mit Waschen leicht unentfernbare, nämlich fest gebundene Schwefelverbindungen wenn auch in geringer Menge vorhanden sind. Diese Schwefelverbindungen stammen zwar aus thermischer Zerlegung des Katalysators, aber ihr Urwesen konnte zufolge mengenmässiger Geringfügigkeit nicht festgestellt werden.

Ferner ist annehmbar, dass noch weitere hochsiedende Polymere mitvorhanden sind.

Zusammenfassung der obigen Ausführungen lautet wie folgt: Wenn Isoamylalkohol in Gegenwart des Zinksulfates als Katalysator das Wasser entzogen wird, entsteht ausser in einem Gemisch befindlichen vieren Mengen Trimethyläthylen mit geringer Menge Methyläthyläthylen sowie Isopropyläthylen, Isovaleraldehyd strukturmässig unbekannte Polymere und Schwefelverbindungen.

Zum Schluss sei noch davon erwähnt, dass die vorliegende Arbeit der Leistung von Herrn Professor Dr. Eiichi Funakubo an der Technischen Fakultät der Universität zu Osaka verdankt ist.

Chemisches Institut der Technischen Fakultät der Universität zu Osaka
Miyakojima-ku Osaka

Forschung über die katalytische Entwässerung des Isoamylalkohols. IV. Quantitative Untersuchung der durch unterm Einsatz des Zinksulfat-Katalysators erfolgende Dehydratisierung gebildeten Produkte auf ihre Bestandteile

Von Akira MITSUTOMI und Eiichi FUNAKUBO

(Eingegangen am 8. April, 1961)

Um die Zusammensetzung der aus Isoamylalkohol dargestellten Olefine zu bestimmen, wurden unterm Einsatz des Zinksulfat-Katalysators, gleich wie in der letzten Mitteilung[1], durch Fluoreszenz-Indikator Adsorotionsanalyse und Silicagel Adsorption die betreffenden gesättigten Kohlenwasserstoffe und Olefine getrennt.

Daraufhin wurde durch Infrarot-Absorptionsspektrum und Gaschromatographie an den Feindestillaten das Wesentliche ermittelt, dann quantitativ der Verbreitungszustand von den Olefinen untersucht, schliesslich die Zusammensetzung derselben klargemacht und gleichzeitig über den Bildungsmechanismus thermodynamische Betrachtung durchgeführt. Die vorliegende Mitteilung beschreibt den Verlauf der Versuchsdurchführung.

Beschreibung der Versuche

Operation.—Die Vorrichtung ist in Abb. 1 gezeigt. Es wird Isoamylalkohol in 100 ccm Glaszylinder (4) mit Skalen eingefüllt. Daraus wird je eine gewisse Menge hiervon in Verdampfer (III) abgegeben und drin mit Mantelerhitzer verdampft. Der Alkoholdampf wird beim Aufsteigen in Wärmeaustauscher (II) durch aus Reaktionsrohr (I) austretendes Gas stets bei 155~165 °C erhitzt und in Reaktionsrohr (I) geführt.

Die Temperatur in Reaktionsrohr konnte während der ca. 6 Tage gedauerten kontinuierlichen Reaktion stets bei 350±3 °C gehalten bleiben.

Die in Wärmeaustauscher kondensierten hochsiedenden flüssigen Substanzen laufen in Vorlage (IV) zusammen, während die übrigen gasförmigen Substanzen von Wärmeaustauscher her in Vorlage (V). Vorlage (V) wird auf Wasserbad auf 80 °C erwärmt, so dass unveränderter Isoamylalkohol und durch Reaktion gebildetes Wasser kondensiert werden, während Olefine und weitere niedrigsiedende flüssige Substanzen, indem sie durch über Erhitzer (6) einlaufendes heisses Wasser in Kühler (VI), von aussen her gewärmt werden, aufsteigen und anschliessend in Kühler stark abgekühlt und in Sammler (VIII) angesammelt werden.

Gase werden über Messer mengenmässig erfasst und in Sammler aufgefangen. Als die Gesamtmenge der Probe eingetan und die Reaktion zum Abschluss gebracht wurde, wurde Stickstoffgas aus Zylinder ins Reaktionssystem eingedrückt, wodurch Reaktionsprodukte alle in Vorlage gebracht wurden, indem jeglicher Verlust weitgehendst verhindert wurde.

Als Katalysator wurde das Gemisch aus 3 Teilen Zinksulfat $ZnSO_4 \cdot 7H_2O$ und 7 Teilen japanischer Säureerde herangezogen, welches mit zugesetztem 28%igen Ammoniakwasser angeteigt, zu Klumpen gemacht, bei 60 °C 2 Std und dann bei 120 °C 5 Std aufgetrocknet, anschliessend in Reaktionsrohr eingepackt und durch 1 stündige Erhitzung bei 500 °C aktiviert wurde.

Als Probe wurde handelsübliche Ware Isoamylalkohol abdestilliert, deren Fraktion bei Sdp 127~130 °C angesammelt wurde.

Bei vorliegendem Versuche wurde darauf Wert gelegt, die Reaktionstemperatur bei 350±5 °C zu behalten. In der Wirklichkeit gelang es uns daher, während der für Reagieren der ganzen Probenmenge von 4800 ccm benötigten Dauer von 115 Std und 50 Min die Temperatur bei 350±3 °C zu sichern.

Durchmesser eines Teilchens vom Katalysator……durchschnittlich 6 mm
Gesamtpackungsmenge des Katalysators……1.505 kg, 1.723.9 ccm
Durchlaufgeschwindigkeit der Proben……41.44 ccm/Std
Raumgeschwindigkeit……1.44 ccm/Min

Versuchsergebnisse

Nach der von uns vorgeschlagenen Methode* wurde die Typenanalyse an rohen Olefinen vorgenommen, deren Ergebnissen in Tabelle I, II, aufgestellt. Daraufhin wurde durch das Silicagel-Adsorptionsverfahren gesättigter Kohlenwasserstoff getrennt und die Gewinnung der reinen Olefinen vorgenommen. Zu diesem Zweck wurden 200 gm Silicagel** in das Adsorptions-Trennungsrohr eingepackt, darauf 80 ccm rohe Olefine zugegeben. Der Ansatz wurde unter

1) A. Mitsutomi, Dieses Bulletin, 34, 1681 (1961).

* Hierbei handelt es sich um ein für Leichtöl-Produkte von Steinkohlenteer anwendbares, durch Modifizierung der FIA-Methode von neuem ausgearbeitetes Verfahren, welches noch später bekanntgegeben wird.

** Tokai Gel F. I. Das Von der Fa. Tokai Kagaku Kogyo K. K. hergestellte, mit dem Olefin-Polymerisation verhindernden Vermögen versehne, für die Chromatographie einsetzbare Silica-gel.

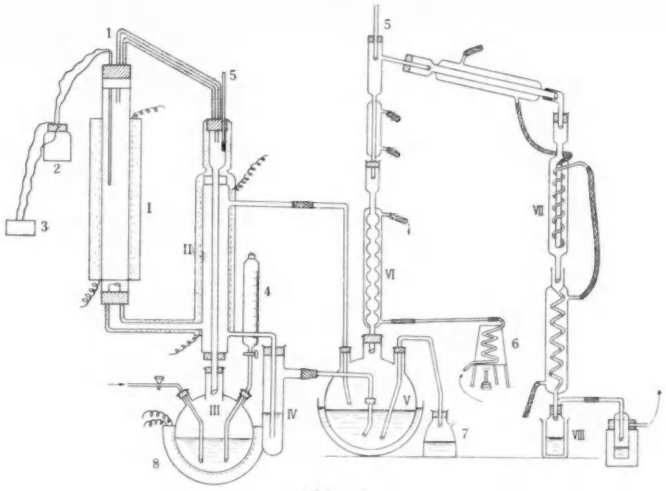

Abb. 1

I……Reaktionsrohr, Aussendurchmesser 70 mm
Innendurchmesser 60 mm
Länge 800 mm
Elektrisch zu erhitzender Reaktionsrohrteil Länge 610 mm
Aussendurchmesser 120 mm
II……Wärmeaustauscher, Innendurchmesser 12 mm
Ausserdurchmesser 43 mm
Länge 430 mm
III……Verdampfer, Kapazität 300 ccm
IV……Vorlage, Durchmesser, 30 mm
Länge 210 mm
V……Trennungsvorlage für unveränderten Alkohol und für Wasser, Kapazität 300 ccm
VI, VII…Kühler
VIII……Vorlage für rohe Olefine.
(1)……Thermoelement
(2)……
(3)……Pyrometer
(4)……Messzylinder von 100 ccm Kapazität mit Skalen.
(5)……Thermometer
(6)……Heizkörper für zirkulierendes Wasser
(7)……Vorrichtung für Entnahme des unveränderten Alkohols und Wassers.
(8)……Falltür.

Tabelle I. Aufstellung der Reaktionsprodukte beim Ansatz von 4800 ccm Alkohol

	Ausbeute ccm	Prozentuale Ausbeute, %		n_{20}^{D}
		bezogen auf Probenmenge	bezogen auf aktuell reagierte Probenmenge	
Rohe Olefine	2988	62.25	75.55	1.3849
Wasser	575	11.98	14.53	
hochsiedende Produkte	30	0.63	0.76	
Wasermenge, kondensierts in Wärmeaustauscher	10	0.21	0.25	
gebildete Gasmenge	319.6 l.		14.3 Mol.	
unveränderter Alkohol	845	17.6		

Tabelle II. Analytische Ergebnisse roher Olefine

Versuchsnummer	1	2	Mittelwert
gesättigter Kohlenwasserstoff, %	2.33	2.38	2.35
Olefine, %	97.67	97.62	97.65

TABELLE III. ERGEBNISSE DER ADSORPTIONSBEHANDLUNG FÜR ROHE OLEFINE

Male der Versuche	1	2	3	4	5	6	7	8	9	10	11	12	13
SO-(I), ccm	11.5	10	10	11	9.5	10	10.5	10.4	10.5	11	10	10	11
rein Olefin-(I), ccm	63.5	64.5	65.5	64	65.5	63	66.5	66.8	63.5	61.5	64	64.5	63.3
OA-(I), ccm	5.5	5	7.5	6.5	5.5	6	5.3	5	7	6	6	5.5	5.2

SO: Gemisch des gesättigten Kohlenwasserstoffs mit Olefin.
OA: Gemisch des Olefins mit Äthanol.

TABELLE IV. ERGEBNISSE DER ADSORPTIONS-REINIGUNG DES GEMISCHES AUS GESÄTTIGTEN KOHLENWASSERSTOFFEN UND OLEFINE SO-(I)

Male der Versuche		1	2	3	4	5
getrennte stoffe	SO-(II), ccm	19.5	20	20	20	20
	rein Olefine (II), ccm	37.5	36	36.5	36.5	36
	OA-(II), ccm	3.5	4	3.5	3.5	4

TABELLE V. GASCHROMATOGRAPHIE DER OLEFINEN

Probenzeichen	Bestandteile, %				
	A	B	C	E	F
O-(I)	3.3	8.1	14.7	74.2	Spur
O-(II)	0.8	11.2	18.4	69.6	
O-(III)	0.7	14.9	23.0	61.1	
O-(IV)	0.8	22.9	22.9	53.3	

TABELLE VI. ERSTE PRÜFUNGSERGEBNISSE VON OLEFINE O-I

Nummer	Destillate Temperatur, °C	Menge, ccm	n_D^{20}	Prozentuales Verhältnis der Bestandteile A, %	B, %	C, %	E, %	F, %
1	18 ~19.5	6	1.3672 (t=15)	0.5	98.4	1.1	—	—
2	19.5~20	11.5		—	92.7	7.3	—	—
3	20 ~28	24	1.3722	1.5	44.6	53.9	—	—
4	28 ~29	11.5		2.3	11.5	86.2	—	—
5	29 ~30	21	1.3779	0.9	1.9	96.2	—	0.9
6	30 ~31	57		0.5	0.5	84	13.5	1.5
7	31 ~35	60		—	—	35.3	63.9	0.8
8	35 ~36.2	21.5		—	—	16.3	82.9	0.8
9	36.2	20	1.3865	—	—	9.4	90.3	0.3
10	36.2~36.8	73.5	1.3870	—	—	3.2	96.8	—
11	36.8	36	1.3872	—	—	2.4	97.6	—
12a	36.8	38	1.3873	—	—	1.6	98.4	—
12b	36.8~36.9	31.5	1.3873	—	—	0.8	99.2	—
13	36.9	101	1.3875	—	—	—	100	—
14	36.9~37	40.5	〃	—	—	—	100	—
15	37	50	〃	—	—	—	100	—
16	37 ~37.1	10	〃	—	—	—	100	—
	Rückstand	14						
	Summe	627, 78.4%						

Anwendung des Äthanols der Austauschentwicklung unterzogen. Tabelle III zeigt die Reinigungsergebnisse.

Dann wurde 60 ccm von dem auf diese Weise erhaltenen SO-(I) weiter abpipettiert und in das mit 200 g Silica-gel eingepackte Rohr eingegossen. Mit Äthanol wurde die Austauschentwicklung ausgeführt. Die erhaltenen Ergebnisse sind in Tabelle IV aufgestellt. Dieses Reinigungs verfahren wurde weiter wiederholt und die Ergebnisse sind in Abb. aufgestellt. Da die Olefine hinsichtlich ihrer Brechungsindizien zusammensetzungsmässige Ähnlichkeit zu zeigen schienen, wurde sie gaschromatographisch auf ihre Zusammensetzung untersucht (Tabelle V).

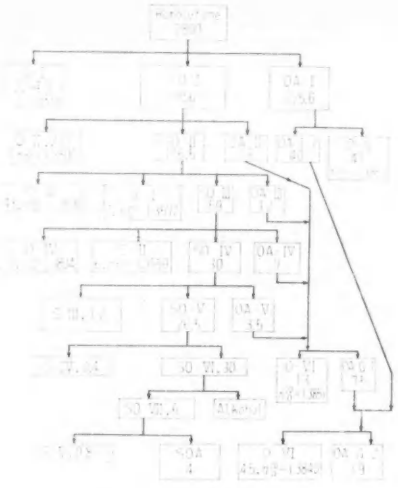

Abb. 2.*

* Nummer in ccm, S: gesättigte Kohlenwasserstoffe, O: Olefine.
Gesamtsumme S: 15.4 ccm, O: 2547.2 ccm.

Wie aus Tabelle V ersichtlich, hat die Probe O-(I) im Vergleich mit drei weiteren Proben anderes Mischverhältnis der Bestandteile aufgezeigt. Dementsprechend wurde darauf eingestellt, dass Olefin O-(I) alleine, O-(II), O-(III) und O-(IV) gemeinsam, auch O-(V), O-(VI), und O-(VIII) gemeinsam, gruppenweise gesondert destilliert werden. Um aber noch festzustellen, wurden die durch vorherige Destillation erhaltenen Fraktionen gaschromatographisch analysiert und der Verbreitungszustand der Bestandteile untersucht. Die Ergebnisse sind in Tabelle VI verzeichnet. Es wurde dabei erkannt, dass die drei Bestandteile B, C und E vorwiegend vorhanden sind, wobei die Beziehung der Siedepunkte auf Gehaltsmenge klar vortritt.

Von diesen Fraktionen sind diejenigen mit Sdp 36.9~37.1°C 100%ig reine E-Bestandteile, deren Brechnungsindies mit den Literaturangabe, von Trimethyläthylen n_D^{20}=1.3874, 1.3876 identisch ist.

Wegen weiterer Feststellung dieser Annahme wurde das Infrarot-Absorptionsspectrum gemessen. Dabei liess es sich finden, dass, wie Abb. 3 zeigt, das ganze Bild mit Standardsbild des 2-Methyl-2-buten übereinstimmt und die spezifische Absorptionswellenlänge 12.53 μ für

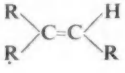

Type intensiv auftritt. Dadurch

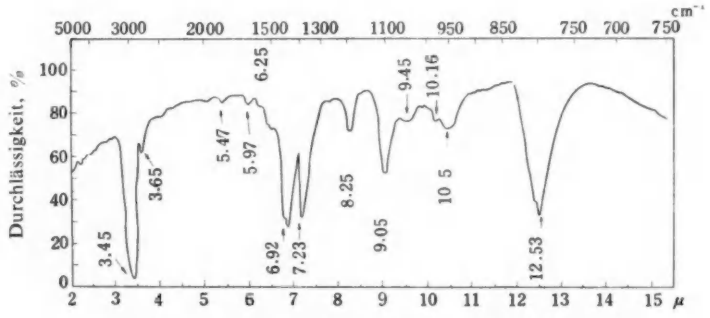

Abb. 2. Infrarot-Absorptionsspektrum von Fraktion Nr. 14.

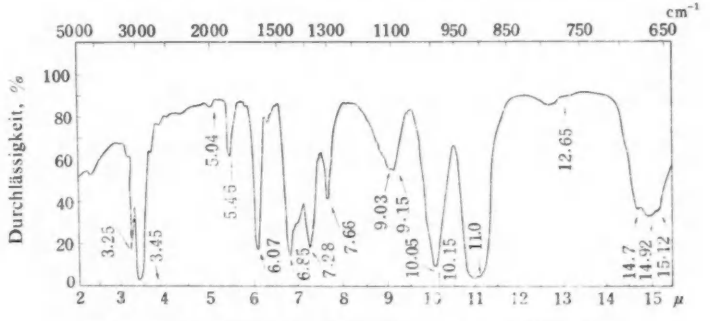

Abb. 3. Infrarot-Absorptionsspektrum von B-Bestandteil.

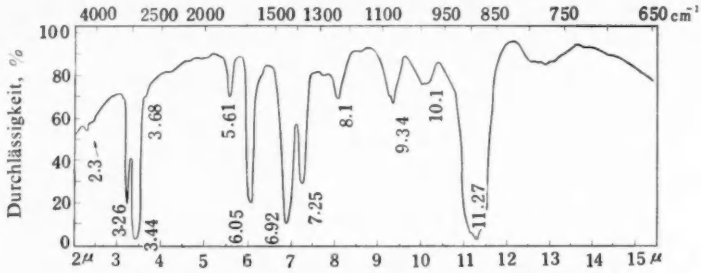

Abb. 4. Infrarot-Absorptionsspektrum von C-Bestandteil.

ist entschieden worden, dass der Bestandteil E Trimethyläthylen darstellt.

Die erste Fraktion, Sdp 18～19.5°C, zeigte das Brechungsindies, welches mit der Literaturangabe von 3-methyl-1-buten $n_D^{15}=1.3677$ übereinstimmt. Ausserdem zeigten die Messungen des Infrarot-Absorptionsspektrums (Abb. 4) einwandfreie Übereinstimmung mit dem Standardsbild für 3-Methyl-1-buten. Als spezifische Absorptionswellenlänge von $\begin{matrix}R\\H\end{matrix}\!\!>\!C$ CH_2 sind die Werte von $10.05\pm0.02\,\mu$, und $10.98\pm0.02\,\mu$ nach K. E. Kitson und $10.98\pm0.02\,\mu$ nach J. A. Anderson order $10.95\pm0.02\,\mu$ nach E. L. Sailer angegeben und diese alle sind auch in unserem Bild als intensive Absorptionen aufgetreten. Demnach haben wir entschieden, dass der Bestandteil B 3-Methyl-1-buten ist. Im Infrarot-Absorptionsspektrum (Abb. 4) der Fraktion Nr. 5 tritt die spezifische Absorption, $11.27\,\mu$, fur $\begin{matrix}R\\R\end{matrix}\!\!>\!C=CH_2$ intensiv auf. Ausserdem stimmt das genze Spektraldiagramm mit dem Standardsdiagramm von Methyläthyläthylen einwandfrei überein. Aus dieser Tatsache und dem Messwerte von Brechungsindies ist entscheiden, dass der C-Bestandteil Methyläthyläthylen darstellt.

Die in Tabelle VI aufgezeichneten gaschromatohraphischen Analysenergebnisse zugrunde nehmend, wurde mengenmässige Verteilung der einzelnen Bestandteile in den einzelnen Fraktionen rechnerisch festgestellt. Kurz gefasst, gaschromatographische und infrarotabsorptionsspektrale Analyse an den durch Feindestillation fraktionierten Destillaten hat ergeben, dass die durch Silicagel-Adsorption gereinigten Olefine folgende Zusammensetzung besitzen: Trimethyläthylen 74.77, Methyläthyläthylen 19.96, Isopropyläthylen 4.78, und Olefine von unbekennter Konstitution 0.49%.

Dann wurden die Olefine O-(II), O-(III) und O-(IV), deren Brechungsindizien einander nähern, zusammengebracht und der Feindestillation unterzogen. Gaschromatographische Analyse an den Fraktionen ergaben die Resultaten in Tabelle VII.

Die Zusammensetzung von rein Olefin in dem Gemisch aus O-(II), O-(III) und O-(IV), war wie folgt: Trimethyläthylen 65.98, Methyläthyläthylen 21.95, Isopropyläthylen 11.63, und Unbekannte Olefin 0.44%.

Die Zusammensetzung von reinem Olefin in dem, Gemisch aus O-(V), O-(VI)und O-(VII), war von Tabelle VIII errechnet wie folgt: Trimethyläthylen 66.35, Methyläthyläthylen 30.17, Isopropyläthylen 0.43, und unbekannte Olefin 3.05%.

TABELLE VII. ERGEBNISSE DER FEINDESTILLATION AN REINEN OLEFINEN

Fraktion				Ergebnisse der gaschromatographische Analyse			
Nummer	Temperatur, °C	Menge, ccm	n_D^{20}	A, %	B, %	C, %	E, %
1	19.9～20	6	1.3644	—	100	—	—
2	20	6	1.3645	—	100	—	—
3	20.1～29.5	14	1.3680	4.5	53.6	42	—
4	29.5～30	9	1.3759	1.2	1.8	97.1	—
5	30 ～30.1	9	1.3778	0.2	spur	99.8	—
6	30.1～35.2	17	1.3808	—	—	50	50
7	35.2～36.6	20	1.3848	—	—	11.1	88.9
8	36.6～36.9	22	1.3857	—	—	7.6	92.4
9	36.9～37	35	1.3803	—	—	3.3	96.7
10	37	37	1.3872	—	—	—	100
	Rückstand	14	1.3921				

Tabelle VIII. Ergebnisse der Feindestillation an reinen Olefine-Gemisch von O-(V), O-(VI) und O-(VII)

Fraktion				Ergebnisse von Gaschromatographie, %				
Nummer	Temperatur, °C	Menge, ccm	n_D^{20}	A	B	C	E	F
1	26.9～30.2	4	1.3807	spur	1.9	94.9	—	3.2
2	30.2～35.5	4	1.3872	—	spur	33.3	59.1	7.4
3	35.5～36.3	3	1.3882	—	—	spur	97.1	2.9
4	36.3～36.6	4	1.3886	—	—	—	100	—
5	36.6	2	1.3889	—	—	—	100	—
	Rückstand, ccm	8	1.3919					

Tabelle IX. Ergebnisse der Destillation vom durch Reaktion gebildeten Wasser

Fraktionen			Spezifikation		
Einteilung	Temperatur °C	Menge ccm	obere Schicht (organische Phase) ccm	unter Schicht (Wasser-Phase) ccm	Anmerkung
1	67～68	3.9	3.7	0.2	Destillation unter normalem Druck.
2	80～94	64.1	6.1	58	unter gering vermindertem Druck destilliert.
3	94～95	370	370	—	gleichmässige Flüssigkeit.
4	95～96	98	98	—	
5	97～99	11	11	—	
6	Rückstand	1	1	—	
	Summe	548	489.8	58.2	

Untersuchung auf das durch Reaktion gebildete Wasser.—Von dem durch Reaktion gebildeten Wasser wurden 550 ccm genommen und destilliert. Verlauf der Destillation und Eigenschaften der Fraktionen sind in Tabelle IX aufgestellt.

Die Fraktionen von Nr. 3 bis 5 waren homogene Flüssigkeiten, enthielten kein Wasser, verhielten den Schiff'schen Reagenz äusserst indifferent.

Bei den Fraktionen Nr. 1 und 2, die der Schiff'schen Reagenz intensiv positiv waren, wurde ihre organische Phase mit *p*-Nitrophenylhydrazin einwirken gelassen.

Von 0.2 ccm der Fraktion Nr. 1 wurden 275 mg *p*-Nitrophenylhydrazon Schmp 101.5～104°C, und von 0.5 ccm der Fraktion Nr. 2 619 mg derselben, aber Schmp 103～108°C, erhalten. Nach Umkristallisation wandelte sich das Vordere in Schmp 105.5～110°C, und das Letztere in Schmp 105～108°C um. Die Beiden wurden durch die Mischschmelzpunktsbestimmung als Isovaleraldehyd mit Sicherheit festgestellt.

Thermodynamische Betrachtung über Isomerisationsgleichgewicht und Zusammenfassung.—Mit der Absicht, aus Isoamylalkohol die vorwiegend aus Trimethyläthylen bestehenden Olefinen kontinuierlich zu fabrizieren, wurde das Gas-Phase Verfahren erforscht.

Zuerst wurden Katalysatoren aus 15 Sorten Substanzen ausgearbeitet, indem diese entweder als Einzelkörper oder als Kombination eingesetzt wurden. In 122 Versuchen wurde auf das katalysatorische Vermögen gründlich untersucht. Dabei haben wir den geeignetesten Katalysator in der Zinksulfat-japanischer Säureerde-Kombination gefunden. Dieser besteht aus 3 Teilen Zinksulfats und 7 Teilen japanischer Säureerde. Dieser Ansatz wird unter Zusatz von Ammoniak angeteigt, zu Kugeln verarbeitet, und aktiviert. Das auf diese Weise behandelte Material entwickelt ausgezeichnetes katalysatorisches Vermögen und zeigt auch nach 246 Std langem kontinuierlichem Einsatz und Behandlung des 52 betragenden Alkohol-Durchsatzes fast kein Nachlassen an der Wirkung.

Unter Anwendung der Reaktionsröhre von mittelgrossem und grossem Format wurden 290 Male Versuche angestellt, um die optimalne Reaktionsbedingungen zu finden. Die durch

Tabelle X. Vergleich der mehreren Versuchsergebnisse von hohen Ausbeuten

Reaktionstemperatur °C	Ausbeute in % der einzelnen Fraktionen			
	～30 C	30～35 C	35～41 C	Summe
330～360	4.6	17.7	67	89.3
330～350	4.0	16.2	67	87.2
285～345	0.7	22.6	67.8	91.1
350～370	2.1	18.9	70	91.0
360～390	3.7	18.3	72.5	94.5
300～315	0	17.3	75.2	92.5

Reaktion erhaltenen rohen Olefine wurden einfach hinsichtlich der Siedepunkte in drei Gruppen eingeteilt, deren Ausbeute festgestellt wurde. Mehrere Sorten mit hohen Ausbeuten wurden beispielsweise in Tabelle X aufgestellt.

Daraus ist die Beurteilung entstanden, dass bei Fabrikation des Trimethyläthylens aus Isoamylalkohol die Ausführung der Reaktion bei 350°C und dergleichen die opimalen Ergebnisse ergibt. Darauf wurde die Reaktion von 4800 ccm Isoamylalkohol bei 350±3°C vorgenommen. Die dabei erhaltenen Reaktionsprodukte wurden durch solche verschiedene Methoden wie Fluoreszenz-Indikator Adsorptionsanalyse, Feindestillation, Infrarot-Absorptionsspektrum, Gaschromatographie usw., auf ihre Bestandteile geprüft, und zwar mit folgenden Ergebnissen: Trimethyläthylen, 74.77～75.14, Methyläthyläthylen, 19.96～20.06, und Isopropyläthylen, 4.78～4.80%.

Für diese dreien Olefine sind schon von Kistiaskowsky[2] zuverlässige thermodynamische Ergebnisse vorgebracht worden. Wir haben anhand dieser Ergebnisse nach folgender Formel theoretische Werte des Isomerisationsgleichgewichtes für die vorliegende Reaktion zu bildende Olefine gesucht.

$$\Delta F = -RT \ln K$$

worin ΔF: Innere Energie, R: Gaskonstante, K: Gleichgewichtskonstante, T: Absolute Temperatur.

Für ΔF haben wir die folgende von Kistiaskowsky gefundene Hydrierungswärme herangezogen.

	$-\Delta F$ (Cal./Mol.)	K bei 350°C
Trimethyläthylen-Methyläthyläthylen	1571	3.56
Trimethyläthylen-Isopropyläthylen	3416	15.8
Methyläthyläthylen-Isopropyläthylen	1845	4.44

Aus diesen Ergebnissen wird das theoretische prozentuale Verhältnis der Bildung für die Dreien wie folgt abgeleitet:

	Theoretische Werte (bei 350°C), %	Experimentelle Werte (bei 350°C), %
Trimethyläthylen	74.45	75.14
Methyläthyläthylen	20.91	20.06
Isopropyläthylen	4.64	4.80

Es ist sehr interessant, dass die genannten theoretischen Werte mit den von uns experimentell erhaltenen Ergebnissen ganz einwandfrei übereinstimmen. Diese Tatsache dürfte eine interessante Hinweisung auf den Mechanismus dieser Reaktion und die Eigenschaften des Katalysators, geben.

Das Bildungsverhältnis von den durch diese Arbeit erhaltenen Olefinen ist nämlich mit dem thermodynamisch zu findenden Verhältnis identisch. Mit anderen Worten, das stimmt mit dem thermodynamisch zu findenden stabilen Gleichgewichtszustand der Isomerisation überein. Die herrschende Annahme ist es, dass der Hauptbestandteil des zu entwässernden Isoamylalkohols Isobutylcarbinol sei, während die Gehalte an *gem*-Methyläthyläthylalkohol geringfügig seien.

Wenn die Entwässerung ohne Isomerisationsreaktion erfolgt, würde aus Isobutylcarbinol Isopropyläthylen und aus *gem*-Methyläthyläthylalkohol Methyläthyläthylen gebildet.

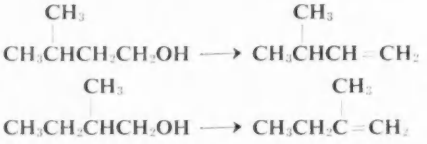

Da nun Isopropyläthylen und Methyläthyläthylen ebenfalls die Isomerisation in Trimethyläthylen mit sich bringen, entstehen die folgenden Formeln.

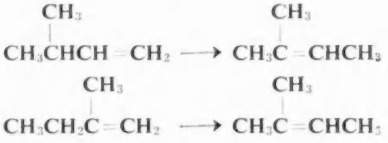

Nun wird die Orientierung dieser Isomerisation im allgemeinen thermodynamisch bedingt. Mit anderen Worten, dies besagt, dass das Unstabile ins Stabile isomerisiert wird. Die Reihenfolge der Stabilität ist nach Kistiakowsky wie folgendes: Trimethyläthylen > Methyläthyläthylen > Isopropyläthylen. Wenn diese Stabilität elektronentheoretisch betrachtet wird, so ist sie abhängig von dem Hyperkonjugationseffekt, wie Ingold[3] bereits erwähnt. Somit ist die Annahme der Isomerisation von Isopropyläthylen in Trimethyläthylen und von Isopropyläthylen in Methyläthyläthylen begründet.

Wenn jetzt ein anderer Gesichtspunkt genommen wird, nämlich über das Isomerisationsvermögen des Katalysators Betrachtung geübt wird, so ist es zu sagen, dass derjenige Katalysator, der Theorie übereinstimmende Isomerisationsverhältnis aufzeigt, der Ausgezeichnete ist. Die Tatsache, dass das Isomerisationsverhältnis mit dem theoretischen

2) G. B. Kistiaskowsky et al., *J. Am. Chem. Soc.* **57**, 65, 876 (1935); **58**, 137, 146 (1936); **59**, 831 (1937).

3) M. L. Dhar, E. D. Hughes, C. K. Ingold, A. M. M. Mandour, G. A. Mow and L. I. Woolf, *J. Chem. Soc.*, **1948**, 2093.

Zahlenwert identisch ist, wie es bei der vorliegenden Arbeit der Fall ist, liefert den Beweis dafür, dass das dabei eigesetze Zinksulfat ausgezeichnetes katalysatorisches Vermögen bei Entwässerungsisomerisation ausübt.

Aus den obigen Betrachtungen ist es anzunehmen, dass bei der vorliegenden Entwässerungsisomerisation das thermodynamische Isomerisationsgleichgewicht erreicht worden ist, indem unabhängig von Verunreinigungen des zu entwässernden Alkohols die gebildeten Olefine isomerisiert werden (obgleich es unklar ist, ob die Isomerisierung gleichzeitig mit der Entwässerung oder erst nach der erfolgten Bildung der Olefine geschieht).

Chemisches Institut der Technischen Fakultät der Universität zu Osaka
Miyakojima-ku, Osaka

Hot-atom Chemistry of Hexamminechromium(III) Nitrate in the Solid State

By Nagao IKEDA, Kenji YOSHIHARA, Hiroshi EBIHARA and Kiyomi SUZUKI

(Received November 21, 1960)

The hot-atom effect in trisethylenediaminechromium(III) nitrate[1,2] and hexamminecobalt-(III) nitrate[3] has been studied, but the same effect in hexamminechromium(III) nitrate has not yet been reported. Recently, the present authors succeeded in enriching ^{60}Co and ^{60m}Co recoil atoms produced in neutron-irradiated hexamminecobalt(III) nitrate with a high efficiency[4]. The method used by the authors was based on the heterogeneous extraction; the neutron-irradiated fine powders were shaken with a liquid which did not dissolve the target but dissolved the recoil species. As this method is very simple and rapid, it has sometimes been used for the enrichment of radioisotopes produced by (n, p)- and (n, α)-reactions[5,6]. In the case of (n, γ)-reaction[7], however, it does not usually give a high yield because of the short recoil range. Therefore the results in the previous paper were rather striking. In this paper, we investigated a similar heterogeneous extraction method on hexamminechromium(III) nitrate and discussed the mechanism of the extraction process. This complex is insoluble in concentrated nitric acid, but chromic ion and chromate or dichromate ion are soluble in it. Therefore, recoil atoms of ^{51}Cr should be extracted and enriched in the aqueous phase by shaking the target powder with concentrated nitric acid.

On the chemical form of the recoil chromium, some results heve already been reported; e.g., in the case of chromium azo-dye Palatine Fast Blue GGN[8], 83% of the radioactive chromium is present as chromium(III) and 11% of it as chromium(VI)*. In the present paper, chemical forms of recoil chromium atoms were also investigated.

Experimental

Target Material. — Hexamminechromium(III) nitrate was prepared by Mori's method[9].

Irradiation.—The cyclotron at the Institute of Physical and Chemical Research, Tokyo, and the nuclear reactor JRR-1 at the Japan Atomic Energy Research Institute were used for irradiation. The hot-atom effect of ^{55}Cr (half-life: 3.5 min.) was investigated by using the cyclotron, and that of ^{51}Cr (half-life: 27.8 day) by using the nuclear reactor. In the cyclotron, neutrons were generated by bombardment of beryllium with accelerated deuterons, and slowed down by a paraffin block. The neutron flux at the position of irradiation was about $10^6 \sim 10^7$ n/cm^2 sec.* The reactor, JRR-1 was operated at 50 kW/hr., and the neution flux

1) A. Turco and M. Scatena, *Ric. Sci.*, **25**, 2651 (1955).
2) A. Turco, *J. Inorg. Nucl. Chem.*, **13**, 200 (1960).
3) G. Kayas, *Bull. soc. chim. France*, **17**, 1145 (1950).
4) N. Ikeda, K. Yoshihara and N. Mishio, *Radioisotopes*, 8, 242 (1959).
5) E. Bleurer and W. Zünti, *Helv. Phys. Acta*, **20**, 195 (1947).
6) P. Jordan, *Helv. Chim. Acta*, **34**, 699, 715 (1951).
7) P. Süe and T. Yuasa, *J. chim. phys.*, **41**, 160 (1944).
8) N. Shibata and K. Yoshihara, This Bulletin, **32**, 422 (1959); K. Yoshihara, M. Arai and T. Ishimori, *Proceedings of the 3rd Isotope Conference of Japan*, S18 (1959).
* In this paper, Cr(III) represents chromic ion, and Cr(VI) represent chromate or dichromate ion.
9) M. Mori, *J. Chem. Soc. Japan, Pure Chem. Sec.* (*Nippon Kagaku Zasshi*), **74**, 253 (1953).
* Contribution of fast neutrons to the radioactivation did not exceed about 5%.

was of the order of 10^{11} n/cm² sec. at the irradiation**. Temperature at the position did not exceed about 50°C.

Measurement of Radioactivity.—As ^{55}Cr emitted only β-particles (2.85 MeV.), the radioactivity was measured by a GM-counter made by the Institute of Physical and Chemical Research, (end window type, mica window thickness: 1.4 mg./cm²). Radioactivity of ^{51}Cr was measured by a single channel γ-ray spectrometer made by the Atomic Instrument Co., Model 810A, (well type, NaI crystal, $1^3/_4'' \phi \times 2''$). γ-Ray of 0.32 MeV. of ^{51}Cr was measured at the photo-peak by this counter.

Measurement of Solubility of Hexamminechromium(III) Nitrate in Nitric Acid.—The solubility of hexamminechromium(III) nitrate in nitric acid was determined in advance. Each 0.2 g. of the sample was shaken with 25 ml. of nitric acid of various concentrations for two or four minutes at 20°C. Results are listed in Table I. The solubility was about 1 mg./25 ml. for the acidity of 8~12 N at 20°C, but it was slightly greater for 6 N. Therefore the acidity of 8~12 N is preferable for this extraction process.

TABLE I. SOLUBILITY OF HEXAMMINECHROMIUM-(III) NITRATE IN NITRIC ACID (20°C)

Concentration of HNO_3, N	Shaking time min.	Solubility, mg. $[Cr(NH_3)_6](NO_3)_3$/25 ml.
6	2	3.1
6	4	3.4
8	2	1.2
8	4	1.1
10	2	1.0
10	4	0.91
12	2	0.89
12	4	0.89

Determination of Chromium.—Amounts of extracted chromium in the liquid phase were determined colorimetrically. After the liquid phase was centrifuged, the complex salt in it was destroyed by boiling with concentrated nitric acid repeatedly, and tervalent chromium was oxidized to the sexivalent state with silver peroxide and the amounts of sexivalent chromium were determined by the diphenylcarbazide method[10]. The enrichment factors, E were calculated by the following formula:

$$E = \frac{a}{a_t} = \frac{M}{m} Y$$

where a and a_t denote specific activities in the liquid phase and in the irradiated complex salt before the process, respectively. M and m denote the amounts of chromium in the original salt and in the liquid phase, respectively. Y is the yield of ^{51}Cr in the liquid phase.

Extraction of Enriched ^{55}Cr.—About 1 g. of hexamminechromium(III) nitrate was bombarded with neutrons produced by the cyclotron for about an hour or two. After irradiation, the target was divided into two portions. One was subjected to the measurement of radioactivity by a GM-counter tracing its decay (Sample I), and the other to the extraction of ^{55}Cr with 20~50 ml. of 8 N nitric acid in an Erlenmeyer flask by being shaken vigorously for 2 min. After the extraction and centrifugal separation, the solid was washed with ethanol and dried in air. Its radioactivity was measured by a GM-counter tracing its decay (Sample II). Samples I and II were weighed, and the retention was calculated from the ratio of the specific activities of the two samples at the same time. The extraction yield was given by subtracting the retention value from 100%. The results are listed in Table II. The extraction yield higher than 60% was obtained and the enrichment factor of 200~400 was obtained. The enrichment of ^{55}Cr has been attained by these simple and rapid procedures.

Preparation of Enriched ^{51}Cr.—Enrichment of ^{51}Cr was studied in the same way as in the case of ^{55}Cr. About 1 g. of the sample was irradiated in the pneumatic tube in the nuclear reactor for 2 hr. After irradiation, the sample was shaken with 50 ml. of 8 N nitric acid in an Erlenmeyer flask for 2 min. After being centrifuged from the solid, an aliquot of the liquid phase was subjected to the measurement of radioactivity by a γ-ray spectrometer. The solid was dissolved in water, and the radioactivity of an aliquot of the solution was measured by a γ-ray spectrometer. The yield of ^{51}Cr was calculated from these values. The results are shown in Table III. A yield of 57~73% was obtained. The enrichment factor was 24~41 which was much lower than the values of ^{55}Cr.

Extraction Curves on Repeated Extraction.—In order to investigate the extraction mechanism, extraction curves on repeated extractions were observed. An outline of the procedures for the repeated extractions is illustrated in Fig. 1. About 0.2 g. of the sample was irradiated in the pneumatic tube in JRR-1, and treated according to the

TABLE II. PREPARATION OF ENRICHED CHROMIUM-55

Amount of target, g.	Irradiation time, hr.	Integrated deuteron current, μA·hr.	Volume of 8 N HNO_3 ml.	Radiochemical yield %	Enrichment factor
1.292	2	20	50	86	230
0.972	2	20	25	66	240
1.270	1	14	20	61	400

** Contribution of fact neutrons to the radioactivation did not exceed about 5%.

10) M. Tanaka, This Bulletin, 23, 165 (1950); E. B. Sandell, "Colorimetric Determination of Traces of Metals", 2nd Ed., Interscience Pub. (1950), p. 260.

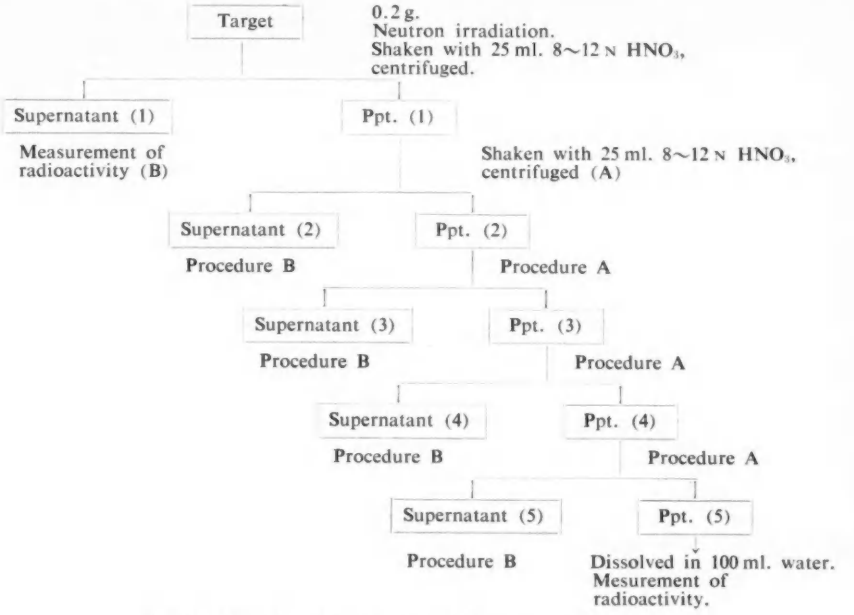

Fig. 1. Procedures in repetition of the extraction.

TABLE III. PREPARATION OF ENRICHED CHROMIUM-51

Amount of target, g	Vol. of 8N HNO_3 ml.	Radiochemical yield %	Enrichment factor
1.0	50	57	24
1.0	50	73	41

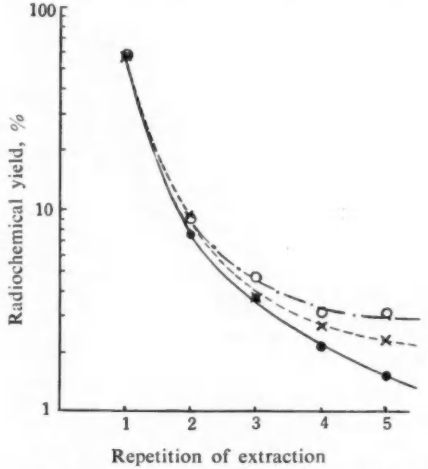

Fig. 2. Relationship between the radiochemical yield and the repetition of extraction (nitric acid only).
—●— 8 N HNO_3 -·-○-·- 12 N HNO_3
···×··· 10 N HNO_3

procedures shown in Fig. 2, where the values of extraction yield at 20°C are plotted against the repetition number of extraction. The extraction yield was very large at the first extraction, and decreased first rapidly and then slowly. As is shown in Fig. 2, tails of the extraction curves are higher with the increasing concentration of nitric acid. The total extraction yield of five fold extraction is shown in Table IV. These values increase

TABLE IV. TOTAL RADIOCHEMICAL YIELD OF CHROMIUM-51 ON REPEATED HETEROGENEOUS EXTRACTIONS

Series	8 N HNO_3 %	10 N HNO_3 %	12 N HNO_3 %
No. 1	71.4	73.8	75.0
No. 2	70.5	71.0	74.5
No. 3	63.6	72.5	78.1

with the increasing concentration of nitric acid. In all experiments mentioned above, nitric acid was used for extraction. Howevere, as the target material is slightly soluble in nitric acid, it is necessary to investigate whether this small solubility plays an important role on the extraction process or not. Nitric acid solution saturated with hexamminechromium(III) nitrate was used as an extracting agent in order to suppress the dissolution of the target. The results are shown in Fig. 3. As a whole, no large difference is found between the results in Figs. 2 and 3, but the tails of the extraction curves seem to be slightly affected by using nitric acid saturated with the complex salt. All the extraction curves in Fig. 3 are similar in shape.

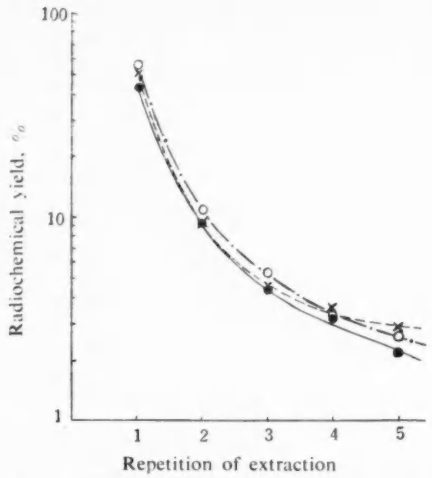

Fig. 3. Relationship between the radiochemical yield and the repetition of extraction (nitric acid saturated with hexamminechromium(III) nitrate).
—●— 8 N HNO_3 –·–○–·– 12 N HNO_3
···×··· 10 N HNO_3

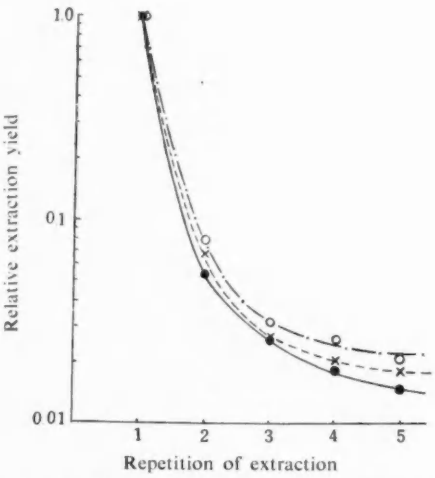

Fig. 4. Effects of shaking time on the extraction. 8 N HNO_3 was used for the extraction; shaking time: —●— 1 min. –·–○–·– 10 min. ···×··· 6 min.

The effect of shaking time on the extraction yield was investigated, using 8 N nitric acid without addition of the complex salt as the extracting agent. The sample was shaken for 6 or 10 min. The results are shown in Fig. 4. The tails of the extraction curves become higher with the increase of shaking time.

Determination of Enrichment Factors. — To calculate the enrichment factor of ^{51}Cr in each extract, chromium was determined colorimetrically as described before. The results are listed in Table V. The chromium found in the aqueous phase is derived from the dissolved complex salt or of radiation- and thermal-decomposition of the complex salt in the reactor. In Table V, "amount of chromium" (in 25 ml. extract) represents the amount of chromium calculated in the form of the complex salt. Comparing the amounts of chromium in Table V with those of dissolved chromium in Table I, it is shown that the solubility of the irradiated complex salt was much greater than that of the salt before irradiation. Even if radiation- and thermal-decomposition of the compolex in the reactor was considered, this could not account for the increase of the amount of chromium in the aqueous phase. At the first extraction, the enrichment factor was the largest, and it fell down with the repetition of extraction. The effect of concentration of nitric acid is distinctly seen on the fourth and the fifth extraction in the table.

TABLE V. ENRICHMENT FACTORS OF CHROMIUM-51 ON EACH EXTRACTION

Extraction number		Amount of chromium, mg. $[Cr(NH_3)_6]\cdot(NO_3)_3$	Enrichment factor
8 N HNO_3	1	5.4	20
	2	2.8	5.4
	3	2.7	2.8
	4	3.0	1.5
	5	3.7	0.9
8 N HNO_3	1	5.6	20
	2	2.9	6.5
	3	2.5	3.2
	4	2.4	2.4
	5	2.1	2.3
8 N HNO_3	1	5.8	20
	2	3.0	5.5
	3	1.8	5.5
	4	1.9	3.7
	5	2.0	3.4

As dissolution of a small amount of the target is inevitable, the enrichment factor drops more or less in the heterogeneous extraction. Therefore, the enrichment factor of chromic ion which is the predominant species produced by the hot-atom effect was determined by the following procedures. The irradiated target was dissolved in water and an iron(III) carrier as well as chromate ion as a hold-back carrier was added to the solution. Ammonia was added to the mixture to precipitate ferric hydroxide with which chromic ion coprecipitates. After being washed with a very dilute aqueous ammonia, the precipitate was dissolved in hydrochloric acid and again ferric hydroxide was precipitated with ammonia. After being washed the precipitate was dissolved in 9 N hydrochloric acid, and the solution was extracted twice tri-*n*-butyl phosphate to remove the iron. The aqueous phase was washed twice with benzene to remove tri-*n*-butyl phosphate. The chromium content in the aqueous phase was determined colorimetrically. The enrichment factor of $^{51}Cr(III)$ thus obtained was 150~230. As an enrichment factor of 20 was

obtained at the first extraction in Table V, dissolution of target material plays an important role in diminishing the enrichment factor of ^{51}Cr in the heterogeneous extraction.

Determination of Chemical Forms of Recoil Products.— In the hot-atom effect of chromium complex salts, formation of chromate ion besides chromic ion was observed[8]. Harbottle[11] suggested that ammonium ion might act as a reducing agent on the recoil event in chromate. As hexamminechromium(III) nitrate has six ammonia molecules in it, it was considered interesting to note whether sexivalent chromium was formed in the target or not.

This was investigated in the following way. At first, the percentage of chromium(III) was determined. After adding 10 mg. of iron(III) carrier as well as 20 mg. of chromate as a hold back carrier to the aqueous solution of the irradiated target, ammonia was added to this mixture to precipitate ferric hydroxide. By this procedure, $[Cr(NH_3)_6](NO_3)_3$ and chromium(VI) were not precipitated while chromium(III) was coprecipitated with ferric hydroxide almost completely. The precipitate was separated and the radioactivity was measured by a γ-ray spectrometer.

Next, formation of chromium(VI) was tested by the following two methods; one is based on the precipitation of lead chromate in the presence of chromic ion as a hold-back carrier, and the other on the extraction of chromate with tri-*n*-butyl phosphate[5]. The latter method was preferable because of its exactness, and was adopted to determine the percentage of chromate. The aqueous solution of the irradiated target was made to 1 N by hydrochloric acid, and it was extracted with tri-*n*-butyl phosphate. Chromate was extracted into the tri-*n*-butyl phosphate phase, while the complex salt and chromic ion were left in the aqueous phase. The radioactivity of the organic layer was measured by a γ-ray spectrometer. Thus the distribution of the chemical forms of the recoil products were determined; chromium(III) fraction 98~99%, chromium(VI) fraction $<0.2\%$ and the retention 1~2%.

Measurement of the Surface Area of the Target*.— The surface area of the target was measured by the nitrogen adsorption method before and after irradiation. Before irradiation, the mean grain size of 140~300 mμ was obtained, and this value was not substantially changed by irradiation.

Discussion

On heterogeneous extraction of recoil atoms in hexammimechromium(III) nitrate, extraction curves were affectd neither by concentration of nitric acid, nor by the extraction time. Therefore the extraction mechanism in this method is considered to be mainly due to the surface process, because if the leaching process from the interior part of the target were a principal feature, great changes would be brought about in the extraction curve by changing the concentration of nitric acid or the extraction time. However, the tail of the extraction curve becomes higher at the higher concentration of nitric acid or at the longer extraction time. These results may be interprete by assuming that the leaching process more or less contributes to the whole process.

If the surface process were a predominant one, the following problems would arise. (1) How does the slight dissolution of hexamminechromium(III) nitrate into nitric acid affect the whole process? The previous experiment will furnish an answer to this problem. The extraction curve is not markedly changed even though the extraction is done with the use of nitric acid saturated with the complex salt. Perhaps this shows that slight dissolution of the target in the aqueous phase does not markedly affect the whole process of the extraction. (2) In order to obtain a large extraction yield such as several times ten per cent by the surface process, the grain size of the target must be vevy small and must be of the comparable order to the recoil range[12]. However, the mean grain size of the target used in these experiments was 140~300 mμ (This value was not substantially changed by irradiation.). This value is much greater than the value of 10 mμ or less which is considered to be a recoil range of the (n, γ)-reaction. How is this fact interpreted?

It is difficult to solve this problem clearly, but we may assume as follows: Hexamminechromium(III) nitrate is relatively unstable to heat and is apt to be decomposed beyond 100°C. In the case of the ^{50}Cr (n, γ) ^{51}Cr reaction, the recoil energy of the order of 300 eV. is dissipated in the neighborhood of the recoil atom, and therefore high temperature appears locally around it. For example, Harbottle[13] suggested that several thousands of atoms around the recoil atom attain to several hundred degrees in a molecular crystal. The thermal decomposition by heat liberated locally is considered to be very probable in this case. Chromium nitrate and ammonia molecules would be irregularly present in this "thermal spike". This part would be easily dissolved into the aqueous phase on contact with nitric acid. This part may be considered to be the path to nitric acid. A recoil atom present in this "thermal spike" would be expected to be carried into the nitric acid solution on extraction, and a crack which reaches the

11) G. Harbottle, *J. Chem. Phys.*, **22**, 1083 (1954).

* This measurement was carried out by Dr. Izumi Higuchi of the Tohoku University.

12) J. Pauley and P. Süe, *J. phys. radium*, **18**, 22 (1957).

13) G. Harbottle and N. Sutin, *J. Phys. Chem.*, **62**, 1344 (1958).

surface after irradiation or on the extraction may be possible. Since ammonia is produced by decomposition of the complex salt, local high pressure may appear in the neighborhood of the "thermal spike". Calculating from the data of the recoil energy of the (n, γ)-reaction and the dissociation energy of the complex salt, ammonia molecules of the order of 10^4 must be present around the "thermal spike". This high pressure may be apt to make a crack at the time of the extraction.

Owing to a thermal spike and/or a crack, the recoil atom would be extractable beyond the recoil range. A similar explanation is possible in the case of the hot-atom effect in hexamminecobalt(III) nitrate.

The heterogeneous extraction is applicale to the rapid separation of recoil atoms. Especially, it is very effective to separate the radioisotope such as ^{55}Cr which has a very short half-life. However, a very high enrichment factor is not expected by this method.

The authors wish to express their hearty thanks to Dr. Kenjiro Kimura, the Director of the Japan Atomic Energy Research Institute for his kind guidance and encouragement throughout this work, to Dr. Izumi Higuchi, Professor of Tohoku University for the measurement of the surface area of the target, to the members of the cyclotron group at the Institute of Physical and Chemical Research, Tokyo, for the bombardment of the samples, and also to Mr. Michimasa Arai for his helpful assistance. A part of the expense for this work was defrayed by a grant from the Ministry of Education, to which the authors' thanks are due.

Tokyo University of Education
Otsuka, Tokyo (N. I. & K. S.)

Japan Atomic Energy Research Institute
Tokai-mura, Ibaragi-ken (K. Y. & H. E.)

Spectroscopic Studies on Molecular Configurations of Some Aliphatic Dinitriles. I. Infrared Spectra of Succinonitrile and Bis(succinonitrilo)copper(I) Nitrate

By Ikuo MATSUBARA

(Received April 24, 1961)

Although the infrared spectra of many substances with polymethylene chains of the type $X-(CH_2)_n-X$ have been studied in relation to their molecular configurations[1], no detailed spectroscopic studies seem to have been made on the series of aliphatic dinitriles except for the case of succinonitrile[2,3]. An interpretation of the spectra of such compounds is always a difficult problem because of the complexity caused by the existence of a number of rotational isomers. By the use of low-temperature techniques, however, the spectra of single rotational isomers in the crystalline solid state may be obtained. It is true that the spectra in the solid state may be explained in part by comparing them with those of like molecules, but it would be of great value if the direct determination of their molecular configurations in the crystalline solid state could be made by other physical methods such as by X-ray crystal structure analysis. Incidentally aliphatic dinitriles form stable copper(I) complexes of the type $[Cu\{NC-(CH_2)_n-CN\}_2]NO_3$ ($n=2, 3\cdots$)[4]. The crystal structures of the first few members of this homologous series were studied recently by X-ray method and the configuration of the ligand dinitrile molecule in the crystals of each complex was determined[5-7]. The infrared spectra of these complexes, which may be analyzed on the basis of these results, would supply much useful data for the complete understanding of the spectra of dinitrile molecules. Naturally a rigorous analysis of the spectrum of a complex compound would be a complicated problem. Therefore, it should

1) N. Sheppard, "Advances in Spectroscopy", Ed. by H. W. Thompson, Vol. I, Interscience Publishers Inc., New York (1959), p. 288; see the references cited there.
2) W. E. Fitzgerald and G. J. Janz, *J. Molec. Spectroscopy*, **1**, 49 (1957).
3) I. Nakagawa and K. Tokumaru, Private communication.
4) H. H. Morgan, *J. Chem. Soc.*, **123**, 2901 (1923); H. Rath, H. Rehm, H. Rummler and E. Specht, *Melliand Textilber.*, **38**, 431, 538 (1957).
5) Y. Kinoshita, I. Matsubara and Y. Saito, This Bulletin, **32**, 741 (1959).
6) Y. Kinoshita, I. Matsubara and Y. Saito, ibid., **32**, 1216 (1959).
7) Y. Kinoshita, I. Matsubara, T. Higuchi and Y. Saito, ibid., **32**, 1221 (1959).

first be assumed that the interaction forces between the ligand molecules are so small that the main features of the spectrum may be explained from the consideration of an isolated ligand molecule[8].

This paper will report on the study of the infrared spectrum of bis(succinonitrilo)copper-(I) nitrate, $[Cu(NC-CH_2-CH_2-CN)_2]NO_3$, in connection with the configuration of the ligand succinonitrile. The result of X-ray analysis[5] shows that in the crystals of this complex the ligand succinonitrile molecule is coordinated tetrahedrally with its nitrogen atoms of both ends to two different copper atoms and takes the gauche configuration. Therefore, the infrared data of this complex may be of interest in relation to the results of the spectroscopic studies on succinonitrile by Fitzgerald and Janz[2], and Nakagawa and Tokumaru[3], who concluded that this molecule exists as a mixture of two rotational isomers, trans and gauche, the latter being the more stable configuration at low temperatures. The spectral changes due to decomposition of the complex as a result of interaction with alkali halides have been of help in assigning the vibrational frequencies of succinonitrile. The assignments of the skeletal deformation vibrations were successfully carried out on the basis of the result of a normal coordinate treatment.

Experimental

The method of preparation and the properties of bis(succinonitrilo)copper(I) nitrate are as described in the previous paper[5].

The infrared spectra of the complex and of succinonitrile in the 4000~400 cm^{-1} region were obtained using a Perkin-Elmer Model 21 and a Perkin-Elmer Model 13 spectrophotometer (with sodium chloride and potassium bromide optics, respectively). Spectra in the cesium bromide region were also obtained using a Perkin-Elmer Model 21 spectrophotometer*. The spectrum of succinonitrile was recorded at room temperature and at −50°C. A low-temperature transmission cell of the type described by Nukada[9] was used to obtain the spectra at low temperatures. The results shown in Figs. 1a and 1b are essentially the same as those obtained by Fitzgerald and Janz[2]. The spectrum of the complex was obtained using both Nujol mull and potassium bromide disk techniques. Nujol mulls of the complex gave different spectra depending on the type of alkali halide cell windows used as supporting plates. The spectrum obtained by using KRS-5 plates and that obtained by using sodium chloride plates were at first identical with each other, but the latter soon began to change gradually with time. This suggests that some interaction exists between the complex and sodium chloride plates. When potassium bromide plates were used the reaction occurred so rapidly that the spectrum changed while it was being recorded. These changes are clearly seen in Fig. 2. The spectrum in Fig. 2a is that obtained by using KRS-5 plates. The spectra in Figs. 2b and 2c are those obtained respectively by the use of sodium chloride and potassium bromide plates. (These were recorded after the specimens had been placed in the laboratory for one day.) These two spectra are in some respects different from each other, showing that the reaction products are not the same in the two cases. The spectrum obtained from a potassium bromide disk of the complex is shown in Fig. 3, which agrees quite well with that obtained from a Nujol mull by the use of potassium bromide plates (Fig. 2c). This means that the same type of reaction occurred between the complex and potassium bromide in the two cases. The absorption frequencies of succinonitrile and bis(succinonitrilo)copper(I) nitrate are listed in Table I together with the assignment.

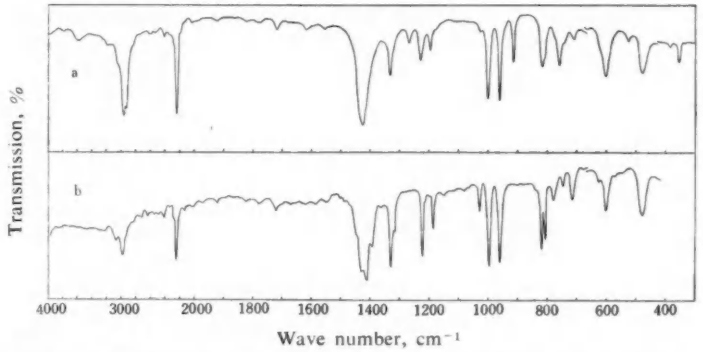

Fig. 1. Infrared spectra of succinonitrile. (a) at room temperature; (b) at −50°C.

8) See for example: F. A. Cotton, "Modern Coordination Chemistry", Ed. by J. Lewis and R. G. Wilkins, Interscience Publishers Inc., New York (1960), Chapter 5.

* By the courtesy of Government Chemical Industrial Research Institute of Tokyo.

9) K. Nukada, *J. Chem. Soc. Japan, Pure Chem. Sec.* (*Nippon Kagaku Zasshi*), **80**, 218 (1959).

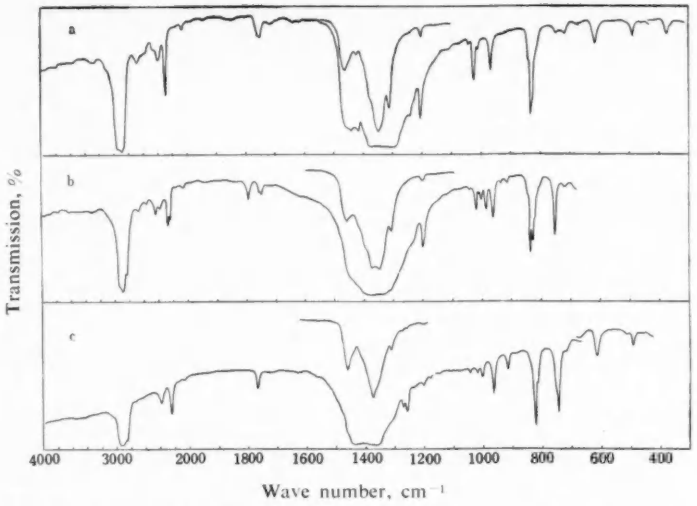

Fig. 2. Infrared spectra obtained from Nujol mulls of bis(succinonitrilo)copper(I) nitrate by using (a) KRS-5, (b) sodium chloride and (c) potassium bromide supporting plates.

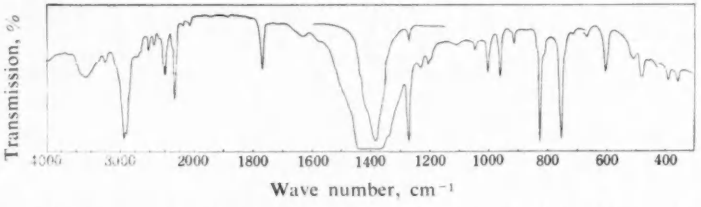

Fig. 3. Infrared spectrum obtained from a potassium bromide disk of bis(succinonitrilo)-copper(I) nitrate.

In Table II are included the absorption frequencies due to the nitrate ion in the complex.

Results and Discussion

The spectral simplification that occurred when succinonitrile was cooled down to -50°C is clearly seen in Fig. 1. In the 1400~400 cm^{-1} region there are four absorption bands that disappear at low temperatures. Fitzgerald et al.[2] and Nakagawa et al.[3] assigned these bands, which are at frequencies of 1271, 917, 761 and 527 cm^{-1}, to the vibrations of the trans form (symmetry C_{2h}) and assigned all the remaining bands to the vibrations of the gauche form (symmetry C_2). As long as the ligand succinonitrile takes the gauche form in the crystals of bis(succinonitrilo)copper(I) nitrate[5], the spectrum of this complex should be closely correlated with that of succinonitrile at low the temperatures. In complete agreement with expectation, the Nujol mull spectrum of the complex (Fig. 2a) corresponds well with the low-temperature spectrum of succinonitrile (Fig. 1b) except for the regions where absorptions due to nitrate vibrations or skeletal vibrations of the complex take place. The fact that no absorptions occur at the four frequencies which were ascribed by the previous authors[2,3] to the vibrations of the trans form gives additional support to their conclusion. On the other hand, the spectra in Figs. 2b, 2c and 3 have absorptions corresponding to the trans vibrations and show spectral features similar to that of succinonitrile at room temperature (Fig. 1a). This means that splitting of copper-nitrogen coordinate bonds occurred and succinonitrile was isolated as a result of the interaction between the complex and alkali halides. The intense bands observed at 1348 and 830 cm^{-1} in Fig. 2a must be ascribed to infrared active fundamentals of the nitrate ion in the complex. The weak doublet with peaks at 1757 and 1751 cm^{-1} must be a certain combination band of the nitrate ion, because some

TABLE I. INFRARED ABSORPTION BANDS OF SUCCINONITRILE AND BIS(SUCCINONITRILO)-COPPER(I) NITRATE

Succinonitrile		Bis(succinonitrilo)copper(I) nitrate		Assignment	
Solid (Room temp.)	Solid (−50°C)	Nujol mull[a)]	KBr disk	Gauche(C_2)	Trans(C_{2h})
		3300 vw	3322 vw sh		
	3226 vw				
3205 w			3205 w		
3058 mw sh	3067 mw				
2985 vs	2994 m		2950 s	C–H stretch.	C–H stretch.
2950 s sh	2959 w sh		2924 s	C–H stretch.	C–H stretch.
2849 vw sh	2849 vw				
			2786 w		
	2732 w	2725 vw sh	2740 vw sh		
		2681 mw			
2646 vw sh	2639 w				
2597 vw	2611 vw		2611 w		
2558 vw	2545 vw	2564 w sh	2551 w		
	2494 vw				
			2475 vw		
	2445 vw	2451 w sh			
2427 w	2421 w		2415 mw sh		
		2398 mw	2398 m		
	2283 w sh	2283 ms	2283 w sh	C≡N stretch. (bound)	
2257 vs	2257 s		2257 ms	C≡N stretch. (free)	C≡N stretch.
2203 vw sh	2203 vw				
2151 vw	2141 w		2155 vw		
2045 vw	2041 vw	2066 w	2066 vw		
		1942 vw	1942 vw		
1923 vw	1923 w				
			1883 vw		
1825 vw	1825 w				
1786 vw	1786 w				
1721 w	1721 mw	1709 vw			
1621 w		1639 vw			
		1613 vw			
	1590 w		1570 vw sh		
1558 w	1550 w	1538 vw sh			
	1445 mw sh				
1425 vs	1431 vs sh			B CH_2 bend.	B_u CH_2 bend.
1416 s sh	1414 vs	1418 ms	1410 m sh	A CH_2 bend.	
	1395 m sh				
	1361 w				
1337 ms	1332 s	1310 vs	1339 s sh	B CH_2 wag.	
1323 w sh	1319 m sh		1307 m sh		
1271 mw			1272 s		B_u CH_2 wag.
1231 ms	1225 s	1242 m sh	1232 w	A CH_2 wag.	
1198 m	1189 m	1202 ms	1206 w	A CH_2 twist.	(A_u CH_2 twist.)
			1199 w sh		
1179 vw sh					
	1152 w				
		1105 vw	1111 vw		
	1081 w	1074 vw			
1027 w	1032 m	1021 m	1021 vw	A C–C stretch.	
1001 s	999 vs	1010 w	1003 m	B C–CN stretch.	

TABLE I. (Continued)

Succinonitrile		Bis(succinonitrilo)copper(I) nitrate		Assignment	
Solid (Room temp.)	Solid (−50°C)	Nujol mull[a]	KBr disk	Gauche(C_2)	Trans(C_{2h})
962 s	963 vs	966 m	963 m	A CH_2 rock.	
	954 mw sh				
			929 vw		
917 ms			917 w		B_u C-CN stretch.
839 vw sh	842 w sh	837 mw sh	838 w sh		
818 ms	820 s	826 ms sh		B CH_2 rock.	
813 ms sh	810 ms	813 mw sh	812 w sh	A C-CN stretch.	
776 vw sh	780 m			603+170[b]	
761 ms			754 s		A_u CH_2 rock.
746 mw sh	750 mw	746 w		385+356	
714 mw	718 m	719 w	714 vw	480+235[c]; 2×356	
668 vw			667 vw		528+145[d]
623 w sh	628 w				
603 ms	603 ms	615 m	602 m	B C-C-C bend.	
578 vw sh	576 vw				
			524 vw sh		
527 w			509 w		B_u C-C-C bend.
480 ms	483 ms	490 mw	480 mw	A C-C-C bend.	
		458 vw			
385 w			389 w	A C-C≡N bend.	A_u C-C≡N bend.
		(369 mw)			
356 m		360 w sh	356 w	B C-C≡N bend.	

a) KRS-5 supporting plates were used to obtain the spectrum.
b) Raman frequency for the A C-C≡N bending mode of the gauche form.
c) Raman frequency for the B C-C≡N bending mode of the gauche form.
d) Calculated frequency for the B_u C-C≡N bending mode of the trans form.

TABLE II. INFRARED ABSORPTION BANDS DUE TO NITRATE IONS IN BIS(SUCCINONITRILO)-COPPER(I) NITRATE

Nujol mull			KBr disk	$NaNO_3$[b]	KNO_3[b]
KRS-5[a]	NaCl[a]	KBr[a]			
	1795 mw			1790 vw	
		1770 m	1770 m		1767 vw
1757/51 mw	1757/51 mw				
		1377 vs	1381 vs		1380 vs
	1375/51 vs			1358 vs	
1348 vs					
1043 w	1043 vw	1047 w	1048 w	—	—
	836 ms			836 m	
830 s	830 ms				
		824 s	826 s		824 m

a) Denotes the type of alkali halide cell windows used to support the mull.
b) See Ref. 10 in text.

inorganic nitrates show weak absorptions in this region[10]. As a result of reaction with sodium chloride these nitrate bands have decreased in their intensities and new absorptions appeared at 1795, 1375/51 and 836 cm^{-1} as shown in Fig. 2b. The reaction with potassium bromide caused the appearance of new bands at 1770, 1377 (or 1381) and 824 (or 826) cm^{-1} as shown in Figs. 2c and 3. These new bands observed in the two cases correspond quite well with those of sodium nitrate and potassium nitrate, respectively (see Table II). Considering these results the reaction of the complex with alkali halides should be ascribed largely

10) F. A. Miller and C. H. Wilkins, *Anal. Chem.*, **24**, 1253 (1952).

to an ion interchange between the two phases. A weak band observed at 1043 cm^{-1} in the spectrum of the complex may correspond to an infrared inactive frequency of the nitrate ion which may have become active due to the effect of the crystalline field of the complex.

The remaining bands of the complex are assigned to the vibrations of the gauche form of succinonitrile with reference to the results of the previous authors[2,3]. Thus the bands observed at 1310 and 1242 cm^{-1} should be assigned to the B and A CH_2 wagging modes, respectively. The bands at 1202 cm^{-1} should correspond to the A CH_2 twisting mode. On the other hand, the B CH_2 twisting mode remains unidentified. According to the result of the normal coordinate treatment by Nakagawa et al.[3] the B CH_2 twisting mode should have a frequency lower than that of the A counterpart, but no appropriate band is found either in the spectrum of the complex or in that of succinonitrile. The weak band at 1027 cm^{-1} and the strong band at 1001 cm^{-1} in the spectrum of succinonitrile are assigned to the A C–C stretching and the B C–CN stretching modes, respectively. This is in agreement with the expectation that a symmetrical skeletal stretching mode is generally weaker than an asymmetrical one in the infrared spectrum. The Raman counterparts of these bands are found at frequencies of 1027 and 1006 cm^{-1} (see Table VIII in Appendix). The fact that the former is much stronger than the latter supports the above assignment because a totally symmetric vibration is expected to be strong in the Raman spectrum. At low temperatures the 1027 cm^{-1} band increases in intensity relative to the 1001 cm^{-1} one (Fig. 1b), showing that the A C–C stretching mode is susceptible to the effect of crystalline field. In the spectrum of the complex a relatively strong band is observed at 1021 cm^{-1}. This band may be assigned to the A C–C stretching mode. To the B C–CN stretching mode may correspond the weak band at 1010 cm^{-1}. The fact that the intensity relation of these two bands is reverse to what is observed in the case of succinonitrile seems not to be in harmony with this assignment, but we may tentatively ascribe it to the effect of the crystalline field of the complex. The strong band at 966 cm^{-1}, which corresponds to the 962 cm^{-1} band in succinonitrile, is assigned to the A CH_2 rocking mode. The 818 cm^{-1} band of succinonitrile with a shoulder at 813 cm^{-1} splits into two components at low temperatures as shown in Fig. 1. One of the components at 820 cm^{-1} is ascribed to the B CH_2 rocking mode and the other at 810 cm^{-1} to the A C–CN stretching mode. In the spectrum of the complex no well-defined band maxima corresponding to these vibrations are observed, due to overlapping by the strong nitrate band at 830 cm^{-1}. However, the shoulder bands at 826 and 813 cm^{-1} are assigned with confidence to the B CH_2 rocking and the A C–CN stretching modes, respectively. The CH_2 rocking frequencies of 1, 2-disubstituted ethanes are known to change conspicuously depending on the azimuthal angle of internal rotation, and therefore can be used to determine the molecular configurations of rotational isomers[11]. The azimuthal angle of internal rotation of succinonitrile in the crystals of the complex has been determined by X-ray analysis to be 53° taking the cis position as the origin[5]. The gauche angle of free succinonitrile must be close to this value, for the two CH_2 rocking frequencies of this molecule agree quite well with the corresponding values of the complex. This conclusion is also in good agreement with what is expected from the calculated frequencies of these vibrations[3].

Assignment of the skeletal deformation vibrations are made with reference to the result of a normal coordinate treatment (see Appendix). The 615 and 490 cm^{-1} bands of the complex correspond each to the 603 and 480 cm^{-1} bands of succinonitrile which are assigned to the B and A C–C–C bending modes, respectively. The weak band at 527 cm^{-1} of succinonitrile which disappears at low temperatures and has no counterpart in the spectrum of the complex (Fig. 2a) corresponds to the B_u C–C–C bending mode of the trans form. The bands at 385 and 356 cm^{-1} of succinonitrile are assigned to the A and B C–C≡N (out-of-plane) bending modes of the gauche form, respectively. The 385 cm^{-1} band may also have some contribution from the A_u C–C≡N out-of-plane bending mode of the trans form. As shown in Fig. 2a the spectrum of the complex has an absorption band at 369 cm^{-1} which probably corresponds to the Cu–N stretching mode, and the shoulder band at 360 cm^{-1} may be correlated with the B C–C≡N bending mode. The absorption corresponding to the A C–C≡N bending mode is not observed, probably due to the overlapping by the 369 cm^{-1} band. The B_u C–C≡N in-plane bending mode of the trans form has a calculated frequency of 145 cm^{-1}, while the A and B C–C≡N (in-plane) bending modes of the gauche form have calculated frequencies of 178 and 247 cm^{-1}, respectively (see Table VIII in Appendix). The values for the gauche form are in good agreement with the observed Raman frequencies, while the infrared data in the region below 300 cm^{-1} are

11) I. Nakagawa, *J. Chem. Soc. Japan, Pure Chem. Sec. (Nippon Kagaku Zasshi)*, **76**, 813 (1955).

not available for this investigation. The fact that the C–C–C bending modes of nitriles such as acrylonitrile[12], malononitrile[13] and propionitrile[14] always appear in a region as high as 600~450 cm^{-1} and that the C–C≡N (in-plane) bending modes lie in a region as low as 250~150 cm^{-1} suggests that there must be considerable mixing of the two bending coordinates in these skeletal deformation vibrations and no single coordinate may be associated with the individual frequencies. Calculation of the potential energy distributions for the skeletal deformation vibrations has shown that the energies associated with the C–C–C bending and the C–C≡N (in-plane) bending motions are of the same order in these two types of vibration (see Appendix). In the spectrum of succinonitrile there are three absorptions in the 800~700 cm^{-1} region other than that corresponding to the CH_2 rocking mode of the trans form. These bands with peaks at 780, 750 and 718 cm^{-1} are observed to increase remarkably in their intensities at low temperatures (Fig. 1b). As Fujiyama and Shimanouchi[15] suggested, these may be attributed to overtones or combinations of some skeletal deformation vibrations of the gauche form. The proposed assignments for these vibrations are included in Table I.

The sharp band observed at 2283 cm^{-1} in the Nujol mull spectrum (Fig. 2a) may correspond to the C≡N stretching vibration of the complex. The C≡N vibrational shift of 26 cm^{-1} towards higher frequencies as compared with the free succinonitrile may be understood by considering the structure of the complex. X-Ray analysis of this complex[5] has revealed that the carbon-nitrogen bond distance is 1.14 Å and that the Cu–N–C–CH_2 group is close to linear, from which it is expected that the carbon-nitrogen bond is essentially of a triple-bond character, the contributions of polar resonance structures such as $-C^+=N^-$ being decreased, and the C≡N stretching frequency is thereby increased. Califano et al.[16] have shown that in the cases of nitriloxides, R–C≡N→O, the C≡N stretching frequencies are about 70 cm^{-1} higher than those of the corresponding nitriles and have explained this as due to the coupling with the N→O stretching vibration. In the case of this complex the effect of the interaction between the C≡N stretching and the Cu–N stretching vibrations, though small, may also contribute to the increase in the C≡N stretching frequency.

12) F. Halverson, R. F. Stamm and J. J. Whalen, *J. Chem. Phys.*, **16**, 808 (1948).
13) F. Halverson and R. J. Francel, ibid., **17**, 694 (1949).
14) N. E. Duncan and G. J. Janz, ibid., **23**, 434 (1955).
15) T. Fujiyama and T. Shimanouchi, Paper presented at the 14th Annual Meeting of the Chemical Society of Japan, Tokyo, April, 1961.
16) S. Califano, R. Moccia, R. Scarpati and G. Speroni, *J. Chem. Phys.*, **26**, 1777 (1957).

Summary

The infrared spectrum of bis(succinonitrilo)-copper(I) nitrate, $[Cu(NC-CH_2-CH_2-CN)_2]NO_3$, has been studied in relation to the molecular configuration of the ligand succinonitrile, which is known from X-ray analysis to be the gauche form. The spectral features of this complex are quite similar to those of free succinonitrile at −50°C in agreement with the conclusion of the previous workers that the gauche isomer of succinonitrile is stable at low temperatures. Thus all the main absorption bands of the complex were satisfactorily explained as due to the vibrations of the gauche isomer. Decomposition of the complex occurs as a result of interaction with alkali halides such as sodium chloride and potassium bromide, which causes the appearance of absorption bands corresponding to the vibrations of the trans isomer. Considering the frequency shifts of the nitrate vibrations the reaction of the complex with alkali halides should be ascribed largely to an ion interchange between the two phases. The increase of 26 cm^{-1} in the C≡N stretching frequency by complex formation may be understood from the linear structure of the Cu–N–C–CH_2 group which suggests that the carbon-nitrogen bond is essentially of a triple-bond character, the contributions of polar resonance structures such as $-C^+=N^-$ being decreased. Assignment of the skeletal deformation frequencies has been made with the help of a normal coordinate treatment which also made possible discussions concerning the nature of these vibrations.

The author wishes to express his sincere thanks to Professor S. Imanishi of Kyushu University for his kind encouragement in the course of this study. He also wishes to thank Dr. H. Murata of Hiroshima University and Dr. I. Nakagawa of the University of Tokyo for many valuable discussions. He is also grateful to Mr. D. Miura of Toyo Rayon Co., Ltd. for carrying out the mechanical calculations and to Messrs. T. Ito, H. Kataoka and K. Shirasaki of Toyo Rayon Co., Ltd. for their assistance in experiments.

Appendix: Calculation of Skeletal Vibrations

The skeletal vibrations of succinonitrile were calculated as a six-body problem. The in-plane skeletal vibrations of propionitrile (symmetry C_s) were also calculated as a four-body problem in order to obtain more information on the nature of the skeletal deformation vibrations of aliphatic nitriles. A potential function of the Urey-Bradley

TABLE III. FORCE CONSTANTS OF PROPIONITRILE AND SUCCINONITRILE (in millidyne/Å)

$K(CH_3\text{-}CH_2)=4.00$[a]	$H(CH_2\text{-}C\equiv N)=0.14_1$[b]
$K(CH_2\text{-}CH_2)=3.70$[a]	$F(CH_3\text{-}CH_2\text{-}C)=0.45$[a]
$K(CH_2\text{-}C)=3.50$[a]	$F(CH_2\text{-}CH_2\text{-}C)=0.45$[a]
$K(C\equiv N)=18.10$[b]	$F(CH_2\text{-}C\equiv N)=0.50$[b]
$H(CH_3\text{-}CH_2\text{-}C)=0.25$[a]	$k(C\text{-}C\equiv N)=0.12$ Å[2] c)
$H(CH_2\text{-}CH_2\text{-}C)=0.25$[a]	

a) Transferred from various hydrocarbons and their derivatives and adjusted to obtain better agreement with the observed values. See for example S. Mizushima, T. Shimanouchi, I. Nakagawa and A. Miyake, *J. Chem. Phys.*, **21**, 215 (1953); M. Hayashi, *J. Chem. Soc. Japan, Pure Chem. Sec. (Nippon Kagaku Zasshi)*, **78**, 222 (1957).

b) Transferred from acetonitrile with some modifications. See I. Nakagawa, "Infrared Absorption Spectrum" (in Japanese), Vol. 7, Nankodo Co., Ltd., Tokyo (1959) p. 1.

c) Interaction term between the C-C≡N in-plane and out-of-plane bending coordinates introduced to obtain better agreement with the observed values.

TABLE IV. SYMMETRY COORDINATES OF PROPIONITRILE

$S_1=(\Delta r_1+\Delta r_2)/\sqrt{2}$	($CH_3\text{-}CH_2\text{-}C$ sym. stretching)
$S_2=(\Delta r_1-\Delta r_2)/\sqrt{2}$	($CH_3\text{-}CH_2\text{-}C$ antisym. stretching)
$S_3=\Delta r_3$	($C\equiv N$ stretching)
$S_4=\Delta\alpha$	($CH_3\text{-}CH_2\text{-}C$ bending)
$S_5=\Delta\beta$	($CH_2\text{-}C\equiv N$ bending)

type[17]) was used, and the values of force constants were transferred from other related molecules as shown in Table III. The symmetry coordinates of propionitrile and succinonitrile listed in Tables IV and V were constructed from the internal coordinates shown in Figs. 4 and 5, respectively. In the trans form of succinonitrile (symmetry C_{2h}) there is no coupling between the C-C≡N in-plane bending and out-of-plane bending motions, because they belong to different classes (see Table V). In the gauche form (symmetry C_2), however, these two motions

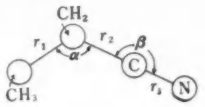

Fig. 4. Internal coordinates of propionitrile.

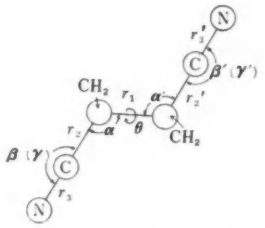

Fig. 5. Internal coordinates of succinonitrile. β (or β') and γ (or γ') denote bending of C≡N bond in and out of the plane of the adjacent C-C-C linkage, respectively. $\theta=180°$ for trans and $\theta=60°$ for gauche.

belong to the same classes and accordingly a coupling occurs between them. In the Urey-Bradley type of potential function no cross term corresponding to the interaction between the two C-C≡N bending coordinates is considered, while such an interaction term, $k(C\text{-}C\equiv N)$, was introduced in this calculation to obtain better agreement with the observed frequencies. The value of $k(C\text{-}C\equiv N)$ used in this case is also included in Table III. For the calculation of the kinetic energy matrices the assumed bond lengths of $r(CH_3\text{-}CH_2)=1.54$ Å, $r(CH_2\text{-}CH_2)=1.54$ Å, $r(CH_2\text{-}C)=1.50$ Å and $r(C\equiv N)=1.15$ Å and the bond angle of 109°28′ were used. The result obtained for the in-plane vibrations (A′) of propionitrile agrees well with the observed values[14] as shown in Table VI. In Table VII are listed the diagonal terms of the potential energy distribution[15], which show that the energies associated with the coordinates S_4(C-C-C bending) and S_5(C-C≡N bending) are of the same order in the two skeletal deformation vibrations. The signs of

TABLE V. SYMMETRY COORDINATES OF SUCCINONITRILE

C_2	C_{2h}		
A	A_g	$S_1=\Delta r_1$	($CH_2\text{-}CH_2$ stretching)
		$S_2=(\Delta r_2+\Delta r_2')/\sqrt{2}$	($CH_2\text{-}C$ sym. stretching)
		$S_3=(\Delta r_3+\Delta r_3')/\sqrt{2}$	($C\equiv N$ sym. stretching)
		$S_4=(\Delta\alpha+\Delta\alpha')/\sqrt{2}$	($CH_2\text{-}CH_2\text{-}C$ sym. bending)
		$S_5=(\Delta\beta+\Delta\beta')/\sqrt{2}$	($CH_2\text{-}C\equiv N$ sym. in-plane bending)
	A_u	$S_6=(\Delta\gamma+\Delta\gamma')/\sqrt{2}$	($CH_2\text{-}C\equiv N$ sym. out-of-plane bending)
B	B_u	$S_7=(\Delta r_2-\Delta r_2')/\sqrt{2}$	($CH_2\text{-}C$ antisym. stretching)
		$S_8=(\Delta r_3-\Delta r_3')/\sqrt{2}$	($C\equiv N$ antisym. stretching)
		$S_9=(\Delta\alpha-\Delta\alpha')/\sqrt{2}$	($CH_2\text{-}CH_2\text{-}C$ antisym. bending)
		$S_{10}=(\Delta\beta-\Delta\beta')/\sqrt{2}$	($CH_2\text{-}C\equiv N$ antisym. in-plane bending)
	B_g	$S_{11}=(\Delta\gamma-\Delta\gamma')/\sqrt{2}$	($CH_2\text{-}C\equiv N$ antisym. out-of-plane bending)

17) T. Shimanouchi, ibid., **17**, 245, 734, 848 (1949).

18) Y. Morino and K. Kuchitsu, ibid., **20**, 1809 (1952).

TABLE VI. CALCULATED AND OBSERVED FREQUENCIES OF PROPIONITRILE (in cm^{-1})

Calcd.	Obs.[a]		Assignment
	Infrared	Raman	
2259	2252	2251	C≡N stretching
1016	1075	1078	C-C-C antisym. stretching
840	836	838	C-C-C sym. stretching
514	545	548	C-C-C bending
241	—	226	C-C≡N bending

a) See Ref. 14 in text.

TABLE VII. POTENTIAL ENERGY DISTRIBUTIONS OF PROPIONITRILE[a]

ν_{calcd}	2259	1016	840	514	241
S_1	− 4	+17	+79	+ 4	0
S_2	+ 4	+82	−14	0	0
S_3	+95	− 1	+ 4	+ 1	0
S_4	0	− 1	−12	+49	+42
S_5	0	− 1	− 1	+41	−57

a) The signs of the corresponding L matrix elements are also included.

TABLE VIII. CALCULATED AND OBSERVED FREQUENCIES OF SUCCINONITRILE (in cm^{-1})

Gauche(C_2)				Trans (C_{2h})				
Class	Calcd.	Obs.		Class	Calcd.	Obs.		Assignment
		Infrared	Raman[a]			Infrared	Raman[a]	
A	2259	2257	2260	A_g	2258		2260	C≡N sym. stretching
	1036	1027	1027		1036		1027	C-C stretching
	812	813	812		883		812	C-CN sym. stretching
	472	480	483		460		514	C-C-C bending
	178	—	170		242		235	C-C≡N bending
	390	385	386	A_u	398	385		C-C≡N bending
B	2259	2257	2260	B_u	2260	2257		C≡N antisym. stretching
	882	1001	1006		874	917		C-CN antisym. stretching
	601	603	604		500	527		C-C-C bending
	247	—	235		145	—		C-C≡N bending
	369	356	359	B_g	398		386	C-C≡N bending

a) Recorded from an aqueous solution with a Cary Model 81 spectrophotometer.

TABLE IX. POTENTIAL ENERGY DISTRIBUTIONS OF THE TRANS FORM OF SUCCINONITRILE[a]

	A_g					A_u
ν_{calcd}	2258	1036	883	460	242	398
S_1	0	+84	+16	+ 5	0	—
S_2	+ 8	−24	+55	+12	+ 5	—
S_3	−95	− 1	+ 3	− 1	+ 1	—
S_4	0	0	−39	+27	+39	—
S_5	0	− 1	− 3	+44	−52	—
S_6	—	—	—	—	—	+100

	B_u				B_g
ν_{calcd}	2260	874	500	145	398
S_7	− 8	+91	− 1	− 2	—
S_8	+95	+ 6	0	0	—
S_9	0	0	+41	−61	—
S_{10}	0	0	+60	−40	—
S_{11}	—	—	—	—	+100

a) See the footnote of Table VII.

TABLE X. POTENTIAL ENERGY DISTRIBUTIONS OF THE GAUCHE FORM OF SUCCINONITRILE[a]

	A					
ν_{calcd}	2259	1036	812	472	178	390
S_1	0	+87	+14	+ 3	0	0
S_2	+ 8	−20	+74	0	0	0
S_3	−95	− 1	+ 4	0	0	0
S_4	0	− 3	− 8	+16	+47	−32
S_5	0	− 2	− 2	+42	−58	−13
S_6	0	0	0	+16	+23	+76

	B				
ν_{calcd}	2259	882	601	247	369
S_7	+ 8	+88	+ 4	+ 1	+ 1
S_8	−95	− 5	− 1	0	0
S_9	0	−14	−48	+25	+15
S_{10}	0	0	+28	−84	+ 3
S_{11}	0	0	+ 6	+17	−93

a) See the footnote of Table VII.

the L matrix elements have revealed that the vibrations assigned to the C-C-C bending and the C-C≡N bending modes correspond respectively to the in-phase and the out-of-phase coupling of the above two coordinates. The calculated and the observed frequencies of succinonitrile are compared in Table VIII, and the diagonal terms of the potential energy distribution for the trans and the gauche forms are listed in Tables IX and X, respectively. In the case of the trans form, where no coupling between the in-plane (A_g and B_u) and out-of-plane (A_u and B_g) vibrations occurs, situation is the same as in propionitrile and energetically the contributions of both the coordinates S_4(C-C-C bending)

and S_5(C-C≡N bending) or those of S_9(C-C-C bending) and S_{10}(C-C≡N bending) are important in producing two each of the skeletal deformation vibrations belonging to class A_g or B_u. It is shown from the signs of the L matrices that the vibrations assigned to the C-C-C bending modes (600~450 cm^{-1}) correspond to the in-phase coupling and those assigned to the C-C≡N bending modes (250~150 cm^{-1}) to the out-of-phase coupling of the two types of bending coordinate. The potential energy distributions show that the A_g vibration which corresponds to the symmetric C-CN stretching mode has a large contribution from the C-C-C bending motion. This is in agreement with the result obtained in the case of 1,2-dichloroethane[19]. In the case of the gauche form coupling occurs between S_4, S_5 and S_8 or S_9, S_{10} and S_{11} to produce three each of the skeletal deformation frequencies belonging to class A or B. However, it may be noted that the contribution of S_6 or S_{11} (C-C≡N out-of-plane bending) is predominant in the vibrations assigned to the C-C≡N bending modes (400~350 cm^{-1}). As in the case of the trans form the energetical contributions of both S_4 and S_5 or of both S_9 and S_{10} are important in two each of the remaining skeletal deformation vibrations belonging to class A or B. The signs of the L matrix elements show that the vibrations assigned to the C-C-C bending modes (600~450 cm^{-1}) correspond to the in-phase coupling and those assigned to the C-C≡N bending modes (250~150 cm^{-1}) to the out-of-phase coupling of the two types of bending coordinate.

Central Research Laboratories
Toyo Rayon Co., Ltd.
Otsu, Shiga-ken

19) I. Nakagawa and S. Mizushima, ibid., **21**, 2195 (1953).

Spectroscopic Studies on Molecular Configurations of Some Aliphatic Dinitriles. II. Infrared Spectra of Glutaronitrile and Bis(glutaronitrilo)copper(I) Nitrate

By Ikuo MATSUBARA

(Received April 24, 1961)

In the preceding paper[1] the author has reported on the analysis of the infrared spectrum of bis(succinonitrilo)copper(I) nitrate, which proved to be quite useful for the understanding of the spectrum of succinonitrile. As a continuation of the spectroscopic studies on the series of aliphatic dinitriles, the infrared spectrum of bis(glutaronitrilo)copper(I) nitrate, $[Cu\{NC-(CH_2)_3-CN\}_2]NO_3$, has been investigated in connection with the molecular configuration of glutaronitrile. This molecule has four possible spectroscopically distinguishable rotational isomers, *TT*, *TG*, *GG* and *GG'*[2], and the complexity of its spectrum in the liquid state, which may be ascribed to the coexistence of these rotational isomers, makes its analysis almost impossible. Recently the author has studied the infrared spectrum of glutaronitrile by the use of low-temperature techniques and found that this molecule forms two different crystalline solid phases, depending on the mode of crystallization[3]. Determination of the molecular configuration of glutaronitrile in each crystalline solid phase has been made possible by comparing the two solid-state spectra with that of bis(glutaronitrilo)copper(I) nitrate, the X-ray analysis of which has revealed that in the crystals of this complex the ligand glutaronitrile molecule takes the *GG* configuration[4]. The detailed analysis of the infrared spectrum of this complex which will be presented in this paper has been undertaken to interpret the whole spectrum of glutaronitrile both in the liquid and in the crystalline solid states. Calculation of the skeletal vibrations for each isomeric form of glutaronitrile also proved useful in determining the configuration of this molecule.

Experimental

Bis(glutaronitrilo)copper(I) nitrate was prepared in the same way as that described in the previous paper[4].

The infrared spectra in the 4000~400 cm^{-1} region of glutaronitrile and the complex were recorded using a Perkin-Elmer Model 21 and a Perkin-Elmer Model 13 spectrophotometer (with sodium chloride

1) I. Matsubara, This Bulletin, **34**, 1710 (1961).
2) For the nomenclature of the rotational isomers see S. Mizushima, "Structure of Molecules and Internal Rotation", Academic Press Inc., New York (1954), Part I, Chapter V.
3) I. Matsubara, *J. Chem. Phys.*, **35**, 373 (1961).
4) Y. Kinoshita, I. Matsubara and Y. Saito, This Bulletin, **32**, 1216 (1959).

and potassium bromide optics, respectively). The spectrum of glutaronitrile in the liquid state is shown in Fig. 1a. As has already been reported[3], glutaronitrile can form two different crystalline solid phases. By rapid cooling of the liquid down to $-60^{\circ}C$ a metastable crystalline form is obtained. This has the spectrum shown in Fig. 1b. When the solid is warmed up to $-40^{\circ}C$ an irreversible transition occurs giving a more stable crystalline form which has the spectrum shown in Fig. 1c. The spectrum of bis(glutaronitrilo)copper(I) nitrate was obtained using both Nujol mull and potassium bromide disk methods. The spectrum obtained from a Nujol mull of the complex by using KRS-5 supporting plates is shown in Fig. 2a. The spectrum in Fig. 2b is that obtained from a Nujol mull of the complex by using potassium bromide plates. (This spectrum was recorded after the specimen had been placed in the laboratory for one day.) These two spectra are very different from each other, showing that a reaction occurred between the complex and potassium bromide as in the case of bis(succinonitrilo)copper(I) nitrate[1]. The use of sodium chloride plates resulted in a spectrum identical with that in Fig. 2a and no time dependent change of the spectrum was observed. Potassium bromide disks of the complex gave different spectra depending on the pressure applied to prepare the disk. In Figs. 3a and 3b are shown the spectra obtained from the disks which were prepare by applying pressures of 8 tons and 10 tons, respectively. The potassium bromide disk having the spectrum shown in Fig. 3a, when repressed under a pressure of 10 tons, undergoes an irreversible change and

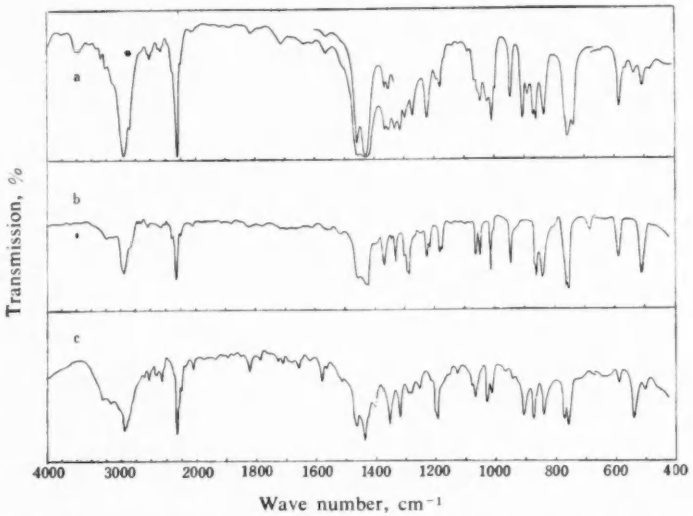

Fig. 1. Infrared spectra of glutaronitrile in various states. (a) liquid; (b) solid (metastable form); (c) solid (stable form).

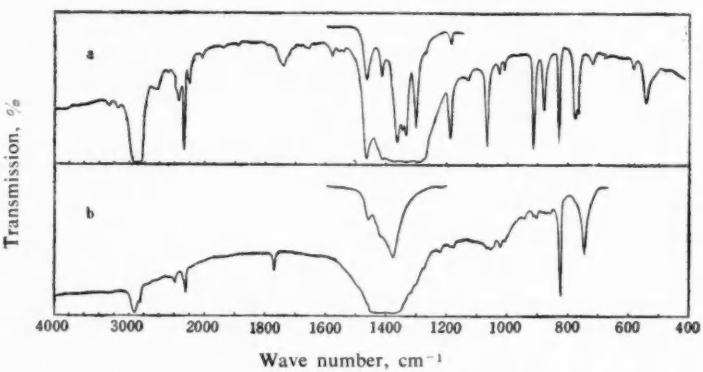

Fig. 2. Infrared spectra obtained from Nujol mulls of bis(glutaronitrilo)-copper(I) nitrate by using (a) KRS-5 and (b) KBr supporting plates.

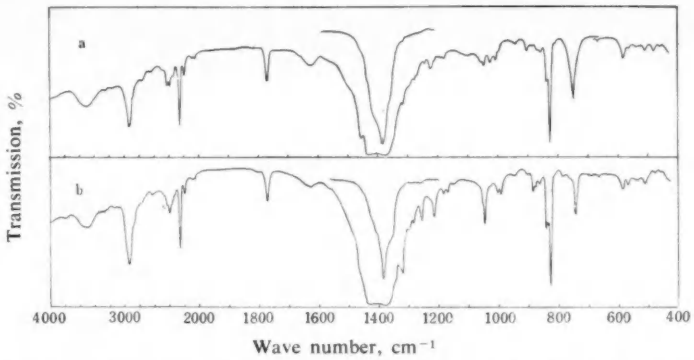

Fig. 3. Infrared spectra obtained from KBr disks of bis(glutaronitrilo)-copper(I) nitrate prepared by applying pressures of (a) 8 tons and (b) 10 tons.

comes to exhibit a spectrum identical with that shown in Fig. 3b. The absorption frequencies of glutaronitrile and bis(glutaronitrilo)copper(I) nitrate are listed in Table I together with the assignment.

Results and Discussion

The symmetry types and the selection rules for the fundamental vibrations of glutaronitrile in the 1400~400 cm^{-1} region[5,6] are given in Table II. All the fifteen fundamental vibrations in this region are expected to be infrared active for the *TG*, *GG* and *GG'* isomers, while for the *TT* isomer two CH_2 twisting and one CH_2 rocking modes belonging to class A_g are infrared inactive. As long as the ligand glutaronitrile takes the *GG* configuration in the crystals of bis(glutaronitrilo)copper(I) nitrate[1], its spectrum should be explained as due to the vibrations of the *GG* form of glutaronitrile. The spectrum obtained from a Nujol mull of this complex by using KRS-5 supporting plates (Fig. 2a) seems to be in good agreement with the selection rules for the *GG* isomer of glutaronitrile. On the other hand, the Nujol mull spectrum obtained by the use of potassium bromide plates (Fig. 2b) and the potassium bromide disk spectrum (Fig. 3a) are very different from the spectrum in Fig. 2a and are quite similar to that of the liquid glutaronitrile (Fig. 1a). This means that free glutaronitrile has been produced as a result of interaction between the complex and potassium bromide. This interaction caused the shifts of the nitrate bands of the complex observed at 1748, 1361 and 830 cm^{-1} in Fig. 2a to 1770, 1385 and 826 cm^{-1}, respectively, as shown in Figs. 2b and 3. The latter frequencies agree quite well with those of potassium nitrate[7], showing that the mechanism of reaction of the complex and potassium bromide should be ascribed largely to an ion interchange between the two phases as in the case of bis(succinonitrilo)copper(I) nitrate[1].

As reported in the previous paper[3] the spectrum of glutaronitrile in the stable crystalline form (Fig. 1c) is closely correlated with that of bis(glutaronitrilo)copper(I) nitrate shown in Fig. 2a. The one to one correspondences between the individual bands of the two spectra are almost complete except for the regions where absorptions due to nitrate vibrations or skeletal vibrations of the complex take place. From this result it has been concluded that glutaronitrile takes the *GG* configuration in the stable crystalline solid state[3]. The vibrational assignment of these two spectra, though tentative in nature, are made with reference to the work of Brown and Sheppard[8] on trimethylene halides which were also found to take the *GG* configuration in the crystalline solid state. Thus, the bands observed at 1350, 1316 and 1250 cm^{-1} in the spectrum of the stable solid form (Fig. 1c) may be assigned to the CH_2 wagging modes and those at 1287/79, 1190 and 1125 cm^{-1} to the CH_2 twisting modes. The behaviors of the CH_2 wagging modes are somewhat anomalous in the case of the complex (Fig. 2a). There are quite intense bands at 1334 and 1300 cm^{-1} but no band is observable around 1250 cm^{-1}. Although this may be ascribed to the effect of the crystalline force field of the complex, no further discussions will be made at this stage. The bands observed at 1271, 1188 and 1130 cm^{-1} in the spectrum

5) J. K. Brown, N. Sheppard and D. M. Simpson, *Phil. Trans. Roy. Soc. London*, **A247**, 35 (1954).
6) E. Funck, *Z. Elektrochem.*, **62**, 901 (1958).
7) F. A. Miller and C. H. Wilkins, *Anal. Chem.*, **24**, 1253 (1952).
8) J. K. Brown and N. Sheppard, *Proc. Roy. Soc.*, **A231**, 555 (1955).

Table I. Infrared absorption bands of glutaronitrile and bis(glutaronitrilo)copper(I) nitrate

Glutaronitrile			Bis(glutaronitrilo)-copper(I) nitrate		Assignment	
Liquid	Solid		Nujol mull[a]	KBr disk[b]		
	Metastable form	Stable form				
		3247 vw	3279 vw	3257 vw		
3205 vw	3195 vw					
			3165 vw			
3115 vw sh		3125 vw		3125 vw		
2959 s	2950 ms	2950 s		2933 ms	*TT*, *TG*, *GG*	C–H stretch.
		2924 s sh		2915 m sh		
2890 m	2874 w	2890 w sh		2874 w sh	*TT*, *TG*, *GG*	C–H stretch.
		2688 vw	2695 vw			
2646 vw sh						
2618 vw	2625 w	2625 w	2632 w	2618 vw		
		2532 vw				
2506 vw		2500 vw	2488 vw			
2463 vw	2451 w					
2445 vw sh		2445 w	2421 vw sh	2427 w sh		
				2398 mw		
			2353 mw	2364 w sh		
2299 vw sh	2304 w	2288 vw sh				
			2278 s		*GG*	C≡N stretch. (bound)
2249 vs	2245 ms	2247 s		2252 ms	*TT*, *TG*, *GG*	C≡N stretch. (free)
2198 vw	2198 w	2198 w	2208 w	2198 mw		
				2096 vw		
2049 vw						
2016 vw	2016 vw	2020 w	2037 w			
		1931 vw	1942 vw			
1890 vw		1890 vw	1890 vw			
1812 w	1818 vw	1818 w				
1786 vw	1773 vw	1783 vw	1776 vw			
		1721 vw	1724 vw sh			
1712 w		1706 vw	1706 w sh			
		1675 vw	1672 vw			
1634 vw		1653 w	1658 vw			
1608 vw	1605 vw	1613 vw				
	1570 vw	1575 w	1580 w			
1563 w	1553 vw	1560 vw	1558 vw	1563 vw		
1548 vw sh	1543 vw	1536 vw sh	1543 vw			
1511 vw sh	1508 w	1508 vw	1506 vw sh			
1458 s	1451 ms	1460 ms			*TT*, *TG*, *GG*	CH_2 bend.
1429 vs	1420 s	1433 s	1414 s		*TT*, *TG*, *GG*	CH_2 bend.
	1395 vw	1399 w				
1366 m	1364 m				*TG*	CH_2 wag.
1355 m		1350 ms	1334 vs		*GG*	CH_2 wag.
	1339 w					
1333 m	1328 m			1328 w sh	*TG*	CH_2 wag.
1314 m		1316 ms	1300 vs	1319 mw	*TT*, *GG*	CH_2 wag.
1299 m	1300 w			1297 vw	*TG*	CH_2 twist.
1289 vw sh		1287 w	1271 ms sh	1280 w	*GG*	CH_2 twist.
	1289 ms sh	1279 w				
1272 m	1282 ms			1272 vw sh	*TG*	CH_2 wag.
		1250 w		1256 mw	*TT*, *GG*	CH_2 wag.
	1241 vw					

TABLE I. (Continued)

Glutaronitrile			Bis(glutaronitrilo)-copper(I) nitrate		Assignment	
	Solid					
Liquid	Metastable form	Stable form	Nujol mull[a]	KBr disk[b]		
1224 ms	1224 m			1224 vw sh	*TG*	CH_2 twist.
	1214 mw			1214 mw	*TT*	CH_2 twist.
		1208 vw				
1193 vw		1190 ms	1188 s		*GG*	CH_2 twist.
1181 m	1181 m			1179 w	*TG*	CH_2 twist.
1170 vw sh	1174 m			1168 w	*TT*	CH_2 twist.
1145 vw	1148 vw			1149 vw		
	1140 vw					
1120 vw		1125 w	1130 w		*GG*	CH_2 twist.
1087 vw		1075 w				
1066 w sh	1060 m	1065 m	1066 s	1064 vw sh	*TG*, *GG*	C–C stretch.
1056 w sh				1050 w sh	*TT*	C–C stretch.
1047 m	1045 m			1044 m	*TT*, *TG*	C–C stretch.
1022 m		1026 m	1027 mw	1026 vw sh	*GG*	C–C stretch.
1008 ms	1009 ms	1010 m	1009 w		*TG*, *GG*	C–C stretch.
	1003 w sh					
998 w				1000 w	*TT*	C–C stretch.
991 vw sh				990 w		
		964 w	971 vw	953 vw		
945 m	943 ms	943 w		943 vw	*TG*	CH_2 rock.
904 ms		903 ms	913 s	902 vw	*GG*	CH_2 rock.
		899 ms sh				
888 w				885 mw	*TT*	C–C stretch.
870 ms		873 ms	880 ms	877 w	*GG*	C–C stretch.
		871 ms				
	864 m sh	864 w sh				
860 ms	859 ms			861 w	*TG*	C–C stretch.
835 ms	839 ms	837 ms	830 s	839 m	*TG*, *GG*	CH_2 rock.
	835 ms sh			833 m		
	800 vw		808 vw	812 vw sh		
757 s	757 s	768 ms	778 ms	784 w	*TG*, *GG*	CH_2 rock.
	751 s	754 ms	767 ms	758 vw sh		
737 ms				742 m	*TT*	CH_2 rock.
	681 mw					
				666 vw		
648 vw						
583 ms	586 ms	588 w	586 w	584 mw	*TG*, *GG*	C–C–C bend.
565 w				564 w	*TT*	C–C–C bend.
535 w		537 ms	544 ms	532 vw	*GG*	C–C–C bend.
507 m	511 ms	503 vw		508 w	*TG*	C–C–C bend.
481 vw			475 vw	473 vw	*TT*	C–C–C bend.
				458 vw		

a) KRS-5 supporting plates were used to obtain the spectrum.
b) The disk was prepared by applying a pressure of 10 tons.

of the complex are assigned to the CH_2 twisting modes. Absorptions corresponding to the C–C stretching modes are found at 1065, 1026, 1010 and 873 cm^{-1} in the spectrum of the stable solid form and at 1066, 1027, 1009 and 880 cm^{-1} in the spectrum of the complex. To the CH_2 rocking modes may correspond the bands observed at 903, 837 and 768/54 cm^{-1} in the spectrum of the stable solid form and those observed at 913, 830 and 778/67 cm^{-1} in the spectrum of the complex.

The configuration of glutaronitrile in the metastable crystalline solid state must be the *TG* form as the *TT* form can be excluded from

TABLE II. THE SYMMETRY TYPES AND SELECTION RULES FOR THE FUNDAMENTAL VIBRATIONS OF GLUTARONITRILE IN THE 1400~400 cm^{-1} REGION

Types of symmetry coordinates		*TT*(C_{2v})				*GG*(C_2)		*TG*(C_1)	*GG'*(C_s)	
		A_1	A_2	B_1	B_2	A	B		A'	A''
CH_2 wagging		1	0	2	0	1	2	3	1	2
CH_2 twisting		0	2	0	1	2	1	3	1	2
C-C stretching		2	0	2	0	2	2	4	2	2
CH_2 roking		0	1	0	2	1	2	3	2	1
C-C-C bending		1	0	1	0	1	1	2	1	1
Selection rules	IR	+	−	+	+	+	+	+	+	+
	Raman	+	+	+	+	+	+	+	+	+

consideration of the selection rules and the existence of the *GG'* form is considered improbable from steric reasons[3]. The vibrational assignment of the spectrum shown in Fig. 1b was made on this basis. Thus, the bands observed at 1364, 1328 and 1289/82 cm^{-1} may be assigned to the CH_2 wagging modes, and those at 1300, 1224/14 and 1181/74 cm^{-1} to the CH_2 twisting modes of the *TG* form. The bands at 1060, 1045, 1009 and 859 cm^{-1} correspond to the C-C stretching modes and those at 943, 839/35 and 757/51 cm^{-1} must be ascribed to the CH_2 rocking modes.

The majority of the bands in the liquid-state spectrum of glutaronitrile (Fig. 1a) can be satisfactorily explained as due to the vibrations of the *TG* and the *GG* isomers, and a few remaining bands must be ascribed to the vibrations of the *TT* form, because one of them at 737 cm^{-1} certainly corresponds to the CH_2 rocking vibration of the methylene chain of the planar all-trans configuration[5,9]. These conclusions are further confirmed by the calculation of the skeletal deformation vibrations for each isomeric form of glutaronitrile (see Appendix). The results of the calculation show that each isomer should have two C-C-C bending frequencies in the 650~450 cm^{-1} region. From the potential energy distributions it is shown that the energetical contributions of both the C-C-C bending and the C-C≡N (in-plane) bending motions are important in these skeletal deformation vibrations as in the case of succinonitrile[1]. The frequencies of 586 and 511 cm^{-1} observed in the spectrum of the metastable solid form (Fig. 1b) agree quite well with the values of 567 and 507 cm^{-1} calculated for the *TG* form. The frequencies of 588 and 537 cm^{-1} observed in the spectrum of the stable solid form (Fig. 1c) and those of 586 and 544 cm^{-1} in the spectrum of the complex (Fig. 2a) are in excellent agreement with the values of 590 and 535 cm^{-1} calculated for the *GG* form. In the spectrum of the liquid glutaronitrile there are weak bands at 565 and 481 cm^{-1} which disappear at low temperatures. These frequencies correspond well with the values of 546 and 441 cm^{-1} calculated for the *TT* form. The values of 616 and 510 cm^{-1} calculated for the *GG'* form seem not to be appropriate to explain the observed frequencies in all cases. The potassium bromide disk spectrum of the complex shown in Fig. 3b is different from the spectrum in Fig. 3a in that the absorptions corresponding to the vibrations of the *TT* form as described above are anomalously intense. It seems that the applied pressure of 10 tons must have favored the selective formation of the *TT* isomer in the reaction of the complex with potassium bromide. The spectrum in Fig. 3b shows a few other anomalously intense bands besides those mentioned above. These bands must also correspond to the vibrations of the *TT* form which could not be identified in the spectrum of the liquid glutaronitrile because of the overlapping of absorptions due to the *TG* or the *GG* form.

Spectral features of the complex in the C≡N stretching frequency region are similar to those of bis(succinonitrilo)copper(I) nitrate[1]. The sharp band observed at 2278 cm^{-1} in the Nujol mull spectrum (Fig. 2a) should correspond to the C≡N stretching mode of the complex. The C≡N vibrational shift of 29 cm^{-1} towards higher frequencies as compared with the free glutaronitrile may be explained from a consideration of the structure of the complex. From X-ray analysis of this complex[4] it has been found that the carbon-nitrogen bond distance is 1.14 Å and that the Cu-N-C-CH_2 group is close to linear. This suggests that the carbon-nitrogen bond is essentially of a triple-bond character, the contributions of polar resonance structures such as $-C^+=N^-$ being decreased, and the C≡N stretching frequency is thereby increased. The effect of coupling between the C≡N stretching and the Cu-N stretching vibrations, though small, may also contribute to the increase in the C≡N stretching frequency. As shown in Figs. 2b and 3, reaction with potassium bromide results in the appearance of the band at 2252 cm^{-1} which corresponds to the C≡N stretching frequency of the free glutaronitrile. The band observed at 2353 cm^{-1} in

9) H. Tschamler, *J. Chem. Phys.*, **22**, 1845 (1954).

the Nujol mull spectrum is considered to be characteristic of the tetrahedral configuration of the complex as in the case of bis(succinonitrilo)copper(I) nitrate[1]. The origin of the band observed at 2208 cm^{-1} is hard to explain, because its intensity tends to vary from specimen to specimen and no other homologues of this series of complex show any absorption at the corresponding frequency. For the present, it may be ascribed to a certain combination vibration or to a vibration of some impurities in the complex.

Summary

The infrared spectra of glutaronitrile and bis(glutaronitrilo)copper(I) nitrate, $[Cu\{NC-(CH_2)_3-CN\}_2]NO_3$, have been studied. The spectrum of the complex has been analyzed on the basis of the result of X-ray analysis which disclosed that the ligand glutaronitrile takes the *GG* configuration in the crystals of this compound. This complex reacts with alkali halides such as potassium bromide, resulting in the isolation of free glutaronitrile. Considering

Table III. Force constants of glutaronitrile (in millidyne/Å)[a]

$K(CH_2-CH_2)=3.70$	$H(CH_2-C\equiv N)=0.14_1$
$K(CH_2-C)=3.50$	$F(CH_2-CH_2-CH_2)=0.45$
$K(C\equiv N)=18.10$	$F(CH_2-CH_2-C)=0.45$
$H(CH_2-CH_2-CH_2)=0.25$	$F(CH_2-C\equiv N)=0.50$
$H(CH_2-CH_2-C)=0.25$	$k(C-C\equiv N)=0.12$ Å^2

a) Transferred from succinonitrile. See Appendix in Ref. 1.

Table IV. Symmetry coordinates of glutaronitrile

C_{2v}	C_2	C_s		
A_1	A	A′	$S_1=(\Delta r_1+\Delta r_1')/\sqrt{2}$	(CH_2-CH_2 sym. stretching)
			$S_2=(\Delta r_2+\Delta r_2')/\sqrt{2}$	(CH_2-C sym. stretching)
			$S_3=(\Delta r_3+\Delta r_3')/\sqrt{2}$	(C≡N sym. stretching)
			$S_4=\Delta\alpha_0$	(CH_2-CH_2-CH_2 bending)
			$S_5=(\Delta\alpha_c-\Delta\alpha')/\sqrt{2}$	(CH_2-CH_2-C sym. bending)
			$S_6=(\Delta\beta+\Delta\beta')/\sqrt{2}$	(CH_2-C≡N sym. in-plane bending)
A_2			$S_7=(\Delta\gamma+\Delta\gamma')/\sqrt{2}$	(CH_2-C≡N sym. out-of-plane bending)
B_1	B	A″	$S_8=(\Delta r_1-\Delta r_1')/\sqrt{2}$	(CH_2-CH_2 antisym. stretching)
			$S_9=(\Delta r_2-\Delta r_2')/\sqrt{2}$	(CH_2-C antisym. stretching)
			$S_{10}=(\Delta r_3-\Delta r_3')/\sqrt{2}$	(C≡N antisym. stretching)
			$S_{11}=(\Delta\alpha-\Delta\alpha')/\sqrt{2}$	(CH_2-CH_2-C antisym. bending)
			$S_{12}=(\Delta\beta-\Delta\beta')/\sqrt{2}$	(CH_2-C≡N antisym. in-plane bending)
B_2			$S_{13}=(\Delta\gamma-\Delta\gamma')/\sqrt{2}$	(CH_2-C≡N antisym. out-of-plane bending)

Table V. Calculated and observed frequencies of glutaronitrile (in cm^{-1})

TT(C_{2v})			*GG*(C_2)			*TG*(C_1)		*GG*′(C_s)	Assignment
Calcd.	Obs. Liquid[a]		Calcd.	Obs. Solid[b]	Obs. Complex[c]	Calcd	Obs. Solid[d]	Calcd.	
A_1 2259		A	2259			2259		A′ 2259	C≡N sym. stretching
993			980			984		980	C-C sym. stretching
909			825			829		826	C-CN sym. stretching
441	481		590	588	586	507	511	616	C-C-C bending
315			358			336		364	C-C-C bending
107			157			205		226	C-C≡N bending
A_2 398			384			368		399	C-C≡N bending
B_1 2259		B	2259			2259		A″ 2259	C≡N antisym. stretching
1069			1062			1067		1062	C-C antisym. stretching
843			853			883		851	C-CN antisym. stretching
546	565		535	537	544	567	586	510	C-C-C bending
230			241			174		169	C-C≡N bending
B_2 398			387			388		365	C-C≡N bending

a) Obtained by subtracting the bands which correspond to the vibrations of the *GG* and the *TG* isomers.
b) Stable crystalline solid state.
c) Obtained from a Nujol mull by using KRS-5 supporting plates.
d) Metastable crystalline solid state.

TABLE VI. POTENTIAL ENERGY DISTRIBUTIONS OF THE *TT* FORM OF GLUTARONITRILE[a]

	A_1						A_2
ν_{calcd}	2259	993	909	441	315	107	398
S_1	0	+82	+11	+ 9	+ 3	+ 1	—
S_2	− 8	− 20	+60	+ 1	+13	0	—
S_3	+95	− 1	+ 3	0	− 1	0	—
S_4	0	− 1	− 20	− 1	+60	−22	—
S_5	0	− 7	− 18	+20	+ 6	+53	—
S_6	0	− 1	− 1	+65	− 7	−26	—
S_7	—	—	—	—	—	—	+100

	B_1					B_2
ν_{calcd}	2259	1069	843	546	230	398
S_8	0	+93	+ 7	0	− 2	—
S_9	+ 8	− 9	+85	+ 1	0	—
S_{10}	−95	0	+ 5	0	0	—
S_{11}	0	0	− 5	+58	+41	—
S_{12}	0	0	0	+40	−59	—
S_{13}	—	—	—	—	—	−100

a) The signs of the corresponding L matrix elements are also included.

TABLE VII. POTENTIAL ENERGY DISTRIBUTIONS OF THE *GG* FORM OF GLUTARONITRILE[a]

	A						
ν_{calcd}	2259	980	825	590	358	157	384
S_1	0	+77	+27	+ 1	− 1	0	0
S_2	+ 8	−29	+61	+ 5	0	0	0
S_3	−95	− 1	+ 3	0	0	0	0
S_4	0	− 7	0	−28	−44	−14	+10
S_5	0	0	−11	+31	− 7	−45	−11
S_6	0	− 1	− 2	+20	−46	−47	0
S_7	0	0	0	+ 5	+20	−15	+74

	B					
ν_{calcd}	2259	1062	853	535	241	387
S_8	0	+96	+ 4	+ 3	0	0
S_9	+ 8	− 7	+85	+ 2	0	0
S_{10}	−95	0	+ 5	0	0	0
S_{11}	0	− 3	−12	+39	+27	−23
S_{12}	0	− 1	− 1	+33	−79	− 2
S_{13}	0	0	0	+ 7	+26	+83

a) See the footnote of Table VI.

TABLE VIII. POTENTIAL ENERGY DISTRIBUTIONS OF THE *TG* FORM OF GLUTARONITRILE[a]

ν_{calcd}	2259	984	839	507	336	205	368	2259	1067	883	567	174	388
S_1	0	+83	+13	+ 5	− 1	0	+ 1	0	+ 1	− 1	− 1	0	+ 1
S_2	− 7	−21	+57	+ 1	+ 2	+ 1	+ 1	+ 1	0	−13	0	0	0
S_3	+80	− 1	+ 3	0	0	0	0	−15	0	− 1	0	0	0
S_4	0	− 4	− 1	− 3	+55	+ 4	+ 1	0	0	+11	− 8	−14	+ 2
S_5	0	− 2	−14	+17	0	+34	+20	0	− 2	+ 1	+ 6	− 8	− 1
S_6	0	− 1	− 1	+26	+ 3	−54	+14	0	0	0	+ 7	− 8	0
S_7	0	0	0	−10	+ 1	+16	−73	0	0	0	+ 2	− 1	+13
S_8	0	+ 1	0	0	0	0	0	0	−93	− 6	− 1	− 1	0
S_9	+ 1	0	−17	0	+ 3	0	0	+ 7	+ 9	−59	− 5	0	+ 1
S_{10}	−15	0	− 1	0	0	0	0	−80	0	− 3	− 1	0	0
S_{11}	0	− 2	0	+ 5	− 1	− 5	+ 1	0	0	+11	−32	−32	+15
S_{12}	0	0	0	+12	−31	+ 6	+ 1	0	+ 1	+ 1	−19	−45	0
S_{13}	0	0	0	− 3	+16	− 2	−10	0	0	0	− 4	−13	−68

a) See the footnote of Table VI.

the frequency shifts of the nitrate vibrations the reaction of the complex with potassium bromide should be ascribed largely to an ion interchange between the two phases. The increase of 29 cm^{-1} in the C≡N stretching frequency by complex formation may be understood from the linear structure of the Cu N–C–CH_2 group which suggests that the carbon-nitrogen bond is essentially of a triple-bond character, the contributions of polar resonance structures such as $-C^+=N^-$ being decreased. Glutaronitrile can form two different crystalline solid phases, depending on the mode of crystallization. From comparison of the two solid-state spectra with that of the complex and from consideration of the vibrational selection rules it has been concluded that glutaronitrile takes the *GG* configuration in one crystalline solid state and the *TG* in the other, and that it exists as a mixture of three isomers, *GG*, *TG* and *TT* in the liquid state. Calculation of the skeletal deformation frequencies for each isomeric form has given the results which support this conclusion. Vibrational assignment of glutaronitrile in various states has been made satisfactorily on the basis of the above results.

The author wishes to express his hearty thanks to Professor S. Imanishi of Kyushu University for his kind encouragement in the course of this study. He is also indebted to Dr. H. Murata of Hiroshima University for many helpful discussions and to Mr. D. Miura

of Toyo Rayon Co., Ltd. for carrying out the mechanical calculations. The assistance of Messrs. T. Ito, H. Kataoka and K. Shirasaki of Toyo Rayon Co., Ltd. in experiments is also acknowledged.

Appendix: Calculation of Skeletal Vibrations

The skeletal vibrations of glutaronitrile were calculated as a seven-body problem. Calculations were carried out on all the four isomeric forms, *TT*(C_{2v}), *GG*(C_2), *GG'*(C_s) and *TG*(C_1). A potential function of the Urey-Bradley type[10] was used, and the values of force constants were transferred from succinonitrile[1] as shown in Table III. The symmetry coordinates of glutaronitrile listed in Table IV were constructed from the internal coordinates shown in Fig. 4. Except for the case

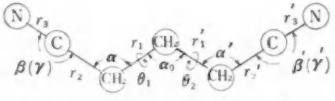

Fig. 4. Internal coordinates of glutaronitrile. β (or β') and γ (or γ') denote bending of C≡N bond in and out of the plane of the adjacent C-C-C linkage, respectively. $\theta_1=\theta_2=180°$ for *TT*, $\theta_1=\theta_2=60°$ for *GG*, $\theta_1=-\theta_2=60°$ for *GG'*, and $\theta_1=180°$ and $\theta_2=60°$ for *TG*.

of the *TT* form, coupling between the C-C≡N in-plane and out-of-plane bending motions occurs. As in the case of succinonitrile[1] a cross term k(C-C≡N) corresponding to the interaction of the two C-C≡N bending coordinates was introduced into the potential function (Table III). For the calculation of the kinetic energy matrices the assumed bond lengths of $r(CH_2\text{-}CH_2)=1.54$ Å, $r(CH_2\text{-}C)=1.50$ Å and $r(C\equiv N)=1.15$ Å and the bond angle of 109°28' were used.

The calculated frequencies are listed in Table V, in which the observed frequencies for the skeletal deformation vibrations are also included, although the observed data are not available for the region below 400 cm^{-1}. For each isomeric form there exist two vibrations corresponding to the C-C-C bending modes in the 650~450 cm^{-1} region. The potential energy distributions listed together with the signs of the corresponding L matrix elements in Tables VI—IX show that these vibrations correspond to the in-phase coupling of the C-C-C bending and the C-C≡N (in-plane) bending motions. The agreement between the observed and the calculated frequencies of these vibrations are satisfactory, showing that the skeletal deformation frequencies of glutaronitrile are quite useful in determining the configurations of rotational isomers of this molecule.

Table IX. Potential energy distributions of the *GG'* form of glutaronitrile[a]

	A'						
ν_{calcd}	2259	980	826	616	364	226	399
S_1	0	+77	+27	+ 1	+ 1	0	0
S_2	+ 8	−29	+59	+ 6	0	0	0
S_3	−95	− 1	+ 3	+ 1	0	0	0
S_4	0	− 8	0	−22	+62	+13	0
S_5	0	0	−13	+41	+ 4	+27	−19
S_6	0	− 1	− 2	+16	+34	−63	0
S_7	0	0	0	+ 3	− 2	+30	−81
	A''						
ν_{calcd}	2259	1062	851	510	169	365	
S_8	0	+96	+ 4	+ 2	0	0	
S_9	− 8	− 8	+85	+ 1	0	0	
S_{10}	+95	0	+ 5	0	0	0	
S_{11}	0	− 3	−10	+23	+49	−18	
S_{12}	0	− 1	− 1	+41	−56	−18	
S_{13}	0	0	0	+13	+11	+91	

a) See the footnote of Table VI.

Central Research Laboratories
Toyo Rayon Co., Ltd.
Otsu, Siga-ken

10) T. Shimanouchi, ibid., **17**, 245, 734, 848 (1949).

*Synthesis and Physical Properties of Normal Higher Primary Alcohols. IV. Thermal and X-Ray Studies on the Polymorphism of the Alcohols of Even Carbon Numbers from Dodecanol to Tetratriacontanol**

By Akira WATANABE

(Received April 20, 1961)

Since X-ray study on a series of normal paraffins was reported by Müller[1], several investigations have been made on the transition phenomenon of many long-chain compounds including acids[2-5], esters[3,6], bromides[7], and alcohols[8]. In these compounds, phase change is known to occur just below their freezing points accompanying the changes in a number of physical properties such as crystal structure, thermal property, and dipole moment in polar compounds. Recently nuclear magnetic resonance studies were also reported[9]. The α phase, which appears at the high temperature side, has been found to possess molecular freedom, the molecule being assumed to rotate about the long axis because of the characteristics of symmetrical crystal structure and high dielectric constant in this phase.

Although Hoffman et al.[10] recently summarized the results of the several investigations mainly on paraffins and bromides, some problems seemed to remain to be solved. The results on the higher alcohols appearing in the literature seemed to be somewhat ambiguous and the data for the alcohols with odd carbon atoms and with more than eighteen carbon atoms are too scanty to permit generalization of the series. On the other hand, the transition phenomenon has been known to be affected by the presence of extremely small amounts of impurities as well as variations in the technique of measurements and in thermal histories of the materials. Therefore it was felt to be important to examine the phenomenon with a series of pure compounds under conditions as comparable as possible. In view of these facts, the author has undertaken a study of synthesis and physical properties of normal higher alcohols with more than ten carbon atoms in order to establish the existence of transition in each member and its dependency on chain length. The reports on the synthesis have been published[11] and in this paper investigation of thermal analyses and X-ray studies on the alcohols of even carbon atoms from dodecanol to tetratricontanol are reported.

Nomenclature of the Phases.—*α-Form.*—This form obtained on crystallization from the melt is somewhat transparent and on further cooling changes to the more opaque β or γ form at the transition point. X-Ray analysis indicates that the hydrocarbon chain is vertical to the plane of the end groups and the dielectric constant is higher than those of the β or γ or liquid phase. It has also been known that this form is unstable and gradually transforms into a more stable γ form on standing.

β-Form.—This form, in which the hydrocarbon chain is vertical to the plane of the end groups, appears below the transition point mainly in odd members and in shorter members of the even alcohols. In the latter case, gradual transformation from β to γ form is known to exist in some of the members.

γ-Form.—This form, in which the hydrocarbon chain inclines to the plane, appears below the transition point only in even compounds and is stable at low temperature.

The correspondence of the present nomenclature to those adopted by other workers is as follows.

* This study has been carried out at the Department of Physics, Faculty of Science, Kyoto University, as a part of the cooperative research on "Synthesis and Physical Properties of Long Chain Compounds".

1) A. Müller, *Proc. Roy. Soc.*, **A138**, 514 (1932).
2) W. E. Garner and A. M. King, *J. Chem. Soc.*, **1929**, 1849.
3) J. D. Meyer and R. E. Reid, *J. Am. Chem. Soc.*, **55**, 1574 (1933).
4) F. Francis et al., *Proc. Roy. Soc.*, **A128**, 214 (1930); ibid., **A158**, 691 (1937).
5) E. Stenhagen and E. Sydow, *Arkiv. Kemi.*, **6**, 309 (1953).
6) W. O. Baker and C. P. Smyth, *J. Am. Chem. Soc.*, **60**, 1229 (1938).
7) R. W. Crowe and C. P. Smyth, ibid., **72**, 1098 (1950).
8) a) J. W. C. Phyllips and S. Munford., ibid., **55**, 1747 (1933). b) K. Higasi and M. Kubo, *Pap. Inst. Phys. Chem. Res.*, **36**, 286 (1939). c) J. D. Hoffman and C. P. Smyth, *J. Am. Chem. Soc.*, **71**, 431 (1949). d) Y. Kakiuchi and T. Sakurai, *J. Phys. Soc. Japan*, **4**, 365 (1949). e) Y. Kakiuchi, T. Sakurai and T. Suzuki, ibid., **5**, 369 (1950). f) D. G. Kolp and E. S. Lutton, *J. Am. Chem. Soc.*, **73**, 5593 (1951). g) K. Asai, *J. Phys. Soc. Japan*, **14**, 1084 (1959).
9) a) E. R. Andrew, *J. Chem. Phys.*, **18**, 607 (1950). b) S. Kojima and O. Ogawa, *J. Phys. Soc. Japan*, **8**, 283 (1953).
10) J. D. Hoffman and B. F. Decker, *J. Phys. Chem.*, **57**, 520 (1953).
11) A. Watanabe, This Bulletin, **32**, 1295 (1959); A. Watanabe, ibid., **33**, 531 (1960); A. Watanabe, ibid., **34**, 398 (1961).

Present paper	Kolp, Lutton	Smyth et al.
α	Alpha	α
β	Sub-alpha	β_1
γ	Beta	β_2

Experimental

Purity of the Materials.—The alcohols used in this study were all prepared by the lithium aluminum hydride reduction of the corresponding fatty acids or their ethyl esters, the acids above octadecanoic being synthesized from the commercially available lower acids which were initially purified by fractional distillation followed by recrystallization. Since it is difficult to purify the compounds in high purity or to obtain a reliable method to establish their purity when the carbon chain is considerably long, the present efforts were made especially toward the purification of the alcohols above tetracosanol.

As is generally known, elemental analysis data which were presented in previous papers[1], are poor criterions for judging the purity of the compounds with more than about eighteen carbon atoms. It was found, however, in the present study that the transition point rather than the melting point proved to be reliable because repetition of the purification process resulted in the raising or disappearance of the transition points though the melting point did not vary noticeably. Table I gives the melting, freezing and transition points of pure and mixed alcohols.

X-Ray examinations also revealed the interesting facts that the presence of as much as 0.5% of hexadecanol in octadecanol resulted in the apparance of β spacing while only γ spacing was found in octadecanol assumed to be pure. Similar states were found in higher members. Fig. 1 shows this phenomenon clearly.

The purification of the final products were carried out extensively by means of high-vacuum distillation followed by recrystallization until the melting points, transition points and X-ray spacings became constant.

The facts that the melting points and transition points of the alcohols obtained fell on smooth curves (Fig. 8) and the X-ray spacings of the alcohols above hexadecanol gave only γ form, indicate the high purity of the materials.

Time-heating Curves. — The melting points and transition points were determined by thermal analysis. A small drop of the molten substance was put on a junction of thermocouple which is made of copper and constantan of about 0.01 mm. in diameter and it was inserted into a doubly air-jacketed tube placed in a water bath.

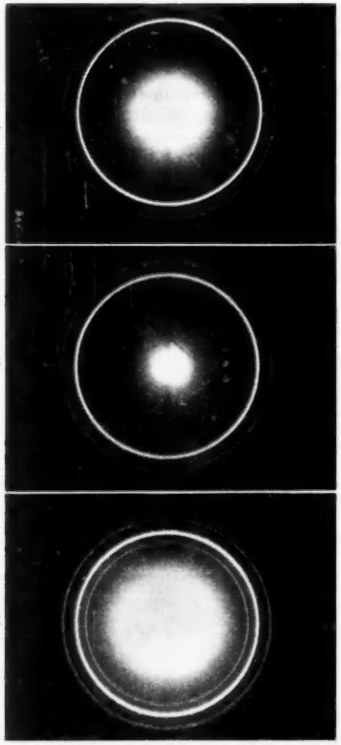

Fig. 1. X-Ray diffraction patterns of pure and mixed alcohols.
A Pure $C_{18}H_{37}OH$
B $C_{18}H_{37}OH$ containing 0.5%$C_{16}H_{33}OH$
C $C_{22}H_{45}OH$ containing 1% $C_{24}H_{49}OH$

Since a higher heating rate was found to be advantageous for good determination of the temperature, the measurements were carried out at the rate of about 2.0°C per minute, readings being taken every 10 sec. Each compound was run at least five times and the reproduciblity of the data was good. Probable errors of the temperatures determined on heating were estimated as being 0.1 to 0.3°C depending on the sharpness of the inflexion points and on the errors on calibration of

Table I. Weight percentage of lower compounds

		0	0.5	1	3	97	99	99.5	100
C_{16}—C_{18}	M.p.	57.3—58.1	57.1—58.0	56.7—57.6	55.7—56.6	48.1—49.7	48.2—49.3	48.1—49.1	48.3—49.3
	F.p.	57.0—56.9	56.8—56.6	56.5—56.4	56.7—56.5	48.0—47.8	48.3—48.1	48.4—48.2	48.4—48.2
	T.p.	51.3—51.1	49.0—48.9	48.6—48.5	47.0—46.7	37.8—37.6	39.2—39.0	40.9—40.8	41.8—41.7
C_{22}—C_{24}	M.p.	74.0—75.0	73.8—75.0	73.8—75.0	73.7—74.6	69.2—69.8	69.5—70.0	69.5—70.1	69.5—70.2
	F.p.	74.3—74.1	74.0—73.8	73.8—73.6	73.6—73.3	69.0—68.8	69.2—69.0	69.8—69.6	69.6—69.4
	T.p.	69.5—69.2	67.9—67.7	66.9—66.6	66.1—65.9	58.6—58.4	60.5—60.2	61.0—60.7	61.7—61.4

The temperature was measured by capillary method and uncorrected.
The heating or cooling speed was 1°C per minute.

the thermocouple, but those of cooling were about 1 C because the high temperature forms tended to supercool before the transitions, as may be seen in Fig. 4.

X-Ray Pattern Measurements.—It is known that the crystal spacings of the alcohols so far investigated here consist of β and or γ modifications in their low temperature forms and α modification in their high temperature form. The three modifications indicate different long spacing depending on different angles of inclination of hydrocarbon chains with respect to the planes of end groups. The most inclined γ form shows the shortest spacing. The short spacing also indicates a greater value in α and β forms because the molecules are more loosely packed in these forms than in the γ form. The data of all the compounds were reported in a previous paper[12] and are represented graphically here (Fig. 2). In the present investigation emphasis was laid on changes of spacings under various conditions especially on the correlations with thermal analyses using the same materials. The X-ray photographs were all taken using Cu-K radiation at 40 KV. and 20 ma. Camera distances and exposure times were varied depending on the chain lengths of the compounds.

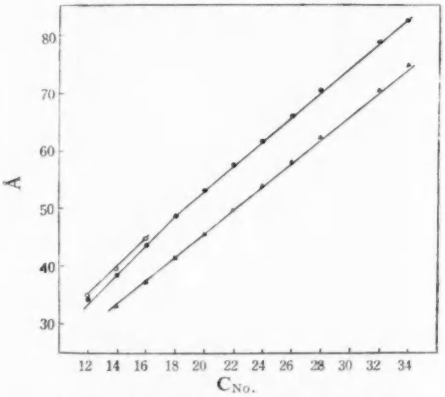

Fig. 2. Long spacings of *n*-higher alcohols.

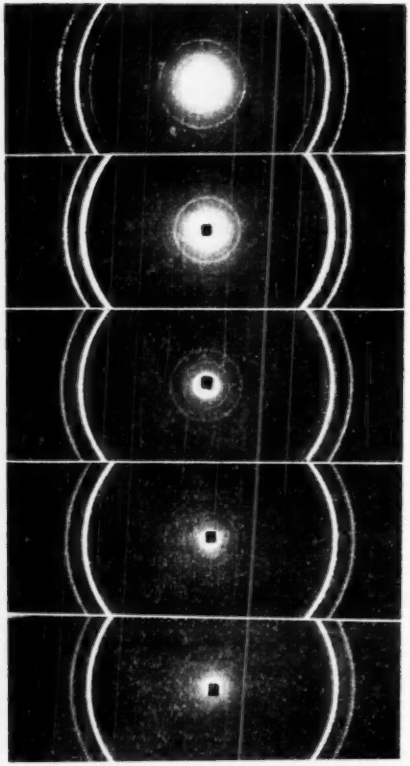

Fig. 3. Representative X-ray diffraction patterns of alcohols. The patterns in discending order are from C_{12}, C_{16}, C_{18}, C_{24}, C_{28} alcohols.

Patterns such as Fig. 3 were taken by the method of sampling as follows. The melted samples were mounted on aluminum rings with about 1.2 mm. diameter and 0.8 mm. width and then solidified in the air. The beam was irradiated perpendicularly to the plane of the sample.

An effective method for the detection of α or β form in γ form was found to be the measurement of the short spacing rather than that of the long spacing. To prepare specimens for these measurements the melted materials were drawn into thin-walled capillary tubes of about 0.2 mm. diameter. The rapidly cooled specimens were obtained by plunging the capillary tube containing the melt into an ice bath. On taking a photograph the capillary tubes were rotated during exposure. An electrically heated brass furnace in which the capillary tube was inserted was used, if necessary. Accuracy of the temperatures measured by means of a copper-constantan thermocouple was within 0.5°C.

Results and Discussion

The transition temperatures on cooling which were obtained by visual observation have been presented in earlier paper[11], but in this method it was experienced to be difficult to

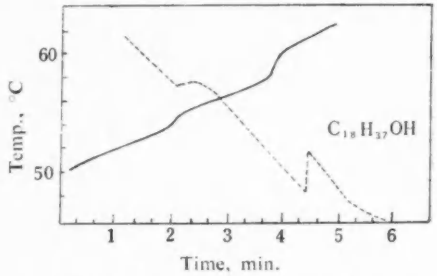

Fig. 4. Time-temperature curves for octadecanol.

12) a) K. Tanaka, T. Seto and T. Hayashida, *Bull. Inst. Chem. Res. Kyoto. Univ.*, 35, 123 (1957). b) K. Tanaka, T. Seto and A. Watanabe and T. Hayashida, ibid., **37**, 281 (1959).

identify the transition point on heating. By the present study more reliable and detailed results could be obtained.

Rotational Transition.—Typical thermograms obtained for octadecanol are given in Fig. 4. Phase transitions, which occur at 54.5°C on heating and at 52.5°C on cooling, are shown by the break in the curves, latent heat absorption or evolution being indicated. Evidently the transition is of the first order and reversible. The previous X-ray diffraction patterns[12] and dipole moment measurements[13] indicated that the transition is rotational. For the alcohols from tetradecanol to hexacosanol similar thermograms were obtained as those presented above in contrast with the results of Phillips and other workers[8a,f] who reported the transitions only on cooling in most of these alcohols. However, the present results were very reproducible even when the thermal histories of the samples had been varied and, furthermore, the data were consistent with those obtained by the previous X-ray patterns[12],*.

Although the present thermal studies for tetradecanol and hexadecanol could not reveal three formes, the previous X-ray studies[12] indicated that these compounds are trimorphic in the solid state and the low temperature forms which consisted of β and γ forms, transform them into high temperature form (α) at the different temperatures, the lower temperatures being the β to α transition point; the alcohols above hexadecanol showed the simple γ to α transitions.

The break in the heating curve of hexacosanol was barely detectable and the interval

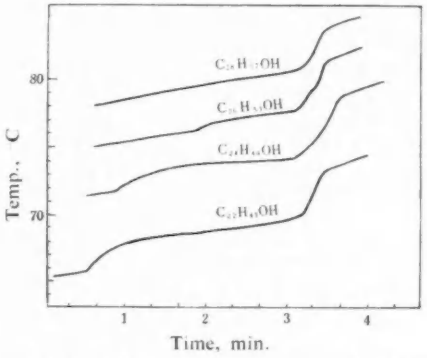

Fig. 5. Time-temperature curves for C_{22}, C_{24}, C_{26}, C_{28} alcohols.

13) K. Asai, E. Yoda and S. Yamanaka, *J. Phys. Soc. Japan*, **10**, 634 (1955).

* Some disagreements will be found between the previous and present results. The former must be revised in view of the use of purer materials and more accurate techniques in measurements in the present study.

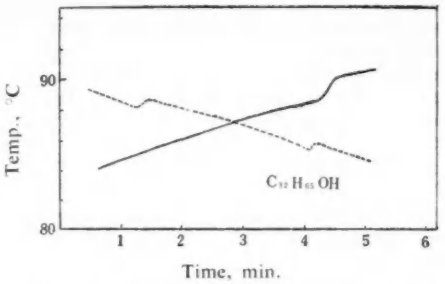

Fig. 6. Time-temperature curves for dotricontanol.

between the melting and transition points is narrow (1.2°C) (Fig. 5). The behaviors of the alcohols above hexacosanol differ markedly from those of the lower members of the series. The curves for octacosanol and dotriacontanol showed that the transitions on heation are missing while those on cooling are still present. However, both transitions were found to disappear at tetratriacontanol. These results are consistent with those by the present X-ray data, according to which in two shorter members (C_{28}, C_{32}) the γ form persisted up to the melting points and in the last member (C_{34}) only the γ form appeared at the temperature just below its freezing point.

Concerning the existence of transition in dodecanol some disagreements can be found in the literature[8ac,9ab,12a,14-16]. In the present study, non-existence of the transition was verified by the method such as thermal analysis using rapidly or slowly cooling technique, or X-ray pattern measurements made just below the freezing point with an exposure time of 15 min., and dielectric constant measurements

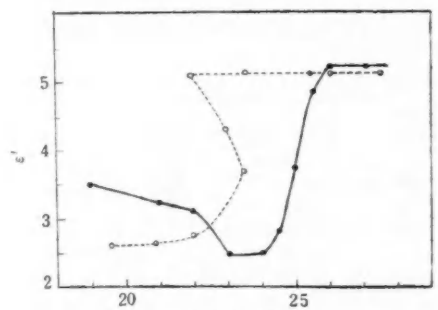

Fig. 7. Temperature dependence of the dielectric constant of dodecanol at 0.5 KC.
● Heating ○ Cooling

14) J. D. Bernal, *Nature*, **129**, 870 (1932).
15) E. Ott, *Z. physik. Chem.*, **193**, 218 (1944).
16) E. Frosch, *Ann. Physik*, **42**, 254 (1942).

at 0.5 (Fig. 7) and 5 KC. in which the results agreed with those of Smyth.

In Table II the data obtained by thermal analyses are given together with those obtained from the literature. The corresponding diagram is shown in Fig. 8.

TABLE II

Alcohol	Carbon No.	M. p. °C	Transition points, °C	
			Heating	Cooling
Dodcyl	12	24.0	—	—(21.6)Ph.
Tetradecyl	14	38.0	36.2	33.5(35.0)Ph. (34.4)S.
Hexadecyl	16	49.5	45.7	43.0(45.0)Ph. (43.2)S. (43.8)K.
Octadecyl	18	58.5	54.5	52.5(53.6)Ph. (53.4)S. (54.7)K.
Eicosyl	20	65.0	63.5	58.2
Docosyl	22	70.5	67.6	63.5(64.5)S.
Tetracosyl	24	75.5	72.8	71.5
Hexacosyl	26	79.3	78.1	73.5
Octacosyl	28	82.5	—	77.5
Dotriacontyl	32	88.5	—	86.2
Tetratriacontyl	34	91.0	—	—

Ph.; Phillips and Munford (Thermal analyses).
S.; Smyth et al. (Dielectric measurements).
K.; Kolp and Lutton (Thermal analyses).

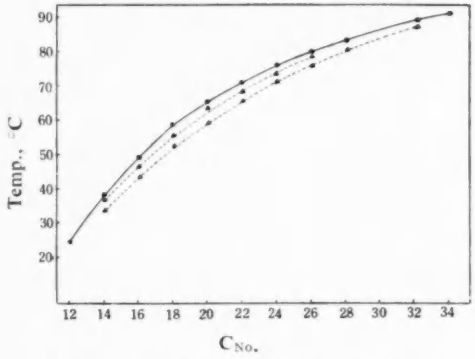

Fig. 8. Melting and transition points of *n*-higher alcohols.
● Melting point
▲ Transition point (heating)
△ Transition point (cooling)

It appears to be interesting that variations in properties of the α forms were observed as the chain length of the compounds increased. In the previous and present studies the following observations have been obtained.

I) Opacities of α forms increase in visual inspections.

II) Inflexions at the transition points become smaller (Fig. 5).

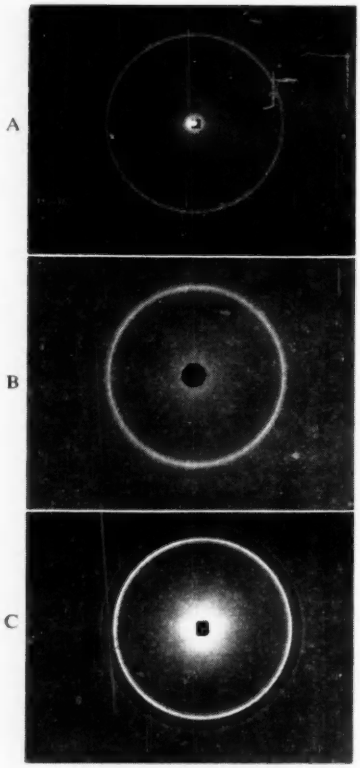

Fig. 9. X-Ray diffraction patterns of the α forms. The photographs were taken after the samples had been standing at the temperatures just below their freezing points for 2 hr.
A $C_{16}H_{33}OH$ C $C_{24}H_{29}OH$
B $C_{20}H_{53}OH$

III) Side spacings of α forms split into two lines (Fig. 9).

IV) In α forms inclination of the hydrocarbon chain to the plane of the ends increases (Fig. 2).

These facts would suggest that deviations in configurations or molecular motions from the typical rotational state may increase as the chain lengthens. Although it is necessary for complete interpretations of the data to await to obtain further data, a possible surmise is that molecular vibration around the axis, rather than rotation, may be caused in such longer compounds.

β to γ Transformation*.—It was reported by Smyth et al.[8c] to explain their result by dielectric constant measurements that in octadecanol and other alcohols rotational transition

* According to Hoffman, the term transformation will be used here to denote phase changes such as β to γ or α to γ which occur spontaneously on storage.

appeared when the sample was heated immediately after it was cooled from the melt while the transition failed to appear on heating the stored sample. Their argument suggests that the β form obtained on cooling may transform into the α form but the transformation of this β form into the γ form which has occurred during the storage, may make it difficult for the transition to take place. The latter X-ray investigation made by Kolp and Lutton[8c] seemed to substantiate this fact although there appeared to remain some doubts in their thermal analysis. As described above, however, the present thermal studies showed that heating transitions invariably appeared in the materials which had been prepared under various conditions such as rapid cooling, slow cooling, or prolonged storage and X-ray data also revealed the existence of γ to α transitions.

Apart from the facts described above, examination with β to γ transformation seemed to be so interesting that more detailed X-ray studies were undertaken. The results of the experiments with tetradecanol and hexadecanol indicated that this transformation took place as evidenced by the increasing intensity of the γ spacings. They appeared to be very gradual, occurring over a wide temperature range. For example, after being kept at 42°C for 24 hr. a sample of hexadecanol showed nearly equal amounts of β and γ forms in their low temperature form which had consisted of about $2/3\beta$ and $1/3\gamma$ forms before the heating. Both compounds indicated no transformation on storage at about 25°C for 24 hr. It was also found that the low temperature forms of these alcohols contained more γ forms when they were cooled slowly from the melt as compared with when they were cooled rapidly. This may be partly due to the β to γ transformations which occurred during the cooling and partly due to the α to γ transformations which will be discussed in the next section.

Because of the absence of the β form in alcohols above hexadecanol, this transformation can not be considered in these compounds. It may be concluded that the β to γ transformation exists only in tetradecanol and hexadecanol but it is so slow as to provide no appreciable effects on rotational transitions in qualitative measurements.

α to γ Transformation.—This transformation, as well as β to γ transformation, was reported by Smyth, Kolp and other workers[8cf]. Recently Asai[13] demonstrated the stability of the α form in octadecanol in his dielectric constant measurements. In the present X-ray investigations the behaviors of α forms in the series were examined by careful control of the temperatures of the samples. It was found that the high temperature form of tetradecanol consists of α and γ forms, the former being the less stable. The data were obtained by holding the compound at the temperature just below its freezing point for about 2 hr., indicating that about 2/3 of the initially existing α form was transformed into the γ form (Fig. 9). In hexadecanol evidence of a smilar behavior was found at the temperature 1°C above its transition point, but at the temperature 1°C below its freezing point the observed spacing indicated only the α form. This α form proved to be stable so that no transformation could be observed within a few hours (Fig. 9). The α forms appearing in the alcohols above hexadecanol showed a considerable stability over the entire region of the temperatures. The relationship described above is illustrated diagrammatically in Fig. 10. It

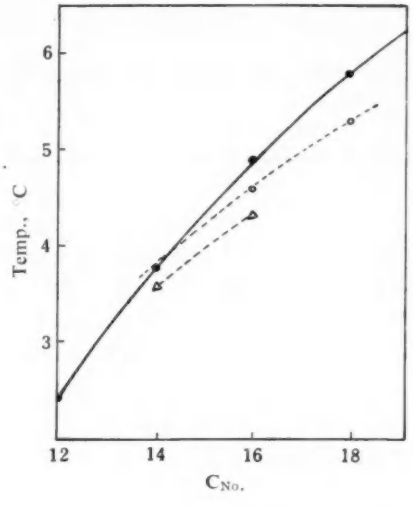

Fig. 10.

● Melting point
○ γ to α transition point
△ β to α transition point

will be apparent that γ to α transition points are higher than β to α transition points and that the α form is unstable only when it coexists with the γ form but once γ to α transformations have taken place the resulting α form is stable.

It is expected that the α form obtained only on cooling may be somewhat unstable. However, the X-ray examinations show that the α form in dotriacontanol is stable at least within about 2 hr.

Summary

1. Determination of the melting points and transition points of the even carbon numbered alcohols from C_{12} to C_{34} was made by thermal analysis. The transition points of the alcohols above C_{18}, except C_{22}, have never been reported.

2. The reversible transition sets in at C_{14} and terminates at C_{26}. The transition of C_{28} and C_{32} is irreversible, appearing only on cooling and both transitions disappear at C_{34}. Probably the pure sample of dodecanol may indicate no transition in any methods of measurements.

3. Properties of the α forms gradually change with increasing chain lengths.

4. The β to γ and α to γ transformations were examined by X-ray pattern measurements and the results were discussed.

5. Transition points and X-ray spacings may be reliable criteria of purity of higher alcohols, and probably of some other long chain compounds.

The author wishes to express his sincere thanks to Professor Ryozo Goto and Professor Kenzo Tanaka of Kyoto University for their continual guidance and encouragement. He is also grateful to Dr. Tsuneo Seto of Kyoto University for his kind direction and criticism in the X-ray diffraction measurements. Thanks are also tendered to Dr. Kenjiro Asai of Kyoto University for his kind direction in the dielectric constant measurements.

Department of Applied Chemistry
Himeji Technical College
Idei, Himeji

SHORT COMMUNICATIONS

A New Rapid Method of Determining Molecular Weight of Water Soluble Linear Polymers by the Measurement of Rate of Settling of Clay Suspensions

By Yūkichi TOYOSHIMA

(Received April 25, 1961)

During the past decade it has been reported that certain water-soluble linear polymers can give rise to the aggregation of clay particles in a state of aqueous suspension[1,2]. In this communication this fact was investigated in a more quantitative manner by observing the relation between the rate of (hindered[3]) settling v of clay suspensions under addition of a linear polymer and the molecular weight of the polymer.

Itaya clay (product of Yamagata Prefecture) levigated and after removing pebbles and large aggregates, was dried and used as suspensoid. Polymers used in this study were purified as described in a previous article[4].

The suspension was introduced in a sedimentation tube of 67.3 cm. long, which was agitated by rotating the tube for 15 min. at a speed of 5 revolutions per minute. After stopping agitation, settling rate of the suspension was measured at 30.0±0.1°C. Intrinsic viscosity of the polymer freshly dissolved in aqueous 1 M sodium nitrate solution was also measured at 30.00±0.01°C in a capillary viscometer of the Ubbelohde type, and the molecular weight of the polymer was determined from it.

In Figs. 1 and 2 $v \sim [\eta]^{30°C}_{1\,M\,NaNO_3}$ relation was shown for thy system in which 0.02% (to the amount of clay) of polymer was added to the 5% clay suspension. A linear relationship between v and $[\eta]^{30°C}_{1\,M\,NaNO_3}$ was confirmed. A similar linearity was also found for a different content of polymers (below 0.02%) and a different concentrations of clay suspensions (above 5%) so long as the other experimental conditions were kept constant. We may discuss in details the mechanism of aggregation

1) A. S. Michaels, *Ind. Eng. Chem.*, **46**, 1485 (1954).
2) M. Noda, *Kōgyō Yōsui*, **30**, 33 (1961).
3) C. Orr, Jr. and J. M. DallaValle, "Fine Particle Measurement", The Macmillan Co., New York (1959), p. 48.
4) Y. Toyoshima, *J. Chem. Soc. Japan, Pure Chem. Sec. (Nippon Kagaku Zasshi)*, **82**, 1295 (1961).

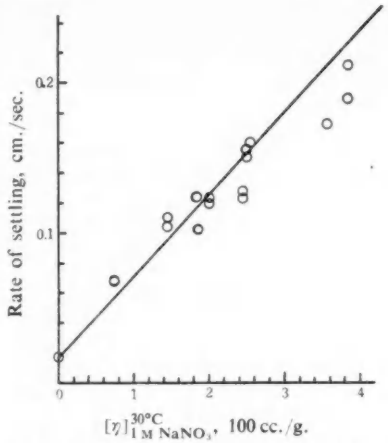

Fig. 1. The relationship between $[\eta]^{30°C}_{1\,M\,NaNO_3}$ and v for polyacrylamides.

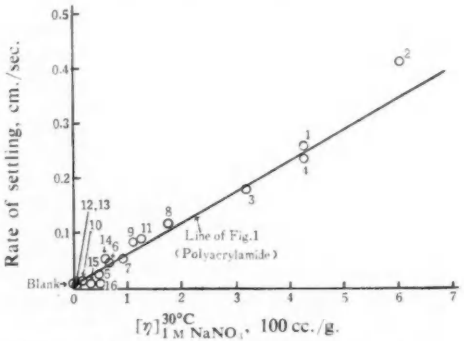

Fig. 2. The relationship between $[\eta]^{30°C}_{1\,M\,NaNO_3}$ and v for various water soluble linear polymers.

1, 2, 3, 4 } Partially hydrolyzed polyacrylamide
5, 6, 7 } Polyvinyl alcohol
8, 9 } Sodium carboxymethylcellulose
10, 11 } Polyvinylpyrrolidone
12, 13 } Dialdehyde starch
14 Agar
15 Gelatin
16 Polyethylene oxide

of clay particles referring to this linearity in a separate reports*. Here we should like rather to draw attention to the fact that using this relation between v and $[\eta]^{30°C}_{1\,M\,NaNO_3}$ together with the known relation between $[\eta]^{30°C}_{1\,M\,NaNO_3}$ and molecular weight M of the polymer, we can correlate v with M, and that using such a relationship we can determine the molecular weight from the measurement of sedimentation velocity, which is easier to practise than a similar and well known method of molecular weight determination by the measurement of intrinsic viscosity.

In the case of polyacrylamide, $v \sim [\eta]$ relation is expressed as

$$v = K[\eta]^{30°C}_{1\,M\,NaNO_3} + a \qquad (1)$$

while that of $[\eta]$ and M is

$$[\eta]^{30°C}_{1\,M\,NaNO_3} = 3.73 \times 10^{-4} M^{0.66} \qquad (2)$$

therefore we obtain from 1 and 2,

$$\log(v-a) = 0.66 \log M + \log(3.73K \times 10^{-4}) \qquad (3)$$

where K is a constant, and a the rate of settling without the addition of polymer. Measurement of $[\eta]^{30°C}_{1\,M\,NaNO_3}$, v and a shows that such a linear relationship really holds as shown in Fig. 3. Hence it enables a rapid

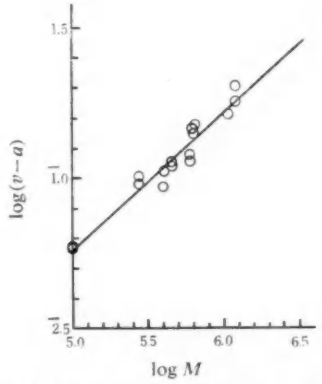

Fig. 3. The relationship between $\log M$ and $\log(v-a)$ for polyacrylamides.

determination of the molecular weight of unknown polyacrylamide from the simple determination of rate of settling under the definite condition of sedimentation test using the clay suspension of the same origin. As for the other various water-soluble linear polymers, for instance, partially hydrolyzed polyacrylamide, polyvinyl alcohol, sodium carboxymethylcellulose, polyvinylpyrrolidone, dialdehyde starch, agar, gelatin, and polyethylene oxide, the same linear relationship as in Fig. 1 was also obtained as shown in Fig. 2. Hence their molecular weights can be rapidly determined from the rate of settling of

5) New Product Bulletin, No. 34, American Cyanamid Co., New York (1955), p. 2.

* The details will be published in a near future.

clay suspensions as in the case of polyacrylamide if the relationships between $[\eta]^{30°C}_{1\,M\,NaNO_3}$ and molecular weights for these polymers are determined previously by the method, for instance, of light scattering or osmotic pressure. As a routine procedure for product control, this new method is perhaps one of the rapid and simple methods for determining molecular weights of water-soluble linear polymers.

The author wishes to express his sincere thanks to Dr. Tsunetaka Sasaki of Tokyo Metropolitan University and Dr. Ryōhei Matsuura of Kyushu University for their advice and criticism, to Dr. Akira Nakatsuchi and Dr. Jirō Kato of our Institute for constant guidance, Mr. Takesada Akiba of our Institute for his permission to publish this work, and to Mr. Mitsuo Ōno for his technical assistance.

Nitto Institute of Chemical Research
Kamikizaki, Urawa

Cation-exchange Properties of Phosphoantimonic(V) Acid

By Takuji Ito and Mitsuo Abe

(Received June 9, 1961)

Limitation of the use of organic ion-exchange resins, in recent years, brought much attention to the development of synthetic inorganic ion exchangers[1,2].

This paper describes some of the ion-exchange properties of phosphoantimonic(V) acid recently discovered. The experimental results indicate that the material is one of the very promising ion exchangers.

Experiment was made with an attempt to obtain the precipitate which was composed of antimony pentoxide and phosphoric acid. When antimony pentachloride was poured in the aqueous solution of phosphoric acid, the rate of formation of the precipitate obtained by the hydrolysis of the said chloride became extremely slow as the concentration of phosphoric acid increased. In case that the concentration of phosphoric acid was suitable relative to that of antimony pentachloride, gelatinous precipitate which was very difficult to filter was gradually formed in warming the solution. After filtering under suction and drying at 80°C, glassy materal was obtained. The material was physically and chemically stable against water, salt solutions and solutions of strong mineral acids, and showed strong cation-exchange properties even in dilute acid solutions.

When the material was added to 0.1 M ammonium nitrate solution its pH fell rapidly at first and then reached to a stational value (approximately 1.8), due to the liberation of H^+ produced by exchange with the cation in the solution. The adsorption of NH_4^+ on the material was 1.4 meq./g.

The analytical results of the glassy material indicate that the mole ratio of antimony pentoxide to phosphorus pentoxide contained was about 2 : 1.

This new material was provisionally given a name of "Phosphoantimonic Acid". This glassy acid was able to exchange reveresibly its H^+ with NH_4^+, alkali, alkaline earth and other metal ions (e. g. Ag, Cu etc.).

As one example of ion-exchange reversibility, 0.1 M ammonium nitrate solution was passed down a column (0.8 $cm^2 \times 7$ cm.) filled with this glassy ion exchanger of H-form. H^+ was liberated as a result of quantitative adsorption of NH_4^+. The adsorbed NH_4^+ was quantitatively eluted by treatment with 3 N nitric acid.

Extremely interesting is the strong adsorption of K^+ on the material in acid solutions. When the 0.01 M potassium chloride solution

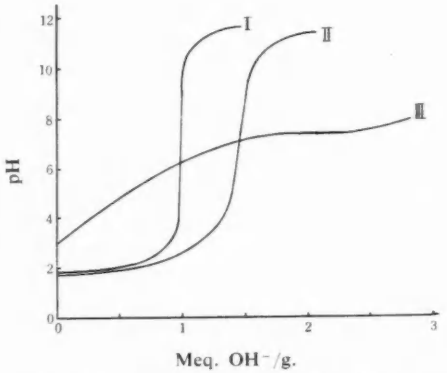

Fig. 1. pH-titration curve for phosphoantimonic acid.
I : 0.01 N H_2SO_4 100 ml.
II : Phosphoantimonic acid
III : Zirconium phosphate (quoted from Ref. 2)

1) K. A. Kraus, H. O. Philips, T. A. Carlson and J. S. Johnson, Paper 1832 presented at the 2nd International Conference of the Peaceful Uses of Atomic Energy, Geneva, 1958.
2) C. B. Amphlett, L. A. McDonald and M. J. Redman, *J. Inorg. & Nuclear Chem.*, 6, 220 (1958).

was added to a column in H-form, K^+ was adsorbed very easily and completely just as NH_4^+ done. The adsorbed K^+ could not eluted even by treatment with 3 N hydrochloric acid or 3 N nitric acid and it was, however, easily eluted with 1 M ammonium nitrate solution. It seemed to us that the abnormal absorbability on this material in strong acid solution might be perhaps attributed to the unordinary structure of phosphoantimonic acid.

The pH-titration curve of the glassy material showed that it was a strong monobasic acid (Fig. 1). It seems extremely possible that phosphoantimonic acid shows strong acid cation-exchange property, because antimonic acid (formally, hexahydroxyl antimonic acid $H[Sb(OH)_6]$) itself is monobasic and has the same strength of acidity as that of acetic acid (viz. dissociation constant; $H[Sb(OH)_6] = 4 \times 10^{-5}$, $CH_3COOH = 1.66 \times 10^{-5}$).

Research Laboratory of
Resources Utilization
Tokyo Institute of Technology
Meguro-ku, Tokyo

Chemical Constitution of Enmein a Bitter Principle from Isodon trichocarpus Kudo

By Takashi KUBOTA, Teruo MATSUURA
Tsutomu TSUTSUI and Keizo NAYA

(Received September 11, 1961)

The partial structure IA was suggested by Takahashi, Fujita and Koyama[1] for enmein[2] (isodonin[3]), $C_{20}H_{26}O_6$, m. p. 274~275°C, $[\alpha]_D$ −156° (acetone). We now wish to propose the structure I for enmein from the following evidences.

Reduction reactions, carried out by us and by other investigators[1,2], of enmein are summarized as follows. Catalytic hydrogenation of enmein (λ_{max}^{EtOH} 232.5 mμ (ε 7400)) affords a mixture of dihydroenmein-a (IIa), $C_{20}H_{28}O_6$, m.p. 256~257°C (decomp.) (λ_{max}^{EtOH} 297 mμ (ε 36); ν_{max} 2.90, 5.72, 5.87 μ), and dihydroenmein-b (IIb), $C_{20}H_{28}O_6$, m. p. 215~216°C (decomp.) (ν_{max} 2.82, 5.72, 5.82 μ). On mild treatment with sodium borohydride IIb is epimerized to IIa. Dihydroenmein-a is also obtained by the sodium borohydride reduction of enmein in methanol at room temperature. Both dihydroenmeins give the same diacetate (III), $C_{24}H_{32}O_8$, m. p. 231~232°C (decomp.), which is obtained also by the reduction of diacetylenmein (IV), $C_{24}H_{30}O_8$, m. p. 221~223°C (decomp.). Both enmein and dihydroenmein are reduced with sodium borohydride in ethanol at 60°C to yield tetrahydroenmein (V), $C_{20}H_{30}O_6$, m. p. 260°C (decomp.) (ν_{max} 2.91, 5.86 μ), (triacetate (VI), $C_{26}H_{36}O_9$, m. p. 193°C (ν_{max} 5.78 μ, no hydroxyl)). Since dihydroenmein-a (IIa) (ν_{max} 5.87 μ; exalted δ-lactone) is recovered unchanged after consuming one mole of alkali on hydrolysis, it is suggested that enmein has a δ-lactone group.

The partial structure IB is deduced from following results. Chromium trioxide-oxidation of dihydroenmein-a (IIa) affords bisdehydrodihydroenmein (VII), $C_{20}H_{24}O_6$, m. p. 251~253°C (decomp.), (monosemicarbazone, $C_{21}H_{27}O_6N_3$, m. p. 225~226°C). Bisdehydrodihydroenmein consumes one mole of dilute alkali (1/60 N) on hydrolysis to yield an acid (VIII),

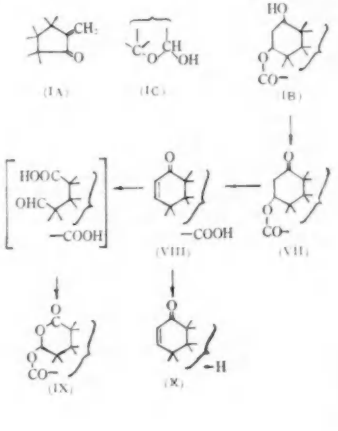

$C_{20}H_{24}O_6 \cdot 1/3H_2O$, m. p. 233°C (decomp.) (ν_{max} 5.64, 5.75, 5.86, 6.01 μ), (monomethylester, $C_{21}H_{26}O_6$, m.p. 245~246°C, monosemicarbazone, $C_{21}H_{27}O_6N_3$, m. p. 265~267°C (decomp.). Inspection of the ultraviolet spectra of VIII (λ_{max}^{EtOH} 225 mμ (ε 9600)) and its monosemicarbazone (λ_{max}^{EtOH} 278 mμ (ε 14300)) shows that the acid VIII possesses an α, β-unsaturated

1) M. Takahashi, T. Fujita and Y. Koyama, *J. Pharm. Soc. Japan* (*Yakugaku Zasshi*), **78**, 699(1958); **80**, 594, 696(1960).
2) T. Ikeda and S. Kanatomo, ibid., **78**, 1123 (1958).
3) K. Naya, *J. Chem. Soc. Japan, Pure Chem. Soc.* (*Nippon Kagaku Zasshi*), **79**, 885 (1958). In comparison of infrared spectra, isodonin was identical with enmein which was kindly supplied by Dr. S. Kanatomo, Kanazawa University.

ketone group, –CO–CH=CH–. Ozonolysis of VIII affords a crystalline neutral substance (IX), $C_{19}H_{22}O_5$, m. p. 249~251°C (decomp.), which consumes two moles of dilute alkali (1/50 N) on hydrolysis, gives positive color reactions for an aldehyde and shows no more absorption of the enone group in its ultraviolet spectrum. On pyrolysis VIII is decarboxylated to yield a neutral substance (X), $C_{19}H_{24}O_4$, m. p. 169~172°C (λ_{max}^{EtOH} 225 mμ (ε 8500)).

Bisdehydrodihydroenmein (VIII) consumes two moles of alkali (1/5 N) to yield an amorphous acid, while the neutral substance X is recovered unchanged after consuming one mole of alkali on hydrolysis. Therefore it is suggested that a lactone group is newly formed in oxidation of IIa to VII. On the other hand, treatment of dihydroenmein-a (IIa) with ethanolic sulfuric acid affords an *O*-ethyl derivative (XI), $C_{22}H_{32}O_6$, m. p. 193~195°C, (monoacetate, $C_{24}H_{34}O_7 \cdot 1/2C_6H_6$, m. p. 103~105°C, (no hydroxyl in its infrared spectrum)). Treatment of IIa with methanolic hydrogen chloride affords *O*-methyldihydroenmein(XII), $C_{21}H_{30}O_6$, m. p. 192~193°C, which reverts to dihydroenmein-a (IIa) on acid-catalyzed hydrolysis. The presence of a methoxyl group in XII was confirmed by the Zeisel analysis and the NMR spectrum (τ 6.68; three protons) of dehydro-*O*-methyldihydroenmein (XIII), $C_{21}H_{28}O_6$, m. p. 218~220°C, which is obtained from XII by chromium trioxide-oxidation. On hydrolysis XIII consumes one mole of alkali to yield a crystalline acid (XIV), $C_{21}H_{28}O_6 \cdot H_2O$, m. p. 190~192°C (decomp.) (λ_{max}^{EtOH} 230 mμ (ε 9700); ν_{max} 5.75, 5.85, 5.97, 6.17 μ), (monomethyl ester $C_{22}H_{30}O_6$, m. p. 189~192°C (λ_{max}^{EtOH} 228 mμ (ε 10400)), monosemicarbazone $C_{22}H_{31}O_6N_3 \cdot H_2O$, m. p. 205°C (decomp.) (λ_{max}^{EtOH} 277.5 mμ (ε 14900)). Conversion of XII to XIV (via XIII) is easily recognized as the transformation, IB→VII→VIII, of the part IB in XII. From these results, it is concluded that the remaining oxygen atoms in the enmein molecule exist as a cyclic hemi-acetal group IC.

Recently two important degradation products were isolated by Kanatomo[4], namely 1-ethyl-4-(3, 3-dimethylcyclohexyl)benzene (XV) on dry distillation of enmein with baryta and retene (XVI) on selenium dehydrogenation of the lithium aluminum hydride-reduction product of dihydroenmein. Kanatomo suggested that enmein has the carbon skeleton of phyllocladene (XVII) and the ketonic and lactonic carbonyl groups exist at the C_{15}- and C_{18}-positions of XVII, respectively.

4) S. Kanatomo, *J. Pharm. Soc. Japan*, (*Yakugaku Zasshi*), **81**, 1049 (1961).

However, from the molecular formula and the partial structure, IA, IB and IC, of enmein, it is apparent that enmein must have a tricarbocyclic ring. Our proposed structure I for enmein is supported by the following evidences. The NMR spectra of diacetyldihydroenmein (III) and dehydro-*O*-methyldihydroenmein (XIII) show that the number of protons attached to the carbon atom, to which one or two oxygen atoms are bonded, is five (at the C_1-, C_3-, C_6- and C_7-positions) in III and four (at the C_3-, C_6- and C_7-positions) in XIII. Furthermore a sharp singlet (τ 3.80; one proton equivalent) attributed to the C_7-proton of the hemiacetal acetate[5] in III shows that the carbon atom adjacent to the hemiacetal group in enmein must have no hydrogen atom. From the biogenetic point of view, it is suggested that the hemiacetal group in the ring B may be formed from a 7-keto-diterpene by the Bayer-Villiger type oxidation followed by the reduction of a lactone formed.

Faculty of Science
Osaka City University
Kita-ku, Osaka

5) J. A. Pople, W. G. Schneider and H. J. Bernstein, "High Resolution Nuclear Magnetic Resonance", McGraw-Hill Book Comp., Inc., New York (1959), p. 395.

Tritium and Carbon-14 in the Tree Rings

By Kunihiko KIGOSHI and Yoshio TOMIKURA

(Received September 25, 1961)

The data on the atmospheric carbon-14 and tritium in recent years can be expected to furnish new information on the circulation problems of geophysics.

There are several data on the concentration of carbon-14 in the atmospheric carbon dioxide and of tritium in the rain water[1-3]. This note presents the results of measurements of the concentration of carbon-14 and tritium in the tree rings of recent years. The purpose of the measurements was to obtain the annual mean concentration of the atmospheric carbon-14 and of the tritium in the rain water.

1) T. A. Rafter and G. J. Fergusson, U. N. Conference on the Peaceful Uses of Atomic Energy, **18**, 526 (1958).
2) F. Begeman and W. F. Libby, AFOSR Report Number: Tn-56-561, ASTIA Document Number AD 110381 (1956).
3) H. v. Buttlar and W. F. Libby, *J. Inorg. & Nuclear Chem.*, **1**, 75 (1955).

TABLE I. TRITIUM AND CARBON-14 CONCENTRATION IN TREE RINGS

Interval of growth of tree ring	Trritium concentration, $T/H \times 10^{15}$		Carbon-14 concentration**	
	Pine ; grown in Hiroshima*	Paulownia ; grown in Tokyo	Pine ; grown in Hiroshima*	Paulownia ; grown in Tokyo
Aug. 1953~Sept. 1954	92.2±6.2		0.975±0.009	
Aug. 1954~Sept. 1955	54.5±4.2	96.3±8.1	0.967±0.009	1.032±0.012
Aug. 1955~Sept. 1956	80.7±8.9		1.006±0.008	
Aug. 1956~Sept. 1957	67.3±2.6	65.6±2.2	1.060±0.009	1.024±0.012
Aug. 1957~Sept. 1958	138.7±3.9		1.101±0.008	1.153±0.012
Aug. 1958~Sept. 1959	304.4±3.0	261 ±3	1.192±0.012	1.196±0.013
Aug. 1959~Sept. 1960	138.7±2.8*	111 ±2.8	1.221±0.013-	1.187±0.013

* This tree was cut down in April 1960, therefore the last tree ring corresponds to the period between Aug. 1959 and April 1960.

** The data are normalized to the concentration of Carbon-14 of the hypothetical modern wood which would not have been affected by industrial effect and nuclear tests.

The tree ring samples were previously dried in a vacuum desiccator at 110°C for several hours. The hydrogen in the tree ring was collected as water by combustion of the gas evolved by strong heating of the dried sample. The water obtained (100~150 ml.) was purified and electrolyzed in order of enrich the tritium. After the reduction of the volume of the water to about one hundredth, the deuterium content of the concentrate was measured by buoyancy method. The tritium disintegration rate was measured by an external quenched Geiger-Counter filled with hydrogen and propane. The preparation of hydrogen from the water and the operation of the counter were done in the similar manner to those developed by Östlund[4].

In Table I the measured tritium concentrations of the tree rings are shown together with the carbon-14 concentrations in the same tree rings. The carbon-14 concentrations were measured in the same manner as described in the previous paper[5]. The concentration of carbon-14 and tritium in the tree ring may be regarded as an annual mean value of the carbon-14 concentration in the atmosphere and that of the tritium concentration in the rain water respectively. The data on the carbon-14 presented here and in previous paper show a tendency of decrease after 1960 and seem to have a maximum value at the beginning of 1960.

The annual mean concentration of tritium in the rain water descreases after 1959 with the half life of about one year. Since the tritium in the troposphere has short mean life[2], the amount of tritium in the troposphere may be proportional to the amount of supply of tritium to the troposphere from the stratosphere. The observed decrease of tritium after 1959 and the annual variation of carbon-14 after 1959 suggest a stratospheric residence time of 1~2 years for these nuclides.

Department of Physics and Chemistry, Gakushuin University
Toshima-ku, Tokyo

4) H. G. Östlund, IAEA Tritium Symposium, Vienna, 1961, Paper TTS/17.

5) K. Kigoshi and T. Tomikura, This Bulletin, 33, 1576 (1960).

Variation of the Atmospheric Carbon-14 in Recent Years at Tokyo

By Kunihiko KIGOSHI and Kunihiko ENDO

(Received September 25, 1961)

This note presents the results of measurements made in recent years of the atmospheric carbon-14. The data are expected to furnish informations about the circulation problems of geophysics as well as to contribute to the evaluation on the hazard from the man-made radionuclides. The atmospheric carbon dioxide was collected in Tokyo by means of the absorption in the sodium hydroxide solution. The radioactivities were measured by an acetylene filled proportional counter as described in the previous paper[1].

The results obtained are shown in Table I. The unit of the values of the carbon-14 concentration listed in the table is a concentration of atmospheric carbon-14 at eighteenth century

1) K. Kigoshi and Y. Tomikura, This Bulletin, 33, 1576 (1960).

TABLE I. ATMOSPHERIC CARBON-14 CONCENTRATION

Collection date	Measured concentration of carbon-14*
1959	
20 Oct.	1.240±0.016
20 Nov.	1.250±0.013
4—5 Dec.	1.172±0.014
1960	
20 Jan.	1.149±0.017
1—5 Feb.	1.113±0.013
22—24 Feb.	1.240±0.027
2 April 9 May	1.121±0.011
25—26 May	1.105±0.010
24—25 June	1.105±0.010
27—29 July	1.140±0.005
5—7 Sept.	1.105±0.014
25—27 Sept.	1.172±0.009
24—26 Oct.	1.121±0.009
24—26 Nov.	1.021±0.009
22—24 Dec.	1.219±0.018
1961	
25—27 Jan.	1.010±0.014
21—23 Feb.	1.072±0.011
21—22 April	1.265±0.016
24—26 May	1.112±0.009

* The unit is a concentration of the atmospheric carbon-14 at eighteenth century.

calculated from the measured concentration of carbon-14 in the tree rings growing at that time.

Rafter and Fergusson[2] reported the carbon-14 concentrations in the atmosphere in New Zealand which showed regular increase of atmospheric carbon-14 concentration between December 1955 and December 1957 by nuclear tests. Compared to these data, Table I shows large fluctuation which might be due to the nature of the air mass at the collection date in Tokyo. The air mass into which carbon-14 from the stratosphere has been supplied at the latest time must have a high concentration of carbon-14. The exchange of carbon dioxide between the air and the surface ocean water may play an important role to surppress the atmospheric carbon-14 concentration. It has been observed by several authors[2-4] that the carbon-14 concentration in the surface ocean water showed large fluctuation due to the mixing of the surface water with the deep sea water. If this fluctuation has strong influence on the atmospheric carbon-14 concentration, the consideration on this line has to be taken for the evaluation of the Suess Effect and of the annual variation of the cosmic ray intensity measured by using the tree ring samples.

Department of Physics and Chemistry, Gakushuin University Toshima-ku, Tokyo

2) T. A. Rafter and C. J. Fergusson, U. N. Con. on the Peacefull Uses of Atomic Energy, **18**, 526 (1958).
3) S. Fonselius and C. Östlund, *Tellus*, **11**, 77 (1959).
4) W. S. Broecker, R. Gerard, M. Ewing and B. C. Heezen, *J. Geophys. Res.*, **65**, 2903 (1960).

Dipole Moment and Infrared Spectrum of 2, 3, 5, 6-Tetraisopropylnitrobenzene

By Ruka NAKASHIMA, Setsuo WATARAI and Toshio KINUGASA

(Received September 30, 1961)

Dipole moment and infrared spectrum of 2, 3, 5, 6-tetraisopropylnitrobenzene were examined. The process of the dipole moment measurement is the same as that described in the articles[1].

The dipole moment of this compound is 3.57D (in benzene solution, at 25±0.01°C), and is actually less than that of nitrobenzene (3.97D)[2], but not so different from that of nitrodurene (3.60D)[3].

The small value of the dipole moment observed is attributed, as generally accepted, to the decrease of the resonance moment of the nitro-group due to steric hindrance.

The infrared spectra were measured with a Perkin-Elmer Model 21 spectrophotometer (with rock salt prism) in chloroform solution in the region from 1670 to 1250 cm^{-1}.

Fig. 1 shows the infrared spectra of nitrodurene and 2, 3, 5, 6-tetraisopropylnitrobenzene, and the data are shown in Table I.

TABLE I

Compound	N–O stretch. vib. Asym. cm^{-1}	Sym. cm^{-1}	Diff. from C_6H_5–NO_2 ΔAs cm^{-1}	ΔS cm^{-1}
C_6H_5–NO_2	1527	1348	—	—
Nitrodurene	1526	1378	−1	30
Nitro-tetra-iso Pr–C_6H_5	1524	1389	−3	41

1) S. Mizushima and K. Higashi, *J. Chem. Soc. Japan (Nippon Kwagaku Kwaishi)*, **54**, 226 (1933).
2) Our observed data.
3) L. E. Sutton et al., *Rec. trav. chim.*, **78**, 790 (1959); In their paper, the dipole moment of nitrodurene was reported as 3.62 D, but they neglected P_A. So we recalculated their value in consideration of P_A (≈5% of P_E) to fit to our data.

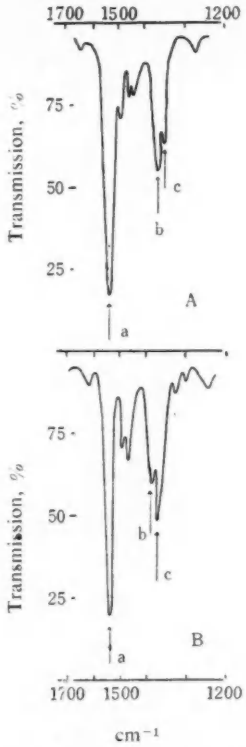

Fig. 1. Infrared spectra of nitrobenzenes (A: Nitrodurene, B: 2,3,5,6-tetra-isopropylnitrobenzene) in chloroform solution.

a: ν_{N-O} asym., b: ν_{N-O} sym., c: δ_{CH} in $-CH_3$

According to our previous observations on the general behavior of N–O sym. and asym. stretching vibrations of alkyl- and halogeno-nitrobenzenes[4], the N–O sym. was sensitive to the co-planarity of the nitro-group with the benzene plane, on the other hand, N–O asym. was affected by the polarity of substituents.

The infrared spectrum data obtained in the present investigation clearly reveal the general features mentioned above.

In comparing the value of ΔS, which seemed to represent the magnitude of steric hindrance, it may be suggested that a larger steric hindrance was in 2,3,5,6-tetraisopropylnitrobenzene than in nitrodurene.

There was a little discrepancy between the results obtained from the study with infrared spectrum and those from dipole moment.

A similar disagreement is found also in the series of the measurements of alkyl- and halogenonitrobenzenes, which will be discussed in elsewhere.

Department of Chemistry
Faculty of Science
Kobe University
Higashinada-ku, Kobe

4) R. Nakashima et al., The 7th. IR and Raman Symposium at Osaka, Proceeding papers, p. 151 (1960).

On the pH Dependence of Transport Behavior of Weak Acids and Weak Bases across Ion-exchange Membranes

By Manabu Senō and Takeo Yamabe

(Received October 10, 1961)

We have pointed out that the transport behavior of weak acids and bases across ion-exchange membranes depends remarkably on the solution pH[1]. It is noticed that there is a range of pH at which the maximum transport takes place. This behavior is due to the suppression of dissociation of acids in the lower pH range, and to the contribution of the competitive transport of hydroxide ions in the higher pH range, in the case of weak acids for example. In this communication, this problem is treated in general and some useful conclusions are derived.

Let us consider the three-component system consisting of strongly dissociated ions A^-, e.g., chloride ions, weak acid ions B^-, and hydrogen or hydroxide ions. It is assumed that the concentration of each component of the sample solution remains unchanged in course of the electrodialysis experiment and all the electrolytes which are adsorbed in the membrane are in the dissociated state. Then, the permselectivity coefficient T^{B}_{A+OH} is defined and written in terms of constant or known quantities as follows:

$$T^{B}_{A+OH} = \left(\frac{t_B}{t_A + t_{OH}}\right) \Big/ \left(\frac{C_{B_0}}{C_A + C_{OH}}\right) = T'^{B}_{A} \cdot \frac{KC_{OH}}{1 + KC_{OH}} \cdot \frac{1 + (C_{OH}/C_A)}{1 + T^{OH}_{A}(C_{OH}/C_A)} \quad (1)$$

4) T. Yamabe, M. Senō and N. Takai, This Bulletin, 32, 1383 (1959); *J. Chem. Soc. Japan, Ind. Chem. Sec.* (*Kogyo Kagaku Zasshi*), **64**, 556 (1961); I. Kamii, T. Tanaka and T. Yamabe, *J. Pharm. Soc.* (*Yakugaku Zasshi*), **81**, 931 (1961).

where t transport number, C concentration, K K_B/K_W, K_B and K_W dissociation constants of weak acid BH and water, and

$$T'^{B}_{A}\left(\begin{matrix}t_B\\t_A\end{matrix}\right)\Big/\left(\begin{matrix}C_B\\C_A\end{matrix}\right),\quad T^{OH}_{A}\left(\begin{matrix}t_{OH}\\t_A\end{matrix}\right)\Big/\left(\begin{matrix}C_{OH}\\C_A\end{matrix}\right)$$

are permselectivity coefficients* which are constant independently of experimental conditions, and the absence and presence of bar above symbols refer to the solution and the membrane phase respectively. Subscript B_0 means total acid molecules in dissociated and undissociated states, and B weak acid ions.

The ratio of transport numbers which expresses the relative amount of weak acid transferred across an anion-exchange membrane is

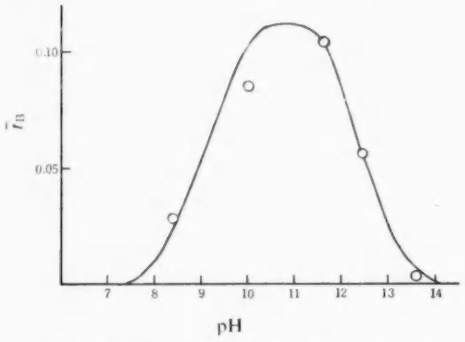

Fig. 1. Transport of boric acid across an anion-exchange membrane.
○ Experimental, —— Theoretical
Experimental conditions; A five-compartment cell, 0.33 mA./cm², 1 hr.; Membranes, heterogeneous ones made from Amberlite IR-120 or IRA-400; Stock solution, 0.05 M H_3BO_3, 0.05 M NaCl, NaOH (for adjustment of pH).

$$\frac{\bar{t}_B}{\bar{t}_A+\bar{t}_B+\bar{t}_{OH}}=\frac{T^{B}_{A+OH}\bar{C}_{B_0}}{\bar{C}_A+T^{B}_{A+OH}\bar{C}_{B_0}+\bar{C}_{OH}} \qquad (2)$$

The experimental verification of these expressions was obtained in the case of boric acid across an anion-exchange membrane as shown in Fig. 1. The experimental procedure was the same as that in the preceding papers[1]. The transport number t_B is the amount (equivalent**) of boric acid transferred across the anion-exchange membrane by passage of the electricity of 1 faraday. The theoretical curve was drawn according to Eqs. 1 and 2, in which quantities were estimated as follows; T^{OH}_{Cl} is 2, T'^{B}_{Cl} is 0.2*, $t_{Cl}+t_B+t_{OH}$, the transport number of anions across the anion-exchange membrane***, is 0.7 and K_B is 7.3×10^{-10}**.

This treatment leads us to the following general conclusion. The minimum pH at which the appreciable transport of a weak acid occurs depends primarily on its dissociation constant and nearly equals to pK_B-1, and the maximum transport takes place in the pH range between pK_B+1 and 12~13. The smaller is T^{OH}_{A} and the larger are C_A and C_B, the higher is the maximum pH. The same treatment can be applied to weak bases. The details will be presented in near future.

The authors express their thanks to Mr. Katuya Yanase for his experimental cooperation.

The Institute of Industrial Science
The University of Tokyo
Yayoi-cho, Chiba

* These are practically dependent on the current densities. T'^{B}_{A} is known from the electrodialysis experiment in the pH range higher than pK_B+1, where

$$T^{B}_{A}=(t_B/t_A)/(C_{B_0}/C_A)=T'^{B}_{A}.$$

** Only the dissociation of boric acid in the first step was considered. Further dissociations are so weak (dissociation constants 1.8×10^{-13} and 1.6×10^{-14}) that these contributions are neglected in the pH range smaller than 13 and in the larger pH range the contribution of hydroxide ions becomes overwhelming.

*** Strictly, it contains the contribution of the transport number of anions across the adjacent cation-exchange membrane.